SOMALIA WATER & LAND INFORMATION PROJECT

FAO

FIAT PANIS

N. 113 A
RELAZIONI E MONOGRAFIE AGRARIE SUBTROPICALI E TROPICALI
NUOVA SERIE

# GEOLOGY AND MINERAL RESOURCES OF SOMALIA AND SURROUNDING REGIONS

(with a geological map of Somalia 1:1,500,000)

edited by
E. ABBATE, M. SAGRI and F.P. SASSI

## A - REGIONAL GEOLOGY

ISTITUTO AGRONOMICO PER L' OLTREMARE
FIRENZE
1993

Cover photograph: the rim of the Somali plateau facing the Gulf of Aden in the Sheikh region. The plain in the foreground is the top of the Precambrian crystalline basement, which is covered by the subhorizontal Cretaceous Yesomma Sandstones (lower and middle part of the cliff) and Maastrichtian to Early Eocene Auradu Limestones (upper part of the cliff).

CONTENTS

## II - SEDIMENTARY AND VOLCANIC COVER

## III - STRUCTURAL GEOLOGY AND GEOPHYSICS

## B - MINERAL AND WATER RESOURCES

### IV - MINERAL RESOURCES AND APPLIED GEOLOGY



### V - HYDROGEOLOGY AND WATER RESOURCES

# FOREWORD

This monograph contains 43 papers presented at the *First International Meeting on the Geology of Somalia and Surrounding Regions* (GEOSOM '87), held in Mogadishu, November 23-30, 1987. It may be therefore considered as the Proceedings of GEOSOM '87.

The GEOSOM '87 Meeting, and the related scientific activity carried out in Somalia in the 1980s and late 1970s, were organized and financed mainly by the Italian Ministry of Foreign Affairs, in the frame of the university cooperation program. The Italian National Council for Research (CNR, *Mechanisms of ocean development: Red Sea - Gulf of Aden system and the Afro-Arabian shield* Project and other projects) and the Ministry for University and Research (MURST) also supported the above-mentioned research activities, which involved the Somali National University on one hand and teams from several Italian universities on the other.

Research concerned both basic and applied geology, as demonstrated by the contents of this monograph, which consists of two parts (A - Regional Geology; B - Mineral and Water Resources). It was also strongly oriented towards field work, and a significant result was the publication of the new *Geological Map of Somalia 1:1,500,000*.

As this monograph appears very late with reference to the date of submission of the papers (1988) and the date of editing (1990), its contents could not benefit by the most recent scientific literature. The great delay is due to the increasing difficulties encountered by Somalia since the late 1980s, and adjustments to the new situation in the activities of the university cooperation between Italy and Somalia. For the same reasons, the present monograph was edited in difficult circumstances and with few financial resources. Due to the lack of funds, its publication was uncertain for several years, but was finally made possible thanks to the open-mindedness of the Director of the *Istituto Agronomico per l'Oltremare*, an important institution for overseas research linked to the Italian Ministry of Foreign Affairs.

However, the great delay with which these two volumes and the related Geological Map of Somalia are published does not imply any decreased significance of the scientific results they present. Both the monograph and the map are rich in new data and, in science, data have a life longer than the five-year delay with which this monograph and map appear.

The support given by A. Bosellini (Italy), C. Faillace (Italy), J.D. Fairhead (Great Britain), J.C. Harms (U.S.A.), C.A. Kogbe (President, African Geological Society), A. Kröner (Germany), P. Omenetto (Italy), A.G. Smith (Great Britain), J. Sougy (France) and B. Zanettin ( Italy) is sincerely acknowledged. Their participation in the GEOSOM '87 Meeting as invited speakers was very important for its scientific success, as well as their help, as members of the Editorial Advisory Board, in editing the present monograph.

Thanks are also due to Laura Bonaiuti for her wise editorial advice in organizing the contributions and in aiding the technical preparation of these two volumes, and to Gabriel Walton, who did much to improve the linguistic aspect of several papers.

Lastly, the editors wish to dedicate this monograph to the young staff of the Somali National University, and particularly to those of the Faculty of Geology who are presently scattered throughout the world. Mostly as guests of universities or other scientific institutions, they are still working on the geology of Somalia with tenacity and hope. May their unforgettable country soon return to a state in which scientific research is again possible, and may their scientific and teaching contributions be determinant for the reorganization and continued development of Somalia.

Ernesto Abbate, Mario Sagri and Francesco Paolo Sassi

From *Geology and mineral resources of Somalia and surrounding regions*, Ist. Agron. Oltremare, Firenze, Relaz. e Monogr. 113, 3-40, 1993.

# THE CRYSTALLINE BASEMENT OF NORTHERN SOMALIA: LITHOSTRATIGRAPHY AND THE SEQUENCE OF EVENTS

F.P. SASSI *, D. VISONÀ *, G. FERRARA **, G.O. GATTO ***, H.A. IBRAHIM ****, A.A. SAID **** and S. TONARINI **

* Department of Mineralogy and Petrology, University of Padova, Corso Garibaldi 37, 35137 Padova, Italy.

** Department of Earth Sciences, University of Pisa, Via S. Maria 53, 56100 Pisa, Italy.

*** Department of Geology, Paleontology and Geophysics, University of Padova, Via Giotto 20, 35137 Padova, Italy.

**** Department of Geology, Somali National University, P.O. Box 1081, Mogadishu, Somalia.

ABSTRACT

New field work, petrographic analyses and radiometric geochronological work were carried out mainly in the western part of the Northern Somali Basement (NSB). Basing on the new results and the data in the literature, a general picture of NSB and a model of its multistage development are presented.

Seven main rock complexes are distinguished in NSB: five of them are metasedimentary sequences bearing some metavolcanic intercalations, two are igneous plutonic complexes.

The metasedimentary complexes are (from the older to the younger): 1) the Qabri Bahar Complex; 2) the Mora C.; 3) the Abdulkadir C.; 4) the Mait C.; 5) the Inda Ad C.. The first two complexes make up the medium to high grade, old polymetamorphic basement. The Abdulkadir and the Mait complexes are greenschist-facies sequences, respectively outcropping in the western and in the central part of NSB. The Inda Ad C. is a low to very-low grade sequence in the eastern part of NSB.

The igneous plutonic complexes are: 1) the Gabbro-Syenite Belt, which consists of several bodies emplaced both in the Qabri Bahar and in the Mora complexes; it underwent a foliation-producing metamorphism which did not obliterate the magmatic features; 2) the Younger Granites, which crosscut all rock complexes; some of them underwent a foliation-producing metamorphism.

The geological and petrological data give several constraints to the interpretation of the chronological relationships among the many petrogenetic events. Such constraints, jointly with some new radiometric age data, suggest the sequence of events schematically shown in Fig. 10. Due to the many metamorphic overprints and the low number of the analysed samples, isotopic chronological results are often affected by large MSWD values. However, they are consistent with the sequence of events reconstructed on geological bases.

All observed petrogenetic processes have been classified in four main thermic pulses or Major Events, the three youngest of which (and perhaps all) fall in the Pan-African time range.

The Major Event I is only recorded by relics of a granulite-facies metamorphism $M_1$ and the very old igneous processes ($B_1$, $B_2$, $G_1$) defessed from some protolith of this rock sequence. It may

represent the vestiges of a possibly pre Pan-African continental crust largely reworked and rejuvenated by the Pan-African event.

**The Major Event II** (older than 700 Ma) includes: regional synkinematic heating, with related amphibolite-facies metamorphism $M_2$ and anatexis $G_2$; related deformational activity; emplacement of the post-tectonic granitoids $G_3$ (e.g. Gebiley);

**The Major Event III** (ca. 700 to 640 Ma): extensional regime; aborted lithospheric rupture, i.e. crustal thinning; deposition of a late Precambrian rock sequence, with a volcanic activity (Abdulkadir Complex: $A_4$, $B_4$) which locally acquired peculiar features, due to local geodynamic situations (Mait Complex: $B_5$); uprise of gabbro and related mainly syenite melts through the thinned crust; therefore, regional metamorphism $M_3$.

**The Major Event IV** (ca. 550-500 Ma) includes: deposition of the Inda Ad sequence; emplacement of I-type, calcalkaline granite melts ($G_6$); further thermic pulse, with regional heating $M_4$ and deformational activity; final emplacement of A-type, postcollisional granitic melts ($G_7$).

In conclusion, the NSB is interpreted to be a Pan-African mobile zone. At the present erosion level, it has all ingredients of a shallow crust whose old parts are slightly deeper levels rehydrated during the Pan-African cycle and rejuvenated not only through regional heating and deformation, but also through the addition of new, quantitatively significant, magmatic masses. The Pan-African "vestigial facet" and "geosynclinal facet" sensu CLIFFORD (1968) coexist in the NSB, the latter being located in the eastern sector, the former in the western sector.

## INTRODUCTION

The crystalline basement outcropping in Northern Somalia (NSB for short) is largely unknown as regards both the descriptive aspects and its interpretation in a wider regional context. Specifically, few data exist in the literature concerning its structural setting, its lithostratigraphy and the sequence of events recorded in it. Furthermore, its relationships with the surrounding crystalline basements (Ethiopia, Kenya, Arabian-Nubian Shield, Mozambique Belt) are almost unknown, because the pertinent hypotheses which can be found in the literature are largely speculative, i.e. based on very few data. Chronological data are particularly scanty: the radiometric age values which were availables before 1987 are extremely few, and their reliability sometimes questionable.

Three stages can be detected in the growth of the literature concerning the NSB:

- the older stage is only represented by the early descriptions published by FARQUHARSON (1924), WYLLIE (1925), BARRINGTON BROWN (1931), PARKINSON (1932) and MACFADYEN (1933);
- the second stage is the product of the very active Geological Survey operating in the 50's in the former Somaliland Protectorate;
- the third stage is related to the activities carried out and/or promoted by the Faculty of Geology of the Somali National University, and includes papers published in the late 70's and in the 80's.

The 24 geological sheets (scale 1:250,000) mapped by the English geologists (J.L. DANIELS, D.C. GELLATLY, J.E. GREENWOOD, J.A. HUNT, J.E. MASON, J.A.B. STEWART, A.J. WARDEN and W.C. WHITE) of the Geological Survey of the former

Somaliland Protectorate in the 50's, and the related explanatory reports, are a very important data base concerning the rock types and sequences, the pattern and extension of the rock complexes, etc.. However, they clearly reveal the time in which they were performed; furthermore, in the legend of these maps some boxes are too much comprehensive, including rock types which today should be mapped separately. The few publications appeared in the 60's represent an extension of this second stage (GREENWOOD, 1960, 1961; GELLATLY, 1961, 1963, 1964; DANIELS et al., 1965; GREENWOOD and BLEACLKEY, 1967; GREENWOOD et al., 1967): they present more detailed analyses and/or interpretation and/or descriptions of some aspects of the NSB, as a conclusion of the research these authors carried out mainly in the 50's. Further developments of these activities were published later by WARDEN and DANIELS (1984), WARDEN and HORKEL (1984).

The third stage, into which the present paper and the whole GEOSOM 87 is to be classified, is the results of the efforts done by the Italo-Somali staff of the Somali National University. It is interesting to point out that these research works, often carried out in very difficult logistic conditions, were planned both for giving a Somali content to the lectures given by the Italian professors to the Somali students, and for training the Somali faculty staff. The results of these research activities are: a not detailed but modern outline of the NSB, a model of the sequence of events recorded in it, some radiometric age values and a proposal concerning the meaning of this basement in the ambit of a wider regional context.

The main conclusion of the present paper is that the NSB is a Pan-African ensialic mobile belt, consisting of a completely rejuvenated older crust (western sector) and juvenile Pan-African terrains (eastern sector). In presenting these results, the authors are aware that a better frame for their conclusions requires a richer set of radiometric age data and structural geological studies.

## THE MAIN ROCK COMPLEXES

Based on many considerations, seven main rock complexes may be distinguished in the NSB following the criteria of SASSI and IBRAHIM (1981) and SASSI and VISONÀ (1985): five of them are metasedimentary sequences bearing various types of intercalations, and two are igneous, plutonic complexes.

The metasedimentary complexes are (from the older to the younger): 1) the Qabri Bahar Complex; 2) the Mora Complex; 3) the Abdulkadir Complex; 4) the Mait Complex; 5) the Inda Ad Complex. The first two complexes in this list make up the medium to high grade, old metamorphic basement. The Abdulkadir and the Mait complexes are greenschist-facies rock sequences, respectively outcropping in the western and the central part of the NSB. The Inda Complex is a low to very-low grade metasedimentary sequence making up the eastern part of the NSB.

The igneous complexes are: 1) the Gabbro-Syenite Belt; 2) the so-called Younger

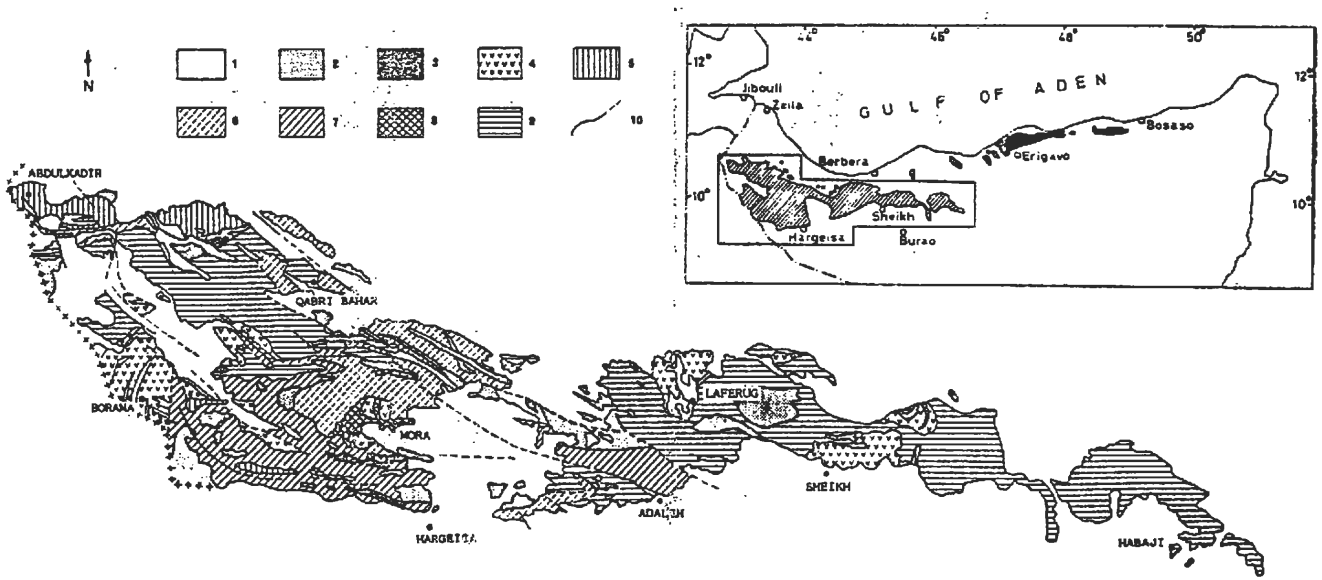


Fig. 1 - Geological sketch of the Northern Somali Basement.
1: Non metamorphic cover; 2: Younger Granites; 3: Gabbro-Syenite Belt: main syenite bodies; 4: Gabbro-Syenite Belt: main gabbro bodies; 5: Abdulkadir Complex: metapelites, acidic and basic metavolcanites; 6: Mora Complex: metapsammites, gneisses and migmatites; 7: Mora Complex: marbles; 8: Mora Complex: amphibolite-rich sequences; 9: Qabri Bahar Complex: paragneisses, migmatites, amphibolites, etc; 10: main tectonic lineaments and faults. Inset: the black areas indicates the Inda Ad and Mait complexes.

Grani·es.

There are not conclusive data concerning the nature of the boundaries between the above mentioned metasedimentary complexes, and for establishing whether they represent elements of an originally unique stratigraphic sequence (later differentiated by peculiar metamorphic-deformational histories), or accreted exhotic terranes, each having an independent history. However, certainly all of these metasedimentary complexes were side-by-side rock suites, roughly in their present relative position since the lowermost Paleozoic, when they were injected by the Younger Granites. Furthermore, the Qabri Bahar and the Mora complexes certainly shared a long common history, at

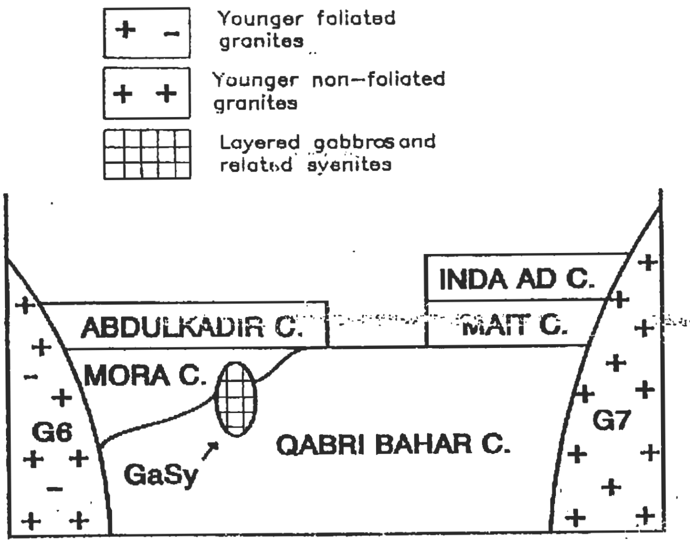


Fig. 2 - Schematic representation of the mutual relationship among the main rock complexes in the Northern Somali Basement. The boundaries at the base of the Inda Ad, Mait and Abdulkadir complexes are interpreted as unconformities.

least since the time of emplacement in them of the Gabbro-Syenite Belt.

Fig. 1 represents the approximate location and extension of the outcropping areas of the seven rock complexes. Their mutual relationship is roughly sketched in Fig. 2.

## The Inda Ad Complex and the Mait Complex

After the studies by MASON and WARDEN (1956) and GREENWOOD (1960, 1961), these two rock complexes have been studied by ABBATE et al. (1981, 1985) and

DAL PIAZ et al. (1987); some new data and observations have been also reported by IBRAHIM and SASSI (1977 and in: D'AMICO et al., 1981), WARDEN and DANIELS (1984), WARDEN and HORKEL (1984). For a more complete picture of the features of these two complexes, readers are referred to these papers, from which all pieces of information given below are taken.

The Inda Ad C. is a metasedimentary rock suite making up the youngest part of the NSB. The main protoliths were sandstones, siltstones, mudstones, intraformational conglomerates and marbles. ABBATE et al. (1985) pointed out the turbiditic character of the Inda Ad sedimentation, and referred it to the erosion of an orogenic volcanic arc.

This complex underwent a foliation-producing metamorphism of low to very-low grade. After having underwent this metamorphism and folding (a single generation of large scale, N to NW trending folds), the Inda Ad Complex was intruded by the Younger Granites (specifically the Arar, Infero and Las Bar bodies).

Some problematic fossil finding (ABBATE et al., 1981) and the radiometric age of the mentioned granite bodies (see the pertinent Section) constrain the range of sedimentation age of the Inda Ad Complex in the uppermost Proterozoic to Cambrian.

The Mait Complex has been described as a narrow, NNE, greenstone belt interposed between the Inda Ad C. and the high grade basement. It was affected by a greenschist-facies metamorphism and two generations of folds. The protoliths were pillow to massive basalts (and related pyroclastics), pelitic to clastic sediments and thin carbonate beds. The present boundary between the Inda Ad and the Mait complexes is tectonic, but, mainly due to the longer deformational history, the Mait Complex has been interpreted as an older (Late Proterozoic) sequence over which the Inda Ad Complex unconformably deposited (ABBATE et al., 1981).

The occurrence of an unconformity between the Inda Ad and the Mait complexes, and another unconformity between the Mait Complex and the high grade basement, are admitted by WARDEN and DANIELS (1984).

## The Abdulkadir Complex

This rock complex makes up the uppermost, less metamorphic part of the NSB to the west of Berbera, and typically outcrops in the area Harirad-Abdulkadir. It is a volcano-sedimentary sequence of unknown age, which is interpreted, consistently with WARDEN and DANIELS (1984), as unconformably deposited on the presently underlying metamorphic basement after its high grade metamorphism.

In fact, as sketched in Fig. 2, the assumed basement of the Abdulkadir Complex, i.e. the high-grade rocks which are in contact with it, commonly belong to the Mora Complex but somewhere belong to the Qabri Bahar Complex (e.g. in the Tog Darkainle, and at approx. 10 Km to the east of Borama: SASSI and VISONÀ, 1985). Such a situation hints an unconformity at the bottom of the Abdulkadir Complex.

It is worthy to point out that the Abdulkadir Complex is never affected by intrusions of the Gabbro-Syenite Belt, but locally is injected by unfoliated Younger Granites.

The main metasedimentary rock types of the Abdulkadir Complex are quartz-phyllites, muscovite-chlorite schists and quartz-rich schists, with minor intercalations of quartzites (sometimes Al-rich: e.g. at Damal) and marbles.

The main volcanogenic rock types are metarhyolites and related acidic metavolcanoclastics (e.g. at Gebiley), associated with minor basic metavolcanics and metavolcanoclastics (e.g. at Ruqi). All these rocks are probably related to a single, two-modal magmatic event characterized by a distinct Daly-gap. Albite-epidote amphibolites and chlorite-epidote-actinolite schists are the main basic orthoderivates.

Some chemical data concerning the metarhyolites (Table 1) indicate a significant compositional alteration due to hydrothermal activity and / or synmetamorphic chemical mobility. Fig. 3 shows the location of the data points in some standard diagrams.

All petrographic data indicate that these rocks only record one metamorphic event, which took place under intermediate pressure conditions, as shown by the occurrence of kyanite in the Al-rich quartzites at Damal. The temperature range recorded in the mineral assemblages occurring in the metabasites is relatively large, covering the whole range of the greenschist facies, from the chlorite-actinolite zone to the albite-epidote-horneblende zone. The strategy of the field works was not suitable for recognizing the pattern of the metamorphic zoneography: however, the range of metamorphic grade is so large that we cannot exclude that parts of the Abdulkadir Complex occur as medium to high grade metamorphics, and may have been confused with parts of the Mora Complex.

Table 1 - Chemical data concerning the Borama metarhyolites (Abdulkadir Complex).

| Sample | 280 | 286 | 286/1 | 287 | 288 | 83-66 | 83-71 | 83-72 | 83-73 | 83-74 | 81-319 |
|---|---|---|---|---|---|---|---|---|---|---|---|
| $SiO_2$ | 71.30 | 76.98 | 78.63 | 76.67 | 76.93 | 74.78 | 78.45 | 73.40 | 71.36 | 78.03 | 74.83 |
| $TiO_2$ | 0.30 | 0.08 | 0.08 | 0.06 | 0.06 | 0.26 | 0.09 | 0.33 | 0.60 | 0.11 | 0.14 |
| $Al_2O_3$ | 13.35 | 12.26 | 12.40 | 12.38 | 12.50 | 12.61 | 12.08 | 12.93 | 13.28 | 11.92 | 13.25 |
| $Fe_2O_3$ | 2.50 | 0.79 | 0.41 | 0.81 | 0.82 | 1.15 | 0.55 | 1.98 | 2.04 | 0.73 | 1.13 |
| FeO | 0.59 | 0.25 | 0.28 | 0.22 | 0.22 | 1.34 | 0.61 | 1.15 | 1.94 | 0.36 | 0.65 |
| MnO | 0.05 | 0.01 | 0.01 | 0.01 | 0.01 | 0.04 | 0.01 | 0.05 | 0.07 | 0.02 | 0.07 |
| MgO | 0.37 | 0.30 | 0.27 | 0.25 | 0.22 | 0.10 | 0.11 | 0.14 | 0.52 | 0.13 | 0.06 |
| CaO | 1.24 | 0.39 | 0.58 | 0.32 | 0.54 | 0.93 | 0.48 | 0.83 | 1.67 | 0.27 | 0.57 |
| $Na_2O$ | 4.08 | 4.01 | 6.05 | 4.25 | 4.96 | 2.67 | 4.35 | 3.60 | 3.76 | 3.22 | 4.71 |
| $K_2O$ | 1.82 | 3.65 | 0.39 | 3.31 | 2.15 | 5.63 | 2.56 | 5.16 | 4.02 | 4.44 | 3.94 |
| $P_2O_5$ | 0.08 | - | - | - | 0.02 | 0.02 | 0.01 | 0.03 | 0.13 | 0.01 | 0.01 |
| LOI | 1.84 | 0.91 | 0.49 | 1.03 | 0.83 | 0.31 | 0.43 | 0.10 | 0.39 | 0.39 | 0.69 |
| Total | 95.68 | 98.72 | 99.10 | 98.28 | 98.43 | 99.53 | 99.30 | 99.60 | 99.39 | 99.24 | 99.36 |
| Rb | 50 | 90 | 17 | 84 | 51 | 119 | 78 | 164 | 126 | 175 | - |
| Sr | 106 | 92 | 149 | 76 | 101 | 80 | 58 | 69 | 147 | 44 | - |

Three low-grade, volcano-sedimentary rock sequences may be tentatively correlated with the Abdulkadir Complex, as concerns both the protoliths and the metamorphic grade.

One of these rock sequences occurs at Jirbi (GATTO et al., 1981, p. 31-32 and Fig. 4). We are deadling there with a layered rock sequence with subvertical, NS trending layers of reddish metarhyolites, minor chlorite-epidote-actinolite schists and quartz phyllites, and subordinate metasiltites, quartzites, Ca-silicate marbles and marbles. This sequence is boundaried by tectonic surfaces: as a consequence, it is speculative to relate it to the Abdulkadir Complex, but it is risky to disregard this possibility. In agreement with WARDEN and DANIELS (1984) we are inclined to admit this correlation.

The second possible correlation is between the Abdulkadir and the Mait complexes (WARDEN and DANIELS, 1984; DAL PIAZ and SASSI, 1987). In this case, the rock association and the metamorphic grade indicate some analogies, but also some differences: acidic metavolcanics prevail in the Abdulkadir Complex, but are lacking in the Mait complex. However, the reconstruction of the mutual relationships among the different complexes in the whole NSB (Fig. 2) assigns an equivalent position to these two complexes, suggesting that such a correlation is highly probable: the very large distance between the two areas may account for the above mentioned differences in their lithologic content.

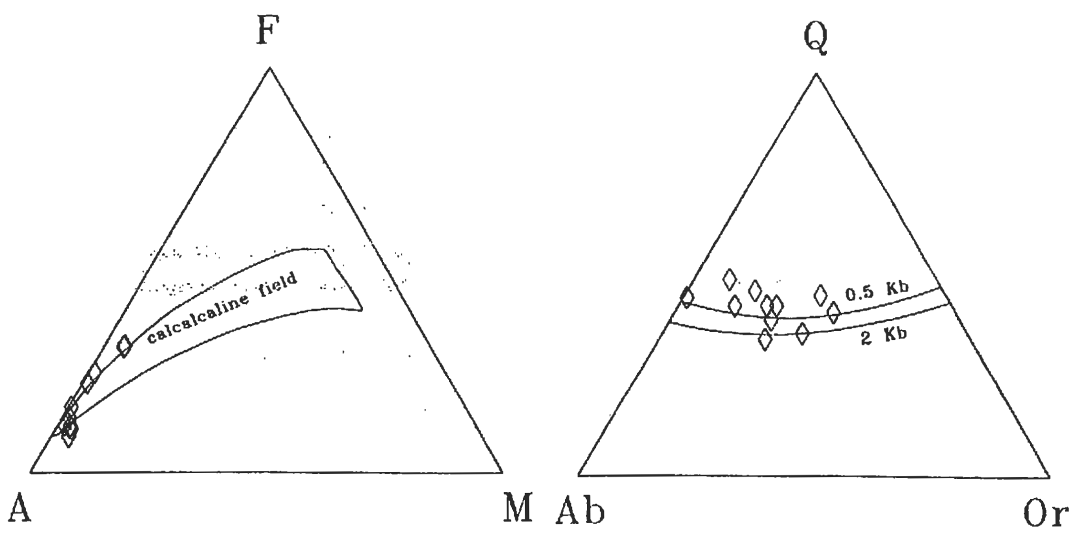


Fig. 3 - Some chemical features of the metarhyolites from Borama (Abdulkadir Complex).

The third rock sequence which may be correlated to the Abdulkadir Complex occurs to the E of Sheik, at Gugux (GATTO et al. 1981, p. 49 and Fig. 2): reddish porphyric gneisses occur there, which have been described as possible acidic metavolcanics. If these reddish gneisses belong to the Abdulkadir Complex, they are located in the middle between the type-areas of the Abdulkadir (to the west) and Mait (to the east) complexes. However, the importance of the situation at Gugux is also the fact that the reddish gneisses have been reported to lie over the Qabri Bahar migmatites: this fact may be a further evidence of a regional unconformity at the bottom of the Abdulkadir Complex, showing that this complex lies somewhere over the Mora Complex and somewhere over the Qabri Bahar Complex.

## The Mora Complex

This rock complex, mainly outcropping in the westernmost part of the NSB, is a medium to high grade metasedimentary rock sequence characterized by the occurrence

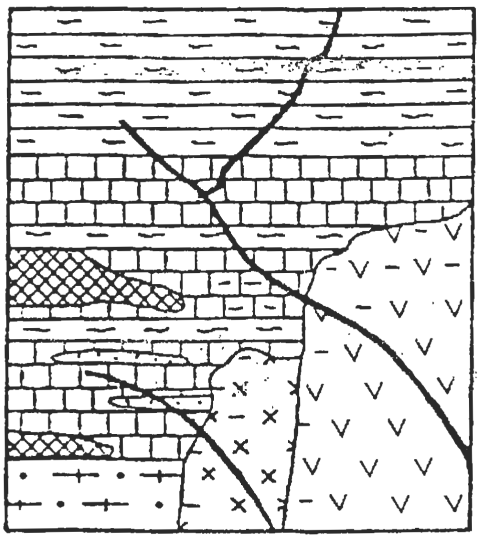

Fig. 4 - Schematic lithostratigraphic column of the Mora Complex, also showing the intrusion relationships in it of the Gabbro-Syenite Belt and the Younger Granites (from SASSI and VISONÀ, 1985). Symbols as in Fig. 5.

of abundant marbles (often Ca-silicate rich), quartzites with Al-rich layers and amphibolites. However, important rock types also are migmatites (e.g. at Ged Deeble: SASSI and VISONÀ, 1985), fine-grained paragneisses and medium-grained gneisses, all of them very similar to those making up the bulk of the Qabri Bahar Complex. This rock complex typically outcrop in the Cadda-Mora area, NNE of Arabsyo.

Fig. 4 is a schematic representation of the lithostratigraphic column of the Mora Complex, also showing that this complex was intruded both by the Younger Granites and the Gabbro-Syenite Belt.

Considering the strong analogies of the metamorphic features between the Mora and the Qabri Bahar rock complexes, the hypothesis is plausible that the former complex belongs to the Qabri Bahar Complex, only representing a protolithologic peculiarity in it (mainly displayed by the abundant marbles). However, it is also possible that the Al-rich quartzites occurring at the bottom of the Mora Complex (e.g. the kyanite-bearing quartzites of Tuke Kulantai: SASSI and IBRAHIM, 1981) represent basal levels of a younger sedimentary suite deposited on the Qabri Bahar Complex. The "conglomeratic" gneisses occurring 2 Km to the west of Jable, between Figi Ayub and Ceelal (GATTO et al., 1981) could also be meaningful from this point of view. Their matrix can be described as a medium to coarse-grained paragneiss, and amphibolites prevail among the pebbles. However, the possible tectonic origin of these "conglomeratic" gneisses should be evaluated.

The Mora Complex displays a polymetamorphic history. The mineral assemblages prevailing in these rocks indicate amphibolite facies to anatectic conditions, but relics of an older, granulite facies event have been found (SASSI and VISONÀ, 1987, and this volume), and a greenschist-facies overprint is also recognizable almost everywhere. Therefore, three metamorphic events are well recognizable in the Mora Complex.

## The Qabri Bahar Complex

The Qabri Bahar Complex is the deepest part of the exposed NSB, and typically outcrops in the Qabri Bahar-Bagai area, as well as along the road between Hargeisa and Berbera (e.g. at Dubato, and to the north of Arabsyio). It mainly consists of banded paragneisses, sometimes bearing kyanite and sillimanite (e.g. at Hudiso), augen orthogneisses (e.g. the country-rocks of the Daimoleh Younger Granite), migmatites (e.g. Hudiso, Tog Kalajab; Ged Deble), amphibolites, metagranitoids (e.g. at Gebiley). Ca-silicate felses also occur locally.

Migmatites often bear large nebulitic leucosomes and amphibolitic melanosomes: the latter are frequently layered, and dismembered in more or less continuous alignments of variously sized boudins.

The metagranitoids of Gebiley make up an intrusive body within the Qabri Bahar Complex. In the field, it looks like an old granitoid body rich in crustal xenoliths (mainly fine-grained paragneisses and minor amphibolites), which was affected by a foliation-producing metamorphism. An evaluation of its metamorphic grade should consider that the igneous zoning of the plagioclases is still preserved, and that chlorite + muscovite seem to be the stable phyllosilicate assemblage: therefore, the metamorphic grade shows a greater affinity with the lower-grade metamorphism of the Abdulkadir Complex than with the higher grade metamorphism of the Qabri Bahar Complex.

Two rock suites may be distinguished in the Qabri Bahar Complex in the Berbera-Hargheisa area: a topographically lower sequence of granitic orthogneisses and a topographically upper sequence of amphibolite-bearing migmatites and metagranitoids.

HUNT (1958, 1960) proposed a distinction between the Barkasan Series (rich in

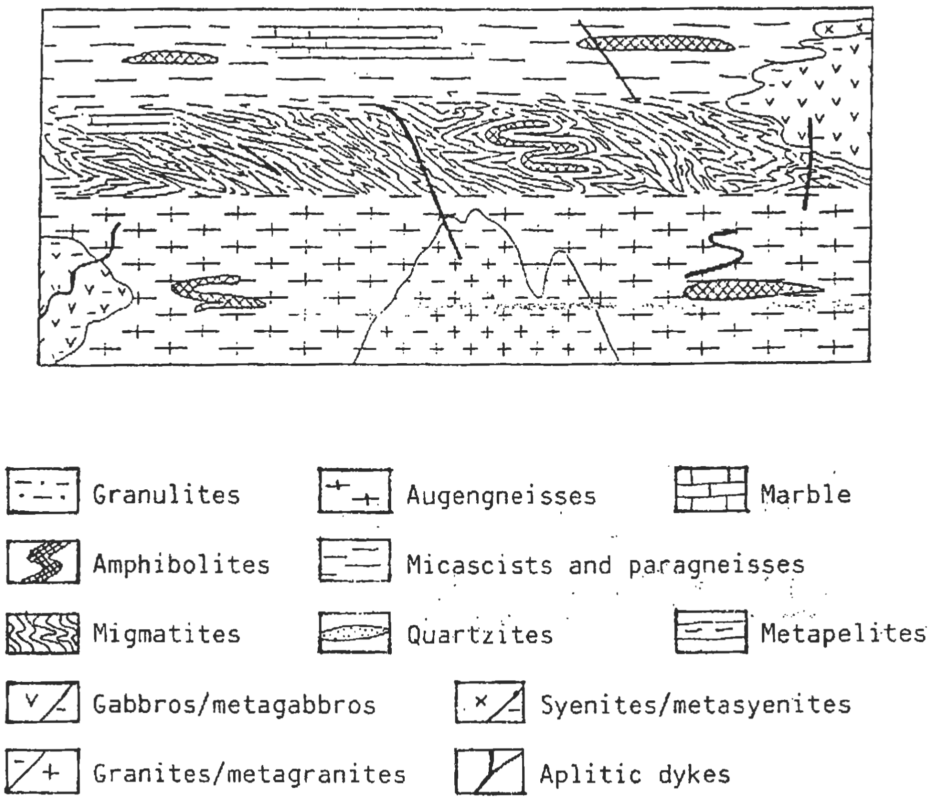


Fig. 5 - Schematic lithostratigraphic column of the Qabri Bahar Complex, also showing the intrusion relationship in it of the Gabbro-Syenite Belt and the Younger Granites (from SASSI and VISONÀ, 1985).

amphibolites) and the Daarburuk and Kalaha Series (both consisting of granitic gneisses and fine-grained gneisses, in different quantitative ratio respectively).

Fig. 5 schematically represents the lithostratigraphic column of the Qabri Bahar Complex, and also shows that it was instruded both by the Younger Granites and by the Gabbro-Syenite Belt.

The Qabri Bahar Complex is polymetamorphic. Specifically, it records three metamorphic events: an older, granulitic metamorphism only represented by mineral relics (SASSI and VISONÀ 1987, and this volume), a prevailing amphibolite-facies metamorphism strictly related to anatexis, and a greenschist facies metamorphic overprint, which also produced the foliation and the low-grade metamorphism in the Gebiley metagranitoids. The metamorphic situation is indistinguishable from that occurring in the Mora Complex, although a younger sedimentation age of the latter cannot be excluded.

Disregarding the folds genetically related to the migmatitic stage, two main deformation stages are recorded in the Qabri Bahar (as well as in the Mora) Complex. The older folding is chronologically related to the amphibolite-facies metamorphism. The younger folding developed after the emplacement of the Gabbro-Syenite Belt. Low-angle shear zones and NE to NW verging thrusts have been observed in the Burao-Las Dureh (GELLATLY, 1960) and Hargheisa-Berbera area (SACCHI et al., 1985, 1987).

## The Gabbro-Syenite Belt

Numerous bodies of layered gabbros occur in the NSB, and their regional distribution induced DANIELS et al. (1965) to use for them the name of Gabbro Belt. They are systematically associated with syenitic bodies over regional scale: consequently SASSI and VISONÀ (1985) described them as the Gabbro-Syenite Belt (Fig. 6) and DAL PIAZ and SASSI (1986) as "gabbro-syenite association".

Syenites sometimes are strictly associated to quantitatively prevailing gabbros (e.g. Sheikh, Lo'jebiye, Hegebo); elsewhere they make up large distinct bodies to which minor gabbros are associated (e.g. Borka Haggar). Carbonatites are also to be mentioned as members, although quantitatively not important, of this gabbro-syenite association: they only locally occur, making up dykelets and/or centimetric to decimetric ovoidal patches within the syenites. The anular shape of the Lo' Jebiye body is worthy of mention.

Field situations indicate that syenites (sometimes nefelinesyenites, e.g. at Darkainle, GELLATLY, 1963) are slightly younger than gabbros, and that alkaline, pyroxene-bearing granites are sometimes associated to them as dykes, stocks and small bodies.

All these rocks were studied by HUNT (1960), MASON (1962), GELLATLY (1963), DANIELS et al. (1965), WARDEN and DANIELS (1984) and DAL PIAZ et al. (1985, 1987): readers may refer to these papers for a more exhaustive description and the original interpretations.

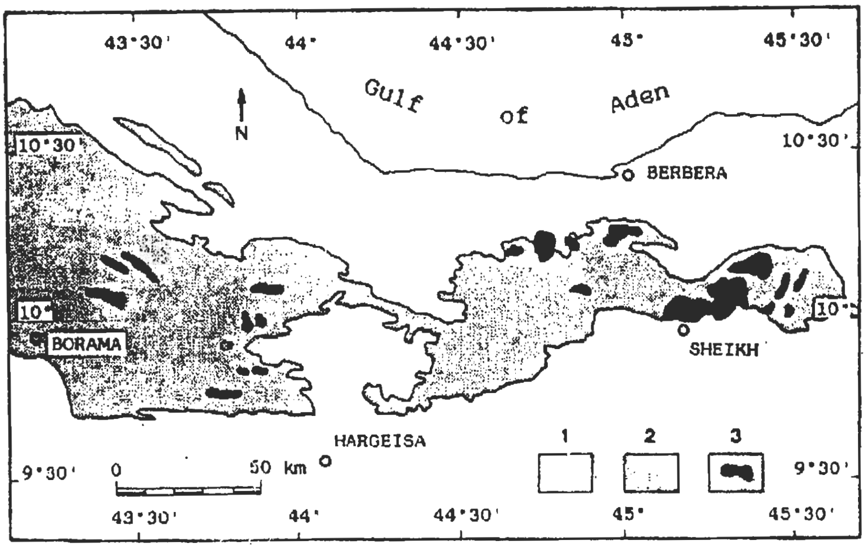


Fig. 6 - Regional distribution of the main bodies making up the Gabbro-Syenite Belt (3) within the Northern Somali Basement (2), 1: non metamorphic cover (taken from DANIELS et al. 1965)

A very important point to stress here is that these gabbros do not represent an ophiolitic suite but record an ensialic magmatic activity (DAL PIAZ et al., 1985, 1987), probably developed under extensional conditions after the main orogenic event, i.e. after the high-grade to anatectic event (DAL PIAZ and SASSI, 1986; GATTO et al., 1987).

Table 2 reports the chemical data concerning the syenites and the alkaline granites belonging to the Gabbro-Syenite Belt. Some chemical features of these rocks are also shown in Figs. 7, 8. These rocks are metaluminous to peraluminous and $SiO_2$ saturated.

Two different types of metamorphic effects are recorded in the rocks of the Gabbro-Syenite Belt. One type is only recorded in the gabbro bodies, and produced pseudomorphic replacements of the igneous mineral grains, totally preserving the igneous textures. The other type consists of a foliation-producing metamorphic alteration, which is recorded in the outer parts of the main gabbro and syenite bodies, and completely affects the small bodies as well as the shear zones crosscutting the major bodies (SAID, 1987, 1988). Usually, these alteration did not obliterate totally the primary, magmatic features, with the exception of the shear zones, where crystalloblastic to blastomylonitic textures prevail.

According to SACCHI et al. (1987) the pseudomorphic replacements could represent

Table 2 - Chemical data concerning the syenites and the alkaline granite (columns 9-10 and 12-16) of the Gabbro-Syenite Belt.

| Sample | 10 | 12 | 13 | 15 | 8 | 9 | 25 | 26 | 27 | 28 | 30 |
|---|---|---|---|---|---|---|---|---|---|---|---|
| $SiO_2$ | 58.91 | 61.52 | 61.70 | 60.84 | 60.50 | 61.09 | 65.28 | 61.77 | 69.40 | 74.44 | 66.22 |
| $TiO_2$ | 0.82 | 0.38 | 0.27 | 0.67 | 0.62 | 0.55 | 0.06 | 0.29 | 0.12 | 0.08 | 0.23 |
| $Al_2O_3$ | 17.26 | 17.99 | 19.02 | 18.20 | 17.63 | 17.73 | 19.31 | 17.70 | 16.39 | 13.55 | 17.71 |
| $Fe_2O_3$ | 1.81 | 4.14 | 3.13 | 2.06 | 1.28 | 1.35 | 0.34 | 1.68 | 1.14 | 0.97 | 1.35 |
| FeO | 5.44 | 2.55 | 1.93 | 3.45 | 4.90 | 4.36 | 0.48 | 3.42 | 1.18 | 0.54 | 1.39 |
| MnO | 0.18 | 0.15 | 0.09 | 0.14 | 0.16 | 0.14 | 0.01 | 0.16 | 0.06 | 0.01 | 0.05 |
| MgO | 0.74 | 0.12 | - | 0.85 | 0.53 | 0.49 | 0.05 | 0.23 | 0.04 | - | 0.19 |
| CaO | 2.99 | 1.67 | 1.33 | 2.30 | 2.41 | 2.37 | 0.92 | 1.91 | 0.95 | 0.55 | 1.30 |
| $Na_2O$ | 4.92 | 4.68 | 5.69 | 5.89 | 5.41 | 5.55 | 6.32 | 5.76 | 5.02 | 3.18 | 5.57 |
| $K_2O$ | 5.16 | 5.93 | 5.84 | 4.16 | 5.72 | 5.85 | 6.56 | 6.21 | 4.99 | 5.39 | 5.08 |
| $P_2O_5$ | 0.24 | 0.07 | 0.03 | 0.27 | 0.15 | 0.13 | 0.01 | 0.20 | - | - | 0.05 |
| LOI | 1.23 | 0.73 | 0.38 | 1.45 | 0.86 | 0.73 | 0.63 | 0.77 | 0.77 | 0.60 | 0.65 |
| Total | 98.47 | 99.20 | 99.03 | 98.83 | 99.31 | 99.67 | 99.34 | 99.33 | 99.29 | 98.71 | 99.14 |
| Rb | 20 | 37 | 40 | 47 | 41 | 44 | - | - | 70 | 77 | 60 |
| Ba | 1533 | 10 | 9 | 340 | 1316 | 1301 | - | - | 10 | 9 | 195 |
| Sr | 493 | 48 | 34 | 410 | 448 | 465 | - | - | 48 | 26 | 121 |
| Nb | 71 | 45 | 25 | 66 | 75 | 72 | - | - | 23 | 21 | 33 |
| Zr | 293 | 1140 | 1820 | 595 | 372 | 231 | - | - | 425 | 310 | 495 |
| Y | 33 | 43 | 43 | 27 | 38 | 38 | - | - | 26 | 17 | 27 |

| Sample | 44 | 45 | 49 | 50 | 51 | 90 | 92 | 93 | 94 | 97 |
|---|---|---|---|---|---|---|---|---|---|---|
| $SiO_2$ | 77.58 | 77.79 | 76.16 | 77.13 | 68.28 | 60.69 | 64.72 | 61.72 | 60.63 | 58.85 |
| $TiO_2$ | 0.13 | 0.08 | 0.12 | 0.12 | 0.63 | 0.76 | 0.38 | 0.62 | 0.72 | 1.25 |
| $Al_2O_3$ | 12.10 | 12.12 | 12.74 | 12.60 | 14.46 | 16.29 | 18.60 | 17.37 | 16.38 | 17.96 |
| $Fe_2O_3$ | 0.81 | 0.78 | 1.08 | 0.88 | 1.46 | 3.86 | 0.60 | 1.64 | 3.25 | 1.15 |
| FeO | 0.44 | 0.26 | 0.59 | 0.56 | 3.09 | 3.63 | 0.92 | 3.51 | 3.98 | 4.38 |
| MnO | 0.01 | 0.01 | 0.01 | 0.02 | 0.09 | 0.23 | 0.06 | 0.14 | 0.22 | 0.11 |
| MgO | 0.07 | 0.03 | 0.03 | - | 0.80 | 0.34 | 0.06 | 0.44 | 0.41 | 1.23 |
| CaO | 0.51 | 0.25 | 0.39 | 0.45 | 2.30 | 2.26 | 0.86 | 1.88 | 2.24 | 2.94 |
| $Na_2O$ | 4.43 | 3.79 | 4.04 | 4.44 | 4.17 | 5.07 | 6.18 | 5.40 | 5.23 | 4.43 |
| $K_2O$ | 3.11 | 4.12 | 4.16 | 3.51 | 3.15 | 5.89 | 6.63 | 6.07 | 5.91 | 5.76 |
| $P_2O_5$ | - | - | 0.01 | - | 0.16 | 0.14 | 0.03 | 0.13 | 0.15 | 0.46 |
| LOI | 0.46 | 0.30 | 0.32 | 0.22 | 0.95 | 0.90 | 0.37 | 0.96 | 0.92 | 0.99 |
| Total | 99.19 | 99.23 | 99.33 | 99.71 | 98.59 | 99.16 | 99.04 | 98.92 | 99.12 | 98.52 |
| Rb | 49 | 103 | 92 | 78 | 104 | 68 | 121 | 523 | 57 | 68 |
| Ba | 80 | 285 | 670 | 570 | 750 | 40 | 720 | 359 | 218 | 210 |
| Sr | 86 | 16 | 30 | 40 | 142 | 36 | 188 | 96 | 50 | 419 |
| Nb | 28 | 17 | 12 | 15 | 17 | 18 | 23 | 114 | 58 | 15 |
| Zr | 325 | 215 | 305 | 310 | 360 | 155 | 227 | 196 | 214 | 179 |
| Y | 137 | 97 | 73 | 79 | 65 | 17 | 21 | 23 | 27 | 20 |

subsolidus alterations developed during the uprise through the crust of these still hot bodies; while SAID (1988) believes that the appearance of the two types of metamorphic alterations was controlled by the deformation partitioning.

The foliation-producing metamorphism which affected the syenites is the same event which produced the younger (locally prevailing) foliation in their country rocks: or, at least, the two foliations have the same attitude, as can be clearly detected observing some dykes of foliated syenites and their country-rocks (GATTO et al., 1981, p. 38-39). An older foliation is however still detectable in the latter rocks.

### The Younger Granites

Two different groups of granitoids are included under this title:

(i) younger granitoids sensu stricto (let label them $G_7$ for short), not foliated, clearly crosscutting their country-rocks, and representing with their dykes (mainly aplites and pegmatites) the latest igneous products in the NSB; specifically, their emplacement was certainly post-tectonic, i.e. younger than the large-scale regional folding;

(ii) more or less distinctly foliated granitoids ($G_6$ for short), for which the intrusion relationships with their country-rocks is still well recognizable. The foliation is well detectable mainly in the outer parts of the granitoid bodies, and may be apparently lacking in the inner parts. Aplites and pegmatites are also associated to the granitoids $G_6$.

The granitoids $G_7$ occur in all the above described rock complexes (i.e. Inda Ad, Abdulkadir, Mora and Qabri Bahar), while granitoids $G_6$ were not found in the Inda Ad Complex, but only in the other three rock complexes. The granitoids $G_7$ are assumed here to be younger than $G_6$.

It is worthy to point out that the granitoids $G_6$ are distincly different in the field (and obviously in thin section) from the older metagranitoids and granitic gneisses belonging to the old basement: the latter rocks are clearly metamorphic rocks, displaying a fully developed crystalloblastic-gneissose texture; the former ones ($G_6$) still preserve their primary igneous texture and their crosscutting character, notwithstanding the often discountinuous and ill-defined foliation which only depends on the orientation of the mica flakes.

The few chemical data existing on the Younger Granites seem to indicate an alkaline character for the youngest granitoids $G_7$, and a calcalkaline affinity for the foliated granitoids $G_6$. These data are reported in Table 3 and in Figs. 9. It is also worthy to point out that the mesonorm data of the analysed granites $G_6$ fall in the low-temperature area along the Q-Or cotectic line at 5 Kb. Of special interest is the location of the $G_7$ data points in the field of the post-orogenic melts as defined by BARCHELOR and BOWDEN (1985), and that of the $G_6$ data points in the field of the syn-collisional melts (Fig. 9d).

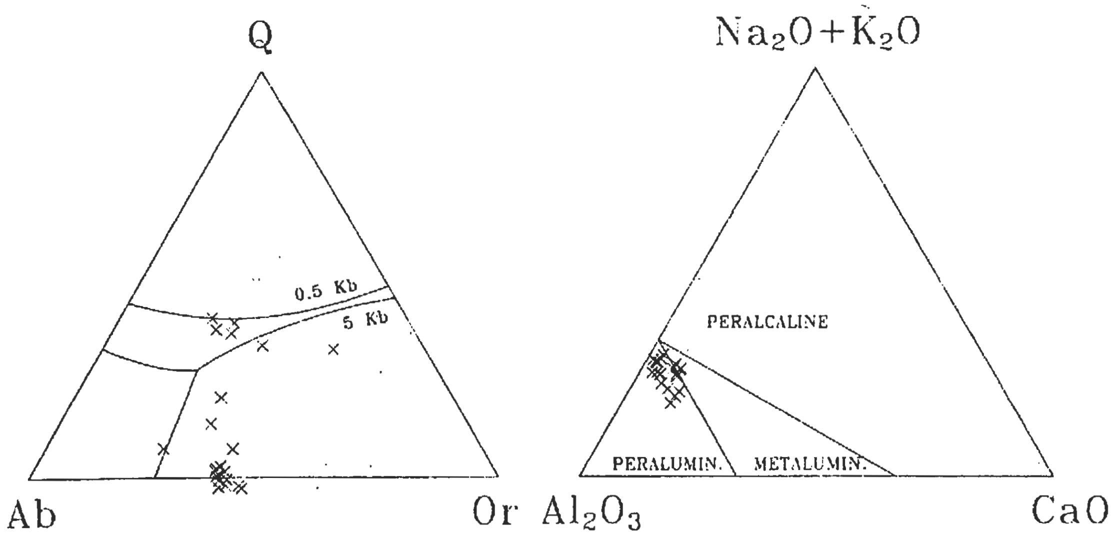


Fig. 7 - Some chemical features of the syenites and alkaline granites belonging to the Gabbro-Syenite Belt .

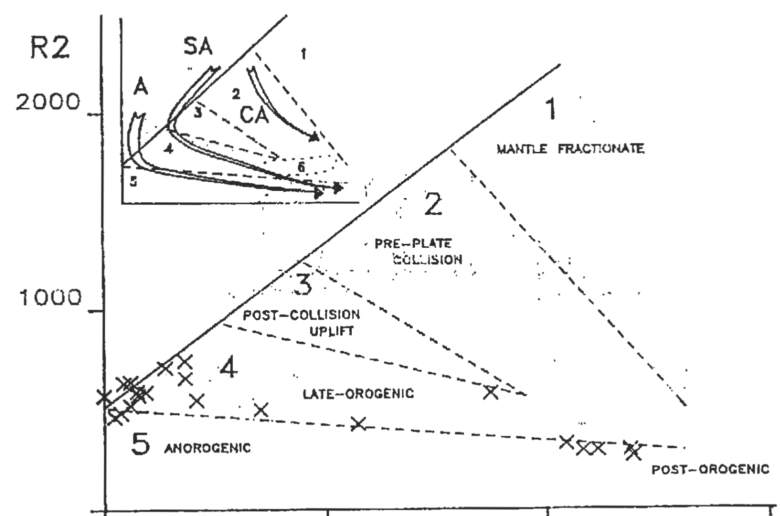


Fig. 8 - Some chemical features of the syenites and alkaline granites belonging to the Gabbro-Syenite Belt.

As concerns the metamorphic overprint occurring in the $G_6$ granitoids, its low grade is worthy to be stressed: the metamorphic mineral assemblages in them are thermodinamically compatible with the mineral assemblages occurring in the Inda Ad Complex and with the retrograde overprints widespread throughout the whole NSB.

## THE SEQUENCE OF THE EVENTS

As turns out very clearly from the previous sections of the present paper, the sequence of the events in the NSB is very complex and long: specifically, numerous igneous and metamorphic events are recorded in NSB. The following pages are an attempt to give a reasonable model of the whole sequence, as a further development of the criteria and proposals given by SASSI and IBRAHIM (1981) and SASSI and VISONÀ (1985). This sequence is sketched in Fig. 10.

In the following discussions and in Fig. 10 each event is labeled using a letter (**M** for metamorphic event or stage, **A** for acidic volcanism, **B** for basic volcanism, **G** for granitoid plutonism, **Sy** for syenite plutonism, **Ga** for gabbro plutonism) and a number (the lower is the number, the higher is the age).

### THE METAMORPHIC EVENTS

Each of the previously described rock complexes records at least one, and often more, metamorphic events (Fig. 10). Specifically:

(i) The Qabri Bahar Complex records a granulitic event (M1), an amphibolite facies to anatectic event ($M_2$) and a foliation-producing greenschist facies metamorphism $M_3$ well recognizable in the Gebiley metagranitoids. Furthermore, it may have been affected by a further retrograde, greenschist-facies overprint $M_4$. The medium-pressure character of the metamorphism $M_2$ is displayed by the occurrence of kyanite.

(ii) The Mora Complex displays an identical metamorphic history: it is reasonable to assume that this rock complex underwent the same events $M_1$, $M_2$, $M_3$ (and $M_4$?) as the Qabri Bahar Complex.

(iii) The Abdulkadir Complex records only one metamorphic event $M_3$, which took place under medium-pressure greenschist facies conditions. Hypothetically, this event $M_3$ could have been the same low-grade event $M_4$ that produced the younger retrograde overprint in the two higher-grade, rock complexes; however, the hypothesis that $M_4$ was a separate, younger event is consistent with the geological constraints. Petrology can supply obvious raisons for understanding why the retrograde overprint $M_4$ is only recognizable within the high-grade rocks and may have been not recorded (or may be not detectable) in the $M_3$ greenschist-facies

Table 3 - Chemical data on the foliated ( columns 1-18: $G_6$) and not foliated ( columns 19-21: $G_7$) Younger Granites.

| Sample | 83109 | 83151 | 83153 | 83154 | 83155 | 83156 | 83182 | 83183 | 83184 | 83185 | 84-87 |
|---|---|---|---|---|---|---|---|---|---|---|---|
| SiO2 | 69.58 | 70.83 | 72.48 | 73.63 | 73.76 | 72.67 | 70.30 | 74.81 | 71.93 | 73.90 | 72.22 |
| TiO2 | 0.43 | 0.35 | 0.29 | 0.22 | 0.22 | 0.22 | 0.33 | 0.09 | 0.34 | 0.06 | 0.30 |
| Al2O3 | 14.28 | 14.50 | 14.32 | 13.85 | 13.92 | 14.42 | 14.74 | 13.61 | 14.26 | 14.16 | 14.45 |
| Fe2O3 | 0.92 | 0.78 | 0.49 | 0.90 | 0.71 | 0.63 | 1.03 | 0.19 | 1.13 | 0.11 | 0.42 |
| FeO | 2.99 | 1.32 | 1.00 | 1.36 | 0.61 | 0.68 | 1.11 | 0.35 | 0.86 | 0.39 | 1.12 |
| MnO | 0.18 | 0.04 | 0.02 | 0.02 | 0.03 | 0.03 | 0.02 | 0.01 | 0.02 | 0.01 | 0.03 |
| MgO | 1.21 | 0.55 | 0.42 | 0.37 | 0.37 | 0.36 | 0.92 | 0.20 | 0.43 | 0.37 | 0.40 |
| CaO | 2.56 | 1.85 | 1.42 | 1.33 | 1.29 | 1.54 | 1.57 | 0.89 | 1.44 | 0.79 | 1.33 |
| Na2O | 3.81 | 3.44 | 3.80 | 3.74 | 3.84 | 4.05 | 3.61 | 3.05 | 3.33 | 3.68 | 3.78 |
| K2O | 2.57 | 5.11 | 5.11 | 4.83 | 4.71 | 4.69 | 5.01 | 5.47 | 4.99 | 5.35 | 4.63 |
| P2O5 | 0.18 | 0.13 | 0.11 | 0.10 | 0.08 | 0.08 | 0.10 | 0.02 | 0.08 | 0.01 | 0.08 |
| LOI | 1.21 | 1.11 | 0.56 | 0.46 | 0.47 | 0.64 | 1.00 | 0.71 | 0.70 | 0.87 | 0.57 |
| Total | 98.71 | 98.90 | 99.46 | 100.35 | 99.54 | 99.37 | 98.74 | 98.69 | 98.81 | 98.83 | 98.76 |
| Rb | 268 | 161 | 177 | 204 | 199 | 195 | - | 223 | 144 | - | 208 |
| Ba | 425 | - | - | - | - | - | - | 1015 | 460 | - | 520 |
| Sr | 170 | 444 | 455 | 296 | 298 | 323 | - | 215 | 425 | - | 255 |
| Nb | 15 | - | - | - | | - | - | 36 | 19 | - | 14 |
| Zr | 180 | - | - | - | - | - | - | 73 | 267 | - | 212 |
| Y | 45 | - | - | - | - | - | - | 19 | 21 | - | 11 |

| Sample | 84-89 | 84-90 | 84-94 | 84-95 | 84-96 | 84-98 | 84-99 | S8136 | S8137 | S8138 |
|---|---|---|---|---|---|---|---|---|---|---|
| SiO2 | 70.48 | 74.13 | 68.95 | 70.74 | 71.10 | 69.40 | 73.08 | 76.53 | 76.20 | 75.94 |
| TiO2 | 0.35 | 0.18 | 0.55 | 0.36 | 0.43 | 0.49 | 0.24 | 0.08 | 0.12 | 0.10 |
| Al2O3 | 14.99 | 13.86 | 15.55 | 15.17 | 14.83 | 15.08 | 14.14 | 11.58 | 11.50 | 11.85 |
| Fe2O3 | 0.74 | 0.32 | 0.68 | 0.78 | 1.20 | 1.00 | 0.58 | 0.86 | 0.80 | 0.71 |
| FeO | 1.39 | 0.75 | 1.62 | 1.27 | 1.15 | 1.62 | 0.88 | 0.92 | 1.14 | 1.03 |
| MnO | 0.05 | 0.03 | 0.05 | 0.04 | 0.05 | 0.05 | 0.02 | 0.02 | 0.02 | 0.02 |
| MgO | 0.55 | 0.20 | 0.75 | 0.52 | 0.52 | 0.69 | 0.39 | 0.05 | 0.01 | 0.01 |
| CaO | 1.78 | 1.24 | 2.16 | 1.58 | 1.64 | 1.84 | 1.25 | 0.44 | 0.52 | 0.43 |
| Na2O | 3.53 | 3.19 | 3.91 | 3.73 | 3.52 | 3.52 | 3.33 | 3.72 | 3.65 | 3.75 |
| K2O | 4.79 | 4.95 | 4.05 | 4.56 | 4.25 | 4.82 | 4.95 | 4.69 | 4.83 | 4.94 |
| P2O5 | 0.11 | [illegible] | [illegible] | 0.12 | [illegible] | 0.15 | 0.08 | 0.01 | 0.01 | 0.01 |
| LOI | 0.84 | 0.47 | 1.11 | 0.64 | 0.96 | 0.96 | 0.64 | 0.89 | 0.91 | 0.95 |
| Total | 98.76 | [illegible] | 98.39 | [illegible] | 98.82 | 98.66 | 98.94 | [illegible] | 98.80 | 98.79 |
| Rb | 179 | 168 | 159 | 164 | 148 | 171 | 183 | 115 | 108 | 115 |
| Ba | 1500 | 740 | 970 | 1315 | 980 | 1530 | 820 | 7 | 20 | 31 |
| Sr | 505 | 265 | 390 | 440 | 350 | 655 | 293 | 4 | 5 | 6 |
| Nb | 17 | 10 | 17 | 15 | 13 | 30 | 12 | 33 | 37 | 29 |
| Zr | 250 | 106 | 257 | 246 | 194 | 298 | 168 | 158 | 268 | 251 |
| Y | 15 | 4 | 12 | 9 | 12 | 42 | 16 | 60 | 56 | 36 |

rocks.

(iv) The Mait and the Inda Ad Complex display only one metamorphism. This event, which is reported here as the Inda Ad metamorphism, should coincide with the retrograde metamorphism $M_4$ above mentioned in the Qabri Bahar and Mora complexes. However, the Mait C. may have also underwent the $M_3$ event

(v) The Gabbro-Syenite Belt records a metamorphic stage of pseudomorphic alterations (only in the core of the major gabbro bodies) and a foliation-producing, low-grade metamorphic event. The latter effects may be reasonably related either to the Abdulkadir metamorphism $M_3$ or to the greenschist-facies Inda Ad metamorphism $M_4$, the latter of which, as previously pointed out, affected the whole NSB. It is also possible that effects of both $M_3$ and $M_4$ are overprinted in the outer, foliated parts of the syenite and gabbros bodies. The metamorphic grade of $M_3$ in the gabbros and syenites may cover a thermic range wider than that of the Inda Ad metamorphism, possibly also reaching the lower amphibolite facies (SAID, 1988).

(vi) The Younger Granites record a low-grade, foliation-producing metamorphism in the granitoids $G_6$. This metamorphism too should be referred to the regional, Inda Ad metamorphism $M_4$.

In conclusion, not less than four metamorphic events are recorded in the NSB. They are:

- $M_1$: it was an old granulite-facies metamorphism; a temperature value close to 700 °C and a pressure value lower than 6 Kb have been estimated (SASSI and VISONÀ, 1987 and in the present volume).
- $M_2$: it was a sinkynematic metamorphism, developed under amphibolite-facies to anatectic conditions; as $M_1$, it is recorded in the Qabri Bahar and Mora complexes. The stability of almandine + kyanite displays intermediate pressure conditions, and the symultaneous appearance of kyanite + sillimanite + leucosomes (e.g. Hudiso, Bixendule, lower stream Miriye) suggests minimum pressure values around 6 Kb and temperature values in the range 620-650 °C.
- $M_3$: it was a synkinematic metamorphism, which altered the sediments and volcanics of the Abdulkadir Complex into greenschist facies rocks, under intermediate pressure conditions (as shown by the occurrence of kyanite), and also affected the Gabbro-Syenite Belt; furthermore, this event should have been responsible for the foliation and greenschist facies alteration of the granitoids $G_3$ (e.g. Gebiley) occurring in the Qabri Bahar Complex, and may have been responsible for the retrograde overprints in the Qabri Bahar and Mora complexes.
- $M_4$: it was a synkinematic metamorphism which affected for the first time the Inda Ad and the Mait complexes and the granitoids $G_4$, and may also have produced retrograde overprints throughout the whole NSB, perhaps also affecting the gabbros and the syenites. This metamorphism took place under low pressure conditions, according to PERUZZO ( this volume).

Fig. 11 sketches the polichrone P-T path which may be inferred from the observed

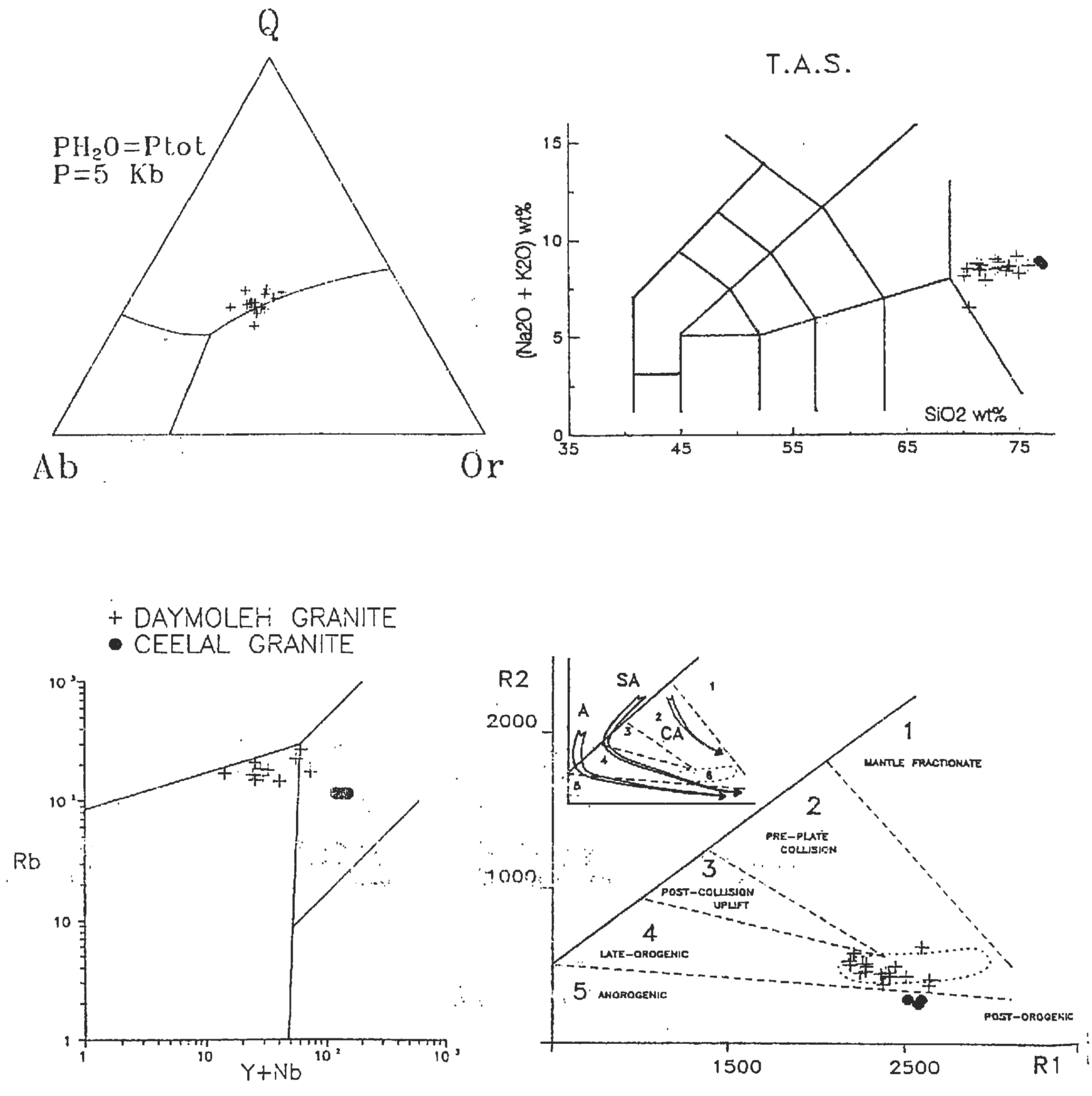


Fig. 9 - Some chemical features of the foliated ($G_6$: crosses) and non-foliated ($G_7$: dots) Younger Granites.

mineral compatibilities: the age values which are discussed below in the pertinent sections have been included for sake of completeness.

## THE MAGMATIC EVENTS

The numerous igneous events recorded in the previously described rock complexes are defined below. Their relative chronological relationships and their chronological location with respect to the metamorphic events are shown in Fig. 10.

(i) The Qabri Bahar Complex records at least four events (besides the Younger Granites):

- the old basic event ($B_1$) to which at least parts of the amphibolites are genetically related;

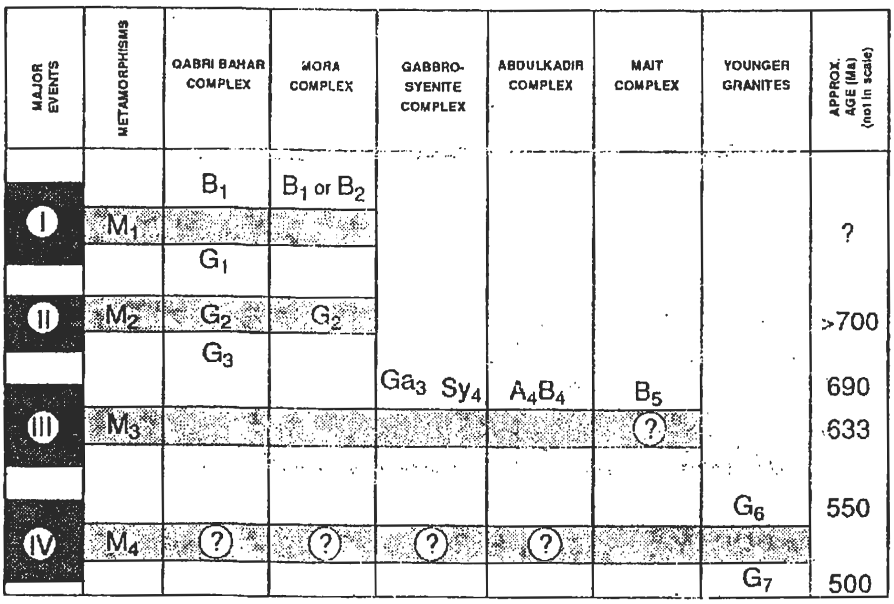


Fig. 10 - Schematic representation of the relative chronology of the igneous and metamorphic events recorded in the different rock complexes making up the NSB. M = metamorphism; A = acidic volcanism; B = basic volcanism; G = granitoid and leucosomes; Ga = gabbro; Sy = syenite. Higher numbers refer to younger events.

- the old granitoid plutonism ($G_1$) represented by the augen orthogneisses into which the Daymoleh massif (a foliated younger granite) is intruded;
- the crustal anatexis $G_2$ which produced the abundant migmatites and related leucosomes;
- the emplacement of granitoid bodies $G_3$, of which the Gebiley metagranitoids is the best known example.

The crustal anatexis $G_2$ is chronologically and genetically linked to the metamorphic event $M_2$. The oldest basic event $B_1$ certainly predates $M_1$ (SASSI and VISONÀ, 1987, and this volume). The old granitoid plutons $G_1$ certainly predates $G_2$ but the occurrence in them of foliated metamorphic xenoliths implies the pre-existence of a metamorphic event ($M_1$?). The granitoids $G_3$ are certainly younger than $M_2$, as suggested by their low-grade metamorphism $M_3$, which was not sufficiently high to obliterate completely the magmatic micro-and mesostructures survived in $G_3$.

(ii)The Mora Complex records at least two events (besides the Younger Granites):
- an old basic magmatism ($B_1$ or $B_2$), to which the thick amphibolite horizons interlayered within the marbles in the Cadda-Mora area are related; it certainly predates both $M_1$ (SASSI and VISONÀ, 1987, and this volume) and $M_2$;
- the crustal anatexis ($G_2$) related to $M_2$.

(iii)The Gabbro Syenite Belt records the emplacement of gabbro ($Ga_3$) and syenite ($Sy_3$) bodies, and related minor alkaline granitoids. These strictly related events took place after the metamorphism $M_2$, but before $M_3$. $Ga_3$ is slightly older than $Sy_3$, although they both belong to a substantially unique plutonic cycle.

(iv)The Abdulkadir Complex records one volcanic event (besides the Younger Granites): this produced acidic and subordinately basic volcanics, and was characterized by a distinct Daly-gap. Let us label them as $A_4$ and $B_4$ respectively.

(v) The Mait Complex records a basic volcanism, which displays ocean-floor affinities (DAL PIAZ et al., 1987). It is completely speculative to state whether this volcanism, with its peculiar features, belongs to the same event $B_4$ recorded in the Abdulkadir Complex or to a different, $B_5$, event. For sake of caution, we prefer to label it as $B_5$ but we do not imply by this any obvious chronological difference between $B_4$ and $B_5$.

(vi) The Younger Granites record two main stages of granitoid emplacement, both clearly postdating the metamorphism $M_3$. One of them ($G_6$) underwent the metamorphism $M_4$. The other one ($G_7$) postdates it, representing the youngest petrogenetic products in the NSB.

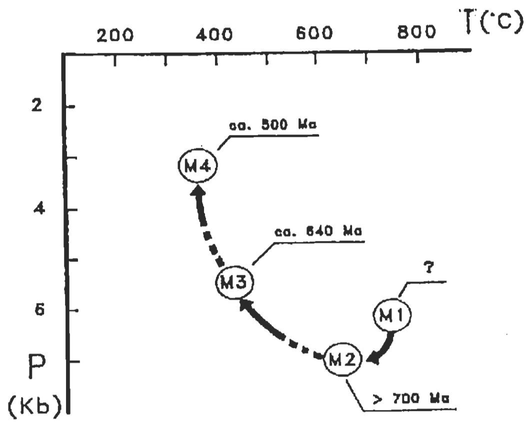


Fig. 11 - P-T polymetamorphic path record in the NSB.

## SOME ISOTOPIC GEOCHRONOLOGICAL CONSTRAINTS

As pointed out earlier, the radiometric geochronological data which were available in the literature before 1987 are very few. Most of them are due to SNELLING (1963, and in: GREENWOOD and BLEACKLEY, 1967) and ABBATE et al., 1985. Some of them is shown in Table 4.

Further few age values have been produced in the last few years by the Italo-Somali team of the Somali National University. Some of them have been previously published (ABBATE et al., 1985; FERRARA et al., 1985), and some are presented here (Table 5 and

Table 4 - Some geochronological data from the literature concerning Younger Granites intruded in the Inda ad Complex.

| Age (Ma) | | Methodology | Massif | Reference |
|---|---|---|---|---|
| 515±25 | K/Ar | Bt | Las Bar | SNELLING, 1967 |
| 500±25 | K/Ar | Bt | Arar | SNELLING, 1967 |
| 490±7 | Rb/Sr | Kfs-Bt | Arar | ABBATE et al., 1985 |
| 510±8 | Rb/Sr | Kfs-Bt | Arar | ABBATE et al., 1985 |
| 525±8 | Rb/Sr | WR-Bt | Arar | ABBATE et al., 1985 |

6). However, some of these new data do not fit, in the Nicholaysen diagram, regression lines which may be considered as true isochrons. Their MSWD values are generally high, probably due to metamorphic overprints which may have reopened the isotopic systems. Furthermore, the number of samples in each attempt at having an isochron is generally low. However, the consistency between the succession of the events recognized on geopetrologic bases and the sequence of the corresponding radiometric age values encourage us to propose such age values, although some of them are poorly defined.

Notwithstanding the above mentioned new contributions, the whole set of radiometric data which is available by now is not sufficient to give an answer to all chronological questions concerning the NSB; it only supplies some important constraints.

## Analytical procedures

Rb and Sr concentrations have been measured by isotopic dilution; the analytical error of the ratio is estimated to be better than $\pm$ 1.5% (95% confidence limit).

The Sr isotopic analyses were made on both VARIAN MAT TH5 and VG ISOMASS 54E mass-spectrometers. $^{87}Sr/^{86}Sr$ ratios were normalized to $^{86}Sr/^{88}Sr$ ratio of 0.1194. Determinations of NSB 987 ($SrCO_3$) yelded an average value of 0.71026 $\pm$ 0.00003 and no strumental bias correction was applaied to the measured Sr isotopic composition. All reported uncertainties on isotopic ratios represent in-run statistics at 95% confidence level. Slope and intercepts for whole-rock isochrons were calculated using ISOPLOT 200 (LUDWIG, 1988).

Ar isotopic analyses were carried using a VARIAN MAT 240 mass-spectrometer. The errors on K/Ar age determinations are 3% because the argon extraction equipment were not on-line with the mass-spectrometer.

K has been determined by standard AAS procedures and estimed error is 0.8%.

IUGS-recommended constants have been used (STEIGER and JÄGER, 1977).

## The younger granites ($G_6$ and $G_7$).

If the presently available data are worthy to be extrapolated over regional scale, a radiometric age close to 550 Ma should be referred to the emplacement of both granites $G_6$ (which underwent the metamorphism $M_4$) and $G_7$ (which do not record any metamorphic overprint). The data supporting such a statement are outlined below:

- the Daymoleh $G_6$ granite gave an age value of 551 $\pm$ 16 Ma (MSWD = 0.8), based on a seven-point Rb-Sr whole-rock isochron (Fig. 12, taken from FERRARA et al., 1985); the relatively low value of the Sr initial isotopic ratio suggests that the crustal contribution to the genesis of these melts was only partial;

- the Ceelal $G_7$ granite gave a Rb-Sr age value of 542 ± 25 Ma (MSWD = 0.1), based on three whole-rock samples (Fig. 13 and Table 5); these samples have very high $^{87}Sr/^{86}Sr$ values, and therefore do not allow the initial Sr isotopic ratio to be reliably estimated. Three K/Ar mineral data (amphibole and biotite) from the same Ceelal granite gave ages from 520 ± 16 to 529 ± 15 (Table 6), and three Wr-Bt Rb/Sr ages between 509 ± 8 and 524 ± 8 Ma, which are referable to the closure of the isotopic system related to the magmatic cooling (Table 5).

Mineral ages obtained from some post-tectonic granites $G_7$ outcropping in the eastern part of the NSB gave lower age values (Table 4). They should also have a similar meaning as the data in Tables 5 and 6, but some influence of $M_4$ cannot be excluded.

The above whole-rock data do not record a significant difference in the emplacement age between $G_6$ and $G_7$. They probably both refer to stages of a short-lasting, unique magmatic cycle. The granites $G_6$ display to have experienced the foliation-producing metamorphism $M_4$, isotopic records of which have also been recognized (see next Section).

### The metamorphic event $M_4$

$M_4$ is the Inda Ad metamorphism, which also affected the granites $G_6$.

The available data which chronologically constrain this metamorphic event point to an age value close to 500 Ma. They are the K-Ar and Rb-Sr data obtained from the foliated Damoleh Massif (Tables 5 and 6). However, numerous other radiometric age values indicate a widespread partial rejuvenation of the older rocks, which may be related to the regional metamorphic heating $M_4$. They are shown in Tables 5 and 6 and refer to:

1) Hudiso paragneisses (Qabri Bahar Complex): muscovite Rb-Sr age 562 ± 9 Ma;

2) Hudiso granodioritic gneisses (Qabri Bahar Complex): three whole-rock Rb-Sr data fit a regression line of about 585 Ma; and a biotite-whole rock Rb-Sr age of 485 Ma has been also obtained;

3) Agabar syenite (Gabbro-Syenite Belt): two K-Ar mineral ages of 562 ± 16 and 591 ± 17, and a Rb-Sr biotite age of 553 ± 9; a similar age value of 600 ± 30 Ma has been reported for the same Agabar syenite by SNELLING (1967);

4) Borka Haggar syenite (Gabbro-Syenite Belt): two K-Ar mineral age of 516 ± 16 and 525 ± 15, which are probably related to a locally strong tectonization.

Therefore, isotopic effects of a more or less complete rejuvenation $M_4$ seem to be widespread throughout the whole NSB.

THE VOLCANISM $A_4$ $B_4$ OF THE ABDULKADIR C. AND THE METAMORPHISM $M_3$

No radiometric data exist concerning the basic volcanism(s) $B_4$ and $B_5$. As concerns the acidic volcanism $A_4$ strictly associated to $B_4$, some Rb-Sr whole rock radiometric data are available. However, these data do not define a well established age value; furthermore, they may only be referred to their metamorphism $M_3$, and only represent a lower boundary value for the age of volcanism (which must be certainly older).

The acidic metavolcanics analysed from this point of view come from two localities: Borama and Damal.

The five Borama samples (Table 5 and Fig. 14) fit an errorchron at 640 ± 67 Ma (MSWD = 39.1; initial isotopic ratio = 0.7082). The data points of four Damal samples fit a regression line at 772 ± 40 Ma MSWD = 2.5; initial isotope ratio = 0.7094. The interpretation of this age value is very difficult.

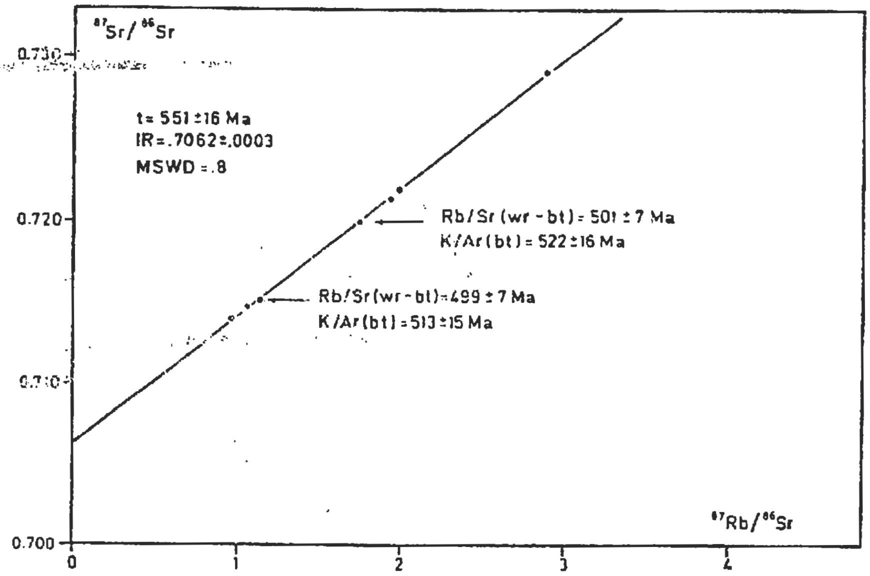


Fig. 12 - Rb-Sr isochron obtained from the Daimoleh foliated granite ($G_6$) (taken from FERRARA et al., 1985).

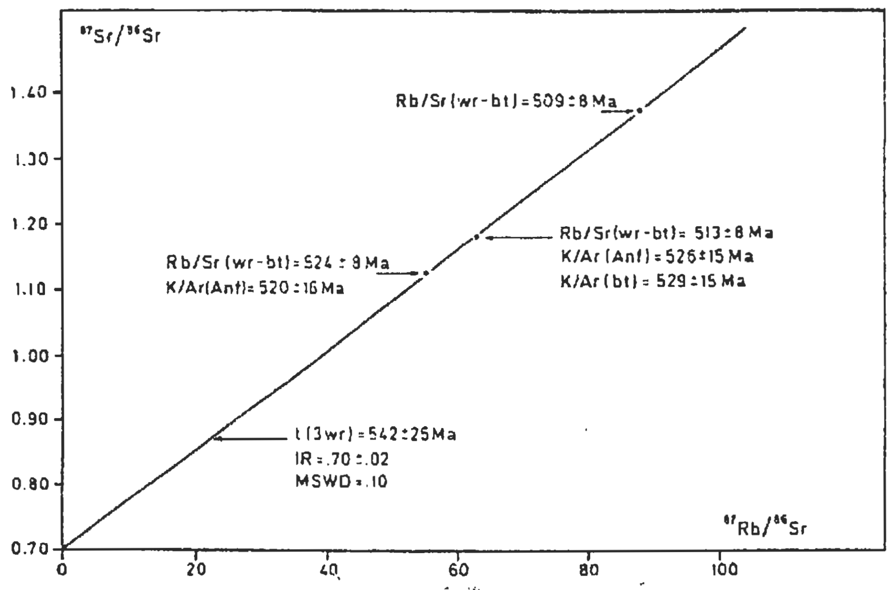


Fig. 13 - Rb-Sr isochron obtained from the Ceelal Massif (not foliated granite $G_7$).

### The Gabbro-Syenite belt

Two Rb-Sr whole rock errorchrons have been obtained from two distinct syenite-gabbro complexes: the Agabar and the Daba Shabeli massifs. They give consistent results, of 695 ± 91 (MSWD = 82) and 694 ± 31 (MSWD = 9.4) respectively, as shown in Tables 5 and 6 and Fig. 15. The high MSWD values may be due to a partial metamorphic reworking of these rocks. The Sr isotopic initial ratio is low in both cases (0.7038 ± 0.0007 and 0.7036 ± 0.0002), showing the subcrustal origin of these melts and their emplacement within a thinned crust.

### The metagranitoids $G_3$

A Rb-Sr whole-rock errorchron has been obtained from four samples of the Gebiley metagranitoids (Table 5, Fig. 16). The indicative age value is 697 ± 101 Ma (MSWD=33;

Table 5 - New Rb-Sr isotopic data.

| | | Rb (ppm) | Sr (ppm) | $^{87}Rb/^{86}Sr$ | $^{87}Sr/^{86}Sr$ $\pm 2\sigma$ | Age Ma |
|---|---|---|---|---|---|---|
| **Younger Granites** | | | | | | |
| *Ceelal Alkaline Granite* | | | | | | |
| S 81-36 | wr | 114 | 4.0 | 87.8 | 1.3761±9 | |
| | bt | 859 | 32.7 | 80.3 | 1.2922±4 | 509±8 |
| S 81-37 | wr | 114 | 5.48 | 62.9 | 1.1824±3 | |
| | bt | 1162 | 16.3 | 243 | 2.4822±9 | 513±8 |
| S 81-38 | wr | 115 | 6.26 | 55.2 | 1.1244±3 | |
| | bt | 1127 | 22.6 | 162 | 1.9169±9 | 524±8 |
| *Daymoleh Granite* | | | | | | |
| S 83-151 | wr | 161 | 444 | 1.05 | 0.71459±6 | |
| S 83-153 | wr | 177 | 455 | 1.13 | 0.71494±6 | |
| | bt | 1027 | 11.3 | 323 | 3.00290±33 | 499±7 |
| S 83-154 | wr | 204 | 296 | 1.99 | 0.72192±12 | |
| S 83-155 | wr | 199 | 298 | 1.94 | 0.72141±9 | |
| | bt | 1224 | 11.4 | 345 | 3.52560±53 | 501±7 |
| S 83-156 | wr | 195 | 323 | 1.75 | 0.71993±6 | |
| S 83-182 | wr | 145 | 431 | 0.96 | 0.71391±12 | |
| S 83-185 | wr | 196 | 197 | 2.89 | 0.72907±16 | |
| **Gabbro-Syenite Belt** | | | | | | |
| *Daba Shabeli* | | | | | | |
| S 84-40 | wr | 86.7 | 169 | 1.48 | 0.71801±6 | |
| S 84-51 | wr | 29.9 | 127 | 0.679 | 0.71048±9 | |
| S 84-35 | wr | 105 | 156 | 1.95 | 0.72342±6 | |
| S 84-50 | wr | 1.33 | 545 | 0.007 | 0.70374±6 | |
| S 84-48 | wr | 41.7 | 334 | 0.361 | 0.70707±6 | |
| S 84-52 | wr | 36.2 | 301 | 0.345 | 0.70699±7 | |
| *Agabar* | | | | | | |
| S 83-8 | wr | [illegible] | 326 | [illegible] | 0.70678±9 | |
| S 83-9 | wr | 37.2 | 338 | 0.328 | 0.70612±12 | |
| S 83-10 | wr | 24.2 | 382 | 0.183 | 0.70573±3 | |
| S 83-25 | wr | 47.3 | 129 | 1.06 | 0.71512±9 | |
| S 83-94 | wr | 51.3 | 30.8 | 4.84 | 0.75071±12 | |
| S 83-26 | wr | 53.6 | 77.2 | 2.01 | 0.72342±6 | |
| | bt | 178 | 12.8 | 41.6 | 1.03563±18 | 553±9 |
| **Metavolcanics** | | | | | | |
| *Damal* | | | | | | |
| S 83-66 | wr | 119 | 804 | 4.30 | 0.75672±12 | |
| S 83-72 | wr | 164 | 68.8 | 6.95 | 0.78700±15 | |
| S 83-73 | wr | 126 | 147 | 2.49 | 0.73682±9 | |
| S 83-74 | wr | 175 | 445 | 11.5 | 0.83473±6 | |
| *Borama* | | | | | | |
| S 81-286 | wr | 89.5 | 92.4 | 2.81 | 0.73382±6 | |
| S 81-287 | wr | 84.1 | 75.9 | 3.22 | 0.73791±6 | |
| S 81-288 | wr | 50.8 | 101 | 1.46 | 0.72204±9 | |
| S 81-280 | wr | 50.0 | 106 | 1.37 | 0.71958±18 | |
| S 81-286/1 | wr | 17.4 | 149 | 0.338 | 0.71131±6 | |
| **Gebiley Orthogneiss** | | | | | | |
| S 83-103 | wr | 216 | 23.3 | 27.6 | 0.98572±9 | |
| S 83-105 | wr | 161 | 87.6 | 5.35 | 0.76463±6 | |
| S 83-106 | wr | 224 | 13.7 | 49.8 | 1.22000±39 | |
| S 83-104 | wr | 173 | 36.8 | 13.75 | 0.84021±9 | |
| **Qabri Bahar Complex** | | | | | | |
| *Hudiso Migmatites* | | | | | | |
| S 84-21 | wr | 137 | 212 | 1.86 | 0.73402±6 | |
| S 84-23 | wr | 110 | 79 | 4.05 | 0.73710±9 | |
| S 84-24 | wr | 87.7 | 130 | 1.95 | 0.73039±8 | |
| S 84-25 | wr | 130 | 64.2 | 5.87 | 0.77144±14 | |
| S 84-22 | wr | 84 | 165 | 1.48 | 0.73704±12 | |
| | ms | 314 | 11.6 | 83.7 | 1.39520±6 | 562±9 |
| *Hudiso Orthogneisses* | | | | | | |
| S 83-258 | wr | 109 | 526 | 0.602 | 0.71042±6 | |
| S 83-305 | wr | 106 | 975 | 0.314 | 0.70807±6 | |
| S 83-257 | wr | 143 | 1005 | 0.411 | 0.70883±6 | |
| | bt | 657 | 16.3 | 127 | 1.58210±9 | 485±7 |

isotopic initial ratio = $0.7106 \pm 0.0142$), and should be related to the emplacement of the protolith. This age value, although very poorly defined, do not conflict with the general chronological frame and the geological constraints.

### The main metamorphism $M_2$ and related anatexis

There are no direct data concerning this event. Therefore, we can only say that: (i) it is older than 695 Ma, because the intrusion of syenites having this age value postdates $M_2$; (ii) it is older than the emplacement of the protolith $G_3$ of the Gebiley orthogneisses ($697 \pm 101$ Ma).

### The metamorphic event $M_1$

No data are available concerning this event. An age of $828 \pm 170$ Ma has been reported by ABBATE et al. (1985), based on a three point Rb-Sr whole-rock errochron from the migmatitic gneisses of Hudiso; and we obtained an age of $970 \pm 100$ Ma from a four-point Rb-Sr whole-rock errorchron on similar rocks in the same area. Therefore, unfortunately, no meaningful age values were obtained from these gneisses after several attemps. The Rb-Sr whole-rock isochron should indicate, in this case, the age of the early heating, therefore an age value related to the early stage of $M_1$.

## CONCLUDING REMARKS

### The evolution of the NSB

On the bases of the above discussed data, the NSB is a polycyclic basement which records four main thermic pulses or Major Events. Let us label them I, II, III, IV, from the older to the younger. At least three of them, the youngest ones, fall in the Pan-African time range (950-450 Ma) defined by KRÖNER (1984), and record "steepening of the thermal gradient which lifted by 200°C or so the ambient temperature of the basement rock" (ALMOND, 1984). We cannot exclude that the older pulse too is younger than 950 Ma, and consequently may fall in the same Pan-African time range. However, due to the lack of any direct evidence, we have to consider the Major Event

I (i.e. the granulitic event) as the record of an older, possibly pre Pan-African, continental crust of which only mineral relics remain. Therefore, NSB is a section of the Proterozoic continental crust largely reworked and rejuvenated by the Pan-African event, as SASSI and IBRAHIM admitted since 1981.

Currently, the Pan-African Event is considered to be a set of processes (including deformation, magmatism, metamorphism, crustal break up, etc) which structurally differentiated the African continent into cratons and mobile zones during the late Precambrian/Early Paleozoic (KRÖNER, 1984). If one accepts this definition, the NSB is one of these mobile zones, or part of it.

Whether this mobile zone in Somalia includes fragments of rearranged, old Proterozoic plate(s), or only newly formed Pan-African rock sequences, is a matter of speculation. We are inclined towards the former alternative, specifically to consider the oldest rock sequence, i.e. the Qabri Bahar Complex, as a pre Pan-African continental crust affected by the **Major Event I**, which later was almost completely re-generated and re-arranged by the Pan-African Event through the following processes, continuously remaining floored by sialic crust:

**Major Event II** (older than 700 Ma): regional synkinematic heating and related amphibolite-facies metamorphism $M_2$ and anatexis $G_2$; related deformational activity; emplacement of the post-tectonic granitoids $G_3$ (e.g. Gebiley);

**Major Event III** (ca. 700 to 640 Ma): extensional regime; aborted lithospheric rupture, e.g. crustal thinning, deposition of a late Precambrian rock sequence, with a volcanic activity (Abdulkadir Complex) which locally acquired peculiar features, due to local geodynamic situations (Mait Complex); related uprise of gabbro and related melts through the thinned crust; therefore, regional metamorphism $M_3$.

**Major Event IV** (ca. 600-500Ma): deposition of the Inda Ad sequence; emplacement of I-type, calcalkaline granite melts; further thermic pulse, with regional heating ($M_4$) and deformational activity; final emplacement of A-type, postcollisional granitic

Table 6 - New K-Ar isotopic data.

| Sample | | Mineral | K% | ml $^{40}Ar^*$/gr sample | $^{40}Ar^*$% | AGE |
|---|---|---|---|---|---|---|
| S 83-155 | Daymoleh | Bt | 7.45 | $1.7189 \times 10^{-4}$ | 91.0 | $513 \pm 15$ |
| S 83-153 | Daymoleh | Bt | 7.89 | $1.7386 \times 10^{-4}$ | 91.0 | $522 \pm 16$ |
| S 81-38 | Ceelal | Amph | 1.03 | $2.4918 \times 10^{-5}$ | 78.0 | $520 \pm 16$ |
| S 81-37 | Ceelal | Amph | 1.02 | $2.4717 \times 10^{-5}$ | 64.0 | $526 \pm 16$ |
| S 81-37 | Ceelal | Bt | 5.96 | $1.4569 \times 10^{-4}$ | 89.2 | $529 \pm 15$ |
| S 83-93 | Borka Aggar | Amph | 1.41 | $3.3813 \times 10^{-5}$ | 85.6 | $516 \pm 16$ |
| S 83-93 | Borka Aggar | Bt | 7.44 | $1.7608 \times 10^{-4}$ | 94.3 | $525 \pm 15$ |
| S 83-9 | Agabar | Amph | 1.72 | $4.6750 \times 10^{-5}$ | 89.2 | $591 \pm 17$ |
| S 83-9 | Agabar | Bt | 4.98 | $1.2769 \times 10^{-4}$ | 86.3 | $562 \pm 16$ |

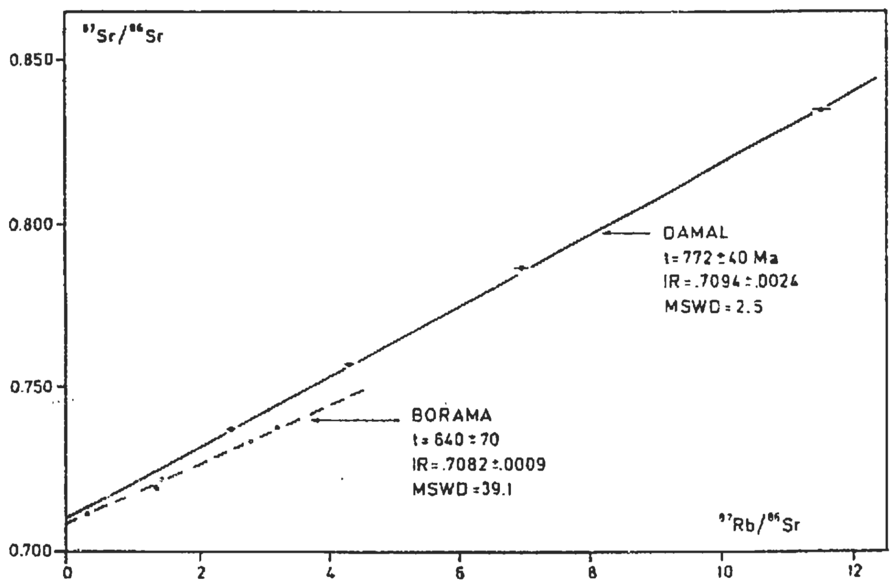


Fig. 14 - Rb-Sr errorchron concerning the Borama and Damal metarhyolites $A_4$.

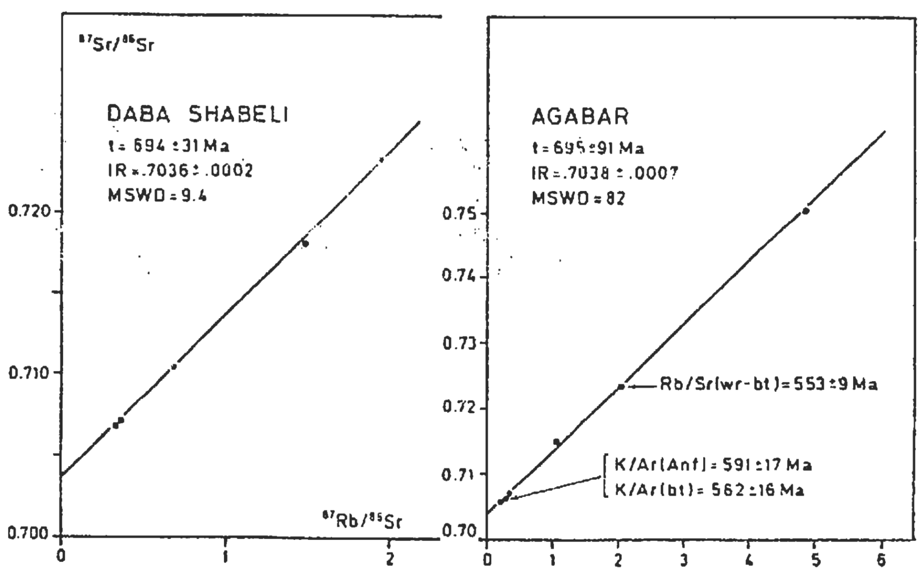


Fig. 15 - Rb-Sr errorchron concerning the Agabar and the Daba Shabeli plutons of the Gabbro-Syenite Complex.

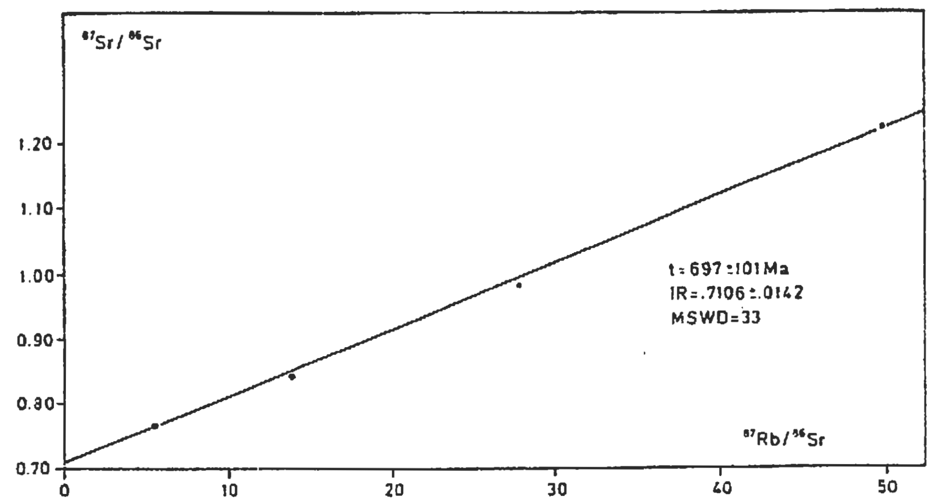


Fig. [illegible] - Rb-Sr errorchron concerning the Gebiley metagranitoids $G_3$.

melts.

During this pervasive and almost continuous reworking, the original stratigraphic boundaries were largely obliterated, and the previously deformed and thinned continental prisms could acquire a new stacking.

## Interregional Comparison

The comparisons with the surrounding basements (i.e. the Ethyopian basement, the Arabian-Nubian shield, the Kenyan basement, the Mozambique Belt) are difficult to be made. They should be done basing on interregional comparison of: 1) the lithostratigraphic sequences; 2) the metamorphic features; 3) the magmatic features; 4) the geochronological data. Each of these elements is often not well defined in the literature, and the regional use of different rock terms and criteria can obscure (or made more clear than it should be the case) differences, analogies and compatibilities. The age data available in the literature are often difficult to be compared: they can be dilated as elastic rubbers. For example, can we believe that an age value of 694 ±31 (Daba Shabeli syenite) really belongs to the unnamed cycle dated at 600 ± 100 in Arabia, rather than to the Hijaz cycle dated at 850 ± 100 (GREENWOOD et al., 1967; RAMSAY, 1979; DUYVERMAN et al., 1982; KRÖNER, 1984).

With these limitations in mind, we can say that NSB really displays some analogies with all above mentioned basements. However, significant differences also occur (e.g. differing from the Arabian-Nubian Shield, ophiolites do not occur in the NSB, and high grade metamorphics are abundant in it; differing from the Mozambique Belt, the occurrence of pre Pan-African rock sequences is not proved in NSB etc.). On the other side, striking analogies can be detected with other basements outside the Mozambique Belt and the Arabian-Nubian Shield: for example, see TACK et al. (1984) as regards the alkaline plutonism in Burundi (Rb-Sr age: 700 Ma), and the data compilation in it (p. 109) regarding the alkaline plutonism in other African regions. Some comparisons can also be attempted with the Sabalok area (Sudan: DÖONER et al., 1987) and Tanzania (MABOKO et al., 1985).

Evaluating the pros and cons, we can agree with WARDEN and HORKEL (1984) when they consider the NSB as the NE branch of the Mozambique Belt. However, we do not agree with their geodynamic model, because records of a trench-arc system, ophiolites, etc. are lacking in NSB. Finally, it should be stressed that NSB is an ensialic mobile zone in which unaltered blocks of a pre Pan-African crust are lacking.

## A FINAL REMARK

As a final remark, and considering the general situation from another point of view, the NSB has all ingredients of a shallow crust (e.g. FOUNTAIN and SALISBURY, 1981), and its old parts are slightly deeper levels rehydrated during the Pan-African cycle and rejuvenated not only thermically and deformationally, but also through the addition of quantitatively significant, new magmatic masses (gabbros, syenites, granitoids). The Pan-African "vestigial facet" and "geosynclinal facet" sensu CLIFFORD (1968) coexist in the NSB, the latter being located in the eastern sector and the former in the western sector.

## REFERENCES

ABBATE E., ALI KASSIM M., DAL PIAZ G.V., GOSSO G., HERSI ADEN IBRAHIM and G. RIGATTI (1981). Note di rilevamento sul basamento cristallino della Somalia settentrionale nell'area Rugay-Maydh-Hiis (Distretto di Ceerigavo). Rend. Soc. Geol. Ital., 4: 333-337.

ABBATE E., BONAZZI A., SAVIOLI MARIANI E., DAL PIAZ G.V., DEL MORO A., GOSSO G. and H.A. IBRAHIM (1985). Il settore dell' unità di Ida Ad ed il granito di Arar (Somalia settentrionale). Univ. Naz. Somala. Quad. Geol. Somalia, 8: 7-25.

ALMOND D.C. (1984). The concepts of "Pan-African Episode" and "Mozambique Belt" in relation to the geology of East and North-East Africa Bull. Fac. Earth Sci. King Abdulaziz Univ. Jeddah 6: 71-87

BARRINGTON BROWN C. (1931). The geology of the north-eastern British Somaliland. Quart. J. Geol. Soc. London, 87: 259-280.

BATCHELOR R.A. and BOWDEN P. (1985). Petrogenic interpretation of granitoid rocks series using multicationic parameters. Chemical Geology, 48: 43-55.

CLIFFORD T.N. (1968). Radiometric dating and the pre-Silurian geology of Africa. In: E.I. HAMILTON and R.M. FARQUHAR (eds.): Radiometric dating for geologist. London, New York. Interscience, 299-416.

D'AMICO C., H. A. IBRAHIM and SASSI F.P. (1981). Outline of the Somalian basement Geol. Rundschau 70: 882-896.

DAL PIAZ G.V. and SASSI F.P. (1986). The crystalline basements of Somalia: A review. Mem. Soc. Geol. It., 31: 351-361.

DAL PIAZ G.V., MARTIN S., RIGATTI G. and VENTURELLI G. (1987). The greenschist pillow lavas of Togga Lo' Aneba, Maydh area, Northeastern Somalia. Geosom 87, Intern. Meeting Geology of Somalia, Mogadishu, 1987, Abstr: 48.

DAL PIAZ G.V., RIGATTI G., GALLI L., MESSIGA B., PICCARDO G.B., GOSSO G., SPALLA M.I. and PECCERILLO A. (1985). Il gabbro di Sheikh (Somalia settentrionale): dati geologici, petrografici, geochimici e geocronologici preliminari. Univ. Naz. Somala. Quad. Geol. Somalia, 8: 151-186.

DANIELS J.L., SKIBA A.J. and SUTTON J. (1965). The deformation of some banded gabbros in the northern Somalia fold belt. Quart. Journ. Geol. Soc. London, 121: 111-142.

DUYVERMAN H.J., HARRIS N.B.W. and HAWKESWORTH C.J. (1982). Crustal accretion in the Pan-African: Nd and Sr isotope evidence from the Arabian shield. Earth Planet. Sci. Lett., 59: 315-326.

FARQUHARSON R.A. (1924). The geology and mineral resources of British Somaliland. London.

FERRARA G., GATTO G.O., H.A. IBRAHIM, A.A. SAID, SASSI F.P., TONARINI S. and VISONÀ D. (1987). Sequence of event recorded in the crystalline basement of Northern Somalia. Geosom 87, Intern. Meeting on Geology of Somalia, Mogadishu, Abstr.: 65.

FERRARA G., TONARINI S., SASSI F.P. and VISONÀ D. (1985). Sull'età del massiccio granitico di Daymoleh (Somalia settentrionale). Quad. Geol. Somalia. Univ. Naz. Somala, 8: 233-241.

FOUNTAIN D.M. and SALISBURY M.H. (1981). Exposed cross-section through the continental crust: implication for crustal structure, petrology and evolution. Earth Planet. Sci. Lett., 56: 263-277.

GATTO G.O., H.A. IBRAHIM, SASSI F.P. and VISONÀ D. (1987). A tentative litostratigraphic classification of the crystalline basement of northern Somalia Geosom 87, Intern. Geology Meeting of Somalia, Mogadishu, Abstr.: 71.

GATTO G.O., H.A. IBRAHIM, SASSI F.P., VISONÀ D. and K.M. ALI (1981). Contributo alla conoscenza del basamento della Somalia (distretti di Berbera e Burao). Univ. Naz. Somala. Quad. Geol. Somalia, 5: 27-41.

GATTO G.O., VISONÀ D. and SAID A.A. (1985). Note di rilevamento sul basamento cristalino della Somalia (distretti di Berbera e Burao).Univ. Naz. Somala. Quad. Geol. Somalia, 8: 243-255.

GELLATLY D.C. (1960). Report on the geology of the Las Dureh area, Burao District. Somaliland Protect. Geol. Survey Report, 6: 1-40.

GELLATLY D.C. (1963). The geology of the Darkainle nepheline syenite complex, Borama District, Somali Republic. Univ. Leeds.

GELLATLY D.C. (1964). Nepheline and feldspar orientation in nepheline syenite complex from Darkainle, Somali Republic. Am. J. Sci. 262: 635-642.

GREENWOOD J.E. (1960). Report on the geology of the Las Khoreh-Elay area, Erigavo District. Somaliland Protect. Geol. Survey Report, 3: 1-36.

GREENWOOD J.E. (1961). The Inda Ad Series of the former Somaliland Protectorate. Overseas Geol. and Min. Res., 8: 288-296.

GREENWOOD J.E. and BLEACKLEY D. (1967). Geology of the Arabian Peninsula, Aden Protectorate. U.S. Geol. Survey Prof. Paper 560-C: 1-96.

GREENWOOD W.R., ANDERSON R.E., FLECK R.J. and SCHMIDT D.L. (1967). Late Proterozoic cratonization in southwestern Saudi Arabia. Phil. Trans. R. Soc. London, A-280, 517 pp.

HUNT J.A. (1958). Report on the geology of the Adadleh area, Hargeisa and Berbera District, quarter degree sheets no. 35. Somaliland Prot. Geol. Survey 2, London.

HUNT J.A. (1960). Report on the geology of the Berbera-Sheikh area, Berbera and Burao District, quarter degree sheets no. 24 and 36. Somaliland Prot. Geol. Survey 4, London.

IBRAHIM H.A. and SASSI F.P. (1977). Il basamento cristallino della Somalia. Univ. Naz. Somala. Quad. Geol. Somalia, 1: 1-18.

KRÖNER A. (1984). Late Precambrian plate tectonics and orogeny: a need to redefine the term Pan-African. In: (eds.) J. KLERKX and MICHOT Geologie Africaine. Tervuren, 23-28.

LUDWIG K.R. (1988). A plotting and regression program for radiogenic isotope data for IBM-PC compatibile computers. U.S. Geol. Survey Open File Rept., 88-557.

MACFADYEN W.A. (1933). The geology of British Somaliland. London: Cown Agents.

MASON J.E. (1954). Report on the geology basement rocks in the Sheikh Auradl Wagger Area. Unpub. Rept. Geol. Survey Somalil. Prot., Hargeisa, London.

MASON J.E. (1958). A preliminary report on the Daba Shabeli ring complex, Burao district. Unpub. Rept. Geol. Survey Somalil. Prot., Hargeisa. London.

MASON J.E. (1962). Report on the geology of the area north of Hargeisa and Laferug, Hargeisa and Berbera District. Somaliland Rep. Geol. Survey Report, 7: 1-34.

MASON J.E. and WARDEN A.J. (1956). The geology of the Heis-Mait-Waqderia area, Erigavo District. Somaliland Protect. Geol. Survey Report, 1: 1-23.

PARKINSON J. (1932). A preliminary note on the Borama schists, British Somaliland. Geol. Mag., 69: 49-65.

PERUZZO L. (This volume). The pressure character of the Inda Ad metamorphism (Northern Somalia).

RAMSAY C.R. (1979). In defense of the Pan-African. In: COORAY G.(ed.) Newsletter, Pan-African crustal evolution in the Arabian-Nubian shield, 2: 22-23.

SACCHI R. and ZANFERRARI A. (1987). Notes on some shear zones of Northern Somalia. J. African Earth Sci., 6: 323-326.

SACCHI R., ZANFERRARI A., DUALEH A. and ABDIRAHMAN H.M. (1985). Osservazioni strutturali del basamento cristallino affiorante tra Hargeisa e Berbera (Somalia settentrionale). Univ. Naz. Somala. Quad. Geol. Somalia, 8: 305-323.

SAID A.A. (1987). Preliminary data on the amphibolization of the layered gabbros NW of Sheik (Northern Somalia). Geosom 87. Intern. Meeting on Geology of Somalia, Mogadishu, Abstr.: 117.

SAID A.A. (1988). Trasformazione gabbro-anfibolite: un esempio dal basamento della Somalia settentrionale. Doct. Thesis. Univ. Padova, 137 pp.

SASSI F.P. and H.A. IBRAHIM (1981). Tentativo di schematizzazione dei problemi litostratigrafici e di correlazione del basamento della Somalia settentrionale Univ. Naz. Somala. Quad. Geol. Somalia, 5: 91-101.

SASSI F.P. and VISONÀ (this volume). Relics of granulitic mineral assemblages in the Somali Basement.

SASSI F.P. and VISONÀ D. (1985). Primo tentativo di inquadramento cronologico globale dei processi magmatici e metamorfici nel basamento della Somalia settentrionale. Univ. Naz. Somala. Quad. Geol. Somalia, 8: 325-335.

SASSI F.P. and VISONÀ D. (1987). Relics of granulitic mineral assemblages in the Northern Somali crystalline basement. Geosom 87, Intern. Meeting on Geology of Somalia, Mogadishu, Abstr.: 118.

SNELLING N.J. (1963). Age determination unit. Ann. Rept. Overseas Geol. Surv. for 1962, London 1963, 30-39.

SNELLING N.J. (1967). Age determination results. In J.E. GREENWOOD and BLEACKLEY (eds): Geology of the Arabian Peninsula, Aden Protectorate.

U.S Geol. Survey Prof. Paper 560-C.: 693-695.

STEIGER R.H. and JÄGER E. (1977). Subcommission on Geocronology: convention on the use of decady constants in geo- and cosmocronology. Earth and Planetary Science Letters, 36: 359-62.

TACK L., DE PAEPE P., DEUTSCH S. and LIEGEOIS J.P. (1984). The alkaline plutonic complex of the upper Ruvubu (Burndi): geology, age, isotopic, geochemistry and implication for the regional geology of the western rift. In: (eds.): J. KLERKX and MICHOT: Geologie Africaine. Tervuren, 91-114.

WARDEN A.J. and DANIELS J.L. (1984). Evolution of the Precambrian of Northern Somalia. Bull. Fac. Earth. Sci. King Abdulaziz Univ. Jeddah, 6: 145-164.

WARDEN A.J. and HORKEL A.D. (1984). The geological evolution of the NE branch of the Mozambique Belt (Kenya, Somalia, Ethiopia). Mitt. Oesterr. geol. Ges. Wien, 77: 161-184.

WYLLIE B.I.N. (1925). Geology of a Portion of British Somaliland. In: J.V. GREGORY (ed.): British Somaliland. London, 8-14.

*Final editing, January 1990*

From *Geology and mineral resources of Somalia and surrounding regions*, Ist. Agron. Oltremare, Firenze, Relaz. e Monogr. 113, 41-58, 1993.

# PAN-AFRICAN METABASALTS FROM THE MAYDH AREA, NORTH-EASTERN SOMALIA

G.V. DAL PIAZ *, HERSI ADEN IBRAHIM **, S. MARTIN *, G.B. PICCARDO ***, G. RIGATTI* and G. VENTURELLI ****

* Dipartimento di Geologia, Paleontologia e Geofisica, Università di Padova, via Giotto 1, 35123 Padova, Italy.

** Department of Geology, Somali National University, P.O. Box 1081, Mogadishu, Somalia.

*** Dipartimento di Scienze della Terra, Università di Genova, Corso Europa 26, 16132 Genova, Italy.

**** Istituto di Mineralogia, Università di Parma, Viale delle Scienze 78, 43100 Parma, Italy.

ABSTRACT

The Late Proterozoic Maydh complex belongs to the Pan-African north-eastern Somali basement and is exposed, north of Ceerigabo, within the Neogene passive margin of the Somali plate bordering the Gulf of Aden. It consists of greenschist facies metatholeiites with normal MORB to transitional affinity and of terrigenous metasediments. The Maydh protoliths post-date the high-grade, partly rejuvenated older continental crust occurring westwards, from the Xiis area to the Ethiopia border, which has been formerly interpreted as the eastern branch of the Mozambique belt.

The Maydh complex is tectonically associated to the west with foliated to strongly sheared younger granites and is overlain by the Latest Proterozoic clastic and carbonate sequences of the Inda Ad complex. These relatively younger sedimentary and magmatic rocks record on the whole very low-grade to greenschist facies signatures of a single tectono-metamorphic episode of Pan-African age which predates the intrusion at a shallow level of Early Cambrian calc-alkaline granitoid plutons.

In spite of the geochemical affinity, the Maydh tholeiitic complex does hardly represent a true ophiolitic suture, due to the absence of other markers as mantle peridotite/serpentinite slices, gabbros and oceanic cover. Further, the Early Pan-African gabbro/monzonite/syenite bodies extensively recorded in the Maydh-Xiis area and in the whole of the northern Somali basement actually were emplaced as ensialic plutons. On the other hand, the Maydh tholeiites cannot even be envisaged as mafic members of a Pan-African volcanic arc, because the underlying foliated intrusives are within-plate granites. No traces of sutured trench-arc systems are exposed in the Maydh area, nor probably in Northern Somalia at all. Rejuvenated older continental crust may be envisaged as buried sole of the relatively younger basement exposed in the Maydh-Boosaso area.

The Maydh mafic complex may be interpreted as a north-trending fold belt of Late Pan-African age, derived from submarine basalts and associated clastic deposits filling graben or deep pull-apart basins which opened during the long-lasting tensive to transtensive attenuation and rupturing of the older continental crust, an extensional lithospheric process which was active since the Early Pan-African emplacement of the ensialic gabbro bodies.

## INTRODUCTION

A greenschist facies mafic volcanic complex locally occurs in the north-eastern sector of the Proterozoic Somali basement. This is exposed along the Neogene rift faults and uplifted blocks of the northern passive margin of the Somali plate, bordering the Gulf of Aden, south of Maydh (Mait), Ceerigabo (Erigavo) District. Also known as the Maydh complex (ABBATE et al., 1981; WARDEN and HORKEL, 1984), it consists of massive to pillow metabasalts and of terrigenous metasediments. This volcano-sedimentary complex was first recognized by MASON and WARDEN (1956) and recorded in the geological map at 1:125,000 scale (sheet 14, Erigavo) of the former Somaliland Protectorate. Subsequently it was tentatively interpreted by WARDEN and DANIELS (1984), WARDEN and HORKEL (1984) as a mafic record of a sutured Upper Proterozoic trench-arc system at the Africa/East Gondwana convergent plate margin.

This paper deals with the interpretation of the Maydh mafic complex, as inferred from field geology, bulk chemistry and microprobe mineral composition of selected pillow and schistose metabasalts collected along the Togga Lo' Aneba and Qoranti valleys during the 1981 and 1985 field surveys supported by the Geological Department of the National Somali University (ABBATE et al., 1981, 1985; DAL PIAZ et al., 1987b).

The reported place-names are from the topographic map of Somalia at 1:100,000 scale, while the English synonyms (in brackets) refer to the geological maps of the former Somaliland Protectorate, quoted in DAL PIAZ and SASSI (1988).

## GEOLOGICAL SETTING OF THE NORTHERN SOMALI BASEMENT

### General Framework

The 700 km long coastal strip of the Upper Proterozoic northern Somali basement mostly consists of the so-called polymetamorphic "older continental crust" that, extending from the Ethiopian border to the Xiis (Heis) area (D'AMICO et al., 1981; WARDEN and DANIELS, 1984; ABBATE et al., 1987; FERRARA et al., 1987; DAL PIAZ and SASSI, 1988, and refs. therein), was seen as the north-eastern branch of the Mozambique belt (WARDEN and HORKEL, 1984). The northern basement is buried beneath the Mesozoic-Tertiary sedimentary cover south of the Somali rift shoulder (BOSELLINI, 1986).

The northern Somali "older continental crust" is represented by polymetamorphic paragneisses with metabasite lenses, granitic orthogneisses and abundant migmatites, and records granulite relics and amphibolite-facies mineral assemblages. Its high-grade regional fabric may be referred to an Early- or pre-Pan-African orogenic cycle (DAL PIAZ and SASSI, 1988, and refs. therein). Polyphase folding, low-angle thrusts (SACCHI and ZANFERRARI, 1987 and refs. therein) and extensional shear zones characterize the structural setting of this belt which may tentatively be related to the collisional processes recorded in Ethiopia by the Adola suture zone (WARDEN and HORKEL, 1984), later collapse and subsequent extensional crustal attenuation. The timing of the basement evolution is not yet well-defined by a sufficient set of radiometric data. The oldest age comes from the Hudiso sillimanite-kyanite-bearing paragneisses south of Berbera; they yield a three-point Rb-Sr whole-rock isochron of 828 ± 170 Ma, which tentatively may record the thermal peak of the amphibolite-facies regional imprint (DAL PIAZ et al., 1985). Huge bodies of homogeneous to layered gabbros and related intermediate to strongly oversaturated rocks (monzonite, Fe-rich diorite, syenite, alkali granite) were emplaced within the "older continental crust" (DANIELS et al., 1965; DAL PIAZ et al., 1985; 1987a). They are cut by swarms of transitional basalt and andesite-basalt dykes which display a typical within-plate affinity (DAL PIAZ et al., 1985, 1987a). Among these bodies, the Lo' Jebyie gabbro-syenite ring complex yields a Rb-Sr isochron age of 688 ± 11 Ma (FERRARA, pers. comm.; FERRARA et al., 1987) while the intercumulus biotite from the Sheikh gabbro-monzonite pluton records a Rb-Sr cooling age of 567 Ma, probably reflecting regional uplifting (DAL PIAZ et al., 1985). From field evidence no doubts arise regarding the ensialic setting of the northern Somali Pan-African gabbro bodies that were emplaced under extensional conditions as igneous underplating beneath and within the "older continental crust" after the penetrative deformation of its high-grade tectono-metamorphic fabric. The composite gabbro bodies in turn display randomly distributed deformations and amphibolite to greenschist facies transformations, mostly as pseudomorphic alterations to recrystallization along mylonitic shear zones (DANIELS et al., 1965; DAL PIAZ et al., 1985, 1987a) that at times may be seen as extensional signatures. The gabbro alteration, which is probably roughly coeval to the retrogression randomly recorded by the high-grade assemblages of the surrounding "older continental crust", probably occurred during the Pan-African attenuation and extensional unroofing of this formerly lower continental crust.

Further, the mafic magmatic activity is locally recorded in Northern Somalia by the greenschist facies Abdulkadir and Maydh volcanoclastic complexes which are located at the western and eastern edges of the "older basement" (WARDEN and HORKEL, 1984; DAL PIAZ and SASSI, 1988, and refs. therein). They are characterized by bimodal and basaltic products respectively and post-date the exhumation of the gabbro bodies. The Maydh complex is overlain by the Inda Ad complex, a very low-grade metaclastic sequence with marble interbeddings which extends from Maydh to Boosaso (MASON and WARDEN, 1956; GREENWOOD, 1960; ABBATE et al., 1981). Both these complexes experienced a single tectono-metamorphic episode of Pan-African age which is partly recorded also in the "older basement".

Finally, the Pan-African evolution of the northern Somali basement records the emplacement of foliated to post-tectonic younger granites at around 550 Ma (ABBATE et al., 1985; FERRARA et al., 1985; DAL PIAZ et al., this volume).

## The Eastern Sector of The Northern Somali Basement

The basement exposed in the eastern sector of Northern Somalia consists mainly of relatively younger upper-crustal section as that recorded by the Maydh and Inda-Ad

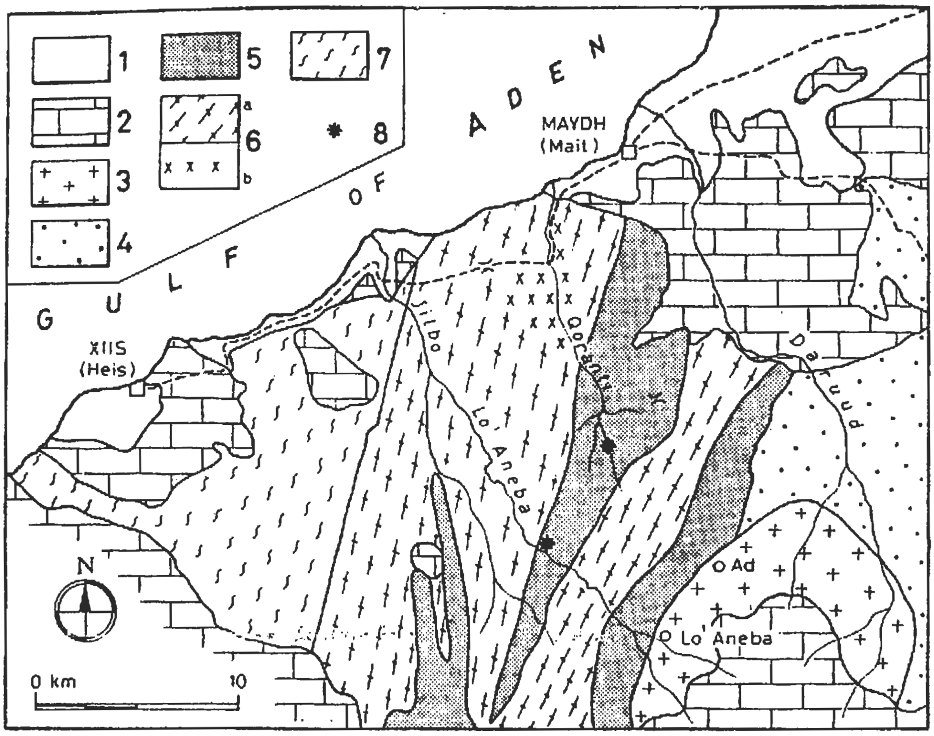


Fig. 1 - Geological sketch map of the northeastern Somali basement in the Maydh-Xiis area, north of Ceerlagabo, simplified and modified from official sources (1:125,000 Erigavo, Heis and Mait maps; MASON and WARDEN, 1956): 1: Recent deposits; 2: undifferentiated Mesozoic-Tertiary cover sequences; 3: Arar post-tectonic granite; 4: Inda Ad very-low grade clastic complex; 5: Maydh greenschist volcano-sedimentary mafic complex; 6: A-type looking foliated granites (a) and associated metamorphic gabbro-monzonite bodies (b); 7: Xiis complex, eastern edge of the Somali "older basement"; 8: location of the analysed tholeiitic metabasalts.

complexes. As reported above, it experienced a single tectono-metamorphic cycle of Pan-African age characterized by greenschist to very low-grade mineral assemblages (MASON and WARDEN, 1956; GREENWOOD, 1960; ABBATE et al., 1981; WARDEN and DANIELS, 1984; DAL PIAZ et al., 1985, 1987b). This monometamorphic continental crust occurs along the low coastal Maydh-Boosaso ranges (Fig. 1), east of the Xiis high-grade basal complex. The latter represents the eastern edge of the polymetamorphic "older basement" here consisting of pelitic and psammitic paragneisses, migmatites, lenses of amphibolite and metagabbro, acidic orthogneisses and various dyke generations (MASON and WARDEN, 1956; ABBATE et al., 1981).

From west to east and from bottom to top, the relatively younger Somali basement in the Maydh-Boosaso area is represented by:

1) An unnamed, tectonically bounded basal complex (6a-b in Fig. 1), which includes greenschist facies foliated to sheared granites, related acidic to lamprophyre dykes and minor metagabbro bodies. This complex extends westward, comprising most of the feldspar-rich "psammitic rocks" reported as "Xs complex" in the Erigavo sheet (MASON and WARDEN, 1956).
2) The intermediate, greenschist facies volcano-sedimentary Maydh complex (5 in Fig. 1), which includes a thick section of submarine metabasalts.
3) The capping Inda Ad complex (4 in Fig. 1), a thick sequence of weakly metamorphosed sandstone, siltstone and mudstone with numerous beds of marbles and a few intraformational conglomerates (MASON and WARDEN, 1956; GREENWOOD, 1960; ABBATE et al., 1981).

The minimum age of the tectono-metamorphic imprint in the Maydh-Boosaso fold belt may be established from field evidence and radiometric data. In fact these low- to very low-grade complexes were sharply intruded at shallow level and thermally metamorphosed by the Arar, Infero and Las Bar undeformed granitoids which yield Early Cambrian radiometric ages (SNELLING, 1967; ABBATE et al., 1985; DAL PIAZ et al., this volume). Swarms of probably coeval post-tectonic quartz porphyry dykes are also extensively recorded. The lower chronological boundary was formerly postulated as Early Paleozoic from the occurrence of ghosts of supposed sponge spiculae and pelmatozoa in the Inda Ad marbles (Gnoli, in ABBATE et al., 1981) and consistently with cooling ages on magmatic micas from the Arar granite at around 515-490 Ma (SNELLING, 1967; ABBATE et al., 1985). This timing is now questioned by the 550 Ma whole-rock isochron obtained from the Arar-Infero plutons which were emplaced after the Inda Ad folding (DAL PIAZ et al., this volume). Accordingly, the Pan-African tectono-metamorphic event recorded by the Maydh and Inda Ad upper-crustal section may go back to the Latest Proterozoic. Further, a Pan-African deposition age of the Inda Ad clastic/carbonate sequence may be indirectly envisaged by comparison with similar covers from the southern Arabia plate (e.g., BEYDOUN, 1970) and by field relationships indicating that the Inda Ad and Maydh sedimentary and volcanic protoliths post-date the high-grade regional metamorphism and anatectic processes recorded in the northern Somali "older basement". The same reasoning points to a Pan-African age for the tectono-metamorphic cycle in the Maydh-Boosaso strip and for the probably coeval (although not yet proved) retrograde evolution of the polymetamorphic Somali "older basement".

## THE MAYDH COMPLEX

The western edge of the Pan-African basement exposed in the Maydh area is the previously reported unnamed complex tectonically juxtaposed to the Maydh volcano-sedimentary complex. East of Togga Jilbo, it mainly consists of pervasively to poorly foliated granites (MASON and WARDEN, 1956; DAL PIAZ et al., this vol.) and of some gabbro-monzonite bodies (Togga Qoranti, Fig. 1). The latters record high- to intermediate-temperature shear zones and are cut by swarms of metabasalt dykes locally preserving chilled margins. All these igneous rocks display ductile to brittle deformations, with numerous cataclastic and mylonitic bands, and are weakly to largely recrystallized under greenschist-facies conditions. Despite pervasive reworking, the former mutual field relationships are locally well preserved, pointing to the relatively older age of the sheared gabbro suite that is sharply intruded by pink granitic and pegmatitic stocks (middle Togga Qoranti). This setting recalls that of the ensialic Sheik and Lo'Jebyie gabbro bodies south of Berbera; the resemblance is implemented by the close analogy of their magmatic assemblages and metamorphic signatures (DAL PIAZ et al., 1987a).

The Maydh complex consists of greenschist metabasalts and of interbedded and overlying terrigenous metasedimentary sequences. The mafic section mostly occurs along the western side of the Maydh metasedimentary strip, within a characteristic Y-shaped (on the plain view) synformal structure (Fig. 1). It is mainly formed of fine-grained massive to foliated and finely banded mafic greenstones; it also encompasses thin bands of sheared chlorite-rich rocks and some interbeddings of calc-schists and albite-chlorite-titanite-rich carbonaceous schists, the latter possibly representing former volcano-clastic layers.

These rocks often display a complete metamorphic fabric, with a very fine felt of greenish to-bluish-green tabular amphiboles including epidote, albite and titanite; opaques, green biotite and carbonate occur as minor to accessory minerals. Otherwise, the less deformed mafic rocks may be seen as homeogeneous dark green metabasalt to diabase types, often preserving a former ophitic texture. In this case, phenocrystic Ca-rich plagioclase, largely replaced by epidote and albite, and greenish calcic amphibole from primary pyroxene constitute the main mineral assemblage. Pillow and minor breccia lavas, which may be recognized everywhere with some uncertainty as textural ghosts within the finely schistose mafic sequences, are locally well preserved, as previously reported by MASON and WARDEN (1956). One of the best pillow lava occurrences is exposed along the upper Togga Lo' Aneba, the main right tributary of Togga Jilbo (Fig. 1). Flattened, fine-grained greenish massive cores (10 to 80 cm long) are wrapped by a dark green chlorite-rich matrix as cm-dm-large anostomosing bands characterized by a penetrative schistosity (Fig. 2). On the microscopic scale, ophitic to intersertal textures are locally preserved in the pillow cores, due to the pseudomorphic attitude of the greenschist imprint. The fine grained metamorphic assemblage includes zoned and homogeneous bluish-green amphiboles, chlorite and minor greenish biotite replacing the magmatic mafic minerals, and albite-epidote $\pm$ carbonate from calcic plagioclase; titanite and opaque accessory minerals also occur. Pillow cores are cut by radial cracks filled by calcite, chlorite and epidote. The matrix displays a chlorite-schist composition, with minor epidote, blue-green amphibole, carbonate and titanite; it sometimes includes thin amphibole-albite-bearing bands. Southwards, the associated metasedimentary section is mostly terrigenous, including very fine-grained blackish, grey and greenish pelitic to clastic phyllites with minor thin beds of calc-schists and

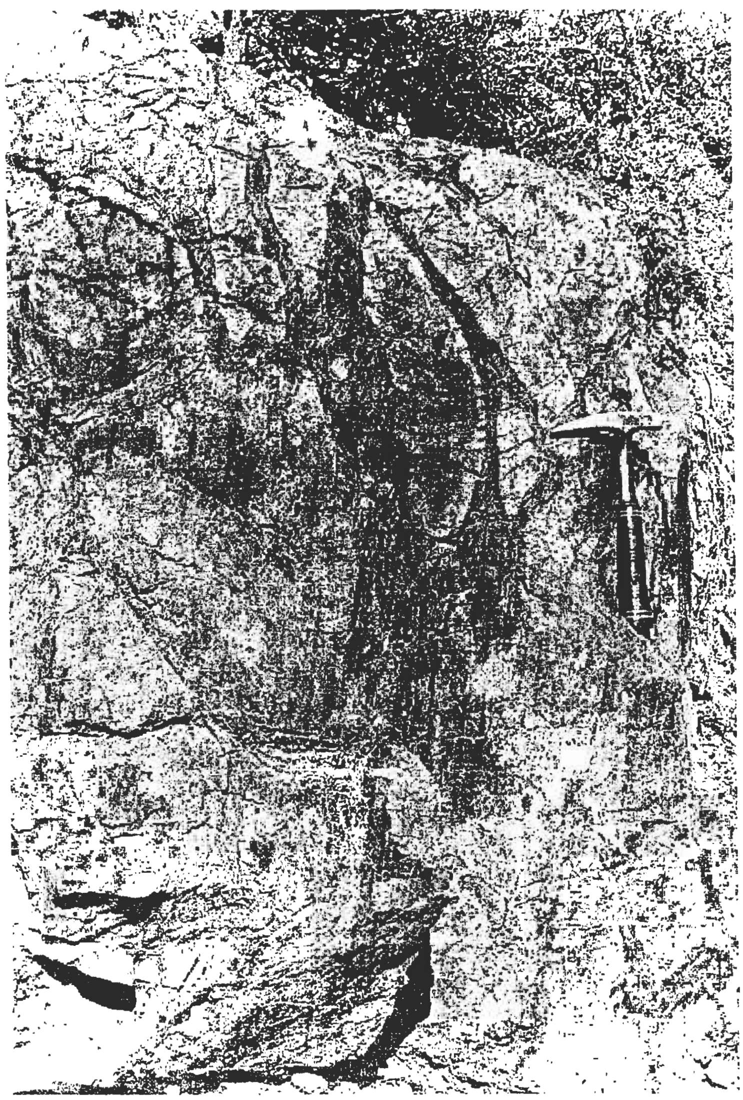

Fig. 2 - Greenschist tholeiitic pillow lavas from Togga Lo'Aneba; location in Fig. 1.

impure marbles; no traces of cherts have been found here. These rocks display a penetrative N/NNW-trending schistosity, defined by a greenschist mineral assemblage with sericite, chlorite, quartz, albite and minor brownish-green biotite. Northwards, along the Togga Qoranty valley (Fig. 1), basal metasiltstones occur, together with repeatedly interbedded marbles, mafic bodies (with ophitic texture and relict brown hornblende), and volcanoclastic layers; they grade upward to fine-grained carbonate-rich phyllites. A second narrow section of the Maydh metasediments is sandwiched between the east arm of the Y- shaped structure and the overlying Inda Ad complex;

it mainly consists of a strongly deformed volcano-sedimentary sequence which includes phyllites, calcschists, impure marbles, chlorite-schists and minor albite-chlorite bearing greenstones. Two deformational phases developed within the Maydh volcano-sedimentary complex under greenschist-facies conditions (ABBATE et al., 1981; DAL PIAZ et al., 1987b). The first is responsible for small isoclinal and rootless folds, shear zones and transposition of the lithological bedding. The second refers to the large-scale folding and related cleavage that are extensively recorded in both Maydh and Inda Ad complexes: it is characterized by N/NNW-trending recumbent, tight and open folds and by a regional shortening which decreases upwards and eastwards, as previously reported by MASON and WARDEN (1956) and GREENWOOD (1960). The lithological and metamorphic features of the Maydh sedimentary sequence were seen to be roughly transitional towards those of the overlying Inda Ad complex (MASON and WARDEN, 1956). Nevertheless, the small metamorphic jump that may be recognized between the greenschist Maydh complex and the very-low grade Inda Ad complex, the different deformational history and the absence of a basal conglomerate

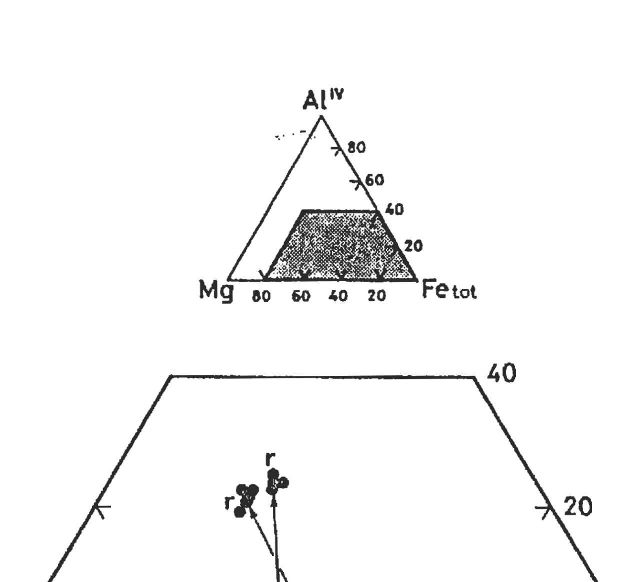


Fig. 3 - Fe-Mg partition and miscibility gap between coexisting greenschist calcic amphiboles from the Maydh tholeiitic metabasalts.

underlying their boundary (GREENWOOD, 1960) may indicate a tectonic or tectonized contact in between. The overall structural setting of the Maydh volcano-sedimentary mafic belt and the surrounding foliated to sheared younger granitoids may be interpreted as a west-vergent fold-and -thrust (?) belt of Pan-African age similar to, although necessarily not coeval with, that reported for Central Northern Somalia by SACCHI and ZANFERRARI (1987).

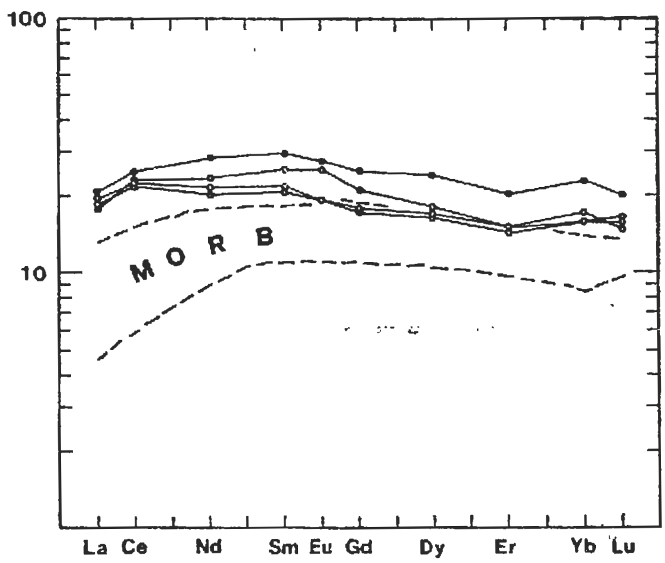


Fig. 4 - REE normalized diagram for the greenschist Togga Lo'Aneba pillow lavas (samples 2-4: open circles) and Togga Qoranti metabasalt (sample 6: dots). MORB field from SUN et al. (1979).

## MINERAL COMPOSITION AND BULK CHEMISTRY

A representative sample of pillow core from Togga Lo' Anèba was selected for electron microprobe study on metamorphic amphiboles. Mineral analyses were performed with the electron E.D.S. microprobe of the Department of Mineralogy and Petrology, University of Padova. Representative analyses of Ca-amphiboles are shown in Table 1. Amphibole analyses were calculated using the method of PAPIKE et al. (1974), assuming $Fe^{3+}$ p.f.u. as mid-point between minimum and maximum $Fe_2O_3$ values. The nomenclature proposed by the I.M.A. (LEAKE, 1978) is adopted. Among

Table 1 - Microprobe analyses of greenschist zoned amphiboles from Togga Lo' Aneba pillow lavas.

| | 1c | 1r | 2c | 2c' | 2r |
|---|---|---|---|---|---|
| $SiO_2$ | 52.74 | 46.32 | 46.68 | 54.57 | 44.64 |
| $TiO_2$ | 0.01 | 0.42 | 0.32 | — | 0.44 |
| $Al_2O_3$ | 4.14 | 10.90 | 9.96 | 1.86 | 12.88 |
| FeO | 13.52 | 17.02 | 17.46 | 13.92 | 17.83 |
| MnO | 1.05 | 0.69 | 1.23 | — | 0.82 |
| MgO | 14.53 | 9.61 | 10.05 | 15.17 | 8.40 |
| CaO | 11.89 | 11.44 | 11.69 | 12.65 | 11.92 |
| $Na_2O$ | — | 1.26 | 0.73 | — | 1.30 |
| $K_2O$ | 0.10 | 0.31 | 0.26 | 0.11 | 0.22 |
| Tot | 97.98 | 98.16 | 98.38 | 98.28 | 98.45 |
| Si | 7.590 | 6.826 | 6.837 | 7.828 | 6.598 |
| Al IV | 0.410 | 1.174 | 1.163 | 0.172 | 1.402 |
| Al VI | 0.293 | 0.719 | 0.557 | 0.142 | 0.843 |
| Ti | 0.001 | 0.046 | 0.035 | — | 0.049 |
| Fe 3+ | 0.095 | 0.211 | 0.457 | 0.009 | 0.173 |
| Fe 2+ | 1.532 | 1.886 | 1.682 | 1.661 | 2.031 |
| Mn | 0.128 | 0.086 | 0.152 | — | 0.103 |
| Mg | 3.116 | 2.110 | 2.194 | 3.243 | 1.850 |
| | 5.165 | 5.058 | 5.077 | 5.055 | 5.049 |
| Ca | 1.834 | 1.806 | 1.834 | 1.944 | 1.888 |
| Na | — | 0.134 | 0.088 | — | 0.063 |
| Na | — | 0.226 | 0.119 | — | 0.310 |
| K | 0.019 | 0.058 | 0.048 | 0.020 | 0.042 |
| Tot | 15.018 | 15.282 | 15.166 | 15.019 | 15.352 |

1: actinolite core (c) to Mg-hornblende rim (r); 2: Mg-hornblende (c) to actinolite (c') inhomogeneous core rimmed by Fe-hornblende (r).

Table 2 - Analyses of representative samples from Lo'Aneba greenschist pillow lavas (1-4), Qoranti massive metabasalts (5-6) and volcanoclastic layer (7).

| | LO'ANEBA | | | | | | QORANTI | | |
|---|---|---|---|---|---|---|---|---|---|
| | 1ec | 1c | 2r | 2ec | 3c | 4c | 5 | 6 | 7 |
| $SiO_2$ | 48.36 | 48.24 | 43.47 | 46.64 | 44.14 | 50.27 | 48.80 | 49.07 | 43.61 |
| $TiO_2$ | 1.77 | 1.82 | 1.95 | 1.95 | 1.91 | 1.88 | 2.19 | 2.34 | 2.37 |
| $Al_2O_3$ | 15.49 | 15.77 | 15.66 | 16.24 | 16.55 | 15.93 | 13.69 | 14.23 | 17.47 |
| $Fe_2O_3$ | 2.84 | 2.78 | 4.45 | 3.26 | 3.07 | 2.61 | 4.80 | 2.93 | 2.50 |
| FeO | 7.70 | 7.48 | 11.28 | 7.66 | 8.40 | 8.25 | 8.58 | 9.13 | 11.11 |
| MnO | 0.18 | 0.17 | 0.22 | 0.18 | 0.18 | 0.17 | 0.23 | 0.22 | 0.26 |
| MgO | 5.27 | 5.12 | 7.87 | 5.16 | 5.67 | 5.71 | 5.45 | 6.26 | 7.17 |
| CaO | 10.21 | 10.51 | 7.24 | 11.08 | 11.61 | 8.85 | 10.89 | 10.28 | 8.05 |
| $Na_2O$ | 2.79 | 2.93 | 1.26 | 3.09 | 2.88 | 2.62 | 2.23 | 3.00 | 2.52 |
| $K_2O$ | 0.24 | 0.22 | 0.24 | 0.28 | 0.28 | 0.13 | 0.22 | 0.26 | 0.30 |
| $P_2O_5$ | 0.21 | 0.18 | 0.23 | 0.21 | 0.21 | 0.19 | 0.27 | 0.26 | 0.35 |
| L.O.I. | 4.39 | 4.23 | 5.67 | 3.93 | 4.67 | 2.92 | 2.17 | 1.80 | 3.96 |
| Tot | 99.45 | 99.45 | 99.54 | 99.68 | 99.57 | 99.53 | 99.52 | 99.78 | 99.67 |
| Trace elements (ppm) | | | | | | | | | |
| Rb | 4 | 8 | 4 | 4 | 7 | 2 | 3 | 4 | 4 |
| Sr | 250 | 242 | 189 | 240 | 272 | 272 | 396 | 261 | 637 |
| Y | 43 | 48 | 46 | 46 | 52 | 45 | 52 | 57 | 42 |
| Zr | 144 | 142 | 148 | 145 | 163 | 159 | 169 | 210 | 249 |
| Nb | 5 | 5 | 4 | 5 | 5 | 5 | 5 | 4 | 5 |
| Cr | 226 | 223 | 261 | 245 | 242 | 247 | 154 | 158 | 38 |

Samples: 1. SML387-388, 2. SML390-391, 3. SML395, 4. SML397, 5. SML 552, 6. SML553, 7. SML561; c. core, ec. external core, r. rim matrix of the pillows.

Table 3 - REE abundances for representative samples of Upper Proterozoic greenschist pillow lavas (A) and massive metabasalts (B) from Togga Lo'Aneba and Togga Qoranti respectively (G).

| | A | | | B |
|---|---|---|---|---|
| | 2r | 2ec | 4c | 6 |
| La | 5.95 | 6.15 | 6.46 | 6.89 |
| Ce | 20.05 | 19.20 | 19.69 | 21.80 |
| Nd | 14.96 | 12.87 | 13.73 | 17.96 |
| Sm | 5.24 | 4.31 | 4.49 | 6.08 |
| Eu | 2.01 | 1.51 | 1.51 | 2.14 |
| Gd | 5.89 | 4.83 | 4.96 | 6.97 |
| Dy | 6.28 | 5.71 | 5.90 | 8.36 |
| Er | 3.37 | 3.25 | 3.43 | 4.64 |
| Yb | 3.49 | 3.51 | 3.80 | 5.07 |
| Lu | 0.56 | 0.54 | 0.51 | 0.69 |

Sample numbers as in Table 2.

the metamorphic amphiboles, those replacing magmatic mafic phases display an unhomogeneous core composition with closely interwoven actinolite and hornblende, and are rimmed by Fe-hornblende; small prismatic amphiboles are zoned, ranging in composition from actinolite core to Mg-hornblende rim, while other crystals are homogeneous hornblende. From these data, the greenschist facies amphibole, probably replacing primary Ca-pyroxene, is actinolite; further, the hornblende rims suggest that a primary amphibole should have been developed in the late magmatic stage after pyroxene. Selected samples from the greenschist Togga Lo'Aneba pillow lavas and Togga Qoranti massive metabasalts and chlorite-rich volcanoclastic layer of the Maydh complex (Tables 2, 3) show bulk rock compositions characterized by relatively high-Ti and low-K contents, broadly overlapping the transitional basalt field. The high L.O.I. values of the pillow lavas reflect alteration by water interaction of submarine basalts. Such processes also involved the pillow cores, prograding inwards through a pervasive net of microscopic fractures.

Assuming that alteration mass transfer did not influence the pattern of some immobile elements (Ti, Nb, Zr, Y), the Maydh metabasalts plot within the normal-

MORB to transitional basalt fields on the pertinent discriminative diagrams not figured here. The almost flat REE spectra (Fig. 4) are consistent with this characterization. The Togga Qoranti metabasalts are systematically higher in P, Ti, Zr and lower in Cr than the Togga Lo' Aneba pillow lavas. The significant positive correlations between incompatible elements (Ti, Zr, Y, P), coupled with their negative correlation with Cr, suggest that the Togga Qoranti group may represent more evolved terms of the same fractionation trend.

## DISCUSSION AND CONCLUSIONS

The greenschist facies foliated granitoids, tholeiitic metabasalts and metamorphic terrigenous sequences occurring in the Maydh area, east of the Xiis complex, are representative of a composite and relatively younger Late Proterozoic crustal section at the eastern edge of the polymetamorphic northern Somali "older basement".

According to WARDEN and HORKEL (1984), these mafic rocks may represent a true ophiolitic suture and/or, together with the underlying foliated granites, the record of a former subduction-related volcanic arc extending from Arabia to Northern Somalia. This hypothesis is a basic regional problem which requires discussion.

The submarine emplacement of the Maydh mafic belt and its geochemical affinity with modern and ancient oceanic crust may be consistent with the model of WARDEN and HORKEL (1984). Nevertheless, areal geology does not supply further evidence of a complete ophiolitic suite, due to the absence in the Maydh area and everywhere in the north-eastern Somali basement of mantle-derived peridotite/serpentinite slices and typical supra-ophiolitic oceanic covers. In our opinion, the lithospheric setting at the time of gabbro intrusion in the northern Somali basement play a basic role in this context. Beside the already discussed field evidences, the following points conclusively support the ensialic emplacement of the gabbro plutons: 1) the chemical features of the gabbro-monzonite and the associated syenite to alkali granite suites and the typical within-plate affinity of the transitional basalt and andesite-basalt dykes in the Sheik area (DAL PIAZ et al., 1985, 1987a); 2) the occurrence among the intercumulus minerals of hydrated magmatic phases such as reddish-brown amphibole and minor biotite, which indicate high X. $H_2O$ operating in the later evolution stages of a closed magmatic chamber; 3) the perfect preservation on a regional scale of the magmatic Ca-plagioclase, pointing to the absence of any oceanic alteration processes in the gabbro bodies (DAL PIAZ et al., 1985, 1987a, and in progress).

In conclusion, no further members of the supposedly northern Somali ophiolite suture exist in addition to the Maydh tholeiitic metabasalts and these, in turn, cannot be univocally interpreted as convincing ophiolitic record. The unique argument for an oceanic interpretation of the Maydh metabasalts rests on their MORB chemical character. However, we may recall that chemical signatures similar to that of the analysed Maydh rocks are also shown by ensialic flood basalts. Moreover the accretionary processes of juvenile crust hypothesized by WARDEN and HORKEL (1984) from the occurrence of the north-eastern Somali younger granitoids can no longer be supported. The chemical affinity of the foliated granites and comparison with well-established extension-related magmatic environments indicate that the melting processes and the emplacement of these plutons happened under regional extension and attenuation of the northern Somali lithosphere (DAL PIAZ et al., 1985, and this volume). The postulated occurrence of sutured subduction-related trench-arc systems of Pan-African age like those occurring in the Arabian-Nubian Shield (e.g. FLECK et al., 1980; GASS, 1981; CAMP, 1984; KRÖNER, 1985; STOESER and CAMP, 1985; KRÖNER et al., 1987; PALLISTER et al., 1987) may consequently be excluded in north-eastern Somalia. It cannot even be supported by the calc-alkaline post-tectonic granitoids of Early Cambrian age exposed in the Maydh-Boosaso area which, notwithstanding their I-type affinity, were emplaced under renewed extensional conditions after the late Pan-African orogenic event recorded in Northern Somalia was exhausted (DAL PIAZ et al., this volume).

In conclusion, the relatively younger basement exposed from Maydh to Boosaso may be seen as a Pan-African upper crustal section overlying the buried "older basement". The Pan-African crustal evolution of the northern Somali basement after the early Pan-African (or older) high-grade tectono-metamorphic signature may be reinterpreted. It has mainly been characterized by lithosphere attenuation and crustal dismembering under long-lasting extensional conditions, coupled with high thermal regimes and partial melting of asthenospheric sources and of the continental crust. These conditions assisted extensive processes of magmatic underplating, through early production, ensialic emplacement, differentiation and slow cooling of huge gabbro-monzonite plutons, closely followed by a bimodal magmatic activity and by younger granitic melts. Fractionation processes in the ensialic gabbro magma chambers and partial melting of the overlying continental crust may be envisaged as main suppliers for the intermediate to acidic magmatic products. The Maydh tholeiites may be related to this extensional scenario too, as a later event which was characterized by locally more active rising of asthenolitic bodies and by the supracrustal opening of north-trending grabens/pull-apart basins, probably still floored by thin continental crust. Lithosphere attenuation through deep-seated low-angle extensional shear zones evolving to asymmetric rift systems and/or transtensive pull-apart intracrustal ruptures may be hypothesized as suitable models for most of the Pan-African evolution of the North-eastern Africa. This scenario is also required in order to solve the space problem of the ensialic magma chamber of gabbros and later intrusive bodies. This may be further supported by the supposed occurrence of extensional unroofing processes allowing uplift and exposure of the composite gabbro batholiths. Tensive to transtensive conditions may have been active in Northern Somalia since the ocean openings in the Arabian-Nubian area, as the southward subduing and possibly delayed ensialic expression of these processes; they may have persisted or been inverted later, during the growth and evolution of the Arabian-Nubian trench-arc-systems, up to continental collision around 650 Ma ago (e.g. CAMP, 1984; STOESER and CAMP, 1985; KRÖNER et al., 1987). In this perspective, a sinistral- and then right-lateral transcurrent zone may have operated in between, bounding the northern margin of the East Gondwana plate. Subsequently, the collision tectonics of the Arabian-Nubian Shield and Late Precambrian Najd wrench fault system (STERN, 1985; STOESER and CAMP, 1985) may have extended soutwards to the northern Somali basement, producing, through transpressive inversion of the former extensional structures, the Late Pan-African tectono-metamorphic event recorded in the Maydh and Inda Ad fold systems and which predates the Early Cambrian intrusion of the calc-alkaline post-tectonic plutons from the Arar-Infero area.

ACKNOWLEDGEMENTS

For facilities made available during the field trips the Somali National University and the geological staff are gratefully acknowledged, as well as the fruitful geological assistance kindly supplied by E. ABBATE and ALI KASSIM. E. CALLEGARI and an anonymous referee are acknowledged for the critical review of the manuscript.

## REFERENCES

ABBATE E., ALI KASSIM M., DAL PIAZ G.V., GOSSO G., IBRAHIM H.A. and RIGATTI G. (1981). Note di rilevamento sul basamento cristallino della Somalia settentrionale nell'area Rugay-Maydh-Xiis, Distretto di Ceerigabo. Rend. Soc. Geol. Ital., 4: 333-337.

ABBATE E., BONAZZI A., DAL PIAZ G.V., DEL MORO A., GOSSO G., IBRAHIM H.A. and SAVIOLI MARIANI E. (1985). Il settore occidentale dell'Unità di Inda Ad ed il granito di Arar (Somalia settentrionale). Univ. Naz. Somala. Quaderni Geol. Somalia 8: 7-25.

ABBATE E., DAL PIAZ G.V., DEL MORO A., GOSSO G., IBRAHIM H.A., RIGATTI G. and SAID A.A. (1987). Review of Late Proterozoic-Cambrian evolution of northeastern Somali continental crust. Intern. meeting Geosom 87. Mogadishu, abstr., 4-6.

BEYDOUN Z.R. (1970). Southern Arabia and Northern Somalia: comparative geology. Phil. Trans. R. Soc. London. A 267: 267-292.

BOSELLINI A. (1986). East Africa continental margins. Geology 14: 76-78.

CAMP V.E. (1984). Island arcs and their role in the evolution of the western Arabian Shield. Geol. Soc. Am. Bull., 95: 913-921.

DAL PIAZ G.V., RIGATTI G., GALLI M., MESSIGA B., PICCARDO G.B., BORGOGNONI S., GOSSO G., SPALLA M.I., PECCERILLO A., POLI G., PARRINI P.L., TODARO M.L., FERRARA G. and TONARINI S. (1985). Il gabbro di Sheikh (Somalia settentrionale): dati geologici, petrografici, geochimici e geocronologici preliminari. Univ. Naz. Somala. Quaderni Geol. Somalia 8: 151-186.

DAL PIAZ G.V., IBRAHIM H.A., GOSSO G., PICCARDO G.B. and RIGATTI G. (1987a). The Sheikh gabbro body and the Hudiso paragneisses. Excursion B Guidebook, Intern. Meeting Geosom 87. Mogadishu, 23-42.

DAL PIAZ G.V., RIGATTI G., ABBATE E., GOSSO G., ALI KASSIM M., IBRAHIM H.A. and SAID A.A. (1987b). Note di rilevamento sul basamento cristallino della Somalia settentrionale tra Heis, Erigavo e Bosaso. Univ. Naz. Somala. Quaderni Geol. Somalia 9, 31 pp.

DAL PIAZ G.V., BIGIOGGERO B., DEL MORO A., IBRAHIM H.A., MARTIN S., RIGATTI G. and SAVIOLI MARIANI E. (this volume). Pan-African foliated alkali granites and post-tectonic granitoids from northeastern Somalia. J. African Earth Science.

DAL PIAZ G.V. and SASSI F.P. (1988). The crystalline basement of Somalia: a review. Mem. Soc. Geol. Ital., 31 (1986): 351-361.

D'AMICO C., IBRAHIM H.A. and SASSI F.P. (1981). Outline of the Somalian basement. Geol. Rundschau, 70: 882-896.

DANIELS J.L., SKIBA W.J. and SUTTON J. (1965). The deformation of some banded gabbros in the Northern Somalia fold-belt. Quart. J. Geol. Soc. London, 121: 111-142.

FERRARA G., GATTO G.O., IBRAHIM H.A., SAID A.A., SASSI F.P., TONARINI S. and VISONÀ D. (1987). Sequence of events in the crystalline basement of Northern Somalia. Intern. meeting Geosom 87, Mogadishu, abstr., 65-66.

FERRARA G., TONARINI S., SASSI F.P. and VISONÀ D. (1985). Sull' età del massiccio granitico di Daymoleh (Somalia settentrionale). Quaderni Geol. Somalia, 8: 233-241.

FLECK R.J., GREENWOOD W.R., HADLEY D.G., ANDERSON R.E. and SCHMID D.L. (1980). Rubidium-strontium geochronology and plate tectonic evolution of the southern part of the Arabian shield. U.S. Geol. Surv. Prof. Paper 1131, 38 pp.

GASS I.G. (1981). Pan-African (Upper Proterozoic) plate tectonics of the Arabian-Nubian shield. In: Precambrian plate tectonics (edited by KRÖNER, A.), 387-405. Elsevier, Amsterdam, Netherland.

GREENWOOD J.E. (1960). Report on the geology of the Las Khoreh-Elayu area, Erigavo District. Somaliland Protectorate. Geol. Surv. Rep. 3, 36 pp.

KRER A. (1985). Ophiolites and the evolution of tectonic boundaries in the Late Proterozoic Arabian-Nubian shield of Northeast Africa and Arabia. Precambrian Res. 27: 277-300.

KRER A., GREILING R., REISCHMANN T., HUSSEIN I.M., STERN R.J., DURR S., KRUGER J. and ZIMMER M. (1987). Pan-African evolution in the Nubian segment of Northeast Africa. In: Proterozoic litospheric evolution (edited by KRER A.), Washington D.C., U.S.A. Geodyn. Series 17: 235-257

LEAKE B.E. (1978). Nomenclature of amphiboles. Soc. franminal. cristall., 101: 453-467.
MASON J.E. and WARDEN A.J. (1956). Report on the geology of the Heis-Mait-Waqderia area, Erigavo District. Somaliland Protectorate. Geol. Surv. Rep. 1, 23 pp.
PALLISTER J.S., STACEY J.S., FISCHER L.B. and PREMO W.R. (1987). Arabian shield ophiolites and Late Proterozoic microplate accretion. Geology, 15: 320-323.
PAPIKE J.J., CAMERON K.L. and BALWIN K. (1974). Amphiboles and pyroxenes: characterization of other than quadrilateral components and estimates of ferric iron from microprobe data. Geol. Soc. Am., Abstracts with programs, 1053.
SNELLING N.J. (1967). Age determination results. Appendix in: Geology of the Arabian Peninsula: Aden Protectorate (GREENWOOD J.E. and BLEACKLEY D.). U.S. Geol. Surv. Prof. Paper 560 C, 93-96.
STOESER D.B. and CAMP V.E. (1985). Pan-African microplate accretion in the Arabian shield. Geol. Soc. Am. Bull., 96: 817-826.
STERN R.J. (1985). The Najd fault system, Saudi Arabia and Egypt: a Late Precambrian rift-related transform system? Tectonics, 4: 497-511.
SUN S., NESBITT R.M. and SARASKIN A.Y. (1979). Geochemical characteristics of mid ocean ridge basalts. Earth Planet. Sci. Lett., 44: 119-138.
WARDEN A.J. and DANIELS J.L. (1984). Evolution of the Precambrian of Northern Somalia. Bull. Fac. Earth Sci., King Abdulaziz Univ. Jeddah, 6: 145-164.
WARDEN A.J. and HORKEL A.D. (1984). The geological evolution of the NE-branch of the Mozambique belt (Kenya, Somalia, Ethiopia). Mitt. öster. geol. Ges. Wien, 77: 161-184.

ADDENDUM. The volume "Research in Sudan, Somalia, Egypt and Kenya" (Berliner Geowiss. Abh, Reihe A, 120.2, 1990), including the contribution of UTKE et al. which deals with the "Geological and structural setting of the Maydh and Inda Ad basement units in Northeast Somalia" has appeared long after this work was presented at the Geosom 87 and submitted to the Editors. The outlined extensional evolution fits in well with our model. Nevertheless, the envisaged oceanic origin of the Maydh metabasalts is not convincingly proved.

*Final editing, January 1990*

From *Geology and mineral resources of Somalia and surrounding regions*, Ist. Agron. Oltremare, Firenze, Relaz. e Monogr. 113, 59-82, 1993.

# THE DABA SHABELI GABBRO-SYENITE COMPLEX: AN ELEMENT OF THE GABBRO BELT IN THE NORTHERN SOMALI BASEMENT

D. VISONÀ

Dipartimento di Mineralogia e Petrologia, Università di Padova, Corso Garibaldi 37, 35123 Padova, Italy.

ASTRACT

An E-W gabbro-syenite belt occurs in the crystalline basement of Northern Somalia, consisting of an alignment of gabbro bodies with minor syenites of about 690 Ma. Among these bodies, the Daba Shabeli (DS) Complex is peculiar, mainly due to the occurrence of a syenitic ring-dyke. Field relations among the different lithotypes in the DS pluton reveal a complex intrusive history. At least four magmatic stages may be recognized, of which the following rocks are representative:

a) olivine gabbros, related cumulates and white syenites;
b) monzonites, qz-syenites and alkali-feldspar granites;
c) ring-dyke syenites;
d) leucogranites.

The qz-bearing acidic rocks (b, d) form mixed assemblages with gabbros and diorites.

Commingling between acidic and basic magmas is shown by the morphology, structure and plasticity of the pillows, and ion exchange between enclaves and hosts in some mixed rocks is indicative of local hybridation. Conversely, the ring-dyke syenites (c) are qz-free or ol-bearing and show no signs of interaction with the more basic magmas.

The presence of "trough structures" and mixed acidic-basic assemblages suggest that the present chamber was filled by several magma pulses coming from deep reservoirs.

Petrography and mineral composition suggest generally low $fH_2O$ conditions during the crystallization of all the lithotypes and $fO_2$ near the QFM, except for the granites. The low value of the iron redox ratio in some granites lacking in Fe-silicates may be due to Fe and Ti alkali stabilization in the metaluminous magma. The progressive increase of $fO_2$ from basic to acidic rocks is coeval with the increase in $fSiO_2$ and $fH_2O$, and causes the formation of titanite crowns on ilmenite and compositional variations in the amphiboles.

Petrographic and microchemical analyses provided a rough scenario for magma evolution, involving several pulses of basic magma at different crustal levels. The fact that the primitive magma became differentiated and later intruded into shallower levels where other magma was already consolidated indicates that it spent relatively prolonged periods of time in chambers at different depths.

## GEOLOGICAL FRAMEWORK

The crystalline basement of Northern Somalia is intruded by an extensive "Gabbro-Syenite Belt" (GATTO et al., 1987). This roughly E-W belt consists of gabbroid bodies with subordinate syenitic plutons and small stocks or dykes of alkali-feldspar granites. It was emplaced about 690 Ma ago (FERRARA et al., 1987) and was involved in later tectono-metamorphic events (SASSI et al., this volume). Structural and metamorphic reworking commonly occurs at the margins of the plutons or in narrow shear zones (DANIELS et al., 1965; SAID, 1987).

The syenite and granites of the Gabbro-Syenite Belt normally intrude the gabbroid plutons with irregularly-shaped stocks and dykes. The Daba Shabeli (DS) pluton differs from the others due to its characteristic ring structure (Fig. 1). Syenites, as well as syenitic and granitic dykes, occur in the ring (MASON, 1954, 1958).

In the DS pluton, field evidence shows the co-existence of gabbroid and granitic magmas in mixing assemblages (nomenclature after WIEBE, 1980) and their multistage intrusion. MASON (1958) pointed out the existence of syenites and granites of different ages after the main gabbro intrusion.

## Stages of Magmatic Emplacement

At least four main intrusive stages including gabbroid, syenitic and granitic magmas have been recognized.

a) The first stage is characterized by large quantities of layered olivine gabbros and old white syenites. Layered, cumulate and ultramafic rocks are present in this older part of the intrusion, inside the ring structure, with layering concordant with the ring shape. The syenites of this stage occur as decimetric blocks or inclusions in the rocks of the later intrusive stages.

b) The second stage is represented by mixed rocks constituted of ball-shaped (pillows-like) mafic bodies and minor interstitial felsic material. The mafic bodies are decimetric to metric, fine-grained gabbro while the felsic rocks are medium-grained monzonite to monzodiorite. The proportion between mafic and felsic rocks is variable; thin fine grained porphiric black border zones around the enclaves (chilled margins) may sometimes be observed. In the eastern part of the pluton, MASON (1958) describes the transition to granitic zones with rare gabbroid ball-shaped enclaves. Zones with marked ellipsoidic enclaves lengthening and having the same orientation of the minerals in the leucocratic portion also occur in Bur Dagahanyo.
The above field relations can be interpreted as a mixing between mafic and felsic magmas to form "pillow zones" similar to the "trough structures" described in the Nain Anorthosite Complex by WEIBE (1988).
Rare decimetric inclusions of coarse-grained white syenite also occur.
The fine- to medium-grained qz-syenites and alkali-feldspar granites also belong to this stage, sometimes in mixed assemblages with gabbroid rocks ("older" syenites of MASON, 1958) which, in the eastern part of the pluton, are in contact with the more recent syenites of the ring dyke. Dark, fine-grained and cm-sized quartz oxide inclusions also occur in these rocks.

c) The above-described intrusions are followed by the injection of the ring dyke, composed of coarse-grained syenites, spotted medium-grained leucosyenites, and

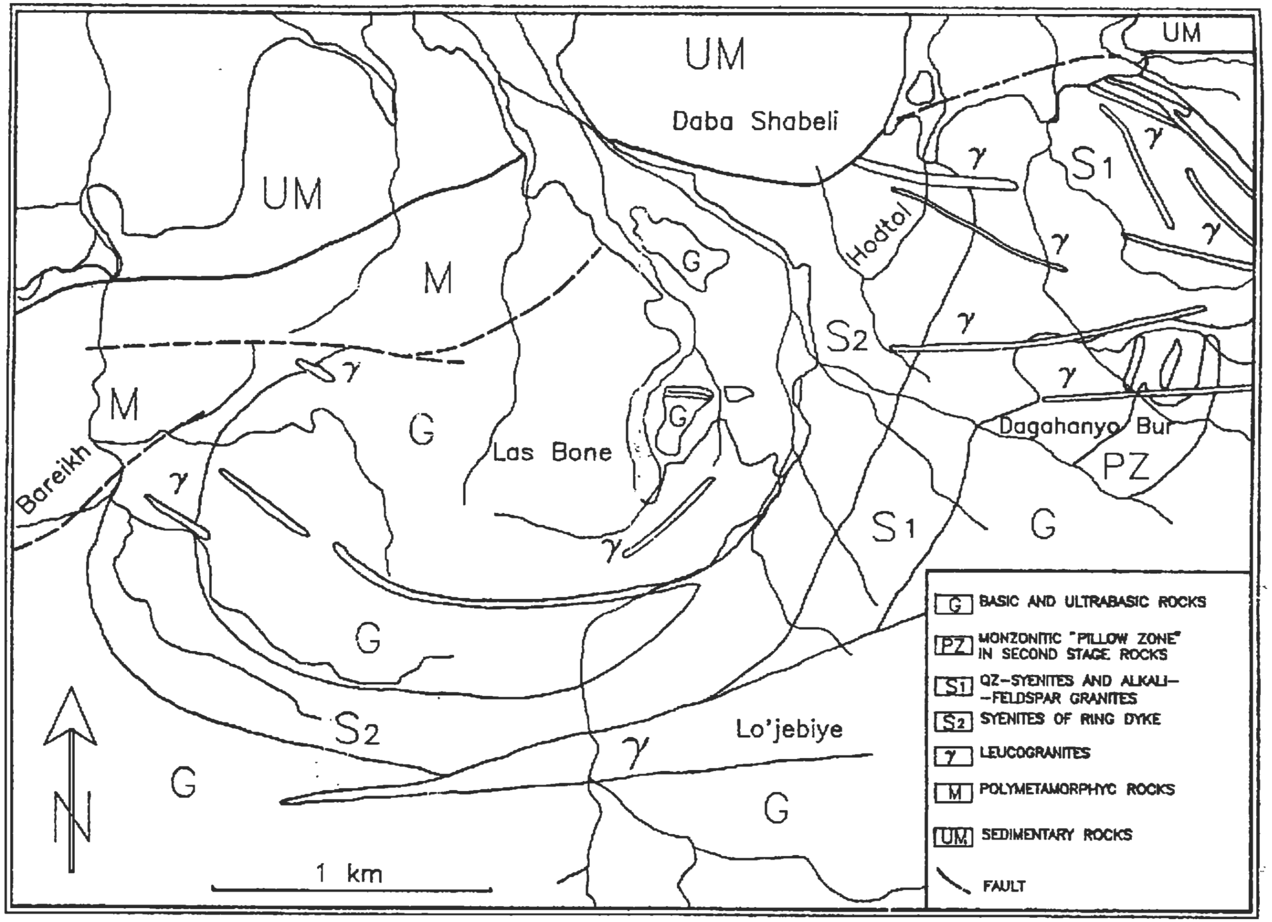


Fig. 1 - Partial geological map of Daba Shabeli Pluton (from MASON, 1958; modified).

leucosyenites. Relations between these rocks and those in stage d) were not observed in the field.

d) The fourth stage is composed of thin E-W dykes of leucogranites containing ball-shaped gabbroid enclaves which, at Bur Dagahanyo, cut the mixed rocks of stage c) (Fig. 2). White syenites of stage a) are found as spiky inclusions near the decimetric pillows, usually subspherical and with lobed contours and crenulate contacts (Fig. 3). Reactions between the commingling magmas (now gabbroid enclaves and host leucogranites) are not recognizable in this case either.

## PETROGRAPHY

### Basic and ultrabasic rocks

The most widespread gabbro is a blackish, medium- to coarse-grained rock with frequent centimetric layering.

The microscope sometimes shows iso-orientation of the plagioclase laths and olivine, interpreted as igneous lamination. Euhedral plagioclase (54% An) and from subhedral to anhedral Ti-augite are the main minerals forming the most frequent ophitic structure. Early magmatic minerals were olivine (70% Fo), sometimes with a thin rim of orthopyroxene, and green spinel associated with Fe-Ti oxides. Inclusions of olivine in clinopyroxene caused local poikilitic textures. Rare biotite (mg = 0.69) is the more frequent late magmatic interstitial mineral; even rarer is brown amphibole (pargasite) growing round pyroxenes or Fe-Ti oxides.

In one case recrystallization of clinopyroxene and the development of abundant neoblastic biotite (mg = 0.50) were observed, interpreted as effects of thermic contact metamorphism. However, no intrusive contacts between gabbros linked to different magmatic phases were observed in outcrops. However, internal contacts between gabbros are widespread in the adjacent Sheckh pluton, with clearcut boundaries, quenching in the more recent gabbro and recrystallization in the host gabbro.

Rare bands of anorthosites, troctolites and peridotites with magnetite are found in the inner part of the ring dyke. They are parallel with the gabbro layering, clearly revealing their origin by *in situ* differentiation.

### Syenites

a) First-stage syenites. These are medium- to coarse-grained, equigranular white rocks. Perthitic K-feldspar is the most abundant mineral, found in large subhedral phenocrysts with lobed plagioclase inclusions or almost complete plagioclase mantles. A little quartz and smaller feldspars are arranged between the perthites and larger plagioclases. Femic minerals are scanty and represented by biotite (mg = 0.25-0.27), often associated with Fe-Ti oxides and blue-green amphibole (Fe-edenite).

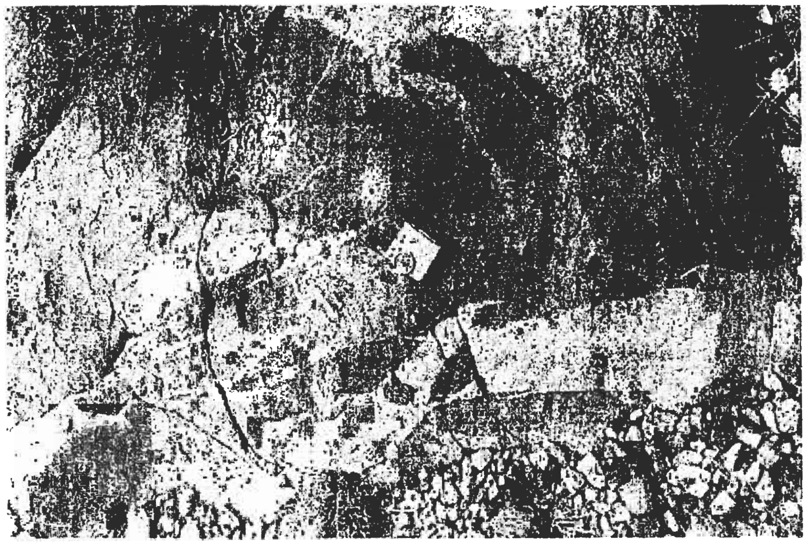

Fig. 2 - Third-stage leucogranitic dyke cutting second-stage rocks in mixed assemblages.

Fig. 3 - Spiky inclusions of white syenite and gabbroid inclusions with lobed contours in third-stage leucogranites.

Accessory minerals (apatite, ilmenite and titanite) are scarce; ilmenite is always crowned with titanite even when it is included in biotite or amphibole. Small euhedral clinozoisites form aggregates in the inner parts of some completely transformed plagioclases included in K-feldspar.

b) Syenites of the ring dyke. These rocks are blue-green, greyish or reddish-mauve, coarse-grained, inequigranular and allotriomorphic. Alkali-feldspars, which are the prevailing minerals in them, contain significant quantities of augite (41-43% Fe), sometimes replaced by a greenish-brown amphibole (pargasite?). The presence of admittedly small quantities of olivine (about 90% Fa) in rounded granules, often associated with pyroxenes or Fe-Ti oxides in small aggregates in the feldspar, is important. There are two generations of clinopyroxenes: one in large isolated crystals and the other in small crystals associated with olivine but always with the same composition (Table 4). Large subhedral crystals of Fe/Ti oxides and apatite in squat euhedral crystals up to 1.5 mm long may be found, sometimes as inclusions in the pyroxene. Interstitial minerals are carbonates accompanying rare pale-green amphibole in the pyroxene transformation products. Rare small red biotite flakes grow at the expense of the Fe-Ti oxides.

MIXED ASSEMBLAGES

1) Second-stage rocks:

a) medium-grained monzodiorites and monzonites make up portions merging into each other, contain basic pillows, or form the thin (cm to dm) film round the pillows (Fig. 2). In the areas with stretched pillows, the minerals of these host rocks are iso-oriented and form flow structures round the pillows. The darker enclaves are sometimes fine-grained and occasionally have a thin, blackish chilled margin. The composition of the enclaves is related to that of the embedding rock: the darker ones are found inside the monzogabbroid portions, the paler ones in the monzonitic portions.
Green amphibole (Fe-edenite) and feldspars (plagioclase: core 9.7% An, rim 6.5% An; K-feldspar 96% Or) are the main minerals defining the subophitic structure of these rocks; Ti-Al biotite (about 0.30 mg) and rare quartz are the minor phases. The characteristic K-feldspar mantles on plagioclase link the inclusions and host rocks. In the case of the monzodiorites, the plagioclases enveloped by K-feldspar (87% Or) contain appreciable quantities of An (max. 12%), while in the monzonites the inner portion is composed of almost pure albite. The monzonites also contain many other structures indicating sharp changes in crystallization conditions, such as plagioclase mantling K-feldspar and biotite crowns on amphibole and titanite on ilmenite.

b) qz-syenites and alkali-feldspar granites are heterogranular rocks, mainly porphyric due to the greater development of subhedral meso-perthites, sometimes with pecilitic rims. Quartz is found in smaller rounded crystals, in a fine intergranular mass of albite and microcline. The rare biotite is interstitial and mainly associated

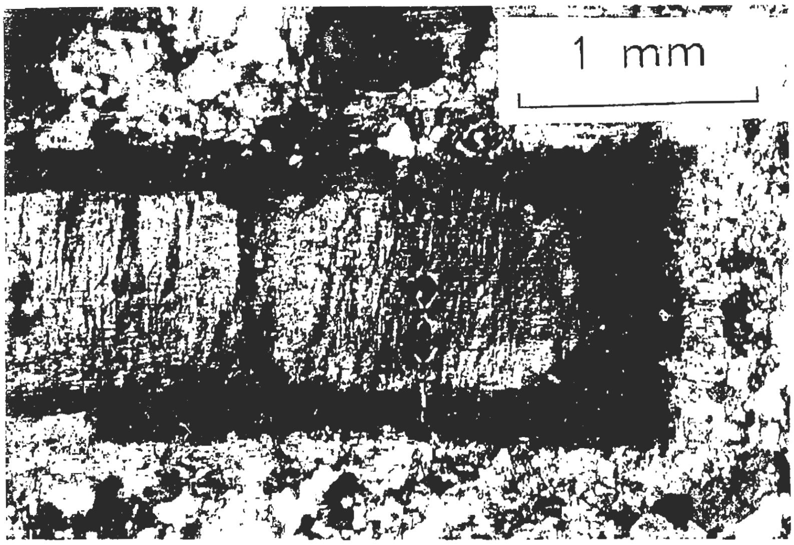


Fig. 4 - Alkali-feldspar granites of second-stage mixing assemblages: shell (dark grey) of plagioclase in K-feldspar phenocrysts. (2 polars).


Fig. 5 - Glomerophyric texture of gabbroid pillows in fourth-stage leucogranites: magmatic mafic phenocrysts are replaced by a felt of actinolitic hornblende; plagioclase is unaltered. (2 polars).

with Fe-Ti oxides. Mantling in feldspars and plagioclase shells in microcline (Fig. 4) is a characteristic common to qz-syenites, alkali-feldspar granites, monzodiorites and monzonites.

Two types of oxide-rich aggregates are peculiar to these rocks:

1) fine rectangular aggregates of quartz and magnetite, with crowns of green amphibole and biotite, which may represent the replacement of an Fe-Mg silicate (pyroxene?), no longer stable in the later $fO_2$ conditions; ii) from mm- to cm-sized inclusions, subspherical or elliptical, equigranular and panallotriomorphic in structure. In this case, magnetite coexists with ilmenite and numerous small euhedral zircons crown the irregularly shaped oxides; apatite is also frequent. Quartz, the other major component of these inclusions, is found in rounded flakes with lobed contours.
2) The often porphyric third-stage leucogranites make up small dykes, mainly in the eastern part of the gabbroid complex. Quartz, K-feldspar and albitic plagioclase (2.6-12% An), with rare rapakiwi structures due to albite mantling (0.5% An) on K-feldspar, are the major components of these rocks. Biotite (mg = 0.24-0.39) and amphibole (with Fe-Hbl/Fe-Ed cores and Fe-Act-Hbl rims), both with remarkably high Cl contents (up to 1.03% in biotite and 1.73% in amphibole) are rare. Magnetite and ilmenite also occur in small separate crystals. Large (up to 3 cm), brown, isodiametric crystals of Danilith are also found rarely (MOLIN and VISONÀ, in prep.).

The structures and mineral chemistry in the gabbroid pillows of these granites are interesting as regards the study of interactions between the two magmas, acidic and basic. Grain-size is fine and texture markedly porphyric in the outer parts, with a thin, biotite-rich chilled margin. The inner parts are medium-grained and rich in phenocrysts.

The magmatic phenocrysts (pyroxene) are replaced by actinolitic hornblende (Fig. 5).

The plagioclase composition is calcic (55-64% An) in the unaltered phenocrysts rich in very fine ore inclusions, while it is sodic (13% An) in the groundmass. It sometimes also shows a thin mantle of K-feldspar.

Amphibole after pyroxene and the growth of biotite and alkaline feldspars reveal chemical interaction with the host magma.

## MINERAL COMPOSITION

The field relations and microstructures described above suggest that gabbroid and granitic (or syenitic) magmas were periodically mixed and intruded in a shallow magmatic chamber containing already consolidated stratified gabbros. The $^{87}Sr/^{86}Sr$ data (FERRARA et al., 1987) of all the rocks described here, including the gabbros, indicate their common subcrustal origin.

These premises lead us to expect that mineral chemistry would show links between the magmas and the processes of fractionated crystallization and mixing which produced the lithotypes now found in the DS pluton.

## Feldspars

Feldspar composition is shown in Fig. 6 and representative analyses in Table 1. The analyses show bimodal distribution of composition: the group of calcic plagioclases (max. 64% An) belongs to the gabbros and pillows, while that of albitic composition (max. 12% An) belongs to the more acidic rocks.

Albitic rims may also be found in the calcic plagioclases of the gabbroid pillows.

Oligoclasic composition (22.5% An) is representative of the unzoned plagioclases in the sample of recrystallized gabbro.

The composition of K-feldspar was determined on not visibly perthitic crystals and gave values of Or> 95%. The only lower value (87.5% Or) regards the plagioclase mantle of a qz-monzodiorite.

Plagioclase (albite) shells on K-feldspar (Fig. 4) also occur (column 5 in Table 1).

Table 1 - Feldspar microanalyses.

Columns 1-6 and 8: second-stage qz-syenites and alkali-feldspar granites;
column 7: their gabbroid enclaves;
columns 9-10: recrystallized gabbro and olivine gabbro;
column 5: plagioclase shell in K-feldspar;
column 2: K-feldspar mantling plagioclase of col. 5.

| | 35 | 35k | 36 | 36k | 37 | 37k | 38 | 45 | 48 | 50 |
|---|---|---|---|---|---|---|---|---|---|---|
| SiO2 | 68.68 | 65.22 | 67.50 | 64.94 | 69.03 | 64.85 | 68.67 | 68.74 | 62.12 | 53.75 |
| Al2O3 | 18.36 | 18.22 | 19.46 | 18.04 | 18.61 | 18.23 | 19.05 | 19.11 | 23.40 | 28.40 |
| FeO | 0.13 | 0.38 | 0.37 | 0.02 | 0.36 | 0.21 | 0.29 | 0.31 | 0.26 | 0.80 |
| CaO | 2.35 | 0.00 | 1.46 | 0.00 | 0.17 | 0.00 | 0.75 | 0.00 | 4.92 | 11.59 |
| Na2O | 10.47 | 1.40 | 10.74 | 0.45 | 11.60 | 0.00 | 11.29 | 11.67 | 9.26 | 5.22 |
| K2O | 0.10 | 14.93 | 0.16 | 16.58 | 0.10 | 16.92 | 0.00 | 0.16 | 0.15 | 0.22 |
| TOT | 100.10 | 100.15 | 99.69 | 100.03 | 99.87 | 100.21 | 100.05 | 100.00 | 100.11 | 99.98 |
| Si+4 | 11.91 | 12.00 | 11.90 | 12.03 | 12.09 | 11.99 | 12.01 | 12.02 | 11.03 | 9.77 |
| Al+3 | 3.96 | 3.96 | 4.02 | 3.94 | 3.83 | 3.99 | 3.93 | 3.94 | 4.90 | 6.08 |
| Fe+2 | 0.02 | 0.06 | 0.05 | 0.00 | 0.05 | 0.03 | 0.04 | 0.05 | 0.04 | 0.12 |
| Ca+2 | 0.44 | 0.00 | 0.27 | 0.00 | 0.03 | 0.00 | 0.14 | 0.00 | 0.94 | 2.26 |
| Na | 3.53 | 0.50 | 3.65 | 0.16 | 3.93 | 0.00 | 3.83 | 3.96 | 3.19 | 1.84 |
| K | 0.02 | 3.51 | 0.04 | 3.92 | 0.02 | 4.01 | 0.00 | 0.04 | 0.03 | 0.05 |
| TOT | 19.88 | 20.03 | 19.94 | 20.05 | 19.97 | 20.02 | 19.95 | 20.00 | 20.13 | 20.13 |
| O-2 | 32.00 | 32.00 | 32.00 | 32.00 | 32.00 | 32.00 | 32.00 | 32.00 | 32.00 | 32.00 |
| AN% | 11.03 | 0.00 | 6.82 | 0.00 | 0.75 | 0.00 | 3.53 | 0.00 | 22.51 | 54.45 |
| OR% | 0.50 | 87.53 | 1.01 | 96.08 | 0.50 | 100.00 | 0.00 | 1.00 | 0.82 | 1.23 |

## Biotite

The microanalyses of Table 2 show negligible variations inside single crystals and significant variations among different crystals in a single sample. In only one case (qz-syenite 45) are the variations very conspicuous, but they may be explained by the fact that one of the two crystals analyzed grows round magnetite.

From the general crystal chemistry viewpoint, increased $Al_{tot}$, Fe and Ti are observed with increasing $SiO_2$ in the host rock. $Al^{IV}$ content is low (2.1-2.5 u.a.f.) and positive correlations are observed between $Al^{VI}$ and Ti and between Ti and Fe. According to ABRECHT and HEWITT (1988), similar behaviour in experimental Fe-Mg biotites is essentially due to the substitution Ti-Tschermakite $Ti^{VI}+Al^{IV} = 2Si^{IV}+(Fe,Mg)^{VI}$.

Table 2 - Biotite compositions, for normalization see Appendix. Columns 1-4: second-stage qz-syenite and alkali-feldspar granites; column 5: their gabbroid enclaves; column 6: third-stage leucogranites; column 7: their gabbroid enclaves; column 8: syenite enclaves; column 9: recrystallized gabbro and (10) olivine gabbro.

| | 35 | 36 | 37 | 45 | 38 | 41b | 41c | 39 | 48 | 50 |
|---|---|---|---|---|---|---|---|---|---|---|
| SiO2 | 35.00 | 34.64 | 34.46 | 35.23 | 37.38 | 37.79 | 36.03 | 35.10 | 36.41 | 36.90 |
| TiO2 | 2.43 | 2.10 | 2.57 | 5.26 | 2.38 | 2.11 | 2.24 | 2.66 | 5.03 | 4.89 |
| Al2O3 | 15.00 | 15.11 | 15.35 | 12.72 | 14.06 | 13.63 | 13.88 | 14.64 | 13.54 | 14.91 |
| FeO | 27.54 | 31.35 | 34.36 | 27.83 | 23.55 | 25.03 | 27.27 | 29.19 | 20.49 | 12.99 |
| MnO | 0.86 | 0.77 | 0.25 | 0.91 | 0.28 | 0.33 | 0.28 | 0.78 | 0.32 | 0.04 |
| MgO | 6.01 | 3.06 | 1.07 | 6.54 | 10.00 | 9.42 | 7.39 | 5.04 | 11.30 | 16.31 |
| CaO | 0.03 | 0.04 | 0.05 | 0.05 | 0.03 | 0.04 | 0.08 | 0.05 | 0.05 | 0.00 |
| Na2O | 0.13 | 0.07 | 0.07 | 0.05 | 0.05 | 0.05 | 0.13 | 0.06 | 0.11 | 0.00 |
| K2O | 8.83 | 8.66 | 7.64 | 7.62 | 8.43 | 7.66 | 8.07 | 8.62 | 8.53 | 10.01 |
| H2O | 3.51 | 3.42 | 3.40 | 3.63 | 3.74 | 3.70 | 3.41 | 3.56 | 3.66 | 3.91 |
| Cl | 0.53 | 0.64 | 0.64 | 0.13 | 0.08 | 0.20 | 0.99 | 0.25 | 0.46 | 0.00 |
| O=Cl | 0.12 | 0.14 | 0.14 | 0.03 | 0.02 | 0.05 | 0.22 | 0.06 | 0.10 | 0.00 |
| TOT | 100.00 | 100.00 | 100.00 | 100.00 | 100.00 | 100.00 | 100.00 | 100.00 | 100.00 | 100.00 |
| Si IV | 5.55 | 5.59 | 5.60 | 5.55 | 5.73 | 5.81 | 5.69 | 5.59 | 5.56 | 5.44 |
| Al IV | 2.45 | 2.41 | 2.40 | 2.36 | 2.27 | 2.19 | 2.31 | 2.41 | 2.43 | 2.56 |
| Ti IV | - | - | - | 0.09 | - | - | - | - | 0.01 | - |
| T site | 8.00 | 8.00 | 8.00 | 8.00 | 8.00 | 8.00 | 8.00 | 8.00 | 8.00 | 8.00 |
| Al VI | 0.36 | 0.47 | 0.53 | 0.00 | 0.27 | 0.28 | 0.27 | 0.33 | 0.00 | 0.03 |
| Ti VI | 0.29 | 0.26 | 0.31 | 0.54 | 0.27 | 0.24 | 0.27 | 0.32 | 0.57 | 0.54 |
| Fe +2 | 3.65 | 4.23 | 4.67 | 3.67 | 3.02 | 3.22 | 3.60 | 3.88 | 2.62 | 1.60 |
| Mn +2 | 0.12 | 0.11 | 0.03 | 0.12 | 0.04 | 0.04 | 0.04 | 0.11 | 0.04 | 0.00 |
| Mg | 1.42 | 0.74 | 0.26 | 1.54 | 2.29 | 2.16 | 1.74 | 1.19 | 2.57 | 3.59 |
| O site | 5.84 | 5.80 | 5.81 | 5.86 | 5.89 | 5.95 | 5.91 | 5.83 | 5.80 | 5.78 |
| Ca | 0.00 | 0.01 | 0.01 | 0.01 | 0.00 | 0.01 | 0.01 | 0.01 | 0.01 | 0.00 |
| Na | 0.04 | 0.02 | 0.02 | 0.01 | 0.01 | 0.01 | 0.04 | 0.02 | 0.03 | 0.00 |
| K | 1.79 | 1.78 | 1.58 | 1.53 | 1.65 | 1.50 | 1.62 | 1.75 | 1.66 | 1.88 |
| A site | 1.83 | 1.81 | 1.61 | 1.56 | 1.67 | 1.52 | 1.68 | 1.78 | 1.70 | 1.88 |
| O | 20.00 | 20.00 | 20.00 | 20.00 | 20.00 | 20.00 | 20.00 | 20.00 | 20.00 | 20.00 |
| OH | 3.86 | 3.83 | 3.82 | 3.96 | 3.98 | 3.95 | 3.74 | 3.93 | 3.88 | 4.00 |
| Cl | 0.14 | 0.17 | 0.18 | 0.04 | 0.02 | 0.05 | 0.26 | 0.07 | 0.12 | 0.00 |
| mg | 0.28 | 0.15 | 0.05 | 0.30 | 0.43 | 0.40 | 0.33 | 0.24 | 0.50 | 0.69 |

One group of biotites shows exceptionally high Ti values (Fig. 7): these are biotites associated with Fe-Ti oxides in gabbros and qz-syenites. In the second case, they are Fe-biotites which, because of the steric effect of the Ti-Tsch substitution, should contain only negligible quantities of $Fe^{3+}$ (ABRECHT and HEWITT, 1988).

The Mg content of the biotite in the pillows is always higher than that of the host granite, and even higher values are typical of the biotites in the inner parts of the pillows (Table 2).

Significant differences in Cl content are noted between the biotites of the gabbroid pillows and those of the host granites. Relatively high Cl values are also found in the biotites of the second-phase mixed rocks.

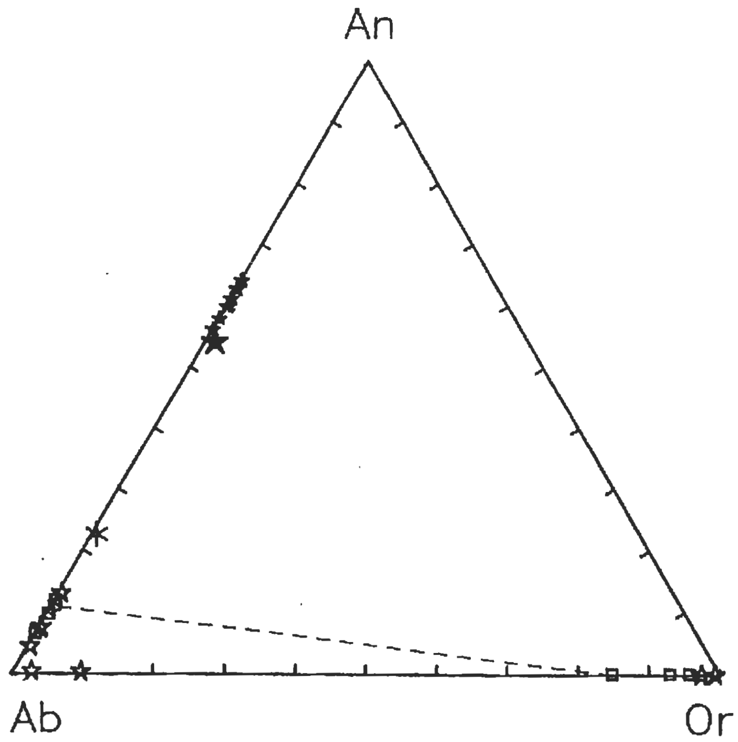


Fig. 6 - Projection of representative analyses of feldspars in An-Ab-Or diagram. Full stars: gabbroid inclusions in third-stage leucogranites; large full star: olivine gabbro; large asterisk: recrystallized gabbro; empty stars: third-stage leucogranites; empty squares: second-stage qz-syenites and alkali-feldspar granites; dashed line joins one plagioclase to its K-feldspar mantle. See text for comments.

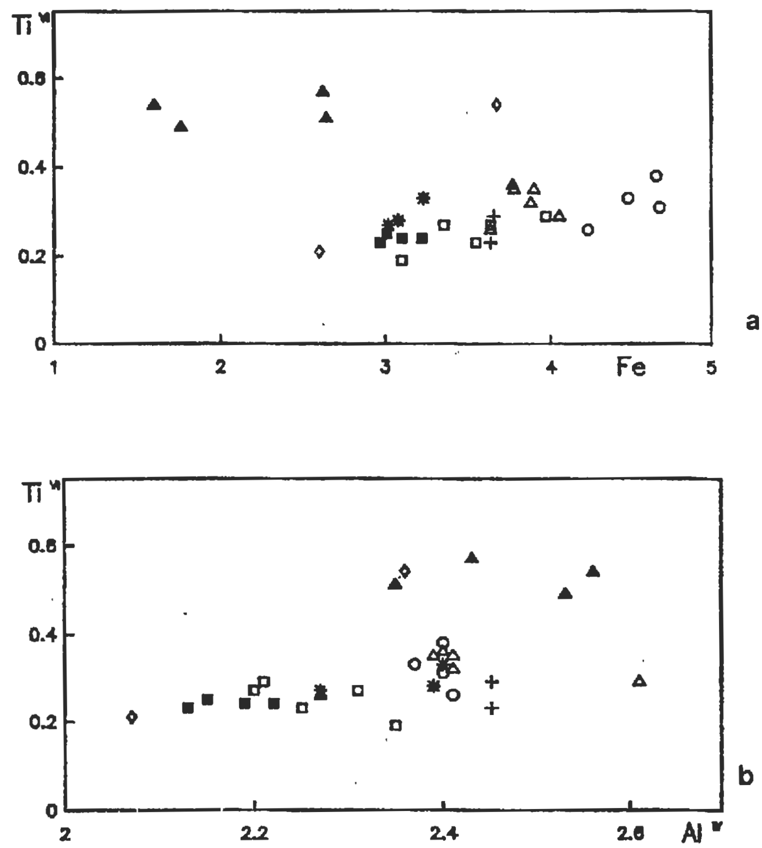


Fig. 7 - Relations between $Ti^{VI}$ and Fe (7a) and between $Ti^{VI}$ and $Al^{IV}$ (7b) in biotites. Crosses, circles and diamonds: second-stage qz-syenites and alkali-feldspar granites and their enclaves (asterisks); triangles: olivine and recrystallized gabbros; empty squares: third-stage leucogranites and their gabbroid enclaves (full squares); reversed triangles: spiky inclusions of white syenite in second- and third-stage rocks. See text for comments.

### Amphibole

Microprobe analysis (selected analyses in Table 3) shows that the amphiboles studied here are all calcic and that their composition varies from actinolite to Fe-pargasite (Fig. 8).

Considering the possible coupled substitutions within amphibole structure

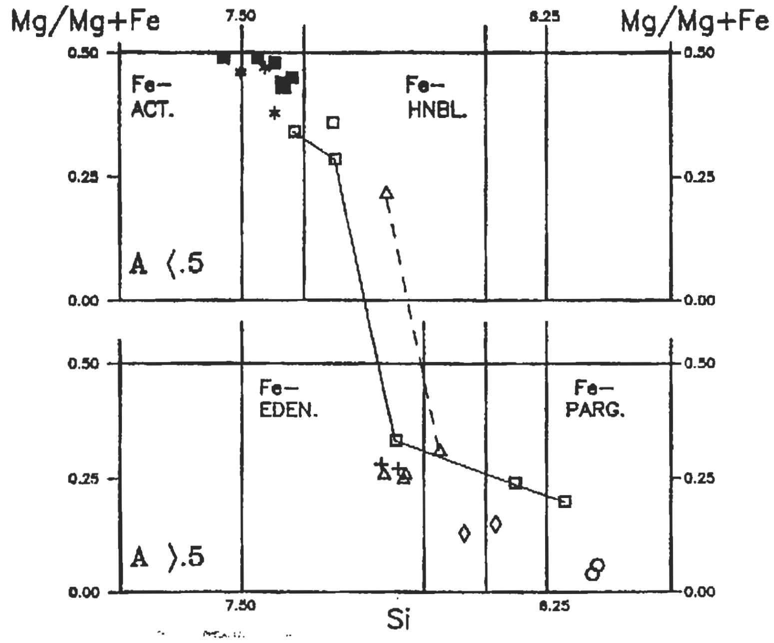


Fig. 8 - Classification of amphiboles after LEAKE (1978). Symbols as in Fig. 7. Lines joining parts of a single crystal represent zonings towards Al-richer and Fe-rich rims.

(CZAMANSKE and WONES, 1973), in the $Al^{IV}$ vs $Al^{T}$ and $Al^{IV}$ vs Ti diagrams (Figs. 9a, 9b), it should be noted that the data points plot along trends compatible with edenitic and Ti-tschermakitic substitutions. In particular, in the rims of amphiboles of differentiated rocks, only edenitic substitution occurs. The observed variations are therefore compatible with increased $fO_2$ and $fSiO_2$ during crystallization (cf. WONES and GILBERT, 1982).

All the amphiboles show low mg values, with extreme Fe-bearing compositions in the acidic differentiates. The mg ratio also varies in the amphiboles of the same sample, with higher values in the pargasitic/edenitic cores and lower ones in the corresponding rims (act.-hbl); this type of zoning has been interpreted as reflecting increased $fO_2$ during magmatic differentiation (CZAMANSKE and WONES, 1973; YAMAGUCHI, 1985).

One important point is that the composition of the pillow amphiboles is very similar to that of the rims of the granitic host rocks (respectively full and empty squares in Figs. 8 and 9).

Table 3 - Amphibole compositions, for normalization see Appendix. Columns 1-3: second-stage qz-syenites and alkali-feldspar granites; column 4: their gabbro enclaves; column 5: first-stage white syenite; columns 6-9: core-rim zoning in third-stage leucogranites and unzoned amphibole in their their gabbro enclave.

| | 35 | 45 | 36 | 38 | 40 | 41a | 41b | 41c | 41d | 41e |
|---|---|---|---|---|---|---|---|---|---|---|
| SiO2 | 43.29 | 40.57 | 36.64 | 48.09 | 43.67 | 47.50 | 46.01 | 44.03 | 37.91 | 49.24 |
| TiO2 | 0.78 | 0.00 | 0.17 | 0.36 | 1.31 | 0.53 | 1.02 | 1.36 | 0.43 | 1.03 |
| Al2O3 | 7.06 | 8.95 | 13.22 | 4.34 | 6.38 | 4.08 | 5.48 | 6.65 | 12.14 | 4.44 |
| FeO | 27.56 | 31.28 | 30.72 | 23.97 | 27.18 | 23.99 | 25.48 | 25.20 | 27.58 | 20.67 |
| MnO | 0.75 | 1.76 | 0.96 | 1.05 | 1.00 | 0.33 | 0.60 | 0.34 | 0.39 | 0.51 |
| MgO | 5.38 | 2.58 | 1.01 | 8.25 | 5.76 | 8.89 | 7.37 | 6.91 | 3.86 | 10.83 |
| CaO | 10.82 | 9.56 | 10.34 | 10.26 | 9.77 | 11.26 | 11.23 | 11.22 | 10.58 | 10.69 |
| Na2O | 1.39 | 2.03 | 2.29 | 1.34 | 1.75 | 0.87 | 0.00 | 1.31 | 1.41 | 0.00 |
| K2O | 0.85 | 1.39 | 1.82 | 0.35 | 0.82 | 0.45 | 0.73 | 0.86 | 2.22 | 0.47 |
| H2O | 1.84 | 1.84 | 1.55 | 1.95 | 1.78 | 1.92 | 1.90 | 1.87 | 1.41 | 1.97 |
| Cl | 0.24 | 0.03 | 1.05 | 0.03 | 0.47 | 0.14 | 0.15 | 0.19 | 1.69 | 0.12 |
| O=Cl | 0.05 | 0.01 | 0.24 | 0.01 | 0.11 | 0.03 | 0.03 | 0.04 | 0.38 | 0.03 |
| TOT | 100.00 | 100.00 | 100.00 | 100.00 | 100.00 | 100.00 | 100.00 | 100.00 | 100.00 | 100.00 |
| Si IV | 6.85 | 6.59 | 6.05 | 7.37 | 6.91 | 7.29 | 7.12 | 6.87 | 6.18 | 7.38 |
| Al IV | 1.15 | 1.41 | 1.95 | 0.63 | 1.09 | 0.71 | 0.88 | 1.13 | 1.82 | 0.62 |
| T site | 8.00 | 8.00 | 8.00 | 8.00 | 8.00 | 8.00 | 8.00 | 8.00 | 8.00 | 8.00 |
| Al VI | 0.16 | 0.31 | 0.62 | 0.15 | 0.09 | 0.03 | 0.12 | 0.09 | 0.51 | 0.16 |
| Ti | 0.09 | 0.00 | 0.02 | 0.04 | 0.16 | 0.06 | 0.12 | 0.16 | 0.05 | 0.12 |
| Mg | 1.27 | 0.63 | 0.25 | 1.88 | 1.36 | 2.04 | 1.70 | 1.61 | 0.94 | 2.42 |
| Fe +3 | 3.48 | 4.07 | 4.11 | 2.92 | 3.39 | 2.87 | 3.05 | 3.14 | 3.50 | 2.30 |
| M1,2,3 | 5.00 | 5.00 | 5.00 | 5.00 | 5.00 | 5.00 | 5.00 | 5.00 | 5.00 | 5.00 |
| Fe +2 | 0.17 | 0.18 | 0.13 | 0.15 | 0.20 | 0.21 | 0.24 | 0.15 | 0.25 | 0.29 |
| Mn | 0.10 | 0.24 | 0.13 | 0.14 | 0.13 | 0.04 | 0.08 | 0.05 | 0.05 | 0.06 |
| Ca | 1.73 | 1.58 | 1.74 | 1.68 | 1.66 | 1.75 | 1.68 | 1.80 | 1.69 | 1.65 |
| Na | 0.00 | 0.00 | 0.00 | 0.03 | 0.01 | 0.00 | 0.00 | 0.00 | 0.00 | 0.00 |
| M4 site | 2.00 | 2.00 | 2.00 | 2.00 | 2.00 | 2.00 | 2.00 | 2.00 | 2.00 | 2.00 |
| Ca | 0.10 | 0.09 | 0.09 | 0.00 | 0.00 | 0.10 | 0.19 | 0.07 | 0.15 | 0.07 |
| Na | 0.43 | 0.64 | 0.73 | 0.36 | 0.53 | 0.26 | 0.00 | 0.40 | 0.45 | 0.00 |
| K | 0.17 | 0.29 | 0.38 | 0.07 | 0.17 | 0.09 | 0.14 | 0.17 | 0.46 | 0.09 |
| A site | 0.70 | 1.02 | 1.20 | 0.43 | 0.69 | 0.45 | 0.33 | 0.64 | 1.06 | 0.16 |
| O | 22.00 | 22.00 | 22.00 | 22.00 | 22.00 | 22.00 | 22.00 | 22.00 | 22.00 | 22.00 |
| OH | 1.94 | 1.99 | 1.71 | 1.99 | 1.87 | 1.96 | 1.96 | 1.95 | 1.53 | 1.97 |
| Cl | 0.06 | 0.01 | 0.29 | 0.01 | 0.13 | 0.04 | 0.04 | 0.05 | 0.47 | 0.03 |

### PYROXENES

Clinopyroxene is the most abundant femic phase in the gabbros and syenites, appears as irregular cores in the amphiboles of the femic enclaves, and is absent in the granitic differentiates. Microprobe analysis (selected analyses in Table 4) shows augitic compositions for the gabbros and Fe-augitic compositions for the syenites. These are augites, according to IMA nomenclature (MURIMOTO et al., 1988), in which significant quantities of acm and traces of urey and ti-tsch are found in only one case (sample 50). In the pyroxene quadrilateral (Fig. 10), the compositional variations inside each lithotype are very small and intermediate rocks between the composition in gabbros and syenites are missing.

As regards the pyroxenes of the recrystallized gabbro sample (columns 1 and 2 in Table 4), when compared with magmatic pyroxenes, they are lacking in Na, Al and Ti and slightly richer in Fe.

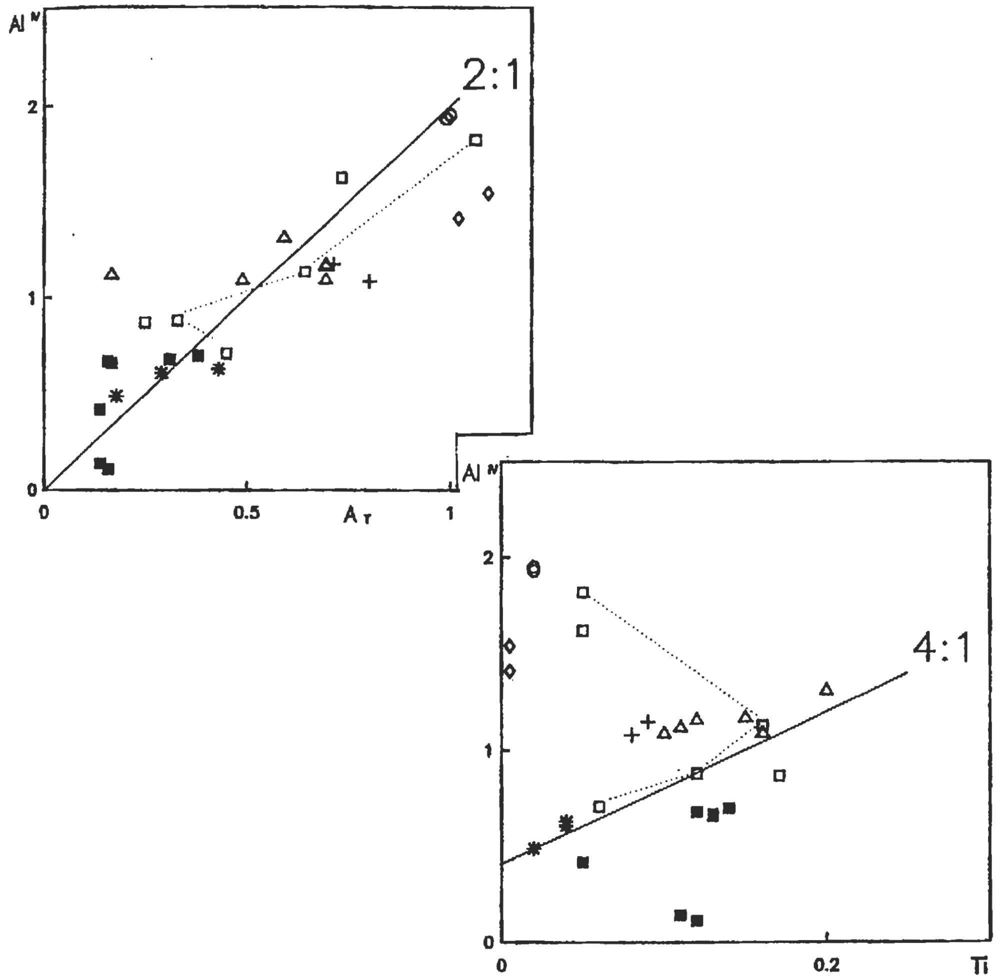


Fig. 9 - Relations between $Al^{IV}$ and $A_T$ (9a) and between $Al^{IV}$ and Ti (9b), highlighting positive correlations 2:1 and 4:1 of edenitic and Ti-tschermakitic substitutions. In acidic differentiates (circles, diamonds and empty squares) only edenitic substitution occurs. Symbols as in Fig. 7.

Table 4 - Pyroxene compositions. Column 1: recrystallized gabbro. Column 2: olivine gabbro, large crystals; column 3: olivine gabbro, small crystals associated with olivine.

| | 48 | 50 | 51a | 51b |
|---|---|---|---|---|
| $SiO_2$ | 53.27 | 49.88 | 49.89 | 50.61 |
| $TiO_2$ | 0.09 | 1.85 | 0.16 | 0.62 |
| $Al_2O_3$ | 0.09 | 2.84 | 0.12 | 0.65 |
| $Cr_2O_3$ | 0.31 | 0.06 | 0.31 | 0.01 |
| FeO | 14.85 | 9.91 | 25.10 | 23.86 |
| MnO | 0.00 | 0.32 | 0.00 | 0.00 |
| MgO | 12.17 | 14.49 | 5.68 | 5.52 |
| CaO | 19.26 | 19.68 | 18.69 | 18.75 |
| $Na_2O$ | 0.00 | 0.96 | 0.00 | 0.00 |
| TOT | 100.04 | 99.99 | 99.95 | 100.02 |
| Si IV | 2.02 | 1.87 | 2.00 | 2.00 |
| Al IV | 0.00 | 0.13 | 0.00 | 0.00 |
| T site | 2.02 | 2.00 | 2.00 | 2.00 |
| Al VI | 0.00 | 0.00 | 0.00 | 0.03 |
| Ti | 0.00 | 0.05 | 0.00 | 0.02 |
| Cr | 0.01 | 0.00 | 0.01 | 0.00 |
| Fe +2 | 0.47 | 0.31 | 0.84 | 0.79 |
| Mn +2 | 0.00 | 0.01 | 0.00 | 0.00 |
| Mg | 0.69 | 0.81 | 0.34 | 0.33 |
| Ca | 0.78 | 0.79 | 0.80 | 0.80 |
| Na | 0.00 | 0.07 | 0.00 | 0.00 |
| M1,M2 | 1.96 | 2.05 | 1.99 | 1.96 |
| WO | 40.00 | 44.00 | 40.00 | 42.00 |
| EN | 36.00 | 46.00 | 17.00 | 17.00 |
| FS | 24.00 | 10.00 | 43.00 | 41.00 |

## Olivine

This mineral occurs only in the syenites of the ring dyke, as well as in the gabbros and cumulates. As Table 5 and Fig. 10 show, the olivines of gabbros are typically rich in Mg (70% Fo), while the olivines of syenites are rich in Fe (90% Fa).
Despite the small number of samples examined, only the fayalitic olivines contain Cr; the others contain Ni.

The relation between the compositions of the olivines and coexisting pyroxenes are shown in Fig. 10, in which the dashed line link minerals from the same sample.

## Fe-Ti oxides

These minerals occur in all the lithotypes studied, and are particularly abundant in the femic cumulates, ring-dyke syenites and second-stage qz-syenites and alkali-

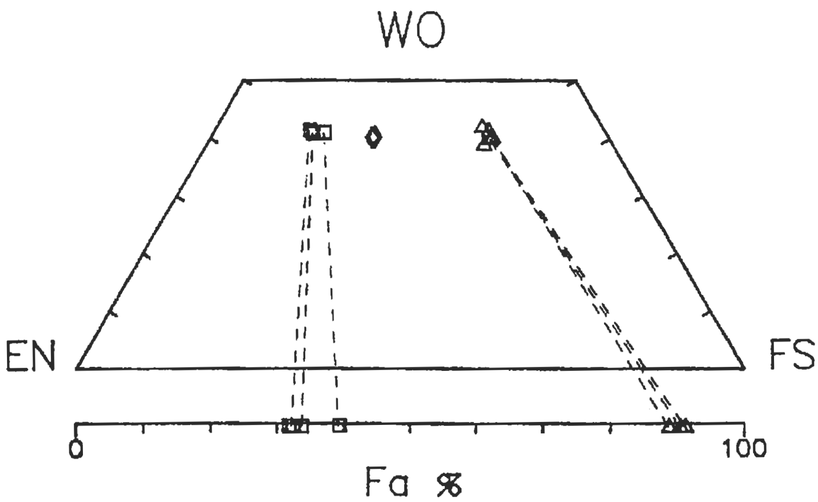


Fig. 10 - En-Fe-Di-Hy quadrilateral composition of pyroxenes and olivines, as Fa% contents. Squares: olivine gabbros; diamonds: recrystallized gabbros; triangles: ring-dyke syenites. Dashed lines join minerals from the same sample.

Table 5 - Olivine compositions. Column 1: olivine gabbros; column 2: syenites of ring dyke.

| | 50 | 51 |
|---|---|---|
| SiO2 | 35.48 | 30.65 |
| FeO | 28.73 | 64.82 |
| MnO | 0.62 | 0.23 |
| MgO | 34.84 | 3.93 |
| CaO | 0.03 | 0.10 |
| NiO | 0.21 | 0.00 |
| Cr2O3 | 0.00 | 0.30 |
| Total | 99.91 | 100.03 |
| Si+4 | 0.95 | 1.01 |
| Fe+2 | 0.64 | 1.78 |
| Mn+2 | 0.01 | 0.01 |
| Mg+2 | 1.39 | 0.19 |
| Ca+2 | 0.00 | 0.00 |
| Ni+2 | 0.00 | 0.00 |
| Cr+3 | 0.00 | 0.01 |
| TOT | 3.00 | 3.00 |
| FO% | 68.00 | 10.00 |

feldspar granites. Magnetite, ilmenite and their weathering products are the main oxides, and green spinel is sometimes found in small masses or as exsolution lamellae in the magnetite of gabbros and cumulates.

In the more femic rocks, crystallization of opaques begins coevally with that of olivine (rare euhedral crystals in olivine) and continues until biotite crystallization (small interstitial masses with biotite crowns). Opaques are preferentially anhedral in the acidic differentiates and inclusions of qz-Fe-Ti oxides. All rocks contain ilmenite and most of them magnetite too. In the ring-dyke syenites, large crystals of ilmenite contain islands of magnetite enveloped in a symplectitic zone of il-mt, while a more or less developed titanite crown encloses the oxides of the seconded third-stage rocks.

As regards minor element contents (Table 6), significant quantities of Cr are characteristic of the magnetites of the gabbros, and relatively high Mn values are found in ilmenites in the qz-oxide and garnet inclusions. However, the quantities of Mn and Mg are not sufficient to invalidate possible indications regarding the oxidation state of the magmas from which the ilmenites crystallized (HAGGERTY, 1976).

*$fO_2$ estimates*: Among the various rocks containing the mt- ilm pair, only in the qz-oxide inclusions of the alkali-feldspar granites did estimates of T-$fO_2$ ratios give results. These parameters were obtained by extrapolation from the curves of BUDDINGTON and LINDSLEY (1964) using the computer algorithm of GHIORSO and CARMICHAEL (1981). Results (Fig. 11) plot between the buffer curves for FMQ and TMQH in the range of normal values for granitic rocks (HAGGERTY, 1976) and in the area of oxidized magmas (WONES and GILBERT, 1982) characteristic of I-type granites (WHALEN and CHAPPELL, 1988). Considering the intrinsic $fO_2$ values of mantle-derived magmas (shaded area in Fig. 11, from WONES and GILBERT, 1982), these values are in line with fractionation of a closed system, starting from more basic magmas.

Table 6 - Ilmenite compositions. Column 1: third-stage leucogranites; column 3: alkali-feldspar granites: column 2: their qz-Fe-Ti oxide inclusions; column 4: olivine gabbros; column 5: syenites of ring dyke.

| | 41a | 45 | 46 | 50 | 51 |
|---|---|---|---|---|---|
| $SiO_2$ | 0.81 | 1.60 | 1.30 | 1.16 | 0.88 |
| $TiO_2$ | 48.27 | 47.69 | 47.81 | 57.84 | 54.28 |
| $Al_2O_3$ | 0.11 | 0.00 | 0.01 | 0.05 | 0.00 |
| $Cr_2O_3$ | 0.00 | 0.26 | 0.10 | 0.00 | 0.17 |
| FeO | 48.24 | 49.12 | 49.59 | 39.42 | 42.88 |
| MnO | 2.49 | 0.93 | 1.08 | 0.00 | 1.62 |
| MgO | 0.00 | 0.52 | 0.05 | 1.49 | 0.20 |
| CaO | 0.06 | 0.00 | 0.00 | 0.02 | 0.00 |
| TOT | 99.97 | 100.12 | 99.93 | 99.98 | 100.03 |
| Si | 0.02 | 0.04 | 0.03 | 0.03 | 0.02 |
| Ti | 0.91 | 0.89 | 0.90 | 1.09 | 1.03 |
| Al | 0.00 | 0.00 | 0.00 | 0.00 | 0.00 |
| Cr | 0.00 | 0.01 | 0.00 | 0.00 | 0.00 |
| Fe +3 | 0.14 | 0.13 | 0.13 | 0.00 | 0.00 |
| Fe +2 | 0.88 | 0.89 | 0.91 | 1.06 | 1.01 |
| Mn | 0.05 | 0.02 | 0.02 | 0.00 | 0.03 |
| Mg | 0.00 | 0.02 | 0.00 | 0.06 | 0.01 |
| Ca | 0.00 | 0.00 | 0.00 | 0.00 | 0.00 |
| Cat. | 2.00 | 2.00 | 2.00 | 2.00 | 2.00 |
| O | 3.00 | 3.00 | 3.00 | 3.00 | 3.00 |

Table 7 - Magnetite compositions. Column 1: third-stage leucogranites; column 3: alkali-feldspar grnaites; column 2: their qz-Fe-Ti oxide inclusions; column 4: olivine gabbros; column 5: composition of green spinel in olivine gabbros.

| | 41 | 45 | 46 | 50 | 50sp |
|---|---|---|---|---|---|
| SiO2 | 3.25 | 1.38 | 1.53 | 1.02 | 0.17 |
| TiO2 | 0.00 | 9.75 | 8.41 | 0.66 | 0.21 |
| Al2O3 | 0.22 | 0.53 | 0.56 | 0.46 | 56.16 |
| Cr2O3 | 0.00 | 0.22 | 0.00 | 1.92 | 1.98 |
| Fe2O3 | 61.18 | 46.17 | 48.65 | 62.86 | 6.10 |
| FeO | 34.91 | 42.00 | 40.48 | 31.78 | 22.42 |
| MnO | 0.05 | 0.05 | 0.10 | 1.33 | 0.54 |
| MgO | 0.00 | 0.00 | 0.29 | 0.00 | 11.22 |
| CaO | 0.36 | 0.00 | 0.00 | 0.00 | 0.00 |
| ZnO | 0.00 | 0.00 | 0.00 | 0.00 | 1.21 |
| TOT | 99.97 | 99.99 | 100.12 | 100.00 | 100.03 |
| Si | 0.12 | 0.05 | 0.06 | 0.04 | 0.00 |
| Ti | 0.00 | 0.28 | 0.24 | 0.02 | 0.00 |
| Al | 0.01 | 0.02 | 0.02 | 0.02 | 1.81 |
| Cr | 0.00 | 0.01 | 0.00 | 0.06 | 0.04 |
| Fe +3 | 1.74 | 1.31 | 1.38 | 1.81 | 0.13 |
| Fe +2 | 1.11 | 1.33 | 1.28 | 1.02 | 0.51 |
| Mn | 0.00 | 0.00 | 0.00 | 0.04 | 0.01 |
| Mg | 0.00 | 0.00 | 0.02 | 0.00 | 0.46 |
| Ca | 0.01 | 0.00 | 0.00 | 0.00 | 0.00 |
| Zn | 0.00 | 0.00 | 0.00 | 0.00 | 0.02 |
| Cat. | 3.00 | 3.00 | 3.00 | 3.00 | 3.00 |
| O | 4.00 | 4.00 | 4.00 | 4.00 | 4.00 |

## DISCUSSION AND CONCLUSION

The field relations among the different lithotypes in the DS pluton reveal a complex intrusive history. At least four magmatic stages may be recognized, of which the following rocks are representative:

a) olivine gabbros, related cumulates and white syenites;
b) monzonites, qz-syenites and alkali-feldspar granites;
c) ring-dyke syenites;
d) leucogranites.

The qz-bearing acidic rocks (b and d) form mixed assemblages with gabbros and diorites. There is commingling between felsic and mafic magmas (WIEBE, 1980), as shown by the morphology, structure and plasticity of the pillows. Moreover, ion exchange (e.g., alkalis and halogens) between enclaves and hosts in the second-stage mixed rocks is indicative of the local loss of identity of the original magmas (hybridation; WIEBE, 1980).

Conversely, the ring-dyke syenites (c) are qz-free or ol-bearing and show no signs of interaction with the more basic magmas.

Field relations and preliminary whole-rock Rb-Sr isochrons (FERRARA et al., 1987) show that the injection of the ring-dyke syenites should fall between distinct intrusive phases of qz-bearing rocks. The common low $(^{87}Sr/^{86}Sr)_i$ values also suggest that the all the differentiates are genetically linked to the first-stage olivine gabbros (a).

It therefore seems reasonable, as a first approach, to attribute the various lithotypes to different evolutionary phases of a basic magma. However, if the ring-dyke syenites (or similar rocks) were the rocks of intermediate differentiation between gabbros and qz-bearing rocks, this would imply the crystallization and separation first of pyroxenes and plagioclase and then of phases poor in or lacking $SiO_2$ (e.g., ol and mt). A similar crystallization sequence contrasts with the case of the olivine gabbros, which show olivine and oxides among the first crystals and pecilitic pyroxene. Differentiation starting from such a magma must therefore have occurred in a shallower chamber than that giving rise to the olivine gabbros, in accordance with the absence of olivine or its transformation products in the gabbros enclosed in the qz-bearing rocks and to the alkaline character of the ring-dyke syenites.

The microtextures of the mixed-assemblage rocks fit the field situation: mantling textures and the pseudomorphosis of amphibole after pyroxene are features to be expected in hybrid rocks of magma mixing origin (HIBBARD, 1981). Although the porphyric textures of the granitic host rocks near the pillows are surprising, it should be remembered that the crystallization kinetics of the system may undergo strong variations near the pillows: heating and water loss greatly influence the growth ratio and density of nucleation of K-feldspar, plagioclase and quartz in host magma (SWANSON, 1977; MUNCILL, 1988), with obvious consequences on the final texture.

It is interesting to note how, in the second-stage mixed assemblages, the typical above-mentioned textures gradually disappear as the compositions of host and enclave approach each other. Compositional similiarities found between the amphiboles of gabbroid enclaves and amphibole rims of host granites (Figs. 10, 11) imply similar conditions of $fO_2$, $fSiO_2$ and alkali activities, indicating intense ion exchange between inclusion and host. The same type of information is provided by the growth of abundant biotite in the rims of the gabbroid pillows. It may be deduced that the gradual disappearance of disequilibrium microstructures in the enclaves accompanied the exchange of elements with the host magma. The result was the progressive loss of mineralogic and chemical identity by the enclave and variations in the host magma as a function of the volume of enclaves contained.

Data on the state of oxidation and degree of hydration during crystallization were obtained by integrating microstructural observations with mineral composition. Petrographic evidence suggests that, in all the lithotypes, biotite was the last Fe-Mg phase to crystallize. This leads to the conclusion that the water content of the magma was always low and that the temperature at the end of crystallization, also in the acidic magmas, was quite high (>850 °C, CLEMENS and WALL, 1988). Cl contents (Table 2),

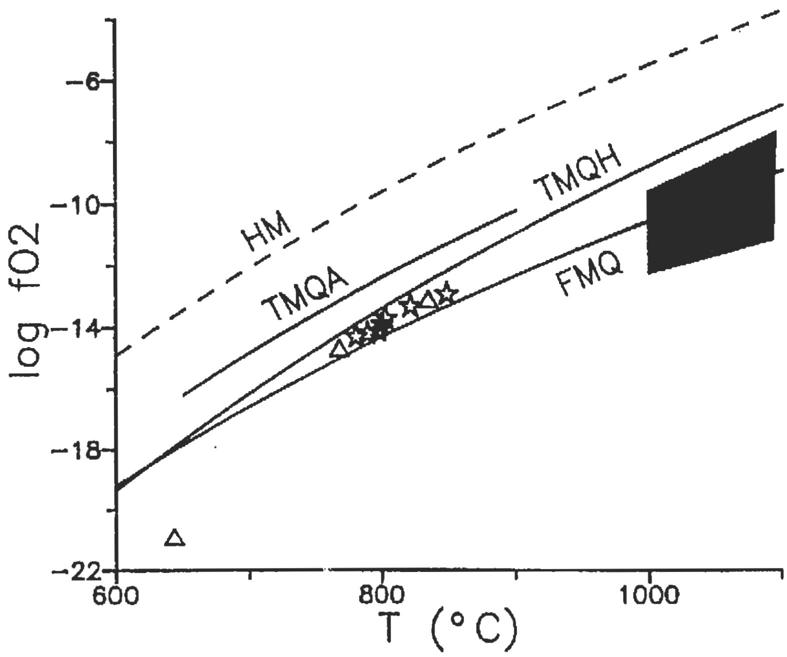


Fig. 11 - Estimated T-$fO_2$ conditions for second-stage qz-syenites. Buffer curves for fayalite+magnetite+quartz (FMQ; HEWETT, 1978), hematite+magnetite (HM; CHOU, 1978), titanite+magnetite+ilmenite+quartz+hedenbergite (TMQH; WONES, 1981), and titanite+magnetite+ilmenite+quartz+amphibole (TMQA, NOYES et al., 1983). All buffer curves are plotted assuming pure phases. Stars: qz-Fe-Ti oxide inclusions in qz-syenite and alkali-feldspar granites; triangles: qz-syenites.

higher in the granitic biotites, show final vapour-phase compositions with relatively low a $H_2O$, and the co-existence of biotite with ilmenite in some of the granites implies low oxygen fugacity (ISHIHARA, 1977).

T-$fO_2$ ratios determined using the mt-ilm pair of the inclusions of qz-Fe-Ti oxides indicate relatively high oxidation conditions for the granitic magmas, characteristic of I-type granites. However, it should be recalled that Fe silicates are often lacking or are extremely scanty in the host granites. The resulting unusual mineralogical association, like the relatively low value of the iron redox ratio, may be due to Fe and Ti stabilization in the metaluminous magma by alkalis (DICKENSON and HESS, 1986; GWINN and HESS, 1989).

Increased $fO_2$ in the advanced phases of crystallization of the granites occurred coevally with increased $f_{SiO2}$ , as shown by the thin crowns of titanite rather than perovskite on the ilmenites. Log$SiO_2$ values of about 1.1 correspond to the estimated temperature of about 800 °C and log$fO_2$ of 12-14 (Fig. Hg 49 in HAGGERTY, 1976). The progressive increase in $fO_2$ and $fSiO_2$ is also recorded by the compositional variation of the amphiboles in the various lithotypes and by their zoning (edenites with actinolitic rims in the granites).

Petrographic and microchemical analyses provided a rough scenario for magma evolution, involving several pulses of basic magma at different crustal levels. The fact that the primitive magma became differentiated and later intruded into shallower levels where other magma was already consolidated may indicate that it spent a relatively long time in chambers at different depths.

## APPENDIX

Microprobe analyses were carried out using an EDS-Ortec system. Accelerating voltages of 15 kV and specimen currents of 10-9 A were employed. Natural crystals of known composition were used as standards. Precision was better than 3% for major elements and better than 8% for minor ones. Microprobe analyses were processed using the MINFILE computer program (AFIFI and ESSENE, 1988) with the following normalizations: feldspar: 32 oxygens; ilmenite: 3 oxygens; spinel: 4 oxygens; olivine: 3 cations; pyroxenes 6 oxygens; amphibole and biotite: 23 oxygens. Bearing in mind that $Fe^{3+}$ and $H_2O$ were not known in the normalization, they were calculated from the charge balance. In particular, reasonable crystal-chemical limits as proposed by ROBINSON et al. (1982) and according to LEAKE (1978) recommendations were borne in mind for the amphiboles.

## REFERENCES

ABRECHT J. and HEWITT D.A. (1988). Experimental evidence on the substitution of Ti in biotite. Am. Mineral., 73: 1275-1284.

AFIFI A.M. and ESSENE E.J. (1988). MINIFILE: A microcomputer program for storage and manipolation of chemical data on minerals. Am. Mineral., 73: 446-448.

ALLEN J.C. and BOETTCHER A.L. (1978). Amphiboles in andesites and basalts: II. Stability as a function of P-T-$fH_2O$-$fO_2$. Am. Mineral., 63: 1069-1085.

BUDDINGTON A.F. and LINDSLEY D.H. (1964). Iron-titanium oxide minerals and synthetic equivalents. J. Petrol., 5: 310-357.

CARMICHAEL C.M., NICHOLLS J. and SMITH A.L. (1970). Silica activity in igneous rocks. Am. Mineral., 55: 246-263.

CLEMENS J.D. and WALL V.J. (1988). Controls on the mineralogy of S-type volcanic and plutonic rocks. Lithos, 21: 53-66.

CZAMANSKE G.K. and WONES D.R. (1973). Oxidations during magmatic differentiation, Finmarka Complex, Oslo area, Norway: Part II, The mafic silicates. J. Petrol., 14: 349-380.

DANIELS J.L., SKIBA W.J. and SUTTON J. (1965). The deformation of banded gabbros in the Northern Somalia fold belt. Quart. J. Geol. Soc. Lond., 121: 111-141.

DICKENSON M.P. and HESS P.C. (1986). The structural role and homogeneous redox equilibria of iron in peraluminous and peralkaline silicate melts. Contrib. Mineral. Petrol., 92: 207-217.

FERRARA G., GATTO G.O., IBRAHIM H.A., SAID A.A., SASSI F.P., TONARINI S. and VISONA' D. (1987). Sequence of events recorded in the crystalline basement of Northern Somalia. Geosom 87 Intern. Geology Meeting of Somalia, Mogadishu, abstr., 65.

GATTO G.O., IBRAHIM H.A., SASSI F.P. and VISONÀ D. (1987). A tentative litostratigraphic classification of the crystalline basement of Northern Somalia. Geosom 87 Intern. Geology Meeting of Somalia, Mogadishu, abstr., 71.

GHIORSO M.S. and CARMICHAEL I.S.E. (1981). A FORTRAN IV computer program for evaluating temperatures and oxygen fugacities from the compositions of co-existing iron-titanium oxides. Computers and Geosciences, 7: 123-129.

GWINN R. and HESS P.C. (1989). Iron and titanium solution properties in peraluminous and peralkaline rhyolitic liquids. Contrib. Mineral. Petrol., 101: 326-338.

HAGGERTY S.E. (1976). Opaque mineral oxides in terrestrial igneous rocks. In D. RUMBLE III (ed): Short course notes, Oxide Minerals. Mineralogical Society of America, 101-300.

HEWETT D.A. (1978). A determination of the fayalite-magnetite-quartz equilibrium between 650°C and 850°C. Am. J. Sci., 278: 715-724.

HIBBARD H.J. (1981). The magma mixing origin of mantled feldspars. Contrib. Mineral. Petrol., 76: 158-170.

ISHIHARA S. (1977). The magnatite-series and ilmenite-series granitic rocks. Mining Geol., 27: 293-305.

LEAKE B.E. (1978). Nomenclature of amphiboles. Can. Mineral., 16: 501-520.

MASON D.R. (1978). Compositional variations in ferromagnesian minerals from porphyry copper-generating and barren intrusions of the Western Highlands Papua New Guinea. Economic Geology, 73: 878-890.

MASON J.E. (1954). Report on the Geology of the basement rocks in the Sheikh Auradl Wagger Area. Unpub. Rept. Geol. Surv. Somalil. Prot., Hargeisa, London.

MASON J.E. (1958). A preliminary report on the Daba Shabeli ring complex, Burao district. Unpub. Rept. Geol. Surv. Somalil. Prot., Hargeisa. London.

MITCHELL R.H. (1973). Composition of olivine, silica activity and oxygen fugacity in kimberlite. Lithos, 6: 65-81.

MUNCILL G.E. (1988). Isothermal crystal growth kineticts of plagioclase in a haplogranodiorite melt at $P(H_2O)$ = 2Kbar. Carnegie Institutions, 40-44.

MURIMOTO N., FABRIES J., FERGUSON A.K., GINZBURG I.V., ROSS M., SEIFERT F.A. and ZUSSMAN J. (1988). Nomenclature of pyroxenes. Mineral. Mag., 52: 535-550.

NOYES H.J., WONES D.R. and FREY F.A. (1983). A tale of two plutons: petrographic and mineralogic constraints on the petrogenesis of the Red Lake and Eagle Peak plutons, Central Sierra Nevada, California. J. Geol., 91: 353-379.

ROBINSON P., SPEAR F.S., SCHUMACHER J.C., LAIRD J., KLEIN C., EVANS B.W. and DOOLAN B.L. (1982). Phase relations of metamorphic amphiboles: natural occurrence and theory. In D.R. VEBLEN and P.H. RIBBLE (eds): Reviews in Mineralogy, Amphiboles: Petrology and Experimental Phase Relations. Mineralogical Socety of America, 1-211.

SAID A.A. (1987). Preliminary data on the amphibolitization of the layered gabbros NW of Sheik (Northern Somalia). Geosom 87 Intern. Geology Meeting of Somalia, Mogadishu, abstr., 117.

SASSI F.P., VISONÀ D., FERRARA G., GATTO G.O., IBRAHIM H.A., SAID A.A. and TONARINI S. (this volume). The crystalline basement of Northern Somalia: lithostratigraphy and the sequence of events.

SWANSON S.E. (1977). Relation of nucleation and crystal-growth rate to the development of granitic textures. Am. Mineral., 62: 966-978.

VERHOOGEN J. (1962). Distribution of titanium between silicates and oxides in igneous rocks. Am. J. Sci., 260: 211.

WHALEN G.E. and CHAPPELL B.W. (1988). Opaque mineralogy and mafic mineral chemistry of I- and S-type granites of the Lachan fold belt, Southeast Australia. Am. Mineral., 73: 281-296.

WIEBE R.A. (1980). Commingling of contrasted magmas in the plutonic environment: examples from the Nain Anorthositic Complex. J. Geol., 88: 197-209.

WIEBE R.A. (1988). Structural and magmatic evolution of a magma chamber: The Newark Island Layered Intrusion, Nain, Labrador. J. Petrol., 29: 383-411.

WONES D.R. (1981). Mafic silicates as indicators of intensive variables in granitic magmas. Mining Geology, 31: 191-212.

WONES D.R. (1989). Significance of the assemblage titanite+magnetite+quartz in granitic rocks. Am. Mineral., 74: 744-749.

WONES D.R. and GILBERT M.C. (1982). Amphiboles in the igneous environment. In D.R. VEBLEN and P.H. RIBBLE (eds): Reviews of Mineralogy, Amphiboles: Petrology and Experimental Phase Relations. Mineralogical Socety of America, 355-390.

YAMAGUCHI Y. (1985). Hornblende-cummingtonite and hornblende-actinolite intergrowths from the Koyama calc-alkaline intrusions, Susa, Southwest Japan. Am. Mineral., 70: 980-986.

*Final editing, January 1990*

From *Geology and mineral resources of Somalia and surrounding regions*, Ist. Agron. Oltremare, Firenze, Relaz. e Monogr. 113, 83-90, 1993.

# RELICS OF GRANULITIC MINERAL ASSEMBLAGES IN THE NORTHERN SOMALI BASEMENT

F.P. SASSI and D. VISONÀ

Dipartimento di Mineralogia e Petrologia, Università di Padova, Corso Garibaldi 37, 35137 Padova, Italy.

## ABSTRACT

The rocks of the Qabri Bahar and Mora complexes are the oldest ones in the Northern Somali Basement. They commonly display migmatitic features and amphibolite facies mineral assemblages, but locally have a granulitic appearance.

Relics of granulite facies mineral assemblages have been found in a few localities. The occurrence of Opx-bearing mineral assemblages was sometimes inhibited by the unsuitable rock bulk composition, but relics of dehydrated mineral assemblages of high temperature indicate environmental conditions similar to those of the rocks in which Opx occurs.

The presence of these relics suggests that, before being affected by the widespread amphibolite facies metamorphism, the Qabri Bahar and Mora complexes were granulitic terrains, similar to those which can be observed in parts of the old African craton which escaped the Upper Proterozoic and Lower Paleozoic reworking.

## INTRODUCTION

The high-grade rock complexes occurring in the Northern Somali Basement (NSB for short), specifically the Qabri Bahar Complex and the Mora Complex (SASSI and IBRAHIM, 1981; GATTO et al., 1987), are polymetamorphic: they record a widespread late Panafrican overprint (FERRARA et al., 1987; SASSI et al., in this volume) and an older metamorphic history (SASSI and VISONÀ, 1985)

In the field, the general features of these rock sequences are in many places those typical of the migmatitic terrains, and usually those of the banded metasedimentary rock sequences affected by a high-grade, water-controlled metamorphic event. The prevailing mineral assemblages belong to the amphibolite facies.

However, relics of some high-grade mineral assemblages which are typical of the granulite facies, or consistent with the environment conditions of the granulite facies, occur in many localities. Usually, those old assemblages are largely obliterated by the overprinted amphibolite-facies metamorphism, the effects of which prevail everywhere. Such a situation was first reported by DANIELS et al. (1965, p. 117) in the area south of Dudub: "... it contains granulite-facies assemblages marked by such minerals as calcic plagioclase (% An 55-78), hyperstene, clinopyroxene and brown horneblende, with accessory iron oxydes, spinel and olivine".

The aim of the present paper is to report some examples of these granulitic relics, attempting at estimating the corresponding P-T conditions and interpreting this metamorphism ($M_1$) as the oldest event recorded in the NSB.

## FIELD AND PETROGRAPHIC DATA

The situations occurring in four areas are described below: two of them concern the Mora Complex and two the Qabri Bahar Complex. The approximate location of each described situation is shown in Fig. 1.

### Relics in the Figi Ayub-Ceelal area (Mora Complex)

This area, labelled as no. 1 in Fig. 1, is located in the sheet no. 38 Habaji (1:125,000).

The prevailing rock types are migmatites and banded gneisses, in which the following lithologies occur as bands and intercalations: K-feldspar-bearing augengneisses, K-feldspar-bearing flaser-gneisses, garnet-horneblende gneisses, clinopyroxene-scapolite felses, clinopyroxene-epidote felses, epidote felses, Ca-silicate marbles, amphibolites (which are interlayered within the marbles), quartzites.

Disregarding some retrograde effects, two different crystallization events can be distinguished in the garnet-hornblende gneisses by means of microtextural analyses and related petrologic interpretations: $M_1$ and $M_2$, $M_1$ being the older.

The mineral assemblages related to $M_2$ are: horneblende + epidote + plagioclase and horneblende + biotite. The occurrence of horneblende, biotite and epidote displays that this $M_2$ metamorphism was controlled by $H_2O$ and took place under amphibolite-facies conditions.

The mineral assemblages related to $M_1$ are: clinopyroxene + plagioclase (scapolite) + almandine; clinopyroxene + plagioclase (scapolite). Plagioclase is antiperthitic. Sillimanite + K feldspar + almandine occur in the associated biotite gneisses and can also be related to $M_1$ basing on microtextural evidence.

All $M_1$ mineral assemblages observed in the Figi Ayub-Ceelal area can be understood basing on the mineral compatibilities shown in Fig. 2. Their crystallization requires anhydrous granulite-facies conditions.

### The situation in the Canjeel area (Mora Complex)

This area is labelled as no. 2 in Fig. 1, and occurs within the sheet no. 33 Gebiley (1:125,000). Migmatites, bearing intercalations of marbles, Ca-silicate marbles, amphibolites and quartzites are the main rock types.

The peculiarity of this area consists in that high-grade mineral assemblages

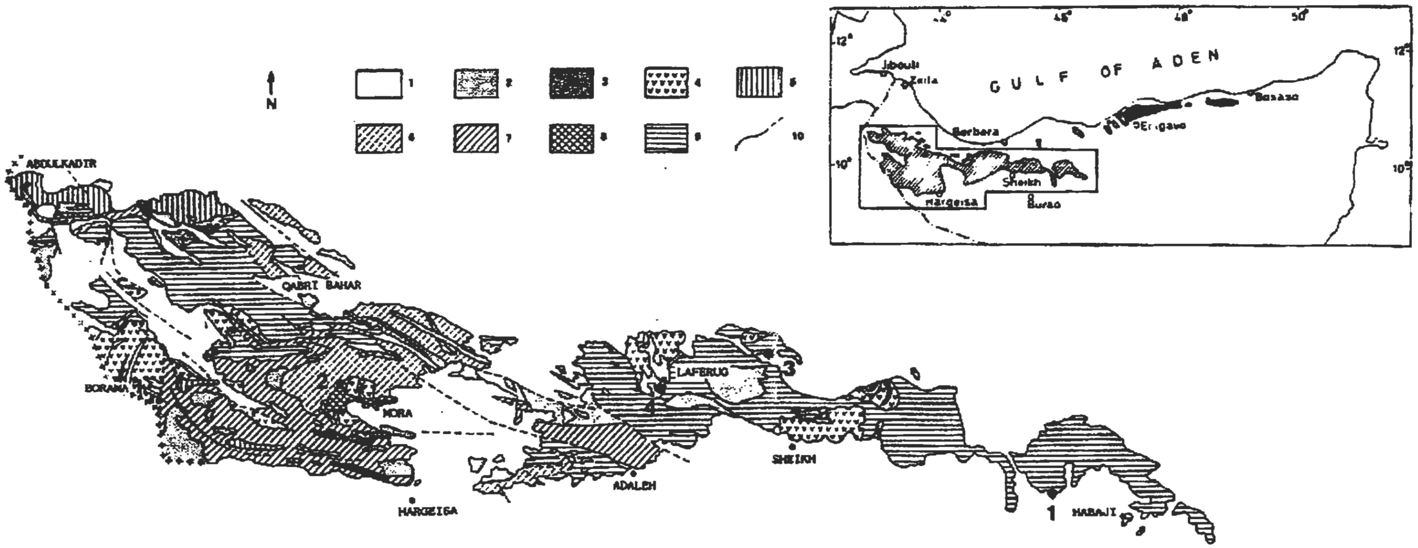


Fig. 1 - Approximate location (asterisks 1, 2, 3, 4) of the described granulitic mineral assemblages (geological sketch taken from SASSI et al., this volume).

Legend. 1: non metamorphic cover; 2: Younger Granites; 3-4: gabbro-syenite belt (3: main syenites; 4: main gabbros, metagabbros and related rocks); 5: Abdulkadir Complex: greenschist facies metapelites *l.s.* and acid to basic metavolcanics; 6 to 8: Mora Complex (6: biotitic and/or amphibolitic schists, undifferentiated schists, migmatites, with intercalations of marbles and schists; 7: quartzites, quartz-feldspathic schists and gneisses; 8: marbles and related rocks; 9: Qabri Bahar Complex: migmatites characterized by prevalence of nebulitic leucosomes and foliated granitoids; 10: main tectonic lineaments and faults.

referable to $M_1$ largely prevail, while younger mineral assemblages referable to $M_2$ are sporadic.

The $M_1$ mineral assemblages occurring within the migmatites are almandine + cordierite + sillimanite + quartz and almandine + cordierite + sillimanite + spinel (Fig. 3). Mineral assemblages referable to the same mineral compatibilities as shown in Fig. 3, but only consisting of two or three mineral phases, also occur (e.g. cordierite + spinel, cordierite + spinel + sillimanite). Aggregates of almandine + sillimanite are also to be mentioned: their shape suggests that they might represent prograde pseudomorphs after staurolite (although relics of this mineral were never observed). The above petrographic data indicate that $M_1$ was high grade: its physical conditions are consistent with those of the granulite facies.

The local occurrence of biotite flakes in the migmatites could represent the only effects of a younger, water-controlled, metamorphic overprint ($M_2$) in these rocks. In the ambit of this interpretation, the rocks of the Canjeel area should represent a fragment of the old, pre-$M_2$ basement, which remained almost unchanged during the $M_2$ amphibolite-facies event. This plausible hypothesis does not require many comments: in fact the $M_1$ mineral assemblages shown in Fig. 3 are also stable in the amphibolite-facies conditions.

### Relics in the Bixindule area (Qabri Bahar Complex)

The Bixindule area is labelled as no. 3 in Fig. 1. It occurs within the sheet no. 24 Berbera (1:125,000). Migmatites are the dominant rock type, and bear intercalations of amphibolites and K-feldspar-bearing augengneisses.

The mineral assemblages prevailing in the amphibolites are: horneblende + plagioclase and horneblende + biotite. However, relics of clinopyroxene and orthopyroxene can also be observed, displaying a complex history consisting of at least two events: the older one of granulite facies ($M_1$) and the younger one of amphibolite facies ($M_2$).

### Relics in the Sheekh Abdal area (Qabri Bahar Complex)

This area is labelled as no. 4 in Fig. 1 and occurs within the sheet no. 35 Adadleh (1:125,000). The prevailing rock types are migmatites and fine-grained gneisses, both with amphibolite intercalations.

Relics of the orthopyroxene + clinopyroxene + plagioclase have been observed within the amphibolites. They are largely obliterated by the prevailing horneblende + plagioclase mineral assemblage.

Therefore the situation is consistent with those above described in the localities 1 and 3: with reference to Fig. 2a, the only difference is the disappearance of the Alm-Cpx tie-line, which is replaced by the Pl-Opx tie-line.

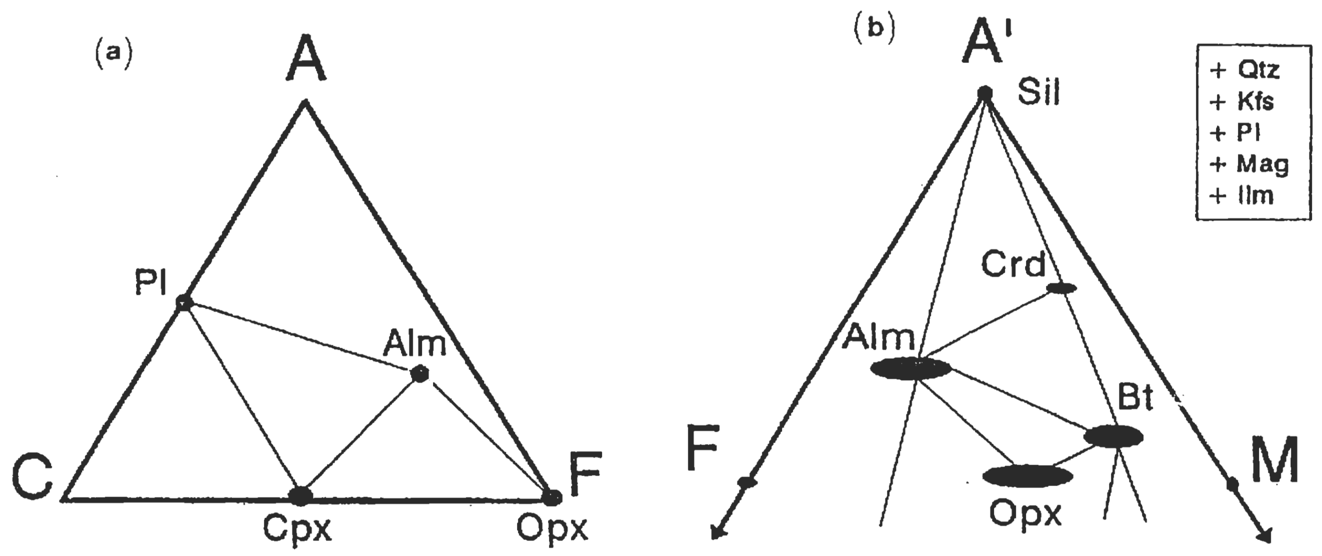


Fig. 2 - Mineral compatibilities related to the $M_1$ metamorphism in the Figi Ayub-Ceelal area.

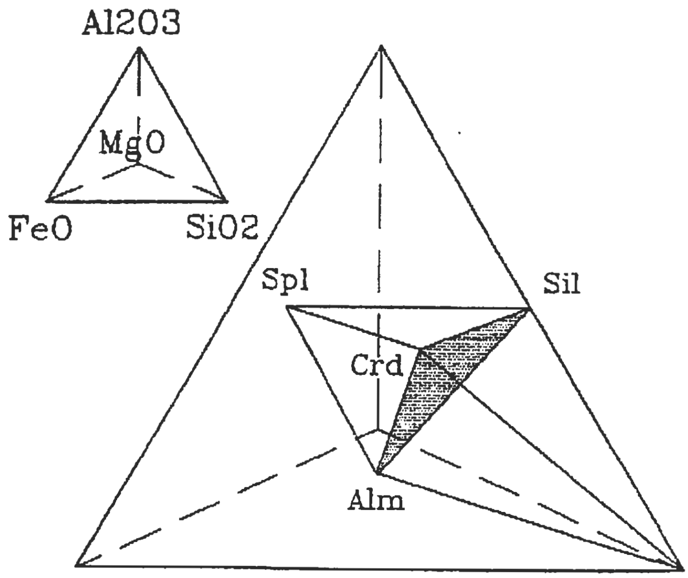


Fig. 3 - Mineral compatibilities related to the $M_1$ metamorphism in the Canjeel area.

## CONCLUSIONS

In the four reported situations, the older mineral assemblages referred to $M_1$ are not compatible with the younger ones referred to $M_2$. The main reason for this incompatibility is the availability of water, which must be admitted during $M_2$ and excluded during $M_1$. However, we cannot exclude that also the P-T conditions were different during these two events.

As concerns pressure, during $M_1$ different values could have prevailed in different rock volumes, as suggested by the different topologies of the ACF diagram (Fig. 2) detected in localities 1 vs. 4: higher pressure values (e.g. about 6 kb) should have stabilized the Cpx-Alm tie line in locality 1, slightly lower P values should have stabilized the Pl-Opx tie-line in locality 4; and the occurrence of cordierite in locality 2 indicate still lower pressure values during $M_1$. As concerns $M_2$, it is reported as a medium-pressure metamorphism (SASSI et al., this volume)

As concerns temperature, the mineral assemblages respectively referred to $M_1$ and $M_2$ do not imply any obvious difference in temperature between these two events, but do not exclude a possible difference, of e.g. 100-150°C.

In order to better focus the geothermobarometric aspects of the detected situations, some P, T estimates have been done basing on the mineral chemistry of the coexisting phases in locality 2. The results suggest the following physical conditions:

- $M_1$: pressure value in the range 3-6 Kb and temperature values in the range 660-795;
- $M_2$: pressure value of about 6 Kb (SASSI et al., this volume) and temperature values in the range 620-655 °C, based on the data obtained from the biotite-garnet pair.

These T-P estimates are neither conclusive nor satisfactory. However, they do not contradict the conclusion of the present paper: before being affected by the Late Panafrican evolution, the NSB was already polymetamorphic, and recorded an evolution from high-grade granulitic conditions to water-controlled amphibolite-facies conditions.

## REFERENCES


BHATTACHARYA A. (1986). Some geobarometers involving cordierite in the FeO-$Al_2O_3$ - $SiO_2$($\pm H_2O$) system: refinements, thermodynamic calibration, and applicability in granulite facies rocks. Contrib. Mineral. Petrol., 94: 387-394.

DANIELS J.L., SKIBA A.J. and SUTTON J. (1965). The deformation of some banded gabbros in the Northern Somalia fold belt. Quart. Journ. Geol. Soc. London, 121: 111-142.

FERRARA G., GATTO G.O., IBRAHIM H.A., SAID A.A., SASSI F.P., TONARINI S. and VISONÀ D. (1987). Sequence of events recorded in the crystalline basement of Northern Somalia. Geosom 87, Intern. Meeting on Geology of Somalia, Mogadishu, Nov. 23-30 1987, Abstr.: 65.

FERRY J.M. and SPEAR F.S. (1978). Experimental calibration of the partitioning of Fe and Mg between biotite and garnet. Contrib. Mineral. Petrol., 66: 113-117.

GATTO G.O., IBRAHIM H.A., SASSI F.P. and VISONÀ D. (1987). A tentative litostratigraphic classification of the crystalline basement of Northern Somalia. Geosom 87, Intern. Geology Meeting of Somalia, Mogadishu, Nov. 23-30, Abstr.: 71.

SASSI F.P. and IBRAHIM H.A. (1981). Tentativo di schematizzazione dei problemi litostratigrafici e di correlazione del basamento della Somalia settentrionale. Univ. Naz. Somala. Quad. Geol. Somalia, 5: 91-101.

SASSI F.P. and VISONÀ D. (1985). Primo tentativo di inquadramento cronologico globale dei processi magmatici e metamorfici nel basamento della Somalia settentrionale. Univ. Naz. Somala. Quad. Geol. Somalia, 8: 325-335.

SASSI F.P., VISONÀ D., FERRARA G., GATTO G.O., IBRAHIM H.A., SAID A.A. and TONARINI S. (this volume). The crystalline basement of Northern Somalia: lithostratigraphy and the sequence of events.


*Final editing, January 1990*

From *Geology and mineral resources of Somalia and surrounding regions*, Ist. Agron. Oltremare, Firenze, Relaz. e Monogr. 113, 91-118, 1993.

# PAN-AFRICAN FOLIATED GRANITES AND POST-TECTONIC GRANITOIDS FROM NORTH-EASTERN SOMALIA

B. BIGIOGGERO*, G.V. DAL PIAZ**, A. DEL MORO***, HERSI ADEN IBRAHIM****, S. MARTIN**, G. RIGATTI** and E. SAVIOLI MARIANI*****

* Dipartimento di Scienze della Terra, Università di Milano, Via Mangiagalli 34, 20133 Milano, Italy.

** Dipartimento di Geologia, Paleontologia e Geofisica, Università di Padova, Via Giotto 1, 35123 Padova, Italy.

*** Istituto di Geocronologia e Geochimica Isotopica, CNR, Via G. Maffi 36, 56100 Pisa, Italy.

**** Department of Geology, Somali National University, P.O. Box 1081 Mogadishu, Somalia.

***** Istituto di Mineralogia, Università di Parma, Viale delle Scienze 78, 43100 Parma, Italy.

ABSTRACT

The northern Somali basement is widely exposed along the passive margin of the Somali plate, bordering the Gulf of Aden. From Maydh to Boosaso, the eastern basement strip corresponds to a section of Pan-African upper crust which post-dates the underlying high-grade polymetamorphic "older basement" occurring westwards, from Xiis to Ethiopia. From west to east and from bottom to top, the Pan-African basement of the Maydh-Boosaso coastal ranges consists of foliated to pervasively sheared younger granites, intermediate Maydh volcano-sedimentary mafic complex and overlying Inda Ad clastic sequence which, as a whole, record tectono-metamorphic signatures of a single Pan- African cycle, grading from greenschist facies to very low-grade metamorphic conditions. This metamorphic imprint post-dates the high-grade fabric of the "older basement". These complexes were in tun intruded and thermally metamorphosed by the post-tectonic Arar, Infero and Las Bar granitoid plutons which yield a Rb-Sr whole rock isochron of 549 $\pm$14 Ma and mineral cooling ages ranging from 525 to 499 Ma.

The foliated and post-tectonic granitoids constitute two groups with different chemical characteristics: 1) oversaturated syn-tectonic granites, mostly meta-alluminous, with A-type affinity, and 2) calc-alkaline granodiorites and granites with I-type affinity. The foliated granites, as well as the tectonically associated Maydh metabasalts and the capping Inda Ad clastic sequences, are not consistent with the postulated occurrence in North-eastern Somalia of a sutured subduction-related trench-arc system of Pan-African age (WARDEN and HORKEL, 1984). This model is not supported even by the occurrence of the undeformed granitoids which, despite their calc-alkaline affinity, are clearly post-kinematic with respect to the last tectono-metamorphic event recorded in the Somali basement.

Crustal attenuation under long-lasting tensive/transtensive conditions and thermal perturbance, acting since the early Pan-African emplacement of ensialic gabbro-monzonite bodies, assisted the melting of different sources and the intrusion of both groups of Pan-African granitoids.

## INTRODUCTION

The paper deals with two groups of Pan-African "younger granites" occurring in the north-eastern Somali basement, i.e. the foliated granites of the Maydh area and the post-tectonic granite- plutons of Arar and Infero.

The northern Somali basement is discontinuously exposed along the Gulf of Aden in the onland section of the northern passive margin of the Somali plate recording the Oligocene-Neogene rifting and drifting evolution of the Arabian-Somali plate margin. Systematic mapping in this area, performed by the GEOLOGICAL SURVEY of the former Somaliland Protectorate, provided a complete set of 1:125,000 geological sheets and some explanatory reports (quoted in DAL PIAZ and SASSI, 1988) which represent the basic support for the geology of the northern Somali basement and Mesozoic-Tertiary cover. The geological evolution of the Precambrian basement in Northern Somalia was recently summarized by D'AMICO et al. (1981), WARDEN and DANIELS (1984) DAL PIAZ and SASSI (1988). Large-scale correlations between Ethiopia, Kenya and Somalia have been discussed by WARDEN and HORKEL (1984), who correlate the northern Somali basement to the NE branch of the Mozambique belt. The place-names reported here are from 1:10,000 Somali topographic maps (English synonyms in brackets).

From the Ethiopian border to the Xiis (Heis) area, Ceerigabo (Erigavo) District, the northern Somali basement mostly consists of the "older continental" crust, partly rejuvenated during the Pan-African cycle (inset of Fig. 1). It includes polymetamorphic paragneisses, amphibolites, orthogneisses, minor silicate-rich to pure marbles and a few quartzites which display granulite relics, high-grade amphibolite facies metamorphic signatures and largely developed anatectic migmatites (WARDEN and DANIELS, 1984; DAL PIAZ and SASSI, 1988, and refs. therein). The high-grade sillimanite-kyanite-bearing paragneisses from Hudiso, south of Berbera, preliminary yield a three-point Rb-Sr whole-rock isochron of 828 $\pm$ 170 Ma, which possibly records the thermal peak of the amphibolite facies re-equilibration at decreasing pressure (DAL PIAZ et al., 1985, this vol.).

After the high-grade regional fabric was imprinted, gabbro-monzonite-syenite were emplaced as layered and composite batholiths in the "older basement" at around 700 Ma (FERRARA et al., 1987). Their ensialic intrusion was regionally assisted by long-lasting extensional conditions of Pan-African age (DAL PIAZ et al., this vol.). The gabbro evolution through progressively shallower structural levels is recorded by subsolidus re-equilibrations and high-T mylonites, followed by shear deformation and metamorphic transformation at decreasing temperature (DAL PIAZ et al., 1985, 1987a). A single Rb-Sr cooling age of 567 Ma is reported for the intercumulus biotite from the Sheikh gabbro (DAL PIAZ et al., 1985), locally recording a late step of regional uplift. Rougly coeval (or shortly later) volcanic activity is represented by the Abdulkadir and Maydh (Mait) complexes which occur at the opposite edges of the Somali "older basement". They include greenschist facies tholeiitic metabasalts, with a few silicic metavolcanics in the first case (WARDEN and DANIELS, 1984; DAL PIAZ and SASSI,

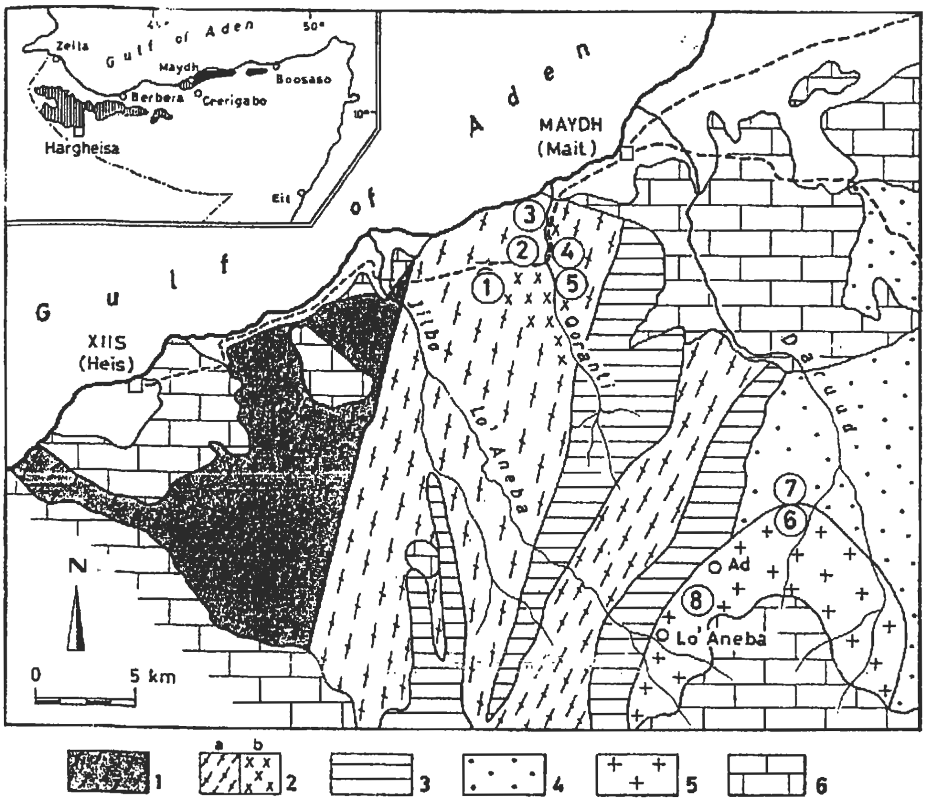


Fig. 1 - Geological sketch map of Maydh-Xiis area, from 1:125,000 Erigavo sheet (MASON and WARDEN, 1956), simplified and modified: 1: Xiis complex, eastern edge of polymetamorphic "older Somali basement"; 2: Foliated to strongly sheared younger granites (a) and associated metagabbros (b); 3: Maydh greenschist facies volcano-sedimentary mafic complex; 4: Inda Ad Complex, capping very low-grade metaclastic sequence of Somali basement; 5: Post- tectonic Arar granodiorite-granite pluton, Early Cambrian; 6: Mesozoic-Tertiary cover sequences. Location of analysed samples: foliated granites: (1) SML 283, (2) SML 314, (3) SML 335, (4) SML 366, (5) SML 373; Arar pluton: (6) SML 1-2-4-5-6-27, (7) SML 7, (8) SML 212-212B-213-214-216. Inset: vertical ruling: "older basement"; black: north-eastern Somali basement.

1988; DAL PIAZ et al., this vol.). The Maydh mafic complex is overlain by the very low-grade Inda Ad metasedimentary complex which, extending eastward up to Boosaso, represents the youngest Proterozoic sequence of the northern Somali basement (MASON and WARDEN, 1956; GREENWOOD, 1960; ABBATE et al., 1985). Leastly the northern Somali basement includes foliated to post-tectonic granitoids and related dykes, commonly known as Pan-African younger granites, which yield whole-rock isochron and mineral cooling ages ranging from 550 (Daymoleh body, Berbera; FERRARA et al.,

1985) to 515-490 Ma (Arar pluton; ABBATE et al., 1985; SNELLING, 1967). A few bulk analyses of these granitoids are reported by ROOKE (1970). In conclusion, two main tectono-metamorphic compressive cycles may be envisaged for the Proterozoic history of Northern Somalia (DAL PIAZ and SASSI, 1988, and refs. therein). The first - Early Pan-African or probably older - is responsible for the high-grade fabric of the polymetamorphic "older continental crust". The second - undoubtedly Pan-African - is recorded by single metamorphic signatures and foldings of the relatively younger complexes from the Maydh-Boosaso area and by reworking of the underlain "older continental crust". These events were separated through a long Pan-African stage of extensional tectonics, underplating of mafic melts, anatectic processes and regional unroofing.

The greenschist facies volcanics and younger granitoids of the northern Somali basement were tentatively interpreted by WARDEN and HORKEL (1984) as markers of Pan-African magmatic arc assemblages supposedly representing the southern extension of the Arabian-Nubian juvenile crust (e.g., ENGEL et al., 1980; STOESER and CAMP, 1985). This magmatic accretion is thought to have developed on the western and eastern active margins of a Somali microplate through opposite subduction of the Ethiopia and East Gondwana lower plates (WARDEN and HORKEL 1984).

As regards the Maydh-Boosaso area, this plate tectonic model is questioned by the absence of adequate indicators of a Pan-African trench-arc suture: the greenschist Maydh tholeiites (DAL PIAZ and al., this vol.) and the younger granites discussed in this paper seem to be inconsistent markers for a sutured convergent plate margin. Field evidence, chemical data and isotope ages are used to discuss whether extensional crustal settings operating in Northern Somalia during the Pan-African evolution may account for their polyphase emplacement.

## GEOLOGICAL FRAMEWORK OF THE MAYDH-BOOSASO AREA

The relatively younger basement units exposed in the Maydh-Boosaso Area may be subdivided into three main groups which post-date the high-grade fabric of the "older basement" (MASON and WARDEN, 1956; GREENWOOD, 1960; ABBATE et al., 1981, 1985; DAL PIAZ et al., 1987 b). From west to east and from bottom to top, they are as follows (Fig. 1):

1) An unnamed basal belt, tectonically juxtaposed to the Xiis Complex (i.e., the easternmost edge of the exposed Somali "older basement"). It mainly consists of foliated to mylonitic intrusive rocks, which represent the first group of younger granites, and of minor older bodies of gabbro-monzonite with hight-T mylonites, both displaying a greenschist facies imprint. As sketched in Fig. 1, this complex extends westwards approximately up to the Togga Jilbo, including the "Xa feldspar-rich metapsammitic Group" of the Erigavo sheet (MASON and WARDEN, 1956) which actually corresponds mostly to acidic orthogneisses and foliated granites with minor metagabbro and amphibolite lenses.

2) The intermediate Maydh Complex, including greenschist facies metatholeiites and associated clastic to pelitic, sometimes carbonate-rich metasedimentary sequences (for their chemical characteristics see DAL PIAZ et al., this vol.).
3) The overlying Inda Ad Complex, a thick, very low-grade sandstone to mudstone sequence, with carbonate interbeddings and minor intraformational conglomerates; illite crystallinity data, reported by ABBATE et al. (1985), partly record the thermal influence of granite intrusions.

The first two complexes make up a NNE-trending west-vergent to steep belt characterized by a penetrative greenschist facies schistosity, shear zones and mylonites, and by large-scale isoclinal to tight folds. The overlying very low-grade Inda Ad Complex displays tight to open folds trending around north, locally coupled with axial plane cleavages. This scenario of compression and metamorphic imprint supports the existence of the so-called Pan-African orogenic event which exhausted here during pre-Cambrian times. In fact, it predates the intrusion at shallow crustal level of the second group of younger granites, represented by the Arar, Infero and Las Bar post-tectonic plutons which yield an Early Cambrian age, as shown by the Rb-Sr whole-rock isochron reported later. The Early Paleozoic age previously inferred for deposition of the Inda Ad clastic and carbonate sequences and the following Pan-African tectonic event by ghosts of supposed Early Paleozoic fossils from the Inda Ad marbles (Gnoli, in ABBATE et al., 1981) consequently becomes unsuitable.

## FOLIATED YOUNGER GRANITES

The first group of younger granites is represented by a set of deformed bodies which display the Pan-African greenschist facies tectono-metamorphic imprint to different extents. In the Togga Jilbo-Togga Qoranti area (Fig. 1), poorly foliated granites and prevailing strongly deformed derivatives with schistose to mylonitic fabric are the end-members of the intrusive suite. In the first case, former sharp contacts with surrounding older metagabbro bodies are often well preserved, locally recorded by intrusive breccias characterized by irregularly-shaped blocks of schistose and amphibolitized metagabbro cemented by stocks of poorly foliated granite (e.g., middle Qoranti valley).

The granite protholiths are medium- to coarse-grained white, greyish and pink types, consisting of perthitic K-feldspar phenocrysts within a matrix of abundant quartz and minor plagioclase, locally zoned. The mafic minerals are represented by scarce amount of ubiquitous red biotite and occasional bluish-green amphibole; titanite, opaques, apatite, zircon and allanite are the common accessory minerals. The deformed types display dynamic recrystallization of quartz and alteration of plagioclase to albite + saussurite and/or epidote, which may be confined to small shear bands or extend to the entire matrix (Fig. 2). Both magmatic biotite and amphibole are poorly to completely replaced by fine aggregates of metamorphic brownish-green biotite which progressively flux to form a well defined greenschist foliation. At increasing deformation, K-feldspar becomes progressively rounded in shape and, together with some mica-

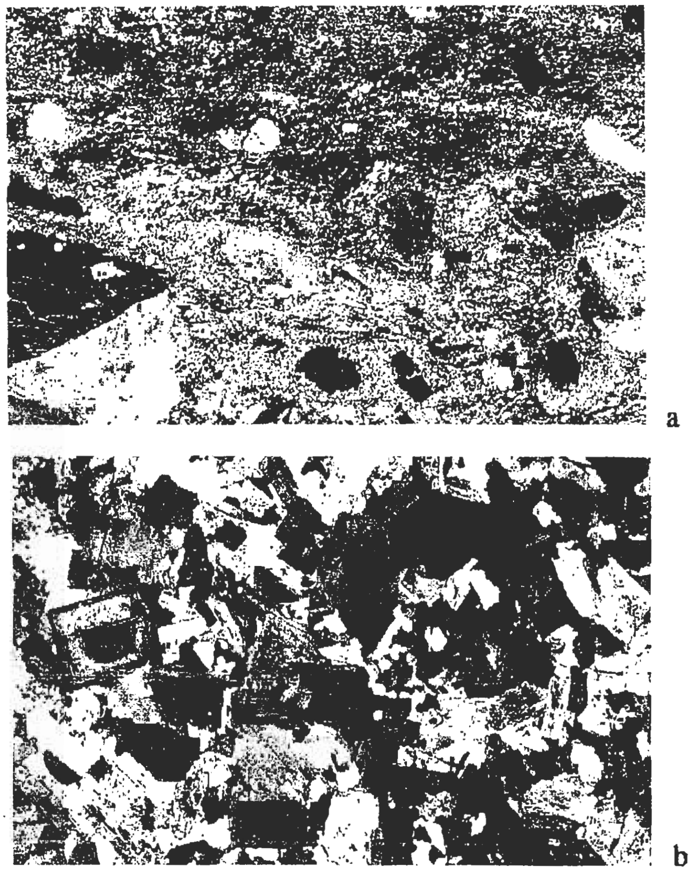

Fig. 2 - Textural comparison between a) mylonitic Maydh granite and b) post-tectonic Infero granodiorite (samples SML 314 and 462; crossed N; 6.5 and 10 x).

fisches, constitutes the only remnants of the magmatic assemblage. The more deformed granites and mylonites occur either as internal shear zones of the complex or as tectonic boundaries towards the surrounding Xiis and Maydh complexes.

No radiometric data are available for defining the age of intrusion and the tectono-metamorphic signature. As previously discussed, the Pan-African age of both intrusive and deformation processes is constrained by field evidence showing that these younger granites were emplaced after the gabbro bodies which in turn post-date the high-grade tectono-metamorphic cycle recorded by the "older Somali basement".

POST-TECTONIC UNDEFORMED GRANITOIDS

The north-eastern Somali post-tectonic granitoids sharply intrude both the folded greenschist facies complexes of the Maydh area (Arar pluton) and the overlying very low-grade Inda Ad sequences (Infero and Las Bar plutons and related dykes), as documented by MASON and WARDEN (1956) and GREENWOOD (1960) and clearly shown in the geological sheets.

The Arar pluton is discontinuously exposed in the Bogon Plain area south of Maydh, and at the base of the Ceerigabo master fault escarpment, displaying a 12 km-wide half-moon shape in map view (Fig. 1); southwards it is unconformably covered and effaced by the Mesozoic-Tertiary sedimentary cover. The intrusive contact and related thermal metamorphism in the surrounding rocks are exposed in the low hills (Bur 549 m) which bound the Bogon Plain northwards, and along the range between the Ad and Lo' Aneba villages. In the first case the contact sharply cuts the north-trending steep sandstone and siltstone sequences of the Inda Ad Complex, which are converted for some tens of meters to very hard black and brownish hornfelses. These rocks include large quantities of random red biotite within a quartz-plagioclase matrix, with minor andalusite and cordierite. In spite of the high-grade thermal imprint, these rocks often preserve former sedimentary textures. In the second case, the intrusive contact, largely covered by Recent deposits, involves metasedimentary sequences with minor mafic interbeddings, probably belonging to the Maydh complex; these rocks are transformed respectively into biotite-andalusite-rich hornfelses (locally with corundum and fibrolite) and to brown hornblende-biotite-plagioclase ± pyroxene and chlorite-bearing amphibolites.

The Arar pluton consists of homogeneous and undeformed medium- to coarse-grained white granite and amphibole-poor granodiorite with a generally well-preserved magmatic mineral assemblage, although altered pink varieties occasionally occur. These rocks include some microgranular mafic enclaves and are cut by thin aplite and pegmatite dykes. They display a granular to porphyric texture (Fig. 2) and consist of prevailing plagioclase, abundant K-feldspar, quartz and minor dark-brown biotite ± amphibole; very scarce amounts of magmatic white mica have occasionally been seen in a few samples from the northern side of the pluton. Plagioclase phenocrysts are strongly zoned and sometimes include readsorbed highly calcic, single or composite nuclei which closely recall, for instance, those from the mantle-derived calc-alkaline Periadriatic plutons of the Alps (e.g., CALLEGARI, 1985). Opaques, apatite, titanite and zircon commonly occur as accessory minerals. Despite the general freshness of the primary assemblage, scarce to discrete late magmatic and hydrothermal alteration products may be seen, mainly as kaolinic patine on K- feldspar, sericite and occasional calcite after plagioclase and a little greenish biotite II or chlorite-titanite after biotite.

The Infero and Las Bar plutons intrude the eastern edge of the Inda Ad Complex, near Xidid, south of Durduri, Laasqoray (Las Khoreh)-Boosaso area (Fig. 3); no older basement units are exposed here, as they are expected to be buried at depth. As shown

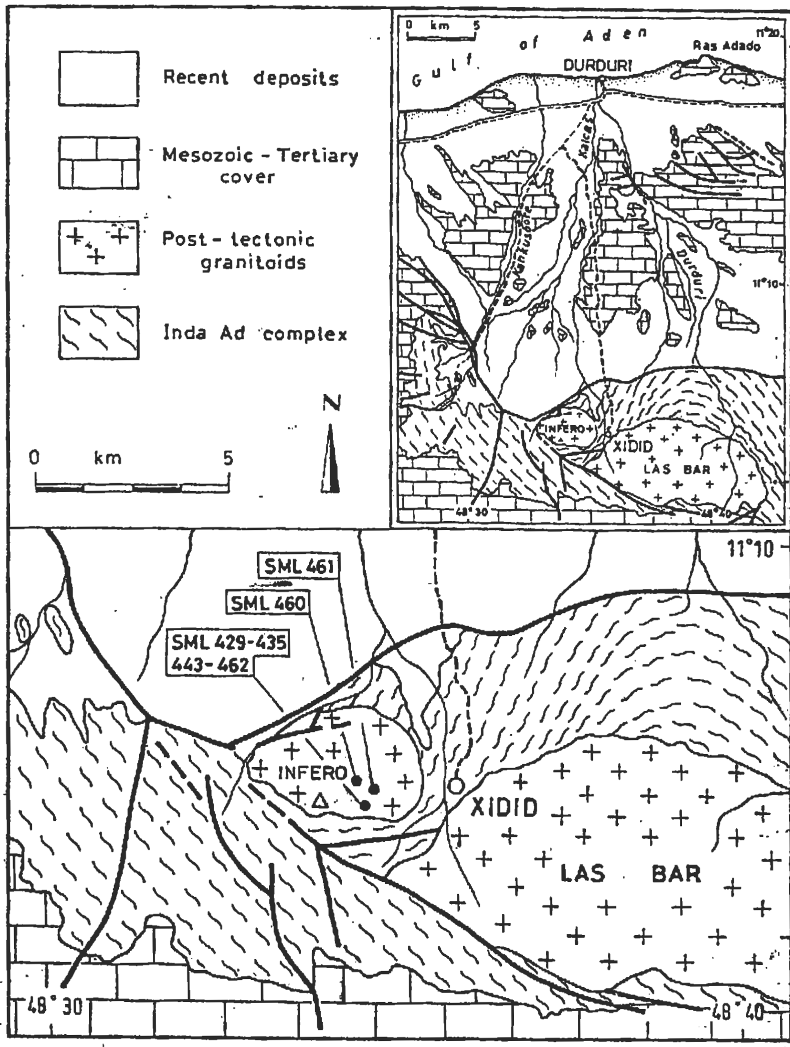


Fig. 3 - Geological sketch map of Infero and Las Bar post-tectonic plutons, from 1:125,000 Elayu and Las Khoreh sheets (GREENWOOD, 1960), and location of analysed samples.

in the Las Khoreh and Elayu 1:125,000 geological sheets (GREENWOOD, 1960), these plutons display an elliptical shape in the plain view, with major axes reaching 4.5 and 13.5 km respectively, suggesting a cauldron subsidence mechanism for their emplacement (STEWARD, in GREENWOOD, 1960). The surrounding Inda Ad sequences are mainly represented here by very low-grade sandstones and siltstones, with interbeddings of marbles and minor variegated mudstones; the sedimentary bedding is mainly NW-trending and steeply dipping, with noticeable variations on the northern side of the plutons (Fig. 3). Large-scale roof pendants are preserved in the Inferò area, together with abundant cm-dm xenoliths, locally occurring as aligned swarms; minor cognate mafic enclaves also occur.

A large thermal aureole encompasses the intrusive bodies; it grades from metasedimentary rocks characterized by increasing granoblastic fabric and the appearance of neogenic little biotite towards different types of hornfelses, mainly biotite-quartz-cordierite- and quartz-biotite-plagioclase-bearing.

The Infero pluton mainly consists of medium-grained biotite-rich granite and granodiorite, with markedly zoned euhedral plagioclase (with readsorbed calcic nuclei), quartz and minor intergranular to poikilitic K-feldspar; mafic minerals are represented by red-brown biotite ± greenish amphibole. Opaques, titanite, apatite, zircon and occasional white mica occur as accessory minerals; chlorite, saussurite and sericite locally develop as alteration products. Microprobe analyses on magmatic biotite, zoned plagioclase and amphibole from the Arar and Infero plutons were performed with the electron E.D.S. microprobe of the Institute of Mineralogy and Petrography, University of Padova. Selected analyses are reported in Table 1.

Biotite displays homogeneous compositions with variations mostly depending on the oxidation state of the samples. As shown in the fe (Fe tot/Fe tot + Mg) vs. Al VI

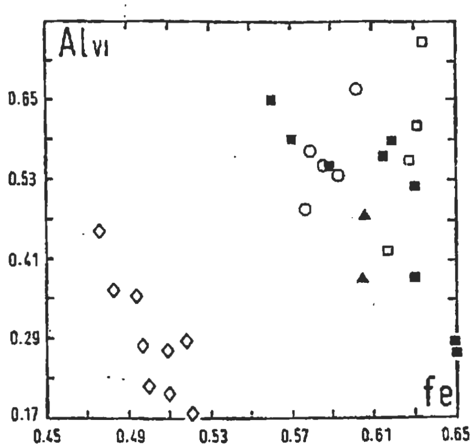


Fig. 4 - Fe vs. Al VI diagram of biotites from post-tectonic granitoids. Arar pluton (open symbols): square: SML 1 granite; circle: SML 198 granite; diamond: SML 214 granite. Infero pluton (filled symbols): triangle: SML 435 granodiorite; square: SML 462 granodiorite.

Table 1 - Representative analyses of biotite, plagioclase and amphibole from post-tectonic Arar and Infero granitoids. Structural formulae calculated on basis of 22 oxygens for biotite, 8 for plagioclase and 23 for amphibole. Iron of biotite was considered to be ferrous; amphibole analyses were calculated according to method of ROBINSON et al. (1982) which normalizes K-free cation sum to 15 and satisfies equation (Na,K) A + Al VI + $Fe^{3+}$ + Cr + $2Ti^{4+}$ = Al IV + Na M4.

| SML | 198 | 214 | | | | 435 | | | | | | 462 | | | | | | |
|---|---|---|---|---|---|---|---|---|---|---|---|---|---|---|---|---|---|---|
| | Bi | Bi | | Pl | | Bi | Pl | | | Amph | | Bi | | Pl | | | Amph | |
| | 1 | 2 | 3 | 4c | 4r | 5 | 6c | 6ir | 6er | 7 | 8 | 9 | 10 | 11c | 11ir | 11er | 12c | 12r |
| $SiO_2$ | 37.46 | 37.18 | 36.09 | 56.46 | 59.68 | 35.88 | 54.22 | 56.58 | 59.12 | 46.78 | 48.33 | 35.66 | 36.07 | 55.44 | 59.11 | 61.32 | 49.07 | 52.40 |
| $TiO_2$ | 3.75 | 3.56 | 4.35 | 0.01 | — | 4.04 | — | 0.02 | 0.18 | 0.92 | 0.78 | 3.73 | 1.16 | — | — | — | 0.29 | 0.02 |
| $Al_2O_3$ | 17.20 | 16.11 | 15.17 | 26.55 | 25.28 | 15.85 | 29.19 | 27.53 | 25.50 | 6.88 | 5.61 | 15.40 | 16.73 | 28.93 | 25.41 | 24.90 | 4.71 | 3.24 |
| FeO | 21.29 | 19.09 | 19.76 | 0.47 | 0.48 | 22.62 | 0.11 | 0.53 | 0.68 | 20.45 | 20.50 | 24.72 | 22.79 | — | 0.09 | 0.20 | 19.76 | 16.59 |
| MnO | 0.55 | 0.72 | 0.61 | 0.28 | 0.12 | 0.45 | 0.24 | 0.05 | — | 1.22 | 0.91 | 0.60 | 0.60 | 0.14 | 0.20 | 0.03 | 1.02 | 1.14 |
| MgO | 8.70 | 11.46 | 10.66 | — | — | 8.30 | — | — | — | 8.72 | 9.37 | 7.48 | 9.44 | — | — | — | 10.56 | 12.42 |
| CaO | — | — | — | 9.28 | 7.03 | — | 10.68 | 9.16 | 6.93 | 11.23 | 11.26 | — | — | 10.23 | 7.99 | 5.47 | 11.96 | 11.92 |
| $Na_2O$ | — | — | 0.17 | 6.85 | 7.17 | — | 5.47 | 6.00 | 7.53 | 1.09 | 0.91 | 0.56 | — | 5.10 | 7.07 | 7.94 | 0.47 | 0.20 |
| $K_2O$ | 9.33 | 9.28 | 9.40 | 0.11 | 0.25 | 8.86 | 0.09 | 0.02 | 0.06 | 0.70 | 0.52 | 9.16 | 9.16 | 0.15 | 0.12 | 0.13 | 0.26 | 0.08 |
| Tot | 98.28 | 97.40 | 96.21 | 100.01 | 100.01 | 96.00 | 100.00 | 99.98 | 100.00 | 97.99 | 98.19 | 97.31 | 95.95 | 99.99 | 99.99 | 99.99 | 98.10 | 98.01 |
| Si | 5.56 | 5.34 | 5.49 | 2.55 | 2.68 | 5.51 | 2.45 | 2.54 | 2.64 | 6.96 | 7.16 | 5.49 | 5.55 | 2.49 | 2.64 | 2.72 | 7.24 | 7.65 |
| AlIV | 2.44 | 2.66 | 2.51 | 1.41 | 1.33 | 2.49 | 1.55 | 1.46 | 1.34 | 1.04 | 0.84 | 2.51 | 2.45 | 1.53 | 1.34 | 1.30 | 0.76 | 0.35 |
| Ti | 0.42 | 0.40 | 0.50 | — | — | 0.47 | — | — | 0.01 | 0.10 | 0.09 | 0.43 | 0.13 | — | — | — | 0.03 | — |
| AlVI | 0.57 | 0.17 | 0.21 | — | — | 0.38 | — | — | — | 0.16 | 0.14 | 0.29 | 0.59 | — | — | — | 0.06 | 0.21 |
| Fe3+ | — | — | — | — | — | — | — | — | — | 0.86 | 0.69 | — | — | — | — | — | 0.72 | 0.18 |
| Fe2+ | 2.64 | 2.38 | 2.51 | 0.02 | 0.02 | 2.91 | — | 0.02 | 0.03 | 1.73 | 1.89 | 3.18 | 2.93 | — | — | 0.01 | 1.75 | 1.86 |
| Mn | 0.07 | 0.09 | 0.08 | 0.01 | 0.01 | 0.06 | 0.01 | — | — | 0.15 | 0.11 | 0.08 | 0.08 | 0.01 | 0.01 | — | 0.11 | 0.05 |
| Mg | 1.93 | 2.54 | 2.42 | — | — | 1.90 | — | — | — | 1.93 | 2.07 | 1.72 | 2.17 | — | — | — | 2.32 | 2.70 |
| Ca | — | — | — | 0.45 | 0.34 | — | 0.52 | 0.44 | 0.33 | 1.79 | 1.79 | — | — | 0.49 | 0.38 | 0.26 | 1.89 | 1.87 |
| Na | — | — | 0.05 | 0.60 | 0.62 | — | 0.48 | 0.52 | 0.65 | 0.32 | 0.26 | 0.17 | — | 0.44 | 0.61 | 0.68 | 0.13 | 0.06 |
| K | 1.77 | 1.76 | 1.82 | 0.01 | 0.01 | 1.74 | 0.01 | — | — | 0.13 | 0.10 | 1.80 | 1.80 | 0.01 | 0.01 | 0.01 | 0.05 | 0.02 |
| Tot | 15.40 | 15.34 | 15.59 | 5.05 | 5.01 | 15.46 | 5.02 | 4.98 | 5.00 | 15.17 | 15.14 | 15.67 | 15.70 | 4.97 | 4.99 | 4.98 | 15.06 | 14.95 |

SML 198: 1. skeletal biotite; SML 214: 2. euhedral biotite flake, 3. interstitial biotite in contact with 4. zoned plagioclase; SML 435: 5. interstitial brown biotite, 6. zoned plagioclase, 7–8. greenamphiboles included in biotite; SML 462: 9. skeletal biotite, 10. late-magmatic biotite, 11. zoned plagioclase, 12. zoned green amphibole. c: core, r: rim, ir: internal rim, er: external rim from zoned minerals. Analyst: S.Martin.

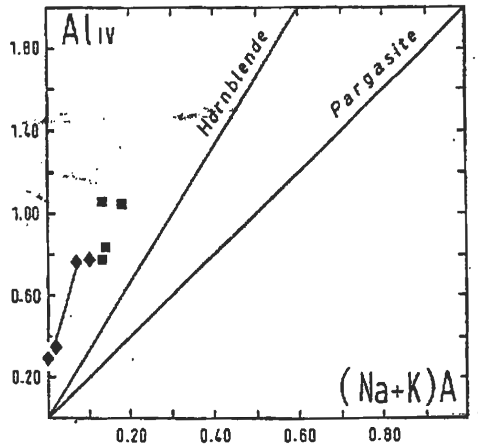


Fig. 5 - Rapresentative diagram of amphiboles from granodiorites of Infero pluton; square: SML 435; diamond: SML 462.

diagram (Fig. 4), biotite from the analysed granite and granodiorite samples has Fe tot / Fe tot + Mg ranging from 0.65 to 0.57; instead, the ratio is lower in the hematite-bearing SML 214 granodiorite from the Arar pluton. The Al VI content varies inversely in fe for SML 214 and SML 462 samples. The small greenish or colourless flakes of late magmatic biotite display a Ti content noticeably lower than in the main red biotites; for instance, also plotting analytical data not reported in Table 1, the rims of the first biotites from the Infero SML 462 granodiorite show high contents of Ti (about 0.35-0.38 p.f.u.), while the new biotite generation has Ti ranging from 0.08 to 0.28 p.f.u.

The composition of zoned plagioclases from the Arar and Infero granodiorites mainly ranges from labradorite to andesine, locally with late magmatic rims of oligoclase.

The analysed green and bluish-green amphiboles from the Infero rocks are hornblende, according to the nomenclature proposed by LEAKE (1978). Their Al IV content ranges from 0.30 to 1.10 at increasing A site occupancy (Fig. 5). Compositional variations of zoned crystals mostly range from hornblende core to actinolite rim.

## GEOCHEMISTRY

The bulk compositions of 5 selected samples of foliated to strongly sheared granites from the Maydh area and 17 of undeformed post-tectonic granites and granodiorites from the Arar and Infero plutons are reported in Tables 2 and 3.

The following samples from the foliated younger granites occurring west of the Maydh complex were selected and analysed (Table 2):

- SML 283: reddish metagranite with K-feldspar porphyroclasts, biotite mica-fisches and minor greenish amphibole within anastomosing bands of recrystallized to mylonitic quartz with small flakes of new greenish biotite II, epidote and albite (160 m pass on watershed between Togga Jilbo and Togga Qoranti, Xiis- Maydh track).
- SML 314: mylonitic granite with ovalized porphyroclasts of perthitic K-feldspar, minor plagioclase and accessory hornblende within a mylonitic matrix which includes quartz $\pm$ albite bands interbedded with folded rows of microlitic greenish biotite II (large stock of reddish granite, approximately half-way between the 160 m pass and the Qoranti valley).
- SML 335: metagranite with perthitic K-feldspar in a medium-grained matrix of quartz, plagioclase, reddish-brown biotite bands and minor amphibole (stock of foliated pink granite, Togga Qoranti, ca. 1 km from coastal plain).
- SML 366: poorly foliated fine-grained alkali granite with K-feldspar, plagioclase (locally zoned), weakly recrystallized quartz, biotite and minor bluish amphibole (intrusive breccias on metagabbros, right side of middle Togga Qoranti).
- SML 373: metagranite with perthitic K-feldspar, saussuritic plagioclase, biotite and hornblende within a well-foliated matrix including recrystallized quartz, small biotite II and amphibole fragments (large body of poorly foliated pink granite, Togga Qoranti, ca. 300 m south of the above sample).

As representative of the post-tectonic Arar and Infero undeformed granitoids the following samples were selected and analysed (Table 3):

**Arar pluton**

a) northern side, Bur 549 m:

- SML 1-2: medium-grained porphyric granite with K-feldspar, zoned plagioclase (weakly altered to sericite and saussurite at the core), quartz, biotite (partly altered to chlorite and titanite), with minor white mica in SML 2.
- SML 4: medium-coarse-grained granite with zoned phenocrysts of plagioclase (poorly altered to sericite, saussurite and calcite), quartz, pink perthitic K-feldspar and large biotite flakes, locally transformed to chlorite.
- SML 5: fine-grained equigranular aplite with scarce biotite.
- SML 6: coarse-grained pink pegmatite with minor biotite.

b) western side, 2-3 km SW of Ad village:

- SML 197: coarse-grained granite with zoned plagioclase, partly altered to white mica and epidote, poikilitic microcline, large crystals of quartz and red biotite.
- SML 198: identical, but medium-grain and scarce chlorite after biotite.
- SML 212-212B-213-214: coarse-grained granites with abundant zoned phenocrysts of plagioclase, including readsorbed calcic nuclei (partly altered), yellow to dark brown biotite, variable amounts of quartz, and K-feldspar in the matrix.

Table 2 - Bulk chemistry and CIPW norms of foliated younger granites from North-eastern Somalia.

| Sample SML | 283 | 335 | 366 | 373 | 314 |
|---|---|---|---|---|---|
| $SiO_2$ | 77.20 | 70.72 | 69.23 | 70.44 | 71.78 |
| $TiO_2$ | 0.38 | 0.46 | 0.57 | 0.47 | 0.37 |
| $Al_2O_3$ | 14.01 | 14.08 | 14.58 | 14.18 | 14.22 |
| $Fe_2O_3$ | 2.74 | 3.52 | 3.86 | 3.48 | 2.62 |
| MnO | 0.04 | 0.07 | 0.08 | 0.07 | 0.05 |
| MgO | 0.49 | 0.60 | 0.68 | 0.61 | 0.34 |
| CaO | 1.42 | 1.88 | 2.31 | 1.81 | 1.26 |
| $Na_2O$ | 3.29 | 3.12 | 3.15 | 3.51 | 3.19 |
| $K_2O$ | 4.73 | 4.89 | 4.89 | 4.89 | 5.72 |
| $P_2O_5$ | 0.10 | 0.12 | 0.14 | 0.11 | 0.07 |
| $H_2O+$ | 0.61 | 0.55 | 0.50 | 0.43 | 0.37 |
| Total | 100.01 | 100.01 | 99.99 | 100.00 | 99.99 |
| Co | 5 | 5 | 4 | 7 | 2 |
| Cr | 5 | 8 | 7 | 10 | 5 |
| Nb | 11 | 13 | 15 | 13 | 10 |
| Ni | 7 | 7 | 6 | 7 | 5 |
| Rb | 80 | 147 | 121 | 136 | 109 |
| Sr | 122 | 149 | 178 | 161 | 117 |
| V | 17 | 30 | 38 | 27 | 12 |
| Zr | 244 | 307 | 363 | 318 | 313 |
| Y | 32 | 39 | 37 | 39 | 27 |
| AN | 18.67 | 24.45 | 28.35 | 21.76 | 17.67 |
| Q | 30.49 | 27.98 | 25.25 | 25.57 | 27.38 |
| or | 27.95 | 28.90 | 28.90 | 28.90 | 33.80 |
| ab | 27.84 | 26.40 | 26.65 | 29.70 | 26.99 |
| an | 6.39 | 8.54 | 10.55 | 8.26 | 5.79 |
| C | 1.14 | 0.52 | 0.24 | 0.09 | 0.66 |
| di | 0.00 | 0.00 | 0.00 | 0.00 | 0.00 |
| hy | 3.36 | 4.33 | 4.70 | 4.29 | 2.90 |
| mt | 1.07 | 1.38 | 1.51 | 1.36 | 1.03 |
| il | 0.72 | 0.87 | 1.08 | 0.89 | 0.70 |
| ap | 0.23 | 0.28 | 0.32 | 0.25 | 0.16 |
| FeO* | 2.47 | 3.17 | 3.47 | 3.13 | 2.36 |
| Rb/Sr | 0.656 | 0.987 | 0.680 | 0.845 | 0.93 |
| K/Rb | 490.7 | 276.1 | 335.4 | 298.4 | 435.6 |

Table 3 - Bulk chemistry and CIPW norms of Arar and Infero post-tectonic granitoids.

| Sample | ARAR ( NORTHERN SIDE ) | | | | | ARAR ( WESTERN SIDE ) | | | | | | |
|---|---|---|---|---|---|---|---|---|---|---|---|---|
| SML | 1 | 2 | 4 | 5 | 6 | 197 | 198 | 212 | 213 | 216 | 212B | 214 |
| SiO2 | 72.74 | 71.55 | 69.23 | 75.27 | 74.42 | 67.53 | 71.61 | 65.94 | 66.20 | 70.10 | 66.10 | 66.18 |
| TiO2 | 0.23 | 0.35 | 0.43 | 0.06 | 0.15 | 0.49 | 0.36 | 0.53 | 0.59 | 0.29 | 0.47 | 0.50 |
| Al2O3 | 14.81 | 14.57 | 15.34 | 13.90 | 13.36 | 16.25 | 14.70 | 16.73 | 16.40 | 15.19 | 16.88 | 16.25 |
| Fe2O3 | 2.01 | 2.94 | 3.34 | 0.58 | 1.22 | 3.43 | 2.96 | 4.23 | 4.27 | 0.83 | 1.27 | 1.48 |
| FeO | 0.00 | 0.00 | 0.00 | 0.00 | 0.00 | 0.00 | 0.00 | 0.00 | 0.00 | 0.00 | 2.18 | 2.27 |
| MnO | 0.09 | 0.11 | 0.09 | 0.02 | 0.05 | 0.10 | 0.07 | 0.10 | 0.11 | 0.03 | 0.07 | 0.08 |
| MgO | 0.55 | 0.82 | 1.14 | 0.12 | 0.34 | 1.31 | 0.97 | 1.58 | 1.60 | 0.67 | 1.61 | 1.77 |
| CaO | 1.41 | 1.22 | 2.45 | 0.50 | 0.54 | 2.50 | 1.34 | 3.37 | 3.40 | 3.39 | 3.14 | 3.02 |
| Na2O | 3.61 | 3.30 | 3.53 | 2.97 | 2.44 | 3.64 | 3.51 | 3.86 | 3.55 | 4.18 | 4.51 | 4.23 |
| K2O | 3.90 | 4.03 | 3.54 | 6.02 | 6.77 | 3.85 | 3.58 | 2.50 | 2.77 | 1.09 | 2.46 | 2.35 |
| P2O5 | 0.09 | 0.16 | 0.13 | 0.06 | 0.08 | 0.16 | 0.08 | 0.18 | 0.19 | 0.12 | 0.14 | 0.13 |
| H2O+ | 0.56 | 0.95 | 0.78 | 0.50 | 0.62 | 0.74 | 0.00 | 0.99 | 0.91 | 3.51 | 1.16 | 1.19 |
| Total | 100.00 | 100.00 | 100.00 | 100.00 | 99.99 | 100.00 | 99.98 | 100.01 | 99.99 | 100.00 | 99.99 | 99.45 |
| Ba | 708 | 991 | 1097 | 492 | | 899 | 570 | 926 | 911 | 349 | | 926 |
| Be | 3 | 3 | 2 | 2 | | 2 | 3 | 2 | 2 | 2 | | 2 |
| Co | 5 | 5 | 5 | 5 | 44 | 5 | 9 | 10 | 13 | 5 | | 13 |
| Cr | 5 | 7 | 16 | 5 | 6 | 18 | 12 | 23 | 20 | 12 | | 20 |
| Cu | 28 | 20 | 35 | 53 | | 41 | 34 | 38 | 18 | 27 | | 54 |
| Ga | 12 | 14 | 7 | 13 | | 24 | 12 | 18 | 14 | 13 | | 5 |
| Nb | 7 | 9 | 5 | 6 | 4 | 5 | 10 | 5 | 7 | 6 | | 5 |
| Ni | 5 | 5 | 15 | 16 | 5 | 17 | 8 | 17 | 21 | 18 | | 36 |
| Rb | 94 | 85 | 66 | 114 | 120 | 82 | 84 | 57 | 56 | 21 | | 58 |
| Sc | 5 | 6 | 8 | 4 | | 8 | 7 | 8 | 8 | 5 | | 9 |
| Sr | 253 | 248 | 379 | 103 | 173 | 418 | 258 | 536 | 543 | 405 | | 521 |
| Th | 5 | 5 | 6 | 10 | | 5 | 24 | 5 | 5 | 8 | | 5 |
| V | 14 | 15 | 36 | 8 | 11 | 48 | 26 | 56 | 59 | 20 | | 51 |
| Zn | 25 | 34 | 50 | 32 | | 57 | 32 | 63 | 74 | 20 | | 63 |
| Zr | 80 | 84 | 126 | 49 | 71 | 120 | 91 | 139 | 138 | 104 | | 129 |
| La | 15.95 | 20.17 | 24.22 | 9.77 | | 11.38 | 17.47 | 13.74 | 11.18 | 24.20 | | 22.61 |
| Nd | 14.70 | 18.07 | 21.47 | 10.02 | | 11.63 | 20.69 | 13.25 | 10.59 | 22.73 | | 19.36 |
| Eu | 0.66 | 0.77 | 0.99 | -0.36 | | 0.92 | 0.72 | 0.98 | 1.03 | 1.02 | | 1.12 |
| Dy | 2.98 | 2.80 | 2.88 | 2.87 | | 2.87 | 6.48 | 2.40 | 2.41 | 2.56 | | 2.76 |
| Yb | 1.74 | 1.56 | 1.38 | 1.83 | | 1.63 | 3.95 | 1.21 | 1.33 | 1.32 | | 1.44 |
| Ce | 34.89 | 43.73 | 51.62 | 23.47 | | 23.70 | 41.14 | 27.97 | 22.42 | 50.58 | | 42.94 |
| Sm | 3.08 | 3.55 | 3.84 | 2.51 | | 2.70 | 5.25 | 2.79 | 2.49 | 3.98 | | 3.77 |
| Gd | 3.04 | 3.37 | 3.62 | 2.42 | | 2.72 | 5.49 | 2.69 | 2.53 | 3.45 | | 3.47 |
| Er | 1.74 | 1.58 | 1.59 | 1.69 | | 1.71 | 3.87 | 1.34 | 1.35 | 1.47 | | 1.50 |
| Lu | 0.33 | 0.24 | 0.28 | 0.33 | | 0.36 | 0.71 | 0.24 | 0.42 | 0.29 | | 0.36 |
| Y | 19.60 | 17.67 | 17.17 | 19.32 | | 19.32 | 44.00 | 14.70 | 15.50 | 15.17 | | 17.07 |
| AN | 17.34 | 15.21 | 27.46 | 7.67 | 9.46 | 26.94 | 17.10 | 32.24 | 34.22 | 34.96 | 27.76 | 28.31 |
| Q | 32.42 | 32.40 | 27.32 | 33.64 | 32.40 | 23.51 | 32.29 | 23.27 | 24.25 | 32.22 | 20.36 | 22.35 |
| or | 23.05 | 23.82 | 20.92 | 35.58 | 40.01 | 22.75 | 21.16 | 14.77 | 16.37 | 6.44 | 14.54 | 13.89 |
| ab | 30.55 | 27.92 | 29.87 | 25.13 | 20.65 | 30.80 | 29.70 | 32.66 | 0.00 | 35.37 | 38.16 | 35.79 |
| an | 6.41 | 5.01 | 11.31 | 2.09 | 2.16 | 11.36 | 6.13 | 15.54 | 15.63 | 19.01 | 14.66 | 14.13 |
| C | 2.30 | 2.94 | 1.56 | 1.73 | 1.23 | 1.93 | 2.81 | 1.98 | 1.84 | 0.17 | 1.42 | 1.57 |
| hy | 3.13 | 4.56 | 5.58 | 0.81 | 1.89 | 6.01 | 4.86 | 7.40 | 7.41 | 2.06 | 6.99 | 7.67 |
| mt | 0.79 | 1.15 | 1.31 | 0.23 | 0.48 | 1.34 | 1.16 | 1.66 | 1.67 | 0.32 | 1.45 | 1.57 |
| il | 0.44 | 0.66 | 0.82 | 0.11 | 0.28 | 0.93 | 0.68 | 1.01 | 1.12 | 0.55 | 0.89 | 0.95 |
| ap | 0.21 | 0.37 | 0.30 | 0.14 | 0.19 | 0.37 | 0.19 | 0.42 | 0.44 | 0.28 | 0.32 | 0.30 |
| FeO* | 1.81 | 2.65 | 3.01 | 0.52 | 1.10 | 3.09 | 2.66 | 3.81 | 3.84 | 0.75 | 3.32 | 3.60 |
| Rb/Sr | 0.372 | 0.343 | 0.174 | 1.107 | 0.694 | 0.196 | 0.326 | 0.106 | 0.103 | 0.052 | | 0.111 |
| K/Rb | 344.4 | 393.5 | 445.2 | 438.3 | 468.3 | 389.7 | 353.7 | 364.0 | 410.6 | 430.8 | | 336.3 |
| La*/Yb* | 6.2 | 8.7 | 11.8 | 3.6 | | 4.7 | 3.0 | 7.6 | 5.7 | 12.3 | | 10.6 |

Table 3 - continued

INFERO

| Sample SML | 435 | 443 | 460 | 461 | 462 |
|---|---|---|---|---|---|
| SiO2 | 65.26 | 63.64 | 64.70 | 64.61 | 63.40 |
| TiO2 | 0.60 | 0.68 | 0.69 | 0.62 | 0.63 |
| Al2O3 | 16.30 | 16.53 | 16.66 | 16.45 | 16.71 |
| Fe2O3 | 0.78 | 0.73 | 1.06 | 0.60 | 0.44 |
| FeO | 3.37 | 3.98 | 3.71 | 3.70 | 4.05 |
| MnO | 0.07 | 0.08 | 0.08 | 0.07 | 0.07 |
| MgO | 1.42 | 1.66 | 1.55 | 1.40 | 1.55 |
| CaO | 3.96 | 4.28 | 4.00 | 3.92 | 4.34 |
| Na2O | 3.85 | 3.81 | 3.99 | 4.10 | 3.99 |
| K2O | 2.95 | 2.94 | 2.31 | 2.67 | 2.59 |
| P2O5 | 0.15 | 0.15 | 0.19 | 0.17 | 0.18 |
| H2O+ | 1.06 | 1.25 | 1.06 | 0.98 | 1.14 |
| Total | 99.77 | 99.73 | 100.00 | 99.29 | 99.09 |
| Ba | 900 | 861 | 712 | 862 | 742 |
| Be | 2 | 2 | 2 | 2 | 2 |
| Co | 7 | 20 | 17 | 51 | 7 |
| Cr | 15 | 16 | 12 | 202 | 8 |
| Cu | 38 | 45 | 31 | 71 | 66 |
| Ga | 8 | 26 | 30 | 21 | 11 |
| Nb | 9 | 11 | 10 | 57 | 51 |
| Ni | 5 | 5 | 6 | 13 | 11 |
| Rb | 80 | 76 | 75 | 60 | 75 |
| Sc | 11 | 12 | 13 | 20 | 12 |
| Sr | 327 | 358 | 331 | 878 | 339 |
| Th | 5 | 5 | 10 | 8 | 5 |
| V | 38 | 39 | 40 | 134 | 47 |
| | 60 | 73 | 57 | 87 | 78 |
| Zn | 172 | 170 | 189 | 222 | 171 |
| La | 23.12 | 24.76 | 26.34 | 36.90 | 21.72 |
| Nd | 20.07 | 24.18 | 24.12 | 33.37 | 21.42 |
| Eu | 1.19 | 1.31 | 1.43 | 1.31 | 0.00 |
| Dy | 4.03 | 4.18 | 4.52 | 5.15 | 4.43 |
| Yb | 2.10 | 2.16 | 2.54 | 2.65 | 2.37 |
| Ce | 46.11 | 52.04 | 52.09 | 75.23 | 44.32 |
| Sm | 4.35 | 5.03 | 5.04 | 6.33 | 4.68 |
| Gd | 4.42 | 4.91 | 5.09 | 6.23 | 4.76 |
| Er | 2.28 | 2.25 | 2.62 | 2.86 | 2.51 |
| Lu | 0.39 | 0.35 | 0.60 | 0.48 | 0.42 |
| Y | 25.28 | 25.23 | 29.26 | 31.08 | 28.17 |
| AN | 36.20 | 37.47 | 35.53 | 34.58 | 37.24 |
| Q | 19.80 | 17.34 | 20.43 | 18.83 | 17.45 |
| or | 17.43 | 17.37 | 13.65 | 15.78 | 15.31 |
| ab | 32.58 | 32.24 | 33.76 | 34.69 | 33.76 |
| an | 18.48 | 19.32 | 18.60 | 18.34 | 20.04 |
| C | 0.00 | 0.00 | 0.78 | 0.10 | 0.00 |
| di | 0.15 | 0.77 | 0.00 | 0.00 | 0.26 |
| hy | 7.05 | 7.84 | 7.97 | 7.23 | 7.68 |
| mt | 1.77 | 2.02 | 2.03 | 1.84 | 1.93 |
| il | 1.14 | 1.29 | 1.31 | 1.18 | 1.20 |
| ap | 0.35 | 0.35 | 0.44 | 0.39 | 0.42 |
| FeO* | 4.07 | 4.64 | 4.66 | 4.24 | 4.45 |
| Rb/Sr | 0.245 | 0.212 | 0.227 | 0.068 | 0.221 |
| K/Rb | 306.1 | 321.1 | 255.6 | 369.4 | 286.6 |
| La*/Yb* | 7.4 | 7.7 | 7.0 | 9.4 | 6.2 |

- SML 216: pink pegmatoid type with prevailing plagioclase (partly altered to sericite and scarce calcite), quartz and minor biotite, mostly converted to aggregates of chlorite, titanite and opaques.

**Infero pluton**

- SML 435-443-462: medium-fine-grained granodiorite with prevailing zoned phenocrysts of plagioclase (poorly altered to saussurite and epidote), biotite (sometimes with chlorite, titanite and rutile as accessory alteration products), quartz, minor greenish amphibole (locally replaced by small late-magmatic biotite and epidote), scarce interstitial K-feldspar (easternmost top of Bur ridge 2 km east of Infero peak).
- SML 460: fine-grained granodiorite with prevailing zoned plagioclase, abundant biotite (partly altered to chlorite), quartz and scarce K-feldspar (south of large marble-rich roof pendant 1 km E-NE of Infero peak).
- SML 461: medium-grained porphyric granodiorite with poorly altered zoned plagioclase, abundant biotite, minor amphibole and a quartz matrix with scarce interstitial K-feldspar (sandy plain between sites SML 435 and 460).

Following the cation classification of DEBON and LE FORT (1988) for common plutonic rocks and their magmatic associations, the analysed foliated younger granites (hereafter FG) of the Maydh area and the post-tectonic Arar and Infero intrusives (PTG) can be fairly well separated into different groups (Fig. 6, a, b, c). The FG may be interpreted as metaluminous oversaturated rocks, exclusively of granitic composition; nevertheless caution may be used in this case due to the mobile beaviour of silica and alkalies which may be expected through metamorphic and mylonitic processes. The undeformed PTG form a granodioritic to granitic suite with an overall calc-alkaline geochemical affinity. The sampled rocks of the Arar pluton range from minor granodiorites to leucogranites in the northern side of the intrusive body and are exclusively granodioritic in its western side; those from the Infero pluton are essentially granodioritic. The highest Al-enrichment trend is shown by the samples from the Arar pluton, clearly Al-enriched with respect to the Infero or FG samples at comparable degrees of differentiatic (Fig. 6 b). Mg/(Mg+Fe) cation ratios (Fig. 6c) further indicate significant differences, with a Mg-richer trend defined by the Arar pluton samples. For an overall comparison, samples are plotted in Fig. 7 in spidergrams, using the normalizing values of the "primordial mantle" proposed by WOOD (1979). Again comparing samples with similar degrees of differentiation, the most noticeable features are: 1) the LILE/HFSE ratios (as Rb/Zr) are clearly lower in the FG than the PTG group; 2) Nb, Zr and REE contents increase slightly but significantly from Arar to Infero granodiorites. Chondrite-normalized REE patterns for Arar and Infero PTG are represented in Fig. 8. REE patterns for Arar samples are similar, although some dispersion of values occurs: a negative Eu anomaly is shown by granitic samples, while a reduced or positive Eu anomaly appears in the less evolved (granodioritic) samples,

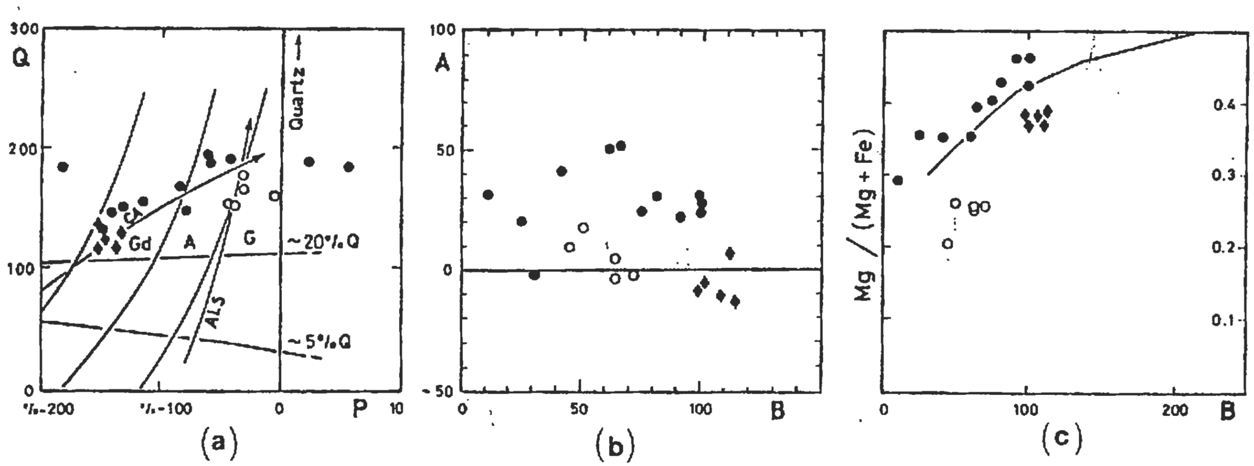


Fig. 6 - 1) Q = quartz (Si/3 - (K+Na+2Ca/3)) vs. P = plagioclase diagram; 2) A = alumina index Al - (Na+K+2Ca) vs. B = mafics (Fe+Mg+Ti) diagram; 3) Mg/(Mg+Fe) vs. B diagram; datum-line separates high-Mg and high-Fe plutonic sequences. Foliated granites (open circles); post-tectonic undeformed granitoids: Infero granodiorites (diamond), Arar granodlorites and granites (filled circles). G: granites; Ad: Adamellites; Gd: granodiorites; CA, ALS: Calc-alkaline and oversaturated alkaline trends, from DEBON and LEFORT (1988).

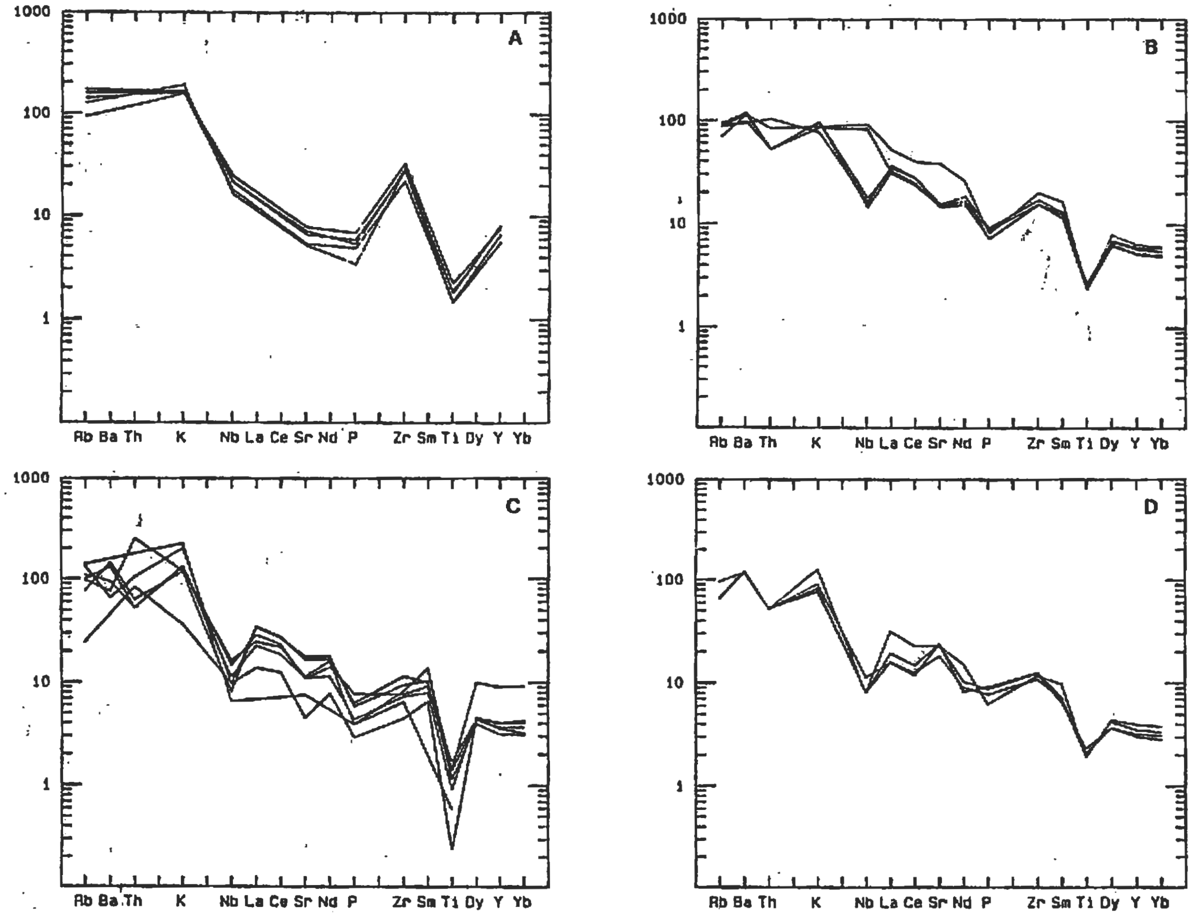


Fig. 7 - Minor and trace element abundances normalized to primordial mantle composition (WOOD, 1979) for foliated younger granites (A) and post-tectonic Infero granodiorites (B), Arar granites (C) and granodiorites (D).

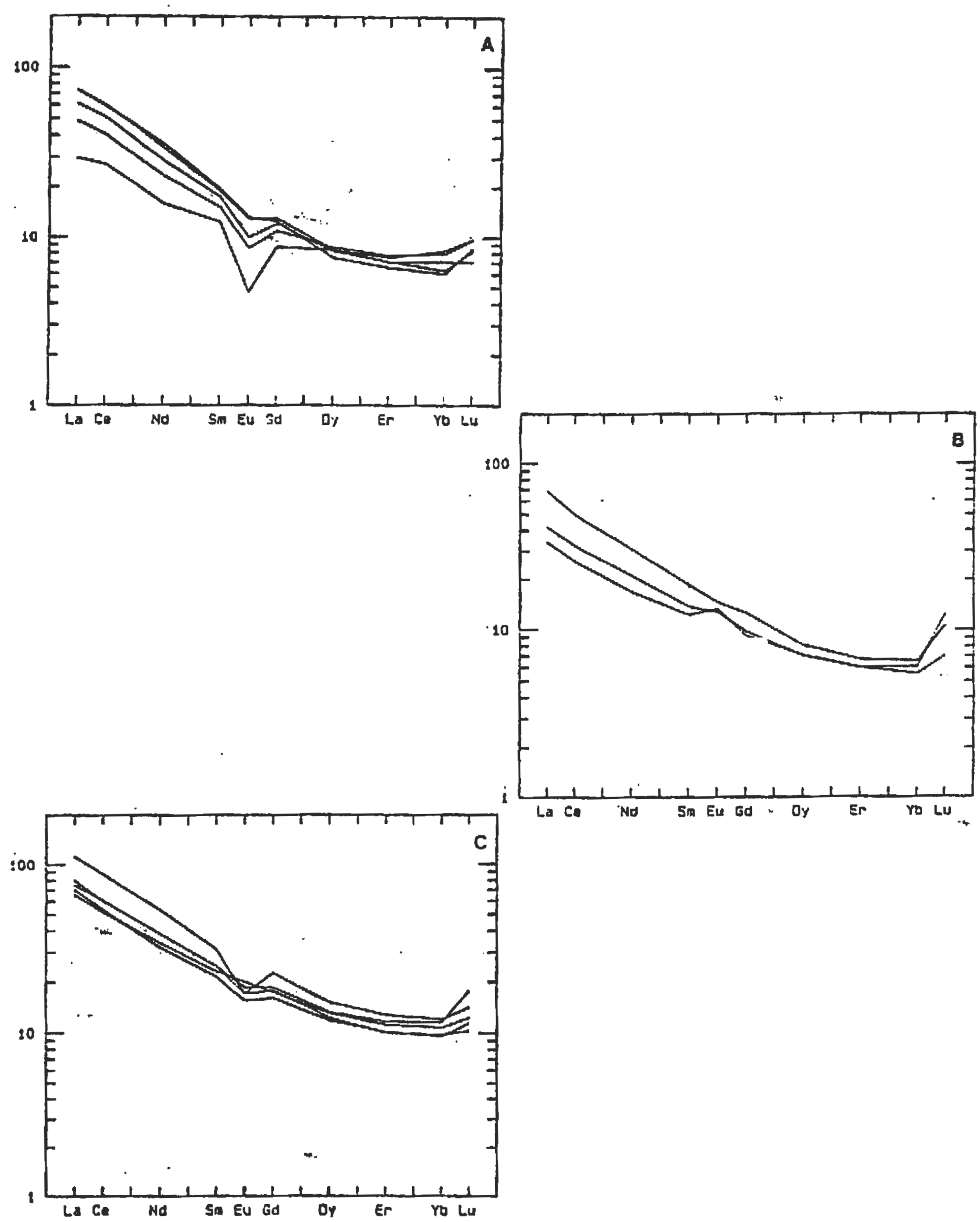


Fig. 8 - REE normalized diagram for Arar (A: granites, B: granodiorites) and Infero (C) post-tectonic plutons.

probably due to cumulus processes or to oxidizing/hydratation conditions. Samples from the Infero body again show significant differences by having greater REE enrichment (mainly middle and heavy REE).

Without any classification purpose, we used the Rb vs (Y+Nb) and Rb/Zr vs $SiO_2$ diagrams proposed by PEARCE et al. (1984) with discriminating fields built-up only for Phanerozoic intrusives (Figs. 9; 10), although elements as Rb may have been mobilized in FG during the tectono-metamorphic imprint: in any case, high Y+Nb contents with moderate Rb/(Y+Nb) ratios may be assumed as indicative of a somewhat "interplate" tendency. The FG and Infero samples appear to be Y+Nb-enriched with respect to the Arar samples.

## Discussion on geochemical data

The geochemical trends of the relatively older FG group area characterized by high Nb and Zr contents and low Mg and Al abundances, pointing to some similarity with A-type (COLLINS et al., 1982) or within-plate (PEARCE et al., 1984) granitoids. The analysed FG samples are representative of a single group of granites which can be hardly interpreted as differentiated types from subcrustal mafic melts. They recall, for instance, some Pan-African granites from Adrar des Iforas (BOULLIER et al., 1986) and the Arabian-Nubian Shield (e.g. HUSSEIN et al., 1982; STERN and HEDGE, 1985; STOESER, 1986) which record post-collisional relaxation and rifting. In particular, they may be compared with western Arabian granites, which have been interpreted as nearly dry melting products of depleted continental crust, thermally assisted by igneous underplating under post-tectonic extensional conditions (JACKSON et al., 1984). This model does fit the late evolution history of the northern Somali basement which, after the high-grade tectono-metamorphic cycle, is thought to be characterized by extensional lithospheric attenuation and related thermal perturbance, rising and partial melting of hot asthenolitic bodies allowing the generation of the gabbro-monzonite batholiths, fast heat transfer into overlying crustal sections, facilitating the anatectic melting. These processes were assisted by tensive or transtensive deformation of the continental crust (DAL PIAZ et al., this volume). The geochemical features of the foliated younger granites seem to exclude any possibility that a subduction-related magmatic arc was recorded by these rocks in North-eastern Somalia.

Instead, the post-tectonic undeformed granitoids display chemical compositions which are partly comparable with those of I-type granites, as defined by CHAPPEL and WHITE (1974) and WHITE and CHAPPEL (1977), although they are lacking of the wide acidic to mafic compositional spectrum which commonly characterizes the I-type plutons. The post-tectonic bodies are similar to calc-alkaline granitoids occurring in active continental margins and to Alpine-type post-collisional ones. In any case, the Arar and Infero undeformed bodies can hardly be referred to a subduction-related magmatic activity, because they were clearly emplaced after the last Pan-African tectono-metamorphic event in North-eastern Somalia which, in turn, cannot be interpreted as collisional suture of a former trench-arc system.

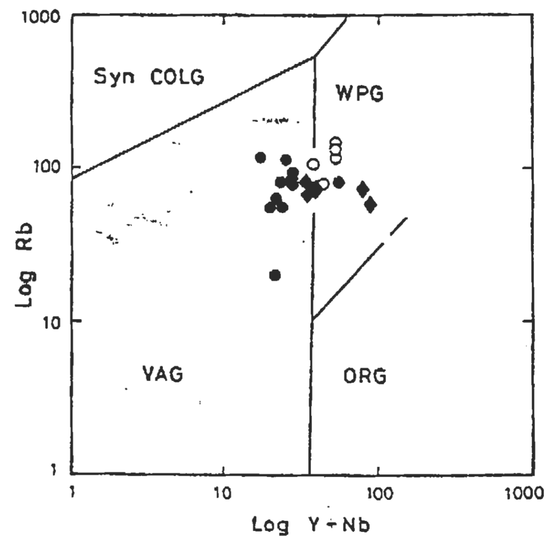


Fig. 9 - Log Rb vs. Log Y+Nb diagram (PEARCE et al., 1984) for foliated and post-tectonic granitoids. ORG: ocean ridge granites; syn-COLG: syn-collisional granites; WPG: within-plate granites; VAG: volcanic arc granites. Symbols as in Fig. 5.

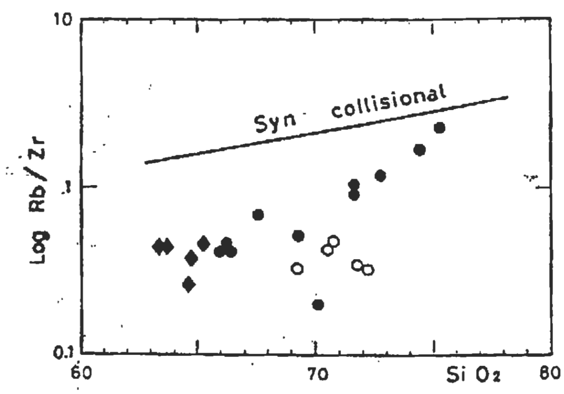


Fig. 10 - Log Rb/Zr vs. $SiO_2$ diagram (HARRIS et al., 1986), discriminating volcanic arc and collisional granites from syn-collisional granites. Symbols as in Fig. 5.

Melt generation processes which assisted the genesis of the PTG group may have involved crustal sources of ultimate intrusive origin (as "classic" I-type granites), but the only moderate Al enrichment rules out any direct involvement of an upper crust of metasedimentary composition. More reliably, according to the above data, the PTG intrusives may be differentiated products of subcrustal mafic melts, with some involvement of crustal components. This interpretation is also supported by the low initial Sr isotope ratio recorded by the Arar intrusives (0.70391; ABBATE et al., 1985, and next chapter).

## GEOCHRONOLOGY

Rb-Sr isotope data have been collected on 13 selected samples from the Arar and Infero post-tectonic granitoids and capping thermally metamorphosed clastic sequences of the Inda Ad Complex, as follows: 3 granites (SML 1, 2, 198), 4 granodiorites (SML 4, 197, 212, 214), 2 aplite dykes (SML 5, 27) and 1 biotite- rich hornfels (SML 7) from the Arar pluton; 2 granodiorites (SML 435, 462) and 1 biotite-cordierite-rich hornfels from the Infero body. Data are reported in Table 4.

Within the evolution diagram of Sr isotope composition, 9 granite and granodiorite samples from the Arar pluton plot around a regression line which, yielding an age of 541 Ma, is graphically indistinguishable from the isochron reported in Fig. 11. Samples plotting relatively farther from the straight line are represented by aplitic dyke SML 5 and the granites SML 1 and SML 2, which cannot be derived from the parent magma generating the other 6 samples. Alternatively, they may record contaminating processes episodically involving the parent magma during its rise or crustal emplacement. The other 6 samples (5 granite- granodiorites and 1 aplite) yield a isochron of 549 $\pm$ 14 Ma (2s; MSWD = 4.6) (Fig. 11), which may be interpreted as the intrusion age within the uppermost continental crust. The low initial Sr isotope ratio (0.70391 $\pm$9) suggests the noticeable contribution of subcrustal melts in generating the Arar granitoids.

If we hypothesize a coeval intrusion age for both the Arar and Infero plutons, Infero granodiorite samples SML 435 and SML 462 appear to have been generated from melts characterized by relatively higher $Sr^{87}$ contents (initial Sr isotope ratios = 0.7056 and 0.7065). These features may be referred to increasing processes of crustal contamination within the Infero magmatic chamber, or to distinct melt sources characterized by different chemical and isotope compositions.

Biotite Rb-Sr ages from the Arar and Infero granitoids record the latest cooling stages of the bodies. They cluster around 513 $\pm$ 15 and 489 $\pm$ 14 Ma for the Arar pluton and 498 $\pm$ 15 and 499 $\pm$ 15 Ma for the Infero body. Biotites coming from high-grade hornfelses of the thermal aureole on the Inda Ad clastic sequence surrounding the Arar (SML 7) and Infero (SML 429) plutons yield Rb-Sr cooling ages of 525 $\pm$ 16 and 516 $\pm$ 16 Ma respectively; these data may indicate that the border zone of these plutons cooled faster than their cores.

Table 4 - Isotope data from Arar and Infero post-tectonic undeformed granitoids.

| Sample | rock type | material | Rb ppm | Sr ppm | $^{87}Rb/^{86}Sr$ | $^{87}Sr/^{86}Sr \pm$ | age (Ma) |
|---|---|---|---|---|---|---|---|
| ARAR PLUTON | | | | | | | |
| SML 1 | GR | WR | 98 | 269 | 1.040 | 0.71276 ± 14 | |
| | | KF | 57 | 279 | 0.589 | 0.70808 ± 18 | 513 ± 15 |
| | | Bi | 624 | 8.4 | 255.004 | 2.55620 ± 153 | |
| SML 2 | GR | WR | 109 | 244 | 1.289 | 0.71348 ± 5 | |
| SML 4 | GD | WR | 69 | 419 | 0.480 | 0.70764 ± 6 | |
| SML 197 | GD | WR | 78 | 463 | 0.491 | 0.70759 ± 8 | |
| SML 198 | GR | WR | 98 | 284 | 1.004 | 0.71211 ± 10 | |
| SML 212 | GD | WR | 58 | 628 | 0.269 | 0.70608 ± 4 | |
| SML 214 | GD | WR | 60 | 614 | 0.284 | 0.70608 ± 6 | |
| | | KF | 20 | 647 | 0.087 | 0.70473 ± 13 | 489 ± 14 |
| | | Bi | 305 | 8.3 | 114.721 | 1.50484 ± 116 | |
| SML 5 | AP | WR | 114 | 69 | 4.836 | 0.73929 ± 28 | |
| SML 27 | AP | WR | 110 | 129 | 2.485 | 0.72300 ± 13 | |
| SML 7 | HF | WR | 114 | 96 | 3.457 | 0.73749 ± 26 | 525 ± 16 |
| | | Bi | 309 | 11.7 | 81.027 | 1.31759 ± 81 | |
| INFERO PLUTON | | | | | | | |
| SML 435 | GD | WR | 80 | 360 | 0.645 | 0.71014 ± 13 | 498 ± 15 |
| | | Bi | 412 | 5.0 | 286.006 | 2.73403 ± 94 | |
| SML 462 | GD | WR | 79 | 391 | 0.588 | 0.71071 ± 17 | 499 ± 15 |
| | | Bi | 406 | 5.1 | 275.464 | 2.66466 ± 93 | |
| SML 429 | HF | WR | 124 | 146 | 2.448 | 0.73567 ± 21 | 516 ± 16 |
| | | Bi | 415 | 19.1 | 65.926 | 1.20252 ± 34 | |

GR: granite; GD: granodiorite; A: aplite; HF: hornfels, Inda Ad; WR: whole rock; KF: K-feldspar; Bi: biotite. Analysts: U.Giannotti and G.Pardini, CNR Pisa.

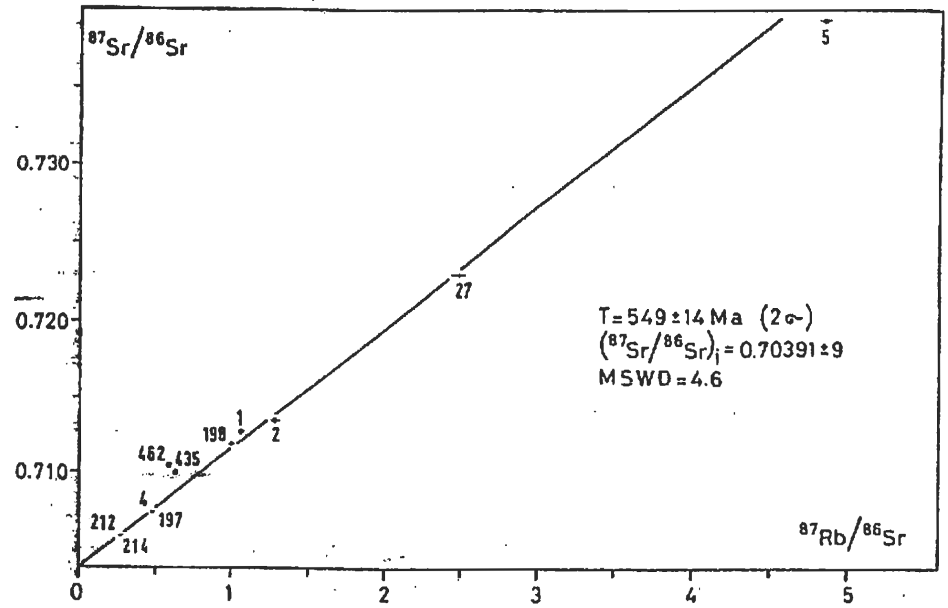


Fig. 11 - Rb-Sr isochron diagram for Arar and Infero post-tectonic plutons. If Arar two-mica granites SML 1-SML 2 and aplite dyke SML 5 (open circle) and two Infero granodiorites (open triangle) are omitted from regression line, remaining Arar rocks define a quite good isochron corresponding to an age of 549 ± 14 Ma.

## CONCLUSIONS

Two diachronous groups of Pan-African younger granites are exposed in North-eastern Somalia along the Maydh-Boosaso coastal strip, east of the polymetamorphic "older basement" which extends from the Ethiopian border to the Xiis area. The first group is represented by poorly foliated to sheared or mylonitic granites, largely exposed within a tectonically bound belt between the underlying Xiis "older basement" and the overlying Maydh volcano- sedimentary mafic complex. Their intrusive emplacement predates a Pan-African tectono-metamorphic event which also overprinted the Maydh and Inda Ad complexes, reaching at the exposed structural levels greenschist to very low-grade physical conditions. The second group is represented by the Arar, Infero and Las Bar post-tectonic undeformed granitoids which were sharply intruded during Early Cambrian at a very shallow crustal level, thermally overprinted the already deformed and regionally metamorphosed Maydh and Inda-Ad roofing complexes and relatively fast cooled down.

The distinction of these groups is further supported by their composition and chemical affinity, which suggest diversified sources and melt-producing mechanisms. The relatively older foliated bodies display a some within-plate or A-type affinity and may be compared with most of the NE African granites which are derived from depressuring continental crustal sources through thermal perturbance and extensional tectonics. For instance, they may be compared to some Pan-African alkali granites from the western Arabian shield which have been referred to nearly dry melting processes of a depleted crust, thermally assisted by rising of subcrustal magmas under extensional regimes (e.g., JACKSON et al., 1984).

Instead, the post-tectonic granitoids display calc-alkaline features and some affinity with I-type granites. Nevertheless, these signatures characterize different geodynamic settings and cannot be exclusively seen as representative of subduction-related magmatic arc activity. The discussed plutons post-date the last Pan-African orogenic cycle recorded in Northern Somalia and cannot be related to formerly subducting lithosphere, as suggested by WARDEN and HORKEL (1984), due to inconsistent timing relationships and the general absence of markers supporting such a hypothesis. By comparison with the extensional geodynamic setting which facilitated, for instance, the emplacement of Late Paleozoic and Tertiary calc-alkaline plutons of the Alps and other similar belts (e.g. DAL PIAZ and VENTURELLI, 1985, and refs. therein), tensive or transtensive regional conditions were probably renewed in Northern Somalia after the compressive or transpressive Pan-African cycle and related metamorphic imprint recorded by the Maydh/Inda-Ad fold belt; these conditions may have facilitated the melting of subcrustal sources and the rising of magmas which were emplaced and differentiated within shallower magmatic chambers where some interaction with continental crust may be envisaged.

In conclusion, we suggest that lithosphere attenuation through tensive/transtensive conditions, crustal underplating of gabbro bodies and related thermal perturbance may have assisted the Early Pan-African depressuring evolution of the "older basement", large production of migmatites, ensialic intrusion and volcanic emplacement of mafic to silicic melts supplied by mantle and lower crustal sources, coupled with tectonic unroofing and the opening of graben or pull-apart basins. The Maydh/Inda-Ad late Pan-African tectono-metamorphic event may have been mainly produced by inversion of these tensive structures. In conclusion, both the foliated granites and post-tectonic undeformed granitoids from North-eastern Somalia represent the latest records of Pan-African repeated extensional pulses which operated in the northern Somali basement, as a whole, from the ensialic gabbro emplacement onwards.

## Analytical Techniques

Major and trace element geochemistry on the foliated younger granites was performed by A. BONAZZI and E. SAVIOLI MARIANI by means of X-ray atomic absorption techniques at the Mineralogical Institute, University of Parma. For post-tectonic granitoids, major elements were detected by G. MEZZACASA and G. RIGATTI through X-ray atomic absorption at the Department of Mineralogy and Petrology, University of Padova; REE abundances were analysed by plasma spectrophotometry at the CGPG Laboratory, Nancy. Geochronological and isotope data were collected by A. DEL MORO at the Istituto di Geocronologia e Geochimica Isotopica, CNR, Pisa. Whole-rock, K-feldspar and biotite samples of usually about 150 mg were analysed by dissolving them in a HF and $HClO_4$ mixture. The dissolved biotite samples were split for separate measurements of Rb concentrations and Sr isotope composition and content. Other samples were spiked with enriched $Rb^{87}$ (98%) and $Sr^{84}$ (99.892%) from the beginning. Sr was separated using the standard cation exchange technique. Isotope analyses were made on a TH5 Varian-Mat mass spectrometer. Analyses of NBS 987 on this machine over a four-year period gave an $Sr^{87}/Sr^{86}$ ratio of 0.71028 $\pm$ 5 (2s; n = 23). All Rb-Sr ages were calculated with a decay constant of 1.42 x E-11/a.

ACKNOWLEDGMENTS

The geological staff of the Somali National University is gratefully acknowledged, as well as the fruitful geological assistance kindly supplied by E. ABBATE and A. KASSIM during the field trips. E. CALLEGARI and an anonymous referee are acknowledged for the constructive review of the manuscript.

REFERENCES

ABBATE E., CALI K.M., DAL PIAZ G.V., GOSSO G., IBRAHIM, H.A. and RIGATTI G. (1981). Note di rilevamento sul basamento cristallino della Somalia settentrionale nell'area Rugay-Maydh-Xiis, Distretto di Ceerigabo. Rend. Soc. Geol. Ital., 4: 333-337.

ABBATE E., BONAZZI A., DAL PIAZ G.V., DEL MORO A., GOSSO G., IBRAHIM H.A. and SAVIOLI MARIANI E. (1985). Il settore occidentale dell'unità di Inda Ad ed il granito di Arar (Somalia settentrionale). Univ. Naz. Somala. Quaderni geol. Somalia, 8: 7-25.

BOULLIER A.M., LIEGEOIS J.P., BLACK R., FABRE J., SAUVAGE M. and BERTRAND J.M. (1986). Late Pan-African tectonics marking the transition from subduction-related calc-alkaline magmatism to within-plate alkaline granitoids (Adrar des Iforas, Mali). Tectonophysics, 132: 233-246.

CALLEGARI E. (1985). Geological and petrological aspects of the magmatic activity in Adamello (Northern Italy). Mem. Soc. Geol. Ital., (1983) 26: 83-103.

CHAPPEL B.W. and WHITE A.J.R. (1974). Two contrasting granite types. Pac. Geol., 8: 173-174.

COLLINS W.J., BEAMS S.D., WHITE A.J.R. and CHAPPEL B.W. (1982). Nature and origin of A-type granites with particular reference to south-eastern Australia.

Contrib. Mineral. Petrol., 80: 189-200.

DAL PIAZ G.V., RIGATTI G., GALLI M., MESSIGA B., PICCARDO G.B., BORGOGNONI S., GOSSO G., SPALLA M.I., PECCERILLO A., POLI G., PARRINI P.L., TODARO M.L., FERRARA G. and TONARINI S. (1985). Il gabbro di Sheikh (Somalia settentrionale): dati geologici, petrografici, geochimici e geocronologici preliminari. Univ. Naz. Somala. Quaderni geol. Somalia, 8: 151-186.

DAL PIAZ G.V., IBRAHIM H.A., GOSSO G., PICCARDO G.B. and RIGATTI G. (1987 a). The Sheikh gabbro body and the Hudiso paragneisses. Excursion B Guidebook. Geosom 87 Intern. Meeting, Mogadishu, 23-42.

DAL PIAZ G.V., RIGATTI G., ABBATE E., GOSSO G., ALI KASSIM M., IBRAHIM H.A. and SAID A.A. (1987 b). Note di rilevamento sul basamento cristallino della Somalia settentrionale tra Heis, Erigavo e Bosaso. Univ. Naz. Somala. Quaderni geol. Somalia, 9: 31 pp.

DAL PIAZ G.V. and SASSI F.P. (1988). The crystalline basement of Somalia: a review. Mem. Soc. Geol. Ital. (1986) 31: 351-361.

DAL PIAZ G.V. and VENTURELLI G. (1985). Brevi riflessioni sul magmatismo post-ofiolitico nel quadro dell'evoluzione spazio-temporale delle Alpi. Mem. Soc. Geol. Ital. (1983) 26: 5-19.

D'AMICO C., IBRAHIM H.A. and SASSI F.P. (1981). Outline of the Somalian basement. Geol. Rundschau, 70: 882-896.

DEBON F. and LE FORT P. (1988). A cationic classification of common plutonic rocks and their magmatic associations: principles, method, applications. Bull. Mineral., 111: 493-510.

ENGEL A.E.J., DIXON T.H. and STERN R.J. (1980). Late Precambrian evolution of Afro-Arabian crust from ocean arc to craton. Geol. Soc. Am. Bull., 91: 699-706.

FERRARA G., GATTO G.O., IBRAHIM H.A., SAID A.A., SASSI F.P., TONARINI S. and VISONÀ D. (1987). Sequence of events in the crystalline basement of Northern Somalia. Geosom 87 Intern. Meeting, Mogadishu, abstr. 65-66.

FERRARA G., TONARINI S., SASSI F.P. and VISONÀ D. (1985). Sull' età del massiccio granitico di Daymoleh (Somalia settentrionale). Quaderni geol. Somalia, 8: 233-241.

GREENWOOD J.E. (1960). Report on the geology of the Las Khoreh-Elayu area, Erigavo District. Somaliland Protect. Geol. Surv. Rep., 3: 36 pp.

HARRIS N.B.W., PEARCE J.A. and TINDLE A.G. (1986). Geochemical characteristics of collision-zone magmatism. In: Collision Tectonics (edited by COWARD M.P. and RIES A.C.), 67-81. Geol. Soc. Spec. Publ., 19.

HUSSEIN A.A., ALI M.A. and EL RAMLY M.F. (1982). A proposed new classification of the granites of Egypt. J. Volcan. Geoth. Res., 4: 187-198.

JACKSON N.J., WALSH J.N. and PEGRAM E. (1984). Geology, geochemistry and petrogenesis of Late Precambrian granitoids in the central Hijaz region of the Arabian Shield. Contrib. Mineral. Petrol., 87: 205-219.

LEAKE B.E. (1978). Nomenclature of amphiboles. Soc. Franç. Minéral. Cristall., 101: 453-467.

MASON J.E and WARDEN A.J. (1956). Report on the geology of the Heis-Mait-Waqderia area, Erigavo District. Somaliland Protect. Geol. Surv. Rep., 1: 23 pp.

PEARCE J.A., HARRIS N.B.W. and TINDLE A.G. (1984). Trace element discrimination diagrams for the tectonic interpretation of granitic rocks. J. Petrol., 25: 956-983.

ROOKE J.M. (1970). Geochemical variations in African granitic rocks and their structural implications. In: African Magmatism and Tectonics (edited by CLIFFORD T.N. and GASS I.G.), 355-417, OLIVER and BOYD, Edinburgh.

SNELLING N.J. (1967). Age determination results. Appendix in: Geology of the Arabian Peninsula: Aden Protectorate (GREENWOOD J.E. and BLEACKLEY D.). U.S. Geol. Surv. Prof. Paper 560 C: 93-96.

STERN R.G. and HEDGE C.E. (1985). Geochronologic and isotopic constraints on Late Precambrian crustal evolution in the Eastern Desert of Egypt. Am. J. Sci., 285: 97-127.

STOESER D.B. (1986). Distribution and tectonic setting of plutonic rocks of the Arabian Shield. J. African Earth Sci., 4: 21-46.

STOESER D.B. and CAMP V.E. (1985). Pan-African microplate accretion of the Arabian Shield. Geol. Soc. Am. Bull., 96: 817-826.

WARDEN A.J. and DANIELS J.L. (1984). Evolution of the Precambrian of the Northern Somalia. Bull. Fac. Earth Sci. King Abdulaziz Univ., 6: 145-164.

WARDEN A.J. and HORKEL A.D. (1984). The geological evolution of the NE-branch of the Mozambique belt (Kenya, Somalia, Ethiopia). Mitt. Oesterr. Geol. Ges. Wien, 77: 161-184.

WHITE A.J.R. and CHAPPEL B.W. (1977). Ultrametamorphism and granitoid genesis. Tectonophysics, 43: 7-22.

WOOD A.D. (1979). A variably veined suboceanic upper mantle. Genetic significance for mid-ocean ridge basalts from geochemical evidence. Geology, 7: 599-603.

ADDENDUM. The volume "Research in Sudan, Somalia, Egypt and Kenya" (Berliner Geowiss. Abh, REIHE A., Band 120.2, 1990), including the contribution of KÜSTER et al. on the "Pan-African granitoid magmatism in Northeastern and Southern Somalia", has appeared long after this paper was submitted to the Editors. Geochemical data and interpretation generally fit in well with our model. Despite, the contrasting U/P age on magmatic zircon reported from the Las Bar pluton does not agree, in our opinion, with the fast cooling evolution expected for the north-eastern Somali intrusive bodies which were emplaced at a very shallow crustal level.

*Final editing, January 1990*

From *Geology and mineral resources of Somalia and surrounding regions*, Ist. Agron. Oltremare, Firenze, Relaz. e Monogr. 113, 119-128, 1993.

# THE PRESSURE CHARACTER OF THE INDA AD METAMORPHISM (NORTHERN SOMALIA)

L. PERUZZO

Dipartimento di Mineralogia e Petrologia, Università di Padova, Corso Garibaldi 37, 35137 Padova, Italy.

## ABSTRACT

The Inda Ad Complex represents the metasedimentary cover of the crystalline basement of the Northern Somalia. It mainly consists of Upper Proterozoic or Cambrian sandstones, siltstones and shales, which only underwent a low-grade metamorphic event, of late Pan-African age.

The aim of this work is to estimate the baric character of metamorphism recorded in this complex.

The method used is based on the measure of the $6d_{33\bar{1},060}$ cell dimension of K-white micas in metapelites. This parameter varies as a function of the metamorphic pressure, significantly at least within the greenschist facies and for metapelites having a specific Al-rich bulk composition. Therefore it has been necessary to define the petrographic characters of the rock samples utilized.

The analytical results support the following conclusions:

1) the Inda Ad metamorphism took place under low pressure conditions;
2) correlating the average value of the $6d_{33\bar{1},060}$ parameter to the metamorphic temperature recorded in these rocks (deduced from the mineral assemblages), it has been possible to estimate a thermal gradient of ca. 20°C/km for the Inda Ad metamorphic event.

## INTRODUCTION

The problems concerning the crystalline basement of the Northern Somalia (NSB for short) are, at present, widely open under many aspects; in fact the basement structural setting and lithostratigraphy, just as the magmatic and metamorphic events which involved it, are only defined in their main outlines.

Some pieces of information on NSB are given below. For more details readers are deferred to SASSI et al. (this volume), from which the statements below are taken, and to the references quoted therein.

This crystalline basement consists of various types of metamorphic and polymetamorphic rocks, mainly Late Proterozoic in age, intruded by granitic and gabbro-syenitic bodies, and unconformably capped by a sedimentary, Mesozoic to Tertiary cover.

Following lithostratigraphic and tectonometamorphic criteria, five rock complexes making up three main supergroups have been distinguished in the NSB. The supergroups

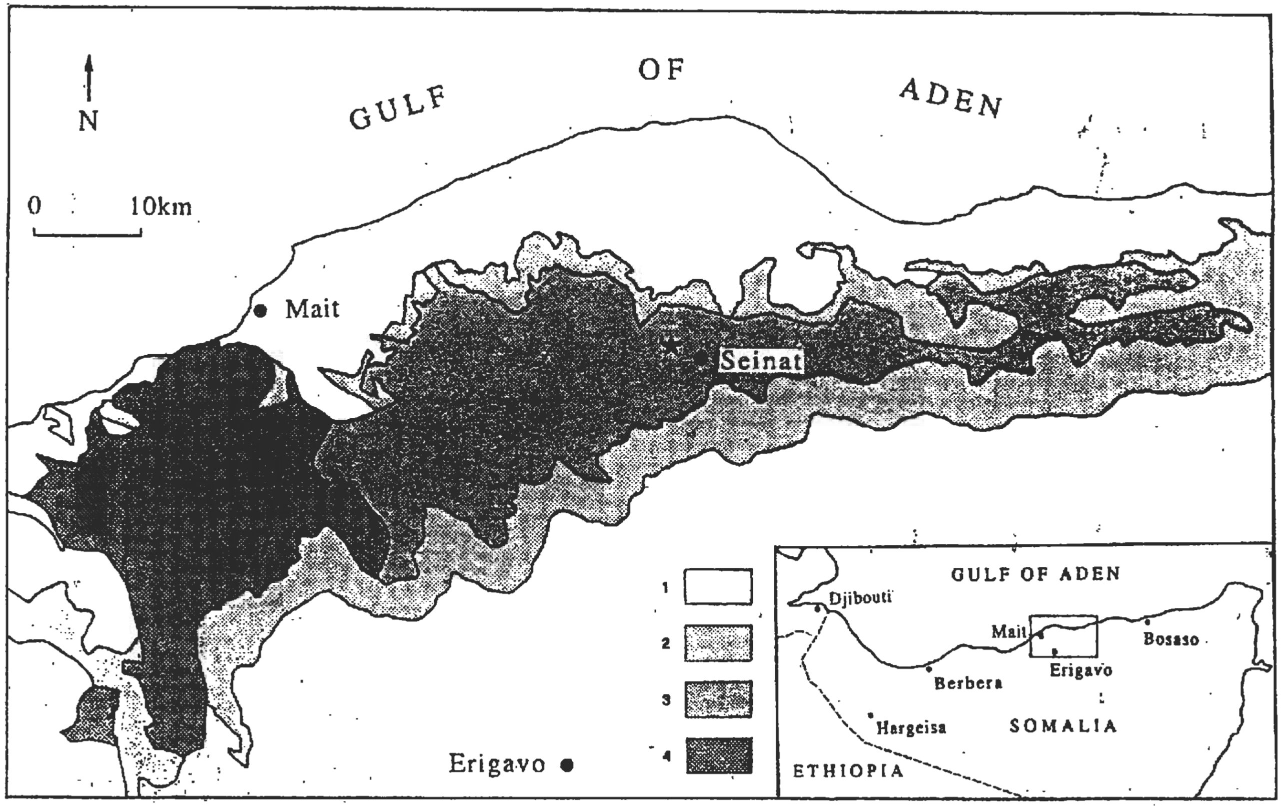


Fig. 1 - Geological sketch of the western part of the Inda Ad Complex in the crystalline basement of the Northern Somalia. 1: Tertiary cover; 2: Mesozoic cover; 3: Inda Ad Complex; 4: older basement and igneous bodies. The asterisk shows the sampled area. (Taken from ABBATE et al., 1981, with some changes).

are: an oldest high grade polymetamorphic basement (which consists of the Qabri Bahar Complex and the Mora Complex), a greenschist facies volcano-sedimentary sequence and a low to very-low grade metasedimentary cover.

The greenschist facies volcano-sedimentary supergroup has been interpreted as a cover unconformably deposited over the above mentioned ancient basement after its high grade metamorphism (WARDEN and DANIELS, 1984). This supergroup consists of two different complexes: the Abdulkadir Complex and the Mait Complex.

The Abdulkadir Complex occurs in the western and central parts of the NSB. It lies on either the Qabri Bahar Complex or the Mora Complex and is capped by the sedimentary Mesozoic cover. The metavolcanic components include metarhyolites and minor metabasites, whereas the metasediments are represented by quartz-phyllites in which minor quartzites and marbles are interlayered.

The Mait Complex is exposed in the eastern part of the NSB, very far from the Abdulkadir Complex outcrops. It lies upon the Qabri Bahar Complex and locally is covered by the younger, very low-grade supergroup. The volcanic protoliths were pillow to massive basalts, while metaclastites with minor quartz-phyllites and marbles represent the metasedimentary components of this complex.

The low to very-low grade supergroup is the Inda Ad Complex. The protoliths were sandstones, siltstones and shales, with minor intraformational conglomerates and carbonate rocks. Their sedimentation took place during the uppermost Proterozoic or Cambrian, as suggested by some problematic fossil findings (ABBATE et al., 1981), and by the radiometric ages of the granites which intruded them after their folding and very-low grade metamorphism.

The aim of the present paper is to provide some analytical data concerning the pressure character of the metamorphism which affected the Inda Ad Complex.

## GEO-PETROLOGICAL SETTING OF THE ROCK SAMPLES

The Inda Ad Complex occurs as a 150 Km long strip outcropping only in the eastern part of the NSB, from Mait to Bosaso, overlying unconformably the Mait Complex.

The rock specimens considered in this paper were collected near Seynat, as roughly shown in the sketch of Fig. 1. They are fine-grained metasediments, light grey coloured and well foliated, and represent the most pelitic layers of the Inda Ad Complex rocks, just as the specific geobarometric method utilized requires (see below).

In thin section these metapelites show a main lepidoblastic microstructure, with a flat to microfolded foliation. Primary compositional banding is sometimes remarkable, especially where quartz-feldspar-rich layers alternate with mica-rich ones: it commonly makes a low angle with the foliation.

The mineral assemblage is relatively simple: muscovite, quartz, chlorite and minor albite occur as main phases; ilmenite and carbonaceous matter are also present. A temperature value around 350 °C may be estimated for this mineral assemblage. Such

Table 1 - Chemical analyses of muscovites and chlorites.

| | Ms1 | Ms2 | Ms3 | Ms4 | Ms5 | Chl1 | Chl2 | Chl3 | Chl4 |
|---|---|---|---|---|---|---|---|---|---|
| SiO2 | 49,03 | 49,84 | 51,19 | 50,63 | 49,80 | 27,81 | 27,38 | 27,41 | 26,61 |
| Al2O3 | 31,99 | 31,08 | 29,81 | 30,93 | 30,93 | 22,39 | 22,50 | 22,14 | 22,52 |
| TiO2 | 0,50 | 0,31 | 0,30 | 0,38 | 0,21 | 0,02 | 0,05 | 0,04 | 0,06 |
| Cr2O3 | 0,05 | 0,02 | 0,00 | 0,00 | 0,00 | 0,04 | 0,00 | 0,00 | 0,00 |
| FeO | 1,38 | 1,46 | 1,49 | 1,35 | 1,31 | 15,78 | 15,66 | 15,81 | 16,23 |
| MnO | 0,00 | 0,00 | 0,03 | 0,01 | 0,06 | 0,24 | 0,34 | 0,46 | 0,29 |
| MgO | 2,15 | 2,44 | 2,88 | 2,66 | 2,39 | 21,18 | 20,72 | 21,18 | 20,49 |
| CaO | 0,00 | 0,01 | 0,01 | 0,02 | 0,01 | 0,03 | 0,04 | 0,02 | 0,00 |
| Na2O | 0,34 | 0,25 | 0,20 | 0,26 | 0,30 | 0,00 | 0,00 | 0,00 | 0,04 |
| K2O | 8,91 | 8,80 | 9,08 | 8,89 | 8,89 | 0,03 | 0,02 | 0,01 | 0,08 |
| | | on the basis of 22 oxygens | | | | | on the basis of 28 oxygens | | |
| Si | 6,51 | 6,61 | 6,74 | 6,65 | 6,63 | 5,55 | 5,52 | 5,51 | 5,42 |
| Al | 5,00 | 4,86 | 4,63 | 4,79 | 4,85 | 5,27 | 5,34 | 5,25 | 5,40 |
| Ti | 0,05 | 0,03 | 0,03 | 0,04 | 0,02 | 0,00 | 0,01 | 0,01 | 0,01 |
| Cr | 0,01 | 0,00 | 0,00 | 0,00 | 0,00 | 0,01 | 0,00 | 0,00 | 0,00 |
| Fe | 0,15 | 0,16 | 0,16 | 0,15 | 0,15 | 2,63 | 2,64 | 2,66 | 2,76 |
| Mn | 0,00 | 0,00 | 0,00 | 0,00 | 0,01 | 0,04 | 0,06 | 0,08 | 0,05 |
| Mg | 0,43 | 0,48 | 0,57 | 0,52 | 0,47 | 6,30 | 6,22 | 6,35 | 6,22 |
| Ca | 0,00 | 0,00 | 0,00 | 0,00 | 0,00 | 0,01 | 0,01 | 0,00 | 0,00 |
| Na | 0,09 | 0,06 | 0,05 | 0,07 | 0,08 | 0,00 | 0,00 | 0,00 | 0,02 |
| K | 1,51 | 1,49 | 1,53 | 1,49 | 1,52 | 0,01 | 0,01 | 0,00 | 0,02 |
| | | | | | | | | | |
| Si+Al | 11,51 | 11,47 | 11,37 | 11,44 | 11,48 | 10,82 | 10,86 | 10,76 | 10,82 |
| Si/(Si+Al) | 0,56 | 0,58 | 0,59 | 0,58 | 0,58 | 0,51 | 0,51 | 0,51 | 0,50 |
| Na+K | 1,60 | 1,55 | 1,58 | 1,56 | 1,60 | | | | |
| Na/(Na+K) | 0,06 | 0,04 | 0,03 | 0,04 | 0,05 | | | | |
| Fe+Mg | 0,58 | 0,64 | 0,73 | 0,67 | 0,72 | 8,93 | 8,86 | 9,01 | 8,98 |
| Fe/(Fe+Mg) | 0,26 | 0,25 | 0,22 | 0,22 | 0,21 | 0,29 | 0,30 | 0,29 | 0,31 |
| Fe/Mg | 0,35 | 0,33 | 0,28 | 0,29 | 0,32 | 0,42 | 0,42 | 0,36 | 0,44 |

a T value is consistent with the values of the illite crystallinity obtained by ABBATE et al. (1985).

The chemistry of 5 muscovite and 4 chlorite flakes (Table 1) have been analyzed by means of a CAMECA/CAMEBAX microprobe, operated at 15 kV with a 15 nA sample current. Similar synthetic and natural standards (provided by CAMECA) were used, and the conversion of X-ray counts into oxide weight percentage were made using a PAP correction program. The analytical data are schematically resumed in the diagrams of Fig. 2 and Fig. 3.

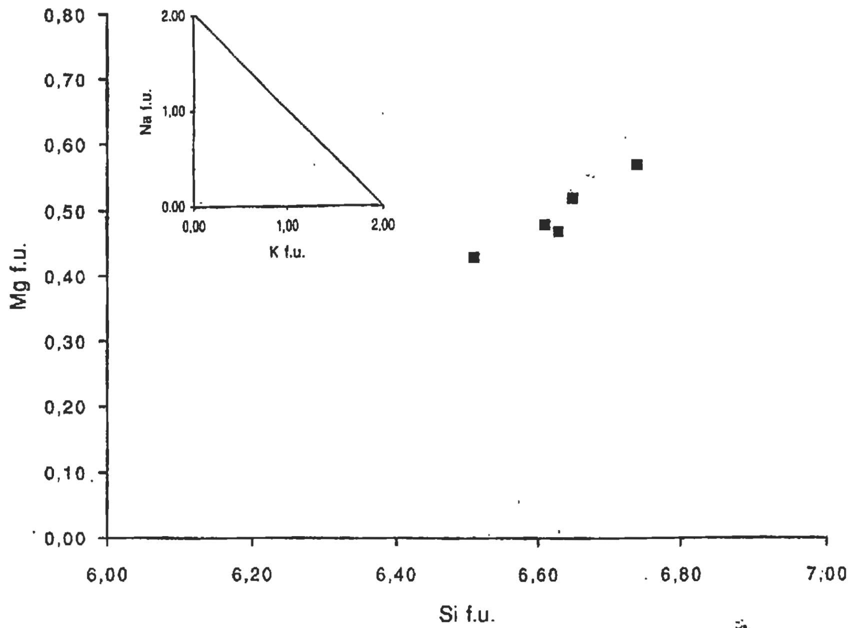


Fig. 2 - Some chemical features of the analyzed muscovites.

## THE BAROMETRIC METHOD AND ANALYTICAL PROCEDURES

The absence in low-grade metapelites, as those considered here, of minerals or mineral assemblages which may indicate the pressure conditions of metamorphism, made necessary to formulate an alternative geobarometric method.

SASSI (1972), SASSI and SCOLARI (1974) proposed such a method, which was successively developed by GUIDOTTI and SASSI (1976, 1986).

It is based on the increase of the phengite content of K-white micas as a function of the metamorphic pressure reached during the greenschist facies metamorphism of pelitic rocks having a specific Al-rich bulk composition. The phengite content is

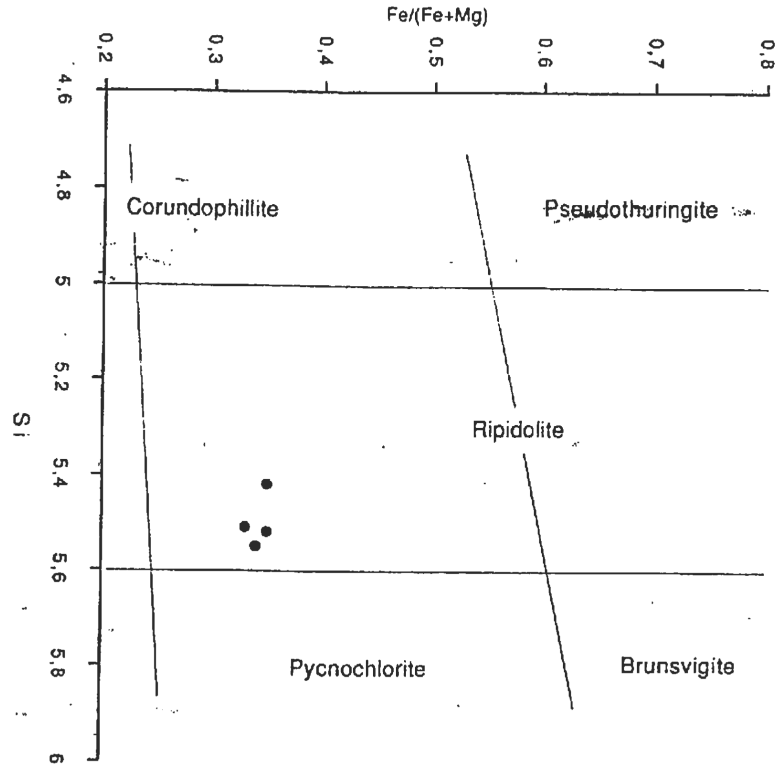


Fig. 3 - Classification of the analyzed chlorites (after HEY M.H., 1954, Min. Mag., 30. p. 277).

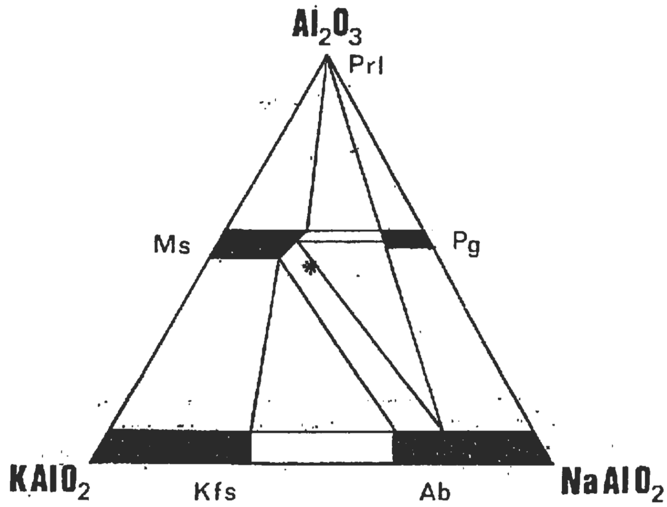


Fig. 4 - The asterisk shows the AKNa minerals assemblage in the analyzed samples, and roughly their chemical composition.

estimated by means the value of the b cell dimension (or, more correctly, the $6d_{33\bar{1},060}$).

The analytical procedure proposed by SASSI and SCOLARI (1974), allows to measure the $6d_{33\bar{1},060}$ spacing directly on rock slices cut perpendicularly to schistosity, using the quartz of the rock and added metallic silicon as standards.

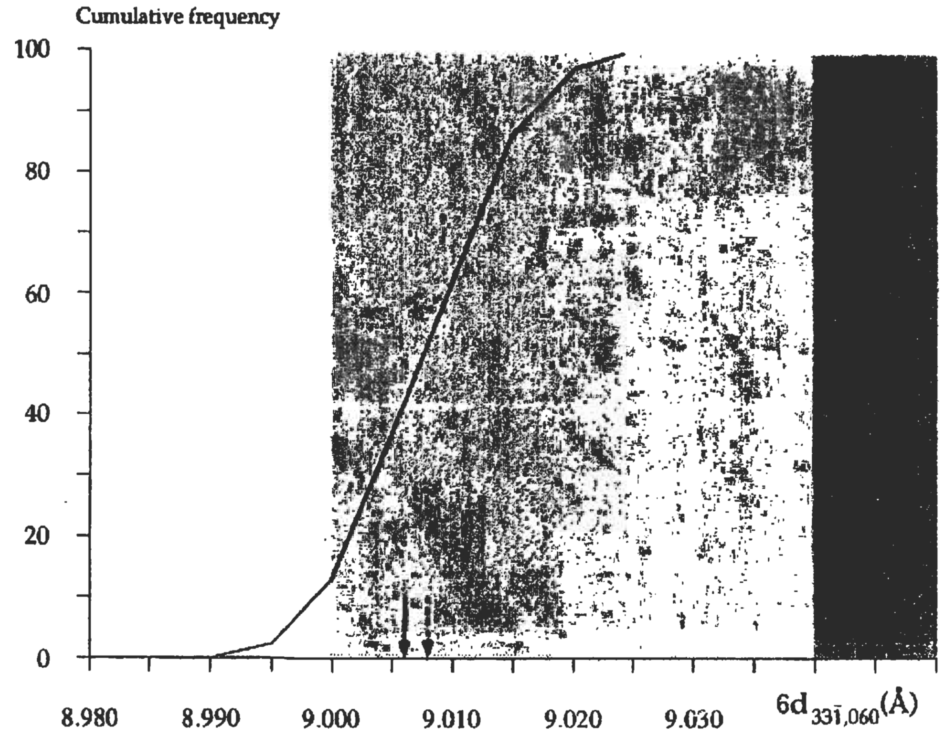


Fig. 5 - Cumulative frequency curve of 38 muscovite $6d_{33\bar{1},060}$ values, the average of which is indicated by the solid arrow. The dashed arrow indicates the average of 31 $6d_{33\bar{1},060}$ values >9.000Å. The boundaries between low (white), intermediate (grey) and high (dark grey) pressure fields are taken from GUIDOTTI and SASSI (1986)

## ANALYTICAL RESULTS

In order to use the above method in the correct way, 38 metapelitic samples have been selected according to the compositional constraints suggested by the above-mentioned authors (Fig. 4).

The $6d_{33\bar{1},060}$ values obtained from them are shown globally in the frequency

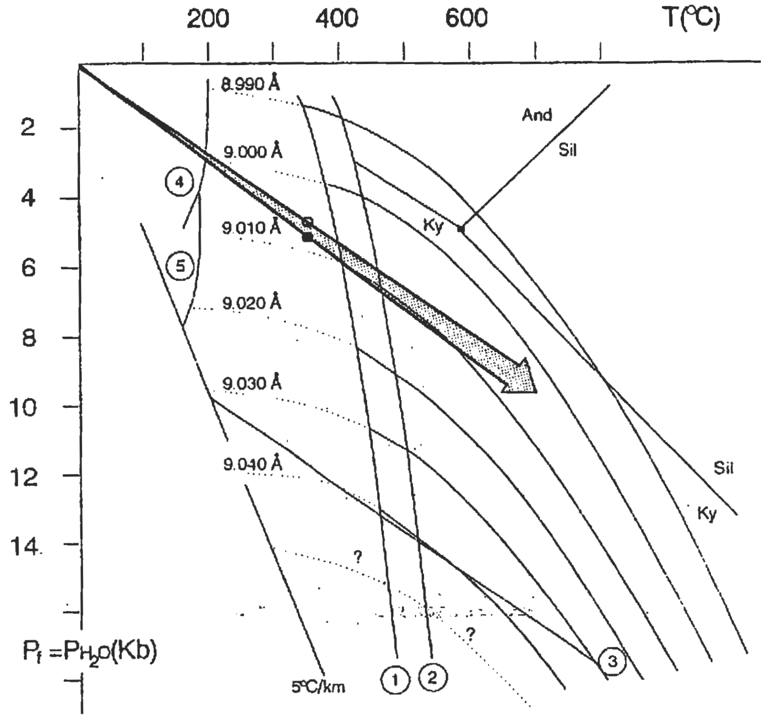


Fig. 6 - Thermal gradient during the Inda Ad metamorphism, as estimated on the basis of T value 350°C and $6d_{33\bar{1},060}$ average values:
o based on the average of 9.006Å (all 38 data);
● based on the average of 9.008Å (31 data).
The isopleths of $6d_{33\bar{1},060}$ are taken from GUIDOTTI and SASSI (1986), modified by SASSI (1987). All curves are redrawn from SASSI (1987): curve 1: Kln+Qtz >Prl+$H_2O$; curve 2: Prl >$Al_2SiO_5$+Qtz+$H_2O$; curve 3: Gln-in; curve 4: Anl+Qtz >Ab; curve 5: Hul >Lws+Qtz; symbols as in KRETZ (1983).

distribution curve of Fig. 5. They range over a relatively wide interval, from 8.992 to 9.020 Å, giving an average value of 9.006 Å, with a sufficiently low standard deviation value (s = 0.007).

As regards the lower values (≤9.000 Å), it is possible that the related samples contain small amounts of paragonite, not enough to be detected by means of X-ray powder analyses, but sufficient to decrease the phengite content in muscovite, and consequently the values of $6d_{33\bar{1},060}$. If this 7 samples are disregarded, the average $6d_{33\bar{1},060}$ value calculated from the remaining 31 data is 9.008 Å, with standard deviation s = 0.005. In every case, these data indicate that the Inda Ad metamorphism took place under intermediate pressure conditions (GUIDOTTI and SASSI, 1986); however, it is necessary to emphasize that the 9.006 Å value falls in the lowest pressure range belonging to the intermediate pressure facies series.

## CONCLUSIONS

Utilizing the temperature value of about 350°C above deduced from the mineral assemblage, and a geobaric gradient of 0.3 Kb/Km, the two average values of $6d_{33\bar{1},060}$ obtained indicate a metamorphic thermal gradient in the range between ca. 20 (corresponding to $6d_{33\bar{1},060}$ = 9.008Å) and 22°C/Km (corresponding to $6d_{33\bar{1},060}$ = 9.006Å). Therefore, as can be deduced from Fig. 6, the metamorphic event recorded in the Inda Ad Complex should have produced kyanite in rocks of suitable bulk composition and metamorphic grade. In the ambit of the NSB, kyanite has been reported within the Qabri Bahar, Mora and Abdulkadir Complexes, but related to older metamorphic events (M2 and M3, in: SASSI et al., this volume).

## ACKNOWLEDGMENTS

The author would like to express his gratitude to Prof. F.P. SASSI for his critical reading of the paper, as well as for the financial support (MURST, 60%). Thanks are due also to C.N.R, Centro di Studio per i Problemi dell'Orogeno delle Alpi Orientali, and to Mr. R. MENEGAZZI for the measurements of the $6d_{33\bar{1},060}$ and Mr. R. CARAMPIN for his assistance in the microprobe analyses.

## REFERENCES

ABBATE E., ALI KASSIM M., DAL PIAZ G.V., GOSSO G., IBRAHIM H.A. and RIGATTI G. (1981). Note di rilevamento sul basamento cristallino della Somalia settentrionale nell'area Rugay-Maydh-Xiis, Distretto di Ceerigabo. Rend. Soc. Geol. It., 4: 333-337.

ABBATE E., BONAZZI A., DAL PIAZ G.V., DEL MORO A., GOSSO G., IBRAHIM H.A. and SAVIOLI MARIANI E. (1985). Il settore occidentale dell'Unità di Inda Ad ed il granito di Arar (Somalia settentrionale). Univ. Naz. Somala. Quaderni Geologia Somalia, 8: 7-25.

GUIDOTTI C.V. and SASSI F.P. (1976). Muscovite as a petrogenetic indicator mineral in pelitic schists. N. Jb. Mineral. Abh., 127: 97-142.

GUIDOTTI C.V. and SASSI F.P. (1986). Classification and correlation of metamorphic facies series by means of muscovite b data from low-grade metapelites. N. Jb. Mineral. Abh., 153: 363-380.

HEY M.H. (1954). A new review of the chlorites. Min. Mag., 30: 277 pp.

KRETZ R. (1983). Symbols for rock-forming minerals. Amer. Mineral., 68: 277-279.

MASON J.E. and WARDEN A.J. (1956). The geology of the Heis-Mait-Waqdeira area, Erigavo District. Somaliland Protect. Geol. Surv., 1: 1-23.

SASSI F.P. (1972). The petrologic and geologic significance of the $b_0$ value of potassic white micas in low-grade metamorphic rocks. An application to the Eastern Alps. Tsch. Mineral. Petrogr. Mitt., 18: 105-113.

SASSI F.P. (1987). Geobarometria basata sul contenuto in celadonite s.s. nella muscovite. In: D'AMICO C., INNOCENTI F. and SASSI F.P. (1987). "Magmatismo e Metamorfismo", UTET, 448-449.

SASSI F.P. and SCOLARI A. (1974). The $b_0$ value of the potassic white micas as a barometric indicator in low-grade metamorphism of pelitic schists. Contrib. Mineral. Petrol., 45: 143-152.

SASSI F.P., VISONÀ D., FERRARA G., GATTO G.O., IBRAHIM H.A., SAID A.A. and TONARINI S. (this volume). The crystalline basement of Northern Somalia: lithostratigraphy and the sequence of events.

*Final editing, January 1990*

From *Geology and mineral resources of Somalia and surrounding regions*, Ist. Agron. Oltremare, Firenze, Relaz. e Monogr. 113, 129-142, 1993.

# PRELIMINARY DATA ON THE MAGMATIC ORIGIN AND EMPLACEMENT CONTEXT OF THE PRECAMBRIAN AMPHIBOLITES OF THE BUUR REGION (SOUTHERN SOMALIA)

A. HAIDER

Department of Geology, Somali National University, P.O. Box 1081, Mogadishu, Somalia.

Present address: ENSG, Laboratoire de Caractérisation des Gîtes Minéraux, 94 Avenue de Lattre de Tassigny, 54000 Nancy, France.

ABSTRACT

The amphibolites of the Precambrian basement of the Buur region outcrop as xenoliths in migmatites and lenses parallel to the main trend of the country rocks. They are interbedded with ultrabasic rocks, garnet quartzites, amphibolitic and biotitic gneisses, quartz-feldspar gneisses, marbles, calc-silicate rocks and iron quartzites.

Their metamorphic grade is amphibolite to granulite facies. A retrograde, greenschist facies metamorphic overprint is also recorded.

Geochemical data on these amphibolites indicate that:

- the protoliths were basic magmatic rocks, with local crystal cumulates (occurrence of metapyroxenites, metagabbros and metabasites);
- trace elements (Nb, Zr, Y, $P_2O_5$, and REE) reveal two types of rocks: one similar to mid-oceanic ridge tholeiites, and one displaying alkaline characteristics (i.e., abundance of light REE, Nb, Zr, $P_2O_5$ and $TiO_2$).

These rocks may indicate either a rifting episode or an ancient Precambrian suture.

## INTRODUCTION

The Precambrian basement of Southern Somalia, in the Buur Region, lies between the regions of Bay and Shabelada Hoose (1° 30' and 3° 20' N, 42° 30' and 45° E), and covers an area of about 26.000 Km². It was recognized for the first time by Italian geologists (STEFANINI and PAOLI, 1916; STEFANINI, 1918, 1925; ALOISI and DE ANGELIS, 1938) and was later studied by other workers: AZZAROLI and PASSERINI (1965); BORSI (1965); DANIELS (1965); ILYIN (1967); BAKOS and SASSI (1978); BELLIENI et al. (1981); HAIDER (1983).

Structurally, this part of the Precambrian basement of Southern Somalia may be divided into two sectors: a north-east sector, with NW-SE isoclinal folds, and a south-west sector, in which younger, NE-SW folds are superimposed on the NW-SE folds.

The latter sector contains the effects of a widespread migmatization and large-scale granitoid intrusions. The second, NE-SW phase deformation is very probably linked to migmatization.

Lithologically, the basement is composed of granito-gneisses, quartz-feldspar gneisses, amphibolitic and biotitic gneisses, amphibolites and marbles associated with calc-silicate rocks and iron quartzites. The whole rock sequences are more or less affected by migmatization involving the emplacement of granitoid stocks, mainly in the south-west sector.

This paper is the first geochemical study dealing with the basic and ultrabasic rocks of the Buur basement. It aims at better knowledge of the geology of this basement, since these rocks may reveal basic magmatism of Precambrian age.

## GEOLOGY OF THE AMPHIBOLITES

The basic rocks in the north-east sector are mainly amphibolites and amphibole pyroxenites, minor pyroxenites and rare tremolitites and cummingtonitites.

These rocks outcrop underneath the alluvial sediments along the river beds (Oueds): Urugey, Godobay, and near the village of Farta. They occur in the form of lenses parallel to the main regional foliation (NW-SE).

These dark-green metabasites are generally medium-to coarse-grained, sometimes foliated and sometimes massive. Layering may appear, due to the occurrence of centimetric bands of different mineral composition. The amphibolites are associated with amphibole-biotite gneisses, garnet quartzites, gneisses, marbles and calc-silicate rocks (Fig. 1).

In the south-west sector, the basic rocks appear embedded in the migmatites and are associated with amphibole gneisses, iron quartzites, marbles and calc-silicate rocks.

## PETROGRAPHY AND MINERALOGY

Under the microscope these basic and ultrabasic rocks show a homogeneous texture, of polygonal granoblastic type. A granonematoblastic texture is defined in the layered types by the preferred orientation of large amphibole and pyroxene laths and aggregates. Pyroxene-bearing and pyroxene-free types may be distinguished. The occurrence of garnet is reported in the literature, but not confirmed during the present research.

In general, these rocks have a simple mineralogy, consisting of three major mineral phases in different proportion: amphibole, plagioclase and pyroxene. Epidote, calcite, and rare muscovite and biotite are minor components. Accessories are magnetite, hematite, ilmenite, sphene, apatite and zircon. Quartz occurs in variable quantities in most samples.

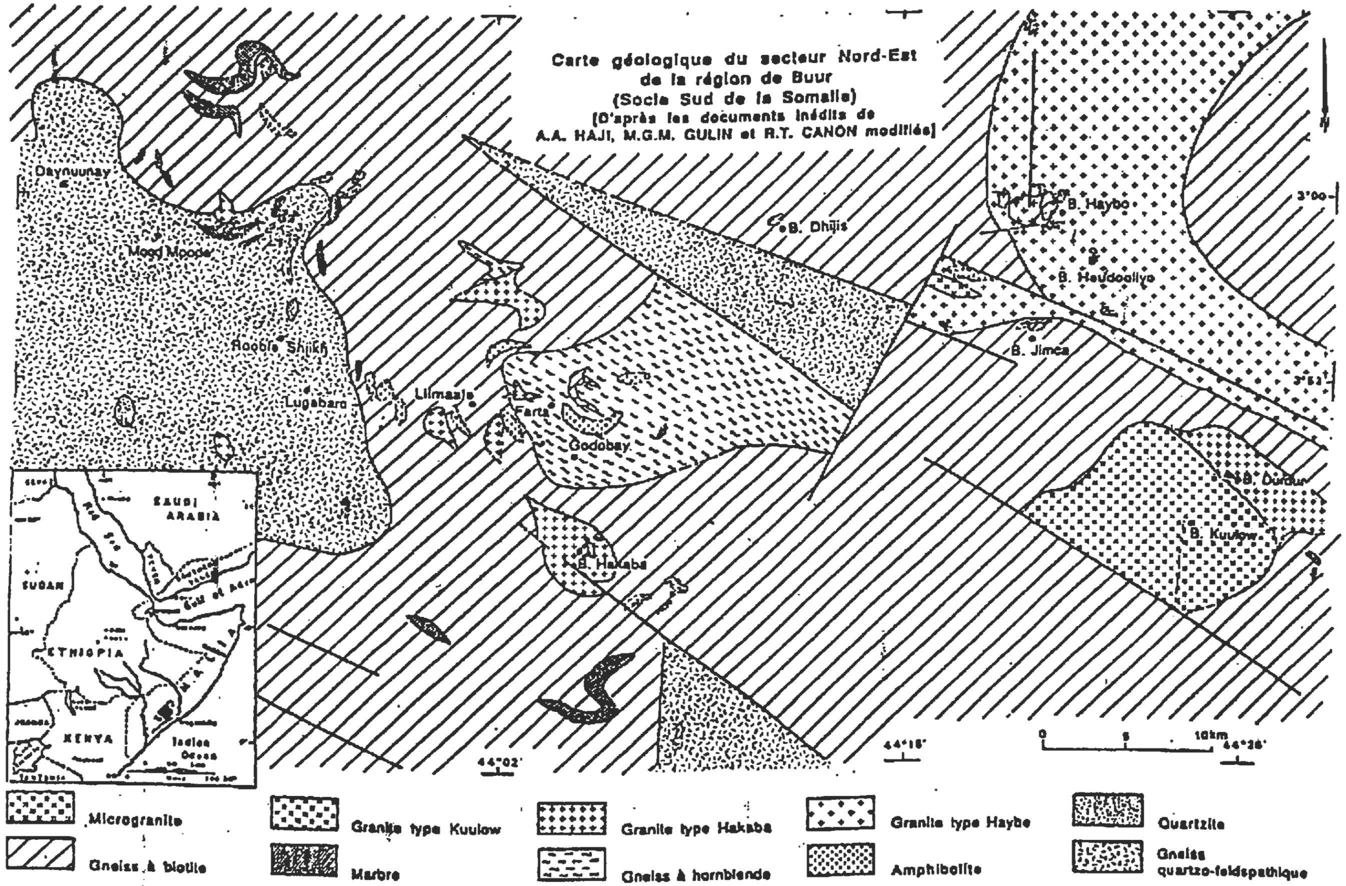


Fig. 1 - Geological sketch of the NE portion of the Buur region

*Amphiboles.* Their crystals are sometimes euhedral, sometimes anhedral. In all cases they are calcic amphiboles according to LEAKE (1978) classification. All rock types bear magnesian hornblende. The pyroxene-bearing types also contain Na-, Fe-, Ti- richer amphiboles, e.g. Fe-hornblende, pargasitic hornblende and/or edenitic horneblende (Table 1).

*Pyroxene.* In the metabasites of the Buur region, pyroxene occurs in increasing proportions, from pyroxene amphibolites to the amphibole-pyroxenites to the pyroxenites. Clinopyroxene belongs to salite group (Table 2), showing slight zoning in some cases (FeO enrichment from core to rim and related MgO and CaO depletion). Retrograde alteration often occurs along the cleavage and the rim of the amphibole crystals.

*Plagioclase.* Plagioclases are more or less sericitized, with development of calcite, epidote and more rarely muscovite. In the clinopyroxene-bearing rock types plagioclase is basic, labradorite or even bytownite (An 82%) in composition. Andesine is more often found in the pyroxene-free rock types (Table 3).

Two metamorphic stages have been recognized in these amphobolites, and the mineral chemistry contributes to better define the mineral assemblage related to each crystallization stage:

1) *stage one*: clinopyroxene, Mg-hornblende, Fe-hornblende, pargasitic hornblende, edenitic hornblende and plagioclase (An 56-82%);
2) *stage two*: magnesian hornblende and plagioclase (An 33-45%), without any traces of pyroxene.

RAASE (1974), and LAIRD and ALBEE (1981) have shown that amphibole composition varies with increasing metamorphic grade. Hornblendes evolve from tschermakitic compositions in low metamorphic grade towards more pargasitic or edenitic types in the higher grades of the amphibolite facies. Bearing in mind the homogeneity of the chemical compositions of the amphiboles, the occurrence of pargasitic and edenitic hornblendes thus records a higher metamorphic grade than that which produced the magnesian hornblendes. Moreover, it is widely known that the anorthite content of plagioclases increases with metamorphic grade: anorthite-rich (labradorite-bytownite) plagioclases may thus be considered as indicating high-grade metamorphism.

As regards pressure, several authors, in particular RAASE (1974), have studied the compositional variations of amphibole as an effect of the metamorphic conditions. The above author has shown that the $A^{IV}$ and Si contents of amphibole increase with pressure and proposed a geobarometric diagram. Our set of samples generally plot close to the reference line P = 5 Kb, with no difference between the mineral assemblage of stage 1 and stage 2.

In the current state of our knowledge of the Southern Somalia basement, it cannot be definitely stated whether the two mineral assemblages detected in the Buur amphibolites correspond to two stages of the same metamorphic event, or to distinct metamorphic events of different age.

Table 1 - Chemistry of the amphiboles from the Buur amphibolites.

| ANALYSE | FR20B/35 | FR20A/27 | FR20A/28 | UR6/29 | UR6/32 | UR6/39 | LIM1/58 | LIM1/60 | LIM1/67 |
|---|---|---|---|---|---|---|---|---|---|
| Si02 | 41.27 | 44.73 | 44.58 | 46,55 | 44.44 | 51,63 | 44,87 | 45,71 | 47.14 |
| Al203 | 12,05 | 10,14 | 10,34 | 9,19 | 10,65 | 4,59 | 10,03 | 9,37 | 8,08 |
| FeO | 18,94 | 16,39 | 15,86 | 16.24 | 17,07 | 14.52 | 14.81 | 13.91 | 15,00 |
| Fe203 | 0,00 | 0,00 | 0,00 | 0.00 | 0,00 | 0,00 | 0,00 | 0,00 | 0,00 |
| MnO | 0,24 | 0.41 | 0.33 | 0,27 | 0,34 | 0,26 | 0,23 | 0,32 | 0.23 |
| MgO | 8,42 | 10,14 | 9,72 | 9,93 | 9.47 | 12,98 | 10,52 | 10,57 | 11,68 |
| CaO | 11,88 | 12,23 | 11,96 | 12,03 | 11,87 | 12,11 | 11,97 | 11,89 | 11,93 |
| Na20 | 1,30 | 1,13 | 1,42 | 1,36 | 1,96 | 0,73 | 1,56 | 1,65 | 1,29 |
| K20 | 1,62 | 0,67 | 0,75 | 0,33 | 0,45 | 0,12 | 0,18 | 0,16 | 0,24 |
| Ti02 | 1,10 | 0,59 | 0,86 | 0,59 | 0,94 | 0,08 | 1,18 | 0,96 | 0,84 |
| Cr203 | 0,00 | 0,02 | 0,00 | 0,00 | 0,00 | 0,00 | 0,08 | 0,00 | 0,00 |
| TOTAL | 96,82 | 96,45 | 95,82 | 96,49 | 97,19 | 97,02 | 95,43 | 94,54 | 96,43 |
| Si | 6,320 | 6,737 | 6,771 | 6,986 | 6,688 | 7,558 | 6,787 | 6,938 | 7,008 |
| Al IV | 1,680 | 1,263 | 1,229 | 1,014 | 1,312 | 0,442 | 1,213 | 1,062 | 0,992 |
| Cr | 0,000 | 0,000 | 0,000 | 0,000 | 0,000 | 0,000 | 0,000 | 0,000 | 0,000 |
| Fe 3+ | 0,000 | 0,000 | 0,000 | 0,000 | 0,000 | 0,000 | 0,000 | 0,000 | 0,000 |
| Ti | 0,000 | 0,000 | 0,000 | 0,000 | 0,000 | 0,000 | 0,000 | 0,000 | 0,000 |
| T | 8,000 | 8,000 | 8,000 | 8,000 | 8,000 | 8,000 | 8,000 | 8,000 | 8,000 |
| Al VI | 0,495 | 0,537 | 0,622 | 0,611 | 0,577 | 0,349 | 0,575 | 0,614 | 0,424 |
| Cr | 0,000 | 0,002 | 0,000 | 0,000 | 0,000 | 0,000 | 0,010 | 0,000 | 0,000 |
| Ti | 0,127 | 0,067 | 0,098 | 0,067 | 0,106 | 0,009 | 0,134 | 0,110 | 0,094 |
| Fe 3+ | 0,331 | 0,183 | 0,000 | 0,000 | 0,035 | 0,047 | 0,000 | 0,000 | 0,162 |
| Mg | 1,922 | 2,276 | 2,200 | 2.221 | 2,124 | 2,832 | 2,372 | 2,391 | 2,588 |
| Fe 2+ | 2,094 | 1,882 | 2,015 | 2,038 | 2,113 | 1,730 | 1,873 | 1,766 | 1,703 |
| Mn | 0,031 | 0,052 | 0,042 | 0,034 | 0,043 | 0,032 | 0,029 | 0,041 | 0,029 |
| C | 5,000 | 5,000 | 4,977 | 4,971 | 5,000 | 5,000 | 4,994 | 4,922 | 5,000 |
| Fe 2+ | 0,000 | 0,000 | 0,000 | 0,000 | 0,000 | 0,000 | 0,000 | 0,000 | 0,000 |
| Mn | 0,000 | 0,000 | 0,000 | 0,000 | 0,000 | 0,000 | 0,000 | 0,000 | 0,000 |
| Mg | 0,000 | 0,000 | 0,000 | 0,000 | 0,000 | 0,000 | 0,000 | 0,000 | 0,000 |
| Ca | 1,949 | 1,974 | 1,946 | 1,934 | 1,914 | 1,899 | 1,940 | 1,934 | 1,900 |
| Na | 0,051 | 0,026 | 0,054 | 0,066 | 0,086 | 0,101 | 0,060 | 0,066 | 0,100 |
| B | 2,000 | 2,000 | 2,000 | 2,000 | 2,000 | 2,000 | 2,000 | 2,000 | 2,000 |
| Na | 0,335 | 0,304 | 0,364 | 0,330 | 0,486 | 0,106 | 0,397 | 0,419 | 0,272 |
| K | 0,316 | 0,129 | 0,145 | 0,063 | 0,086 | 0,022 | 0,035 | 0,031 | 0,046 |
| A | 0,652 | 0,432 | 0,510 | 0,393 | 0,572 | 0,129 | 0,432 | 0,450 | 0,318 |
| X Mg (1) | 0,442 | 0,524 | 0,522 | 0,521 | 0,497 | 0,614 | 0,559 | 0,575 | 0,581 |
| X Mg (2) | 0,479 | 0,547 | 0,522 | 0,521 | 0,501 | 0,621 | 0,559 | 0,575 | 0,603 |

(1) Mg/ (Fe2 (B,C) (C)+Mg (B,C))     (2) Mg/ (Fe2 (B,C)+Mg (B,C)

| | | | | | | | | | |
|---|---|---|---|---|---|---|---|---|---|
| Fe203 | 2,87 | 1,62 | 0,00 | 0,00 | 0,31 | 0,43 | 0,00 | 0,00 | 1,45 |
| FeO | 16,35 | 14,94 | 15,86 | 16,24 | 16,79 | 14.13 | 14,81 | 13,91 | 13.70 |
| H20 | 1,96 | 1,99 | 1,97 | 2,00 | 1,99 | 2,05 | 1,98 | 1,97 | 2,02 |
| Total | 99,06 | 98,60 | 97,79 | 93,49 | 99,21 | 99,11 | 97,41 | 96,51 | 98,59 |

## GEOCHEMISTRY OF AMPHIBOLITES

With the aim of revealing the origin of the Buur amphibolites, fourteen chemical analyses (major and trace elements), seven zirconium and niobium determination and three REE analyses were carried out (Table 4).

The amphibolites have a chemical composition characteristic of slightly differentiated basic rocks, with $SiO_2$ contents in the range 44-49% and a $Fe_2O_3/MgO$ ratio equal to or less than 2%. Alkali contents are instead relatively low, less than 5%.

The chemical data are plotted in the geochemical diagrams usually used in the study of basic rocks. In MOINE and DE LA ROCHE (1968) diagram (Fig. 2), the data points plot in the field of the magmatic rocks. The magmatic origin of the protoliths of these amphibolites is confirmed by VAN DE KAMP (1969) diagram (Fig. 3), which shows a positive correlation between log $C_{Cr}$ and the ratio $MgO/(MgO+FeO_{tot})$, together with high Cr contents; on the contrary, sediments usually show a negative correlation and low Cr contents.

Also, the Rb/Sr ratio of the Buur amphibolites (average 0.07) is closer to that of the basic and intermediate magmatic rocks (0.003-0.33), and different from that of shales (average 0.50).

Table 2 - Chemistry of the clinopyroxenes from the Buur amphibolites.

| ANALYSE | FAR20B/30 | FAR20B/31 | FAR20B/32 | FAR20B/33 | FAR20/34 | UR5/44 | UR5/45 | YR5/46 | UR7/56 |
|---|---|---|---|---|---|---|---|---|---|
| SiO2 | 51.07 | 50.86 | 51.16 | 50.46 | 51.39 | 52.38 | 52.57 | 52.21 | 53.02 |
| Al2O3 | 1.82 | 2.10 | 2.02 | 2.54 | 1.94 | 0.98 | 0.94 | 0.96 | 1.03 |
| FeO | 10.01 | 10.72 | 10.32 | 10.73 | 10.27 | 9.26 | 9.39 | 8.62 | 9.44 |
| Fe2O3 | 0.00 | 0.00 | 0.00 | 0.00 | 0.00 | 0.00 | 0.00 | 0.00 | 0.00 |
| MnO | 0.50 | 0.57 | 0.32 | 0.43 | 0.35 | 0.23 | 0.36 | 0.30 | 0.47 |
| MgO | 11.27 | 11.08 | 11.29 | 10.85 | 11.44 | 12.23 | 12.51 | 12.31 | 12.39 |
| CaO | 23.36 | 23.56 | 23.56 | 22.92 | 23.32 | 23.80 | 23.58 | 23.82 | 23.69 |
| Na2O | 0.41 | 0.43 | 0.43 | 0.54 | 0.51 | 0.30 | 0.31 | 0.33 | 0.31 |
| K2O | 0.00 | 0.00 | 0.06 | 0.06 | 0.00 | 0.00 | 0.00 | 0.03 | 0.00 |
| TiO2 | 0.16 | 0.16 | 0.17 | 0.12 | 0.13 | 0.00 | 0.00 | 0.03 | 0.03 |
| Cr2O3 | 0.00 | 0.59 | 0.00 | 0.00 | 0.17 | 0.00 | 0.00 | 0.00 | 0.01 |
| TOTAL | 98.60 | 100.07 | 99.33 | 98.65 | 99.52 | 99.18 | 99.66 | 98.61 | 100.39 |

| | | | | | | | | | |
|---|---|---|---|---|---|---|---|---|---|
| Si | 1,956 | 1,931 | 1,948 | 1,938 | 1,951 | 1,983 | 1,982 | 1,985 | 1,984 |
| Al IV | 0,044 | 0,069 | 0,052 | 0,062 | 0,049 | 0,017 | 0,018 | 0,015 | 0,016 |
| T | 2,000 | 2,000 | 2,000 | 2,000 | 2,000 | 2,000 | 2,000 | 2,000 | 2,000 |
| Cr | 0,000 | 0,018 | 0,000 | 0,000 | 0,005 | 0,000 | 0,000 | 0,000 | 0,000 |
| Ti | 0,005 | 0,005 | 0,005 | 0,003 | 0,004 | 0,000 | 0,000 | 0,001 | 0,001 |
| Al VI | 0,039 | 0,025 | 0,039 | 0,053 | 0,038 | 0,027 | 0,023 | 0,028 | 0,029 |
| Mg | 0,644 | 0,627 | 0,641 | 0,607 | 0,634 | 0,683 | 0,687 | 0,698 | 0,679 |
| Fe 2+ | 0,321 | 0,340 | 0,329 | 0,337 | 0,319 | 0,290 | 0,289 | 0,274 | 0,290 |
| M2 | 1,008 | 1,015 | 1,013 | 1,000 | 1,000 | 1,000 | 1,000 | 1,000 | 1,000 |
| Mn | 0,016 | 0,018 | 0,010 | 0,014 | 0,011 | 0,007 | 0,011 | 0,010 | 0,015 |
| Ca | 0,959 | 0,959 | 0,961 | 0,943 | 0,949 | 0,966 | 0,952 | 0,970 | 0,950 |
| Na | 0,030 | 0,032 | 0,032 | 0,040 | 0,038 | 0,022 | 0,023 | 0,024 | 0,022 |
| K | 0,000 | 0,000 | 0,003 | 0,003 | 0,000 | 0,000 | 0,000 | 0,001 | 0,000 |
| Mg | 0,000 | 0,000 | 0,000 | 0,002 | 0,002 | 0,004 | 0,010 | 0,000 | 0,009 |
| Fe 2+ | 0,000 | 0,000 | 0,000 | 0,001 | 0,001 | 0,001 | 0,004 | 0,000 | 0,004 |
| M1 | 1,006 | 1,009 | 1,006 | 1,003 | 1,000 | 1,000 | 1,000 | 1,006 | 1,000 |
| X Mg | 0,667 | 0,648 | 0,661 | 0,643 | 0,665 | 0,702 | 0,704 | 0,718 | 0,701 |
| Act. Mg | 0,000 | 0,000 | 0,000 | 0,001 | 0,001 | 0,002 | 0,007 | 0,000 | 0,006 |
| R Fe+Mg | 0,013 | 0,024 | 0,016 | 0,020 | 0,018 | 0,006 | 0,009 | 0,004 | 0,004 |
| R Sites | 0,000 | 0,000 | 0,000 | 0,000 | 0,000 | 0,000 | 0,000 | 0,000 | 0,000 |

Table 3 - Chemistry of the plagioclases from the Buur amphibolites.

| ANALYSE | GODI/32 | GODI/33 | UR6/41 | FR20A/1 | LIMI/54 | UR4A/9 | LIMI/48 | UR6/42 | FR19/73 | FR19/74 |
|---|---|---|---|---|---|---|---|---|---|---|
| $SiO_2$ | 59,89 | 59,64 | 57,11 | 54,27 | 52,47 | 52,61 | 50,03 | 47,42 | 48,82 | 49,76 |
| $Al_2O_3$ | 24,66 | 25,13 | 27,31 | 29,15 | 30,10 | 30,26 | 31,78 | 32,71 | 33,32 | 32,57 |
| FeO | 0,12 | 0,07 | 0,06 | 0,03 | 0,09 | 0,10 | 0,15 | 0,02 | 0,00 | 0,12 |
| MnO | 0,00 | 0,00 | 0,02 | 0,00 | 0,00 | 0,00 | 0,04 | 0,05 | 0,03 | 0,00 |
| MgO | 0,01 | 0,01 | 0,00 | 0,00 | 0,00 | 0,00 | 0,00 | 0,01 | 0,00 | 0,00 |
| CaO | 6,81 | 7,13 | 9,46 | 11,33 | 12,65 | 12,80 | 14,44 | 16,03 | 16,90 | 15,86 |
| $Na_2O$ | 7,23 | 7,18 | 6,42 | 4,85 | 4,49 | 4,37 | 2,92 | 2,46 | 2,08 | 2,50 |
| $K_2O$ | 0,30 | 0,46 | 0,00 | 0,06 | 0,00 | 0,02 | 0,01 | 0,02 | 0,00 | 0,03 |
| $TiO_2$ | 0,00 | 0,00 | 0,00 | 0,00 | 0,01 | 0,00 | 0,01 | 0,00 | 0,00 | 0,00 |
| $Cr_2O_3$ | 0,07 | 0,00 | 0,00 | 0,03 | 0,00 | 0,01 | 0,00 | 0,00 | 0,00 | 0,00 |
| TOTAL | 99,09 | 99,62 | 100,38 | 99,72 | 99,81 | 100,17 | 99,38 | 98,72 | 101,15 | 100,84 |

| | | | | | | | | | | |
|---|---|---|---|---|---|---|---|---|---|---|
| Si | 2,692 | 2,671 | 2,554 | 2.453 | 2,383 | 2,381 | 2,291 | 2,202 | 2,211 | 2,254 |
| Ti | 0,000 | 0,000 | 0,000 | 0,000 | 0,000 | 0,000 | 0,000 | 0,000 | 0,000 | 0,000 |
| Al | 1,306 | 1,326 | 1,439 | 1,553 | 1,611 | 1,614 | 1,715 | 1,790 | 1,778 | 1,739 |
| $Fe^{3+}$ | 0,005 | 0,003 | 0,002 | 0,001 | 0,003 | 0,004 | 0,006 | 0,001 | 0,000 | 0,005 |
| Mn | 0,000 | 0,000 | 0,001 | 0,000 | 0,000 | 0,000 | 0,002 | 0,002 | 0,001 | 0,000 |
| Mg | 0,001 | 0,001 | 0,000 | 0,000 | 0,000 | 0,000 | 0,000 | 0,001 | 0,000 | 0,000 |
| Z | 4,004 | 4,000 | 3,996 | 4,007 | 3,998 | 3,999 | 4,014 | 3,996 | 3,990 | 3,997 |
| Ca | 0,320 | 0,342 | 0,453 | 0,549 | 0,616 | 0,621 | 0,709 | 0,798 | 0,820 | 0.770 |
| Na | 0,630 | 0,623 | 0,557 | 0,425 | 0,395 | 0,383 | 0,259 | 0,222 | 0,183 | 0,220 |
| K | 0,017 | 0,026 | 0,000 | 0,003 | 0,000 | 0,001 | 0,001 | 0,001 | 0,000 | 0,002 |
| X | 0.975 | 0,992 | 1,010 | 0,977 | 1,011 | 1,005 | 0,968 | 1,020 | 1,003 | 0,991 |
| Total | 4.979 | 4,992 | 5,006 | 4,985 | 5,009 | 5,004 | 4,983 | 5,016 | 4,993 | 4,988 |
| Ab | 64,61% | 62,86% | 55,12% | 43.50% | 39.11% | 38,14% | 26,77% | 21,71% | 18,22% | 22,16% |
| An | 33,63% | 34,49% | 44,88% | 56,15% | 60,89% | 61,74% | 73,17% | 78,17% | 81,78% | 77,67% |
| Or | 1,76% | 2.65% | 0,00% | 0,35% | 0,00% | 0,11% | 0,06% | 0,12% | 0,00% | 0,17% |

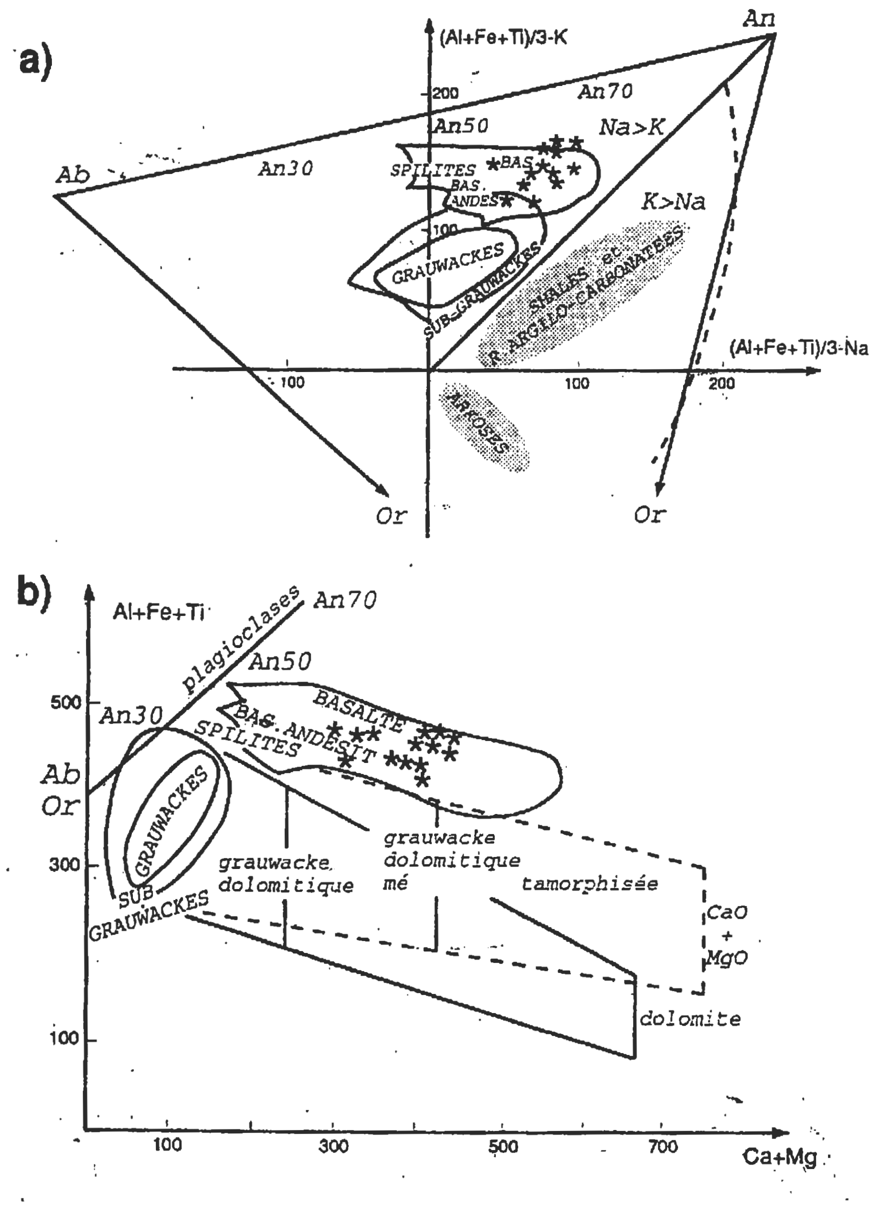


Fig. 2a, b - Location of the Buur amphibolites in the diagram of MOINE and DE LA ROCHE (1968).

Table 4 - Chemical composition of the Buur amphibolites

| | GOD2 | BQ5 | FAR9 | GOD3 | UR7 | GOD13 | LIM1 | FAR20B | UR8 | FAR19 | FAR20 | UR6A | UR4A | UR5 |
|---|---|---|---|---|---|---|---|---|---|---|---|---|---|---|
| SiO2 | 48.29 | 47.97 | 49.17 | 48.02 | 45.82 | 46.1 | 46.28 | 47.22 | 48.08 | 48.16 | 47.28 | 44.36 | 46.24 | 44.53 |
| Al2O3 | 13.28 | 13.46 | 13.69 | 14.48 | 13.18 | 13.64 | 13.53 | 15.07 | 15.72 | 14.47 | 13.6 | 14.44 | 14.37 | 13.76 |
| Fe2O3 Total | 14.67 | 15.09 | 14.23 | 13.00 | 14.26 | 14.02 | 13.89 | 12.37 | 9.96 | 12.67 | 11.61 | 14.42 | 13.5 | 14.79 |
| MnO | 0.22 | 0.22 | 0.24 | 0.23 | 0.27 | 0.23 | 0.21 | 0.28 | 0.19 | 0.26 | 0.26 | 0.18 | 0.21 | 0.17 |
| MgO | 6.06 | 6.5 | 6.29 | 7.08 | 9.24 | 8.94 | 8.4 | 6.7 | 6.76 | 5.64 | 7.56 | 7.7 | 7.13 | 9.72 |
| CaO | 10.15 | 10.12 | 9.47 | 10.73 | 12.85 | 12.78 | 12.61 | 14.37 | 11.84 | 14.13 | 13.89 | 13.39 | 14.52 | 12.41 |
| Na2O | 2.48 | 3.47 | 3.32 | 2.51 | 1.88 | 2.02 | 1.95 | 2.25 | 2.96 | 2.12 | 2.17 | 2.12 | 1.8 | 1.93 |
| K2O | 0.65 | 1.00 | 1.08 | 0.48 | 0.36 | 0.27 | 0.19 | 0.77 | 0.64 | 0.24 | 0.38 | 0.48 | 0.13 | 0.36 |
| TiO2 | 2.02 | 1.44 | 1.42 | 1.25 | 1.02 | 0.95 | 0.87 | 0.86 | 0.86 | 0.85 | 0.78 | 0.75 | 0.72 | 0.64 |
| P2O5 | 0.24 | 0.21 | 0.16 | 0.13 | 0.8 | 0.09 | 0.09 | 0.06 | 0.03 | 0.06 | 0.09 | 0.09 | 0.06 | 0.05 |
| Pf | 0.57 | 0.73 | 0.6 | 0.66 | 0.87 | 0.89 | 0.65 | -0.52 | 1.46 | 0.59 | 0.94 | 0.72 | 0.37 | 1.01 |
| Total | 98.63 | 100.21 | 99.67 | 98.57 | 99.83 | 99.93 | 98.67 | 100.47 | 98.5 | 99.19 | 98.56 | 99.25 | 99.05 | 99.37 |
| Ba | 215,00 | 226,00 | 160,00 | 374,00 | 279,00 | 58,00 | 64,00 | 328,00 | 507,00 | 1130,00 | 734,00 | 338,00 | 164,00 | 311,00 |
| CO | 85,00 | 65,00 | 57,00 | 114,00 | 92,00 | 75,00 | 96,00 | 136,00 | 65,00 | 70,00 | 76,00 | 76,00 | 89,00 | 81,00 |
| Cr | 71,00 | 103,00 | 100,00 | 98,00 | 276,00 | 230,00 | 218,00 | 287,00 | 259,00 | 209,00 | 256,00 | 203,00 | 246,00 | 196,00 |
| Cu | 128,00 | 37,00 | 46,00 | 98,00 | 49,00 | 133,00 | 162,00 | 76,00 | 27,00 | 40,00 | 23,00 | 83,00 | 181,00 | 81,00 |
| Ni | 123,00 | 106,00 | 93,00 | 139,00 | 127,00 | 185,00 | 175,00 | 166,00 | 137,00 | 145,00 | 172,00 | 146,00 | 164,00 | 128,00 |
| Sr | 250,00 | 213,00 | 223,00 | 148,00 | 210,00 | 178,00 | 153,00 | 185,00 | 241,00 | 205,00 | 226,00 | 175,00 | 151,00 | 216,00 |
| V | 344,00 | 323,00 | 322,00 | 298,00 | 319,00 | 325,00 | 297,00 | 296,00 | 212,00 | 278,00 | 267,00 | 313,00 | 11,00 | 329,00 |
| Rb | 22,00 | 12,00 | 18,00 | 16,00 | 10,00 | 11,00 | 12,00 | 17,00 | 12,00 | 10,00 | 12,00 | 9,00 | 11,00 | 10,00 |
| Zr | n.d. | 116.15 | n.d. | 76.74 | n.d. | 28.69 | n.d. | 36.41 | n.d. | 38.32 | n.d. | 35.03 | n.d. | 31.99 |
| Nb | - | 20.39 | - | 14.07 | - | 9.48 | - | 13.83 | - | 10.84 | - | 11.3 | - | 9.04 |
| Y | - | 29.50 | - | n.d. | - | n.d. | - | 17.83 | - | n.d. | - | n.d. | - | 19.41 |
| La | - | 11.02 | - | - | - | - | - | 2.03 | - | - | - | - | - | 2.43 |
| Ce | - | 25.83 | - | - | - | - | - | [illegible].40 | - | - | - | - | - | 10.94 |
| Nd | - | 14.17 | - | - | - | - | - | 4.83 | - | - | - | - | - | 5.72 |
| Sm | - | 4.20 | - | - | - | - | - | 1.82 | - | - | - | - | - | 2.00 |
| Eu | - | 1.34 | - | - | - | - | - | 0.90 | - | - | - | - | - | 0.66 |
| Gd | - | 3.92 | - | - | - | - | - | 2.03 | - | - | - | - | - | 2.41 |
| Dy | - | 4.20 | - | - | - | - | - | 2.41 | - | - | - | - | - | 2.68 |
| Er | - | 2.26 | - | - | - | - | - | 1.40 | - | - | - | - | - | 1.53 |
| Yb | - | 2.34 | - | - | - | - | - | 1.50 | - | - | - | - | - | 1.67 |
| Lu | - | 0.28 | - | - | - | - | - | 0.20 | - | - | - | - | - | 0.23 |

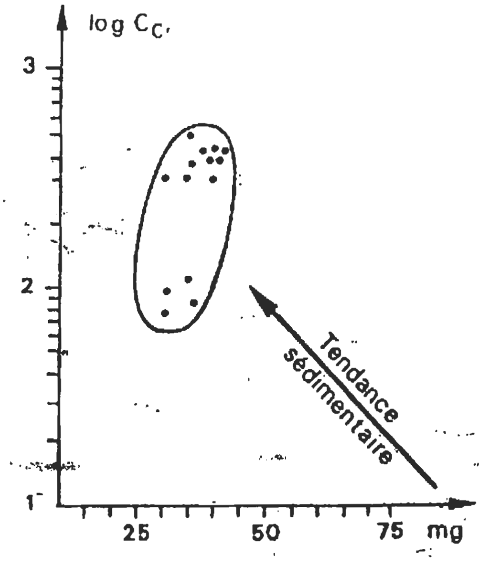


Domaine de tendance des roches sédimentaires.
• Les amphibolites de Buur.

Fig. 3 - Location of the Buur amphibolites in the diagram of VAN DE KAMP (1969).

The interpretation of the geochemistry of metabasites must also take into consideration the possible mobility of some elements during metamorphism. This problem has been faced by various authors, including PEARCE (1974), MIYASHIRO SHIDO (1975), BECCALUVA et al. (1979), SHERVAIS (1982). The following points briefly summarize their results:

- chemical migration is important in greenschist-facies metamorphism, but less so in amphibolite-facies metamorphism;
- the elements considered to be most mobile are K, Na, Rb, Ca, etc., while Ti, V, Cr, Zr, Nb and Y are considered to be relatively immobile.

Rare earths are also considered to be immobile. However, HELLMAN et al. (1979) have shown that, during greenschist-facies metamorphism, some mobilization may occur.

Due to the relative immobility of zirconium, in contrast with the well known mobility of potassium during post-magmatic alteration, the Zr-K pair in a rock may record secondary alterations. In the case of the Buur amphibolites, the analyzed samples do show a linear correlation between zirconium and potassium, which means that the initial K/Zr ratio of these basic rocks may have been preserved. Their chemical composition may thus be considered similar to that of the basic igneous protoliths from which they derived.

However, it is difficult to understand the type of magmatism of these protoliths. Many indications suggest the presence of cumulates: the occurrence of ultrabasic rocks and the banding of some amphibolites.

From the chemical point of view, the Buur amphibolites may be classified into two groups:

- Group 1 (first 4 samples of Table 1), characterized by high Ti and P contents and low Cr, Ni and Ca. The REE in one sample from this group ($BQ_5$) shows LREE enrichment;
- Group 2 (last 10 samples in Table 1), characterized by low Ti and P contents and high Cr, Ni and Ca contents. REE in two samples from this group shows a flat profile.

Group 1 shows the features of transitional to alkaline basalts, while Group 2 shows ocean-ridge tholeiitic affinity. However, relatively high Nb contents may indicate a certain transitional character, much less marked than that of the Group 1 (Figs. 4, 5).

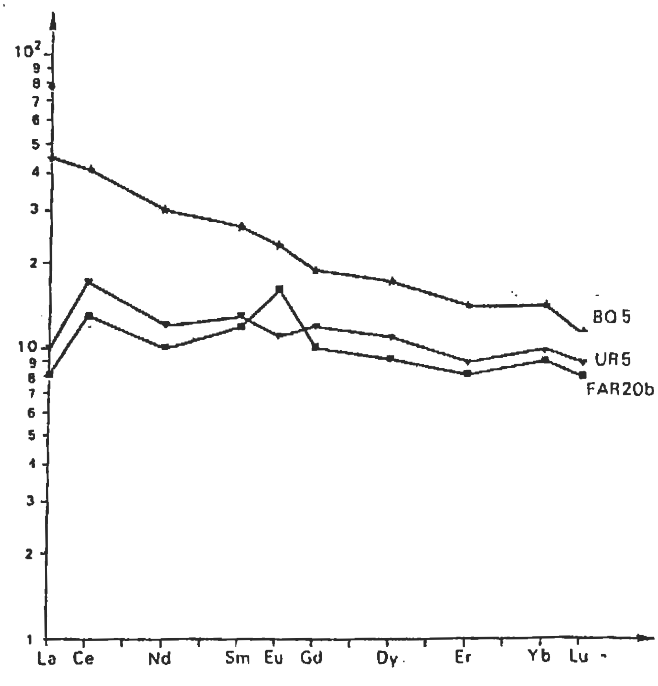


Fig. 4 - Pattern of the REE of the Buur amphibolites (normalization according to $C_1$ in EVENSEN et al., 1978).

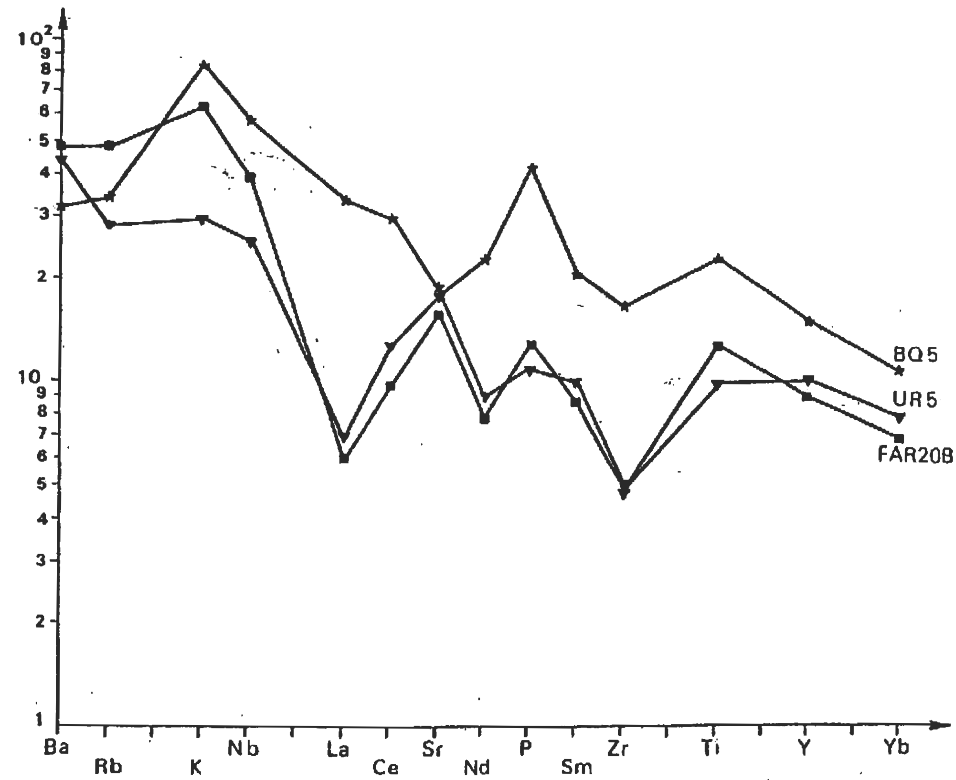


Fig. 5 - Spider diagram of the Buur amphibolites (normalization according to THOMPSON, 1984).

## CONCLUSIONS

Although these results are only preliminary and require further and more detailed work, they may already suggest that the Buur amphibolites probably derive from an ancient, slightly differentiated basic protholith, metamorphosed under conditions at the amphibolite/granulite facies boundary. We hypothesize that these ancient basic rocks were of tholeiitic to alkaline affinity, and were emplaced in a Precambrian extension domain of rift or ocean-ridge type. Consequently, the Buur amphibolites may reveal an ancient suture comparable to other Precambrian sutures known in the Mozambique Belt (East Africa).

REFERENCES

ALOISI P. and DE ANGELIS A.M. (1938). Le rocce della Somalia. Geologia della Somalia. R. Soc. Geogr., 2: 1-166.

AZZAROLI A. and PASSERINI P. (1965). Lineamenti geologici della regione dei Bur in Somalia. Att. Soc. Tosc. Nat., a., 72: 537-547.

BAKOS F. and SASSI F.P. (1978). The crystalline basement in the Bur area (Southern Somalia). Somali National University.

BECCALUVA L., OHNENSTETTER D. and OHNENSTETTER M. (1979). Geochemical discrimination between ocean-floor and island-arc tholeiites. Application to some ophiolites. Can. J. Earth Sci., 16: 1874-1884.

BELLIENI G., HAYDER A., IBRAHIM H.A., SASSI F.P. and ZIRPOLI G. (1980). Caratteri geochimico-petrografici dei graniti dei Buur (Somalia meridionale).Univ. Naz. Somala. Quad. Geol. Som., 4: 98-114.

BORSI S. (1965). Determinazione di età con il metodo Rb/Sr di alcune rocce della regione di Buur in Somalia. Att. Soc. Tosc. Sc. Nat., 71: 4 pp.

CECIONI G. (1940). I Buur della Somalia. Riv. Colonie, 14/10: 1427-1437.

D'AMICO C., IBRAHIM H.A. and SASSI F.P. (1981). Outline of the Somalian basement. Geol. Rundsch., 70: 882-896.

DAINELLI G. (1943). Geologia dell'Africa Orientale. Acc. Ital., 4.

DANIELS J.L. (1965). A photogeological interpretation of the Buur region, Somali Republic. Overseas geology and mineral resourses. 2, 4: 427-437.

EVENSEN N.M., HAMILTON P.J. and O'NIONS R.K. (1978). Rare earth abundance in chondritic meteorites. Geochim. Cosmochim. Acta, 42: 1199-1212.

FLEET A.J., HENDERSON P. and KEMPE D.R.C. (1976). Rare earth element and related chemistry of some drilled Southern Indian ocean basalts and volcanogenic sediments. J. Geophys. Res., 81: 4257-4268.

FLOYD P.A. and WINCHESTER J.A. (1975). Magma type and setting using immobile elements. Earth Planet. Sc. Lett., 27: 211-218.

GALE G.H. and PEARCE J.A. (1981). Geochemical pattern in Norwegian greenstone. Can. J. Earth Sci., 19: 385-397.

HAIDER A. (1983). Contributo alla conoscenza delle masse granitoidi dei Buur (Somalia meridionale). Univ. Naz. Somala. Quad. Geol. Som., 7: 39-53.

HELLMAN P.L., SMITH R.E. and HENDERSON P. (1979). The mobility of the rare earth elements: evidence and implications from selected terrains affected by burial metamorphism. Contrib. Mineral. Petrol., 71: 23-44.

ILYIN A. (1967). Geology of the Buur area. Explanatory note to the geological map of Buur area Scale 1:200.000. Geol. Surv. Som., unpub. Rept.

LAIRD J. and ALBEE A.J. (1981). Pressure, temperature and time indicators in mafic schists: their application to reconstructing the polymetamorphic history of Vermont. Am. J. Sc., 281: 127-175.

LEAKE B.E. (1978). Nomenclature of the amphiboles. Min. Mag., 42: 533-563.

MIYASHIRO A. and SHIDO F. (1975). Tholeiitic and calc-alkalic series in relation to the behaviours of titanium, vanadium, chromium and nickel. Am. J. Sc., 275: 265-277.

MOINE B. and DE LA ROCHE H. (1968). Nouvelle approche du problème de l'origine des amphibolites à partir de leur composition chimique. C. R. Acad. Sc. Paris, 267: 2084-2087.

PEARCE J.A. (1974). Basaltic geochemistry used to investigate post-tectonic environments on Cyprus. Tectonophys., 25: 41-67.

RAASE P. (1974). Al and Ti contents of hornblende, indicators of pressure and temperature of regional metamorphism. Contr. Mineral. Petrol., 45: 231-236.

SHERVAIS J.W. (1982). Ti-V plots and the petrogenesis of modern and ophiolitic lavas. Earth Planet. Sc. Lett., 59: 101-118.

STEFANINI G. (1918). Osservazioni geologiche nella Somalia italiana meridionale. Boll. Soc. Geol. Ital., 32, Roma.

STEFANINI G. (1925). Sulla costituzione geologica della Somalia italiana meridionale. C. R. 13 Cong. Geol. Intern., Liège.

STEFANINI G. and PAOLI G. (1916). Ricerche idrogeologiche, botaniche, etnologiche fatte nella Somalia meridionale. Ist. Agr. Colon., 25: 172-224.

TRIBOULET C. and AUDREN C. (1985). Evolution des amphibolites et de leur associations au cours d'un métamorphisme progressif polyphase dans les métabasites de Vilaine (Bretagne méridionale). Schweiz. Mineral. Petrogr. Mitt. 65: 279-298.

VAN DE KAMP P.C. (1969). Origin of amphibolites in the Beart mountains, Montana, Wyoming: new data and interpretation. Geol. Soc. Am. Bull., 80: 1127-1136.

WARDEN A. (1960). Brief note on the geology of the South-western part of the Buur region, near Dinsor. Somaliland Protect. Geol. Surv., Unpub. Rept.

*Final editing, January 1990*

From *Geology and mineral resources of Somalia and surrounding regions*, Ist. Agron. Oltremare, Firenze, Relaz. e Monogr. 113, 143-152, 1993.

# GEOLOGY OF THE LOWDER-MUDIAH AREA, YEMEN

M.A. BA-BTTAT *, B.F. WINDLEY **, A.T. AL-MISHWT *, D.C. ALMOND *

* Geology Department, Kuwait University, P.O. Box 5969, Kuwait 13060.
** Geology Department, Leicester University, Leicester LE1 7RH, U.K.

## ABSTRACT

The geology of the Lowder-Mudiah area is dominated by Precambrian basement rocks, which are unconformably overlain by Jurassic limestone and partly covered by Quaternary basalts of the Shugra volcanic field. The basement rocks consist of three major lithological units that are separated by two northeast-striking ductile shear (thrust) zones. The three lithological units are gneissose granites underlying a central belt, a sequence of bimodal metavolcanic rocks in the south-east and a weakly altered granite, diorite and gabbro intruded by mafic to felsic dyke swarms in the north-west. A third ductile shear (thrust) zone is located within quartz-biotite gneisses of the central belt.

Multiple deformation has affected the area and is represented by three recognisable deformation episodes, each with its own distinctive style and orientation. Northeast trending isoclinal folding is followed by open folds with vertical axial planes and northwest trending cross-and kink-folds.

Several occurrences of carbonatite dyke intrude the grey gneiss of the central belt. Sulphide gossans are developed on mineralized quartz veins in the metamorphosed quartz-rhyolite porphyry.

## INTRODUCTION

The Lowder-Mudiah area is situated in Yemen between longitudes 45°40′ E and 46°10′ E and latitudes 13°40′ N and 14°00′ N (Fig. 1). The area covers approximately 2200 km$^2$. and is underlain by a basement of granitic gneisses and a sequence of metavolcanic rocks regarded by GREENWOOD et al. (1967) as part of the Aden Metamorphic Group. These rocks are unconformably overlain by Jurassic limestone (GREENWOOD et al., 1967) and Quaternary volcanic basalt of the Shugra volcanic field (COX et al., 1977). Elevation in the mapped area varies between 1100 m and 1200 m above sea level, except at the Mukeras Escarpment, where elevations exceed c. 2500 metres above sea level. The escarpment separates the Lowder-Mudiah lowlands from the Mukeras Plateau to the North.

This paper is part of Ph. D. research project (first author) and is only a preliminary account of the geology of the area. Mapping is based on aerial photographs at a scale of 1:60,000.

## GENERAL GEOLOGY

The Lowder-Mudiah area lies within southern extension of the Arabian Shield and is made up dominantly of crystalline basement rocks that can be divided into three main lithological units which are separated by two main ductile shear zones developed on major thrusts (Fig. 1). The first of these three units is a highly metamorphosed unit underlying two thirds of the area in its central part. This northeast-trending belt is composed of grey and pink granitic gneiss including lenses and patches of sheared quartz-biotite gneiss and amphibolite. It is intruded by grey and pink pegmatitic granites containing garnet and tourmaline. Within the gneiss belt, migmatites occur locally at Asswedah and Um-Sallamiah (Lowder) but show no evidence of high grade aluminium silicate minerals, probably due to lack of appropriate pelitic rocks. This localized migmatization affected the quartz-biotite gneiss and amphibolite and may be related to the emplacement of the grey granite associated with it.

The second lithological unit occupies the eastern part of the area and forms a northeast-trending belt of metamorphosed, intermediate and acidic volcanic rocks interlayered with subordinate marble bands. These rocks were metamorphosed under low-grade greenschist facies conditions and are composed of quartz-biotite-chlorite schists interlayered with amphibolites and alternating with schistose quartz-rhyolite porphyry. The sequence is disposed in open synformal and antiformal folds (Fig. 3) with vertical axial planes that trend northeast.

The third lithological unit of the basement occupies the western part of the area and forms a northeast trending 1 km high escarpment that reaches elevations of 2500 m above sea level. The main rock unit underlying the escarpment is a weakly altered, medium-grained white granite, diorite and gabbro which is extensively injected by a dense swarm of northeast-trending mafic and felsic dykes. The dyke rocks are metamorphosed to low-grade greenschist facies, are weakly sheared and strongly epidotized. Thickness measurements of dykes along traverses perpendicular to their trend revealed that they represent approximately 70% of the rock volume, indicating a high degree of extension. WINDLEY and TARNEY (1986), when discussing the structural evolution of the crust in general, stated that exposed basic dyke swarms often represent feeders of lavas within aulacogens under continental forelands. The Mukeras Escarpment dykes may mark a major late Precambrian extensional episode in this segment of the Arabian Shield.

Carbonatite occurs as dykes intruded into the grey granitic gneiss with sharp, cross-cutting intrusive contacts in the vicinity Um-Sallamiah, Al-Arakbi and Durib. The dykes are associated with uranium, thorium and potassium anomalies (ABOUOV et al., 1981).

Sulphide-bearing veins are common within the metamorphosed quartz-rhyolite porphyry, and are shown as gossans in the field.

Jurassic limestone unconformably overlies the basement and is well-bedded, with dips of 35 degrees to the southeast. It forms discontinuous, northeast ridges which are

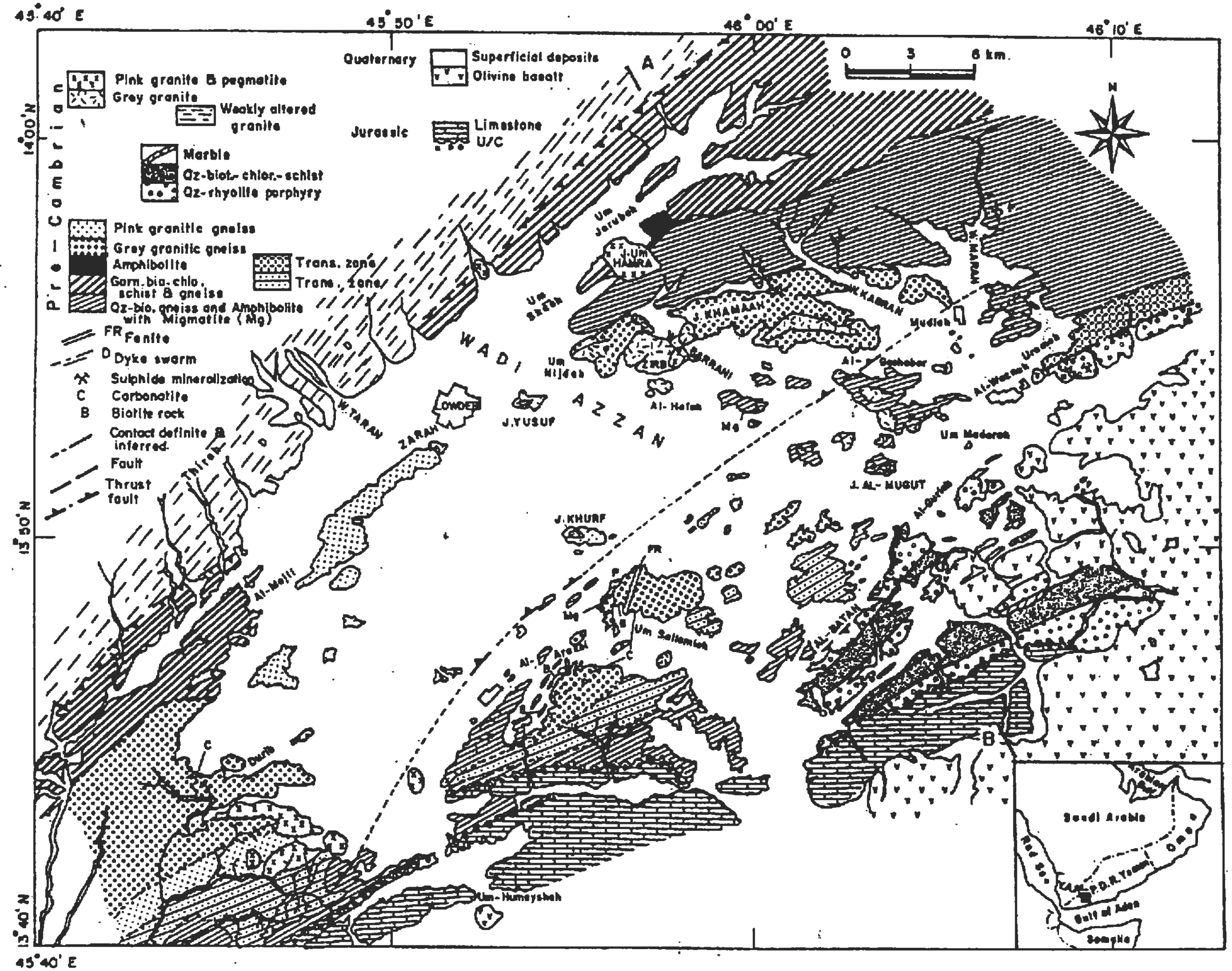


Fig. 1 - Geological map of the Lowder-Mudiah Area.

white in colour and of considerable length. Quaternary olivine basalt flows of the Shugrah Volcanic Field occupy the south-eastern part of the area.

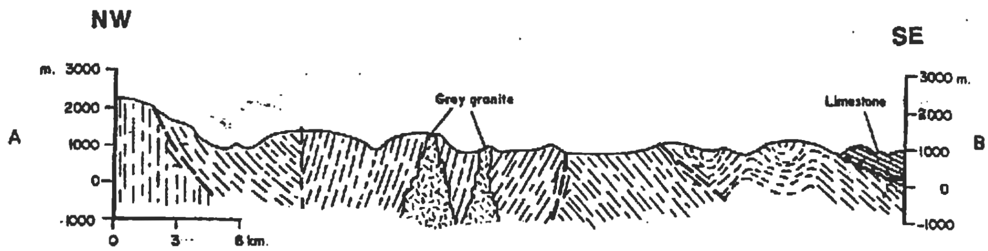


Fig. 2 - Structural cross-section along A-B.

## STRUCTURAL GEOLOGY

Multiple deformation has affected the whole area, as documented by three phases of folding. The earliest episode produced recumbent, tight isoclines with semi-horizontal axial planes, probably indicating the presence of nappe structures. This episode was followed by the development of large-scale open folds with vertical axial planes trending northeast, illustrated well by synforms and antiforms in the layered sequences. Folding during the third phase is manifested by open, cross, microfolds and kink folds with northwest-trending, subvertical axial planes. These folds deform both the isoclines and northeast-trending open folds. The three phases of folding are envisioned as developing at successively shallower crustal levels.

Two main ductile shear zones developed on major thrusts, striking northeast. The first is located in the eastern part of the area and separates the metavolcanic lithological unit to the east from the granitic gneisses and amphibolites in the central part of the area. The second is located in the western margin of the area, sparating granitic gneisses and amphibolites from the dyke swarms and their granite, diorite and gabbro host rocks. Shearing along these zones is evidenced by mylonitization, lensoidal fragmentation and sigmoidal textures as characteristic shear fabrics.

A third major shear (thrust?) zone is located within the gneiss belt, marked by sheared quartz-biotite gneiss and amphibolite which have been folded into a northeast-plunging antiform. Dislocation is indicated by strong shearing in the quartz-biotite gneisses and amphibolite and their disruption into lens-shaped fragments, and by the interlayering of slices of different rock types. The above assumptions about thrusts follow the definitions of PARK (1983).

Although the dip of the two major thrust planes is mainly southeast, the majority of preserved lineations plunge NE and represent an overprint of the latest movements. However, there are indications of an older lineation plunging to the SE and preserved

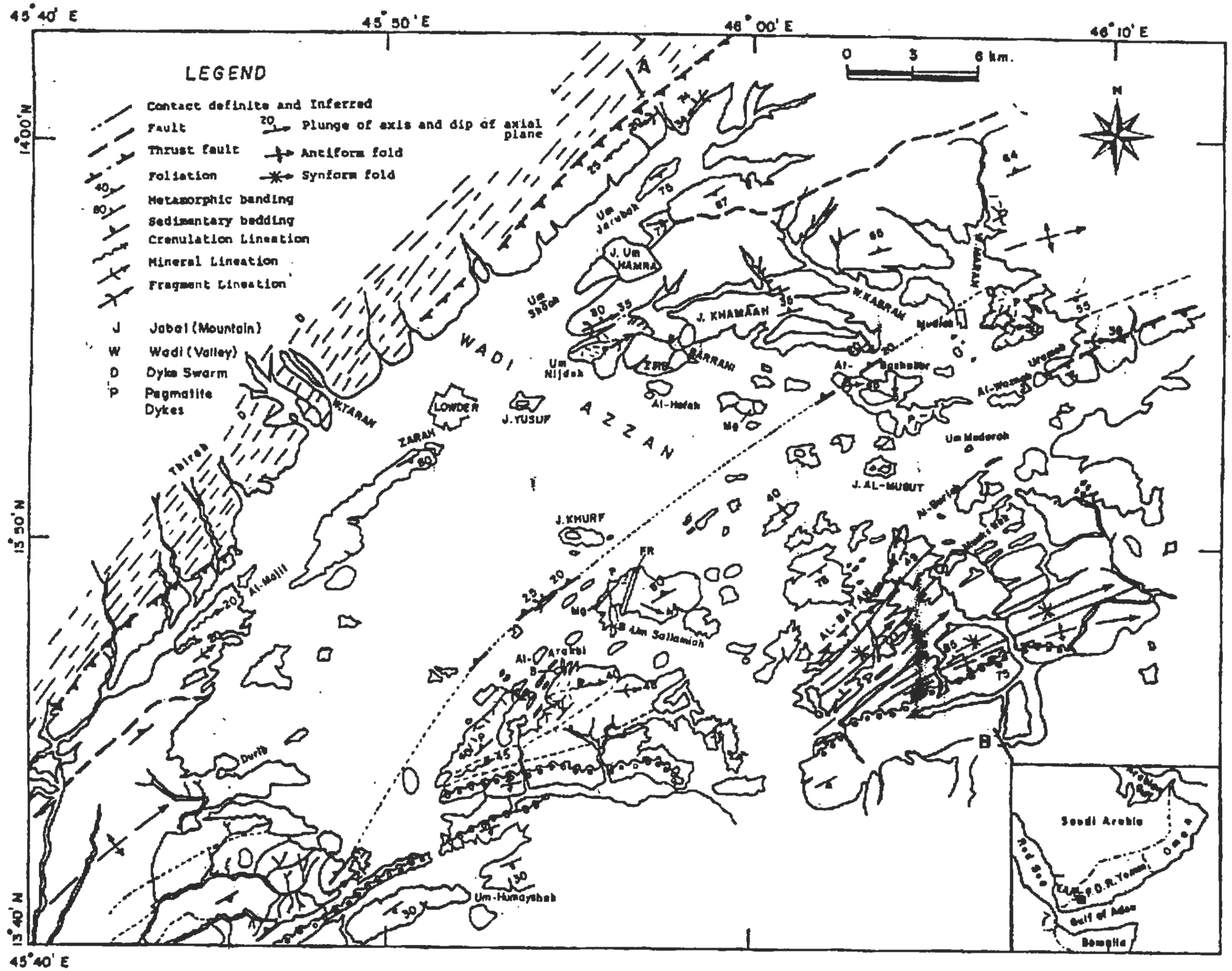


Fig. 3 - Structural map of Lowder-Mudiah Area.

Table 1 - Tentative correlation of the Precambrian basement of Yemen and North Somalia (Modified after GREENWOOD et al., 1967; WARDEN et al., 1984)

| Yemen | Lowder-Mudiah Yemen | N. Somalia |
|---|---|---|
| Ghabar Group (Beydoun 1961)<br>Arenaceous clastics, quartzite, shale, dolomite and limestone with gypsum. Tuffaceous lavas and basal conglomerate with volcanic clasts. | | Inda Ad Series<br>(Shelf-Miogeosynclinal)<br>Banded mudstones, arenaceous clastics and carbonates. Basal conglomerate with metamorphic clasts. |
| INTERTECTONIC IGNEOUS ROCKS<br>Dike rocks intruded mainly as a late phase of intertectonic igneous activity<br>Calc-alkaline granite of Mukeiras area<br>Intermediate mafic plutonic intrusions — Older volcanic rocks-mainly andesites and keratophyres with pyroclastic rocks | Mafic-Felsic dyke swarm<br>Weakly altered granite<br>Metamorphosed Andesite-Rhyolite and Marble | Abdul Qader Volcanic Series<br>Mait Greenstones |
| Syntectonic granite<br>Concordant granites and granitized rocks, approximately coeval with the main phase of regional metamorphism. Pegmatites and feldspathic bands associated with granitic rocks.<br>Aden Metamorphic Group<br>Diorite gneiss; marble, metacalcareous rocks, pelite, metamorphose mafic volcanics, quartzite and meta-arkosic rocks; migmatite. | | Haridad-Mora Calcareous Series<br>Marble, orthoquartzite, talc schist and pelite.<br>Borama-Ubali Pelitic Series<br>Mica schist, ortho-and paraamphibolite<br>Gebile Psammitic Series<br>Meta-quartzofeldspatic sediments; minor amphibolite, mica schist, rare marble; migmatite. |
| Older Gneiss | Granitic gneiss amphibolites and schist | ?Gneissic remnants in the Adadleh area. |

only in a few localities, namely at Al-Arakbi (Lowder), Al-Moshshah and Al-Waznah Mudiah).

If we accept and apply the idea of SHACKLETON (1986), that the disintegration of ophiolites into lenses and repetition of their units imply the presence of major crustal shear zones, then the presence of a tectonized and dismembered ophiolite sequence about 100 km to the south-west of the Lowder-Mudiah area and along the strike (AL-DERWEESH, 1988) can be considered as further evidence for the presence of major shear zones in the region.

## CONCLUSIONS

The general structural trends in the area are almost perpendicular to those in the nearest parts of the Arabian Shield, although the lithology is generally similar to some major rock units in Saudi Arabia (GREENWOOD et al., 1980; ROBOOL et al., 1983; STOESER et al., 1983). It is even more closely comparable to that of Northern Somalia, where the structural trends are also northeast. This suggests that the geology of the Lowder-Mudiah area may be directly correlated with the Mozambique belt of east Africa (WARDEN and DANIELS, 1983). WARDEN and HORKEL (1984) consider that the northeast branch of the Mozambique belt extends into Southern Arabia and constitutes a distinct geotectonic entity, characterized by a predominantly ensialic structural setting and lengthy polycyclic evolution.

HAWKINS et al. (1981) stated that a small segment of the Pan-African Shield in Dhofar is composed of acid-gneisses, granites, pegmatites, aplites and a basic dyke swarm underlies the Mirbat plain. Furthermore, two windows of basement rocks occur in south-west Dhofar.

Based on field observation and petrography, the gneiss belt of Lowder-Mudiah may be equivalent to the older granitic orthogneiss of GREENWOOD et al. (1967) of Southern Yemen (Table 1). We suggest that the metavolcanic unit may correlate with the Older Volcanic Rocks of both GREENWOOD et al. (1967), WARDEN and HORKEL (1984) and also with the Abdul Qadar Volcanic Series, Mait Greenstones of North Somalia (WARDEN and DANIELS, 1983). That is, the Lowder-Mudiah metavolcanic unit is not part of, but younger than, the so-called Aden Metamorphic Group, and perhaps equivalent to the Thaalab Group of Southern Yemen (BEYDOUN, 1966). The weakly altered granite of the Mukeras (Thireh) escarpment is probably part of the calc-alkaline batholith around Mukeras itself (GREENWOOD et al., 1967). The dyke swarm along the escarpment may then be considered as part of GREENWOOD "Intertectonic Igneous Rocks", which preceded the volcanic events recorded by the Ghabar Group.

All the suggested correlations of Table 1 are tentative and need confirmation by isotopic age dating. However, if these correlations prove valid there must be, in general terms, an unconformable relationship between the Lowder-Mudiah metavolcanic rocks and the gneiss unit, since the Aden Metamorphic Group is absent from this area.

Any field evidence for this relationship will have been obscured or destroyed by later shearing associated with thrusting. That is, this contact is certainly now highly tectonized.

Although some features of the geology of Lowder-Mudiah are similar to those of the Precambrian of the Arabian Shield in Saudi Arabia, there are closer comparisons, in both lithology and structure, with the Precambrian basement of Northern Somalia. Thus, the possibility that the South Yemeni basement is distinct from that of Saudi Arabia and represents a continuation of the Mozambique Belt into Southwest Arabian cannot be ruled out.

## ACKNOWLEDGMENTS

The first author is very grateful to the government of Yemen, Ministry of Oil and Minerals, for help during field work; to The British Council for a Foreign and Commonwealth Office Award Scholarship, to Kuwait and Leicester Universities and to Kuwait Foundation for Advancement of Sciences for funding participation of the first author in the "GEOSOM 87" Conference. Thanks are also due to the technical staff of the Departments of Geology in Kuwait and Leicester Universities. We also thank Mr. A. SHAH and M. KAMBAL for typing and drafting.

## REFERENCES

ABOUOV A.K., LYSITSIN E.S., POTROUKHIN I.I., LYCHKOVSKY B.P. and ABDUL AZIZ,J.S. (1981). Report on the results of prospecting and estimation within the Lawder field of carbonatites for 1977-1981. Unpublished technical report. Board of Petroleum and Minerals. Dept. of Geol. and Miner. Exploration. Aden, R.Y.

AL-DERWEESH K.A.S. (1988). Geology and hydrogeology of Batais Al-Husn area (Upper Abyan Delta) Abyan Governorate R. of Yemen. M. Sc. Thesis (unpub.). Kuwait University, Kuwait.

BEYDOUN Z.R. (1966). Geology of the Arabian Peninsula. Eastern Aden Protectorate and Part of Dhufar. U.S.G.S. Professional Paper 560-H. Washington, U.S.A.

COX K.G., GASS I.G. and MALLICK D.I.J. (1977). The western part of the Shugra volcanic field, South Yemen. Lithos; 10 (3): 185-191. Oslo.

GREENWOOD J.E.G.W. and BLEACKLEY (1967). Geology of the Arabian Peninsula. Aden Protectorate. U.S.G.S. Professional Paper 560-C. Washington, U.S.A.

GREENWOOD W.R., ANDERSON R.E., FLECK R.J. and ROBERTS R.J. (1980). Precambrian geologic history and plate tectonic evolution of the Arabian Shield. Bull. 24 D.G.M.R., Jeddah, Saudi Arabia.

HAWKINS T.R.W., HINDLE D. and STRUGNELL R. (1981). Out lines of the stratigraphy and structural framework of South Dhofar (Sultanate of Oman). Geologie en Mijinbou, 60 (2): 247-256.

PARK R.G. (1983). Foundations of structural geology. Blackie Son Ltd., Glasgow, Scotland, U.K.

ROBOOL M.J., RAMSAY C.R., JACKSON N.J. and DARBYSHIRE D.P.F. (1983). Petrological aids to stratigraphic correlation of volcanosedimentary successions in the Central Arabian Shield. Bull. Fac. Earth Sci. King Abdulaziz University. Jeddah, Saudi Arabia, 6: 165-194.

SHACKLETON R.M. (1986). Precambrian collision tectonics in Africa. Geological Society Special Publication No. 19: 329-349. From COWARD M.P. and RIES A.C. (eds.). Collisions Tectonic, Blackewell, Scientific Oxford, U.K.

STOESER D.B., FLECK R.J. and STACEY J.S. (1983). Geochronology and origin of an early tonalite gneiss of the Wadi Tarib batholith and the formation of syntectonic gneiss complexes in the Southeastern Arabian Shield, Kingdom of Saudi Arabia. Bull. Fac. Earth Sci. King Abdul Aziz Univ., 6: 351-364.

WARDEN A.J. and DANIELS J.L. (1983). Evolution of the Precambrian of Northern Somalia. Bull. Fac. Earth Sci. King Abdul Aziz Univ., 6: 145-164.

WARDEN A.J. and HORKEL A.D. (1984). The Geological Evolution of the NE-Branch of the Mozambique Belt (Kenya, Somalia, Ethiopia). Mitt. Osterr. Geol. Ges., 78.

WINDLEY B.F. and TARNEY J. (1986). The structural evolution of the lower crust of orogenic belts, present and past. Geological Society Special Publication, 24: 221-230. London. U.K. sp. Pub. on "The Nature of the Lower Continental Crust" DAWSON J.B., CARSWELL D.A., HALL J. and WEDEPOHL K.H. (eds.).

*Final editing, January 1990*

From *Geology and mineral resources of Somalia and surrounding regions*, Ist. Agron. Oltremare, Firenze, Relaz. e Monogr. 113, 153-168, 1993.

# CONTRIBUTIONS TO THE STRATIGRAPHY OF THE EARLY TO MIDDLE JURASSIC FORMATIONS OF THE EASTERN SIDE OF THE LUUQ-MANDERA BASIN, BAY AND GEDO REGIONS, SOUTH-WESTERN SOMALIA

L. BUSCAGLIONE *, M. FAZZUOLI *, M. CHIOCCHINI ** and G. PAVIA ***

* Dipartimento di Scienze della Terra, Università di Firenze, Via La Pira 4, 50121 Firenze, Italy.

** Dipartimento di Scienze della Terra, Università di Camerino, Viale Betti 1, 62032 Camerino, Italy.

*** Dipartimento di Scienze della Terra, Università di Torino, Via Valperga Caluso 37, 10123 Torino, Italy.

## ABSTRACT

In the Bay and Gedo regions of South-western Somalia the units of the Mesozoic Luuq-Mandera sedimentary Basin are well exposed.

Above the basal Adigrat Sandstones, three lithostratigraphic units, which we suggest to rank as formations, crop out, namely: Uanei, Baidoa and Goloda; these units may be framed in the Iscia Baidoa Group.

Within these Early-Middle Jurassic units, several sub-units can be recognized.

A) The Adigrat Sandstones consist of coarse to fine quartz sandstones. The inferred age is Early Liassic. The environment of sedimentation was fluviatile to shallow marine.

B) The Uanei Formation is constituted by three sub-units:

B 1) dark grey marly limestones and marls;

B 2) thick bedded grey calcilutites, thin bedded grey calcilutites and marls, laminated fine calcarenites;

B 3) grey marls, reddish shaly marls, reddish nodular calcilutites, yellowish marls, ferruginous calcarenites.

The age of the Uanei Formation is ?Late Pliensbachian-Toarcian. The environment of deposition is initially referable to a restricted platform, then passes to a shallow shelf and later on to a proximal ramp.

C) The Baidoa Formation is characterized by two sub-units:

C 1) grey brown bioturbated calcarenites, grey oncoidal calcilutites;

C 2) grey brown bioturbated calcilutites.

The age of the Baidoa Formation is Aalenian-Bajocian. The environment changes from open platform to partially restricted platform.

D) In the Goloda Formation three sub-units are recognizable:

D 1) grey calcilutites and yellow pink dolomites;

D 2) bioturbated calcilutites alternating with grey brown calcarenites;

D 3) yellowish brown calcarenites.

The age of the Goloda Formation is Bathonian-Early Callovian. The environment of sedimentation of the sub-unit D 1 can be referred to a partially restricted platform, while that of the sub-units D 2 and D 3 to an open platform.

## INTRODUCTION

The Luuq-Mandera basin, extending northwards from the coast of Southern Somalia and trending SSW-NNE, is comprised between the crystalline basements of the North Eastern District of Kenya, on the west, and of the Bur Region, on the east. In this area a Jurassic-Early Cretaceous succession crops out within a large synclinal structure; older sediments are present in subsurface, within a deep linear trough, found by oil wells.

The sedimentary succession of this area may be summarized as follows (BELTRANDI and PYRE, 1975; BARBIERI, 1978; CANUTI et al., 1980; CANUTI et al., 1983; ANGELUCCI et al., 1983; MONTANARI, 1986; BUSCAGLIONE and FAZZUOLI, 1987; ALI KASSIM et al., 1987; BOSELLINI, 1989):

1) ?Late Triassic-Early Jurassic clastic, evaporitic and carbonate deposits of continental, transitional and restricted marine environments, related to a phase of continental rifting.
These deposits, filling a narrow graben or semi-graben structure found by geophysical prospections, have been reached only in the Hol 1 well, placed in the axial part of the basin (BURMAH OIL CO, 1973).
2) Early to Middle Jurassic carbonate and shaly sediments, connected with the marine transgression which started during the Lias in the Arabian-Madagascan arm of the Tethys. Open sea environments are recorded by the deposition of marls with ammonites during Early Toarcian (CANUTI et al., 1983). Then a regression with minor oscillations ensued, but a widespread emersion was never reached.
3) Middle to Late Jurassic, possibly extending up to the Early Cretaceous, shaly, carbonate and clastic sediments (CANUTI et al., 1980). In this time, when the detachment of the Madagascar from East Africa occurred, the sea invaded the East Africa, overlapping large areas previously covered mostly by continental deposits. Marly sediments and pelagic faunas (ammonites and belemnites), of Late Callovian-Early/middle Oxfordian age, record the deeper water environment (open but quite shallow epicontinental sea).

In previous works (DOMINCO, 1966a, 1966b; BARBIERI, 1968; BELTRANDI and PYRE, 1975) the stratigraphic succession of South-western Somalia, above the crystalline basement, was established as follows, from bottom:

- Iscia Baidoa Formation, of inferred ?Early-Middle Jurassic age, subdivided in four members, namely Deleb, Uanei, Baidoa, Goloda Members, of clastic and carbonate lithology;
- Anole Formation, a marly unit of Callovian age;
- Uegit Formation, a calcareous unit of Late Jurassic age.

More recently, according to the regional nomenclature, basal clastics of the Deleb have been referred to the Adigrat Sandstones (HILAL et al., 1977).

This paper exposes the paleontological and sedimentological preliminary results of a regional study on the Early and Middle Jurassic units of the South- western Somalia. According with these data, the above cited four members are clearly recognizable and mappable on a regional extent and therefore they should be ranked as formations. The name "Iscia Baidoa" may indicate the Group, comprehensive of three mostly carbonate formations.

## The Early And Middle Jurassic Formations

Above the crystalline basement, the Jurassic sedimentary succession of South-western Somalia crops out in a crescent shape, forming a prominent "cuesta" that extends for many tens of kilometres between the Bur Region and the Jubba River (Fig. 1). The scarps of the cuesta permit to observe several stratigraphic sections, in particular in the neighbourhood of the Isha Baydhabo (Iscia Baidoa) town. The study of these sections, as well that of others sections along the roads Baydhabo-Luuq, Baydhabo-Xuddur, Diinsoor-Bardheere (Fig. 1), led to recognize four lithologic units that, from bottom, are:

A) Adigrat Sandstones;
B) Uanei Formation;
C) Baidoa Formation;
D) Goloda Formation.

### Adigrat Sandstones (Unit A)

On the peneplained crystalline basement, the Jurassic sedimentation starts with a thin level of basal clastics, referable to the Adigrat Sandstones (HILAL et al., 1977). This unit grades upwards from a conglomerate with quartz pebbles at the contact with the basement to a medium to fine-grain size, light grey sandstones (DOMINCO, 1966). The sandstones are thin to medium bedded, generally poorly cemented, with angular grains, well sorted in the upper part of the section, rich in pyrite and mica crystals. The thickness varies from 12 m at Deleb (type- section 14 km NE of Baydhabo) up to 30 m, 100 km SW of Baydhabo.

The sedimentary environment, up to now not studied in detail, was probably transitional from continental (braided to meandering rivers) to deltaic and probably near-shore shallow marine.

The age is not definible, due to the lack of fossils; but, according with the age of the overlying formation, an Early Liassic age may be feasible.

### Uanei Formation (Unit B)

This formation is constituted at Waaney (type-section) (cf. CANUTI et al., 1983), and near the town of Isha Baydhabo, by three superimposed sub-units, from bottom:

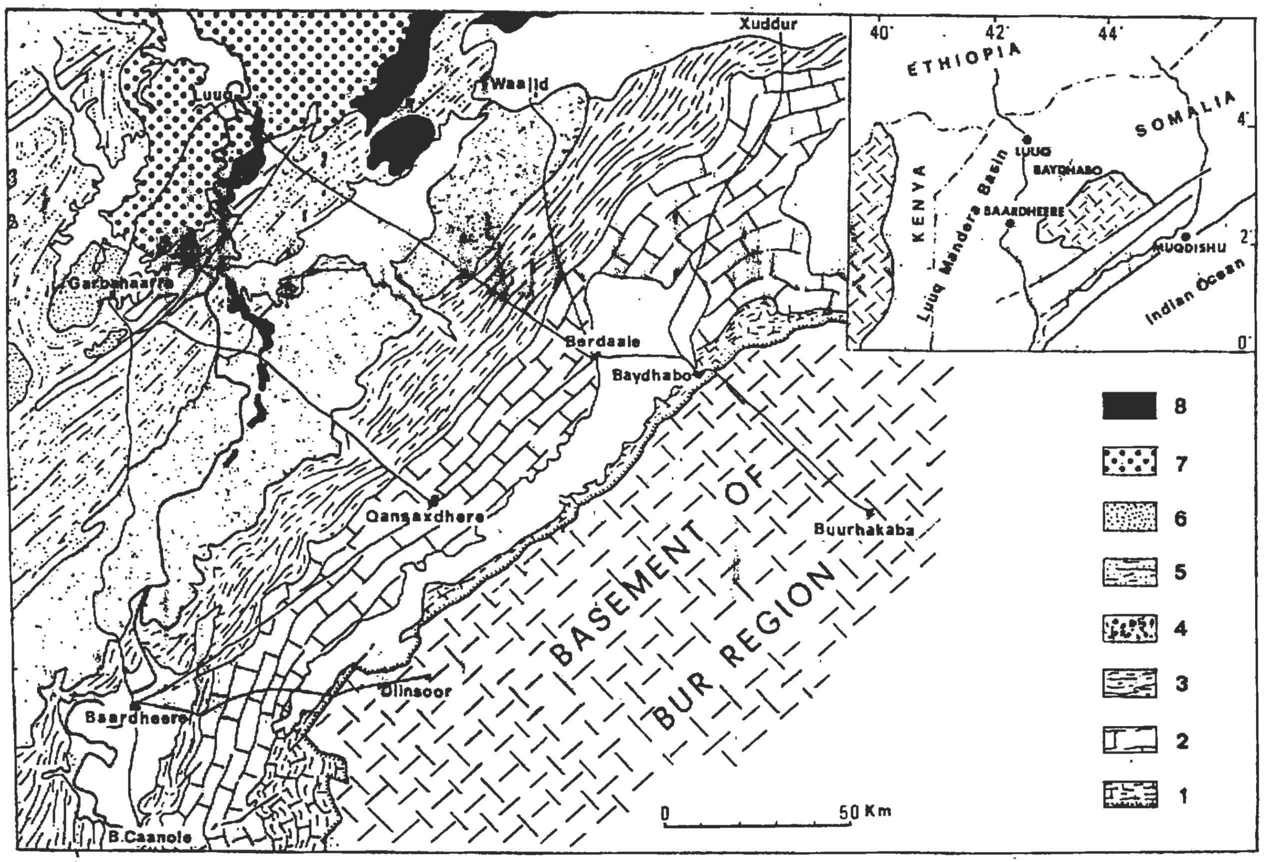


Fig. 1 - Geological sketch map of South-western Somalia (from ALI KASSIM et al., 1987, modified). 1 - Adigrat Sandstones, Uanei Formation, Baidoa Formation; 2 - Goloda Formation; 3 - Anole Formation; 4 - Uegit Formation; 5 - Garbaharre Formation, Busul Member; 6 - Ambar Sandstones; 7 - Garbaharre Formation, Mao Member; 8 - Tertiary basalts.

Sub-unit B1: dark grey marly limestones with abundant quartz grains (20 m); grey green marls (10 m).

Both in the marly limestones and in the marls, fossils have been not found; the age, according to the stratigraphic position, is pre-Toarcian, possibly Late Pliensbachian. The sedimentary environment may be inferred as the protected side of a coastal lagoon with restricted circulation and with a fine and rarely coarse terrigenous imput.

Sub-unit B2: thick bedded, dark grey calcilutites (4.5 m); thin bedded, grey marly limestones and marls with laminated grey-brown calcarenitic bed at the top (3.5 m).

In the sub-unit B2, the dark grey limestones, in beds 20-80 cm thick, consist of bioclastic wackestones, often bioturbated, with some levels of lumachellas; the thin (5-10 cm) marly limestone beds are also strongly bioturbated. The calcarenitic bed, 10-15 cm thick, consists of bioclastic and peloidal packstones and grainstones. Fossils are represented by pelecypods, gastropods, echinoderms, benthic foraminifera: *Vidalina? martana* FARINACCI, *Pseudocyclammina liasica* HOTTINGER, *Lingulina* gr. *tenera* BORNEMANN, *Globochaete alpina* LOMBARD, "*Siphovalvulina*" *sensu* SEPTFONTAINE 1981, *Glomospira* sp.1, *Glomospira* sp.2, *Ammobaculites* sp., *Dentalina* sp., *Spirillina* sp., *Lenticulina* sp., *Glomospirella* sp., *Cornuspira* sp., *Nodosariidae*, ostracods, coprolites (*Favreina* sp.) and "filaments".

The age could be referred to the lower part of the Early Toarcian.

The environment is subtidal, generally under wave base, and it is referable to a transition area (ramp) between the platform and the shallow shelf, with carbonate and fine clastic deposition.

Sub-unit B3 : grey fossiliferous marls (1-3 m); reddish shaly marls with ammonites (13-15 m); grey brown and pink nodular calcilutites (6-8 m); grey yellow marls with ammonites (10 m); thick bedded reddish brown (ferruginous) calcarenites ( 6 m).

The marly levels are massive, possibly by bioturbation and they are characterized by a relatively abundant fossil content, namely by ammonites and pelecypods. In the middle (reddish) marly level, in some places, calcareous concretions are present, consisting mostly of an agglomerate of cemented shells of pelecypods of the genus Opis.

The lower calcareous level consists of well stratified (5-30 cm), brown yellowish calcilutites, rich in iron-stained stylolites that give a nodular feature; bioturbation structures are widespread. Texture is represented by recrystallized mudstones with abundant small crystals of iron oxides. In some places, levels of ferruginous calcarenites, similar to those of the upper calcareous level (see below) are present.

The upper calcareous level includes well stratified (10-40 cm) yellowish brown calcarenites and calcilutites. Sedimentary structures are represented by graded bedding and cross bedding in the calcarenites, wavy bedding in the calcilutites; some levels show a brecciated feature. The textures of the calcarenites consist mostly of grainstones with pellets, peloids and coprolites; substitution of grains with iron oxides is widespread (ferruginous calcarenites). In the calcilutites, recrystallized mudstones prevail.

As regards fossils, the lower grey marly level contains following forms: *Spiriferina madagascariensis* THEVENIN, ?*Ovaticeras* sp., *Glyptarpites* cf. *glyptus* Buckman, *Hildaites gautieri* (THEVENIN), *Hildaites* cf. *serpentiniformis* BUCKMAN, *Parahildahites* aff. *jolyi* (THEVENIN), *Parahildaites madagascariensis* (THEVENIN), *Bouleiceras arabicum* ARKELL, *Bouleiceras elegans* ARKELL, *Bouleiceras nitescens* THEVENIN, *Bouleiceras rectum* ARKELL, *Bouleiceras* n. sp., ?*Grammatodon kenyanus* COX, *Modiolus* spp., *Lima* sp., *Opis* aff. *parvicarinata* THEVENIN, *Astarte* sp., *Protocardia africana* COX, *Anisocardia arkelli* COX, *Anisocardia* cf. *didimtuensis* COX, *Discohelix* n. sp., ?*Africonulus* sp., *Hypodiadema* sp.

The middle, reddish shaly marly level contains the following ammonites, pelecypods and gastropods:
*Hildaites gautieri* (THEVENIN); cf. CANUTI et al., 1983, t. 2, f. 6, *Parahildaites jolyi* THEVENIN, ibidem, t. 2, ff. 4, 9, *Parahildaites* cf. *termieri* BLAISON, *Parahildahites* n. sp. ind.; *ibidem*, t.2, ff. 7, 8, 10-12, *Parahildahites namakiensis* BLAISON, *Anisocardia arkelli* COX, Nuculanids, Trigonids.

The lower (as well the upper) calcareous level contains only rare microfossils: *Glomospira* sp., *Ammobaculites* sp., unidentifiable coprolites (*Favreina* sp.) and "filaments".

The upper, yellow green marly level contains:
*Hildaites gautieri* (THEVENIN) (cf. CANUTI et al., 1983, t. 2, f. 1), *Parahildaites jolyi* (THEVENIN), *Parahildahites madagascariensis* THEVENIN (*ibidem*, t. 2, f. 2), *Parahildahites namakiensis* BLAISON, *Parahildaites* cf. *Termieri* (BLAISON), *Lucina* sp., *Opis* aff. *parvicarinata* THEVENIN, *Anisocardia Arkelli* COX, *Anisocardia* cf. *didimtuensis* COX.

The inferred age of the marly levels, on the ground of the fossils cited above, is the upper part of the Early Toarcian (Serpentinus Zone); in the ferruginous calcarenites, for stratigraphical position, the age may extends to the Middle and the Late Toarcian.

The sedimentary environment of the marly levels as well as that of the nodular calcilutites is referable to an open shelf, under wave base, with periods of abundant fine clastic supply. The nodular calcareous level represents a period of starvation of that supply. The ferruginous calcarenites appear to be resedimented (PICCOLI et al., 1986). However, even if gravity flows processes may be feasible in some instances, we think that most calcarenites deposited under action of storms, as they present sedimentary structures referable to proximal tempestites (AIGNER, 1980, 1985).

The sequence marls-calcarenites marks therefore a shallowing of the environment of deposition.

### Baidoa Formation (Unit C)

This formation is well exposed on the top of the scarp in the neighbourhood of Isha Baydhabo; the hard limestones are quarried as building stone.

Two sub-units can be recognized, from bottom:

Sub-unit C1: grey-brown bioclastic and oncoidal calcarenites (20 m); grey oncoidal calcilutites (20 m); oolitic calcarenites.

The rock is well bedded; the bed thickness is 15-40 cm.

Textures of the calcarenites consist of bioclastic, peloidal, oncoidal packstones/ grainstones; the beds are often cross laminated, but they are also bioturbated on the top by vertical burrows. Also the bioclastic, peloidal and oncoidal wackestones present bioturbation features. A ferruginous hardgrounds has been observed, on the top of a calcarenitic bed, near Isha Baydhabo. Some levels of oolitic grainstones are present only in the south western area.

Fossils are represented by pelecypods, gastropods, echinoderms and:

*Globochaete alpina* LOMBARD, *Favreina* cf. *eiggensis* BRONNIMAN, *Favreina fendiensis* BRONNIMANN and ZANINETTI, *Mesoendothyra croatica* GUSIC (typical form), *Nubecularia reicheli* RAT, *Glomospira* spp., *Ammobaculites* sp., *Valvulinidae*, *Nodosariidae*, ostracods, rare radiolaria and sponge spicules, "filaments".

The environment is referred to an open carbonate platform, with medium to high energy conditions.

Sub-unit C 2 : bioturbated, grey brown calcilutites (40 m); grey calcarenites (10 m).

The thickness of the beds is 15-40 cm .

Textures consist mainly of bioturbated mudstones and bioclastic wackestones, while oolitic, peloidal and bioclastic grainstones are subordinate.

Fossils present are : pelecypods, gastropods, echinoderms and

*Sarfatiella dubari* CONRAD and PEYBERNES, *Nubecularia reicheli* RAT, *Mesoendothyra croatica* GUSIC (typical form), *Spiraloconulus* sp., *Ophtalmidium* sp., *Glomospira* sp.1, *Nodosariidae*, coprolites *Favreina* cf. *eiggensis* BRONNIMANN, *Palaxius* aff. *triasicus* (ELLIOTT), rare ostracods, radiolaria and sponge spicules.

The environment of the sub-unit C 2 seems to be variable, from a shallow shelf, mainly for the occurrence of pelagic forms, to a partially restricted platform, mostly below wave base. Only in the south-western area, some episodes of higher energy are present.

The inclusive age of the sub-units C 1 and C 2 is Early Dogger (Aalenian-?Early Bajocian), though the upper time boundary is at present uncertain.

### Goloda Formation (Unit D)

This unit is the thickest of the Jurassic succession of South-western Somalia (about 600 m of thickness). It is well exposed south west of Isha Baydhabo and particularly in the area between Diinsoor and Bardheere.

Studied stratigraphic sections are present in two areas, more than 120 Km apart: the north-eastern area (roads Baydhabo-Luuq, Baydhabo-Waajid, Baydhabo-Xuddur) and the south-western area (road Diinsoor-Bardheere) (Fig. 1). In the north-eastern area the lower part of the stratigraphic sections is generally covered. The two areas show lithological features quite different; up to now, informations about the intermediate area are not available.

The lithostratigraphical features of two areas are examined separately.

## SOUTH WESTERN AREA

Sub-unit D 1: grey calcilutites, yellow pink dolomites (thickness about 300 m).

This sub-unit consists mostly of medium bedded (20-60 cm thick) calcilutites of dark grey colour, sometimes with bioturbation structures. Textures of calcilutites are constituted by mudstones and wackestones with rare bioclasts and quartz grains. Calcilutites are often partly or completely recrystallized and dolomitized. The dolomitic levels have a reddish colour; textures consist of coarse mosaics of recrystallization and dolomitization.

Only rare pelecypods, echinoderms and "filaments" have been found in this sub-unit.

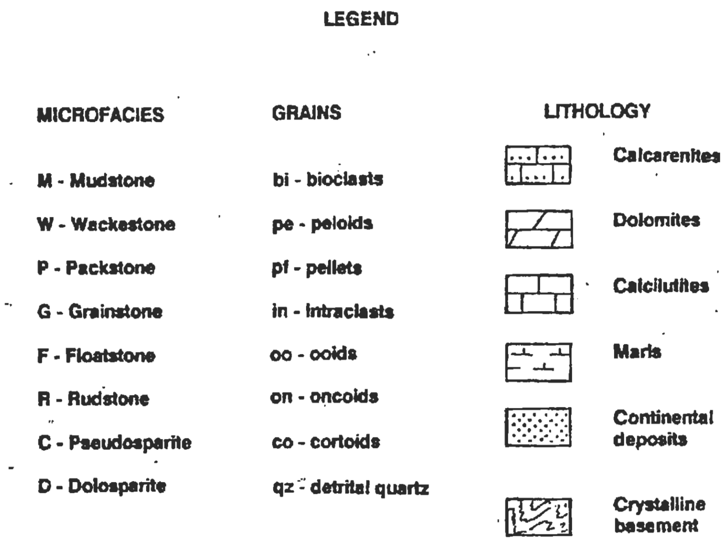


Legend of Figs. 2a and 2b

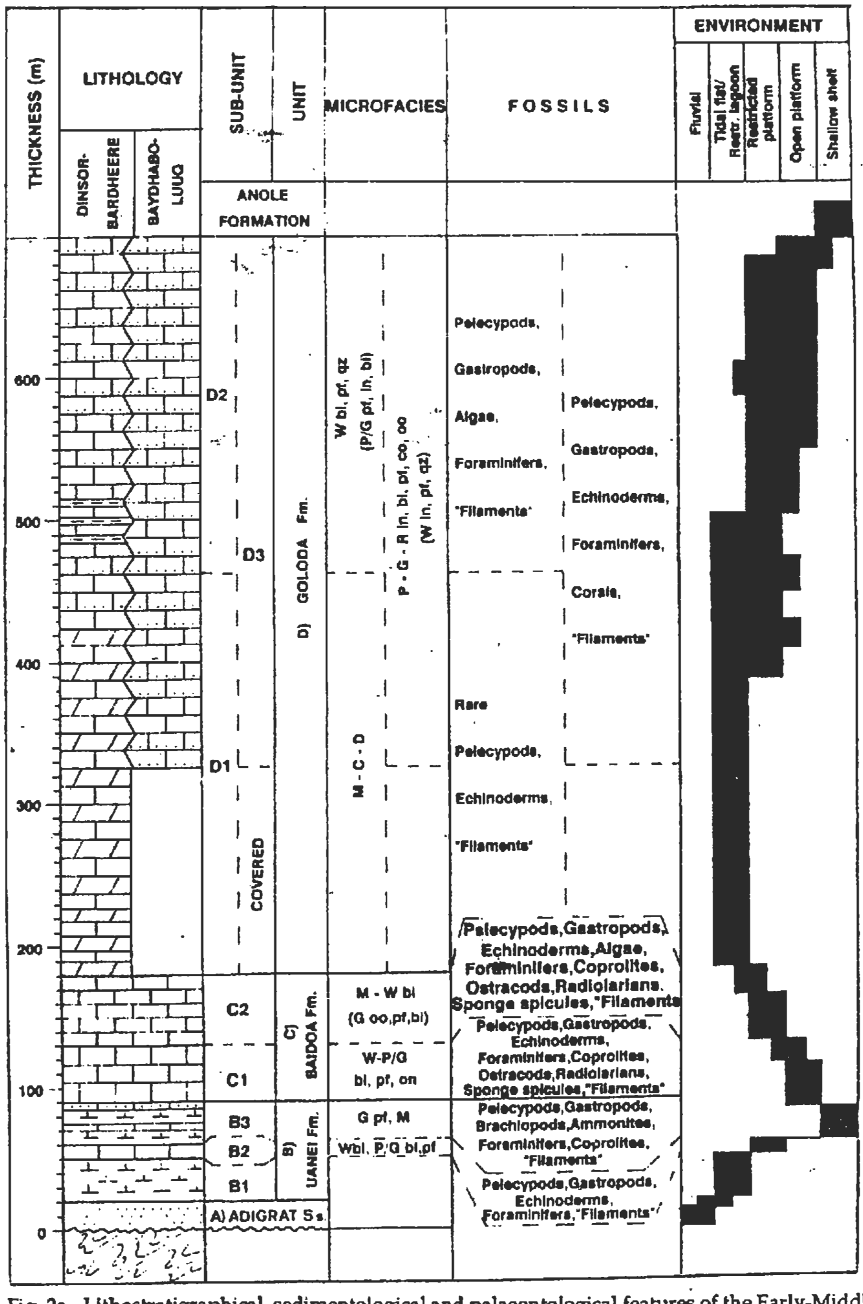


Fig. 2a - Lithostratigraphical, sedimentological and palaeontological features of the Early-Middle Jurassic succession of South-western Somalia (continued to Fig. 2b).

The age cannot be established directly; most probable age, inferred only for the stratigraphic position, could be ?Late Bajocian-Bathonian p.p..

The barren mudstones deposited in subtidal conditions below the wave base, whereas the dolomitized levels possibly originated in hyperaline conditions. These features seem to indicate a restricted environment (platform?), but the presence of filaments, on other hand, can suggest a connection with deeper sea. The common occurrence of quartz grains can be related with a close emerged land.

This sub-unit may represents, on the whole, the peak of the regressive phase, which led in particular the south-western area in shallow water conditions, but without generalized episodes of emersions. Probably, during the lowering of the sea level, this area remained at time isolated from the open sea by the development of barrier island complex; so, features of restricted environment developed.

Sub-unit D 2: grey bioturbated calcilutites; grey brown calcarenites (about 250 m).

This sub-unit consists of dark grey calcilutites, in beds to 40 cm thick, with frequent bioturbation structures.

Rare thin shaly beds are present. Textures are represented by mudstones and wackestones with bioclasts, fecal pellets and quartz grains; levels of recrystallized mudstones, sometimes dolomitized, and of bioclastic packstones (lumachellas) are also present. In particular in the upper part of the section, rare calcarenitic beds are present, intercalated between calcilutite beds. In some instances, calcarenitic levels seem to be channelized within the calcilutites. Textures of calcarenites consist of grainstones/rudstones with bioclasts, intraclasts, cortoids and fecal pellets. In the calcarenitic levels, sedimentary structures as horizontal laminations; due to isohorientation of shells and "umbrella" structures are frequent. The fossil content includes pelecypods, gastropods, foraminifers and algae:

*Nautiloculina oolithica* MOHLER, *Pfenderella arabica* REDMOND, *Trocholina* gr. *palastiniensis* HENSON, *Alzonella cuvillieri* NEUMANN, *Cayeuxia* sp., *Nodosariidae*, "filaments".

It is to be noted that all forms of foraminifers and algae seem to appear abruptly in the calcarenitic levels.

The microfossils are indicative of a Late Bathonian-Early Callovian age. The environment of deposition of the calcilutites of the sub-unit D2 is referable to a subtidal, under wave base, shallow shelf, whereas the calcarenites correspond to storm deposits (tempestites).

NORTH EASTERN AREA

Sub-unit D 3: brown calcarenites (about 400 m, outcropping).

This sub-unit is constituted mostly by calcarenites; calcilutites are rare, but present in particular in the lower part of the section Baydhabo-Luuq.

The calcarenites of the sub-unit D 3 are thick bedded (up to 200 cm thick), white

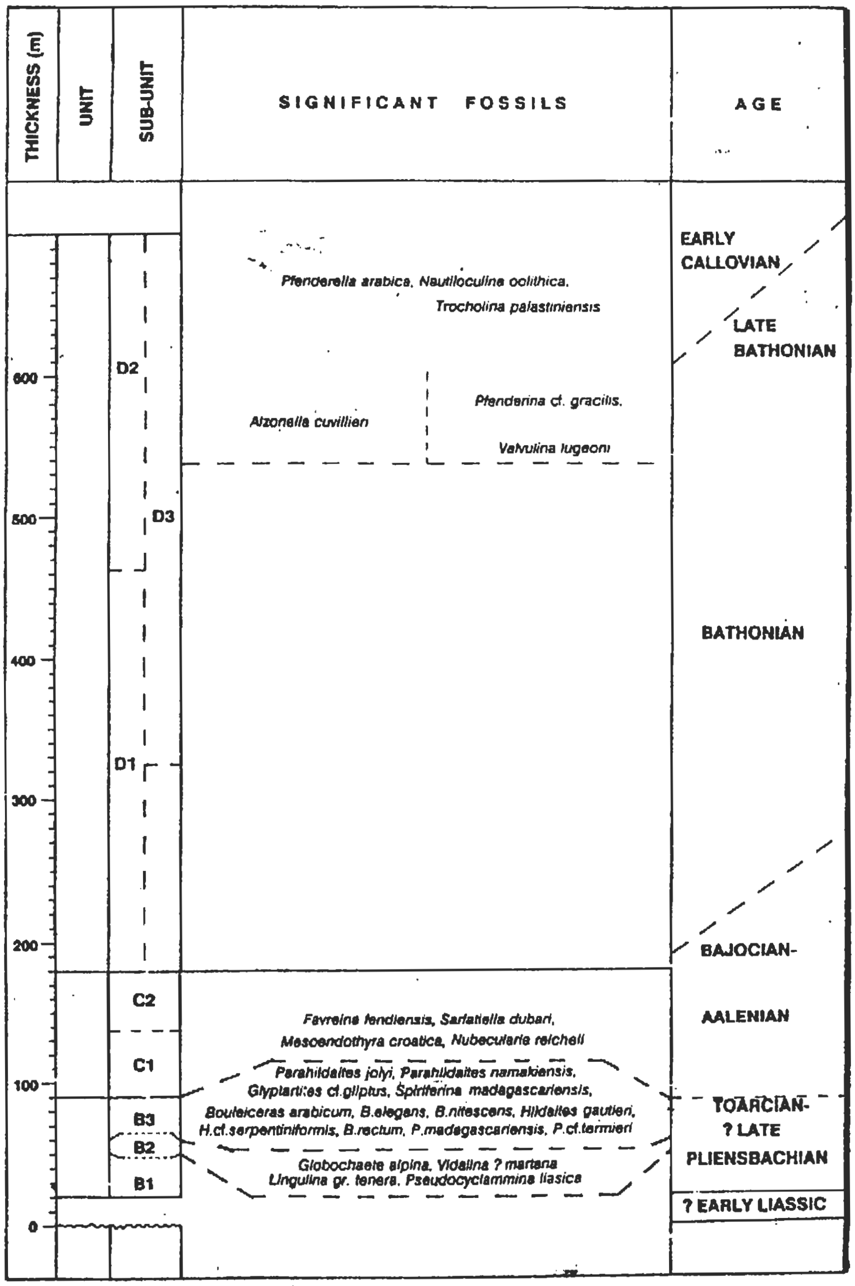


Fig. 2b - Lithostratigraphical, sedimentological and palaeontological features of the Early-middle Jurassic succession of South-western Somalia.

yellowish to the percussion but dark brown if weathered; they show horizontal, cross and wavy laminations. Textures consist of grainstones/packstones and rudstones with intraclast, bioclasts, fecal pellets, cortoids and rare ooids; often grains are substituted by iron oxides.

The calcilutites have a dark grey colour, and, in some occurrences, are partially or completely recrystallized or dolomitized. Textures consist of mudstones and bioclastic, intraclastic, pellettiferous and quartzose wackestones.

Along the whole section the fossil content includes pelecypods, gastropods, echinoderms, and corals.

Near the middle of the exposed section, the fauna becomes also rich in foraminifers and algae :

*Nautiloculina oolithica* MOHLER, *Pfenderella arabica* REDMOND, *Trocholina* gr. *palastiniensis* HENSON, (these forms are commom with the sub-unit D 2), and moreover:

*Mesoendothyra croatica* GUSIC (form B by PELISSIER and PEYBERNES, 1982), *Valvulina lugeoni* SEPTFONTAINE, *Pfenderina* cf. *gracilis* REDMOND, *Thaumatoporella parvovesiculifera* RAINERI, "*Siphovalvulina*" sp. (*sensu* SEPTFONTAINE, 1981), *Cladocoropsis mirabilis* FELIX, *Pfenderina* sp., ostracods and rare "filaments".

The rich micropaleontological record permit to assign the uppermost fossiliferous calcarenites of the sub-unit D 3 to the Late Bathonian-Early Callovian. Therefore, for fossil content and age, as well as for stratigraphical position (both sub-units D 2 and D 3 passe upwards to the Anole Formation), the sub-unit D 3 is heteropic, in their upper part, with the sub-unit D 2 and in their lower part, also with the sub-unit D 1.

As to the environment of deposition, the calcarenites of the sub-unit D 3 deposited in a moderately to higly agitated, open platform.

On the whole, the sub-units D 2 and D 3 indicate the return to a more open sea, even if shallow. However, whereas in the north-eastern area the calcarenites of the sub-unit D 3 indicates the development of a high energy marginal zone, in the south-western area, the calcilutites of the sub-unit D 2 deposited in a subtidal, low energy environment, closer to the continent and protected sea wards by the marginal zone.

## CONCLUSIONS

The preliminary results of the stratigraphic and sedimentologic researches, carried out in the Early to Middle Jurassic units of South-western Somalia, give new and important informations about the age of the units, and therefore about the age of the phases of the marine transgression that interested this area (as well as the whole East Africa) and about the sedimentation processes, linked with that transgression.

The macrofossils, mainly ammonites, found in the Uanei Formation confirm and detail the previous dating (CANUTI et al., 1983) to the Early Toarcian; moreover, the age of the microfossils of the Uanei Formation agrees well with the age of the ammonites. The occurrence of significant microfossils permit to attribute to Aalenian-Bajocian the age of the Baidoa Formation and to Late Bathonian-Early Callovian the age of the upper part of the Goloda Formation.

As regards the evolution of the sedimentary environment in the South-western Somalia during Early and Middle Jurassic, in particular from Early Liassic to Callovian, it presents several variations in time and in space.

Three phases can be distinguished in the sedimentary evolution, corresponding to the following periods:

i) pre-Toarcian to Late Toarcian; ii) Early Aalenian to Early Bathonian; iii)? Middle / Late Bathonian to Early Callovian.

In the first period, at the beginning of the transgression, the sedimentation is clastic, of continental and transitional (lagoonal) environment (Adigrat Sandstones and sub-unit B 1 of the Uanei Formation).

At the beginning of the Early Toarcian, the sedimentation become carbonatic and marly (sub-units B 2 and B 3 of shallow shelf environment, more or less open, even if not very deep). In fact, a shallow seaway developed, connected towards north east with the Tethys, which permitted the occurrence of the ammonites of the genus Bouleiceras and Parahildahites, present also in NE Kenya, NE Somalia, NW Madagascar and Central Arabia (Arabo-ethiopian-madagascan Province).

The carbonate level sandwiched between the marly levels would correspond to a bathymetric variation or, more probably, to a period of higly reduced fine terrigenous supply, with following deposition of a fine carbonate sediment, at low sedimentation rate.

With the ferruginous calcarenites (upper part of the sub-unit B 3, the second (regressive) phase starts, probably at the top of the Toarcian, and the environment comes again in shallow water conditions, with carbonate sedimentation (Baidoa Formation, of Aalenian-Bajocian age). In this unit, a regressive sequence occurs: the environment changes from high energy conditions of the open platform (sub-unit C 1) to low energy conditions of partially restricted platform (sub-unit C 2).

Later on the regressive phase pursued. Probably this phase was not a continuous process, but it seems to be the final results of some minor oscillations, probably due to short-period eustatic variations. The apex of the regression, even if evidences of emersions have been not found, may be recorded, in particular in the south western area, by features of shallow water environment, with restricted circulation and even possible episodes of high carbonate concentration (calcilutites with extremely poor fauna and dolomites of the sub-unit D 1).

However, during this time, the environment of deposition was not uniform in the whole region. In fact, the south western area, placed closer to the continent, was probably protected by the north eastern area, that shows features of marginal zone. During Bathonian (up to now it is not possible to define more accurately the time), in the upper part of the Goloda Formation, the third, transgressive, phase starts.

On one side it is possible to observe, together with an increase of higher energy calcarenitic levels in the calcilutitic sub-units D 2, a "bloom" of faunas, that is both the type of microfossils and their density show an abrupt increase.

On the other side, in particular in the north eastern area, it is remarkable the occurrence of the same kind of "bloom", with the same microfossils, within the calcarenites D 3. This fact confirmate the lateral transition between the upper part of the sub-unit D 2 and that of D 3 and document an opening of the sea, that permitted the bloom of microfossils.

It consists therefore of the development of anew transgressive phase, which will reach its apex during the Callovian - Early Oxfordian, with the deposition of marls with pelagic fauna in a shelf environment (Anole Formation).

The Liassic transgression occurred in East Africa in a relatively shallow channel, just in correspondence of the present coastline of the Indian Ocean, with some small embayments: Lamu, Mandera-Luuq, "Somali embayment". The NE-SW and N-S trends of the main sea arm and of the embayments were connected with the trends of the previous Karroo basins (KENT et al., 1971; CANNON et al., 1981; RAIS ASSA, 1988) and heralded the trends both of the transform margin and of the rifted margin, that developed between East Africa and Madagascar since Late Jurassic (RABINOWITZ et al., 1982; BOSELLINI, 1986). Therefore, as during the Toarcian an important eustatic rise occurred (HALLAM, 1978; VAIL et al., 1977; HAQ et al., 1987), the origin of the transgression was both tectonic and eustatic. In fact the transgression was controlled by the eustatic rise, but the flooding interested mostly the depressed areas, corresponding to the Karroo grabens (BOSELLINI, 1989).

During the Bathonian, another important transgressive phase started again, that interested large areas of East Africa (Ethiopia, Somalia, Kenya and Tanzania).

In the Luuq-Mandera Basin, this phase reached its apex in the Oxfordian (BUSCAGLIONE and FAZZUOLI, 1987), when in a shelf environment took place the sedimentation of the marls with ammonites of the Anole Formation.

Later on, starting from Early Kimmeridgian up to Portlandian, the sedimentation of the carbonate Uegit Formation occurred in a platform environment (FAZZUOLI, 1985). Shallow water conditions prevailed, even with oscillations. Finally, the sea retreated from South-western Somalia during Early Cretaceous.

The transgressive phase of the Middle-Late Jurassic seem to fit well with the eustatic curve of HAQ et al., 1987; the regressive phase, on the contrary, shows some differences. In fact, according with HAQ et al., 1987, the highest sea level was reached during Late Kimmeridgian; but in the studied area, the return to shallow water conditions occurred during Early Kimmeridgian, that is during the eustatic rise.

The maximum sea depth was connected with the regional subsidence more than with the rise of the sea. The maximum subsidence rate was probably reached during the detachment of the Madagascar from East Africa (at the beginning of Late Oxfordian, according with RABINOWITZ et al., 1983), and it was caused by the crustal stretching of the continental margin.

Possibly, hysostatic readjustments followed to the detachment of the Madagascar led to a positive warping of the South-western Somalia; the subsidence rate lowered and shallow water conditions, with carbonate platform sedimentation, were established again.

According to BOSELLINI (1989), the succession of the Uanei, Baidoa and Goloda formations constitutes a depositional sequence, namely the Hamanley Sequence. The Goloda Formation would correspond to the prograding highstand system tract of the sequence and the sharp transition between the calcarenites of the Goloda Formation and the marls with ammonites of the overlying Anole Formation to the transgressive surface of the younger depositional sequence (namely the Uarandab D.S.) and therefore the sequence boundary; his age is Upper Callovian.

According to the above exposed data, we think that the transgression of Middle-Late Jurassic began earlier, during Bathonian, and that it is recorded in particular by the "bloom" of faunas observed in the Goloda Formation, as this "bloom" is connected with a sea level rise.

## REFERENCES


AIGNER T. (1980). Storm deposits as a tool in facies analysis: I Calcareous tempestites. I.A.S. 1st European Meeting, Bochum, 1980, Abstr., 44-46.

AIGNER T. (1985). Storm Depositional System. In: G.M. FRIEDMAN, H.J. NEUGEBAUER and A. SEILACHER. Lecture Notes in Earth Sciences, 3, Springer Verlag.

ALI KASSIM M., CARMIGNANI L. and FAZZUOLI M., with the collaboration of BRUNI P., FANTOZZI P., HAWA HERZI H, SASSI F.P. (1987). Geology of the Luuq-Mandera Basin. Excursion A. Guidebook GEOSOM 87, Mogadishu, 43 pp.

ANGELUCCI A., BARBIERI F., CABDULQAADIR M.M., FAADUMA C.C., FRANCO F., ARUSH C.A. and PICCOLI G. (1983). The Jurassic Stratigraphic series in Gedo and Bay Regions (South-western Somalia). Mem. Soc. Geol. It., 36: 73-94 .

BARBIERI F. (1968). Jurassic microfacies in Western Somalia. Riv. Ital. Paleont. Strat., 74: 805-862.

BELTRANDI M.D. and PYRE A. (1973). Geological evolution of South-western Somalia. In: G. BLANT (Ed.). Sedimentary Basins of the African Coasts, pt. 2, South and East Coast. Assoc. African Geol. Surveys, 181-191

BOSELLINI A. (1986). East Africa continental margins. Geology, 14: 76-78.

BOSELLINI A. (1989). The Continental Margins of Somalia: their Structural Evolution and Sequence Stratigraphy. Memorie di Scienze Geologiche, 41: 373-458.

BURMAH OIL Co. (1973). Hol No. 1. Complete Report. Burmah Oil Somalia Ltd., Mogadishu, 71 pp. (unpublished)

BUSCAGLIONE L. and FAZZUOLI M. (1987). Jurassic Carbonate Microfacies of Somalia. Dipartimento di Scienze della Terra, Università di Firenze, 107 pp.

CANNON R.T., SIMIYU SIAMBI W.M.N. and KARANGA F.M. (1981). The Proto-Indian Ocean and a probable Paleozoic/Mesozoic triradial rift system in East Africa. Earth and Planetary Earth Science Letters, 52: 419-426.

CANUTI P., FAZZUOLI M. and TACCONI P. (1980). Photogeological Map of the Region between Juba and Webi Shebeli Rivers (South-west Somalia). In: Geodynamic Evolution of the Afro-Arabian Rift System. Accademia Nazionale Lincei. Atti, 47: 209-217.

CANUTI P., FAZZUOLI M., FICCARELLI G. and VENTURI F. (1893). Occurrence of Liassic faunas at Waaney (Uanei), Province of Bay, South-western Somalia. Riv. Ital. Paleont. Strat., 89: 31-46.

DOMINCO E. (1966a). Report on the Geology of the Bur Uplift area. Hammar Petroleum Co., Mogadishu. Unpublished Report, 19 pp.

DOMINCO E. (1966b). Final Report. Geology of the Garbaharre area (Western Somalia). Hammar Petroleum Co., Mogadishu. Unpublished Report, 22 pp.

FAZZUOLI M. (1985). Sedimentological features of the Gawan Limestone and of the Uegit Formation (Upper Jurassic) in Somalia. Quad. Geol. Somalia, 8: 221-231.

HALLAM A. (1978). Eustatic cycles in the Jurassic. Palaeogeography, Plaeoclimatology, Palaeoecology, 23: 1-32

HAQ B.U., HARDENBOL J. and VAIL P.R. (1978). Chronology of fluctuating sea levels since the Triassic. Science, 235: 1156- 1167

HILAL A.F., PAVAN G. and ROBBA E. (1977). Geologia stratigrafica della Somalia. Univ. Naz. Somala. Quad. Geol. Somalia, 19-50 .

KENT P.E., HUNT J.A. and JOHNSTONE D.W. (1971) - The geology and geophysics of coastal Tanzania. Geophysical Paper No. 6, Inst. Geol. Sci.

MONTANARI L. (1984). Orientamenti per la Geologia della Somalia. 50 pp., Università Nazionale Somala, Mogadishu.

PICCOLI P., BOCCALETTI M., ANGELUCCI A., ROBBA E., ARUSH M.A. and CABDULQAADIR M.M. (1986). Geological History of Central and Southern Somalia since the Triassic. Mem. Soc. Geol. It., 31: 415-425.

RABINOWITZ P.D., COFFIN M.F. and FALVEY D. (1983). The separation of Madagascar and Africa. Science, 220: 67-69.

RAIS-ASSA R. (1988). Stratigraphy and geodynamics of the Mombasa Basin (Kenya) in relation to the genesis of the proto-Indian Ocean. Geol. Mag., 125: 141-147.

VAIL P.R., MITCHUM R.M. and THOMPSON S. (1977). Global cycles of relative changes of sea level. In: C.E. Payton (Ed.), Stratigraphic Interpretation of Seismic Data. Am. Ass. Petr. Geol. Mem., 26: 83-97.

*Final editing, January 1990*

From *Geology and mineral resources of Somalia and surrounding regions*, Ist. Agron. Oltremare, Firenze, Relaz. e Monogr. 113, 169-180, 1993.

# TECTONIC SIGNIFICANCE OF QUARTZ-TYPE IN JESOMMA SANDSTONE, SOMALIA

MOHAMUD ABDI ARUSH * and ABHIJIT BASU **

* Department of Geology, Somali National University, P.O. Box 1081, Somalia.
** Department of Geology, Indiana University, Bloomington, IN 47405, USA.

ABSTRACT

Distribution of quartz types in the Upper Cretaceous-Paleocene Jesomma Sandstone from four diverse locations in Somalia is determined by point counting more than 50 thin sections. Two distinct clusters are obtained indicating (a) a granitic and/or a gneissic source and a low grade metamorphic source for these sandstones. It is inferred that relative block uplifts to the west and to the north provided much of the siliciclastic detritus. This suggests that the late Mesozoic marine transgression in Somalia came from the east and south as Madagascar pulled away from East Africa and migrated southward.

## INTRODUCTION

The upper Mesozoic marine sequence in Somalia forms a package enclosed between clastic beds which are for the most part, terrestrial or littoral deposits. These are the Adigrat Sandstone below and the Jesomma Sandstone above. The succession has attracted considerable attention both academically for its relation to the break-up of the Gondwana super continent, and economically because of its hydrocarbon potential. Despite this increased interest there are many still unanswered fundamental questions. For example, did this marine transgression come from the north (ARKELL, 1956), or from the south and east (BOSELLINI, 1986), or both? In this short note an attempt is made to address the problem of the origin of Jesomma Sandstone, and to provide a first indication of provenance by use of the distribution of quartz types. The recognition of provenance provides an important constraint on the direction of marine transgression, and this in turn greatly affects assessments of areas with a hydrocarbon potential, especially in terms of source-rocks and reservoirs.

## THE JESOMMA SANDSTONE

### GENERAL DESCRIPTION

Although the most extensive outcrops of the Jesomma Sandstone are in Northern Somalia, it also crops out in the central and southern parts of the country. It takes its

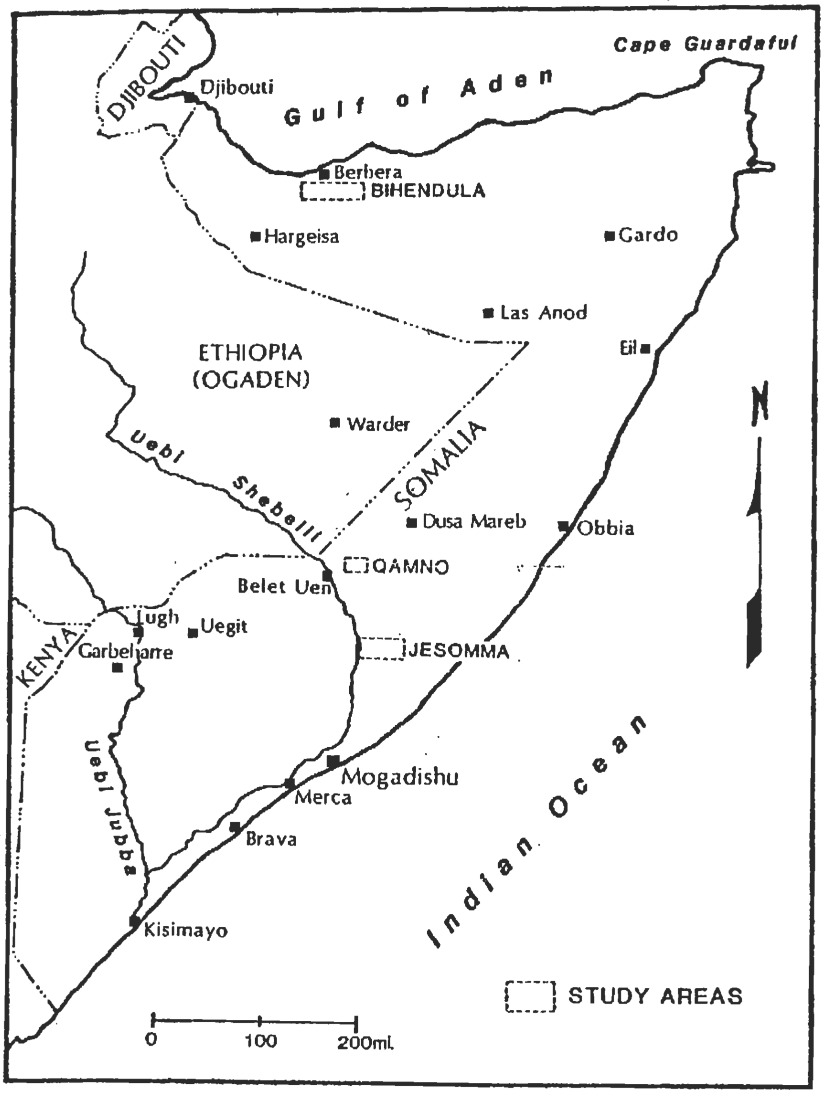


Fig. 1 - General map of Somalia showing the distribution of sites of sampling Jesomma Sandstone. Note that samples have been collected from Bihendula in the north to Qamno and Jesomma in the south.

name from a location in south-central Somalia (Fig. 1). It may reach a thickness as great as 1700 m in the north, near Guban (MERLA et al., 1979) but in the south it is reduced to about 80 m in outcrop (ALTICHIERI et al., 1982) near the Jesomma village, although in subsurface the presence of 450 m in the Sinclair hole XF5 has been reported (BARNES, 1976). In the south, near Bur Qamno and Bur Jesomma outcrops tend to be few and expose only parts of the sequence .

In the north the Jesomma Sandstone is found in the Bihendula-Borama basin, the Almado-Darroor basin, and over the Erigavo High. MERLA et al. (1979) measured the greatest recorded thickness in the Guban area where they showed that it transgressed over the older Gawan Limestone Formation of Jurassic age. In the Bihendula Basin too it follows the Jurassic marine section but over the Erigavo high it rests on basement rocks. In the 1250 m Dubar section BRUNI and FAZZUOLI (1976) showed that the Jesomma Sandstone was deposited in coastal plain environment passing up to an inferred littoral environment marked also by meandering streams. This suggests a generally regressive sequence. In the Almado-Darroor basin to the east, however, it passes laterally into marine beds, which in contrast would suggest a transgressive sequence. Unfortunately descriptions of the sandstone in other parts of Somalia are generally inadequate for environmental interpretation, although at Jesomma the descriptions are consistent with, but not diagnostic of, a lower coastal plain environment.

### Lithologic Description

Mature quartz and is the principal component of the Jesomma Sandstone. The heavy mineral assemblage is dominated by rutile, zircon, tourmaline and opaque iron oxides minerals; some apatite and rarely collophane is reported. Feldspar and rock fragments generally form less than 10% of the thin sections examined, 80 that the rocks may be classified as quartz arenites. The feldspars, predominantly potash feldspar, shows various degrees of alteration to kaolinite and illite. Microcline is found in the northern sections but is rare or absent in the south. Part of the maturity of the sandstones is due to diagenetic alteration of labile grains (cf. MC BRIDE, 1987). However, we do not find any over-sized pores and/or those with characteristically deformed shapes indicating large scale secondary dissolution and subsequent compaction (SHANMUGAM, 1985). Therefore, we infer that much of the maturity of the framework mineralogy could be primary. However, floating detrital grains are common in some sandstones, indicating that development of secondary porosity must have been pervasive in at least some horizons. Many sandstones show a distinct bimodal grain size distribution; the coarse mode is characterized by well rounded quartz grains whereas the fine mode is usually made up of very angular quartz and some feldspar grains. There is considerable variation in the cementing material from place to place. Calcite is predominant, but siliceous (opal or chalcedony) and ferruginous cements are also common. The sand are probably second or third cycle deposit which explains the lack of compositional variety whether collected in the north or south.

Because the sandstones are relatively mature, we have used only detrital quartz for the purpose of deciphering the provenance of these sandstones. Therefore, as long as the quartz population is representative of parent rocks, it is immaterial if the maturity of the sandstones is diagenetic or if it is primary. Provenance interpretation on the basis of quartz-types would not be affected.

### Age and correlation

The Jesomma Sandstone has been correlated with the Tawilah Group of Saudi Arabia (BEYDOUN, 1964), and the Amba Aradam Sandstones of Ethiopia (MERLA et al., 1979) and with the Nubian Sandstone (GUERRERA, 1983). Yet with the general absence of fossils apart from burrows and non-diagnostic plant debris at a few places the correlations are tenuous at best. Most if not all the ages suggested for the Jesomma Sandstone are maximum ages based upon stratigraphic position. In the south, ALTICHIERI et al. (1982) assign a Conacian-Campanian age for the basal units/contact and a probable Paleocene age for the top of the formation. Similar chronostratigraphic interpretation is also made by ALTICHIERI et al. (1981) for the Qamno section. However, in the Guban area the Jesomma Sandstone transgresses over Upper Jurassic (Guwan) Limestone and hence a Late Cretaceous age for basal Jesomma Sandstone cannot be ruled out.

### Tectonic Evolution

An Early Jurassic activity of uplift, fracturing, and development of embryonic basins may be associated with the deposition of Lower Jurassic Adigrat Sandstone. At least two important tectonic episodes affect Somalia during the time of "Jesomma" deposition. First, in Late Jurassic Madagascar split off along with the rest of East Gondwana (Madagascar, India, Antartica and Australia) and moved away from the rest of Gondwanaland (BOSELLINI 1986; COFFIN and RABINOWITZ, 1987). Second, in Middle Cretaceous Madagascar was isolated from East Africa following a ridge jump; this affected Northeast Somalia (DUALEH and NAIRN, in press). Madagascar migrated southward with a narrow belt of transform faults in between East Africa and Madagascar (BOSELLINI, 1986). These faults also likely affected the Somalian basement. It is generally dated that the major deposition of Jesomma Sandstone occurred during the interval between the Late Cretaceous and presumably before the Paleocene phases of tectonic activity. It appears that block faulting associated with the break up of Gondwanaland was the cause of initiation of Adrigat and Jesomma deposition. The principal effects of these movements most probably affected different parts of Somalia resulting in uplifts of different blocks, each of which might have acted as a source of siliciclastic detritus. However, environmental conditions of deposition may not have been altogether different in the resulting basins.

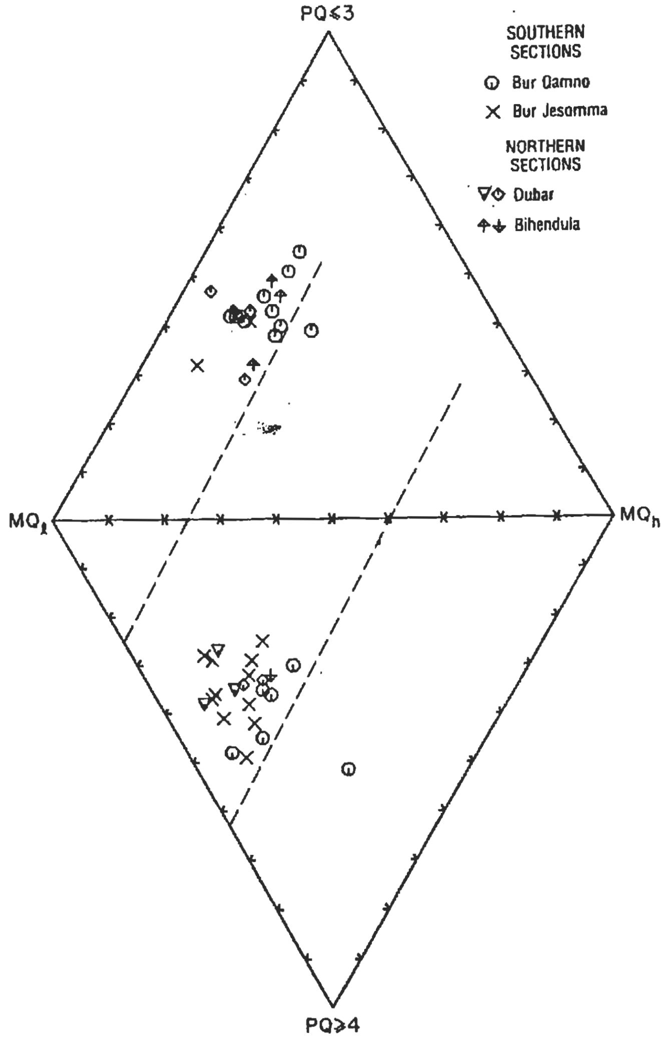


Fig. 2 - Plots of quartz type population in Jesomma sandstone in the diamond diagram of BASU (1985). Two distinct clusters indicate two distinct source rocks for the Jesomma Sandstone. Note that geographic location of the samples have no bearing on the clusters.

Table 1a - Summary of analyses of quartz types: Bur Qammo, Southern Somalia.

| Sample No. | Monocryst. Quartz | | Po[redacted]talline Quartz | | Total Polycrystalline Quartz |
|---|---|---|---|---|---|
| | L | H | F | M | |
| 205 | 39 | 18 | 31 | 12 | 43 |
| 208 | 32 | 15 | 38 | 13 | 51 |
| 198 | 39 | 15 | 30 | 16 | 46 |
| 197 | 28 | 17 | 36 | 19 | 55 |
| 195 | 43 | 21 | 30 | 6 | 36 |
| 194a | 34 | 27 | 26 | 13 | 39 |
| 191 | 41 | 21 | 28 | 10 | 38 |
| 131 | 44 | 8 | 37 | 11 | 48 |
| 138 | 42 | 28 | 24 | 6 | 30 |
| 193 | 40 | 15 | 36 | 9 | 45 |
| 199 | 39 | 21 | 30 | 10 | 40 |
| 200 | 46 | 12 | 30 | 12 | 42 |
| 201 | 45 | 14 | 30 | 11 | 41 |
| 202 | 47 | 11 | 27 | 15 | 42 |
| 192 | 45 | 20 | 31 | 4 | 35 |
| 207 | 45 | 19 | 30 | 6 | 36 |
| yy5 | 57 | 16 | 23 | 4 | 27 |
| yy6 | 54 | 8 | 32 | 6 | 38 |
| yy8 | 50 | 15 | 30 | 5 | 35 |

## METHODS

### Distribution of Samples

Samples used in this study were collected far and apart from (a) the Bihendula and Dubar sections close to the Gulf of Aden in Northern Somalia, (b) the Qamno section in south-central Somalia, and (c) from near the Jesomma village also in south-central Somalia (Fig. 1).

*Bihendula and Dubar sections.*

The Dubar section consists of 1.250 m of red, brown, white or occasionally yellow mudstone, siltstones, and interbedded sandstones which BRUNI and FAZZUOLI (1976) interpreted as lower coastal plain and meandering stream deposits. Five samples from Dubar, spread at approximately 100 m intervals through the succession were examined. Additionally, five samples were also collected from the Bihendula area.

Jesomma Village sections. A thickness of 80 m is exposed. The succession is divisible into three parts. The lower part consist of alternation of siltstones and fine to medium grained sandstones and some conglomeratic lenses. Cross bedding is common, and fining upward beds are usually truncated at the top by succeeding coarser horizons. The middle section consists of parallel bedding sandstones and siltstones. Burrowing is common and cross bedding is less important. The top section shows an increase in coarser sediments, and conglomerates predominate near the top. A total of 14 samples were collected from this area.

*Qamno section*

The Qamno section is 75 m thick and shows some similarities with the Jesomma village section but the sediments are generally finer in grain size. The lower third consists of fine non-laminated sandstones and siltstones. The middle sandy section is much burrowed while the top third is made up of siltstones, the upper parts of which are cross-bedded. Manganese nodules are found in both the upper and lower parts. A total of 19 samples were examined.

Table 1b - Summary of analyses of quartz types: Bur Jesomma, Southern Somalia

| Sample No. | Monocryst. Quartz | | Polycrystalline Quartz | | Total Polycrystalline Quartz |
|---|---|---|---|---|---|
| | L | H | F | M | |
| 294 | 50 | 25 | 19 | 6 | 25 |
| 293 | 46 | 12 | 31 | 11 | 42 |
| 292 | 49 | 19 | 26 | 6 | 32 |
| 291 | 43 | 15 | 34 | 8 | 42 |
| 285 | 41 | 10 | 41 | 8 | 49 |
| 284 | 44 | 15 | 30 | 11 | 41 |
| 185 | 49 | 10 | 32 | 9 | 41 |
| 184 | 57 | 14 | 25 | 4 | 29 |
| 183 | 58 | 10 | 23 | 9 | 32 |
| 283 | 59 | 13 | 22 | 6 | 28 |
| 288 | 53 | 11 | 30 | 6 | 36 |
| yy1 | 53 | 10 | 28 | 9 | 37 |
| yy3 | 50 | 21 | 24 | 5 | 29 |
| yy4 | 46 | 16 | 31 | 7 | 38 |

## Laboratory Methods

Eight polished thin sections and over fifty regular thin sections of Jesomma Sandstones were examined. Each thin section was petrographycally described noting

especially the cements. Heavy minerals in the polished thin sections were identified on an electron microprobe using energy dispersive x-ray analysis. One hundred randomly selected medium sand-size (250-500 m) quartz grains in thin sections of the samples were classified according to the scheme first developed by BASU et al. (1975). We used four types of quartz the details of which are given in BASU (1985); the types are:
Monocrystalline quartz:
low undulosity (extinction of whole grain in <5° rotation of stage)
high undulosity (extinction of whole grain in >5° rotation of stage)
Polycrystalline quartz:
few subgrains (2-3 subgrains)
many subgrains (4 or more subgrains)

The distribution of quartz types in these sandstones are given in Table 1 and are plotted in Fig. 2.

Table 1c - Summary of analyses of quartz types: Dubar section, Northern Somalia.

| Sample No. | Monocryst. Quartz | | Polycrystalline Quartz | | Total Polycrystalline Quartz |
|---|---|---|---|---|---|
| | L | H | F | M | |
| D307 | 49 | 17 | 29 | 5 | 34 |
| D321 | 48 | 5 | 34 | 13 | 47 |
| D303 | 46 | 21 | 27 | 6 | 33 |
| D325 | 43 | 14 | 28 | 15 | 43 |
| D304 | 51 | 20 | 21 | 8 | 29 |

Table 1d - Summary of analyses of quartz types: Bihendula section, Northern Somalia.

| Sample No. | Monocryst. Quartz | | Polycrystalline Quartz | | Total Polycrystalline Quartz |
|---|---|---|---|---|---|
| | L | H | F | M | |
| D295 | 45 | 23 | 28 | 4 | 32 |
| D293 | 36 | 18 | 26 | 20 | 46 |
| D299 | 48 | 20 | 24 | 8 | 32 |
| D233 | 36 | 15 | 28 | 21 | 49 |
| D231 | 46 | 11 | 32 | 11 | 43 |

## DISCUSSION AND CONCLUSION

There is a danger that the term the Jesomma Sandstone Formation may become an all-embracing term for all post Upper Jurassic Sandstones in Northeastern Africa regardless of age and depositional environment much as the terms Nubian Sandstone or Karroo Sandstone have become catch-all terms. The age of the Jesomma Sandstone is poorly constrained at best. Because it is transgressive over Jurassic Gawan Limestone as well as over Lower Cretaceous rocks and Precambrian basement rocks, the base of Jesomma is clearly diachronous. Lithologically it is composed of both fresh and reworked sands but appears to lack any distinctive characteristics regardless of where it has been collected. Depositional environments have seldom been determined, and although these may help to determine a consistent paleogeographic pattern, they are of little chronological assistance. We have restricted the use of the term to the Late Cretaceous to Paleocene mappable siliciclastic unit of AZZAROLI and CANUTI (1979).

The purpose of this article as stated above is to apply a quantitative technique based upon the distribution of quartz types in order to characterize the sandstone and establish its provenance and regional variations. Samples from the several locations in Jesomma Sandstone described above were examined. Using modal analysis of quartz types based on our measurements, presence of two distinct non-overlapping clusters on the diamond diagram may be seen (Fig. 2). One cluster, rich in polycrystalline quartz with few subgrains, plots in the plutonic field of the diamond diagram indicating a granitic and/or gneissic source for the quartz. The other cluster, rich in polycrystalline quartz with many subgrains, is located in a field that may be considered an extension of the low grade metamorphic field. Thus a very distinct second source is indicated. Note that the populations of quartz types are not geographically controlled; all sections from Northern and South-central Somalia have similar quartz type distributions. Previous studies employing the quartz type approach (e.g. ARRIBAS et al., 1985; GARZANTI, 1985) for source rock determination suggest that it is unusual for the same siliciclastic unit to have such widely disparate populations of quartz types.

Granites and granite gneisses of Paleozoic and Precambrian age are presently exposed some 200 km to the west of the Jesomma Sandstone outcrops, and along the northern coast of Somalia. These granite and granitic gneisses are the obvious source of the first cluster noted above. These source rocks are commonly exposed in Somalia (e.g Bur Acaba) and in Kenya. The source rocks of the second cluster may be the low grade metamorphic rocks that are generally poorly exposed to the west. The alternative, to derive the latter quartz type from deformed and sheared granites seems less likely given the Phanerozoic history of the region. If this provenance interpretation is correct, i.e. if relative block uplifts to the west and north of the basins provided the bulk of the upper Mesozoic siliciclastic detritus, then a transgression from the south, and east seems likely. This is compatible with the tectonic scenario proposed recently by BOSELLINI (1986) for the Upper Mesozoic evolution of the continental margin of East Africa.

## ACKNOWLEDGMENTS

We are indebted to Professors ABBATE, SAGRI, and BRUNI of Florence University, and Professors ANGELUCCI of Rome University and MEZZADRI of Parma University for furnishing samples and providing field assistance. Professor MC BRIDE of the University of Texas at Austin and Professor A.E.M. NAIRN advised at various stages of the research. The Department of Geology at Indiana University and Earth Sciences and Resources Institute of South Carolina University made their laboratory facilities available to MAA. Ms. JUDY GITTINGS and Ms. CINDY HEATON are thanked for assisting in ms. preparation. The study was supported by the Faculty of Geology, Somali National University, Research Incentive Program of Indiana University, and through Grant #86-08212 of the United States Information Agency under the Fulbright African Senior Research Scholar Program (MAA).

## REFERENCES

ALTICHIERI L., ANGELUCCI A., ARUSH M., BOCCALETTI M., CABDULGADIR M., PICCOLI G. and ROBBA E. (1982). Preliminary study on the Paleogene Formation of Central Somalia (Hiiraan Galgaduud Mudug and Nugaal Regions). Univ. Naz. Somala. Quaderni Geologia della Somalia, 6: 83-204.

ARKELL W.J. (1956). Jurassic Geology of the World. OLIVER and BOYD, London, 806 pp.

ARRIBAS J., MARFIL R. and DE LA PENA J. (1985). Provenance of Triassic feldspathic sandstones in the Iberian Range (Spain): Significance of Quartz. Journal of Sedimentary Petrology, 5: 864-868.

ARUSH M.A. (1981). Osservazioni petrografiche sulle arenarie di Garbaharre (Giurassico Superiore-Cretacico Inferiore). Univ. Naz. Somala. Quaderni Geologia della Somalia, 5: 49-56.

AZZAROLI A. and CANUTI P. (1979). The Mesozoic of Somalia. In: A Geologic Map of Ethiopia and Somalia (1973). C.N.R. Italy, 4: 33-44.

BARNES S.U. (1976). Geology and oil prospects of Somalia, East Africa. Bull. Amer. Assoc. Petrol. Geol., 60: 389-413.

BASU A. (1985). Reading provenance from detrital quartz. In: ZUFFA G. ed., Provenance of Arenite. NATO-ASI. C-148. Reidel Publishing. Dordrecht, 231-248.

BASU A., YOUNG S.W., SUTTNER L.J., JAMES W.C. and MACK G.H. (1975). Re-evaluatian of the use of undulatory extinction and polycrystallinity in detrital quartz for provenance interpretation. Journal Sed. Petrology, 45: 873-882.

BELLIENI G., HAYDER A., SASSI P.F., IBRAHIM H. and ZIRPOLI G. (1982). Caratteri geochimici-petrografici dei graniti dei Bur, Somalia Meridionale. Univ. Naz. Somala. Quaderni Geologia della Somalia, 6: 33-50.

BELTRANDI M. and PYRE A. (1973). Geological evolution of Southwest Somalia. In BLANT C., ed. Sedimentary Basins of African Coast. 2: South and East Africa. Assoc. Surv. Geol. Africa. Paris, 152-178.

BEYDOUN Z. R. (1970). Southern Arabia and Northern Somalia: Comparative geology. Phil. Trans. Roy. Soc., London. Ser. A: 267-292.

BOSELLINI A. (1986). East Africa continental margins. Geology, 14: 76-78.

BRUNI P. and FAZZUOLI M. (1976). Sedimentological observation on Jurassic and Cretaceous sequences from Northern Somalia. Boll. Soc. Geol. Italiana, 45: 1571-1588.

BUNCE E.T. and MOLNAR P. (1977). Seismic reflection profiling and basement topography in the Somali Basin: possible fracture zones between Madagascar and Africa. Journal of Geophysical Research, 82: 305-5311.

COFFIN M.F. and RABINOWITZ P.D. (1987). Reconstruction of Madagascar and Africa: evidence from the Davie Fracture Zone and Western Somali Basin. Journal of Geophysical Research, 92(B9): 9385-9406.

DUALEH A. (1986). Geological and stratigraphic evolution of Northeast Somalia continental margin and adjacent areas. Unpublished Thesis. Univ. of South Carollna, 312 pp.

DUALEH A.H.A. and NAIRN A.E.M. (in press). The continuing story of the fragmentation of Gondwana: a contribution from Somalia.

GARZANTI E. (1985). The sandstone memory of the evolution of a Triassic volcanic arc in the Southern Alps, Italy. Sedimentology, 32: 423-433.

GUERRERA F. (1983). The Jesomma Sandstone in Somalia: a possible southern equivalent of the Nubian Sandstone. Rendiconti della Società Geologica Italiana, 6: 34-37.

KOZERENKO V.N. and LARTSEV V.S. (1978). Block tectonics of the East African activation region. Geotectonic, 12(1): 34-40.

MC BRIDE E.F. (1987). Diagenesis of the Maxon Sandstone (Early Cretaceous), Marathon region, Texas: a diagenetic quartz arenite. Jour. Sedimentary Petrology, 57: 98-107.

MERLA G., ABBATE E., AZZAROLI A., BRUNI P., CANUTI P., FAZZUOLI M., SAGRI M. and TACCONI P. (1979). A Geoloyical Map of Ethiopia and Somalia (1973) and comment with a Map of major Land Forms. C.N.R. Italy, 95 pp.

MOHR P.A. (1962). The Geology of Ethiopia. University College of Addis Ababa Press. Addis Ababa, Ethiopia, 268 pp.

RABINOWITZ P.D., COFFIN M.F. and FALVEY D. (1983). The separation of Madagascar and Africa. Science, 220: 67-69 pp.

SACCHI R. and ZANFERRARI A. (1987). Notes on some shear zones of Northern Somalia. Journal of African Earth Sciences, 6: 323-326.

SHANMUGAM G. (1985). Types of porosity in sandstones and their significance in interpreting provenance. In: ZUFFA G.G. (ed.). Provenance of Arenites. NATO-ASI C-148. Reidel Publishing, Dordrecht, 115-137.

*Final editing, January 1990*

From *Geology and mineral resources of Somalia and surrounding regions*, Ist. Agron. Oltremare, Firenze, Relaz. e Monogr. 113, 181-196, 1993.

# PALEOCENE TO EOCENE PLANKTONIC FORAMINIFERAL BIOZONES IN CORIOLEI 1 WELL (MOGADISHU COASTAL BASIN, SOMALIA)

ABDI SALAH HUSSEIN

Department of Geology, Somali National University, P. O. Box 1081, Mogadishu, Somalia.
Present address: Dipartimento di Scienze della Terra, Università di Firenze, Via La Pira 4, 50121 Firenze, Italy.

## ABSTRACT

Results of the planktonic foraminifers investigations on the Paleocene-Eocene sequences met by the Coriolei 1 Well (Mogadishu Basin) are presented. Foraminiferal events are correlated to planktonic foraminiferal standard biozones (BOLLI, 1962, 1969, 1979; BERGGREN et al., 1985, MC GOWARN, 1978; TOUMARKINE and LUTERBACHER, 1985).

Although with the uncertainties due to sample collection (only cuttings were available), the following biostratigraphical data, from top to bottom, can be put forward using the Tertiary zones of BLOW (1969) and BERGGREN et al. (1985).

The basal part of Obbia Fm. (Late Eocene, mainly argillites with calcareous interbeds) is assigned to Zone P16.

The Shabele Fm. (Middle to Late Eocene, mostly sandstones with rare argillites) includes Zones P13?/P14 to P16.

In the Coriolei Fm. (Paleocene to Middle Eocene, dolostones and limestones with marly interbeds) the Zones P13 to P12 seem to rest unconformably above Zone P9. Also between Zones P7 to P4 there is a stratigraphic gap. Thus, most of the Late Paleocene and the base of the Early Eocene as well as the lower part of the Middle Eocene are missing.

These hiatuses can be matched with some deep-sea drillings results in the western Indian Ocean.

Furthermore, the evolutionary trend of *Turborotalia cerroazulensis* allows more detailed interpretation of the Late Eocene section of the well.

## NUXUR

Nolool-daafyada fooraminiferada sabbeeya (plankton foraminifera) ee Baaleyooseen-Eyooseen ee ceelka Qoryooleyga-1aad ee bedda Muqdisho.

Halakan waxaa la soo bandhigayaa natiijooyinka ka soo baxay fooraminiferada sabbeeya ee da'doodu tahay Baaleyooseen-Eyooseen lagalana kulmay ceelka Qoryooleyga-1aa ee bedda Muqdisho.

Fooraminiferada sabbeeya ee ceelkaas waxaa la barbardhigay nolool- daafafyo (biozones) hal

beeg (standard) ah (BLOW, 1969, 1979; BERGGREN et al., 1985; MC GOWRAN, 1978.)

Walow, muunadihi la soo ururiyay ay san dhammeyn waayo waxaa la helay oo iceli ah muunadaha jajaban (cuttings), haddana nolool lakab-derisyaasha (biostratigraphy) soo socda koor ila hoos waxaay u dhigan yihiin sideey u kala dambeyeen da'doodu iyado la'adegsa naayo daafyada (zones) tersiyaariga (Tertiary) ee BLOW, 1969 iyo BERGGREN i.k. kale, 1985.

Abuuranka Hobyo (Eyooseenka sare), qayb hoosaadka abuuranka Hobyo, badidiisu waa dhadhaab dhoobeed soona dhexgalaayaan lakab qala xeed, waxaa lagu sunta daafta P16.

Abuuranka Shabeele (Eyooseenka dhexe-sare), badidiisu waa dhadhaab ciideed soona dhexgalayaan sí naadir ah dhadhaab dhoobeed; waxaa loo asteeya daafaha ?P13/P14-P16.

Abuuranka Qoryooley (Baaleyooseenka-ila Eyooseenka dhexe), wuxu ka koobma qalax iyo doloomiid soona dhexgalayaan heerar darro (marl) ah. Waxaa loo asteeya daafaha P13, P12 oo dulsaaran daafta P9, waxaa algu mala'awaala in ay ku dhexjirto iin (hiatus).

Xata, u dhaxeeynta daafaha P7 ila P4 waxaa ku dhexjirta dalool lakab-deris (stratigraphic gap) ah.

Sido kale waxaa ma qan ugu badnaan qeyb ka mid ah Baleyooseenka sare, dhamman Eyooseenka hoose iyo qayb ka mid ah Eyooseenka dhexe.

Iinahan waxaa lo asteeya in laga helay natiijooyinki ka soo baxay qaar ahaan ceelashi laga qoday Galbeedka Badweeynta Hindiya (Deep- sea drilling project).

Taddawurka ku siqaaya (evolutionary trend) Turborotalia cerroazulensis waxay si muujinayaan qayb ka mid ah ceelkaas in lagu til maamo Eyooseenka sare.

## INTRODUCTION AND SCOPE OF THE WORK

The Mogadishu basin is part of the depression along the Indian Ocean coast of Somalia, which extends from El-Dhere (about 250 km NE of Mogadishu) to Brava (200 km SW of Mogadishu) (Fig. 1). This basin is separated from the Bur crystalline basement by a fault system which bounds it towards NW where the Bur crystalline basement outcrops. The latter is covered by Jurassic to Cretaceous sequences (Fig. 1). The crystalline basement and its Mesozoic to Tertiary sedimentary cover have been deeply downfaulted and the Mogadishu basin is covered by recent alluvial deposits. The sedimentary cover has been penetrated by a number of oil wells which show the development of the Tertiary deposits.

Well-preserved planktonic forams found in well cuttings motivated this research.

The examined intervals belong to the Coriolei-1 well (100 km W of Mogadishu) drilled by Sinclair Co.in 1961. The penetrated sedimentary sequence was regrouped from top to bottom as follows: Obbia, Shabele and Coriolei formations. Summarized lithological descriptions of the above mentioned formations and their chronostratigraphic relations as in the SINCLAIR reports are as follows (from top):

OBBIA FORMATION (Late Eocene)

- Dark-grey shales with thin levels of limy shale. Thickness 141 m. Deposited in moderately deep marine environment.

SHABELE FORMATION (Middle-Late Eocene)

Light-grey limy sandstone with occasional conglomeratic and shaly levels. Thickness 355 m.

Deposited in shallow to deep marine environment.

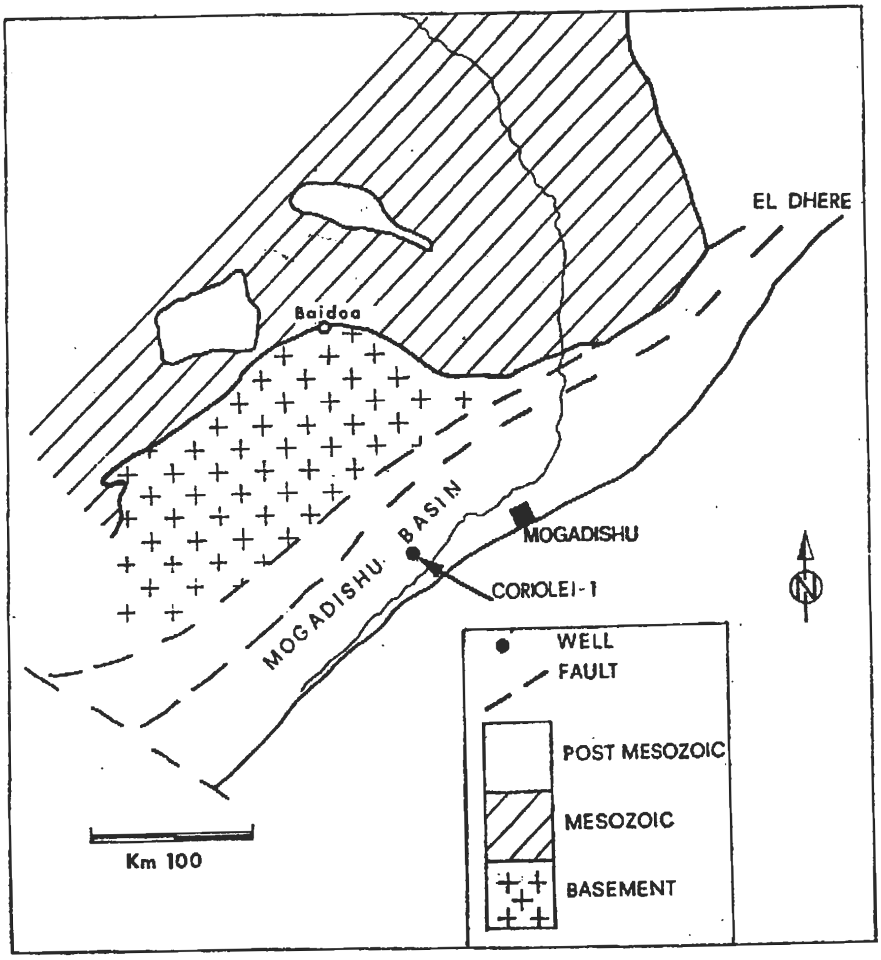


Fig. 1 - Geological map of the Mogadishu area.

CORIOLEI FORMATION (Paleocene-Middle Eocene)

Marly fossiliferous, cherty grey limestone with glauconitic and dolomitic levels. Thickness 611 m. Deposited from the open sea to platform.

The age assigned to these formations by SINCLAIR SOMALI COORPORATION (1960) is Paleocene-Middle/Late Eocene on the basis of occurrences of: *Hantkenina alabamensis, Globigerina bulloides, Globorotalia cf. cocoaensis, Globorotalia formosa, Globorotalia formosa gracilis, Alveolina elliptica* and *Nummulites discorbinus*.

The scope of this research is to give a more precise age to the above mentioned formations and to recognize standard planktonic foram biozones.

## MICROPALEONTOLOGICAL CONTENT

The micropaleontological content has been examined in the three mentioned formations (Obbia, Shebele and Coriolei) Fig. 2. Microfaunas have been reported for each sample.

It should be noted that microfossil assemblages might have suffered mechanical reworking, since the study has been carried out only through cuttings analyses.

### Obbia Formation

All the fossiliferous samples come from the lowest levels of the unit and are composed of shale and limy shale (7 m thick).

The available cuttings cover two intervals: 1466-1470 m and 1470-1476 m. The first interval represents the base of the formation, while the second part represents the transition between the Obbia and Shabele formations.

1466-1470 m:

*Turborotalia cerroazulensis cerroazulensis* (COLE); *T.c. pomeroli* (TOUMARKINE and BOLLI); *Globigerina utilisindex* JENKINS; *Globigerina praebulloides* BLOW; *"Globigerina" prasaepis* BLOW; *G.* sp. *Globorotaloides permicra* (BLOW and BANNER); *Globoquadrina tripartita* (KOCH); *Catapsydrax martini scandretti* (BLOW and BANNER); *Pseudohastigerina micra* (COLE); *Nummulites* sp.; *Alveolina* sp.

Only are sample is available for the whole interval 1470-1476 m, which includes the transition between the Obbia and Shabele formations. It contains:

1470-1476 m:

*Turborotalia cerroazulensis cerroazulensis* (COLE); *T.c. pomeroli* (TOUMARKINE and BOLLI); *T.c. cocoaensis* (CUSHMAN); *T.c. cunialensis* (TOUMARKINE and BOLLI); *Subbotina linaperta* (FINLAY); *S. eocaena* (GUEMBEL); *S. corpulenta* (SUBBOTINA); *Catapsydrax africana* (BLOW and BANNER); *Catapsydrax martini martini* (Blow); *C.* sp. *Globigerina* cf. *euapertura* (JENKINS); *G. officinalis* (SUBBOTINA); *G. index tropicalis* (BLOW and BANNER); *Globoquadrina galavisi* (BERMUDEZ).

### Shabele Formation

The samples come from sandy units (118 m thick) from the upper part of the formation and from shaly sand units (90m thick) from the lower part of the formation.

1479-1482 m:

*Turborotalia cerroazulensis cerroazulensis* (COLE); *T.c. pomeroli* (TOUMARKINE and BOLLI); *T.c. cocoaensis* (CUSHMAN); *T.c. cunialensis* (TOUMARKINE and BOLLI); *Subbotina corpulenta* (SUBBOTINA); *S. eocaena* (GUEMBEL); *Catapsydrax africana* (BLOW and BANNER); *C. howei* (BLOW and BANNER); *C. simulans* (BERMUDEZ); *T. pseudoampliapertura* (BLOW and BANNER); *Globoquadrina galavisi* (BERMUDEZ); *G. pseudovenezuelana* (BLOW and BANNER); *Globigerinatheka index tropicalis* (BLOW and BANNER); *G. semiinvoluta* (KEIJZER).

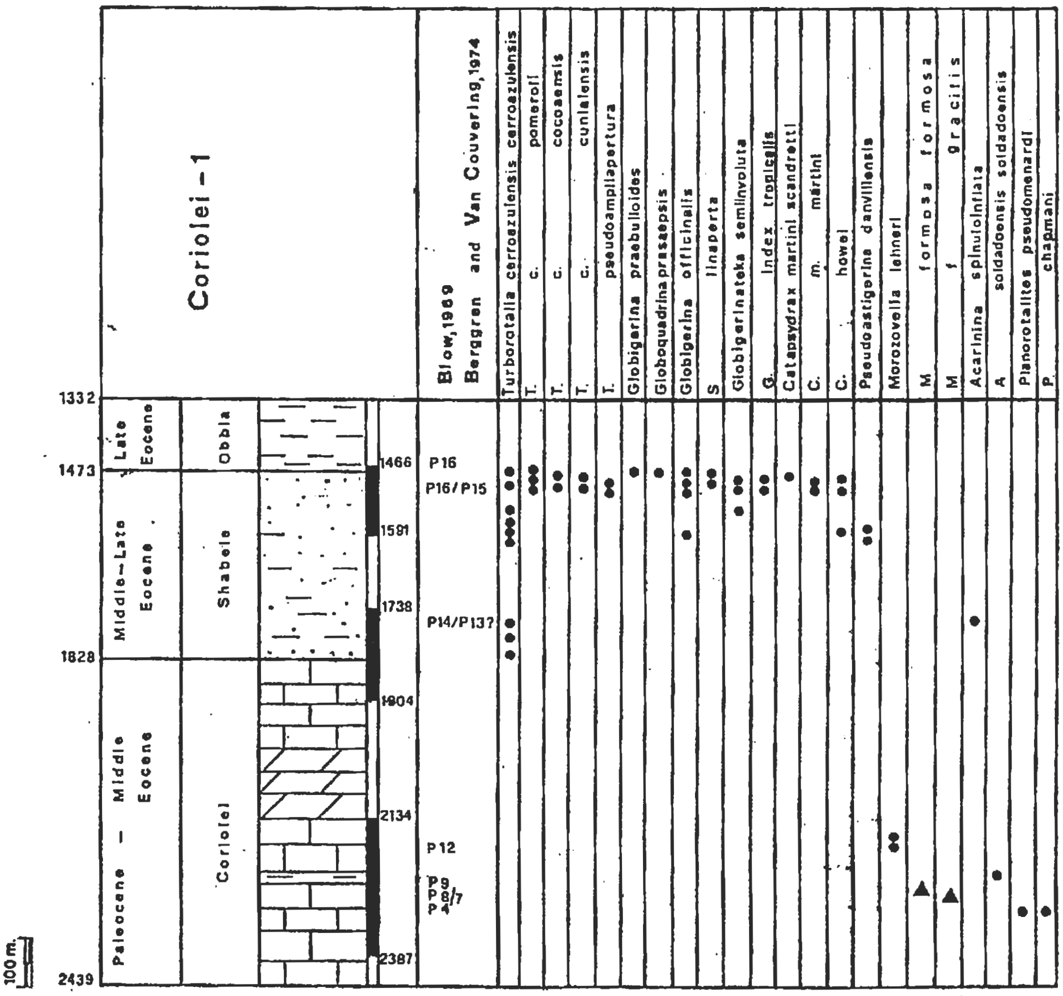


Fig. 2 - Lithological column and Planktonic foraminiferal range in Coriolei-1 well. Solid triangles indicate Sinclair data.

1482-1485 m:

*Turborotalia cerroazulensis cerroazulensis* (COLE); *T.c. pomeroli* (TOUMARKINE and BOLLI); *Globigerina ampliapertura* (BOLLI); *G. officinalis* (SUBBOTINA); *G. utilisindex* (JENKINS); *T.c. cocoaensis* (CUSHMAN); *Globoquadrina tripartita* (KOCH); *G. galavidis*

(BERMUDEZ); *Catapsydrax martini martini* (BLOW); *Globigerinatheka semiinvoluta* (KEIJZER); *Cribrohanthekenina* cf. *lazzarii* (PERICOLI); *Globigerina* sp.; *Globorotalia* sp..

1485-1488 m:

*Turborotalia cerroazulensis cerroazulensis* (COLE); *T. pseudoampliapertura* (BLOW and BANNER); *Subbotina linaperta* (FINLAY); *S. gortanii* (BORSETTI); *Globoquadrina galavisi* (BERMUDEZ); *G. yeguaensis* (WEINZIERL and APPLIN); *Catapsydrax howei* (BLOW and BANNER).

1491-1494 m:

*Turborotalia cerroazulensis cerroazulensis* (COLE); *Globigerina* sp.; *Globoquadrina tripartita* (KOCH); *G. galavisi* (BERMUDEZ); *G. Yeguaensis* (WEIZIERL and APPLIN).

1500-1503 m:

*Globigerina* sp.; *Nummulites* sp.; *Alveolina* sp..

1534-1537 m:

*Turborotalia cerroazulensis cerroazulensis* (COLE); *Globigerina* sp.; *Globigerinatheka semiinvoluta* (KEIJZER).

1552-1555 m:

*Turborotalia cerroazulensis cerroazulensis* (COLE); *Globigerina* sp.; *Globoquadrina pseudovenezuelana* (BLOW and BANNER).

1570-1576 m:

*Turborotalia cerroazulensis cerroazulensis* (COLE); *Catapsydrax howei*; *Globigerina* sp..

1576-1582 m:

*Turborotalia cerroazulensis cerroazulensis* (COLE); *Subbotina angiparoides* (HORNIBROOK); *Globigerina* sp..

1581-1585 m:

*Turborotalia cerroazulensis cerroazulensis* (COLE); *Globigerina officinalis* (SUBBOTINA); *Pseudohastigerina barbadoensis* (BLOW); *Subbotina eocaena* (GUEMBEL); *Tenuitella gemma* (JENKINS); *P. micra* (COLE).

1585-1588 m:

*Turborotalia cerroazulensis cerroazulensis* (COLE); *Globigerina officinalis* (SUBBOTINA); *Pseudohastigerina micra* (COLE); *P. danvillensis* (HOWE and WALLACE); *Globigerina* sp..

1588-1591 m:

*Turborotalia cerroazulensis cerroazulensis* (COLE); *Globigerina* sp..

1741-1744 m:

*Acarinina spinuloinflata* (BANDY); *Acarinina* sp.; *Globigerina* sp..

1753-1756, 1785-1788 and 1814-1817 m:

*Turborotalia cerroazulensis cerroazulensis* (COLE); *Globigerina* sp..

-Coriolei Formation

Fossiliferous samples containing few planktonic forams were found in two levels. One level consists of limestone and is 76 m thick, while the other has about 253 m and

is more marly.
1854-1858 m:
*Nummulites* sp.; *Alveolina* sp..
2152-2162 m:
*Morozovella lehnerii* (CUSHMAN and JARVIS); *Morozovella* sp.; *Globorotalia* sp.; *Globigerina* sp..
2162-2171 m:
*Turborotalia cerroazulensis cerroazulensis* (COLE); *Morozovella lehnerii* (CUSHMAN and JARVIS); *Morozovella* sp.; *Globorotalia* sp.; *Globigerina* sp..
2256-2286 m:
*Acarinina* cf. *soldadoensis-soldadoensis* (BRONNIMANN); *Globigerina* sp..
2332-2341 m:
*Globigerina* sp.; *Planorotalites* sp.; *Planorotalites chapmani* (PARR); *P. pseudomenardii* (BOLLI); P. sp.; *Morozovella* sp.; *Nummulites* sp.; *Alveolina* sp..

## BIOZONATION

Fig. 3 includes the most indicative middle Paleocene to Eocene forams found in the Coriolei-1 well. They are referred to BLOW (1969), BERGGREN and VAN COUVERING (1974) zonations.

As we are dealing only with cuttings, we will take into consideration the last occurrences (L.O.). From the top of the well to the bottom, the most important L.O. and other bioevents are the following:

1) L.O. of *Catapsydrax howei* and *Globigerinatheka index tropicalis* (P16) at 1466-1473 m in the Obbia Formation.
2) L.O. of *Globigerinatheka semiinvoluta* (P15) at 1479-1482 m in the Shebele Formation.
3) L.O. of *Acarinina spinuloinflata* and *A.* spp. (P14-?P13) at 1741-1744 m in the Shebele Formation.
4) Presence of *Morozovella lehneri* (P12) at 2152-2162 m in the Coriolei Formation.
5) L.O. of *Acarinina* cf. *soldadoensis soldadonensis* (P9) at 2256-2286m in the Coriolei Formation.
6) L.O. of *Planorotalites pseudomenardi* (P4) at 2332-2341 m in the Coriolei Formation.

Taking into account the SINCLAIR investigations, and the stratigraphic distribution of the most significant forams encountered in the examined sequence, the following age determinations can be presented:

### Coriolei Formation

The lower part of the sequence studied may be assigned to the Late Paleocene zone P4 (*Planorotalites pseudomenardi*). Besides the index species, *P. chapmanii*, *Planorotalites* sp. and *Morozovella* sp. occur. The species indicating the uppermost portion of the Paleocene (zone P5) are missing.

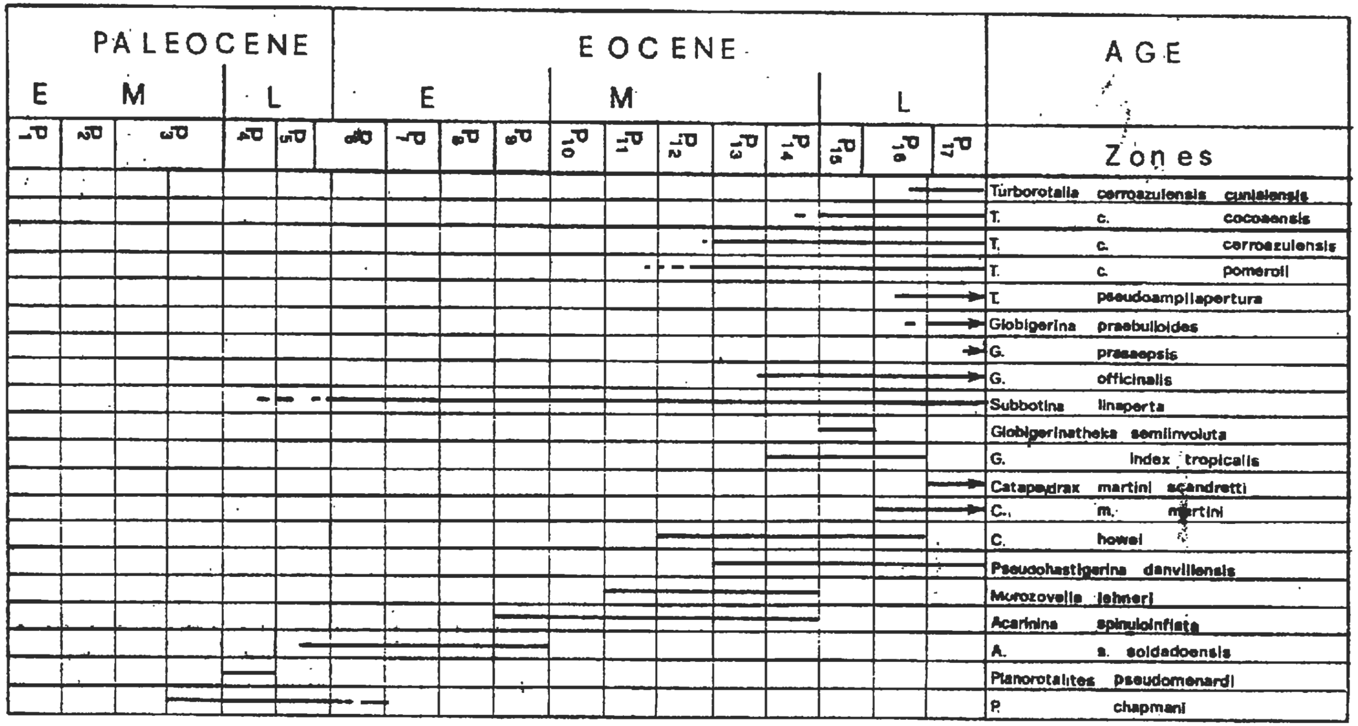


Fig. 3 - Range of most indicative Middle Paleocene to Eocene forams found in the Coriolei-1 well, referred to BLOW (1969); BERGGREN and VAN COUVERING (1974) bionations.

In the overlying sediments the presence of *Acarinina soldadoensis soldadoensis* at a depth of 2256 m and of *Morozovella formosa formosa* and *Morozovella formosa gracilis* at 2280 and 2300 m allows to assign this interval of the Coriolei Formation to zones P7-P9 (Early Eocene). Indicators of the zone P6, i.e. the base of the Eocene period are missing. Thus, the hiatus would include the Paleocene/Eocene boundary (P5/P6).

Middle Eocene Zone P12 (*Morozovella lehneri*) rests unconformably above zone P9.

Therefore, the lower part of the Middle Eocene (zones P10/P11) are not present in the succession.

The upper part of the formation lacks planktonic forams, and the presence of *Nummulites* sp. and *Alveolina* sp. testifies to the shifting of the depositional environment from the open sea to platform.

### Shabele Formation

The lower part of the Shabele Formation can be assigned to zone ?P13-P14 (Middle Eocene) due to L.O. *Acarinina spinuloinflata* and *Acarinina* spp.

The assemblage of *Turborotalia cerroazulensis cerroazulensis, Globigerina officinalis, Pseudohastigerina micra, P. danvillensis, Tenuitella gemma, Globigerinatheka semiinvoluta* and *G. index tropicalis*, are characteristic of P15-P16 (Late Eocene). The presence of *Turborotalia cerroazulensis cunialensis* in this interval, allows to assign the terminal part of the Shabele Formation to the *T.c. cunialensis* zone of TOUMARKINE.

### Obbia Formation

Only the lower part of the Obbia formation has been investigated. The L.O. of *Catapsydrax howei* and *Globigerinatheka index tropicalis* permits assignment to Zone P16 (Late Eocene).

## HIATUSES DURING PALEOCENE AND EOCENE

The occurrence of hiatuses in the Coriolei-1 Well, has in part frustrated attempts to recover a continuous biostratigraphical record.

The absence of the latest Paleocene and earliest Eocene interval is pointed out by the super-position of Zone P7 above Zone P4, and could be due to submarine erosion related to frequent sea level fluctuations reported for this time interval (HAQ et al., 1987). In addition, Zone P12 rests unconformably above Zone P9. This hiatus can be matched with some deep-sea drilling sites in the Western Indian Ocean (MCGOWRAN, 1978). Although the geological contexts are different (continental margin vs. true ocean basin), a common oceanographic cause can be recognized in the actively eroding bottom currents, which, after the separation of Madagascar from NE Africa, were circulating North-South and connecting the Tethys with the Mozambique Channel.

A concomitant cause could be the coeval, episodic catastrophic slidings of sediments from the continental margin toward the Somali abyssal plain (COFFIN and RABINOWITZ, 1988).

## SYSTEMATICS

Because of the absence or scarce distribution of the major part of the planktonic foram standard zonation markers in the high latitudes, TOUMARKINE and BOLLI (1970), with later amendments by TOUMARKINE in TOUMARKINE and LUTERBACHER (1985), introduced an alternative zonation for the Eocene. This was based on the evolutionary line of the *Turborotalia cerroazulensis* subspecies which have a wide paleogeographic distribution and are more resistant to the dissolution than most of the tropical markers.

In the studied samples, it was possible to identify some forams indicated by TOUMARKINE and BOLLI (1970), as follows: *Turborotalia cerroazulensis pomeroli, T.c. cerroazulensis, T.c. cocoaensis* and *T.c. cunialensis.*

In consideration of their stratigraphic value, below are their specific descriptions.

a) *T.c. Pomeroli* (Plate 1; Fig. 5/a-b-c)
   Type species: *Globorotalia c. pomeroli* (TOUMARKINE and BOLLI, 1970).
   Synonym: *Globorotalia centralis* (CUSHMAN and BERMUDEZ, 1973).
   *T.c. pomeroli* differs from its ancestral *Possagnoensis* by having more room in the last loop and being bigger and more rounded.

b) *T.c. cerroazulensis* (Plate 1; Fig. 4/a-b-c)
   Type species: *Globorotalia cerroazulensis* (COLE, 1928).
   Synonym: partially *Globorotalia centralis* (CUSHMAN, 1937).

**Plate 1**

The evolutionary trends of Turborotalia cerroazulensis SEM pictures. a = lateral side; b = umbilical side; c = dorsal side.

Fig. 1/a-b-c: *Turborotalia cerroazulensis cunialensis* (TOUMARKINE and BOLLI) sample 1470-1476 m, magnification x 200.

Fig. 2/a-b-c: *Turborotalia cerroazulensis cocoaensis* (CUSHMAN) sample 1470-1476 m, magnification x 200.

Fig. 3/a-b-c: *Turborotalia cerroazulensis cerroazulensis* - T. c. cocoaensis, transition. sample 1470-1476 m. magnification x 180.

Fig. 4/a-b-c: *Turborotalia cerroazulensis cerroazulensis* (COLE) sample 1466-1470 m, magnification x 180.

Fig. 5/a-b-c: *Turborotalia cerroazulensis pomeroli* (TOUMARKINE and BOLLI) sample 1466-1470 m, magnification x 180.

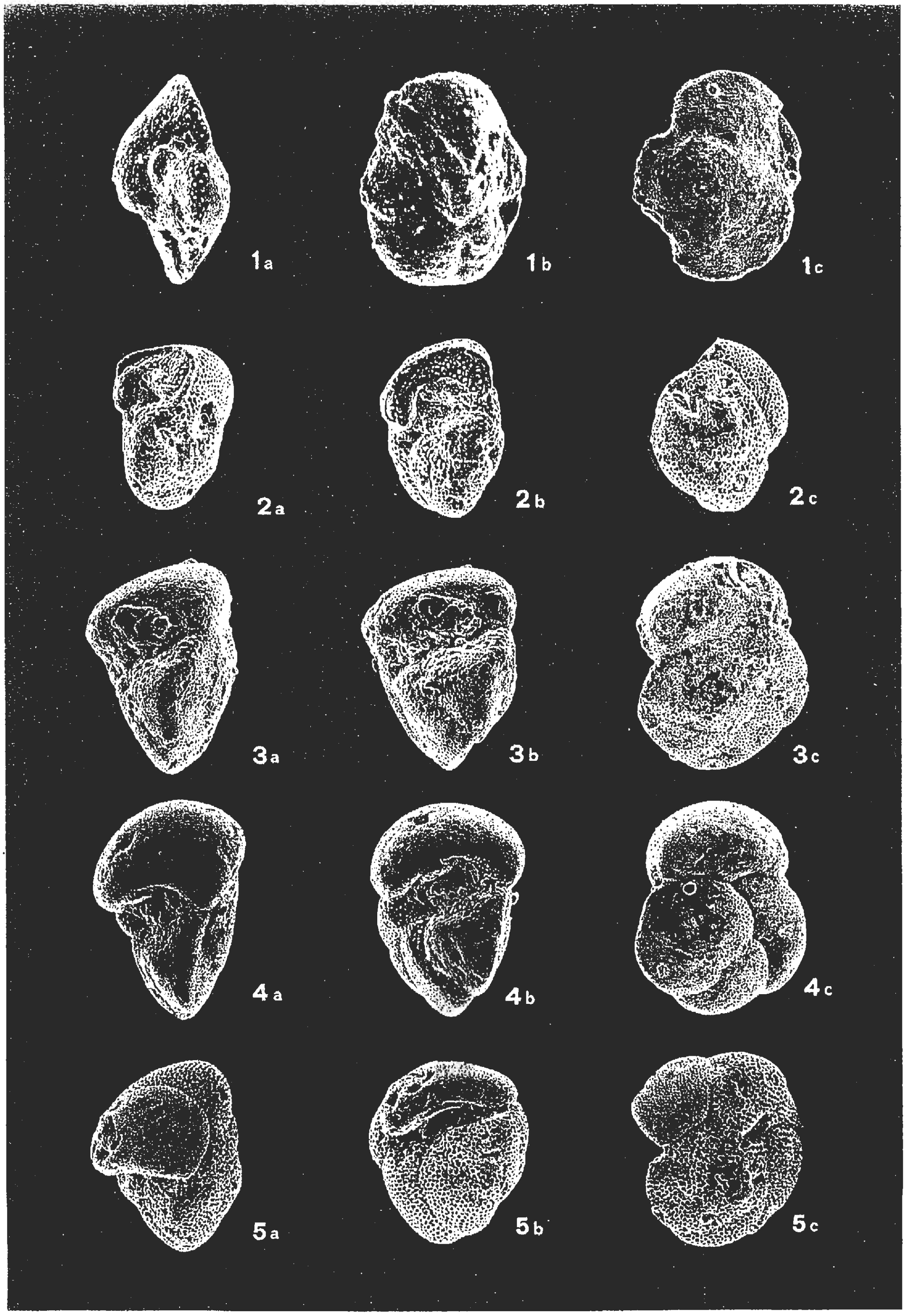
1a
1b
1c
2a
2b
2c
3a
3b
3c
4a
4b
4c
5a
5b
5c

*T.c. cerroazulensis* differs from *T.c. pomeroli* for its flat dorsal side which gives a more angular shape to its lateral view, and the high aperture which migrates towards the umbelicus and reaches the terminal.

c) *T.c. cerroazulensis* transition *T.c. cocoaensis* (Plate 1; Fig. 3/a-b-c).
d) *T.c. cocoaensis* (Plate 1; Fig. 2/a-b-c).
   Type species: *Globorotalia cocoaensis* (CUSHMAN, 1928).
   *T.c. cocoaensis* resembles the subspecies cerroazulensis from the flattened dorsal side, but in the lateral view the last chamber margin is more acute. Its aperture is high arch between the umbelicus and the terminal.
e) *T.c. cunialensis* (Plate 1; Fig. 1/a-b-c).
   Type species: *Globorotalia cunialensis* (TOUMARKINE and BOLLI, 1970).
   *T.c. cunialensis* is the final form of the *T.c.* family and is characterized by a very acute profile and a weak imperforate carena.

## CONCLUSIONS

The examined intervals belong to the succession met by the Coriolei-1 Well, 100 km W of Mogadishu. Their detailed study evidenced several events from Late Paleocene to Late Eocene.

From bottom to top, the sedimentary sequence includes Coriolei, Shebele, and Obbia Formations.

The lowest part of the Coriolei Formation can be assigned to Zone P4 by the presence of *Planorotalites pseudomenardi*. The overlying sediments are characterized by the presence, of *Acarinina soldadoensis soldadoensis*, *Morozovella formosa formosa*, and *Morozovella formosa gracilis* which define Zones P7-P9. A hiatus covering Zones P5 and P6 is suggested.

Further upward in the sequence, the overlying Zone P12 characterized by the presence of *Morozovella lehneri* seems to rest unconformably above Zone P9.

Therefore, most of Late Paleocene up to the basal part of the Early Eocene and the lower part of the Middle Eocene are missing. Eroding bottom currents and mass slidings are inferred as responsible for these hiatuses.

The upper part of the Coriolei Formation lacks planktonic forams, and the presence of *Nummulites* sp., and *Alveolina* sp. testifies to the shifting of the depositional environment from the open sea to platform.

The lower part of the Shebele Formation can be assigned to Zone P14/P?13 due to L.O. of *Acarinina spinuloinflata*, whereas the upper part of the Shebele Formation is characterized by the association of *Turborotalia cerroazulensis cerroazulensis*, *Globigerina officinalis*, *Pseudohastigerina micra*, *P. danvillensis*, and *Globigerinatheka semiinvoluta*. The presence of *Turborotalia cerroazulensis cunialensis* permit assignment of the upper portion of the Shebele Formation to Zone P15/P16.

The lower part of the Obbia Formation is recognized through the L.O. of *Catapsydrax howei* and *Globigerinatheka index tropicalis* Zone P16.

## ACKNOWLEDGMENTS

I am especially grateful to Profs. S. MONECHI, M. NOCCHI, I. PREMOLI SILVA and A. RUSSO for help in determination of foraminiferal biozones and access to laboratory facilities.

Particular thanks are to be addressed to Prof. E. ABBATE for critical reading of the manuscript. The kind assistance of M. ULIVI for SEM observations in Laboratorio di Microscopia Elettronica del Dip. Sc. della Terra, Università di Firenze, is also acknowledged.

## REFERENCES

ABBATE E., BRUNI P. and SAGRI M. (1987). The Mesozoic and Tertiary deposits. Geosom 87, Mogadishu. Excursion guide book c, 12-22.

ABDI SALAH HUSSEIN (1989). Stratigraphic analysis of the sequences drilled in the Mogadishu basin (Somalia), with particular reference to the Cretaceous and Eocene (Ph. D. thesis).

ABDI SALAH HUSSEIN. Stratigraphic of some Cretaceous-Eocene sequences drilled in the Mogadishu basin (Somalia). Data from plankton foraminifera and calcareous nannoplankton (In press).

ABDISAMAD SHEIKH OSMAN, HILAL ABDALLA FARAJ and MOHAMED SAID ABDI (1985). Geology of Somalia. Ministry of Mineral and Water Resources. Mogadishu, Somalia, 32 pp.

AZZAROLI A. (1971). Geologia della Somalia. Enciclopedia del petrolio e del gas, 111: 778-789.

BARNES S.U. (1976). Geology and Oil prospects of Somalia, East Africa. A.A.P.G. Bulletin, 60: 390-413.

BELTRAND M.D. and PYRE A. (1974). Geological Evolution of South-west Somalia. In: Basins sedimentaires du litoral african-sedimentaire basin of the African coasts, pt.2, litoral austral et oriental south and east coast. Paris, Assoc. Serv. Geol. Afr., 159-178.

BERGGREN W.A. and VAN COUVERING J.A. (1974). Biostratigraphy, geochronology and paleochimatology of the last 15 million years in marine and continental sequences. Palaeogeogr. Palaeoclimatol. Palaeoecol., 16: 1-216.

BERGGREN W.A., KENT D.V. and FLYN Y.Y. (1985). Paleogene Geochronology and Chronostratigraphy. In: N.J. SNELLING (ed.). The Chronology of the Geological Record. Geological Society London, Special Paper, 110: 141-194.

BLOW W.H. (1969). Late Middle Eocene to Recent planktonic foraminiferal biostratigraphy. Proc. 1 Int. Conf. Plankton Microfossils, Geneva 1967. I, 199-421 pls. 1-54.

BLOW W.H. and BANNER F.T. (1962). The mid-Tertiary (Upper Eocene to Aquitanian), Globigerinacea. In: Fundamentals of mid-Tertiary stratigraphical correlations. (Edited by F.E. EARNES, F.T. BANNER, W.H. BLOW, W.J. CLARKE and L.R. COX). Cambrige University Press, 61-151.

BOSELLINI A. (1986). East Africa continental margins. Geology, 14: 76-78.
BOSELLINI A. (1989). The continental margins of Somalia: Their structural evolution and sequence stratigraphy. Mem. Sci. Geol. Padova, 41: 373-458.
COFFIN M.F. and RABINOWITZ P.D. (1982). A multichannel seismic transect of the Somalian continental margin. Proceeding 1982 Offshore Technological Conference, 2, 421-430.
COFFIN M.F. and RABINOWITZ P.D. (1984). Rifting of the East African continental margin: EOS Transaction of the American Geophysical Union, 65: 900.
COFFIN M.F. and RABINOWITZ P.D. (1988). Evolution of the conjugate East Africa-Madagascar margins and the western Somali Basin. The Geological Society of America. Special Paper, 226: 1-78.
DEUTSCHE TEXACO AKTIENGESELLSCHAFT (1973). Somalia, Coriolei Basin interpretation. Ministry of Mineral and Water Resources, Mogadishu, Somalia.
GIRDLER R.W. and STYLES P. (1974). Drifting and rifting of Africa. Nature, 217: 1102-1106.
HAQ B.U., HARDENBOL J. and VAIL P.R. (1987). Chronology of fluctuating sea levels since the Triassic. Science, 235: 1156-1167.
HEIMAN M.E., FRERICH W.E. and VICENT E., (1974). Paleogene planktonic foraminifera from the Western Tropical Indian Ocean, D.S.D.P. Leg 24. In: FISHER R.L., BUNCE E.T. et al., Init. Rep. D.S.D.P., 24: 851 pp.
LUTERBACHER H.(*) and STAINFORTH M.(**), (*)Illustrated review of Paleocene to Middle Eocene index species, 163-244. (**) Illustrated review of Late Eocene to Middle Miocene index species, 245-332. In: Cenozoic planktonic foraminiferal zonation and characteristic of index forms. (Edited by R.M. STAINFORTH, J.L. LAMB, HANSPETER LUTERBACHER, J.H. BEARD, and R.M. JEFFORDS). The Univ. of Kansas Paleont. Inst.. Harold Norman Fisk Memorial Papers. Exxon Company, USA.
MC GOWRAN B. (1978). Stratigraphic record of Early Tertiary ocean and continental events in the Indian Ocean region. Marine geology, 26: 1-39. MOORE JR T.C., VAN ANDEL T.J.H., SANCETTA C. and PISIAS N. (1978). Cenozoic hiatuses in pelagic sediments. Micropaleontology, 24: 113-138.
NOCCHI M., PARISI G., MONACO P., MONECHI S. and MADILE M. (1988). Eocene and Early Oligocene micropaleontology and paleoenvironment SE Umbria, Italy. Paleogeog. Paleoclim. Paleoec.. Elsevier Amsterdam, 67, 64.
RABINOWITZ P.D., COFFIN M.F. and FALVEY D.A. (1983). Salt diapirs bordering the continental margin of Northern Kenya and Southern Somalia. Science, 215: 663-665.
SINCLAIR SOMALI COORPORATION (1960). Somalia, Geological-Geophysical Report. Ministry of Mineral and Water Resources. Mogadishu, Somalia, unpublished report.

TOUMARKINE M. and LUTERBACHER H. (1985). Paleocene and Eocene planktonic foraminifera. In: Plankton Stratigraphy (Edited by H.M. BOLLI, J.B. SAUNDERS, K. PERCH-NIELSEN), Cambridge University Press, 87-154.

VAIL P.R., MITCHUM R.M. JR., TODD R.G., WIDMIER J.M., THOMPOSON S.III, SANGREE J.B., BUBB J.N. and HATLELID W.G., (1977). Seismic stratigraphiy and global changes of sea level, in Payton, C.E. (eds.). Seismic stratigraphy Application to hydrocarbon exploration. American Association of Petroleum Geologists Memoir, 26: 49-212.

*Final editing, January 1990*

From *Geology and mineral resources of Somalia and surrounding regions*, Ist. Agron. Oltremare, Firenze, Relaz. e Monogr. **113**, 197-210, 1993.

# A CONTRIBUTION TO THE STRATIGRAPHIC KNOWLEDGE OF CENTRAL SOMALIA WITH SPECIAL REFERENCE TO THE AREA OF GAALKACYO

C. FAILLACE * and P. GRANATA **

* Consulting Hydrogeologist, Via Fontana dei Monaci Prima 7, 00043 Ciampino, Roma, Italy.

** Mr. Granata's address is not known to the other author. His contribution to this paper derives from his unpublished report "Galcaio Water Well, Lithological and Paleontological Description", Mogadishu, 1961.

ABSTRACT

The widespread gypsum in Central Somalia was dated as Eocene (Taleex Formation) in the official geological map of East Africa. A more recent study attributes the gypsiferous crusts and terrigenous sediments covering the Mudug and the Galgadud Plateau to the Miocene (Mudug Beds). The satellite imagery interpretation carried out by FAILLACE for the "Water Quality Data Book of Somalia" clarifies that the widespread gypsum covers ancestral drainage systems, most probably of Pleistocene age, in the Mudug Region (Gaalkacyo System) and in the Galgadud Region (Dhuusamarreeb System). The gypsiferous crusts cover fluvio-lagunal sediments belonging to the Miocene (Mudug Beds).

A stratigraphic sequence of 320 m of sediments in Gaalkacyo was investigated in the early 1960s by means of an exploratory borehole. According to the lithological and paleontological determination, the sediments penetrated by this borehole are constituted by 90 m of undifferentiated sandy clay, gypsum, and marls (Oligocene-Miocene), topped by Pleistocene gypsiferous alluvial deposits. From 90 to 180 m, fossiliferous shallow marine sediments are predominant (Karkar Formation - Middle Eocene). The section from 180 to 320 m is mainly constituted by an evaporitic sequence, probably belonging to the Taleex Formation (Lower/Middle Eocene).

This paper presents the results of the Gaalkacyo exploratory borehole and reports its lithological and paleontological sequence. It also includes two cross-sections derived from the lithological correlation of several water wells drilled in the Central Rangelands.

## INTRODUCTION

According to the geological map of KOZERENKO (1970) the limestone overlying the Yasoomman Formation constitutes the lower member of the Mudug-Marka Formation (Oligocene/Miocene) and the large area covering Central Somalia previously mapped as Taleex Formation belongs to the upper member of the same formation, which is dated as Miocene. POPOV and KARRANI (1973) adopted KOZERENKO interpretation. The lower part of these sediments is generally constituted by white limestone, marls, and dolomite deposited in a rather shallow sea; the upper part is constituted by sand, sandy limestone, sandstone, gypsum, gypsiferous clay in varying colours, and clay of semi-continental and lagunal environments named "Mudug Beds" by RAMPETROL (1975).

In recent years POZZI et al. (1984), on the basis of the above-mentioned sources and on the results of the age determination of basalt (25.3 $\pm$ 0.4 m.y.) struck in a borehole drilled near the village of Xananbur northwest of Dhuusamarreeb, established that the sediments above the basalt were younger than the Oligocene.

This paper presents the results of the Gaalkacyo exploratory borehole and reports its lithological and paleontological sequence. It also reports two cross-sections derived from the lithological correlation of water wells and the general geological and structural conditions of the Central Rangelands.

## LITHOLOGICAL DESCRIPTION OF THE GAALKACYO EXPLORATORY WELL

In 1961, B. WALTHALL, geologist of SINCLAIR OIL, probably based on data obtained from geophysical studies, suggested the drilling of a 350 m deep well for the water supply of Gaalkacyo. The reason that justified such a depth was most probably based on geophysical interpretation. According to the previsions of WALTHALL, the gypsiferous sequence outcropping in the area should have been about 200 m thick, it was overlying the Auradu limestone, where groundwater of good quality was expected. The water of the gypsiferous sequence dated as Taleex Formation should have been isolated.

Most probably the top 32 m, however, are alluvial materials deposited along an ancestral drainage system (visible from satellite imageries) during the Pleistocene.

The lithological sequence of this borehole is briefly described below.

| Depth (m) | Description |
|---|---|
| 0 - 12 | selenitic white gypsum with some granules of quartz sand; |
| 12 - 16 | reddish sandy, clayey, and gypsiferous conglomerate, slightly cemented. The quartz sand is medium to coarse, slightly rounded; gravelly quartz, from 14 to 16, mixed with selenitic gypsum; |
| 16 - 28 | reddish clayey, gypsiferous sand, from fine to coarse and well-rounded; crystals of selenitic gypsum; |
| 28 - 32 | reddish coarse quartz sand, slightly rounded with some gypsum crystals; |
| 32 - 34 | whitish arenaceous limestone with quartz granules; |
| 34 - 42 | coarse quartz sand, calcareous and quartz pebbles grading into quartz gravel (36 - 38 m), (40 - 42 m); |
| 42 - 44 | coarse rounded quartz sand and quartz grains mixed with white gypsiferous marls; |
| 44 - 46 | coarse quartz sand, quartz grains, selenitic gypsum crystals, and calcareous gypsiferous nodules; |

46 - 60 quartz sand as above, mixed with abundant basalt fragments and rare limestone fragments in a greyish silty-clay matrix (46 - 48 m), grading into basalt with rare arenaceous limestone fragments in a silty-clay matrix;
60 - 66 mixture of greyish-black basaltic, calcareous, quartzose, and gypsiferous sand;
66 - 78 whitish-yellowish compact angular, semi-crystalline limestone; rounded and smooth quartz grains;
78 - 80 basalt;
80 - 86 white, slightly porous, angular fragments of limestone; some layers of brownish limestone, soft and marly;
86 - 102 yellow, hard calcareous marls, with some thin limestone layers; fossils at 98 m;
102 - 140 grey fossiliferous clay, intercalated with layers of grey limestone and basalt especially from 120 to 140 m;
140 - 170 slightly clayey sub-rounded quartz sand, with limestone and basaltic sand along with pieces of gypsiferous sandstone, small layers of grey clay with pyrite crystals and rare foraminiferous fossils; clay content increases in the bottom 4 m;
170 - 177 dark - grey clayey, sandy, porous, soft, tuff-like limestone, light and frequent fragments of compact limestone and basalt; intercalations of grey clay layers, some crystals of gypsum, pyrite and calcite;
177 - 185 undefined, slightly fibrous white rock fragments;
185 - 190 coarse, grey sandy - clay with fragments of basalt, limestone, and gypsum crystals;
190 - 192 grey fossiliferous clay with small basalt fragments;
192 - 196 light grey clay, gypsiferous and slightly sandy;
196 - 198 as from 190 - 192 m;
198 - 200 as from 192 - 196 m;
200 - 206 whitish to brown gypsiferous and calcareous sand; frequent quartz sand;
206 - 246 white, hard gypsiferous marls with intercalations of thin layers of marls and gypsum;
246 - 316 white sandy gypsiferous marls; sand increases progressively towards the bottom.

The depth or 350 m was not reached due to drilling problems. The borehole was completed at 316 m by the former "Well Section" of the MINISTRY of PUBLIC WORKS under the supervision of FAILLACE. The paleontological determination was carried out by GRANATA (at that time a paleontologist of SINCLAIR OIL CO.), who subdivided the penetrated sediments as follows:

| Depth (m) | Description |
|---|---|
| 0 - 90 | undifferentiated sediments (Oligocene-Miocene) |
| 90 - 180 | Karkar Formation (Upper Eocene) |
| 180 - 316 | Taleex Formation (Middle Eocene) |

Most of the sediments of the Gaalkacyo well were deposited, from top to bottom, under continental/lagunal, shallow marine, and lagunal/evaporitic environments. In Godinlabe a water well drilled to a depth of 86 m had a lithological sequence similar to that met in the upper part of the well in Gaalkacyo. In Cadaado a water well penetrated 80 m of continental deposits consisting of gypsiferous clay with calcareous and arenaceous nodules, sandy clay, and sand. The underlying sediments were deposited in a lagunal or shallow sea environment and are constituted by white marls, cherty limestone, with intercalations of clay and marly clay followed by yellow marls, clay, and sandy clay. Grey sandy clay with intercalations of black sandy clay with organic matter was met between 125 and 138 m; no fossils were found. The water well in Mareer-Gur met the following sequence of sediments:

| Depth (m) | Description |
|---|---|
| 0 - 15 | gypsiferous limestone, white to pink marls |
| 15 - 57 | gypsiferous clay of various colours and sandy clay |
| 57 - 73 | calcareous gravel and marly clay |
| 73 - 83 | soft white limestone |
| 83 - 100 | grey and green sandy clay with intercalations of soft limestone and cherty limestone. |

The sequence from 0 to 73 m is of continental origin, while the section between 73 and 100 m was deposited in a lagunal or shallow sea environment.

In the Hobyo Sinclair oil well the Upper Tertiary deposits were penetrated for a thickness of 732 m and were constituted mainly by sandstone with green-grey shales and porous chalky white limestone.

Oligocene-Miocene sediments have been met in several wells drilled recently by LBI in the Central Rangelands. The well in Wargaloh penetrated 162 m of gypsiferous sand and sandy clay with fine gravel which was deposited on top of about 50 m of basalt, which in turn was deposited on yellow soft limestone, most probably of the Karkar Formation.

The wells drilled by LBI in Afgaduudle, Dhajimaale, Bud Bud (north of Hobyo), and Quracley met sediments belonging to the Oligocene-Miocene similar to those overlying a thick sequence of basalt met in various wells in the Mudug - Galgadud Plateau. A rather detailed description of the geological formations of Central Somalia is given by FAILLACE in "Hydrogeology and Water Quality of Central Somalia" (1986). The geological conditions of the Central Rangelands and the considerable lithological changes, both vertically and horizontally, especially in the upper section of the Mudug Beds, are represented in Fig. 2 and Fig. 3 (FAILLACE, 1986). They show the cross-sections of Gal Dogob-Wisil and Matabaan-Dhuusamarreeb-Gaalkacyo-Buur Yaqab, respectively. The location of these cross-sections is shown in Fig. 1.

Fig. 1 - Central Somalia. Location of cross-section A - A and B - B'.

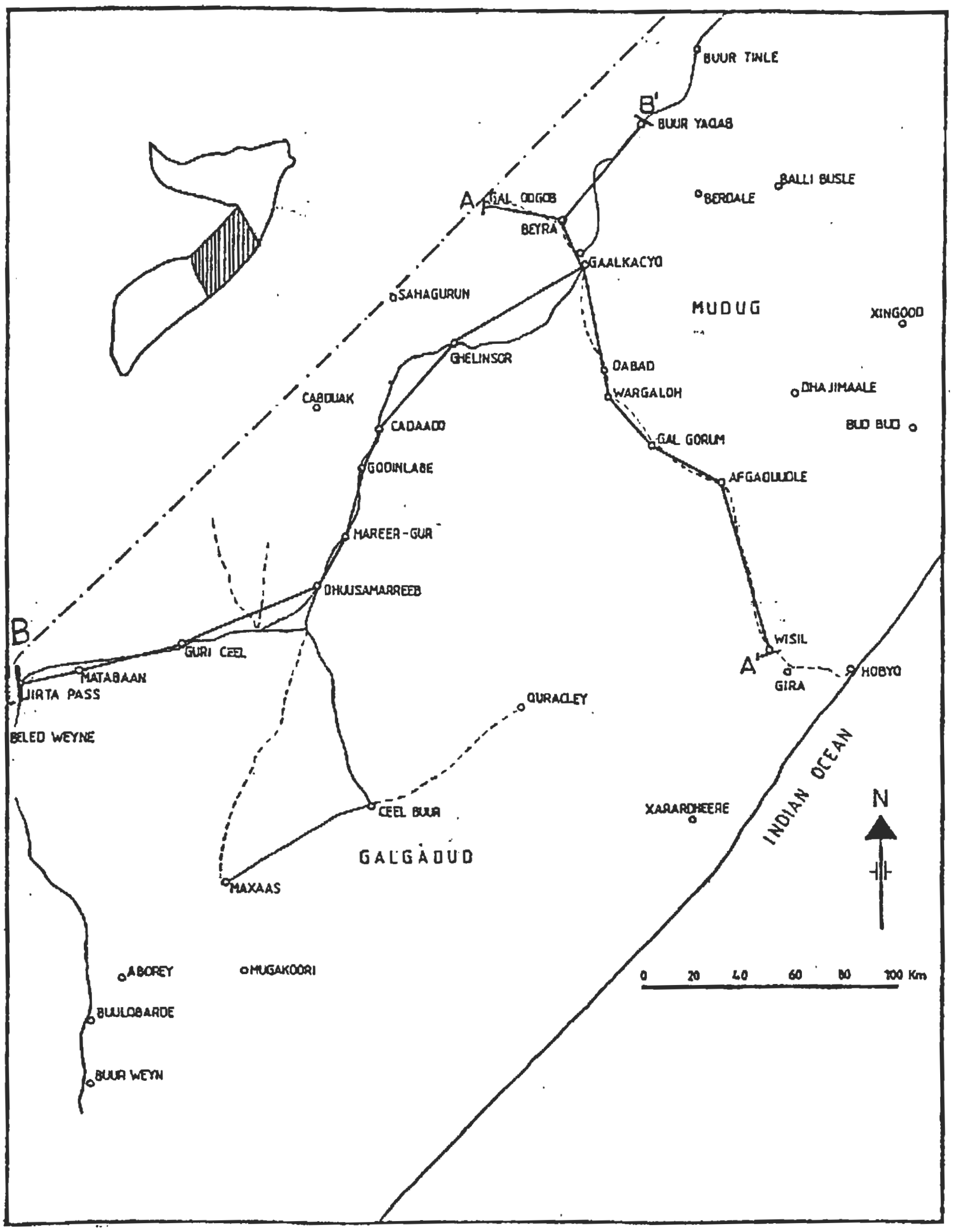
BUUR TINLE
B'
BUUR YACAB
BERDALE
BALLI BUSLE
A
GAL OOGOB
BEYRA
GAALKACYO
SAHAGURUN
MUDUG
XINGOOD
GHELINSOR
OABAD
WARGALOH
CABDUAK
DHA JIMAALE
CADAADO
BUD BUD
GAL GORUM
GODINLABE
AFGADUUDLE
MAREER-GUR
DHUUSAMARREEB
B
WISIL
GURI CEEL
A'
GIRA
HOBYO
MATABAAN
JIRTA PASS
QURACLEY
BELED WEYNE
INDIAN OCEAN
N
CEEL BUUR
XARARDHEERE
GALGADUD
MAXAAS
ABOREY
MUGAKOORI
0 20 40 60 80 100 Km
BUULOBARDE
BUUR WEYN

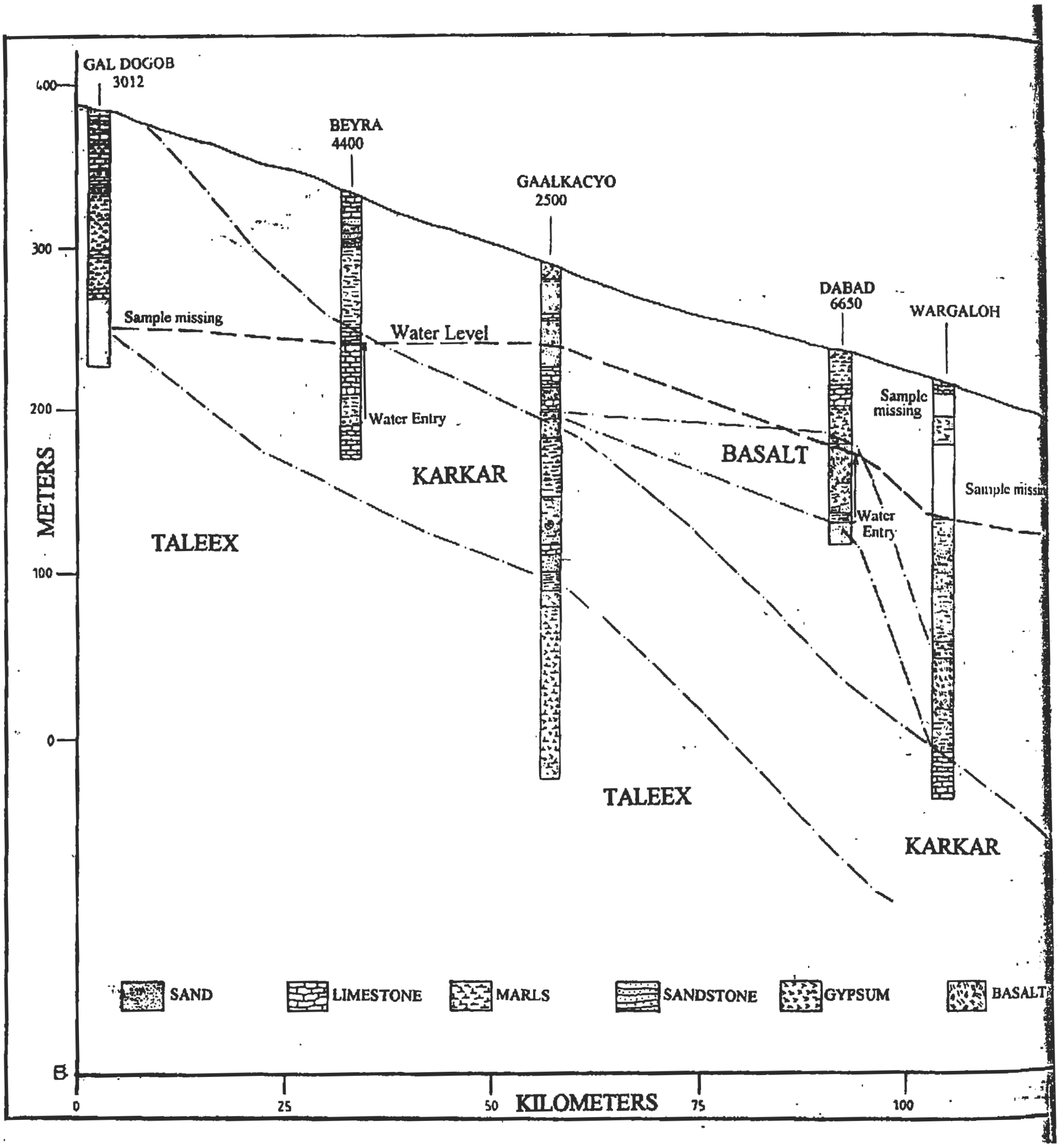


Fig. 2 - Central Somalia. Hydrogeological cross-section: Gal Dogob-Wisil. Note: E.C. in micromhos/cm indicated below well name.

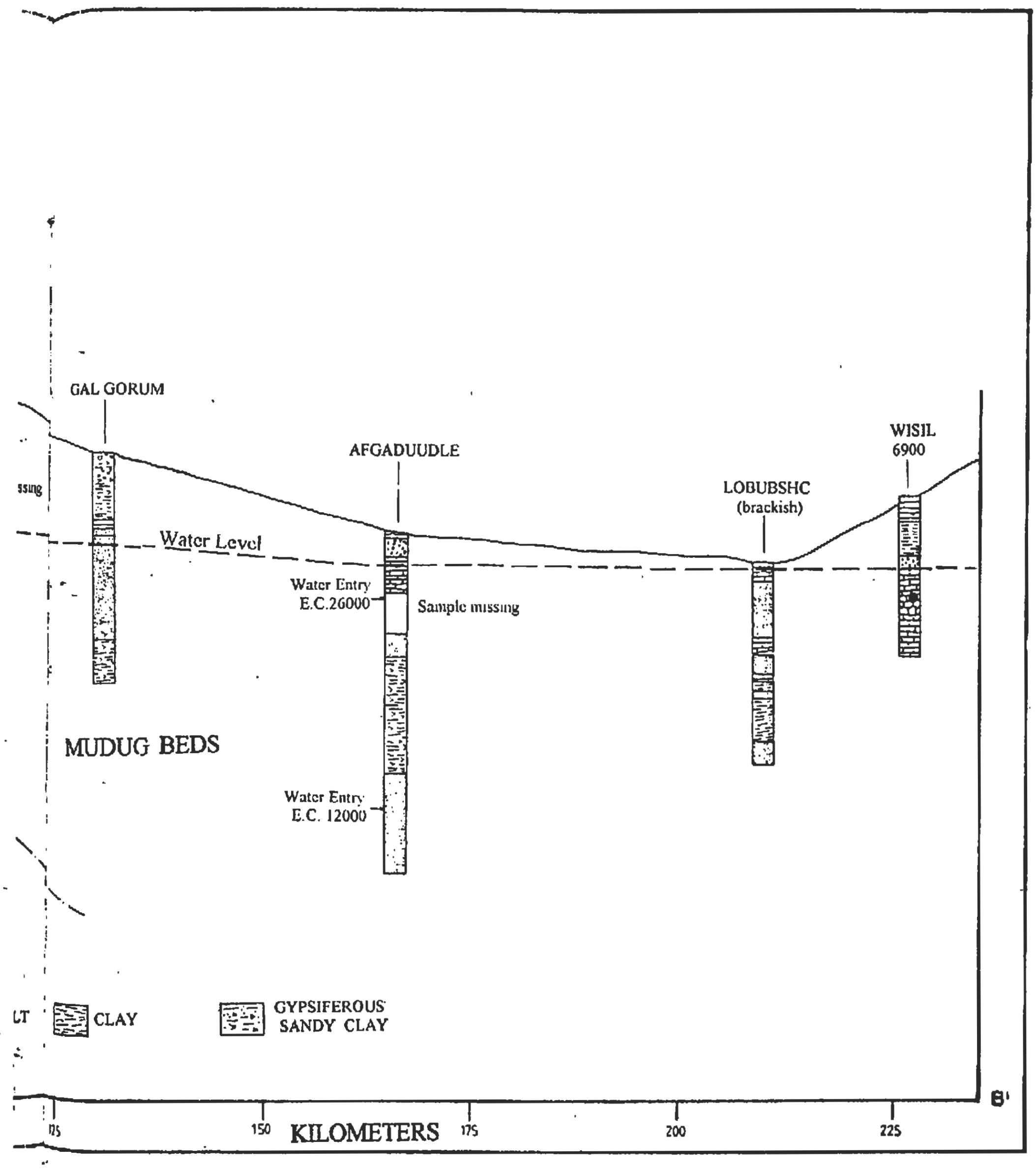
GAL GORUM
AFGADUUDLE
LOBUBSHC
(brackish)
WISIL
6900
ssing
Water Level
Water Entry
E.C.26000
Sample missing
Water Entry
E.C. 12000
MUDUG BEDS
LT
CLAY
GYPSIFEROUS
SANDY CLAY
B'
125
150
KILOMETERS
175
200
225

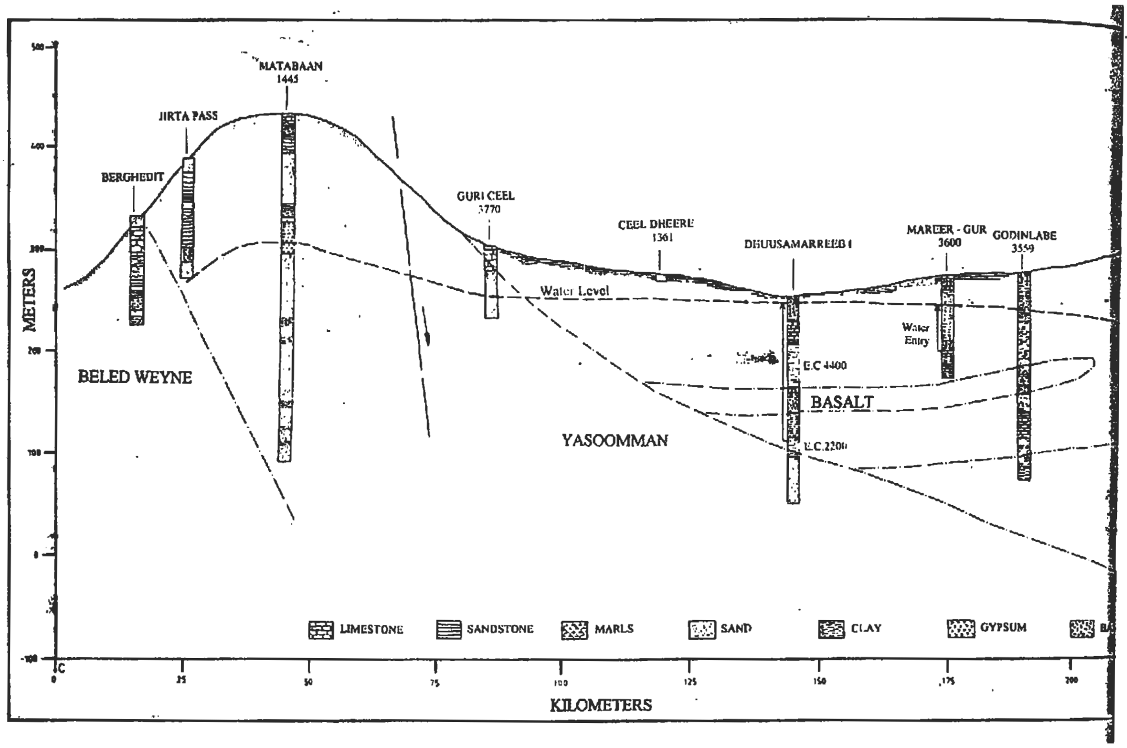


Fig. 3 - Central Somalia. Hydrogeological cross-section: Matabaan-Dhuusamarreeb-Gaalkacyo-Buur Yaqab. Note: E.C. in micromhos/cm indicated below well name.

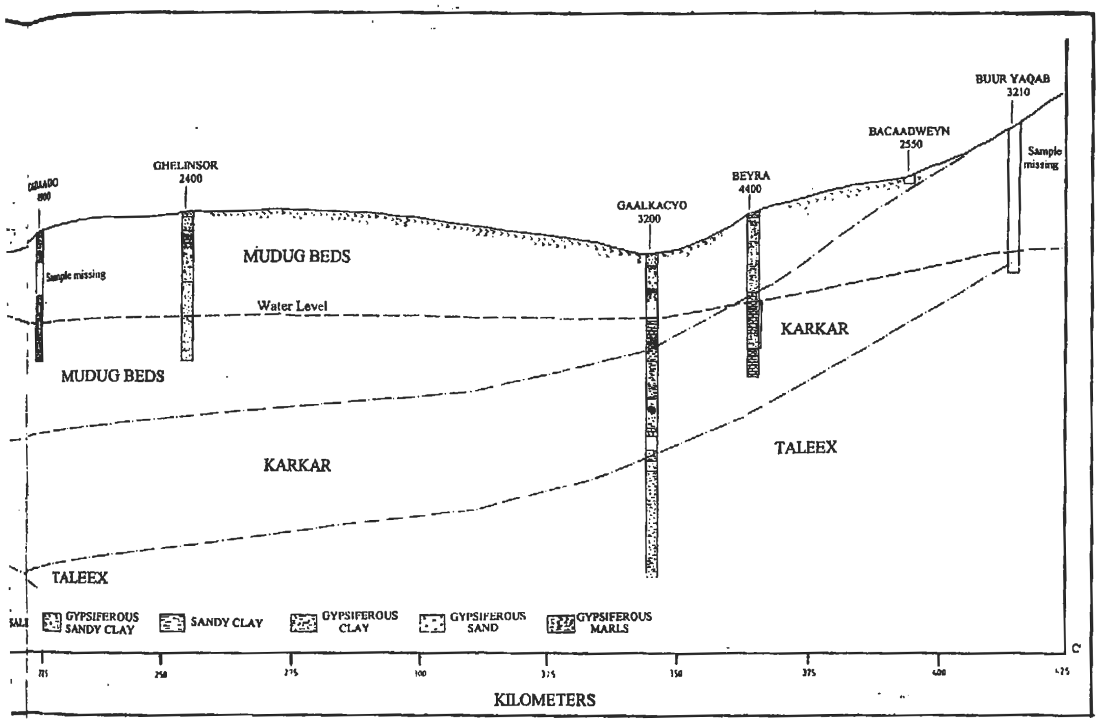
BUUR YAQAB
3210
BACAADWEYN
2550
Sample missing
GHELINSOR
2400
BEYRA
4400
GAALKACYO
3200
Sample missing
MUDUG BEDS
Water Level
KARKAR
MUDUG BEDS
TALEEX
KARKAR
TALEEX
GYPSIFEROUS SANDY CLAY
SANDY CLAY
GYPSIFEROUS CLAY
GYPSIFEROUS SAND
GYPSIFEROUS MARLS
KILOMETERS

## PALEONTOLOGY

Fossils were first encountered in abundant numbers in this water well from about a depth of 90 m. Fifteen different species of foraminifera and four different genera of ostrocodes were recognized. A more detailed taxonomic study of this fauna would have probably revealed the presence of more species than identified but it was felt that this endeavour would be more of academic than practical value.

The species of foraminifera found in this well indicate that this section at least in part belongs to the Middle Eocene Karkar Formation. The following microfossil forms substantiate this conclusion:

1. *Dictyoconus daviesi:* this species is confined to levels II to IV of the Karkar Formation according to AZZAROLI (1952) and has also been reported by SILVESTRI (1939) from the Middle Eocene of Somalia. The genus *Dictyoconus* in Somalia is considered by some eminent workers in the area to be confined to the Middle Eocene (BENNISON 1962, El Hamurre # 1 report) but it has also been reported in limited numbers from the Auradu Formation (RUGGERI, 1955).

2. *Linderina buranensis:* this species was first described by NUTTALL and BRIGHTON (1931) from the Middle Eocene of Somalia. It was also reported from the Middle Eocene by SILVESTRI (1948) and AZZAROLI (1952). The genus *Linderina* is rather widespread; it is found in rocks ranging from Cretaceous to Miocene age but most species have been described from the Middle Eocene. In Somalia it is reported only from rocks of Middle Eocene age (SILVESTRI, 1948; AZZAROLI, 1952; NUTTALL and BRIGHTON, 1931; SMOUT, 1954).

3. *Pellatispira tudensis*: the genus *Pellatispira* according to SILVESTRI (1939) ranges in age from Middle Lutetian to Oligocene. The species *Pellatispira tudensis* has been reported in Somalia only from the Middle and Upper Eocene (AZZAROLI, 1958). AZZAROLI (1952) in his original description of this species placed it in the genus ASSILINA but in a later publication (AZZAROLI, 1958) he changed the generic name to *Pellatispira.*

4. *Nummulites* cf *discorbinus*: there is a long history of confusion between the above-named species and *N. beaumonti* D'ARCHIRAC and HAIME. It is stated in the original description of *N. beaumonti* that it has a very straight septa at about the whorl height while the septa of the *N. discorbinus* are closer marking the chamber height about twice the length. It is felt that the specimens in this well resemble more closely the *N. discorbinus* although at times it is difficult to distinguish between these two species. The species *Nummulites discorbinus* is confined in range to the Middle Eocene in the Mediterranean Region, India, Qatar, and Somalia, while *N. beaumonti* is typical of the Late Middle and Upper Eocene of these regions (SMOUT, 1954; AZZAROLI, 1952; SILVESTRI, 1948; NUTTALL and BRIGHTON, 1931).

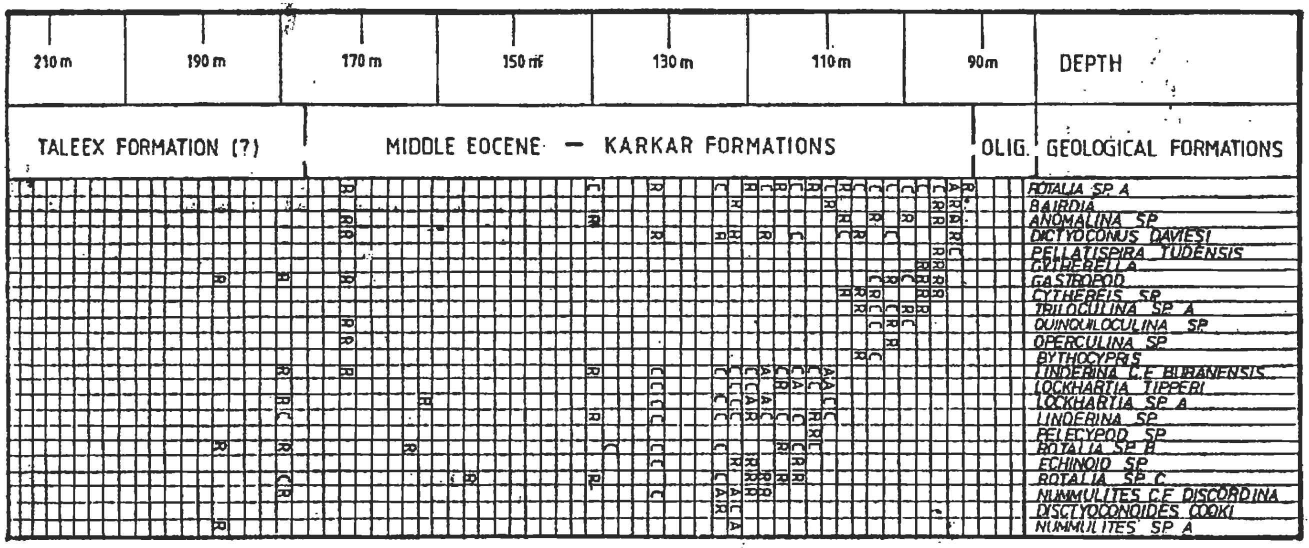


Fig. 4 - Quantitative faunal log of Gaalkacyo exploratory well. A = Abundant C = Common R = Rare
Note: no fossils were found above 90 m and below 190 m.

A consideration of the abundant literature available on *Nummulites* in Somalia reveals that this genus does not range below the Taleex. RUGGERI (1955) in his study of the Auradu made a definite statement saying that *Nummulites* in Somalia made their first appearance at the base of the Taleex Formation and not before. SILVESTRI (1942) does not record any *Nummulites* from the Lower Eocene but just from the Lutetian. STEFANINI (1937) in reviewing the stratigraphy of the Eocene reports *Nummulites* from the Karkar and some small forms from the Taleex but none from the Auradu Formation. NUTTALL and BRIGHTON (1931) found abundant *Nummulites* in the Middle Eocene but did not report any *Nummulites* from the Lower Eocene sections examined. SILVESTRI (1942) described many species of *Nummulites* but none of these were found in beds older than Karkar. The work of BENNISON on subsurface samples in Somalia and Ethiopia also seems to substantiate this same conclusion. Upon an examination of the sample logs and faunal lists made by BENNISON it was found that in all the tests that spudded in the Auradu *Nummulites* were not present and in the ones that spudded in younger sediments *Nummulites* were confined in formations to formations younger in age than the Auradu.

5. *Dictyoconoides cooki*: this species is restricted in range to the Middle Eocene of Somalia, Northern India, Southwestern Iraq, and the Qatar Peninsula (SMOUT, 1954; NUTTALL and BRIGHTON, 1931; AZZAROLI, 1952; SILVESTRI, 1942; STEFANINI, 1927).

   Further evidence that this section belongs to the Middle Eocene Karkar Formation and not to the Lower Eocene-Paleocene Auradu is the absence of typical Auradu fossils such as *Sakesaria cotteri, Lockharia diversa, Miscellanea meandrina,* and others which are very common in the Auradu Formation in Ethiopia.

FAUNAL LIST OF THE GAALKACYO WATER WELL

| (meters) | |
|---|---|
| 90 - 92 | *Rotalia* sp. A |
| 92 - 94 | *Bairdia* sp., *Anomalina* sp., *Rotalia* sp. A, *Dictyoconus daviesi, Pellatispira tudensis* |
| 94 - 96 | *Pellatispira tudensis, Cytherella* sp., *Anomalina* sp., *Rotalia* sp. A, *Gastropod* sp., *Bairdia* sp., *Cythereis* sp. |
| 96 - 98 | *Cythereis* sp., *Rotalia* sp., *Gastropod* sp., *Triloculina* sp. A, *Cytherella* sp. |
| 98 - 100 | *Triloculina* sp. A, *Rotalia* sp. A, *Quinquiloculina* sp., *Gastropod* sp., *Anomalina* sp. |
| 100 - 102 | *Dictyoconus daviesi* , *Gastropod* sp., *Rotalia* sp. A, *Operculina* sp., *Quinquiloculina* sp., *Triloculina* sp. A |
| 102 - 104 | *Quinquiloculina* sp., *Gastropod* sp., *Rotalia* sp. A, *Anomalina* sp., *Cythereis* sp., *Triloculina* sp. A |

104 - 106 *Dictyoconus daviesi* , *Triloculina* sp. A, *Rotalia* sp. A, *Bythocypris* sp., *Cythereis* sp.

106 - 108 *Dictyoconus daviesi, Rotalia* sp. A, *Cythereis* sp., *Anomalina* sp.,

108 - 110 *Linderina* cf. *buranensis, Lockhartia tipperi, Bairdia* sp., *Lockhartia* sp. A, *Linderina nuttalli, Rotalia* sp. A

110 - 112 *Pelecypod* sp., *Lockhartia tipperi, Linderina* cf. *buranensis, Rotalia* sp. B, *Rotalia* sp. A, *Linderina nuttalli*

112 - 114 *Rotalia* sp. C, *Dictyoconus daviesi, Lockhartia tipperi, Echinoid* sp., *Linderina* cf. *buranensis, Rotalia* sp. A, *Rotalia* sp. B, *Linderina nuttalli*

114 - 116 *Linderina* cf. *buranensis, Rotalia* sp. A, *Rotalia* sp. B, *Linderina nuttalli, Rotalia* sp. C, *Lockhartia tipperi*

116 - 118 *Rotalia* sp. A, *Lockhartia* sp. A, *Nummulites* .cf. *discorbinus, Dictyoconus daviesi, Linderina* cf. *buranensis, Linderina nuttalli, Rotalia* sp. C

118 - 120 *Echinoid* sp., *Linderina* cf. *buranensis, Lockhartia* sp. , *Lockhartia tipperi, Rotalia* sp. A, *Nummulites* cf. *discorbinus, Linderina nuttalli, Rotalia* sp. C

120 - 122 *Dictyoconus* sp., *Nummulites* cf. *discorbinus, Lockhartia tipperi, Dictyoconoides* sp., *Linderina* cf. *buranensis, Echinoid* sp., *Bairdia* sp., *Nummulites* sp. A, *Lockhartia* sp. A, *Linderina nuttalli*

122 - 124 *Rotalia* sp. B, *Nummulites* cf. *discorbinus, Lockhartia* sp. A, *Dictyoconus* sp., *Linderina* cf. *buranensis, Dictyoconoides* sp., *Linderina nuttalli, Rotalia* sp. C, *Rotalia* sp. A

129 - 130 *Echinoid* sp., *Lockhartia* sp. A, *Nummulites discordina, Daviesina* sp., *Linderina* cf. *buranensis, Rotalia* sp. B, *Lockhartia* cf. *tipperi, Dictyoconus* sp., *Linderina nuttalli, Rotalia* sp. A

138 - 140 *Linderina* cf. *buranensis, Linderina nuttalli, Rotalia* sp. A, *Anomalina* sp.

146 - 147 *Rotalia* sp. B

154 - 156 *Rotalia* sp. C

160 - 162 *Lockhartia* sp. A

162 - 164 *Rotalia* sp. B

170 - 172 *Dictyoconus* sp., *Rotalia* sp. A, *Linderina* cf. *buranensis, Gastropod* sp., *Quinquiloculina* sp., *Operculina* sp., *Anomalina* sp.

178 - 180 *Rotalia* sp. C, *Lockhartia* sp. A, *Linderina* cf. *buranensis, Gastropod* sp., *Rotalia* sp. B, *Linderina nuttalli, Nummulites* cf. *discordina*

186 - 188 *Gastropod* sp., *Nummulites* sp. A, *Rotalia* sp. B.

The quantitative faunal logs of the Gaalkacyo well are shown in Fig. 4.

ACKNOWLEDGMENTS

Sincere appreciation is expressed to Prof. RUGGERO MATTEUCCI, Department of Earth Sciences, Rome University, for reviewing the paper.

REFERENCES


FAILLACE C. (1961). Situazione geoidrologica del pozzo in perforazione per il centro abitato di Galcaio. Unpublished Report, Mogadishu.

FAILLACE C. (1986). Hydrogeology and water quality of Central Somalia, In: "Water Quality Data Book of Somalia". Rome.

GKW (1982). Water scheme for Ceerigabo, Quardho-Garowe-Gaalkacyo-Dhuusamareeb. Mogadishu.

GRANATA P. (1961). Galcaio water well. Lithological and paleontological description. Sinclair Unpublished Report, Mogadishu.

KOZERENCO V.N. (1970). Geological map of Somalia. Scale 1:1,000,000. U.N.D.P.

LOUIS BERGER INTERNATIONAL (1985). Comprehensive groundwater development Project. Final Report, Vol. III Appendix, Mogadishu.

POPOV A.P., KIDWAI A.L. and KARRANI S.A. (1973). Mineral and ground water survey (Phase II), ground water in the Somali Democratic Republic. Vol. III. Technical Report, UNDP.

POZZI R. et al. (1983). Groundwater resources in Central Somalia. Mem. Sc. Geol. Padova, 35.

POZZI R. and XUSSEN SALAAD M. (1984). Groundwater resources in Hobyo Area (Mudugh Region, Central Somalia). Mem. Sc. Geol. Padova, 36.

POZZI R. et al. (1985). Late Paleogene-Early Middle Miocene Formation in Obbio Area (Mudugh Region) Central Somalia. Mem. Sc. Geol. Padova, 37.

RAMPETROL (1975). Consideration on the oil prospects of the Democratic Republic of Somalia. Unpublished Report, Bucarest.


*Final editing, January 1990*

From *Geology and mineral resources of Somalia and surrounding regions*, Ist. Agron. Oltremare, Firenze, Relaz. e Monogr. 113, 211-240, 1993.

# PRE- AND SYN-RIFT SEDIMENTATION IN A TERTIARY BASIN ALONG THE GULF OF ADEN (DABAN BASIN, NORTHERN SOMALIA)

E. ABBATE, ABDI SALAH HUSSEIN, P. BRUNI and M. SAGRI

Dipartimento di Scienze della Terra, Università di Firenze, Via La Pira 4, 50121 Firenze, Italy.

ABSTRACT

The Daban Basin is located 25 km SE of Berbera (Northern Somalia) and is filled with 2,700 m of Middle Eocene to Oligocene clastic deposits. From the base of the sequence upward the environments listed below are distinguished: restricted lagoon, delta, open lagoon, alluvial plain, ephemeral and perennial lakes. The perennial lake sediments are lateral transitional to a coarse-grained delta sequence. The Daban Basin was a rapidly subsiding trough parallel to the Gulf of Aden. It was active during the beginning of the breakup of the Somali-Arabian continental block and the rifting of the Gulf of Aden. The sedimentary evolution of the Daban Basin was controlled by tectonic, paleogeographic and paleoclimatic changes induced by this event.

## INTRODUCTION

Since the Early Mesozoic the development of sedimentary sequences on the Somali continental margins is the response to plate movements of Africa, India and Arabia and the opening of the Indian Ocean and of the Gulf of Aden.

Mesozoic to Early Tertiary continental and shallow marine deposits, that rest unconformably on Precambrian to Early Paleozoic basement, outcrops extensively in Northern Somalia (Fig. 1) and can be easily correlated across the Gulf of Aden (SWARTZ and ARDEN, 1960; BEYDOUN, 1970; ABBATE et al., 1974; BRUNI and FAZZUOLI, 1979). These sedimentary sequences were deposited on the East Africa-Arabia continental margin during and after the Gondwana dismemberment. The Late Eocene to Neogene sedimentary sequences, instead, are distributed only along a narrow coastal belt (Fig. 1) (S.O.E.C., 1954; AZZAROLI, 1958; BEYDOUN, 1970; MERLA et al., 1979; ABBATE et al., 1988). They were deposited in fast subsiding faulted basins during the rifting and the opening of the Gulf of Aden and the development of the northern Somalia continental margin.

A continuous succession of Middle Eocene to Oligocene deposits outcrops SE of Berbera, in the Daban basin (Fig. 2). This Daban sequence preserves a fairly continuous record of the tectonic and paleogeographic changes induced by the early phases of evolution of the Gulf of Aden.

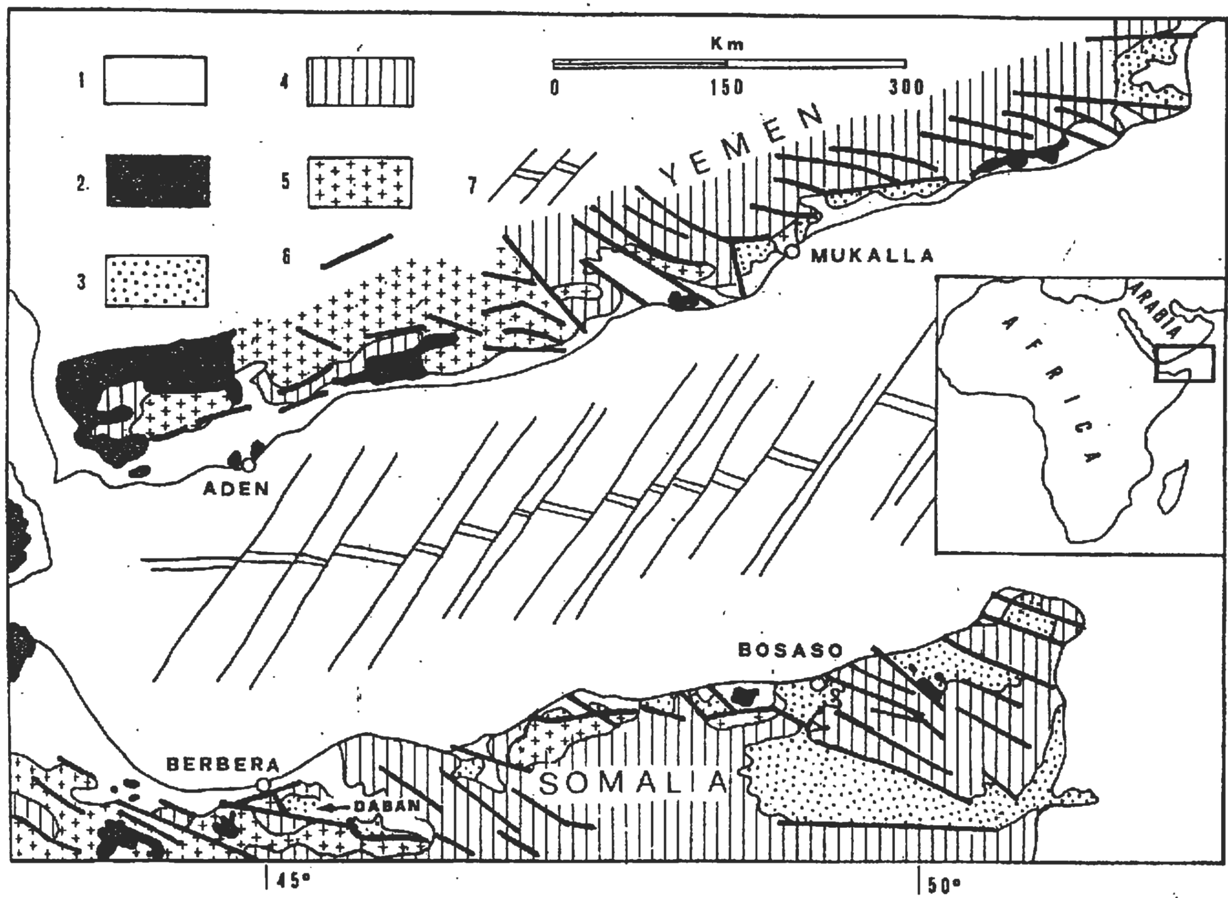


Fig. 1 - Simplified geology of the Somali and Yemenite coasts of the Gulf of Aden. 1 - Quaternary deposits; 2 - Neogene volcanites; 3 - Oligo-Miocene sedimentary deposits; 4 - Mesozoic to Early Tertiary deposits; 5 - Precambrian to Early Paleozoic basement; 6 - major faults; 7 - Sheba ridge.

As far as we know, in Northern Somalia, there is only the Daban sequence which shows such a thick and continuous succession, but, according to unpublished oil companies studies, similar deposits exist in the offshore prospicient to the Somali and Yemenite coasts of the Gulf of Aden.

In the Daban Basin we have carried out two field surveys and the geological map alleged to this volume has been produced (BRUNI et al., 1987). Preliminary facies analyses were also made and two sections were measured along the Togga Biyoguure and Togga Kalajab streams (Figs. 2, 4).

The purpose of this paper is to provide a detailed description and paleoenvironmental interpretation of the Daban sequence and to identify the principal controls on sedimentation induced by structural and paleogeographic changes connected with the breakup of the Somali-Arabian continental block and the development of the Gulf of Aden.

## GEOLOGY OF THE DABAN BASIN

The Daban Basin, located 25 km southeast of Berbera, is filled with Middle Eocene to Oligocene predominantly clastic deposits (Fig. 2). More than 2,700 m of sediments accumulated in the basin during 20-25 Ma, giving an average sedimentation rate of 10.8-13.5 cm/1000 y.

MACFADYEN (1933) described the Daban sequence and brilliantly interpreted its different environments. Other information on the Daban Basin has been reported by WILLIE (1925), S.O.E.C. (1954), HUNT (1960) and more recently by ABBATE et al. (1983) and SAGRI et al. (1989). The Daban succession shows a variation from shallow marine at the base to continental sediments at the top (Fig. 4) (MACFADYEN, 1933; ABBATE et al., 1983; BRUNI et al., 1987; SAGRI et al., 1989). Fossils were collected at the base of the sequence in the shallow marine deposits (MACFADYEN, 1933). They consist of nautiloids (HAAS and MILLER, 1952), Middle Eocene Nummulites (NUTTAL and BRIGHTON, 1931), ostracods, gastropods and vertebrates. The upper portion of the sequence contains only few fossils, such as fresh-water fishes (Cichlids) (VAN COUVERING, 1982), ostracods and silicified trees of probable Oligocene age (MACFADYEN, 1933).

The Daban Basin is a half-graben elongated in an east-west direction and is from 20 to 40 km wide. The original size of the basin was wider than the present one, since the marginal portions of the basin are covered by Quaternary sediments (HUNT, 1960; BRUNI et al., 1987).

A broad syncline is recognized in the Daban deposits; the northern limb has a gentle southerly dip and rests conformably on the Middle Eocene Taleh Evaporites, while the beds of the southern margin have steeper dip and are truncated by the Dagah Shabele major border fault which places them against the Mesozoic and the crystalline basement, or are covered by Plio-Quaternary terraced deposits (Fig. 2).

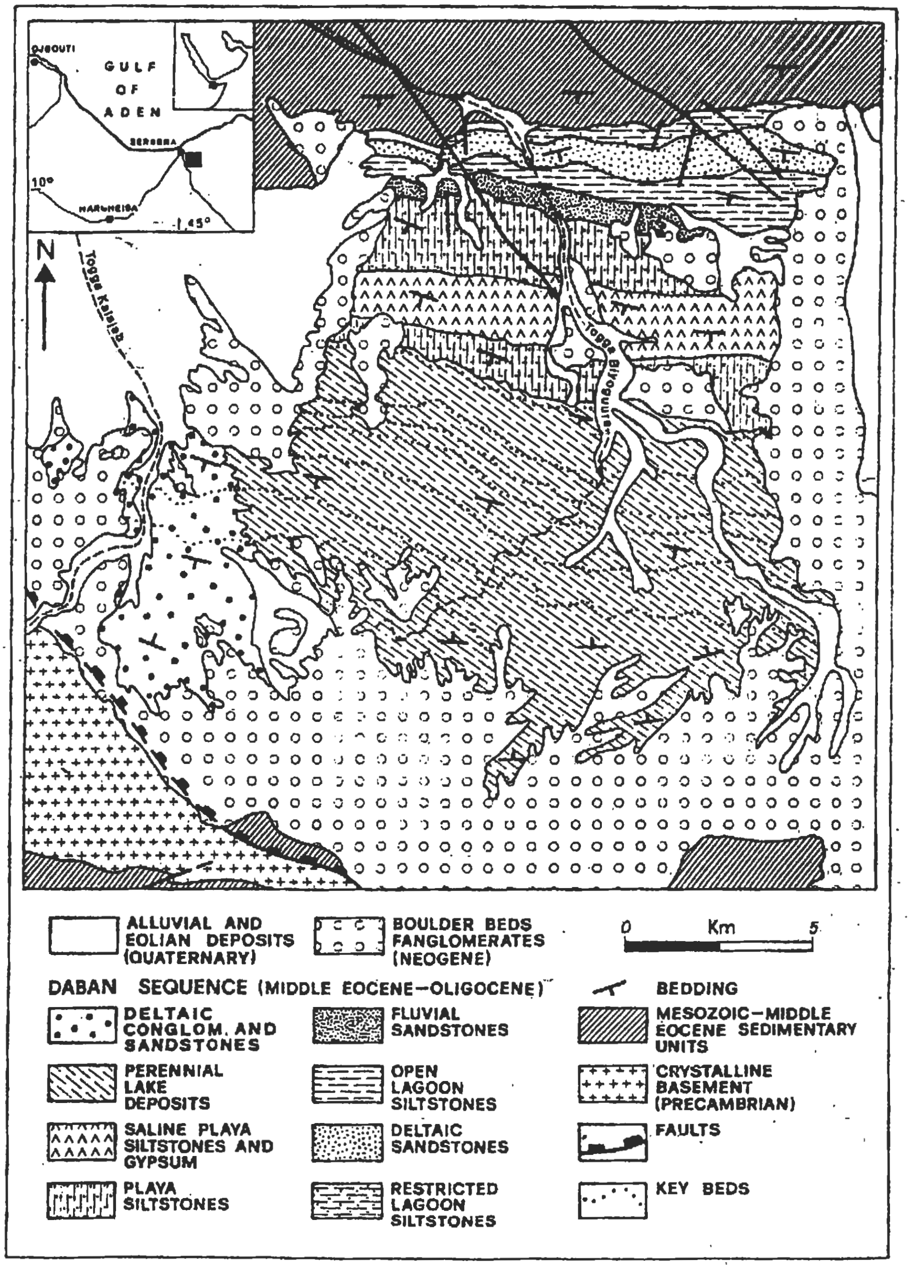


Fig. 2 - Simplified geology of the Daban Basin (after the 1:100,000 geological map of BRUNI et al., 1987).

The Daban sequence is unconformably cut by alluvial fanglomerates (Boulder Beds) of Pliocene age (MACFADYEN, 1933) whose deposition is related to the uplift of the Somali plateau.

## SEDIMENTARY SEQUENCE AND FACIES

The sedimentary succession of the Daban Basin can be subdivided into seven units (Fig. 4). From the base of the sequence upward the following environments can be distinguished: restricted lagoon, delta, open lagoon, alluvial plain, ephemeral lake and perennial lake. The latter shows westward a lateral transition in to a coarse-grained lacustrine delta sequence (Fig. 2, 3).

**Restricted lagoon** - The lower unit of the Daban sequence, 45 m thick, is characterized by fine grained clastic sediments (Fig. 5, log A) deposited in shallow-water marine environment. They consist of:

1 - grey to green structureless silty claystones intensely bioturbated, containing thin layers (5 cm thick) of fine sand and highly burrowed silt;

2 - yellow limestones, in beds up to 200 cm thick (Fig. 6) containing marine gastropods and pelecypods, are locally interbedded in the claystone. They are bioclastic mudstones and wackestones with few disseminated quartz grains and glauconite laid down in low energy environment in absence of terrigenous inflow;

3 - nodular to wavy laminated gypsum beds (20-200 cm thick) containing siliceous nodules occur at the base of the sequence. They correspond to periods in which the restricted lagoon experienced conditions of high salinity. During the deposition of the restricted lagoon sediments, the environment gradually shifted from true evaporitic (Taleh Evaporites) to brackish lagoon with the inflow of fresh water loden with very fine terrigenous sediments. The lagoon experienced abnormal and fluctuating water salinities. The upward salinity decrease allowed favorable life conditions for gastropods and pelecypods.

**Delta** - The restricted lagoon sediments grade upward into 320 m thick deltaic deposits (Figs. 4, 5, log A). They consist of upward-thickening and coarsening mouth-bar sequences, 10-50 m thick (Fig. 5, logs A, B, C; Fig. 7), composed of three main facies, from bottom to top:

1 - massive and intensely bioturbated, grey to green siltstones, rich in plant debris and, locally, wavy and cross laminated. They are interpreted as deposition from suspension or low energy currents in mouth-bar front;

2 - medium to fine sandstones with plane and trough cross laminations, wave and climbing ripples, in beds up to 50 cm thick. They were deposited during river flood on the mouth-bar crest;

3 - channelized, trough and cross bedded, coarse red sandstones and pebbly sandstones, in layers up to 5 m thick with load casts and escape structures.

Paleosols and rooted horizons are locally present. These sediments are interpreted to represent distributary channel fills experiencing frequent emersions.
Thin lignite levels and detritic limestones with gastropods and pelecypods are frequently interbedded with the siltstone facies expecially in the basal portion of the deltaic sequence.
Paleocurrent data indicate north-western clastic supply (Fig. 4).
The features of the deposits suggest an highly constructive fluvial dominated delta system (COLEMAN and WRIGHT, 1975; GALLOWAY, 1975; ELLIOTT, 1986; COLEMAN, 1981) prograding in shallow marine water.

**Open lagoon** - The transition between deltaic and open lagoon sediments is marked by a coquina bed, containing abundant ostreids (Fig. 8), immediately overlain by herringbone cross bedded sandstones (Fig. 5, log C). Up in the lagoon sequence, the sediments contain abundant remains of pelecypods, gastropods, nautiloids (Fig. 9) (HAAS and MILLER, 1952), Middle Eocene Nummulites (NUTTHAL and BRIGHTON, 1931), vertebrates and silicified tree trunks (MACFADYEN, 1933).

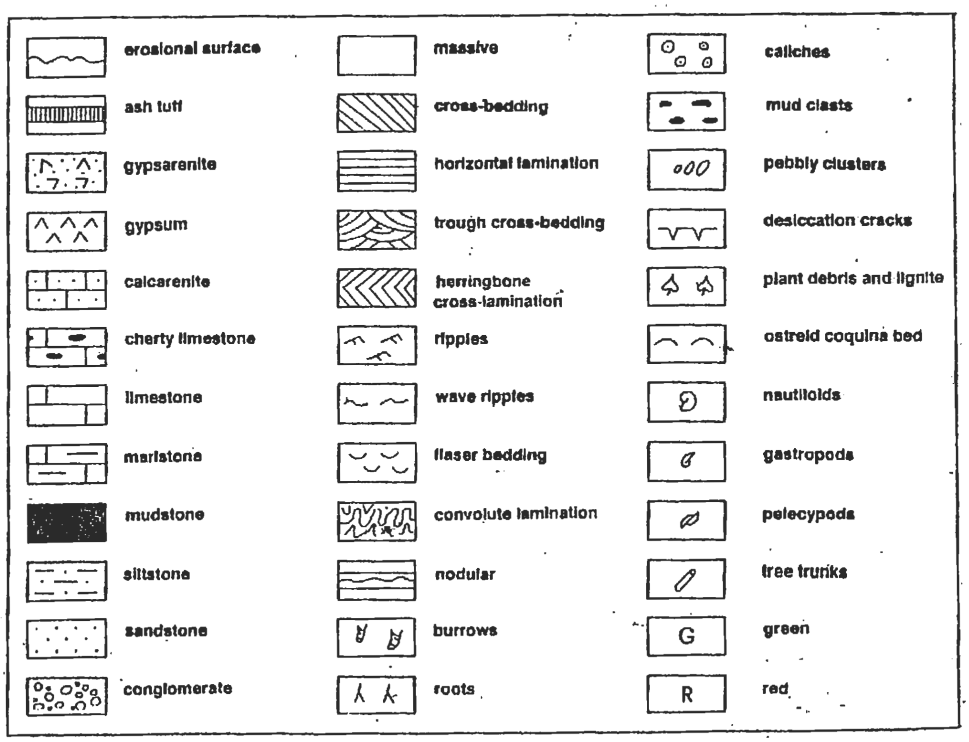


Fig. 3 - Legend for the sedimentological logs.

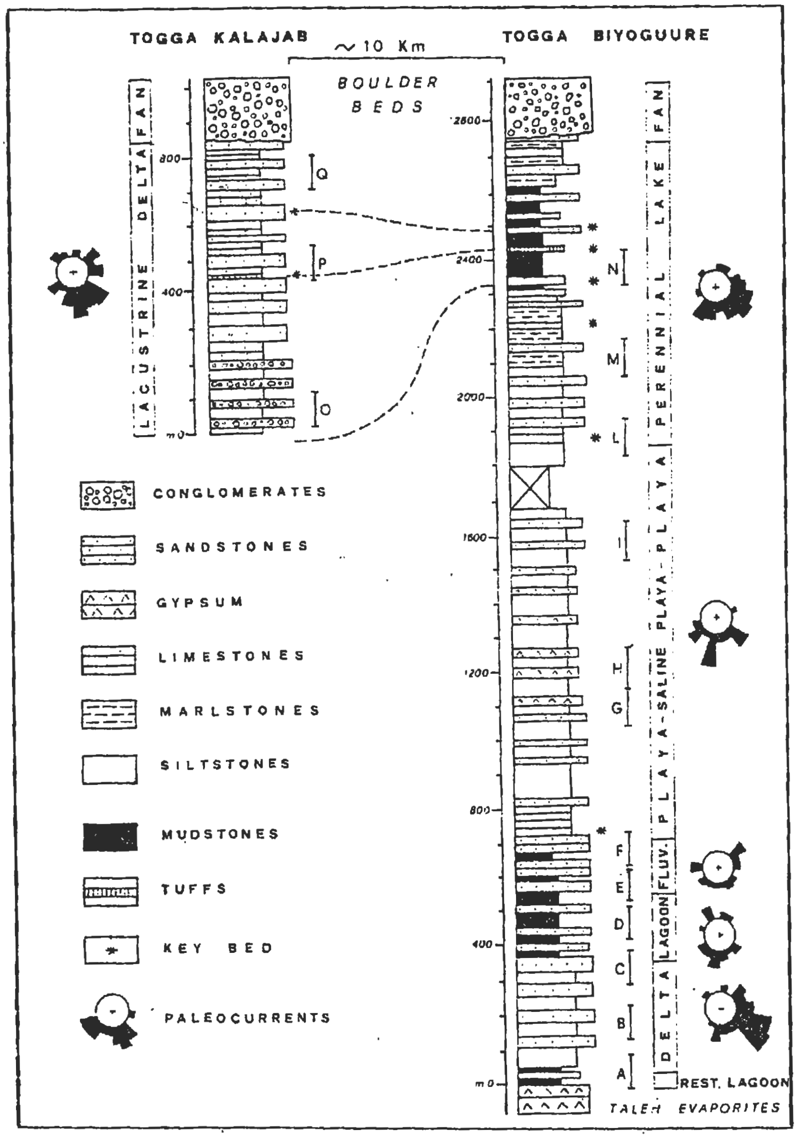


Fig. 4 - Lithological sequences and environmental interpretation of the Daban Basin fill in the Kalajab and Biyoguure sections. Paleocurrent data are summarized in rose diagrams. Capital letters on the right side of the sections indicate the stratigraphic position of the sedimentological logs reported in this paper (Figs. 5, 10, 13, 16 and 21). Dashed lines indicate key beds correlations.

Open lagoon deposits, 185 m thick, include medium to fine grained clastic sediments (Fig. 5, log C; Fig. 10, logs D, E) laid down in brackish, shallow water composed of:

1 - grey to green, massive silty clays, with plant debris, pelecypods, gastropods and fish remains. In some place they show colour bands and manganese nodules;
2 - fine grained sandstones in beds up to 50 cm thick, slightly bioturbated, wavy and planar laminated and flaser bedded, locally rich in plant debris;
3 - rare beds up to 400 cm of intensely burrowed, medium to fine grained calcareous sandstones containing chaotic accumulations of fossil shells (mainly ostreids). They locally alternate with the silty clays. They derive from wave reworking of shell and clastic materials in a shallow-water environment successively homogenized by bioturbation;
4 - lenticular beds of medium to coarse sandstones. They are well sorted, cross-laminated and bidirectionally (herringbone) cross-laminated, with wave ripples, containing fragments of shells, clay chips and silicified trunk remains. The sandstone beds, 50-500 cm thick, rest on erosional surfaces marked by a lag of shell fragments and clay chips and can be interpreted as tidal channel deposits.
   Bimodality of paleocurrent data indicate current from north and south (Fig. 3). Lithology, structures, fossils and paleocurrent pattern indicate a brackish lagoon environment (DICKINSON et al., 1972; PLINT, 1983; ELLIOT, 1986), sometimes subjected to subaerial conditions.

**Alluvial plain** - The alluvial sediments, 175 m thick, are represented by typical red beds of coarse and fine clastic material deposited in fluvial channels and in floodplain (Fig. 10, logs E, F). They consist of:

1 - red, coarse to pebbly quartzose sandstones with subordinate amounts of fine sandstones and conglomerates. Strata are 50 to 500 cm thick and are lenticular. Trough and tabular cross bedding are the principal sedimentary structures. Silicified tree trunks, red clay clasts and rooted horizons occur frequently in the sandstones. Beds form erosive based lenticular sequences 5-20 m thick, stacked one over the other (Fig. 11) or separated by fine sediments. The sedimentary structures, lithology and geometry of the beds are typical of braided channel deposits (FRIEND, 1983; MIALL, 1977);
2 - red, massive silty clays intensely bioturbated and pedogenized. They show mottling (red, orange, purple and grey), mud craks and contain abundant manganese spherules and caliche nodules. Rooted horizons and silicified wood remains are common. These sediments represent overbank material deposited in the flood plain;
3 - grey and black, carbonaceous siltstones, rich in plant debris. Lignite levels and manganese spherules are common. They occur mainly in the upper portion of the alluvial sequence (Fig. 10, log F) and were deposited in swamps and shallow-water lakes;

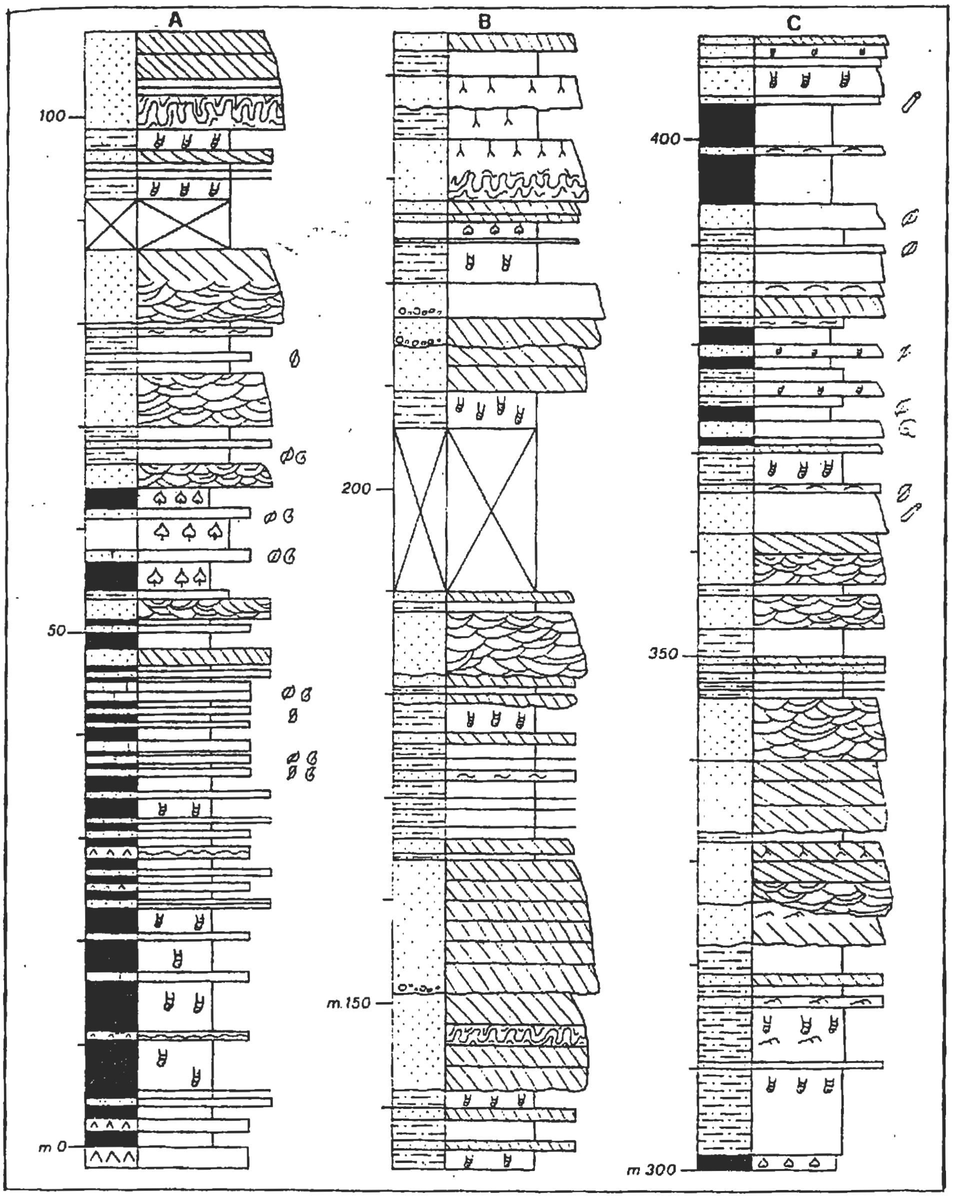


Fig. 5 - Sedimentological logs in the Biyoguure succession. A = restricted lagoon and basal deltaic sediments. B = deltaic deposits. C = transition between deltaic and open lagoon deposits. Logs position in the Biyoguure section in Fig. 4; legend in Fig. 3.

4 - two lenticular bodies, 5-10 m thick, of pale to yellow, very well sorted medium grained, quartzose sandstones are interbedded in fluvial deposits. They are cross-bedded in 1-2 m thick, mainly trough-shaped sets (Fig. 12). Ripples occur superimposed on foreset surfaces. These sandstones represent eolian deposits (GLENNIE, 1970; WALKER and HARMS, 1972; BROOKFIELD, 1977; CLEMMENSEN and ABRHAMSEN, 1983) deriving from wind reworking of fluvial sands during periods of major aridity. Scattered paleocurrent data indicate main flow toward SW and SE at the base of the alluvial sequence and toward NE in the upper portion (Fig. 4).

**Ephemeral lake** - The ephemeral lacustrine succession, 1.145 m thick, rests conformably on fluviatile deposits. It consists of clastic playa mudflat sediments with an intercalation (Fig. 4) of an evaporitic and clastic sequence deposited in a saline playa or inland sabkha (SAGRI et al., 1989). The inception of lacustrine deposition is marked by the appearence of a 3 m thick key bed (Figs. 4, 5, log F) consisting of micritic chalklike silicified limestone containing ostracods, algae remains and ooids. The main facies recognized in the playa mudflat are (Fig. 13, logs G, I):

1 - red and green massive siltstones and mudstones, intensely bioturbated with abundant gypsum and manganese concretions and desiccation cracks. These sediments are interpreted as having been deposited in a mud flat periodically subjected to drying (EUGSTER and HARDIE, 1978; HUBERT and HYDE, 1982);
2 - red and brown, tabular sandstone bodies, cross-stratified pebbly sandstones and imbricated channelized fine grained conglomerates, with clay clasts, in beds 1-5 m thick, occur at the top of the playa mudflat sequence (Fig. 13, log I). They are deposited by unconfined sheet flows and channelized flows which crossed the playa mudflat (HUBERT and HYDE, 1982) during intense flood events;
3 - thin levels of green mudstones, siltstones, marls and lignitic shales deposited in water ponds are present at the top of the sequence.

The saline playa sediments, intercalated within the playa mudflat deposits, consist of three principal facies arranged in cycles of about 5-15 m thick (Figs. 13, logs G, H; 14) reflecting lacustrine expansion and contraction (SAGRI et al., 1989). From bottom to top they are:

1 - red massive siltstones intensely bioturbated, containing gypsum veins and carbonate caliche horizons. They were deposited in a dry mudflat;
2 - green massive, mottled and bioturbated siltstones, deposited in a shallow water lake that experienced reducing conditions as suggested by the green coloration (COLE and PICARD, 1981);
3 - gypsum / shale layers, up to 2 m thick, that consist of alternating gypsum laminae (0.5-2 cm thick) and green shales (Fig. 15) with algal remains.

The cyclically arranged facies in the saline playa sequence reflect longterm climatic fluctuations that changed the hydrological status of the lake (SLAY, 1978; EUGSTER and HARDIE, 1978). Red silstones represent periods of prolonged

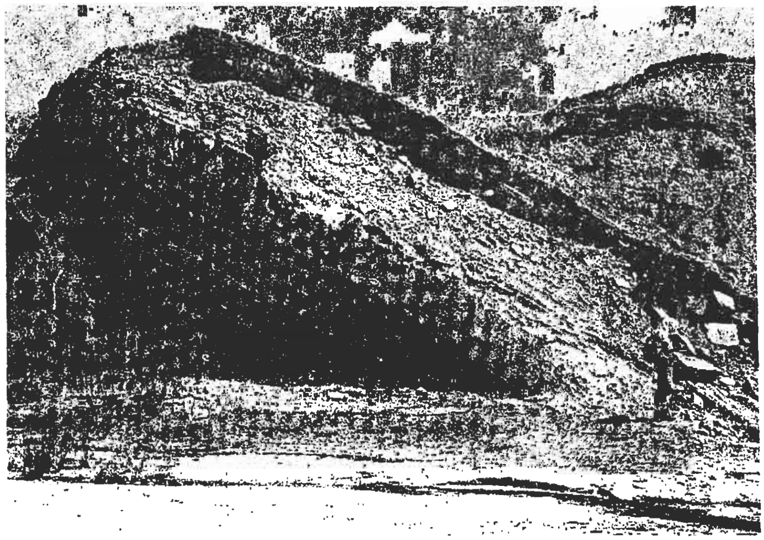

Fig. 6 - White calcareous bed with marine gastropods and pelecypods interbedded in the restricted lagoon grey claystones at the base of the Biyoguure section.

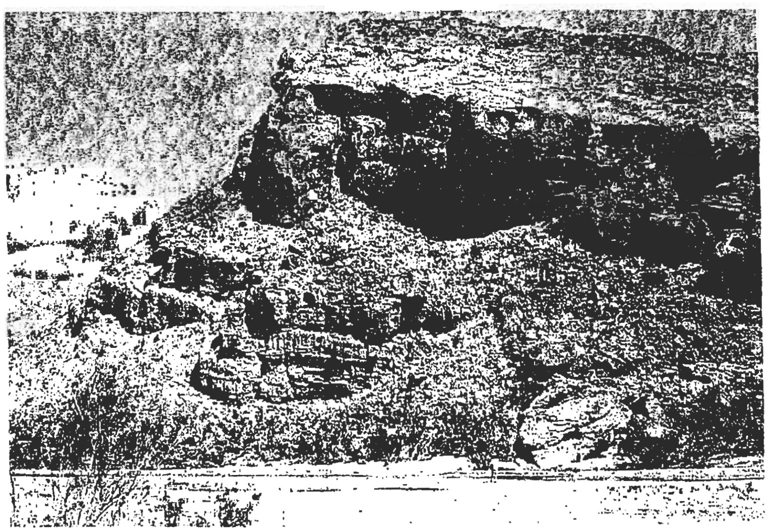

Fig. 7 - Thick mouth-bar sequence in the upper portion of the deltaic succession, Biyoguure section.

regional aridity with the permanent emergence of the lake bottom. As the climate became more humid, increased stream discharge led to the inundation of the mudflat and green siltstone accumulated. With the approach of a new dry period intense evaporation caused the deposition of gypsum/green shales beds in a chemically stratified lake (SMITH, 1965; BOYER, 1982). Gypsum dominated evaporites in the saline playa cycles were due to the predominance of gypsum (Taleh Evaporites) in the contemporary catchment.
The clastic supply in the ephemeral lake deposits are from NE and NW (Fig. 4).

**Perennial lake** - Perennial lake deposits, 870 m thick, occur in the upper portion of the Daban sequence (Fig. 4) and consist of terrigenous sediments with subordinate amounts of limestones and marls (SAGRI et al., 1989) belonging to a siliciclastic type of lake (ALLEN and COLLINSON, 1986).
Central and marginal lake facies can be distinguished (SAGRI et al., 1989). Marginal facies outcrop only in the western side of the basin and are represented by the deposits of a coarse grained delta. Central lake facies (Fig. 16) consist of:

1 - green massive siltstones and mudstones with rare dark lignitic shales laid down in shallow water. This facies is volumetrically the most significant;
2 - paper-thin interlamination of green marls and siltstones characterized by a paucity of burrowing. These varve-like sediments probably were deposited under reducing conditions in a stratified water body protected from bioturbation, bottom currents and influx of coarse detritus;
3 - laminated to poorly laminated chalky limestones in units up to 10 m thick (Fig. 17), containing well preserved fresh water fishes (Fig. 18) (cichlids, VAN COUVERING, 1982), ostracods and brown chert nodules. The limestone layers are traceable across the entire basin and are good stratigraphic markers (Figs. 2, 4, 17). Laminated carbonate beds are due to chemical inorganic precipitates and to subordinate phytoplancton blooms. They formed in fresh-water stratified lakes (BRADLEY, 1973) in response to seasonal or cyclic variations in chemical and biological conditions (KELTS and HSU, 1978; DEAN, 1981);
4 - horizontal or cross-laminated fine to coarse green-grey sandstones in bed up to 2-4 m thick (Fig. 16, log M) containing clay clasts, and current-rippled or wave-rippled fine grained sandstones. These occur as isolated beds or in thickening and coarsening upward sequences and represent the distal portion of the delta episodically prograding into perennial lake;
5 - rare graded sandstones, in bed up to 1 m thick, with well developed Bouma subdivisions. They represent deposits from turbidity currents probably triggered by sporadic river storm floods or by seismic events;
6 - basin-wide, whitish, porous tuffs, up to 7 m thick, locally interbedded in the perennial lacustrine deposits (Fig. 16, logs L, M);
7 - massive red siltstones and mudstones with silicified wood occur in the upper portions of the lacustrine sequence. They indicate periods of intense oxigenation of the bottom waters and fall of the lake level with the emergence of the bottom.

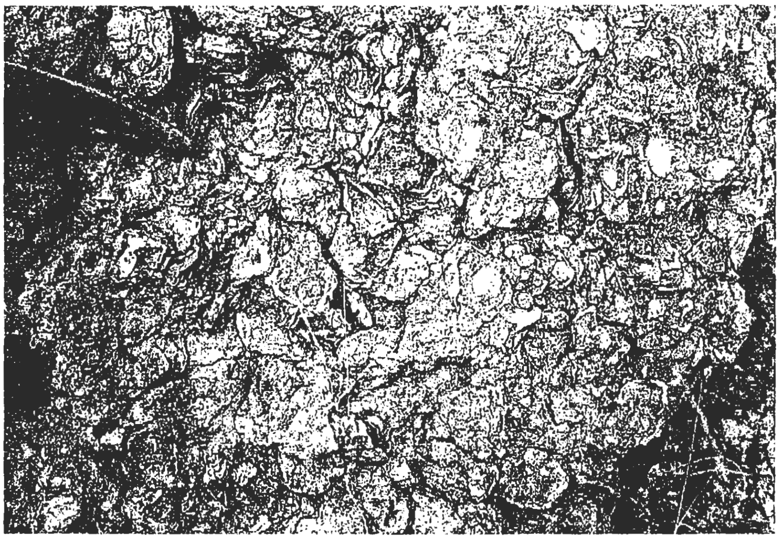

Fig. 8 - Ostreid coquina bed that marks the transition between delta and open lagoon deposits, Biyoguure section.

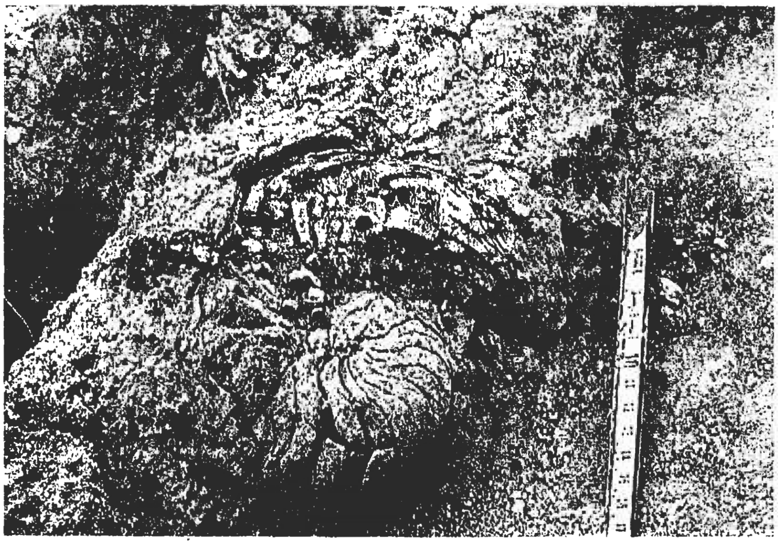

Fig. 9 - Nautiloid from the basal portion of the open lagoon deposits, Biyoguure section.

Fine-grained clastic sediments and carbonate deposits occur mainly in the upper portion of the perennial lacustrine sequence (Fig. 16, log N), whereas sandstones intercalations prevail in the lower portion (Fig. 16, logs L, M).

The perennial lake of the Daban sequence was probably a shallow-water basin. As suggested by the paucity of burrowing and diffuse parallel lamination of some facies (cfr ANADON et al., 1988) it experienced periods where the water mass was well mixed and periods of thermal stratification (SAGRI et al., 1989). The latter condition was favoured by the tropical setting of the Daban basin (ALLEN and COLLINSON, 1986).

Paleocurrent data indicate N and NW inflow (Fig. 4).

**Coarse-grained lacustrine delta** - The upper portion of the perennial lacustrine sediments shows a lateral transition to a thick and coarse grained delta sequence (Figs. 2, 4), which represents marginal deposits of the western lacustrine shore. The lowermost part of the delta system is covered by Boulder Beds fanglomerates and Quaternary deposits (Fig. 2). The middle and upper portions are particularly well exposed.

Thick beds of chalky limestones and tuffs can be traced along the Daban basin (BRUNI et al., 1987) and permit good correlations between the lacustrine and fan delta sequences (Figs. 2, 4). The lacustrine delta system can be divided in to two parts: a coarse-grained mouth-bar delta (Fig. 19) at the base overlain by thick sandstone units (Fig. 20) of a terminal fan.

The coarse-grained mouth-bar delta, 250 m thick, consists of upward thickening and coarsening sequences, ranging from 5 to 10 m thick (Fig. 19). Each sequence is composed of three main facies, which are, from bottom to top (Fig. 21, log O):

1 - wave rippled, cross or horizontally laminated green siltstones and marlstones, which are locally intensely bioturbated, deposited in the mouth-bar front. Nodular, massive chalky fresh water limestones are locally interbedded with these fine grained sediments;

2 - coarse to pebbly sandstones beds, varying in thickness from 50 to 100 cm. Trough and planar cross-stratification dominates in this facies, although horizontal lamination also occur. Wave ripples are locally present at the top of the beds. This facies is interpreted as mouth-bar deposits;

3 - coarse-grained, clast-supported conglomerates in beds 1-5 m thick. Clast are well rounded, imbricated and their maximum size reach 50 cm. They are poorly to moderatly sorted with sand matrix. The conglomeratic beds show lenticular shape and generally erosional bases. They are massive, normal and reverse graded, and trough-cross stratified. The foresets meet tangentially the basal erosional surface. Clasts derive from the Mesozoic to Eocene limestones and from the basement. The conglomerate beds are deposited in distributary channels at the top of mouth-bar sequences.

Downcurrent, toward the center of the lake, the mouth-bar succession grades into typical distal mouth-bar sequences.

The upper 600 m of the delta system is characterized by thick stacked sandstone

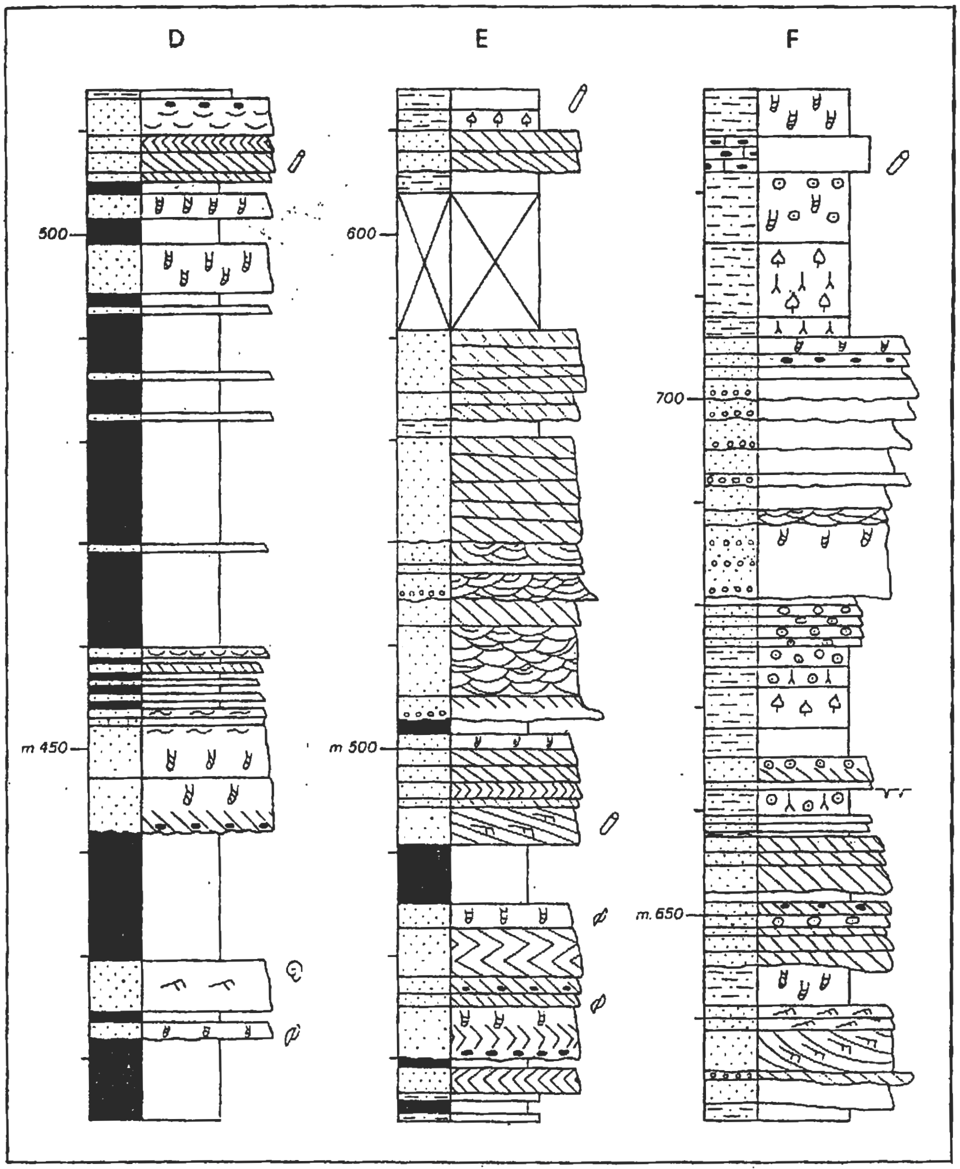


Fig. 10 - Sedimentological logs in the Biyoguure section. D = lagoon deposits. E = lagoon-alluvial plain transition. F = upper portion of alluvial plain deposits topped by a chalky limestone which marks the transition to the ephemeral lacustrine sediments. Logs position in the Biyoguure section in Fig. 4; legend in Fig. 3.

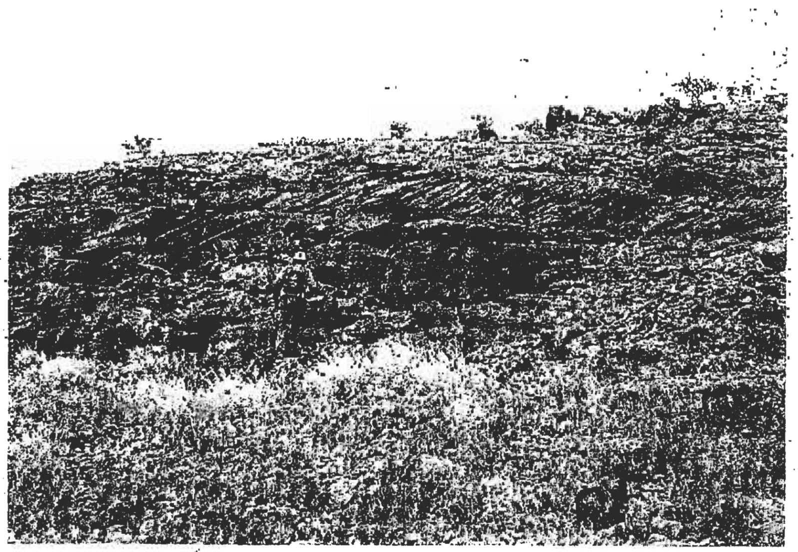

Fig. 11 - Tabular cross-bedded, red sandstone layers, stacked one upon the other, and deposited in braid bars, Biyoguure section.

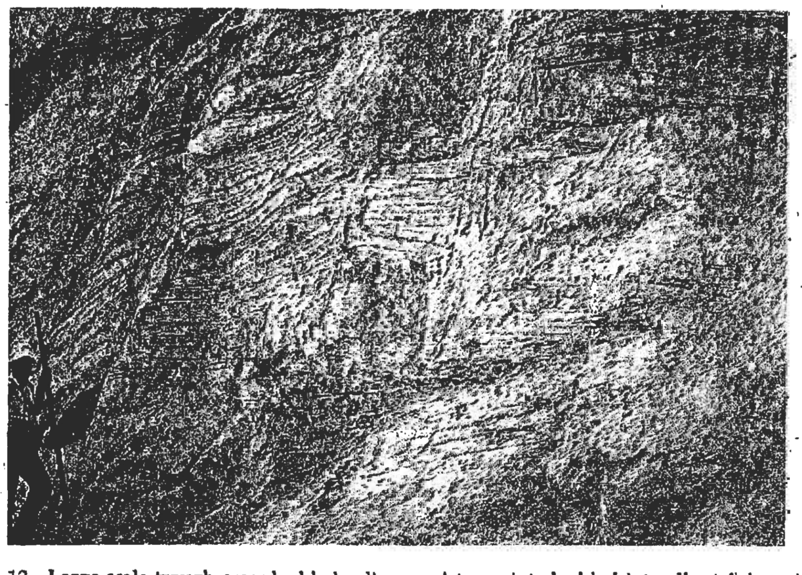

Fig. 12 - Large-scale trough cross-bedded eolian sandstones interbedded into alluvial deposits, Biyoguure section.

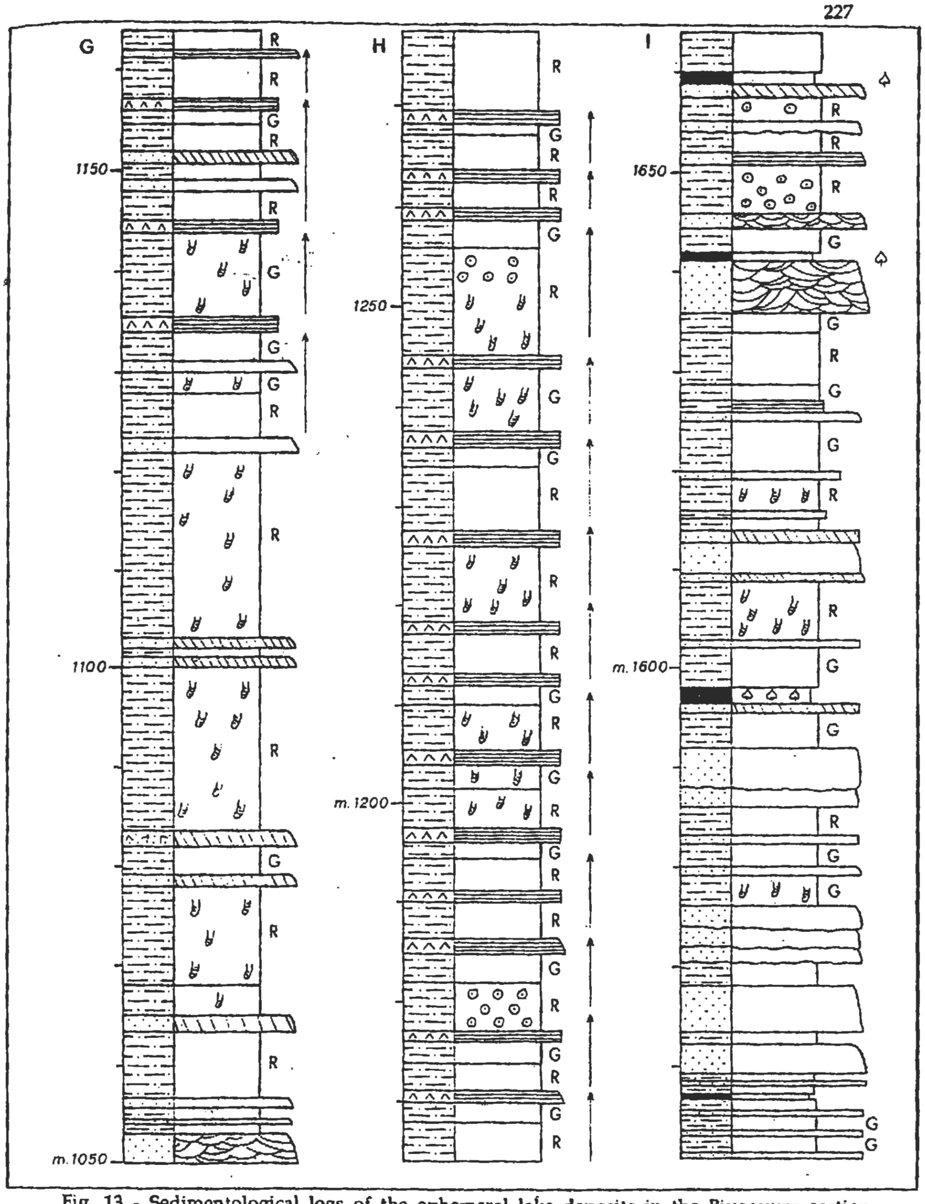


Fig. 13 - Sedimentological logs of the ephemeral lake deposits in the Biyoguure section. G = transition between playa mudflat and saline playa sediments. H = saline playa sediments. I = playa mudflat deposits. Arrows indicate cycles in the saline playa deposits. Logs position in the Biyoguure section in Fig. 4, legend in Fig. 3.

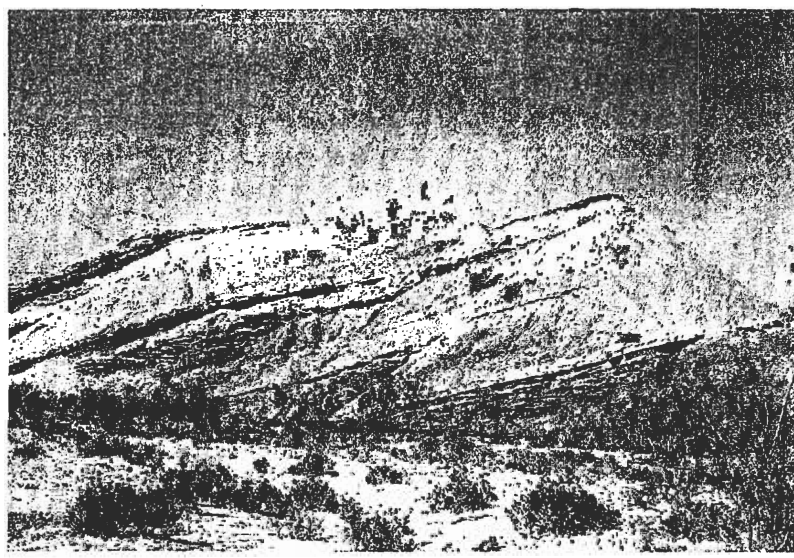

Fig. 14 - Cycles in the salina playa deposits composed of red and green siltstones, and gypsum beds (detail in Fig. 15), Biyoguure section.

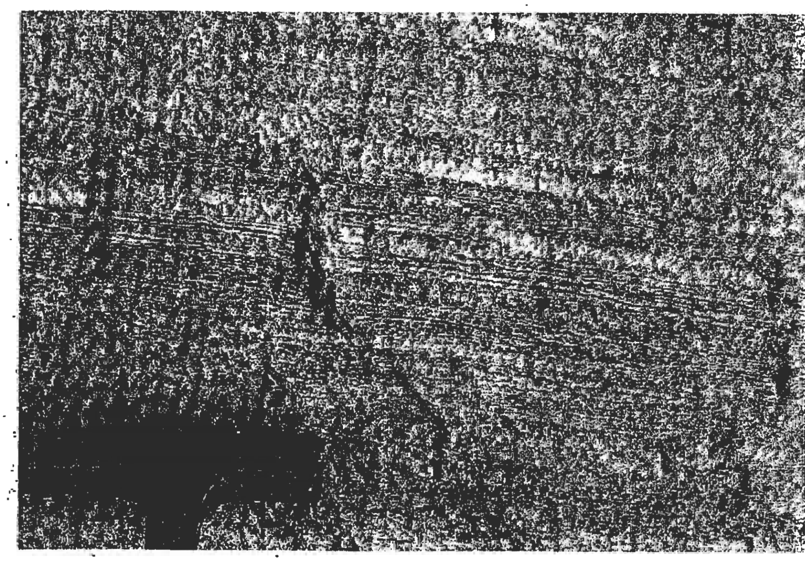

Fig. 15 - Alternating centimetric gypsum laminae and shales in the gypsiferous layers of the salina playa deposits (see Fig. 14), Biyoguure section.

units (Fig. 20), deposited in a terminal fan at the margin of the perennial lake, interbedded with siltstones and fresh-water limestones (Fig. 21, logs P, Q):

1 - the sandstone facies consist of very thick units ( up to 30 m), of brown, medium to coarse sandstones, laterally continuous and unchannelized with basal surfaces slightly erosive or nearly planar. Imbricated conglomerates are locally present in pockets at the base of the erosive beds. Angular intraformational clasts, composed of nodular cherty limestones and green siltstones are common. Horizontal plane-lamination is the dominant sedimentary structure (Fig. 20). Plane-laminated units are sometimes capped by cross-laminated fine sandstones. Dish and fluid escape structures and soft sediment convolutions have been found. The top of the beds show intense red pedogenic alterations and rooted horizons.
   The diffuse horizontal lamination suggests deposition through repeated sheet floods widely spreading in a terminal-fan type system (MUKERJI, 1976; FRIEND, 1983; TUNBRIDGE, 1984).
   The horizontally laminated sandstone bodies pass, toward the central lake, into single beds of parallel laminated fine sandstones or into turbidite beds;

2 - beds, 1-3 m thick, of green siltstones are interbedded within the thick sandstone units. They are massive and intensely bioturbated and were deposited into interlobe ponds or during periods of scarce clastic supply;

3 - fresh-water nodular limestones locally associated with siltstones levels. They are massive and contain brown chert lenses, ostracods, fresh-water fishes, algal remains, silicified tree trunks. Locally mud-craks and roots of aquatic plants have been found. These calcareous sediments represent lake margin deposits in areas sheltered from influx of terrigenous detritus.
   Whitish, porous ash tuff layers, up to 7 m thick are interbedded in the deltaic sediments. The source of this volcanic material can be recognized in the acidic effusions of the Late Oligocene-Early Miocene age in the Ali Sabieh area (southern Afar, ref. in MERLA et al., 1979).
   Clastic inflows from N, NW and SW are recognized in the lacustrine delta sequence (Fig. 3). The repetitive alternations of thick sandstone bodies within finer sediments and the stacking of conglomeratic mouth-bar sequences may indicate a rapid subsidence of the basin during the deposition of the coarse-grained delta sequence.

**Boulder Beds** - The Daban sequence is unconformably overlain by alluvial fanglomerates (Boulder Beds, Fig. 2; 4) of Pliocene age (MACFADYEN, 1933). They are poorly stratified, massive, clast-supported conglomerates with rounded boulders in a reddish sandy matrix with some interbeds of coarse massive sandstones. The clasts derive from the crystalline basement and its sedimentary cover (Mesozoic to Middle Eocene units).

They are terraced and are deposited during three distinct sedimentary cycles (BRUNI et al., 1987). The deposits of the first cycle are slightly tilted.

The Boulder Beds are connected with the main phases of the uplifting of the Somali plateau.

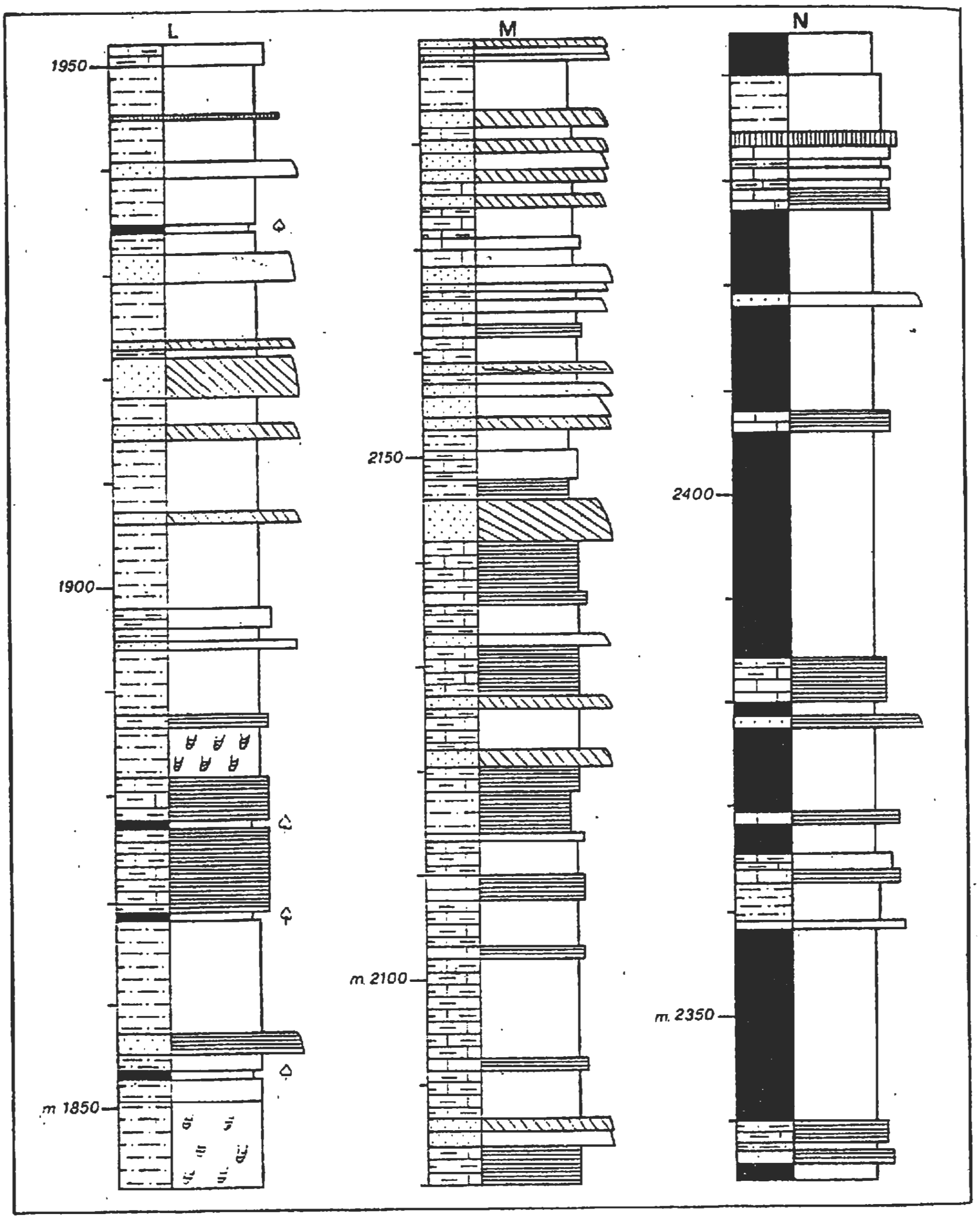


Fig. 16 - Sedimentological logs in the lacustrine deposits of the Biyoguure succession.
L = playa mudflat-perennial lake transition marked by horizontally laminated thick limestone key bed (see Fig. 17). M = perennial lake deposits consisting of marlstones, limestones, sandstones and siltstones. N = upper portion of the perennial lake sediments composed mainly of mudstones. Logs position in the Biyoguure section in Fig. 4, legend in Fig. 3.

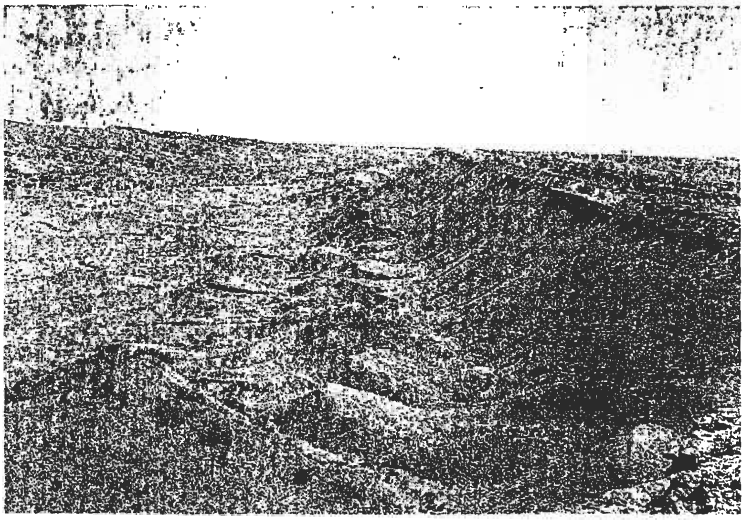

Fig. 17 - Red and green siltstones in the upper portion of the playa mud-flat deposits. The transition to perennial lake units is marked by a whitish, thick, fresh-water limestone key bed outcropping at the top of the cliff, Biyoguure section.

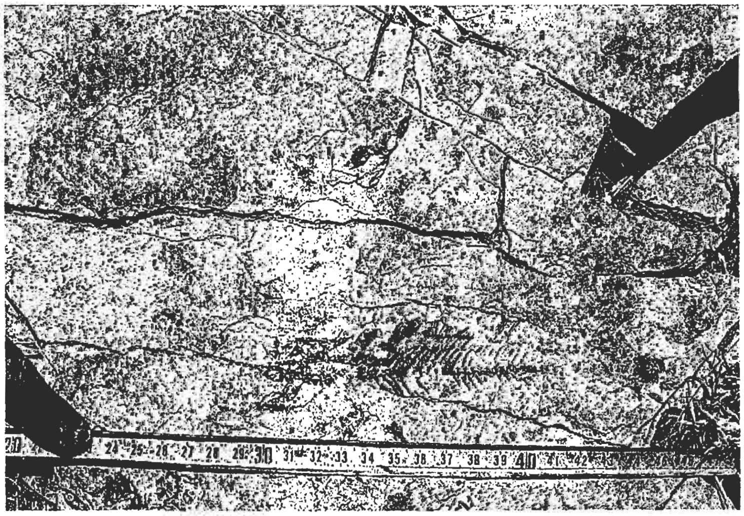

Fig. 18 - Fresh-water fish (cichlid) in a finely laminated limestone bed of the perennial lake deposits, Biyoguure section.

## THE DABAN BASIN EVOLUTION AND THE GULF OF ADEN RIFTING

The relationships between the rifting of the Gulf of Aden and the evolution of the Daban basin can be summarized as follows (Fig. 22).

During Middle Eocene, after the deposition of the Taleh Evaporites, the sea retreated eastward (AZZAROLI and FOIS, 1964) some ten of kilometres from the Daban area, and the coastal line run NE-SW at the eastern margin of the Somali-Arabian continental block. This straight coastal line was interrupted by an embayment (ABBATE et al., 1983) where the sea penetrated into the Somali-Arabian continent, at least up to the Daban area. This embayment probably developed in corrispondence of an east-west trending belt of crustal weakness (lineaments centrafricains, CORNACCHIA and DARS, 1983) along which successively the Gulf of Aden was formed (see later).

Shelf limestones (Karkar Limestones and Habishiya Formation in Northern Somalia and Southern Yemen, respectively) were deposited during Middle and Late Eocene on the margin of the Somali-Arabian continental area, whereas in the embayment, deltaic and lagoon deposits were laid down.

The restricted lagoon was frequently subjected to super saline conditions during which evaporitic episode occured with the deposition of gypsum layers. These conditions were due to the low input of fresh-water in the lagoon as suggested by the occurrence of very fine terrigenous sediments.

Successively, a stream, flowing from north-west, interested the Daban area. Abundant waters, laden of coarse terrigenous materials, built up a river-dominated delta and deposited 320 m of stacked mouth-bar sequences. Owing to a reduced water inflow or a shifting of the deltaic mouth, an open lagoon developed in the Daban area and brackish waters favoured the life of ostreids, gastropods and nautiloids.

At the beginning of the Oligocene the sea retreated further east (AZZAROLI and FOIS, 1964); the Daban area lost its connection with the Indian Ocean and continental sediments were deposited in the basin (Fig. 22 B).

At the same time the breakup of the Somali-Arabian continental block began to develop. The Arabian plate moved toward northeast and along the west-east line of crustal weakness (lineaments centroafricains, CORNACCHIA and DARS, 1983) an oblique rifting developed (YAIRI, 1975; WITHJACK and JAMINSON, 1986; ABBATE et al., 1988). This crustal movement induced tensional stresses in the Daban area and a subsiding basin in shape of a WNW trending halfgraben was formed (Fig. 22 B) and occupied by ephemeral and perennial lakes.

During the first phase of lacustrine deposition (ephemeral lakes) the Daban basin experienced arid continental conditions (SAGRI et al., 1989) and the lake was permanently dry (playa mud flat) or was subjected to fluctuations in water level, evaporation and periodic dessiccations (saline playa). The ephemeral lakes were fed by channelized flows and sheet flows carrying coarse and fine clastic material from north and north-west.

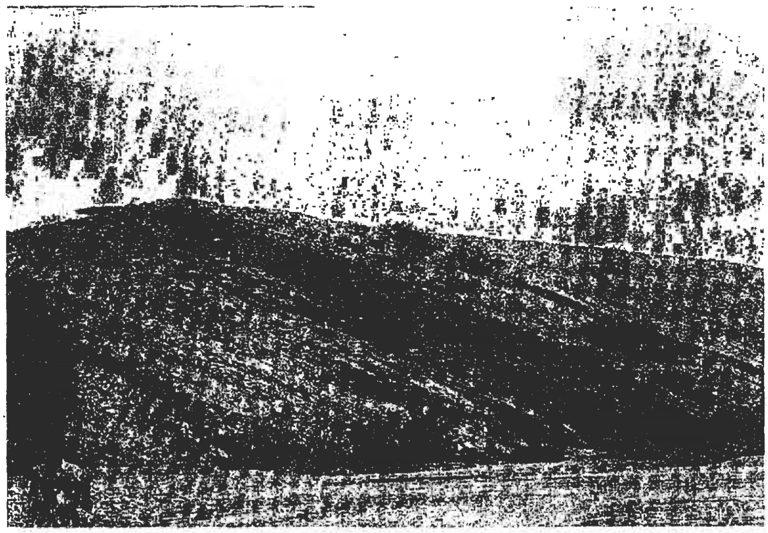

Fig. 19 - Coarse-grained mouth-bar sequence of the lacustrine delta consisting, from base to top, of green siltstones with interbedded nodular limestones, sandstones and channelized conglomerates, Kalajab section.

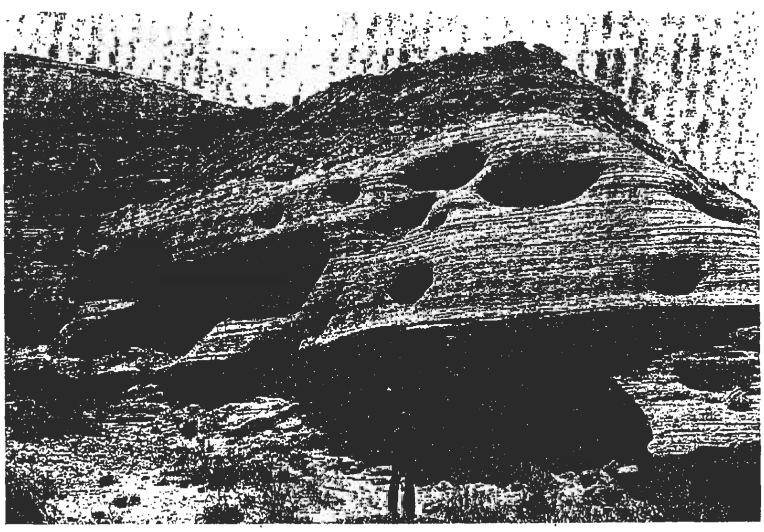

Fig. 20 - Horizontally laminated thick sandstone unit deposited in the terminal fan developed at the western margin of the perennial lake, Kalajab section.

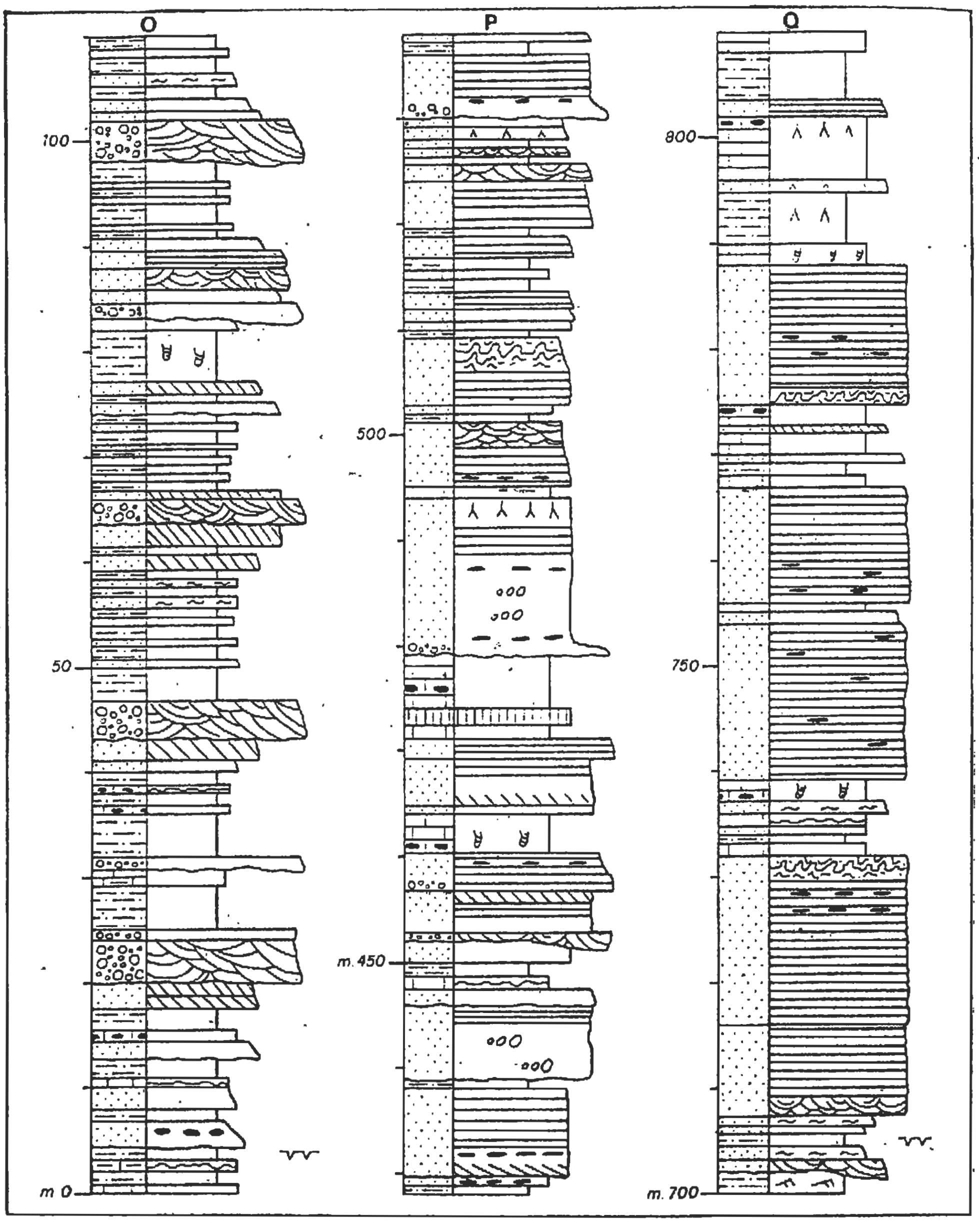


Fig. 21 - Sedimentological logs of the fan delta deposits in the Kalajab succession.
O = lower portions characterized by conglomeratic mouth-bars. P = middle portion of the sequence composed by conglomeratic bodies and horizontal laminated sandstone units. Q = upper portion of the sequence composed mainly by horizontally laminated sandstone units. Logs position in the Kalajab section in Fig. 4; legend in Fig. 3.

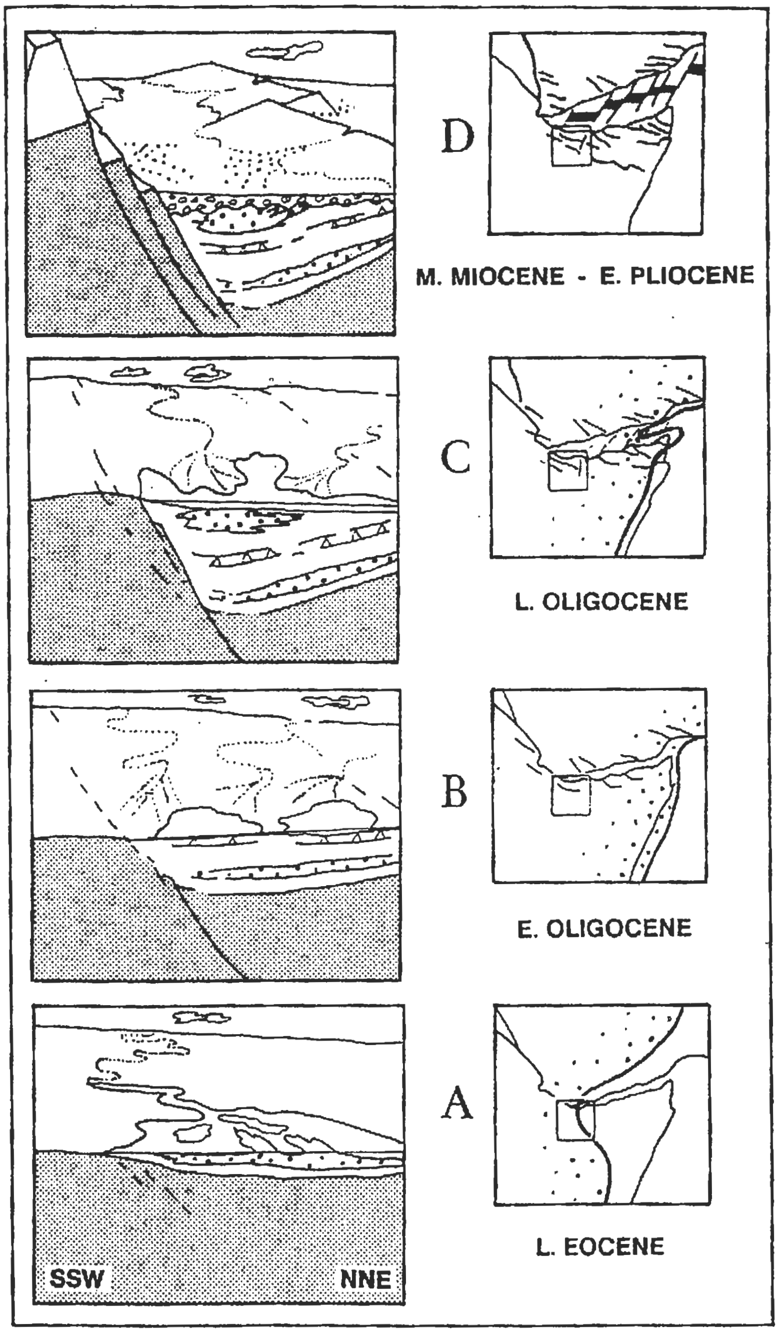


Fig. 22 - Successive steps in the evolution of the Daban Basin and of the Gulf of Aden since Late Eocene. From left to right: block diagrams depicting paleoenvironments and structures in the Daban Basin; structural sketch of the Gulf of Aden evolution; paleogeography of the Somali-Arabian continental blocks: heavy line = shore line, dotted area = land; for major details see text.

In the Late Oligocene the Gulf of Aden rifting continued to develop and an elongate narrow gulf was formed in the axial area of the proto-Gulf of Aden (Fig. 22 C). The sea approached the Daban area, giving rise to less severe arid climatic conditions. The concomitant uplift of the rim of the Somali plateau, bordering the proto-Gulf of Aden, induced the condensation of moist air-masses coming over this water body and from the Indian ocean. Consequently, fresh-water inputs to the Daban basin augmented and a perennial lake was formed (SAGRI et al., 1989). Huge clastic inflows coming from faulted blocks built up the coarse-grained delta which prograded from north-west in to the perennial lake. The thickness and the coarseness of the delta system and the clast lithology (crystalline basement and Mesozoic sedimentary cover) suggest a significant relief in the adjoining regions (Fig. 22 C).

At the end of the perennial lake deposition a period of aridity affected again the Daban area (probably connected with a regression in the proto-Gulf of Aden induced by the dramatic Chattian fall of the sea level, HAQ et al.,1987). Part of the lake bottom emerged as indicated by the occurrence of massive red siltstones and mudstones. The affluent streams of the lake became ephemeral and gave rise to a terminal fan system at the NW lake margin. At the end of Oligocene sedimentation ceased in the Daban area and the basin itself was involved in the uplift of the Somali escarpment. The Daban fill sediments were deformed into an asymmetric syncline and successively covered unconformably by very coarse fanglomerates (Boulder Beds) coming from the southward rising Somali plateau (Fig. 22 D).

## CONCLUSIONS

The Daban basin, filled with 2,700 m of Middle Eocene to Oligocene clastic deposits, was a fast subsiding basin (mean clastic accumulation 10.8-13.5 cm/1000 y) developed during the first stages of the evolution of the Gulf of Aden

During the Middle-Late Eocene regression, that affected the Somali-Arabian continental block, in the Daban area transitional environments developed and 550 m of lagoon and deltaic sediments were deposited. Successively, in Early Oligocene, the Daban area lost its connection with the Indian Ocean and 175 m of fluvial and 2.000 m of lacustrine deposits filled the basin. During this continental episode the Daban basin was a well developed half- graben trending WNW and fed mainly from N and NW by clasts deriving from the basement and its sedimentary cover outcropping along the rising Somali escarpment.

As reported for many rift basins (e.g. DUNNE and HEMPTON, 1984; COHEN et al., 1986; REID and FROSTICK, 1986; CAVAZZA, 1989), also in the Daban half graben the clasts derived mainly from the hanging-wall dip-slope facing the major boundary fault (Dagha Shabele fault) and from the axial streams.

At the end of the Oligocene the basin itself was deformed during the uplift of the Somali plateau and successively unconformably covered by Boulder Beds fanglomerates.

Their clasts were supplied by the southward raising escarpment.

The evolution of the Daban basin was strictly controlled by the tectonic, paleogeographic and paleoclimatic changes induced by the rifting of the Gulf of Aden and the uplift of the Somali plateau.

ACKNOWLEDGMENTS

Early version of this work benefitted from discussion and review by I.P. MARTINI. This research was made possible through the financial support of the Ministero Pubblica Istruzione, Consiglio Nazionale delle Ricerche and Ministero Affari Esteri. The authors would like to thank all the Somali Government Official who helped them in their field work. Special acknowledgments are due to the Somali National University.

REFERENCES

ABBATE E., BRUNI P., FAZZUOLI M. and SAGRI M. (1983). Le facies di transizione e continentali nel bacino terziario del Daban, Somalia settentrionale. Dati preliminari. Univ. Naz. Somala. Quaderni Geologia della Somalia, 7: 7-32.

ABBATE E., BRUNI, P., FAZZUOLI M. and SAGRI M. (1988). The Gulf of Aden continental margin of Northern Somalia: Tertiary sedimentation, rifting and drifting. Mem. Soc. Geol. Ital., 31: 427-445.

ABBATE E., FICCARELLI G., PIRINI RADDRIZZANI C., SALVIETTI A., TORRE D. and TURI A. (1974). Jurassic sequences from the Somali Coast of the Gulf of Aden. Riv. Ital. Paleont. Stratigr., 80: 409-478.

ALLEN P.A. and COLLINSON J.D. (1986). Lakes. In: READING H.G. (ed): Sedimentary environments and facies. Blackwell Scientific Publications, Oxford, 63-112.

ANADON P., CABRERA L. and JULIA R. (1988). Anoxic-oxic cyclical lacustrine sedimentation in the Miocene Rubielos de Mora Basin, Spain. In: FLEET A.J., KELTS K. and TALBOT M.R. (eds): Lacustrine Petroleum Source Rocks. Geol. Soc. London, Spec. Publ., 40: 353-367.

AZZAROLI A. (1958). L'Oligocene e il Miocene della Somalia. Stratigrafia, tettonica, paleontologia (Macroforaminiferi, Coralli, Molluschi). Paleaontographica Italica, 52: 1-142.

AZZAROLI A. and FOIS V. (1964). Geological outlines of the Northern and of the Horn of Africa. Proceed. 22nd. Int. Geol. Congr., New Delhi, 4: 293-314.

BEYDOUN Z. R. (1970). Southern Arabia and Northern Somalia comparative geology. Phil. Trans. Roy. Soc. London, Ser. A, 267: 267-292.

BOYER B. W. (1982). Green River laminites: does the playa-lake model really invalidate the stratified-lake model? Geology, 10: 321-324.

BRADLEY W. H. (1973). Oil shale formed in desert environment: Green River Formation, Wyoming. Bull. Geol. Soc. Am., 84: 1121-1124.

BROOKFIELD M. E. (1977). The origin of bounding surfaces in ancient aeolian sandstones. Sedimentology, 24: 303-332.

BRUNI P., ABBATE E., ABDI SALAH HUSSEIN, FAZZUOLI M. and SAGRI M. (1987). Geological map of the Daban Basin, Northern Somalia. S.E.L.C.A., Firenze.

BRUNI P. and FAZZUOLI M. (1979). Mesozoic structural evolution of the Somali Coast of the Gulf of Aden. Accad. Naz. Lincei. Atti Convegni Lincei, 47: 192-207.

CAVAZZA W. (1989). Sedimentation pattern of a rift-filling unit, Tesuque Formation (Miocene), Espanola Basin, Rio Grande Rift, New Mexico. Jour. Sed. Petrology, 25: 99-111.

CLEMMENSEN L.B. and ABRAHAMSEN K. (1983). Aeolian stratification and facies association in desert sediments, Arran Basin (Permian) Scotland. Sedimentology, 30: 311-339.

COHEN A.S., FERGUSON D.S., GRAM P.H., HUBLER S.L. and SIMS K.W. (1986). The distibution of coarse-grained sediments in modern Lake Turkana, Kenya: implications for clastic sedimentation models in rift lakes. Geol. Soc. London., Spec.Publ., 25: 127-139.

COLE R.D. and PICARD M.D. (1981). Sulfur-isotope variations in marginal lacustrine rocks of the Green River Formation, Colorado and Utah. In: ETHRIDGE F.G. and FLORES R.M. (eds): Recent and ancient nonmarine depositional environments: Models for exploration. Soc. Econ. Paleont. Miner., Spec. Publ., 31: 213-231.

COLEMAN J.M. (1981). Deltas: processes and models of deposition for exploration. Burgess Publ. Co., CEPCO Division, Minneapolis, 124 pp.

COLEMAN J.M. and WRIGHT L.D. (1975). Modern river deltas: variability of processes and sand bodies. In: BROUSSAND M.L. (ed): Deltas, models for exploration. Houston Geol. Soc., 99-149.

CORNACCHIA M. and DARS R. (1983): Un trait structural majeur du continent africain. Les linéaments centroafricaines du Camerun au Golfe d'Aden. Bull. Soc. Geol. Fr., 25: 101-109.

DEAN W.E. (1981). Carbonate minerals and organic matter in sediments in modern north temperate hard-water lakes. In: ETHRIDGE F.G. and FLORES R.M. (eds): Recent and ancient nonmarine depositional environments: Models for exploration. Soc. Econ. Paleont. Miner., Spec. Publ., 31: 213-231.

DICKINSON K.A., BERRYHILL H.L. and HOLMES C.W. (1972). Criteria for recognizing ancient barrier coastlines. In: RIGBY J.K. and HAMBLIN W.K. (eds). Recognition of ancient sedimentary environments. Soc. Econ. Paleont. Miner., Spec. Publ., 16: 192-214.

DUNNE L.A. and HEMPTON M.R. (1984). Deltaic sedimentation in the Lake Hazar pull-apart basin, south-eastern Turkey. Sedimentology, 31: 401-412.

ELLIOT T. (1986). Siliciclastic shorelines. In: READING H.G. (ed): Sedimentary environments and facies. Blackwell Scientific Publications, Oxford, 155-188.

EUGSTER H.P. and HARDIE L.A. (1978). Saline lakes. In: LERMAN A. (ed): Lakes, chemistry, geology, physics. Springer-Verlag, New York, 237-293.

FRIEND P.F. (1983). Towards the field classification of alluvial architecture or sequence. In: COLLINSON J.D. and LEWIN J. (eds): Modern and ancient fluvial systems. I.A.S, Spec. Publ., 6: 345-354.

GALLOWAY W.E. (1975). Process framework for describing the morphologic and stratigraphic evolution of deltaic depositional systems. In: BROUSSAND M.L. (ed): Delta, models for exploration. Houston Geol. Soc., 87-98.

GLENNIE K.W. (1970). Desert sedimentary environments. Development in Sedimentology. Elsevier, Amsterdam, 14: 222 pp.

HAAS O. and MILLER A.K. (1952). Eocene Nautiloids of British Somaliland. Bull. Am. Mus. Nat. Hist., 99: 317-354.

HAQ B.U., HANDERBOL J. and VAIL P.R. (1987). Chronology of fluctuating sea level since the Triassic. Science, 235: 1156-1166.

HUBERT J.F. and HYDE M.G. (1982). Sheet-flow deposits of graded beds and mudstones in an alluvial sandflat-playa system: Upper Triassic Blomidon redbeds, St. Mary's Bay, Nova Scotia. Sedimentology, 29: 457-474.

HUNT J.A. (1960). Report on the geology of the Berbera-Sheikh area, Berbera and Burao districts. Geol. Surv. Somaliland, Rep. 4: 27 pp.

KELTS K. and HSU K.J. (1978). Freshwater carbonate sedimentation. In: LERMAN A. (ed): Lakes- chemistry, geology, physics. Springer Verlag, New York, 295-323.

MACFADYEN W.A. (1933). The geology of British Somaliland with a geological map 1:1,000,000. Crown Agents, London, 87 pp.

MERLA G., ABBATE E., AZZAROLI A., BRUNI P., CANUTI P., FAZZUOLI M., SAGRI M. and TACCONI P. (1979). A geological map of Ethiopia and Somalia (1973) 1:2,000,000 and comment with a map of major landforms. CNR Italy, Centro Stampa, Firenze, 95 pp.

MIALL A.D. (1977). A review of the braided-river depositional environment. Earth Sci. Rev., 13: 1-62.

MUKERJI A.B. (1976). Terminal fans of inland streams in Sutlej-Yamuna plain, India. Z. Geomorph., 20: 190-204.

NUTTAL W.L.F. and BRIGHTON A.G. (1931). Larger Foraminifera from the Tertiary of Somaliland. Geol. Mag., 68: 49-65.

ORI G.G. (1986). The nature of Permian rivers in Southern Alps. Mem. Soc. Geol. Ital., 34: 155-160.

PLINT A.G. (1983). Facies, environments and sedimentary cycles in the Middle Eocene, Bracklesham Formation of the Hampshire Basin: Evidence for global sea-level changes? Sedimentology, 30: 625-653.

REID I. and FROSTICK L.E. (1986). Slope processes, sediment derivation and land form evolution in a rift valley basin, Northern Kenya. Geol. Soc, London, Spec. Publ., 25: 99-111.

SAGRI M., ABBATE E. and BRUNI P. (1989). Deposits of ephemeral and perennial lakes in the Tertiary Daban Basin (Northern Somalia). Palaeogeography, Palaeoclimatology, Palaeoecology, 70: 225-233.

SLAY P.G. (1978). Sedimentary processes in lakes. In: LERMAN A. (ed): Lakes-chemistry, geology, physics. Springer Verlag, New York, 65-87.

SMITH G.I. (1965). Geology of Searles Lake. A guide to prospecting for buried continental salinas. 2nd. Symp, Salt, North Ohio Geol. Soc., 167-180

SOMALILAND OIL EXPLORATION COMPANY (S.O.E.C.). (1954). A geological reconnaissance of the sedimentary deposits of the Protectorate of British Somaliland. Crown Agents, London, 42 pp.

SWARTZ D.H. and ARDEN D.D. (1960). Geologic history of Red Sea area. A.A.P.G. Bull., 44: 1621-1637.

TUNBRIDGE I.P. (1984). Facies model for a sandy ephemeral stream and clay playa complex; the Middle Devonian Trentishoe Formation of North Devon, U.K. Sedimentology, 31: 697-715.

VAN COUVERING J.A. (1982). Fossil Cichlid Fish of Africa. Palaeont., Palaeont. Assoc., London, Spec. Pap., 29: 103 pp.

WALKER T.R. and HARMS J.C. (1972). Eolian origin of flagstone beds, Lyons Sandstone (Permian), type area, Boulder Country, Colorado Mount.. Geol., 9: 279-288.

WYLLIE B.K.N. (1925). Geology of a portion of British Somaliland. In: GREGORY J.W. (ed): The collection of fossils and rocks from Somaliland. Monograph. Geol. Dept. Hunterian Museum, Glasgow University, 8-14.

WITHJACK M.O. and JAMISON W.R. (1986). Deformation produced by oblique rifting. Tectonophysics, 126: 99-124.

YAIRI K. (1975). Geometry and mechanics of an échelon faulting with application to the East African Rift System. 1st. Prelim. Rept. African Studies, Nagaya Univ., 29-38.

ADDENDUM. The geological map of the Daban Basin, Northern Somalia by BRUNI P., ABBATE E., ABDI SALAH HUSSEIN, FAZZUOLI M. and SAGRI M. (1987) is appended to volume 113 B.

*Final editing, January 1990*

From *Geology and mineral resources of Somalia and surrounding regions*, Ist. Agron. Oltremare, Firenze, Relaz. e Monogr. 113, 241-250, 1993.

# THE GEOMORPHOLOGICAL EVOLUTION OF THE UPPER JUBBA VALLEY IN SOUTHERN SOMALIA

ABDIRAHIM M. M. *, ALI KASSIM MOHAMED *, L. CARMIGNANI ** and M. COLTORTI ***

* Department of Geology, Somali National University, P.O. Box 1081, Mogadishu, Somalia.
Present address: Department of Earth Sciences, University of Siena, Via delle Cerchia 3 , 53100 Siena, Italy.

** Department of Earth Sciences, University of Siena, Via delle Cerchia 3 , 53100 Siena, Italy.

*** Department of Earth Sciences, University of Camerino, Viale E. Betti 1, 62032 Camerino, Italy.

## ABSTRACT

Geological and geomorphological surveys on recently discovered Tertiary-Quaternary formations and associated morphologies in the Upper Jubba Valley allowed reconstruction of the late Tertiary-Quaternary evolution of this area.

After the Upper Cretaceous the region was affected by peneplanation which levelled all formations, followed by the evolution which produced the present landscape, probably in connection with generalized uplifting movements.

The Faanweyn Formation, lacustrine in origin and composed of whitish sandy clays, was deposited in a huge NE-SW-trending depression between Baardheere and Garbahaarrey. The influent of this lake came from at least two large rivers trending NW-SE: one situated in the same position as the present Jubba Valley in the Luuq area, and the other represented by the Paleo-Dawa. The drainage network deepened and the lacustrine depression was cut almost at a right angle by the Paleo-Jubba, a paleo-river with a course similar to that of the present Jubba, filled with alluvial and pyroclastic materials (Kuredka Formation) and capped by basalt lava flows. The most important downcutting episode of the valley subsequently occurred, modelling an alluvial terrace 5 m above the present thalweg during the end of the Upper Pleistocene. Further downcutting, resulting in the shaping of the present thalweg, occurred after this period.

During these phases, an important episode of piracy affected the Dawa river, creating a dead valley more than 100 km in length, from Garbahaarrey to Kenya, beyond Mandera.

## INTRODUCTION

This work is the result of a geological survey of the Gedo Region promoted by the Somali National University (CARMIGNANI et al., 1983) and of more recent geo-archeological researches carried out in the same region (COLTORTI and MUSSI, 1987).

The data emerging from these researches allowed a first attempt at reconstructing the Tertiary-Quaternary evolution of the Jubba Valley between the border with Kenya and Ethiopia at Doolow (almost 4° N) and Baardheere (almost 2° 20' N).

## GEOMORPHOLOGICAL AND GEOLOGICAL BACKGROUND

The Jubba River originates at the confluence of the Ganane and Dawa rivers (Fig. 1). After the confluence near Doolow, the Jubba flows SE as far as Luuq, where it takes on a decidedly N-S course which, after some variations, it maintains as far as Baardheere. The region is characterized by a planation surface deeply cut by the Jubba. North of Luuq the thalweg lies at 160 m a.s.l. and, almost 170 km further south at Baardheere, at about 100 m a.s.l., so that the water-course has a very slight gradient.

From the geological viewpoint, the area is a wide synclinorium of sedimentary Jurassic and Lower Cretaceous rocks (BARBIERI, 1968; BELTRANDI and PYRE, 1975, ANGELUCCI et al., 1981).

The oldest sedimentary formation outcropping in the Upper Jubba Valley is the Canoole Formation (Late Callovian-Late Oxfordian), mainly consisting of marls and shales about 400 m thick. This is followed by the Uegit (Waajid) Formation (Late Oxfordian-Early Portlandian), composed of bedded limestone about 350 m thick. In turn, this is followed by the Garbahaarrey Formation, occupying most of the area studied and subdivided into two members: the Bossul Member (lower part), consisting mainly of limestone, dolomitic limestone and sandstone, and the Macow Member (upper part), consisting mainly of gypsum and anhydrite with marl and shale intercalations (Lower Cretaceous). In the SE part of the area the Macow member passes laterally to the Cambar Formation, which consists of sandstones with shale and siltstone intercalations.

The structure of the Jurassic-Cretaceous sequences is simple. NW of the Buur Region basement the sedimentary cover dips 1°-2° NW for more than 100 km as far as the Luuq and Garbahaarrey areas. Further W the average dip is SE and E, so that the crystalline basement outcrops again beyond the border with Kenya. The structure of the whole Jubba Valley upstream from Baardheere is therefore a wide NE-SW-trending synclinorium enclosed between two crystalline outcrops. This simple structure is complicated by NE-SW faults and folds concentrated along the Sengif and Garbahaarrey Belts (Figs. 1, 2) (BELTRANDI and PYRE, 1975).

Fig. 1 - Geological sketch-map of Upper Jubba Valley. 1: Basalt; 2: Faanweyn Formation; 3: Garbahaarrey and Cambar Formations; 4: Waajid Formation; 5: Canoole Formation; 6: Bedding attitude; 7: Fault; 8: Fossil drainage.

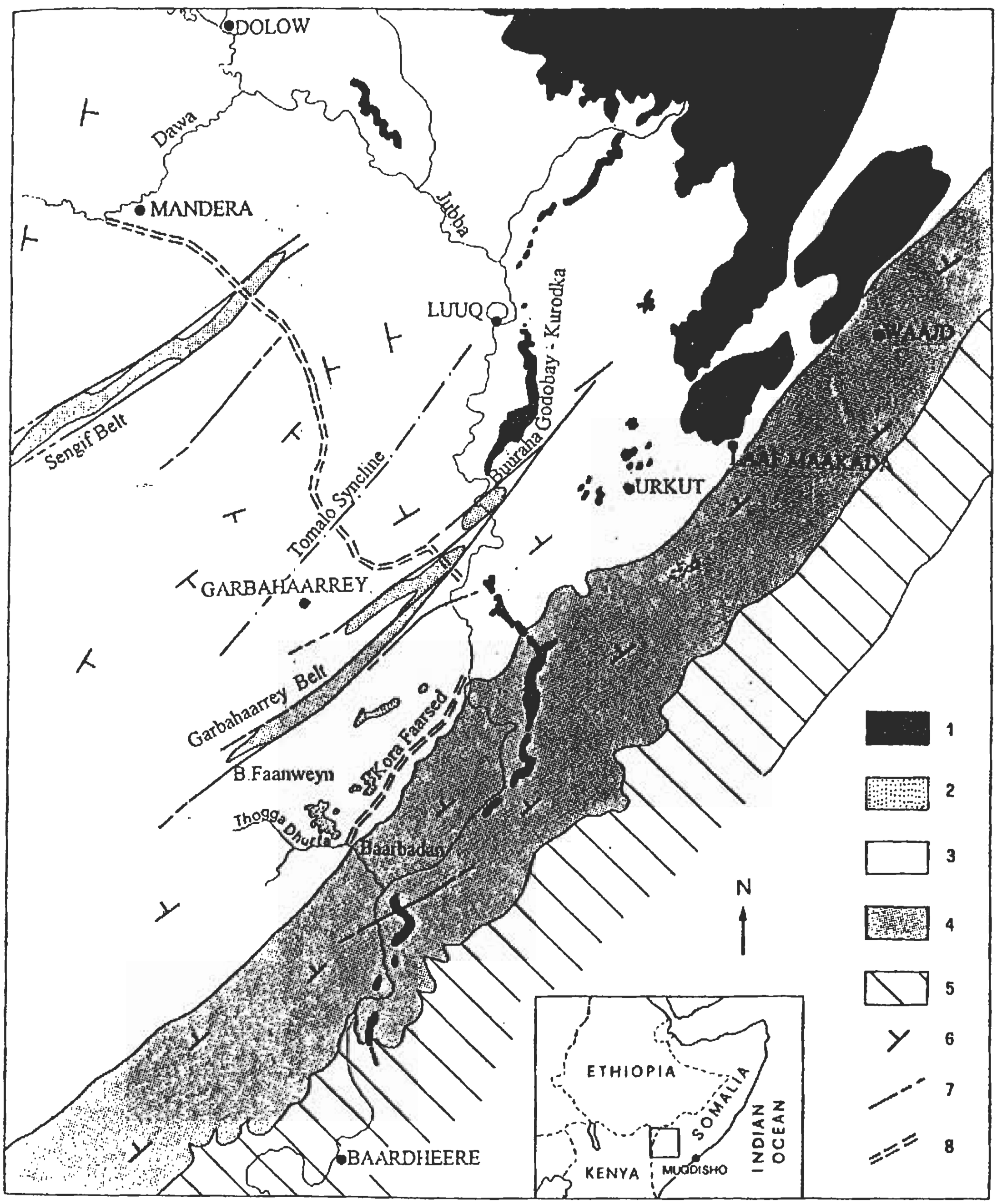
DOLOW
Dawa
MANDERA
Jubba
LUUQ
Buuraha Godobay - Kurodka
Sengif Belt
Tomalo Syncline
URKUT
GARBAHAARREY
Garbahaarrey Belt
Kora Faarsed
B.Faanweyn
Thogga Dhurla
Baarbadan
BAARDHEERE
1
2
3
4
5
6
7
8
N
ETHIOPIA
SOMALIA
KENYA
MUQDISHO
INDIAN OCEAN

The Sengif Belt is composed of a long anticline bounded on both sides by two faults, extending from the Luuq area for about 100 km as far as Kenya.

The Garbahaarrey Belt develops for about 130 km, characterized by many faults and folds. The hard limestone of the Waajid Formation outcrops on the core of the anticlines which rise above the soft Cretaceous rocks.

ALI KASSIM M. et al. (this volume) have hypothesized that the two belts may be due to right-wrenching tectonics associated with a transpressional component.

Discordant Tertiary continental sediments and volcanics overlie the Jurassic-Lower Cretaceous deformed sequence and will be illustrated in more detail later.

## GEOLOGICAL AND GEOMORPHOLOGICAL ELEMENTS OF TERTIARY EVOLUTION

Data on the Tertiary evolution is limited to the outcrop of a few discontinuous continental formations and morphological features which allow fragmentary reconstruction of the evolution of the landscape.

### Planation remnant

Evidence of a levelled surface, with average altitudes of 400 m a.s.l. and often covered by calcrete, silcrete and laterite soils several metres thick, is preserved in the higher areas of the whole of SE Somalia. Scattered rounded quartz pebbles and granules are frequently found on this surface, testifying that the smoothing was mainly associated with river erosion during a phase of tectonic stability.

It is difficult to reconstruct the precise initial morphology of the area, and to establish the extent of denudation to which it was subjected and, in particular, if some of the currently present depressions were active or, as seems more likely, were created after the gradual deepening of the base level. The second hypothesis is favoured by the extraordinary degree of smoothing of some parts of the area, which may even suggest the presence of an "ultiplain" (TWIDALE, 1983).

The modelling of a planation surface requires a long period of tectonic stability and conditions favouring aerial erosion, and KING (1976) has indicated numerous levelling phases which may have affected the land surface. Among these is the "Moorland Planation", corresponding to the "African Planation", which may have developed between the Late Cretaceous and the Upper Miocene. This planation is characterized by "extraordinary smoothness, developed over enormous areas, encrusted with a senile soil profile of laterite, calcrete or bauxite which is normally diagnostic" (op. cit.). The smoothness of the region and the occurrence of well-developed calcrete and laterite soils may indicate this levelling phase.

The Jubba Valley started to form when an overall variation in the morphodynamic balance occurred: in other words, after a phase of general "aerial modelling" came a phase of more intense "linear modelling".

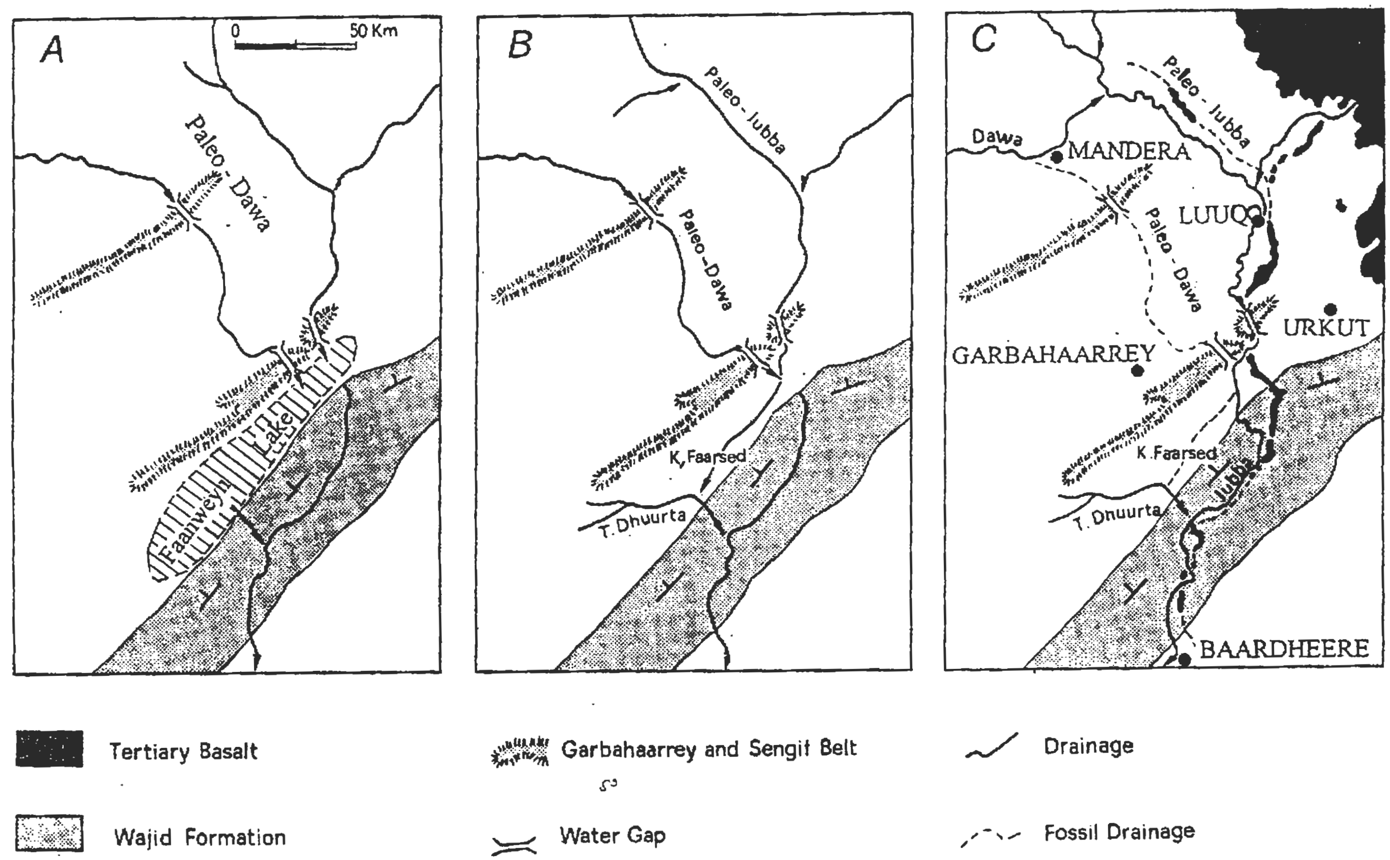


Fig. 2 - Evolution of hydrographic network of Upper Jubba Valley.

## Faanweyn Formation

This is the oldest discordant formation on Jurassic-Cretaceous rocks in the Jubba Valley. It is composed of whitish, clayey, silty sediments with sandy lenses, outcropping at Buuraha Faanweyn and other isolated hills located further N, always on the hydrographic right of the Jubba (B. Afar Irdood, B. Cadaad Caano, B. Dhooliaao, B. Carabiyaha, etc.). Maximum thickness is about 10 m. The highest altitude at which these sediments outcrop is around 330 m a.s.l. and the summits of the hills are always covered by silcrete several metres thick. These hills represent the remains of a wider cover that extended for at least 1000 km² over a depressed area bounded to the NW by the reliefs of the Garbahaarrey Belt and to the SE by the surveyed area, along which the limestones of the Waajid Formation outcrop (Fig. 2). This morphology and the prevalence of fine-grained parallel-laminated sediments lead to the assumption that the sediments were deposited in a shallow lacustrine environment.

## The Paleo-Dawa and Koora Faarseed conglomerates

A dry valley, over 100 km long and almost as wide as the present Jubba Valley, runs N from the Garbahaarrey area to the Dawa River, W of Mandera (Paleo-Dawa in Fig. 2). Where it cuts the Garbahaarrey and Sengif belts, the valley narrows to form two gorges at the point where the hard Waajid limestone outcrops.

There is another fossil drainage S of the Garbahaarrey Belt, near Hufay in the Koora Farseed area. The existence of this ancient watercourse is proven by a paleo-valley running between the softer sediments of the Garbahaarrey Formation and the limestones of the Waajid Formation, and by cemented fluvial conglomerates with igneous elements. These sediments lie lower than the Faanweyn lacustrine sediments, demonstrating that the threshold of the basin was already cut at the time of their deposition.

## The Paleo-Jubba and Kuredka Formation

A well-preserved paleo-valley, cut in the limestones of the Waajid Formation and suspended several dozen metres above the current thalweg (Fig. 2c), is found N of Baardheere. Its course does not differ greatly from the present course of the Jubba, and is partially filled with alluvial deposits overlain by basalt or sometimes with basalt alone. In the Luuq area, the softness of the Cretaceous rocks has meant that almost every trace of this paleo-valley has been obliterated by erosion. The alluvial deposits protected from erosion by the overlying basalts have remained as aligned reliefs, allowing reconstruction of the fossil course.

Previously called "Continental Pre-Basaltic Deposits" (CARMIGNANI et al., 1983), the alluvial deposits outcrop near Luuq in the Buuraka Godobay-Kuredka relief which, since it has been studied in more detail, we prefer to call the Kuredka Formation.

The Kuredka Formation is composed of alternating pebbly deposits, some of which are coarse, with sandy or more seldom silty layers and lenses. The gravels are well-rounded and mainly composed of volcanic material. However, in some places similarly well-rounded siliceous and quartzose pebbles clearly indicate that they were transported over long distances and underwent many cycles, since continental formations containing such materials do not occur in this region of Somalia. The pebbly deposits testify to the presence of an alluvial plain crossed by shallow braided channels. Instead, the sandy deposits are plane-laminated, sometimes giving way to cross-laminated layers, indicating a water-course with a less important bedload and considerable lateral migration, with sandy bars on the bottom.

The sequence contains silicified fossil trunks, sometimes of considerable size, and layers of acid volcanic ashstone also occur in various sections (ALOISI and DE ANGELIS, 1938; CARMIGNANI et al., 1983). The upper part of one section contains two levels of obsidian 50-100 cm thick, indicating that an eruptive centre was situated not far from this area.

The whole sequence was deposited during a period of intense volcanic activity and was perhaps strongly influenced by it. The composition of the volcanic pebbles indicates that they originated from the reworking of more alkaline volcanites, up to phonolites (ALI KASSIM M. and FANTOZZI, 1985), representing a magmatic event completely different from that to which the basalts capping the sequence belong.

### The basalts

Extensive basalt lava flows were identified in the Gedo Region by the expeditions of BOTTEGO and STEFANINI (DE ANGELIS D'OSSAT and MILLOSEVICH, 1900; MANASSE, 1916; ALOISI, 1927; ALOISI and DE ANGELIS, 1938). These flows are also indicated on the "Geological Map of Ethiopia and Somalia" (MERLA et al., 1979) and in more detail in CARMIGNANI et al. (1983). ALI KASSIM M. and FANTOZZI (1985) demonstrated that the basalts aligned along the paleo-Jubba and classified as "olivine tholeiites" may be distinguished petrographically from those outcropping extensively N of Laaf Maakada, which are slightly more alkaline. The distribution of the former suggests that they derived from lava flows canalized inside the paleo-course of the Jubba. As yet, no other elements indicate whether they may be attributed to two completely separate periods of basalt flow or to a single period.

On the basis of some preliminary radiometric investigations (Prof. G. TRAVERSA, pers. comm.), the age of the basalts outcropping near Luuq is Oligocene, but data from the Institute of Geochronology of the Italian National Council for Research, Pisa, have recently demonstrated the presence of excess $Ar^{40}$ in several basalt samples. The apparent age values must therefore be considered older than the real ones (ALI KASSIM M. et al., this volume).

## ALLUVIAL DEPOSITS OF THE PRESENT JUBBA VALLEY

### Recent alluvial deposits

These concern mainly sandy and silty sediments, interstratified with lenses of fine pebbles and granules. The beds display both plane-and cross-stratification with clearly visible ripple structures, located on the edges of the present course of the Jubba and sometimes stretching for hundreds of metres, e.g., N of Luuq, while S of the city their extent is limited to several tens of metres. Their maximum height on the thalweg near Luuq is 3 m. At certain points they subtend recent morphologies, such as channels or small closed depressions, and constitute alluvial sediments deposited during major floods, both in periods close to the pre-sent and in the recent Holocene. Laterally they rest against the cliffs cutting into the older alluvial formation. In some places, present-day and recent fragments of ceramic may be found on top of the sediments, demonstrating that part of the alluvial plain has not been affected by floods, at least in recent times.

### Terraced alluvial deposits

Another alluvial unit is located above the previous one, separated by a fluvial erosion escarpment more than 4 m high. The bedrock occasionally outcrops between the two units (e.g., E of Luuq) and the alluvial material, composed of coarse sand and medium-fine pebbles, is thin. However, in places the river cuts directly into this alluvial unit (e.g., at Luuq) to a depth of more than 8 m, down to the present-day course. Where this happens wavy plane-or cross-laminated sands outcrop, separated by massive sands and plane-laminated silts and clays.

It is therefore probable that the lower surface of this unit is irregular and eroded by paleo-channels. The upper surface is generally flat, but is cut at some points by channels which have progressively lowered it so that it is now close to the present riverbed, as is the case of the Luuq meander. The upper deposition surface progressively rises to form a pediment towards the hills, covered here and there by a veneer of medium-coarse debris with subrounded and sub-angular edges.

Prehistoric artefacts have been found on the surface. Attributed mainly to the Late Stone Age and some probably to the Middle Stone Age (COLTORTI and MUSSI, 1987), they allow the deposition of the sediments and the modelling of the pediment to be attributed to the Late Pleistocene. This unit is informally called the Litho-morphostratigraphic Unit of Luuq.

One of the above-mentioned dry valleys (Paleo-Dawa) is located at a similar height.

## CONCLUSIONS

The sea did not return to the region after the Cretaceous regression. A lengthy period of peneplanation followed, responsible for the modelling of the Southern

Somalia Plateau.

The morphological evolution of the Jubba Valley began subsequently and in conjunction with general uplifting movements. These movements are probably linked to the general uplifting attributable to the early phases of evolution of the Rift Valley (NYAMWERU, 1980). In this initial evolutionary phase of the hydrographic network, a lacustrine basin, elongated in a NE-SW direction, was formed between the Garbahaarrey Belt and a plateau lying in the same direction, modelled on the limestone monocline of the Waajid Formation (Fig. 2a). In these depressions the sandy clays of the Faanweyn Formation were deposited, the latter being the oldest discordant formation on the Jurassic-Cretaceous sequences of the Jubba Valley. The main affluents of this lake were probably two rivers which resulted from the above-mentioned consequent NW-SE-trending hydrography. One of these affluents must have corresponded to the present-day course of the Jubba in the Luuq Region; the other was represented by the Paleo-Dawa. Traces of this paleo-channel remain, particularly in the Garbahaarrey and Sengif Belts where the river has cut two deep gorges (Fig. 2a). Subsequently, the hydrographic network deepened and, from the lake outlet, probably coinciding with the course of the Jubba downstream from Baarbadan, the erosional process moved up along the Togga Dhuurta, clearing out the lake until it joined the affluents (Fig. 2b). This link-up is demonstrated by the fluvial conglomerates containing igneous elements found in the Koora Farseed paleo-valley.

A hydrographic network substantially similar to the actual one only came into existence with the Paleo-Jubba, whose course between Luuq and Baardheere is still easy to reconstruct (Fig. 2c). The main difference between the Paleo-Jubba and the network described above may be seen in the stretch between the Garbahaarrey Belt and the Baarbadan area. The regressive erosion of a subsequent affluent along a clayey layer of the Waajid formation allowed the capture of the water-course upstream from Koora Farseed. The Paleo-Jubba was subsequently filled by alluvial deposits (Kuredka Formation) and sealed by a basalt lava flow, after which the valley was deepened almost to the present-day thalweg. Successive stages of this downcutting process are shown by the terraced alluvial deposits found in the Luuq area.

The capture of the Dawa upstream from Mandera is also to be attributed to this recent evolution, and gave rise to a dead valley more than 100 km long, running from the Garbahaarrey area to beyond Mandera in Kenya.

ACKNOWLEDGMENTS

The research of M. COLTORTI was carried out with grants from the Italian Ministry of Public Education, 60% funds, assigned to M. MUSSI, Italian Institute of Paleontology, Rome.

The research of L. CARMIGNANI was carried out with grants from the Dipartimento per la Cooperazione allo Sviluppo, Italian Ministry for Foreign Affairs.

REFERENCES

ALI KASSIM M., BELLIENI G., CARMIGNANI L., FANTOZZI P., FERRARO G., JUSTIN VISENTIN E., TONARINI S. and ZANETTIN B. (this volume). Flood basalts of the Gedo Region (Southern Somalia): geology, petrology and isotopic geochemistry.

ALI KASSIM M., CARMIGNANI L. and FANTOZZI P. (this volume). Tectonic transpression in the Gedo region (Southern Somalia).

ALI KASSIM M. and FANTOZZI P. (1985). Studio geologico-petrografico preliminare dei basalti della regione di Gedo (Somalia Meridionale). Univ. Naz. Somala. Quad. Geol. Somalia, 8: 257-268.

ALOISI P. (1927). Rocce della Somalia raccolte dalla seconda missione Stefanini. Mem. Soc. Tosc. Sc. Nat., 38: 132-157.

ALOISI P. and DE ANGELIS A.M. (1938). Le rocce della Somalia. In: Geologia della Somalia, 166 pp., R. Soc. Geogr., 2.

ANGELUCCI A., BARBIERI F., MAXAMED C.M., CARUUSH M.C. and PICCOLI G. (1981). Preliminary report on the Jurassic sequence in the Gedo and Bay regions (South-western Somalia). Univ. Naz. Somala, Quad. Geol. Somalia, 4: 115-154.

BARBIERI F. (1968). Jurassic macrofacies in western Somalia. Riv. It. Paleont. Strat., 74: 805-826.

BELTRANDI M.D. and PYRE A. (1975). Geologic evolution of south-west Somalia. In: Sedimentary Basins of African Coasts, Part 2: South and East Coasts (Edited by BLANT G.), 159-178. Ass. Serv. Geol. Afr.

CARMIGNANI L., ALI KASSIM M. and FANTOZZI P. (1983). Nota preliminare sul rilevamento della regione di Gedo (alta valle del Giuba, Somalia Meridionale). Univ. Naz. Somala, Quad. Geol. Somalia, 7: 85-109.

COLTORTI M. and MUSSI M. (1987). Late Stone Age hunter-gatherers of the Juba Valley. Nyame Akuma, 28-32.

DE ANGELIS D'OSSAT G. and MILLOSEVICH F. (1900) Studio geologico sul materiale raccolto da M. Sacchi (seconda spedizione Bottego). Soc. Geogr. It., 212 pp.

KING L. (1976). Planation remnants upon high lands. Z. Geomorph., 20, 2: 133-148.

MANASSE E. (1916). Rocce della Somalia italiana raccolte dalla missione scientifica Stefanini-Paoli, 1913. Mem. Soc. Tosc. Sc. Nat., 31: 1-74.

MERLA G., ABBATE E., AZZAROLI A., BRUNI P., CANUTI P., FAZZUOLI M., SAGRI M. and TACCONI P. (1979). A geological map of Ethiopia and Somalia. C.N.R., Italy, 95 pp.

NYAMWERU C. (1980). Rifts and Volcanoes. Nelson Africa, 128 pp.

SUMMERFIELD M.A. (1983). Silcrete as a palaeoclimatic indicator: evidence from southern Africa. Palaeogeogr. Palaeoclim. Palaeoecology, 41: 65-79.

TWIDALE C.R. (1983). Pediments, peneplains and ultiplains. Rev. Géol. Dun. Géogr. Phys., 24: 52-62.

*Final editing, January 1990*

From *Geology and mineral resources of Somalia and surrounding regions*, Ist. Agron. Oltremare, Firenze, Relaz. e Monogr. 113, 251-258, 1993.

# FISSURAL BASALTS OF THE LUUQ AREA (CENTRAL-SOUTHERN SOMALIA): GEOLOGY, PETROLOGY AND ISOTOPE GEOCHEMISTRY

ALI KASSIM MOHAMED *, L. CARMIGNANI **, P. FANTOZZI **, G. FERRARA ***, S. TONARINI ***, G. BELLIENI ****, E. JUSTIN-VISENTIN **** and B. ZANETTIN ****

* Department of Geology, Somali National University, P.O. Box 1081, Mogadishu, Somalia.
Present address: Dipartimento di Scienze della Terra, Università di Siena, Via delle Cerchia 3, 53100 Siena, Italy.

** Dipartimento di Scienze della Terra, Università di Siena, Via delle Cerchia 3, 53100 Siena, Italy.

*** Istituto di Geocronologia, C.N.R., Via C. Maffi 36, 56100 Pisa, Italy.

**** Dipartimento di Mineralogia e Petrologia, Università di Padova, Corso Garibaldi 37, 35123 Padova, Italy.

## ABSTRACT

Flow and sills of basic volcanites have been studied in the Luuq and Buulobarde Regions (Central Somalia). They are transitional basalts with tholeiitic affinity.

## INTRODUCTION

Basic volcanites represented by flows and sills, outcrop in the Luuq and Buulobarde regions (Central-southern Somalia) (DE ANGELIS D'OSSAT and MILLOSEVICH, 1900; MANASSE, 1916; ALOISI, 1927; ALOISI and DE ANGELIS, 1938; CARMIGNANI et al., 1984) (Fig. 1).

In the Luuq area the volcanites outcrop both in the plateau between Luuq and Waajid (Laaf Maakada basalts) and on the left side of the Juba River (Juba basalts).

The Laaf Maakada striated basalts of maximum thickness of 15 m rest on the Mesozoic substrate. The Juba basalts with a measured maximum thickness of 32 m, fill a paleo-river bed that cuts the Upper Jurassic limestone north of Baardheere for about 100 km (ALI KASSIM and FANTOZZI, 1985).

In the Buulobarde area the volcanites outcrop along the right bank of Shebelle River (Webe Shebelle basalts). These outcrops (70 km lenght) occur to the south of Buqda Caqable and are formed at least in part (more than 30 km) by a sill injected at shallow depth. Minor outcrops, 10 m thick, form the top of neighbouring hills (BARBIERI et al., 1979).

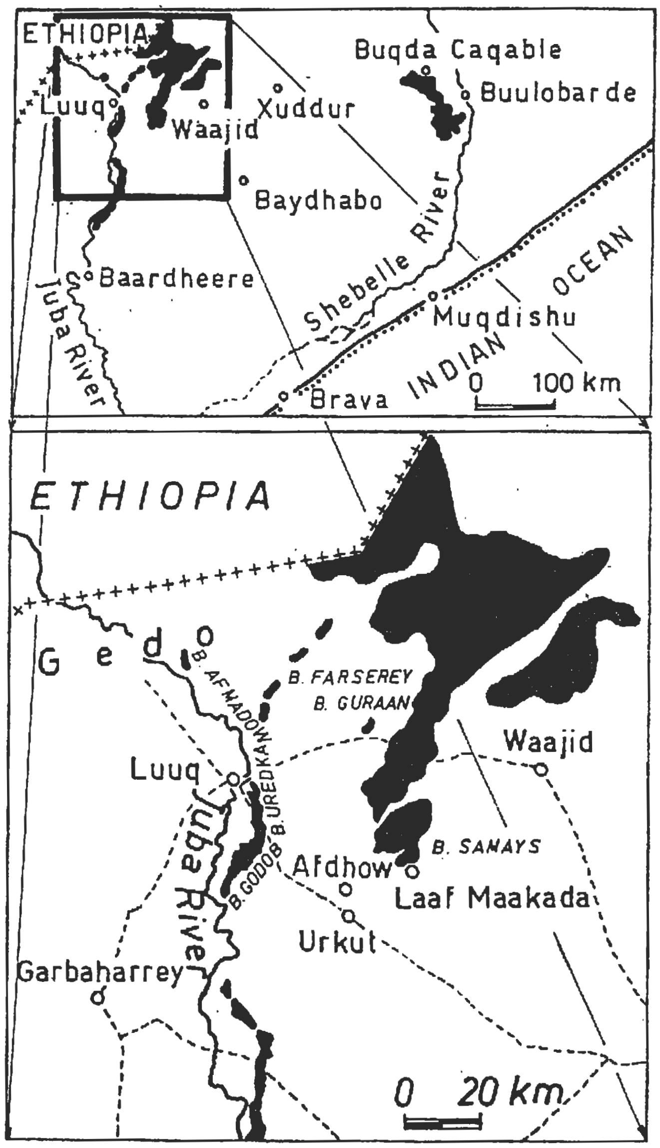


Fig. 1 - Geological sketch map of Southern Somalia. Black areas represent the basalt outcrops.

LAAF MAAKADA AND JUBA BASALTS (LUUQ AREA)

These two groups of basalts are very similar. They are fine-grained, aphyric or microporphyritic with phenocrysts of plagioclase (An 86-60%) and microphenocrysts of augite (Wo 42-39%). Groundmass is formed by plagioclase (An 70-58), clinopyroxene (Wo 44-36%), opaques and partially altered olivine (Fo 71-60%).

In general the pyroxene composition is typical of transitional basalts. The only

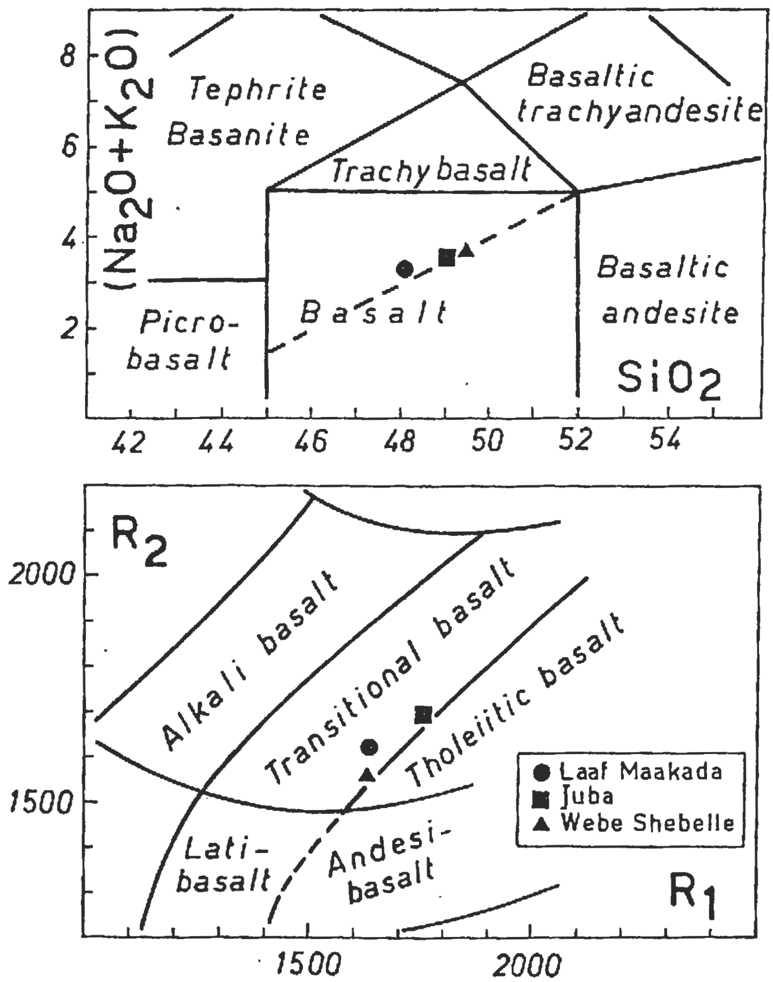


Fig. 2 - Distribution of average Laaf Maakada, Juba and Webe Shebelle volcanites in the Total Alkali-Silica (TAS) (ZANETTIN, 1984) and R1 vs. R2 classificative diagram (DE LA ROCHE et al., 1980, modified by BELLIENI et.al., 1981). $R1 = 4Si - 11(Na+R) - 2(Fe+Ti)$; $R2 = 6Ca + 2Mg + Al$.

Table 1 - Average chemical (major, trace elements and REE) and Sr isotopic composition of Laaf Maakada, Juba and Webe Shebelle basalts. Aver. = average, s.d. = standard deviation, N = number of samples. $(^{87}Sr/^{86}Sr)_i$ = initial Sr isotope ratios.

| | Laaf Maakada | | Juba | | Webe Shebelle | |
|---|---|---|---|---|---|---|
| | (N=13) | | (N=16) | | (N=2) | |
| | aver. | s.d. | aver. | s.d. | aver. | s.d. |
| $SiO_2$ | 47.39 | 0.52 | 49.11 | 0.34 | 48.53 | 0.25 |
| $TiO_2$ | 3.28 | 0.18 | 2.65 | 0.09 | 3.92 | 0.03 |
| $Al_2O_3$ | 15.04 | 0.97 | 14.95 | 0.56 | 15.07 | 0.10 |
| $Fe_2O_3$ | 3.02 | 1.13 | 2.65 | 1.07 | 1.95 | 0.06 |
| FeO | 10.41 | 1.14 | 9.06 | 1.17 | 10.19 | 0.02 |
| MnO | 0.22 | 0.01 | 0.19 | 0.01 | 0.20 | 0.02 |
| MgO | 5.75 | 0.33 | 5.76 | 0.16 | 4.18 | 0.30 |
| CaO | 9.73 | 0.26 | 10.44 | 0.19 | 10.04 | 0.10 |
| $Na_2O$ | 2.68 | 0.07 | 2.70 | 0.11 | 2.84 | 0.06 |
| $K_2O$ | 0.50 | 0.06 | 0.72 | 0.07 | 0.65 | 0.02 |
| $P_2O_5$ | 0.57 | 0.21 | 0.39 | 0.10 | 0.56 | 0.01 |
| L.O.I | 1.42 | 0.40 | 1.38 | 0.21 | 1.86 | 0.07 |
| mg | 0.470 | 0.017 | 0.504 | 0.011 | 0.414 | 0.017 |
| | (N=2) | | (N=2) | | (N=1) | |
| La | 18.73 | 0.14 | 25.95 | 2.04 | 23.65 | |
| Ce | 47.51 | 1.52 | 57.56 | 1.51 | 62.08 | |
| Nd | 26.79 | 0.49 | 28.72 | 0.64 | 34.43 | |
| Sm | 7.15 | 0.09 | 7.02 | 0.34 | 8.46 | |
| Eu | 2.65 | 0.13 | 2.03 | 0.08 | 2.88 | |
| Gd | 6.04 | 0.13 | 5.66 | 0.53 | 7.26 | |
| Dy | 5.76 | 0.10 | 5.10 | 0.18 | 6.48 | |
| Er | 2.67 | 0.06 | 2.37 | 0.14 | 3.05 | |
| Yb | 2.59 | 0.01 | 2.22 | 0.11 | 2.93 | |
| Lu | 0.37 | 0.01 | 0.32 | 0.01 | 0.40 | |
| | (N=7) | | (N=6) | | (N=3) | |
| Sr | 427 | 10 | 486 | 5 | 490 | 50 |
| Rb | 8.08 | 1.15 | 18.53 | 1.09 | 12.15 | 5.14 |
| $(^{87}Sr/^{86}Sr)_i$ | 0.70405 | 0.00010 | 0.70508 | 0.00012 | 0.70440 | 0.00038 |

difference between the pyroxenes from these two groups of rocks is the presence in the Laaf Maakada basalts of brown augite with an higher iron content (average $Fe^{2+} + Fe^{3+} + Mn = 30 \pm 3$ vs. $18 \pm 5$).

From the chemical point of view, (Table 1) both the Laaf Maakada and Juba basalts correspond to transitional basalts with tholeiitic affinity (Fig. 2). However, geochemical differences allow to distinguish Juba from Laaf Maakada basalts since the former are

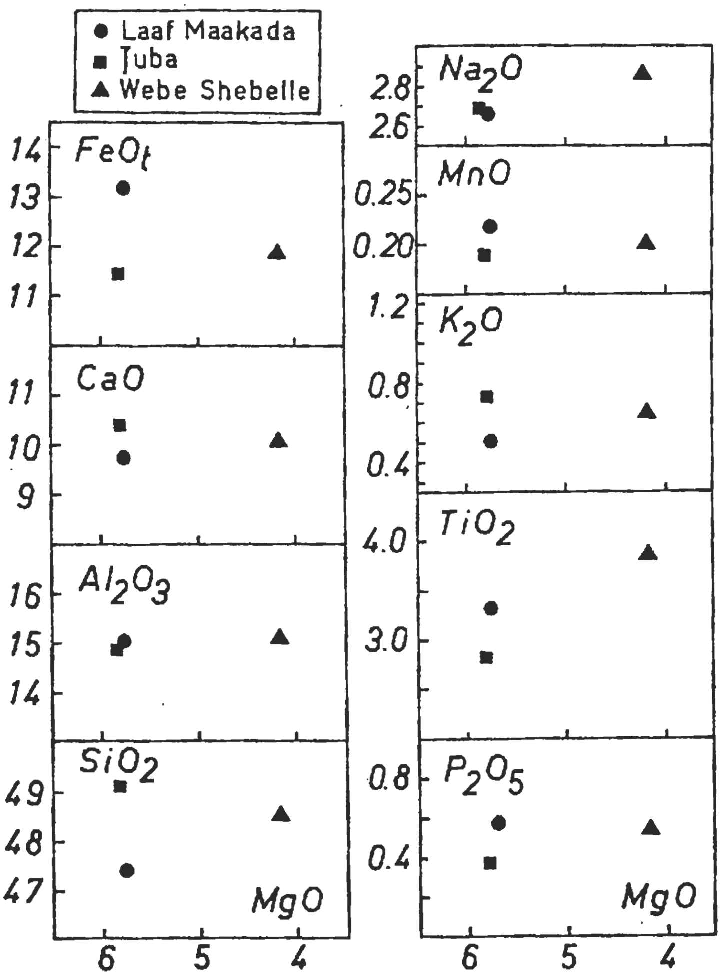


Fig. 3 - Plots of average Laaf Maakada, Juba and Webe Shebelle basalts in major elements (% wt.) vs. MgO (% wt.) variation diagrams.

richer in $SiO_2$, CaO, $K_2O$, Sr, Rb, La, Ce and poorer in $FeO_t$, $P_2O_5$, $TiO_2$ and MnO (Table 1 and Figs. 3, 4). The mg values (at. $Mg/Mg+Fe^{2+}$ assuming $Fe_2O_3/FeO = 0.15$) indicate that the Juba basalts are slightly less evolved than the Laaf Maakada ones (i.e., aver. $0.504 \pm 0.011$ vs. $0.470 \pm 0.017$).

These geochemical features clearly indicate that the Laaf Maakada basalts cannot be derived from Juba basalts through gabbro fractionation process.

## WEBE SHEBELLE BASALTS (BUULOBARDE AREA)

The Webe Shebelle basalts are similar to those from the Luuq area but are generally slightly more evolved (Table 1 and Figs. 3, 4).

The Sr initial isotope composition ranges from 0.70388 to 0.70530 (ALI KASSIM M. et al., 1992). Besides the possibility of source heterogeneity, this variation may very probably be ascribed to slight crustal contamination.

The higher mg values for Juba basalts and their higher Sr isotopic ratios (0.7053-0.7050) with respect to the Laaf Maakada basalts (0.7042-0.7040) suggest contamination by granitic rocks for the former. The Juba basalts show a remarkable increase in $K_2O$,

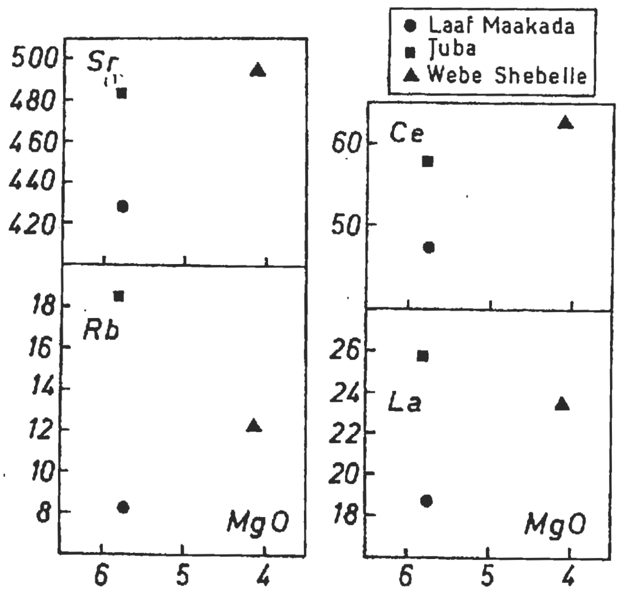


Fig. 4 - Plots of average Laaf Maakada, Juba and Webe Shebelle basalts in trace elements (ppm) vs. MgO (% wt.) variation diagrams.

Rb and Sr, and a slight increase in LREE, without showing important variations in the other components. This may be due to selective contamination by a granitic rock component (WATSON, 1982). The increase in Sr content (not referable to fractional crystallization) associated with increased Sr isotope composition, $K_2O$ and Rb is consistent with a K-feldspar (Orthoclase-Microcline) contaminant identifiable among the main components of the granitoid rocks of the Somalian basement.

The Webi Shebelle basalts show an intermediate degree of contamination ($^{87}Sr/^{86}Sr$ = 0.7047-0.7040).

## ACKNOWLEDGMENTS

This work was supported by grants from C.N.R. (40%) "Evoluzione tettonica e magmatologica del sistema di rift del blocco Afro-Arabico", MURST (60%) "Evoluzione magmatologica e strutturale nel blocco Afro-Arabico" and Department of Geology (Somali National University).

## REFERENCES

ALI KASSIM M. and FANTOZZI P. (1985). Studio geologico e petrografico preliminare dei basalti della regione di Gedo (Somalia meridionale). Univ. Naz. Somalia. Quad. Geol. Somalia, 8: 257-268.

ALI KASSIM M., CARMIGNANI L., FANTOZZI P., FERRARA G., TONARINI S. and ZANETTIN B. (1992). Flood basalts of the Gedo Region (Southern Somalia): Geology, petrology and isotopic geochemistry. Mem. Accad. Lincei, (in press).

ALOISI P. (1927). Rocce della Somalia Italiana raccolte dalla seconda missione Stefanini. Mem. Soc. Tosc. Sci. Nat., 38: 132-157.

ALOISI P. and DE ANGELIS A.M. (1938). Le rocce della Somalia. Vol. Geologia della Somalia. R. Soc. Geogr., 2: 1166.

BARBIERI F., CABDULQAADIR M.M., DI GERONIMO I., FAADUMA C.C., GIULINI P., CARUSH M.C., MICHELIN G. and PICCOLI G. (1979). Il Cretaceo della regione di Hiraan in Somalia (valle dello Webi Shebelle), con appendice sulla foresta fossile di Sheekh Guuze. Mem. Sci. Geol. Padova, 32: 1-23.

BELLIENI G., PICCIRILLO E.M. and ZANETTIN B. (1981). Classification and nomenclature of basalts. I.U.G.S. Subcommission on the Systematics of Igneous Rocks. Circ. 34, Contribution 87: 1-19.

CARMIGNANI L., ALI KASSIM M. and FANTOZZI P. (1984). Nota preliminare sul rilevamento della regione di Gedo (alta valle del Giuba, Somalia meridionale). Univ. Naz. Somala. Quad. Geol. Somalia, 85-109.

DE ANGELIS D'OSSAT G. and MILLOSEVICH F. (1900). Studio geologico sul materiale raccolto da M. Sacchi (seconda spedizione Bottego). Soc. Geogr. It., 1-212.

DE LA ROCHE H., LETTERIER J., GRANDCLAUDE P. and MARCHAL M. (1980). A classification of volcanic and plutonic rocks using R1-R2 diagram and major elements analyses, its relationships with current nomenclature. Chem. Geol., 29: 183-210.

MANASSE E. (1916). Rocce della Somalia italiana raccolte dalla missione scientifica Stefanini-Paoli del 1913. Mem. Soc. Tosc. Sci., 31: 1-74.

WATSON E.B. (1982). Basalt contamination by continental crust: some experiments and models. Contr. Miner. Petrol., 80: 73-87.

ZANETTIN B. (1984). Proposed new chemical classification for volcanic rocks. Episodes, 7: 19-20.

*Final editing, January 1990*

From *Geology and mineral resources of Somalia and surrounding regions*, Ist. Agron. Oltremare, Firenze, Relaz. e Monogr. 113, 259-278, 1993.

# STRATIGRAPHY, FACIES DEVELOPMENT, AND TRACE FOSSILS OF THE UPPER CRETACEOUS OF SOUTHERN TANZANIA (KILWA DISTRICT)

G. ERNST and J. ZANDER

Institut für Paläontologie, Freie Universität Berlin, Schwendener Strasse 8, D-1000 Berlin 33, Germany.

ABSTRACT

Newly exposed Upper Cretaceous sequences of marls and clayey-marls interbedded with sandstones are described from the coastal zone of Southern Tanzania, East Africa. A series of road cuts exhibit a usable standard section from the Santonian to the uppermost Upper Campanian or Maastrichtian, as determined through foraminifera assemblages. Large stratigraphic gaps cannot be established except for a possible break in the "middle" Campanian. This sequence of rocks contains an exceptional trace fossil assemblage identified as a *Nereites* ichnofacies, characteristic of flysch deposits. Geological and microfaunal evidence suggests that these sedimentary sequences were deposited in a shelf paleo-environment, affected by storms, while the ichnological evidence indicates perhaps the presence of small-scale troughs or basins on the shelf.

## INTRODUCTION

In the southern coastal region of Tanzania (South Mainland coast zone of KENT et al. (1971), a broad stripe of Jurassic, Cretaceous, and Tertiary sedimentary rocks occur (AITKEN, 1961). These rocks are regarded as a regressive succession onlapping a continental margin. Exposure is generally poor and discontinuous in the area. This is especially so for the Upper Cretaceous in the District of Kilwa between Dar es Salaam and Lindi which is little known or studied due to the lack of exposure. Only MOORE (1963, 1965) published a geological map with short comments of the Kilwa area.

In 1985-1987 west of the towns of Kilwa-Masoko and Kilwa-Kivinje, new road construction has for the first time exposed fresh continuous outcrops of the Upper Cretaceous (Fig. 1). Some of the new sections were observed during two excursions to the dinosaur beds of Tendaguru. These sections are exceptional in the fact that they contain a diverse ichnofauna which does not fit into the depositional model derived from the paleontological and general geological analysis.

## LOCALITIES

Along the main road from Kilwa-Masoko through Nangurukuru toward Dar es Salaam, new road construction has produced about a dozen fresh road cuts (Fig. 1). Northwest of the bridge over the Mantandu River, grey to variegated lowermost Upper Cretaceous marls with sandstone intercalations predominate. Interesting sections from a ichnological point of view were found southeast of Matandu up to the road junction at Nangurukuru. These sections were numbered according to stratigraphic age, younging toward Nangurukuru. Within these road cuts, up to 500 meters long, interstratified sandstones and marls contain the mentioned ichnofauna. The thick marl sequences are interrupted irregularly by singular calcareous sandstone layers or grouped packages of thin sandstone layers. Three sections (n. 1, 2, 5; Fig. 1) were only superficially surveyed. Three other sections were measured in detail (n. 3 , 4; Figs. 1, 2; Plate 1, Figs. 1, 2). Section 3 is located near the locality of Kigombo, approximately northwest of the valley containing Matezampi Brook. In Section 4, about 1.200 m NW of the road junction at Nangurukuru, two separate sections on either side of the road (Nangurukuru A, B) were measured.

The Upper Cretaceous sedimentary rocks in the rolling hills of the region between Nangurukuru and Mantandu exhibit gently sloping synclines and anticlines.

Section 2 cuts into the core of a syncline, while anticlinal doming is projected to occur in the covered area between Section 2, 3. General strike direction varies between NW and NNE, mainly toward the NNE. Dip directions are mostly toward the east while dip slopes are generally only a few degrees, with a maximum dip of 20° SE measured at Section 2. Exact measurement of stratigraphic thicknesses are difficult in this tectonically disturbed area. About 300-400 meters of section was estimated between Mantandu and Nangurukuru as Santonian Campanian, and perhaps Maastrichtian, while MOORE (1963, 1965) established about 2000 feet (~ 600-700 meters) of thickness for the Conacian to Maastrichtian in the region of Kilwa.

## STRATIGRAPHY AND MICROFAUNA

Stratigraphic subdivision and correlation among the described sections are based on lithostratigraphy and microfaunal evidence.

### Lithostratigraphy

A detailed lithologic comparison over the short distance between Nangurukuru A and B is possible with the thin calcareous sandstone layers interstratified with the marls and clayey to sandy marls (Fig. 2). However, the rapid lateral changes in thickness and bedding makes lithostratigraphic correlation tenuous. A unique feature of these two sections, layers of "Topf-Konkretionen" or pot-shaped concretions or nodules, are

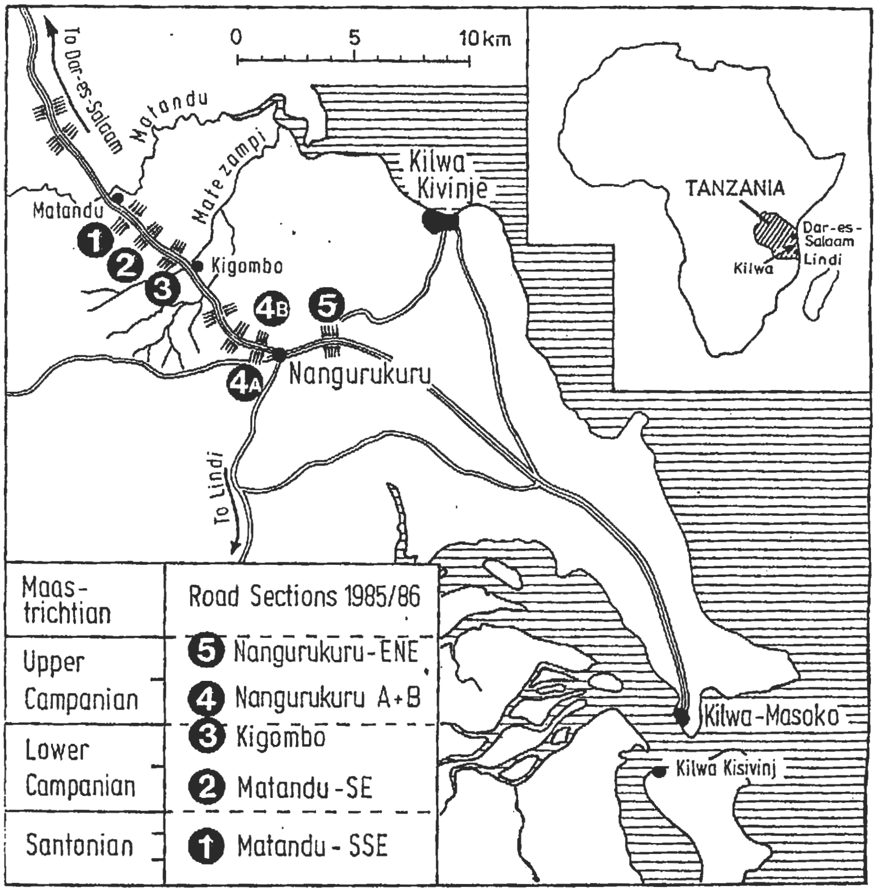


Fig. 1 - Map of the study area in the Kilwa District with the location and stratigraphic position of the road cuts. Topographical data and local names after MOORE (1963).

present in the upper portion of the Nangurukuru sections and contributes stratigraphic control. Correlation between the Nangurukuru sections and Kigombo section is tenuous. It appears to be possible that the thick uncemented fine yellow sand body at Kigombo corresponds stratigraphically with comparable sand bodies between Kigombo and Nangurukuru.

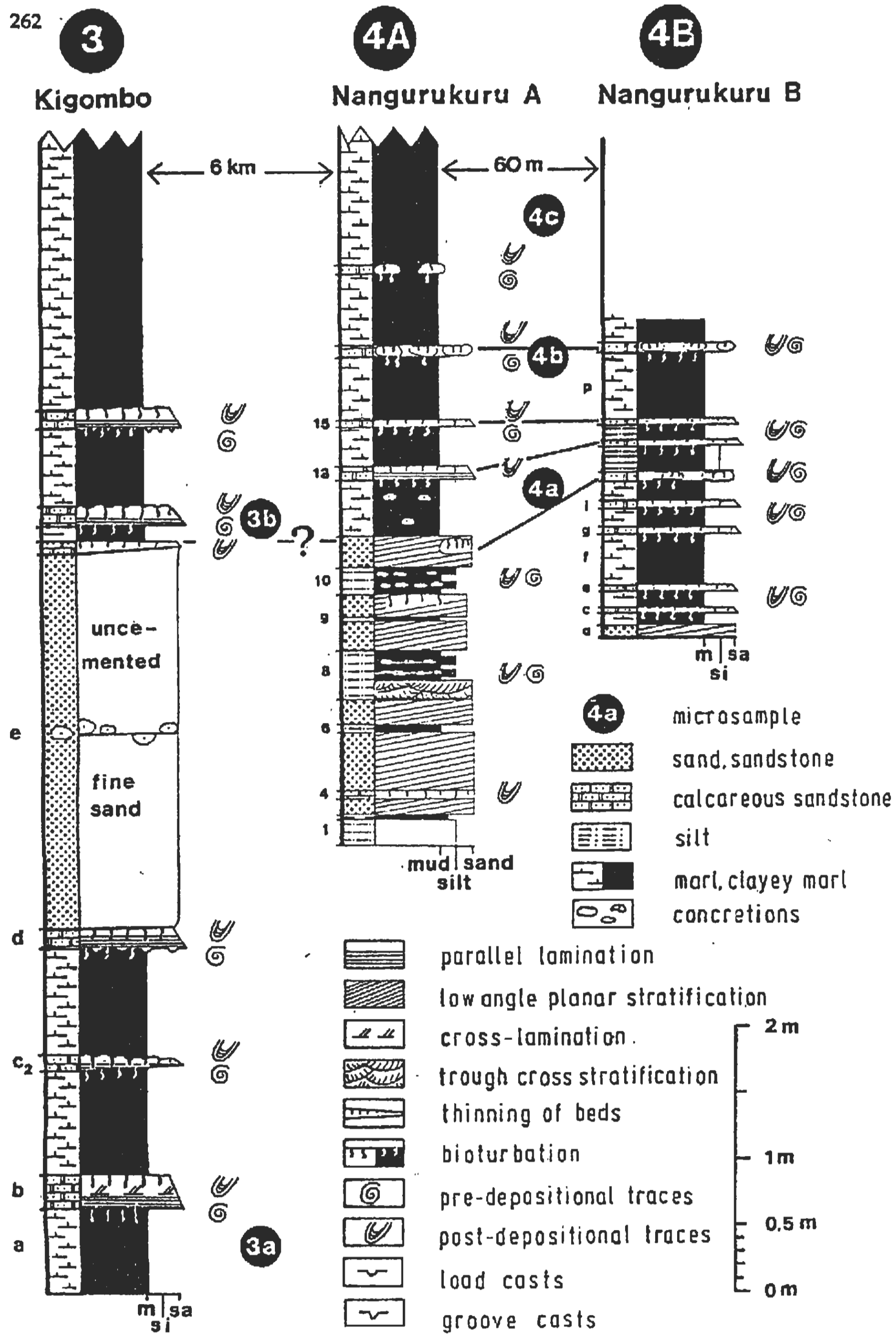


Fig. 2 - Measured sections from the road cuts near Nangurukuru (Sections 4A and 4B) and the lower part of Kigombo (Section 3) with the thick "middle" Campanian sand package in mid-section.

## Biostratigraphy

The marls and clayey to sandy marls of the described sections contain a somewhat diverse foraminifera fauna, from which stratigraphic and paleoecological data can be obtained. Reported here are the results derived from ten samples from Sections 1 through 5, highlighting a cross section through the uppermost Upper Cretaceous. The preservation and composition of the fauna is variable which indicates different stratigraphic and bathymetric controls.

### Santonian

Two samples from Section 1 (1a and 1b from Mantandu S-SE) are placed into the Santonian. Planktonic forms include:

| | | | |
|---|---|---|---|
| | *Dicarinella concavata* (BROTZEN) (abundant): | 1a | |
| * | *D. asymetrica* (SIGAL): | 1a | 1b |
| | *Marginotruncana undulata* (LEHMANN): | 1a | |
| | *M. sinuosa* (PORTHAULT): | 1a | |
| | *M. paraconcavata* (PORTHAULT) (rare): | 1a | |
| * | *M. sigali* (REICHEL) (rare): | 1a | |
| * | *Globotruncanita* cf. *elevata* (BROTZEN): (mainly preserved as compressed forms) | | 1b |
| | *Globotruncana ex gr. arca*: | | 1b |
| | *G. linneiana* (D' ORBIGNY): | | 1b |
| | *Rosita fornicata* (PLUMMER): | | 1b |

The forms marked by an asterisk (*) are important index fossils.

The association of Sample 1a belong to the *asymetrica*-zone of the Santonian. The forms of Sample 1b, taken some ten meters above Sample 1a, are assigned to the uppermost Santonian where *G. elevata* and *D. asymetrica* overlap. Planktonic forms dominate in both samples, comprising up to 90% of the samples. The plano-convex morphotypes *Dicarinella concavata*, *D. asymetrica*, and *Marginotruncana paraconcavata*, which dominate the association, indicate "deeper water" conditions (HART and BAILEY, 1979).

The benthic forms within Sample 1b is evenly distributed among calcareous Nodosariacea (e.g., *Lenticulina* sp.) and Cassidulinacea (e.g., *Gyroidinoides* sp.), and arenaceous Lituolacea (e.g., *Marsonella* sp.) forms. Within Sample 1a, the calcareous Nodosariacea dominate. The benthic foraminifera, especially the rare form *Gyroidinoides* sp., likewise suggest a deeper shelf paleoenvironment.

### Lower Campanian

Two samples from Section 2 (2a, 2b from Mantandu-SE) and one from the bottom portion of Section 3 (3a from Kigombo) are dealt with here. Plankter representatives include:

| | | | | |
|---|---|---|---|---|
| * | *Globotruncanita elevata* (BROTZEN): | 2a | 2b | 3a |
| | *Globotruncana linneiana* (D'ORBIGNY): | 2a | 2b | 3a |
| * | *Marginotruncana coronata* (BOLLI): | 2a | 2b | |
| | *M. sinuosa* ( PORTHAULT): | 2a | 2b | |
| | *Rosita fornicata* (PLUMMER): | 2a | 2b | 3a |
| | transitional forms between | | | |
| | *M. sinúosa* and *R. fornicata*: | 2a | | |
| | Heterohelicidae, div. gen, div. sp.: | 2a | 2b | 3a |

*Globotruncanita elevata* is the index fossil of the *elevata*-zone in the Lower Campanian. *Marginotruncana coronata* and the transitional form *M. sinuosa-R. fornicata* from Section 2 characterize the lower *elevata*-zone.

Benthic foraminifera in all three samples are under-represented (Sample 2a, 2b: only ~ 10%; Sample 3a: ~ 40%). In Sample 3a, there appears to be an even proportion between calcareous and arenaceous benthics.

The general composition of the planktonic association exhibits significant differences. This is illustrated in the ratio between the representatives of the Heterohelicidae and those of the Globotruncanidae (*Globotruncana, Globotruncanita, Marginotruncata, Rosita*, etc.). In the red marls of Sample 2a, the ratio is 30% : 70%, while in the grey marls of Sample 2b, it is 60% : 40%. Even though grey and red marls alternate over a few meters distance in the upper part of Secton 2, microfaunal composition from neighbouring layers present reversed ratios.

It is important to also note that the number of taxa from the Heterohelicids from Sample 2a to 2b drops from five to two. Associations dominated by Heterohelicids may originate from differing water temperatures and/or shallower water shelf paleoconditions (CARON, 1985; HAIG, 1979).

Plate 1

Fig 1 - View of Section 4A, Nangurukuru A, W-NW road cut, beds 1-18. Note the poorly cemented, thick sandstone layers in the lower part and the thin calcareous storm sandstone layers and concretions intercalated with marls and clayey to sandy marls in the upper part.

Fig. 2 - View of Section 4B, Nangurukuru B, beds a - r. Note the well-exposed thin calcareous storm sandstone layers topped by concretion layers.

Fig. 3 - Calcareous sandstone bed (Facies 2), bed b from Section 3 (Kigombo). Note small Fe-concretions and trace fossils at the base followed by parallel lamination and topped by ripple cross-lamination. Uppermost Lower Campanian.

Fig. 4 - Sole of bed h from Section 3 (Kigombo). Note the distinct groove casts (left to right), the partially destroyed honeycomb network of the pre-depositional *Paleodictyon*, and the various post-depositional traces.

Fig. 5 - Sandstone bed 5 from Section 4A, Nangurukuru A. The low-angle planar stratification is marked by mm thin laminae of heavy minerals.

Fig. 6 - Fresh excavation in the Recent beach sands ca. one km north of the Jubba River mouth in southern Somalia. Note the dark parallel laminae of heavy minerals. Backshore region of the beach.

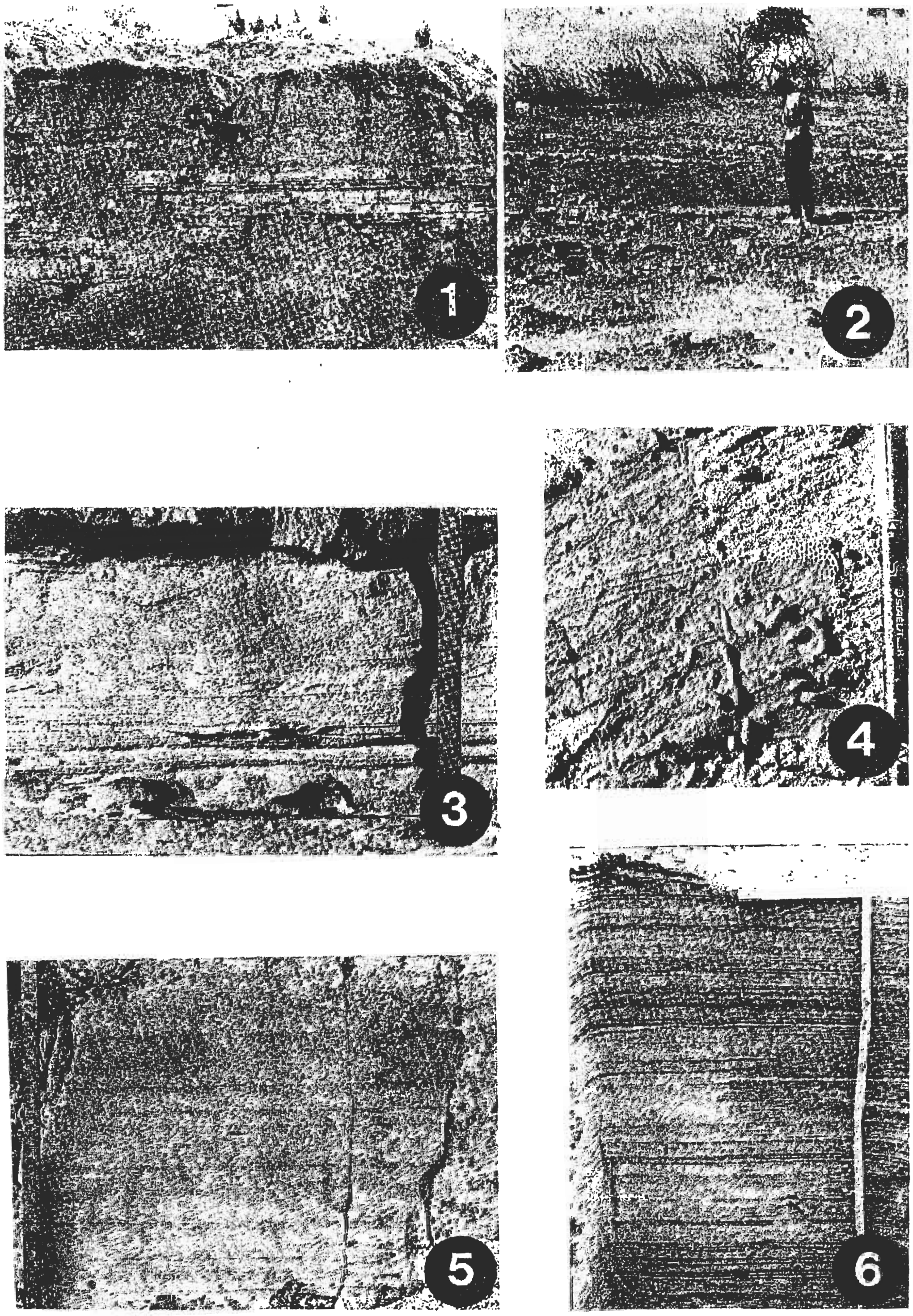
1
2
3
4
5
6

## Upper Campanian

Section 4 (4a to 4c from Nangurukuru) and perhaps the upper portion of Section 3 (3b from Kigombo) represent the Upper Campanian. The composition of the foraminifera association shows a dependence upon relative position to the thick poorly cemented sand horizons at Kigombo and Nangurukuru (Fig. 2). Sample 3b and 4b contains no plankters, Sample 4a a few, and Sample 4c about a third of the fauna. The following planktonic foraminifera were identified in Sample 4c.

* *Globotruncana ventricosa* WHITE (common)
* *G. rosetta* (CARSEY) (abundant)
*G. linneiana* (D'ORBIGNY) (abundant)
*G. bulloides* VOGLER (common)
*G. orientalis* EL NAGGER (rare)
*Globotruncanita stuartiformis* (DALBIEZ) (very abundant)
*Rugoglobigerina rugosa* (PLUMMER) (rare)
*Rosita fornicata* (PLUMMER) (rare)
* *R. patelliformis* (GANDOLFI) (rare)

The double-keeled genus *Globotruncana* dominates with five species. The asterisked forms are indicative of the *ventricosa*-zone. Since the exact boundary of the sub-stages in the Campanian are still controversial, the *ventricosa*-zone can be placed completely within the Upper Campanian or it begins at the transition between the Upper and Lower Campanian.

The rich benthic fauna contains a rare index fossil form, *Neoflabellina rugosa* (D'ORBIGNY). Much more abundant are the calcareous Nodosareacea (*Lenticulina* sp.; *Dentalinoides* sp.) and Lituolacea as well as the arenaceous Ammodiscacea (e.g. *Ammobaculites sp.*). The Ammodiscacea comprise mostly simple rolled forms or elongated agglutinated forms. Their dominance in Sample 4a, 4b suggests coastal shelf paleoconditions, with Sample 4c further off-shore (HAIG, 1979). In Sample 3b, the Ammodiscacea represent nearly the entire benthos microfauna while in Sample 4a they comprise a majority. Within Sample 3b the ratio of arenaceous Ammodiscacids to calcareous benthics is 1:1.

## Uppermost Campanian To Maastrichtian.

Section 5 (Nangurukuru E-NE) probably represents, through geological position and microfaunal evidence, the youngest part of the Upper Cretaceous exposed in the road cuts. After MOORE (1963), this section lies at the boundary or within the Paleocene. Within its sandy marls, the calcareous planktonic foraminifera could not be determined due to partial dissolution of shells. The benthics include the following forms:

*Bolivina incrassata incrassata* REUSS (abundant), *B. incrassata crassa* VASILENKO and MYATLIUK (rare), *Neoflabellina rugosa caesata* (WEDEKIND) (rare), *Lenticulina* sp.

(rare), *Gavelinella* sp. (abundant), *Verneuilina tricarinata* (D' ORBIGNY) (abundant). *B. incrassata incrassata* range from the uppermost Upper Campanian to Upper Maastrichtian and *B. incrassata crassa* from the most uppermost portion of the Upper Campanian to the Upper Maastrichtian (KOCH, 1977). Therefore, Section 5 is placed either within the uppermost Upper Campanian or, more likely, in the Maastrichtian.

### Microfauna And Paleoenvironment

The foraminifera fauna from the road cuts in all cases represents a shelf paleoenvironment. The table below summarizes the paleoecological inferences, such as water depth and shelf position, from the above discussed microfaunal samples.

| | | | |
|---|---|---|---|
| MAASTRICHTIAN to uppermost UPPER CAMPANIAN | | Sample 5 | near shore |
| UPPER | *ventricosa* -zone | Sample 4c | deeper, "middle" shelf |
| CAMPANIAN | | Sample 4a, 4b | off shore |
| | | ? Sample 3b | near shore |
| "middle" CAMPANIAN | | thick sand bodies and sand layers | shore to inner shelf |
| LOWER | upper *elevata*-zone | Sample 3a | nearer to shore |
| CAMPANIAN | lower *elevata*-zone | Sample 2a, b | deep water, outer shelf |
| SANTONIAN | upper *asymetrica*-zone | Sample 1b | deep water, zone outer shelf |
| | lower *asymetrica* -zone | Sample 1a | deep water, outer shelf |

A reduction in water depth appears to have occurred during the Lower Campanian. Above the dividing thick fine sand bodies (Sect. 3) or the sand layers (Sect. 4), water depth may have increased into the Upper Campanian. This may suggest that the deposition of the thick sand bodies occurred during the regression of the "middle" Campanian. This time slice is also recognized in Europe (e.g. northern Spain and northwest Germany) as a regressive phase (ERNST and SCHMID 1979, and unpublished data of ERNST G.).

KENT et al. (1971) postulates that the limited microfauna and small forms of the Upper Cretaceous along the Tanzanian coast were a result of lower salinities and limited circulation on the shelf. However, our foraminiferal analysis presented here conflicts with this hypothesis.

### Macrofauna

Besides the trace fossils, only large, mostly fragmented inoceramids were found at Section 5; they occur in layers within the marls or their fragments are reworked at the base of sandstone layers. The inoceramid shells are rarely colonized with oysters. Likewise, MOORE (1965) mentioned the occurrence of reworked *Inoceramus* fragments along the Nangurukuru-Kilwa Kivinje road and in the Ukuli valley. He placed them at the base of the Paleocene. According to our results, *Inoceramus* was found to co-exist with Upper Campanian to Maastrichtian foraminifera at Section 5. This calls into question the positioning of the Cretaceous/Tertiary boundary by MOORE (1963). In our opinion, the boundary represents a stratigraphic gap.

## SEDIMENTARY STRUCTURES

The road sections between Matandu and Nangurukuru are composed of grey or tan marls and clayey to sandy marls interbedded with fine to medium-grained sandstones. Four facies types dominate:

Facies 1 - clayey marls, marls, or silty to sandy marls.
Facies 2 - thin calcareous sandstone beds.
Facies 3 - fine sandstone beds (heavy minerals define layers).
Facies 4 - fine sandstone bodies
Facies 1 contains the described foraminifera fauna and can be decimetres to tens of meters in thickness.

The thin calcareous sandstone beds (Plate 1, Fig. 3, 4) of Facies 2 vary from centimetres to decimetres in thickness with great lateral changes. The lower contacts are abrupt with current and scour markings on the soles. Broken pieces of *Inoceramus* shells, as mentioned above, were found at the base of several sandstone layers at Section 5. Most sandstone layers exhibit normal grading. These thin sandstone beds commonly contain parallel lamination or relatively thicker layers have parallel lamination topped by ripple cross-lamination. Lamination is mostly defined by heavy minerals. Most of these sandstones layers are bioturbated, especially toward the top. (See Sec. 5 for trace fossil descriptions.)

At the road cut east of Nangurukuru (Section 5), several sandstone beds appear to have been deposited as large-scale cut and fill structures. Also, the sandstone layers are normally not continuous layers but pinch out over a few meters distance. Some of them change laterally into separate nodules or concretions. In some cases, especially layer 11 and 17 at Nangurukuru A and layer k at Nangurukuru B, these concretions have a pot-shaped form ("Topfkonkretionen"). Under the "cover" of these concretions, a rich ichnofauna is present. It is preserved as concave epireliefs and dominated by *Buthotrephis* (Plate 3, Fig. 6).

The poorly cemented thicker yellow sandstone layers of Facies 3 (Nangurukuru A) contain very low angle planar cross-stratification, parallel lamination, and rare trough cross-stratification. Bioturbation is rare in these thick sandstone layers. Most of the layers contain a significant amount of heavy minerals which define layering (Plate 1, Fig. 5).

The sand bodies of Facies 4 are longitudinally-shaped with an average length of 100 m. Also composed of uncemented fine sand, the layering is difficult to see due to the lack of heavy minerals. Parallel lamination can be recognized in some parts of the exposure. Some vertical to oblique trace fossils are present.

## TRACE FOSSILS

Bioturbation occurs generally in the upper portions of the thin calcareous sandstone layers and concretions (Facies 2), but can also be found throughout. Many are present on the soles of the sandstone beds. Preservational forms include full reliefs, concave epireliefs, and convex hyporeliefs. The trace fossil association of the Campanian sections can be divided into types: pre-depositional and post-depositional ichnofauna.

### Pre-depositional ichnofauna

The trace fossils that appear to be pre-depositional in nature were formed by animals within the marls and clayey marls (Facies 1). These traces were sometimes partially eroded and infilled through catastrophic sand deposition and preferentially preserved on the soles of the sandstones. Evidence for this lies in the fact that these trace fossils are rarely complete and appear to have been partially destroyed by depositional currents (Plate. 1, Fig. 5). Pre-depositional association includes *Paleodictyon*, *Spirorhaphe*, *Urohelminthoida*, *Cosmorhaphe*, *Paleomeandron*, and *Protopaleodictyon* ( see Plate 2). The diversity appears to be relatively high since several "species" of *Paleodictyon* and *Spirorhaphe* can be differentiated on the basis of size. However, *Paleodictyon*, *Spirorhaphe*, as well as *Cosmorhaphe* are relatively rare and appear to be restricted to certain layers.

Whether this is due to variation in preservational potential or true diversity is unclear. (Trace fossils are identified here only by genera; detailed descriptions will be published elsewhere.)

### Post-depositional ichnofauna

Post-depositional trace fossils or those traces which were made subsequent to the deposition of the thin sandstone layers are found distributed throughout these beds. Some are identified as *Scolicia, Zoophycos, Diplocraterion, Granularia,* and *Buthrotrepkis* (see Plate 3). This ichnofauna is abundant and specific genera are hard to recognize due to the amount of bioturbation within some of the sandstone beds and concretions. Certain forms appear to be restricted to certain layers or within concretions. For example, *Buthotrephis* was found only within the concretion layers of Section 4 and 5, while *Scolicia* was only abundant in some layers at Section 1.

### Paleoecology

The ichnogenera of these sequences in general are diagnostic of the *Nereites* ichnofacies (FREY and PEMBERTON, 1984). This trace fossil assemblage or ichnofacies is normally characteristic of deep water flysch sequences (CRIMES, 1973; KERN, 1980; CRIMES et al., 1981). Considering the paleoecological implications, the animals of the pre-depositional ichnofauna of the Kilwa District required muddy, quiet, very low energy conditions to build their traces, similar to conditions in the deep sea. The organisms of the post-depositional ichnofauna required sandy, relatively higher energy conditions to survive. Within "flysch" environments, the high energy

Plate 2
Pre-depositional trace fossils
Fig 1 - ***Paleodicyton*** ichnosp. Section 2, Mantandu-SE; lowermost Lower Campanian.
Fig. 2 - ***Protopaleodicyton*** ichnosp. Section 3, Kigombo, bed $c_2$; uppermost Lower Campanian.
Fig. 3 - ***Spirorhaphe*** ichnosp., smaller form. Section 3, Kigombo, bed h; "middle" Campanian.
Fig. 4 - ***Spirorhaphe*** ichnosp., larger form. Section 4, Nangurukuru B, bed i; lowermost Upper Campanian.
Fig. 5 - ***Granularia*** ichnosp. Section 1, Mantandu-SSE; Santonian.
Fig 6 - ***Cosmorhaphe*** ichnosp. Section 3, Kigombo, float from below bed e; uppermost Lower Campanian.

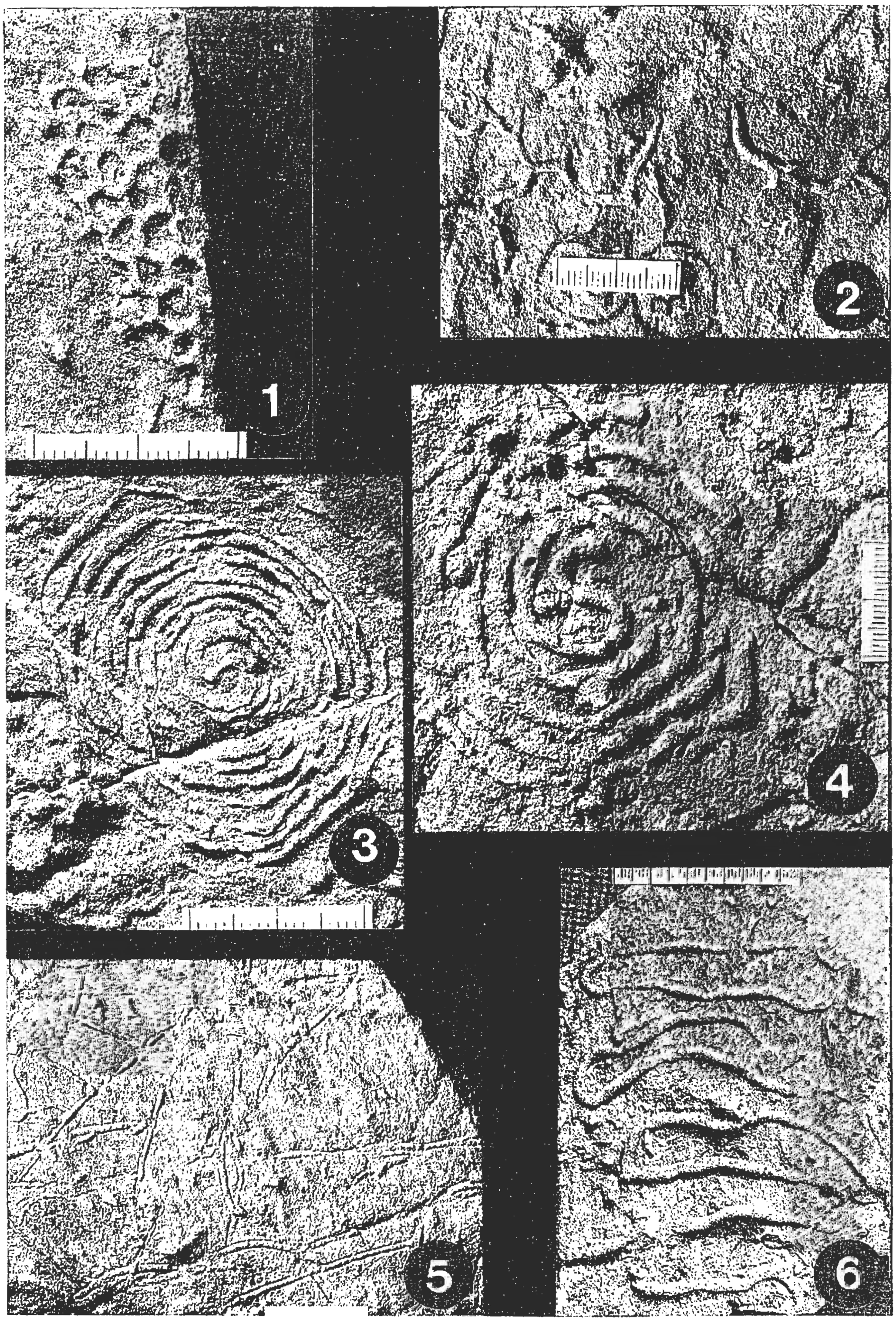
1
2
3
4
5
6

requirements are met within the channels of a turbidite fan while the low energy conditions exist between depositional events. In such a low energy environment, deposition comprises settle out of suspended-fine material, such as clays and marls.

## REGIONAL GEOLOGY AND TECTONICS

A stable, epeiric continental shelf is postulated to have existed along the coastal zone of Tanzania since the Middle Jurassic (KENT, 1972). Marine conditions were probably initiated through the southeastward rifting of the Madagascar-Indian plate away from Africa (c.f. RABINOWITZ et al., 1983; HULVER, 1985). Rifting ceased perhaps in the Lower Cretaceous and a long period of "exceptional stability" lasted through the Early Tertiary (KENT et al., 1971).

The regressive nature of the Tanzanian shelf succession, though oscillatory, was probably due to the seaward build-up of onlap sediments (KENT et al., 1971). Minor faulting in the study area is described by KENT et al.(1971) in the Upper Cretaceous. Eastward tilting and hinging on old fault lines may have produced irregularities on the shelf. Some major scale slumping has been documented from an area south of Kilwa (KENT et al., 1971 from HENNIG, 1914) where "steeper" zones may have existed because of these irregularities. Small-scale slump features are also present in some of our road cuts.

## DEPOSITIONAL MODEL

From the sedimentary structures, stratigraphy, ichnology, regional geology, and tectonics of the study area, a general depositional model can be constructed for the Upper Cretaceous west of Kilwa. According to regional geology and tectonic data, deposition occurred on an epeiric continental shelf.

**Plate 3**

Post-depositional trace fossils

Fig. 1 - Burrows within the thick sandstones (bed 9 and 10) of Section 4, Nangurukuru A; lowermost Upper Campanian.

Fig. 2 - *Scolicia* ichnosp. Section 1, Mantandu-SSE, Santonian.

Fig. 3 - *Zoophycos* ichnosp., giant form. Section 1, Mantandu-SSE; Santonian.

Fig. 4 - *Zoophycos* ichnosp., small form. Section 4B, Nangurukuru B; lowermost Upper Campanian.

Fig. 5 - *Skolithos* ichnosp. Section 5, Nangurukuru ENE; uppermost Upper Campanian to Maastrichtian.

Fig. 6 - *Buthotrephis* ichnosp. Section 4A, Nangurukuru A; concretion layer; lowermost Upper Campanian.

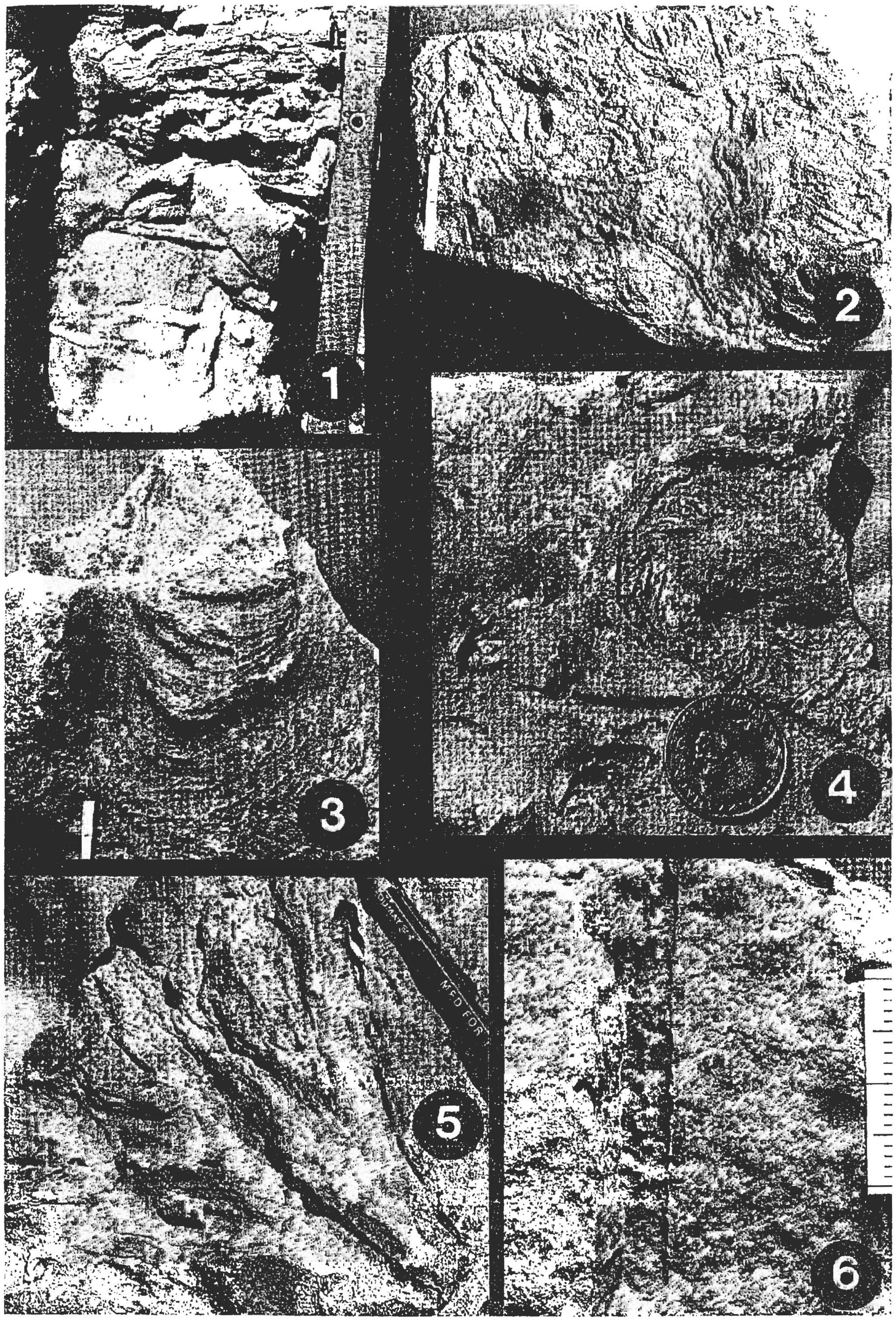
1
2
3
4
5
6

The foraminiferal evidence from stratigraphic data also points to a shelf paleoenvironment where background sedimentation of clays and marls normally predominates (Facies 1).

The thinner allochthonous calcareous sandstone layers (Facies 2) are comprised of incomplete Bouma sequences (BOUMA, 1962); waning flow sequences are suggested by the parallel to cross-lamination sequences. These sedimentary structures are common within turbidites and tempestites (WALKER, 1984) and can be best described as storm sand-layers within the context of a shelf paleoenvironment (ALLEN, 1982). Deposition would occur during a major storm in which sandy material pushed shoreward would become liquified by mixing and then would move again seaward to be deposited. The sand deposited below storm wave base would resemble turbidites with incomplete waning flow sequences. Since the term turbidite suggests grain flow fluidized flow in a deep basinal environment while the term tempestite implies traction-deposited sequences containing shell layers and hummock cross-stratification, storm sand-layers might be a more appropriate interpretative, descriptive expression. Lateral differences in storm sand-layers across a shelf would be dependent upon such variables as storm duration, wind speed, slope angle of shelf, and distance from shore (ALLEN, 1982). Cut and fill channels would be common.

The thicker fine sandstone layers (Facies 3) are more difficult to analyze due to the limited exposure. They superficially resemble the beach deposits that are found along the modern coast of East Africa, especially in Southern Somalia near the mouth of the Jubba River (Plate 1, Fig. 6).

The fine sandstone bodies (Facies 4) may represent linear sand ridges or sand waves that are commonly found on ancient and modern continental shelves (e.g. Modern shelves: e.g. HOUBOLT, 1968; SWIFT et al., 1978; STUBBLEFIELD et al., 1984; SWIFT et al., 1984; Cretaceous seaway: SHURR, 1984; SWIFT and RICE, 1984). Though the exact origin for these sands is still under debate; these sand ridges and sand waves can be basically described as sand bodies reworked on a shelf by currents tidal, oceanic, or storm-generated (WALKER, 1984) into dune-like structures and/or are relict regressive sand bodies. Sedimentary structures within these ridges include cross-stratification and parallel lamination. Since exposure is poor, the exact geometry of the Campanian thick sand bodies is difficult to reconstruct. Their longitudinal axis seem to be parallel to the former shore line.

From an ichnological point of view, a shelf paleoenvironment is unsatisfactory since the animals of the pre-depositional ichnofauna required a quiet, very low energy paleoenvironment with background sedimentation which was periodically but catastrophically inundated with sands. Continental shelf deposits are normally influenced by different types of currents (WALKER, 1984). KENT et al. (1971) limited circulation shelf theory is appealing but difficult to prove.

However, the ichnological and paleontological interpretations can be reconciled with the presence of "steep zones" caused by irregularities due to hinging and minor faulting, as proven by the existence of slumping features (KENT et al., 1971). Perhaps these steep zones are small-scale troughs or basins on the shelf. Quiet, low energy conditions in these depressions probably would prevail, protected against normal shelf currents and waves. During large storms liquefied sand could be transported from shore and pour into these shelf basins under turbiditic hydrodynamic conditions.

## CONCLUSIONS

New road exposures west of Kilwa, between Matandu and Nangurukuru, in the coastal area of southern Tanzania reveal Upper Cretaceous sequences of marls and clayey to sandy marls interbedded with fine to medium-grained sandstones. Stratigraphic determinations based on foraminifera indicate a usable standard section from the Santonian to the Upper Campanian or Maastrichtian. Six stratigraphic levels are established: Santonian, uppermost Santonian, lowermost and uppermost Lower Campanian, lowermost Upper Campanian, and uppermost Upper Campanian to Maastrichtian. This sequence appears to be relatively continuous except for a break in the "middle" Campanian. A shelf paleoenvironment is postulated from tectonic, regional geology, and microfaunal evidence. Sedimentation conditions appear to have remained similar from the Santonian until the Upper Campanian with the marls and sandy to clayey marls punctuated at irregular intervals by sand layers or packages of thin distal sand layers.

Four facies can be differentiated. The marls and clayey to sandy marls (Facies 1) represent background sedimentation on a continental shelf. Thin calcareous sandstone beds (Facies 2) contain parallel lamination or parallel lamination to ripple cross-lamination sequences. Lower contacts are abrupt and contain current scour markings. These sandstones are interpreted to be off-shore storm sand-layers. The thicker sandstone beds (Facies 3) contain low angle cross-stratification to parallel lamination and trough cross-stratification. These rocks could be interpreted as beach deposits. The fine sandstone bodies (Facies 4) probably represent shelf linear sand ridges or sand waves of a hundred meter scale. Their longitudinal axis seems to be parallel to the former coast line.

A trace fossil assemblage is described for the first time from the Upper Cretaceous of East Africa. A pre-depositional ichnofauna consists of *Paleodictyon, Spirorhaphe, Urohelminthoida, Cosmorhaphe, Paleomeandron* and *Protopaleodictyon*. The tracemakers needed quiet, very low energy conditions to construct their complex burrow systems. The post-depositional ichnofauna includes *Scolicia, Zoophycos, Diplocraterion, Granularia,* and *Buthotrepis*. Higher energy conditions were required by the tracemakers of this ichnofauna. The depositional environment of these sequences in southern Tanzania was probably an epeiric continental shelf which was cyclically affected by large storms and could have had small-scale troughs or basins.

ACKNOWLEDGMENTS

Special thanks to Dr. PETER ICKLER (Dusseldorf-Neuss) who provided logistical help in the field-planning expeditions and providing vehicles. SABINE ZIX (Berlin) and SAMUEL KAMBONA IBRAHIM (Dar es Salaam - now deceased) assisted in the field. Also, the Department of Geology at the University of Dar es Salaam, especially Dr. KAPILIMA and Prof. Dr. SCHLÜTER, contributed support in the field and with laboratory work. Many thanks to Dr. RISCH (Munich) and DORTE SALOMON (Berlin) for their assistance in foraminifera identification, and Prof. Dr. BROMLEY (Copenhagen) for trace fossil identification. We are particularly grateful to Dr. E. GIERLOWSKI-KORDESCH (Berlin) for analyzing the ichnological and sedimentological features, and especially for translating and revising the manuscript.

REFERENCES

AITKEN W.G. (1961). Geology and Paleontology of the Jurassic and Cretaceous of southern Tanganyika. Geol. Surv. Tanganyika Bulletin n. 31, 144 pp.

ALLEN J.R.L. (1982). Sedimentary Structures: Their character and Physical Basis. Volume II. Developments in Sedimentology 30 B, Elsevier, Amsterdam, 663 pp.

BOUMA A.H. (1962). Sedimentology of some flysch deposits. Elsevier, Amsterdam, 168 pp.

CARON M. (1985). Cretaceous planktonic foraminifera. In: Plankton stratigraphy. BROLL H.M. et al. (eds), Cambridge Univ. Press. Cambridge, London, New York, 17-86.

CLIFTON H.E., HUNTER R.E. and PHILLIPS R.L. (1971). Depositional structures and processes in the non-barred high energy nearshore. Jour. Sed. Petrol., 41: 651-670.

CRIMES T.P. et al. (1981). Trace fossil assemblages of deep-sea fan deposits, Gurnigel and Schlieren flysch (Cretaceous-Eocene), Switzerland. Eclogae Geol. Helv., 74(3): 953-995.

CRIMES T.P. (1973). From limestones to distal turbidites: a facies and trace fossil analysis in the Zumaya flysch (Paleocene-Eocene), North Spain. Sedimentology, 20: 105-131

ERNST G. and SCHMID F. (1979). Multistratigraphische Untersuchungen in der Oberkreide des Raumes Braunschweig-Hannover. Aspekte der Kreide Europas, IUGS Ser. A, 6: 11-46.

FREY R.W. and PEMBERTON S.G. (1984). Trace fossil facies models. In: Facies Models. (Edited by WALKER R.G.) Geol. Assoc. Canada Reprint Series 1: 189-207.

GIERLOWSKI-KORDESCH E. and ERNST G. (1986). A flysch trace fossil assemblage from the upper Cretaceous shelf of Tanzania. In: Current Research in African Earth Sciences. (Edited by MATHEIS G. and SCHANDELMEIER H.) A.A. Balkema, Rotterdam, 217-221.

HAIG D.W. (1979). Global distribution patterns for Mid-Cretaceous foraminiferids. Jour. Foram. Res., 9(1): 29-40.

HART M.B. and BAILEY H.W. (1979). The distribution of planktonic foraminiferida in the Mid-Cretaceous of NW Europe. Aspekte der Kreide Europas. IUGS Ser. A, 6: 527-542.

HENNIG E. (1914). Beitrage zur Geologie und Stratigraphie Deutsch-Ostafrika. Arch. Biontol., 3(3): 1-72.

HOUBOLT J.J.H.C. (1968). Recent sediments in the southern bight of the North Sea. Geologie en Mijnbouw, 47: 245-273.

HULVER M.L. (1985). Cretaceous Marine Paleogeography of Africa. Masters Thesis, The University of Chicago.

HUNTER R.E., CLIFTON H.E. and PHILLIPS R.L. (1979). Depositional processes, sedimentary structures, and predicted vertical sequences in barred nearshore systems, northern Oregon coast. Jour. Sed. Petrol., 49: 711-726.

KENT P.E., HUNT J.A. and JOHNSTONE D.W. (1971). The geology and geophysics of coastal Tanzania. IGCG n. 6. National Environment Research Council, London.

KENT P.E. (1972). Mesozoic history of the east coast of Africa. Nature, 238: 147-148.

KERN J.P. (1980). Origin of trace fossils in the Polish Carpathian flysch. Lethaia, 13: 347-362.

KOCH W. (1977). Biostratigraphie in der Oberkreide und Taxonomie von Foraminiferen. Geol. Jb., A 38: 11-123.

MOORE W.R. (1963). Quarter degree sheet 256 and 256E, Kilwa. Scale 1:125.000. with a brief explanation of the geology. Map Geol. Surv. Tanganyika, G.S. 1727.

MOORE W.R. (1965). Geological notes on quarter sheets 256/256E, Kilwa and 255, Njinjo, Southern Region. Records Geol. Surv. Tanganyika, 11(1961): 21-31.

RABINOWITZ P.D., COFFIN M.F. and FALVEY D. (1983). The separation of Madagascar and Africa. Science, 220: 67-69.

SCHURR G. (1984). Geometry of shelf sandstone bodies in the Shannon Sandstone of southeastern Montana. In: Siliciclastic Shelf Sediments, (Edited by TILLMAN R.W. and SIEMERS C.T.), SEPM Spec. Publ. n. 34: 63-83.

STUBBLEFIELD W.L., MC GRAIL D.W. and KERSEY D.G. (1984). Recognition of trasgressive and post-transgressive sand ridges on the New Jersey continental shelf (and reply) In: Siliciclastic Shelf Sediments, (Edited by TILLMAN R.W. and SIEMERS C.T.), SEPM Spec. Publ. n. 34: 1-23 and 37-41.

SWIFT D.J.P., PARKER G., LANFREDI N.W., PERILLO G. and FIGGE K. (1978). Shoreface connected sand ridges on American and European shelves: a comparison. Estuarine Goast. Mar. Sci., 7: 257-273.

SWIFT D.J.P., MCKINNEY T.F. and STAHL L. (1984). Recognition of transgressive and post-transgressive sand ridges on the New Jersey continental shelf: discussion. In: Siliciclastic Shelf Sediments, (Edited by TILLMAN R.W. and SIEMERS C.T.), SEPM Spec. Publ. n. 34: 25-36.

SWIFT D.J.P. and RICE D.D. (1984). Sand bodies on muddy shelves: a model for sedimentation in the Western Cretaceous Seaway, North America. In: Siliciclastic Shelf Sediments, (Edited by TILLMAN R.W. and SIEMERS C.T.), SEPM Spec. Publ. n. 34: 43-62.

WALKER R.G. (1984). Shelf and shallow marine sands. In: Facies Models, (Edited by WALKER R.G.), Geol. Assoc. Canada Reprint Series n. 1: 141-170.

*Final editing, January 1990*

From *Geology and mineral resources of Somalia and surrounding regions*, Ist. Agron. Oltremare, Firenze, Relaz. e Monogr. 113, 279-310, 1993.

# ON THE EVOLUTION OF THE ETHIOPIAN VOLCANIC PROVINCE

B. ZANETTIN

Dipartimento di Mineralogia e Petrologia, Università di Padova, Corso Garibaldi 37, 35137 Padova, Italy.

ABSTRACT

This paper schematically summarizes:

a) the volcanic successions recognized until now in the "type area", i.e., central-eastern Ethiopian plateau, northern Ethiopian rift, and Afar;

b) the fundamental geochemical features of the various volcanic formations, indicating the systematic serial differences between the widespread fissural flood basalts (transitional) and the basalts of the shield volcanoes (alkaline);

c) the main tectonic episodes (formation of the rifts) and their role in the migration of volcanism.

Furthermore, the approximate areal extension of the volcanites emitted at different stages of the cycle is shown in simplified sketch maps.

Geochemical comparison between the transitional flood basalts occurring in the plateau and in the rift floor indicates that, in the course of the long-lasting Ethiopian volcanic cycle, the composition of the emitted magmas did not change appreciably. The same conclusion is also valid for alkaline basalts of different ages.

The Afar basalts are the most primitive and crystallized under the lowermost $fO_2$; is fact is interpreted as a consequence of the fact that the crust is thinner in Afar than elsewhere.

Similarity of composition also exists for the alkaline basalts, independently of their age, e.g., Oligocene to Miocene Termaber basalts from the plateau; basalts of the Recent Transversal Ranges in Afar.

## INTRODUCTION

The Tertiary volcanics of Ethiopia, although largely eroded, cover an area of about 600,000 km$^2$ (Fig. 1). Only few sectors of the territory have been studied, so far insufficiently. We will mention here the central-eastern part of the Ethiopian Plateau (hereafter "type area"), the northern part of the Ethiopian rift, and the central-northern part of the Afar rift. Other sectors are either largely or almost totally unknown.

This fact implies uncertainty in making correlations among the volcanic sequences of the type area and the coeval sequences of the other sectors, and the geological picture given here for the entire Ethiopian province must be considered as largely tentative.

In order to avoid misunderstanding in the terminology of the volcanic rocks, we will adopt here the classification diagram total-alkalis vs. silica (TAS) (Fig. 2). Alkali

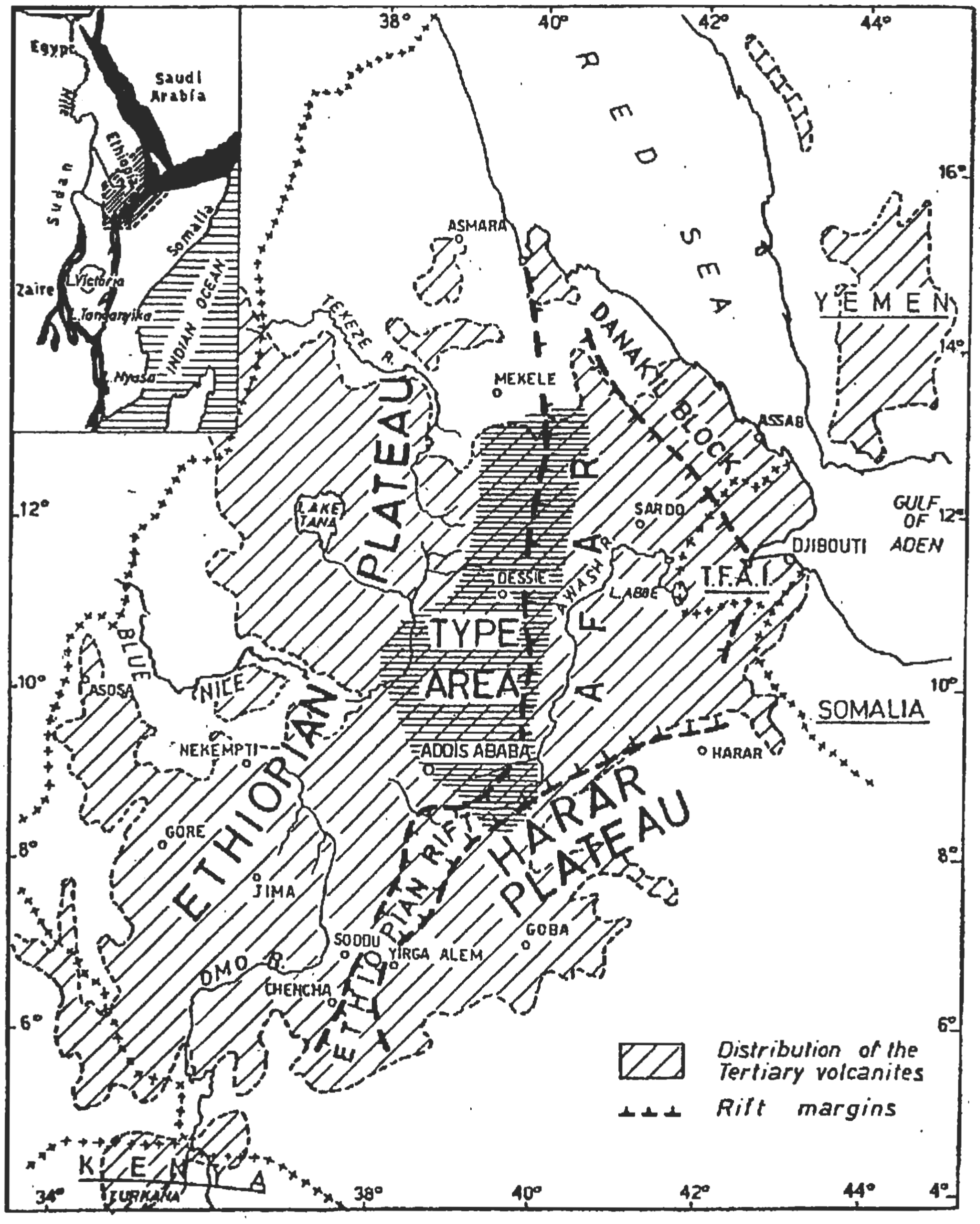


Fig. 1 - Ethiopian volcanic province. Location of "type area". Asymmetrical distribution of Tertiary volcanites with respect to present rifts may be explained by existence of an older, more westerly rift (see Fig. 5).

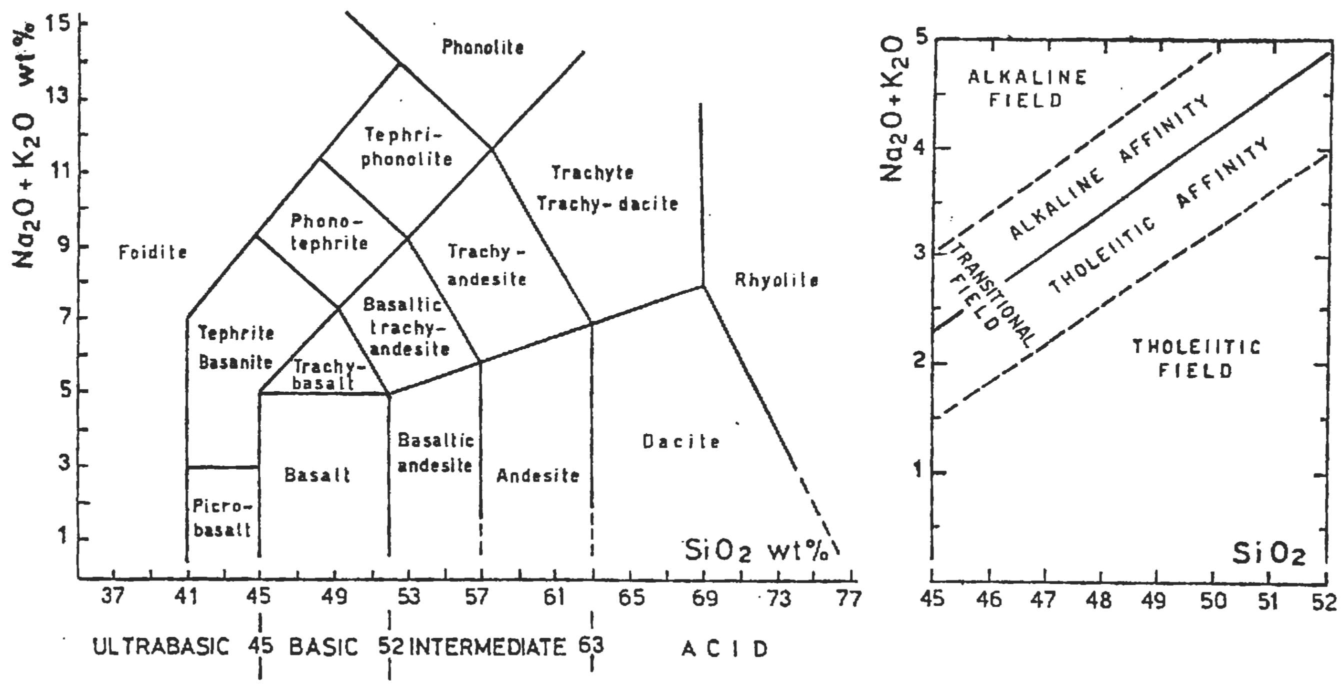


Fig. 2 - a) Total alkalis vs. silica (TAS) diagram (after LE BAS et al., 1986); b) on basalt field, Ethiopian flood basalts plot mainly in belt between dashed lines. These are transitional basalts with either alkaline or tholeiitic affinity (simplified after PICCIRILLO et al., 1979).

basalts are distinct from subalkali basalts according to the respective presence or absence of normative nepheline. Moreover, the term "transitional basalts" will be applied, as an approximation, to rocks that, in the TAS diagram, are confined within 1% total alkalis from the line separating some Hawaiian alkaline from subalkaline basalts. Transitional basalts plotting above that line are said to have alkaline affinity, those below the line, tholeiitic affinity.

Other chemical features of typical Ethiopian transitional basalts are: moderate values of $Al_2O_3$ (c. 13-14) and $TiO_2$ (2.5-3.1), and $K_2O$ contents (c. 0.4-1.1%) that, for a given percentage of silica, lie between those for alkaline and MORB tholeiitic basalts.

## STRATIGRAPHY

Until recently, the Ethiopian volcanics were divided into two main series: 1) Trap (= Plateau) Series; 2) Rift Series (Fig. 3). It is now generally accepted that, in the type area, the Trap Series was formed in the course of two clearly separate cycles or stages: the Ashangi cycle (50-35 Ma) and the older part of the post-Ashangi cycle (32-15 Ma). The Rift Series is younger than 15-13 Ma.

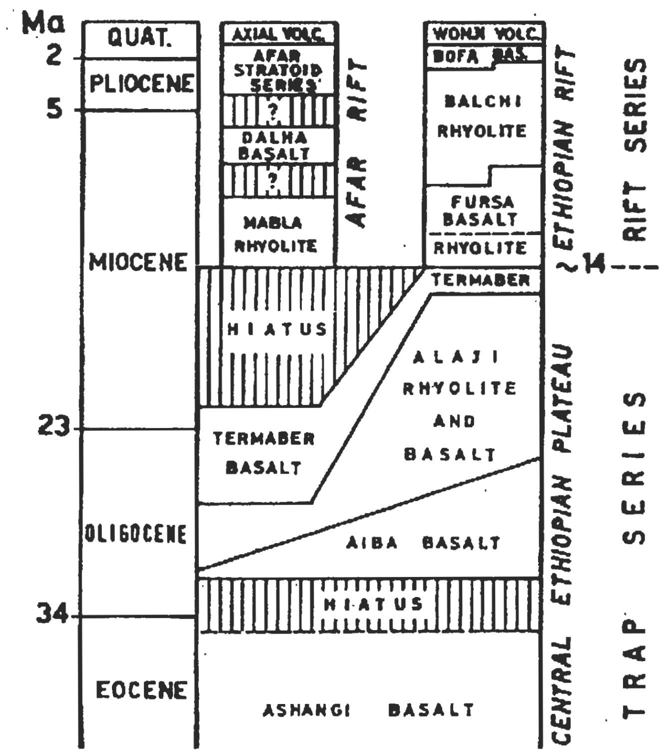


Fig. 3 - Schematic stratigraphic sequence of volcanics from type area and Afar rift (after ZANETTIN et al., 1978a, with modifications).

The chronological correspondence with the volcanic sequences recognized by other authors in the type area or in other sectors of Ethiopia is shown in Fig. 4.

## VOLCANISM OF THE TYPE AREA

### Plateau series

The following information on the type area is taken essentially from ZANETTIN and JUSTIN-VISENTIN (1974, 1975); ZANETTIN et al. ( 1974, 1978) and PICCIRILLO et al. (1979).

#### Ashangi Cycle (50 ? - 35 Ma).

Knowledge on the rocks of this cycle, which may have begun about 50 Ma ago, are fragmentary. They occur in Wollega (W Ethiopia) (MERLA et al., 1973; BERHE et al., 1987) and in the SW Ethiopian plateau (DAVIDSON et al., 1973), as well as in the type area. This areal occurrence is connected with a rift system now buried under younger volcanics. Its northern branch trends E-W, i.e., almost perpendicular to the present W Afar escarpment. Another rift branch is presumed to have run from Lake Tana on the Kenyan border (ZANETTIN et al., 1980) (Fig. 5).

Information on the nature of the Ashangi rocks is also scanty. In the type area, the "fissural" basalts are represented by transitional basalts with tholeiitic affinity, while the more frequent "moderately fissural" basalts are still transitional but with alkaline affinity, and are characterized by a lower $Na_2O/K_2O$ ratio and lower content in $Al_2O_3$ (9-12%) (Table 1, cols. 1-2; Figs. 6, 7).

In SW Ethiopia silicic rocks were also emitted (MOORE and DAVIDSON, 1978).

#### Post-Ashangi cycle

Plateau sequences: Aiba and Alaji fissural volcanism (32-15 Ma).

The new cycle began with the emission of huge volumes of lavas, flooding the peneplain which formed after the end of the Ashangi cycle. These lavas - the Aiba basalts 32-25 Ma old - are typical transitional basalts, very homogeneous in composition (Fig. 6). They are generally followed by the Alaji volcanics, represented by interlayered silicic rocks and transitional basalts, but sometimes only by silicic rocks, mostly slightly peralkaline rhyolites. In the type area (Fig. 8) the Alaji rhyolites occur only close to the eastern edge of the Ethiopian plateau and in the underlying escarpment: a demonstration that their emission was controlled by tectonics (see also Fig. 19). In the course of time the Alaji volcanism died out in the northern areas and was progressively confined to the south. This fact allowed us to clarify that the Afar escarpment began to form in the north 30-25 Ma ago and then progressed to the south, approaching the parallel of Addis Ababa about 15 Ma ago.

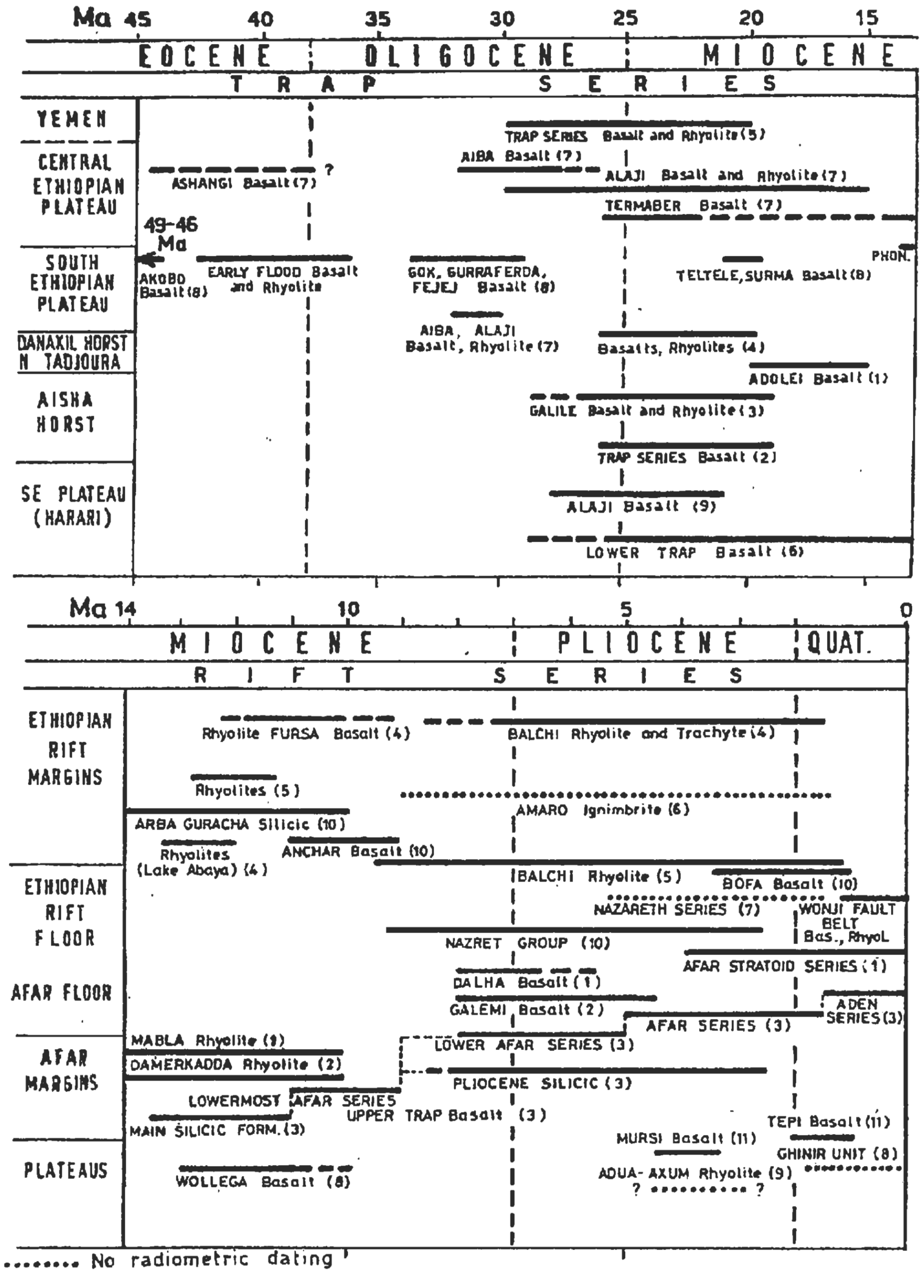


Fig. 4 - Chronological correspondence among volcanic formations of type area and those described by other authors in different sectors of Ethiopia (after ZANETTIN et al., 1980a).

Coeval and lithologically similar volcanic sequences are known, under local names, in many parts of the Ethiopian province: Yemen, Danakil Alps, Aisha horst, northern and southern Harar Plateau, southern Ethiopian Plateau and northern Turkana (Kenya) (Fig. 4).

### Termaber central volcanism

In the type area the fissural Alaji volcanism was followed by central volcanism which built up large shield volcanoes decreasing in age from N to S (Fig. 9). The change in volcanic regime is matched by a change in lava composition: no longer transitional basalts, but alkali basalts and basanites (Figs. 6, 7; Table 1, cols. 6-9).

This stage ended with a strong uplift which caused the appearance of the proto-Ethiopian rift (Fig. 17).

### Rift series

Knowledge of the volcanic sequences of the Rifts is taken essentially from: a) BROTZU et al. (1974a, b, 1980a, b); KAZMIN et al. (1980); ZANETTIN and JUSTIN-VISENTIN, (1974); ZANETTIN et al. (1980); JUCH, (1975), for the Ethiopian rift and southern Afar escarpment; b) BARBERI et al. (1975a); DE FINO et al. (1973; 1978), for central and northern Afar.

After the formation of the escarpments fissural volcanism was confined to the rifts. This new volcanic stage began with the emission of the Mabla rhyolitic ignimbrites (14-11 Ma) and the voluminous Fursa flood basalts (12-9 Ma). The latter occur (Fig. 10) at the base of the Ethiopian and Harar escarpments and in a supposed transversal rift, which later failed, running from the Addis Ababa area west as far as Wollega. Near the Ethiopian Plateau they correspond to transitional basalts (Table 1, col. 10), similar to the Aiba basalts; near the Harar Plateau, where they are better known as Anchar basalts (KAZMIN et al., 1980), they show a more alkaline composition (Table 1, col. 11).

In the last 8 Ma the volcanism was of different character in the Afar and in the Ethiopian rift: basic lavas largely prevailed in Afar and silicic products in the Ethiopian rift (Fig. 11).

Mainly transitional basalts with affinity varying from tholeiitic to alkaline were emitted in Afar (Table 1, cols. 18-25). They form the Dalha basalts (8-6 Ma), the Afar stratoid series (4-1 Ma) and the younger volcanoes built on the axial fissure system of Afar (BARBERI et al., 1975). Instead, the volcanoes placed on tectonic lines transversal to the axial fissures have a clearly alkaline composition (DE FINO et al., 1973; 1978), (Fig. 12).

Huge volumes of ignimbrites, mainly peralkaline rhyolites (Balchi Formation), locally interlayered with basalts, were emitted in the Ethiopian rift and in southern Afar, from 8 to 2 Ma ago. The Balchi rhyolites are covered by the Bofa transitional alkaline basalts (KAZMIN et al., 1980; BROTZU et al., 1980b), and still younger basalts

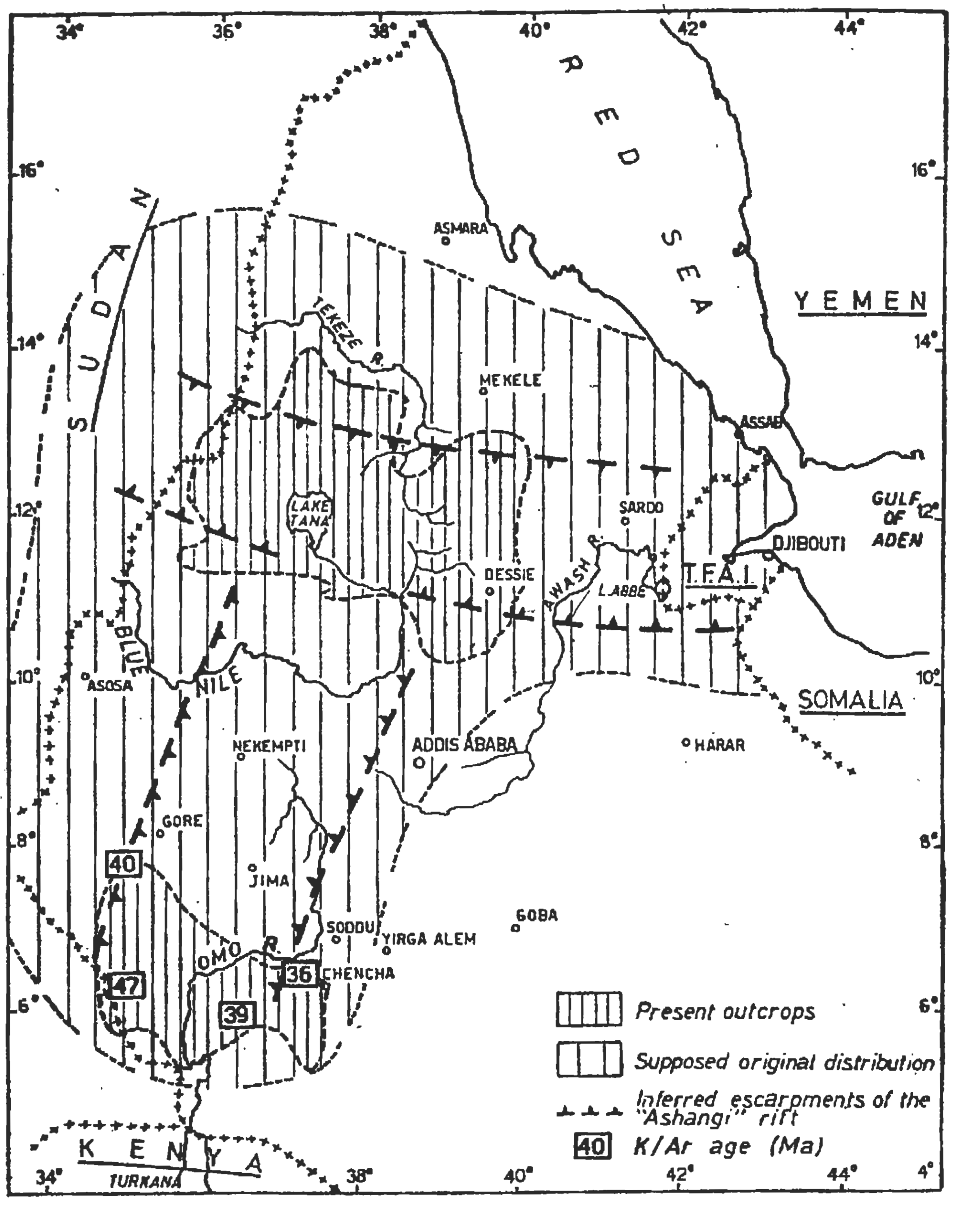


Fig. 5 - Distribution of Ashangi basalts and coeval volcanites (c. 50-35 Ma). In type area, Ashangi basalts outcrop on escarpment (tilted flows) and in floor of an old (Ashangi) rift, now buried under horizontal Aiba flood basalts. Old rift has been interpreted as extension of a former Aden continental rift (ZANETTIN et al., 1980b): Triple junction would have fallen in Lake Tana area.

and peralkaline silicics built up volcanic edifices in the axial zone of the Ethiopian rift (Wonji Group) (Table 1, cols. 12-16; Fig. 13).

Many well-known volcanoes occurring in the area south of Addis Ababa belong to the Balchi Formation, but those rising in the axial zone are Quaternary in age (Fig. 14).

## COMPARISON BETWEEN PLATEAU AND RIFT VOLCANITES

### TRANSITIONAL BASALTS

As already mentioned, the most common fissural basalts occurring both in the plateau and in the rift are transitional in character.

As regards major elements, the basalts from the plateau and Afar are broadly similar. In fact, the TAS as well as the De La Roche diagrams (Fig. 15) show that all the highly fissural basalts plot in a restricted area, independently of age or structural setting (Aiba-Alaji: 32-20 Ma, plateau series; Afar stratoid series, 4-1 Ma). The Fursa basalts (12-9 Ma) are slightly more evolved, and the recent basalts that build the volcanoes of the Afar axial ranges also have the same serial features, although they are poorer in $SiO_2$. A stronger tholeiitic affinity is present both in the oldest rocks from the Ethiopian plateau (Ashangi basalts, c. 50-35 Ma) and in the Afar rift (Dalha basalts, 8-6 Ma).

No appreciable differences are found in trace elements (PICCIRILLO et al., 1979).

Some differences are shown by the Plio-Quaternary Bofa and Wonji basalts of the northern Ethiopian rift. In general they are still transitional in character, but with a clear alkaline affinity, and are richer in $Al_2O_3$ (15-16% vs. 13-14%). Instead, some incompatible elements (Ta, Hf, Zr, Tb, La) are slightly lower than in Afar (BROTZU et al., 1980a).

The most common rocks of the Ashangi Formation are also classified by the diagrams as transitional-alkaline basalts, but they clearly differ from the Bofa and Wonji basalts due to their much higher $K_2O$ (ca. 1.5% vs. c. 0.8%) and much lower $Al_2O_3$ contents (9-12% vs. 15-16%).

It is worth noting that the transitional basalts from the rifts show a more primitive character, having fractionated only olivine, while the plateau basalts formed by fractionation of 30-35% olivine + plagioclase + pyroxene (PICCIRILLO et al., 1979).

This fact may be explained by the different thickness of the crust, which is thinner under the rifts.

### SILICIC PERALKALINE ROCKS

The silicic volcanites associated with transitional basalts have a peralkaline index (mol. $Na_2O + K_2O/Al_2O_3$) close to one. Peralkaline trachytes and rhyolites (pantelleritic comendites and pantellerites) prevail (80%) in the Ethiopian rift (Balchi Formation and Wonji Group) in association with transitional basalts with clear alkaline affinity (Bofa and Wonji basalts), while in the Afar rift (Afar stratoid series and axial ranges) and

Table 1 - Average chemical composition of the rocks belonging to the Ethiopian volcanic formations cited in the text. Localities: Col. 1 to 9, type area, plateau; 10, Addis Ababa, Fursi, Ethiopian rift, Ghibie; 11, Auash Station, Southern Afar, Miesso; 12 and 13, Balchi, Ethiopian rift, Assabot Center; 14 to 16, Ethiopian rift, Boseti Center; 17 and 18, western Afar, Eloha, Eda Ali; 19, Central and Southern Afar; 20, Central Afar, Sardo, Aramuda, Borauli Center; 21, Central (Tandaho, Gablaitu, Curub) and Southern Afar; 22 and 23, Central (Gablaitu) and eastern Afar (La Mauda); 24 and 25, Eastern Afar, Assab, Edd, Bahar Assoli. Source of the analyses: Col. 1 to 9, ZANETTIN et al. (1974); 10 to 13, JUSTIN-VISENTIN and ZANETTIN (unpublished); 14 to 16, BROTZU et al. (1980); JUSTIN-VISENTIN and ZANETTIN (unpublished); 17 to 23, JUSTIN-VISENTIN and ZANETTIN (unpublished); 24 and 25, DE FINO et al. (1973, 1978).

TRAP SERIES - CENTRAL ETHIOPIAN PLATEAU

| VOLCANIC FORMATION | ASHANGI | | AIBA | ALAJI | | TERMAHER | | | |
|---|---|---|---|---|---|---|---|---|---|
| Column | 1 | 2 | 3 | 4 | 5 | 6 | 7 | 8 | 9 |
| $SiO_2$ | 50.70 | 47.50 | 49.83 | 49.14 | 70.45 | 42.10 | 47.67 | 55.01 | 64.40 |
| $TiO_2$ | 2.72 | 4.07 | 3.07 | 3.17 | 0.59 | 3.39 | 2.46 | 0.93 | 0.53 |
| $Al_2O_3$ | 14.33 | 11.40 | 13.50 | 13.84 | 12.99 | 12.38 | 15.43 | 18.55 | 15.66 |
| $Fe_2O_3$ | 4.36 | 6.13 | 4.42 | 4.07 | 2.52 | 6.25 | 5.35 | 3.32 | 3.49 |
| FeO | 7.92 | 7.10 | 7.56 | 8.59 | 0.88 | 7.86 | 6.61 | 2.07 | 1.30 |
| MnO | 0.18 | 0.22 | 0.19 | 0.21 | 0.13 | 0.23 | 0.18 | 0.26 | 0.17 |
| MgO | 5.11 | 6.83 | 5.98 | 5.73 | 0.49 | 8.30 | 5.48 | 1.08 | 0.49 |
| CaO | 9.34 | 9.62 | 9.20 | 9.01 | 0.74 | 11.70 | 9.08 | 3.74 | 0.56 |
| $Na_2O$ | 2.92 | 2.78 | 2.91 | 3.08 | 3.82 | 2.77 | 3.64 | 5.88 | 6.47 |
| $K_2O$ | 0.69 | 1.48 | 0.86 | 1.08 | 4.73 | 0.96 | 1.35 | 4.91 | 4.89 |
| $P_2O_5$ | 0.35 | 0.59 | 0.52 | 0.49 | 0.09 | 0.80 | 0.69 | 0.34 | 0.07 |
| $H_2O+$ | 1.13 | 1.89 | 1.50 | 1.34 | 2.46 | 2.85 | 1.60 | 3.61 | 1.61 |
| Total | 99.75 | 99.61 | 99.64 | 99.75 | 99.89 | 99.59 | 99.54 | 99.70 | 99.64 |
| ANALYSED ROCKS N° | 11 | 30 | 35 | 43 | 82 | 16 | 53 | 19 | 18 |
| Q | 5.67 | 2.17 | 4.15 | 1.65 | 28.83 | — | — | — | 7.31 |
| C | — | — | — | — | 0.46 | — | — | — | — |
| Or | 4.07 | 8.74 | 5.67 | 6.38 | 28.66 | 5.67 | 7.97 | 30.19 | 29.48 |
| Ab | 24.70 | 23.52 | 24.62 | 26.06 | 33.17 | 14.89 | 30.80 | 40.06 | 54.41 |
| An | 23.95 | 14.25 | 20.94 | 20.75 | 3.18 | 18.51 | 21.77 | 10.08 | — |
| Ne | — | — | — | — | — | 4.63 | — | 6.39 | — |
| Ac | — | — | — | — | — | — | — | — | 1.26 |
| Wo (Di) | 8.39 | 12.36 | 8.89 | 8.66 | — | 14.32 | 7.83 | 2.89 | 0.98 |
| En (Di) | 5.15 | 9.94 | 5.99 | 5.33 | — | 10.75 | 5.53 | 2.50 | 0.85 |
| Fs (Di) | 2.75 | 0.97 | 2.22 | 2.82 | — | 2.13 | 1.61 | — | — |
| En (Hy) | 7.56 | 7.05 | 8.89 | 8.93 | 1.24 | — | 2.32 | — | 0.38 |
| Fs (Hy) | 4.03 | 0.68 | 3.29 | 4.73 | — | — | 0.68 | — | — |
| Fo (Ol) | — | — | — | — | — | 6.94 | 4.05 | 0.20 | — |
| Fa (Ol) | — | — | — | — | — | 1.51 | 1.30 | — | — |
| Mt | 6.32 | 8.88 | 6.40 | 5.90 | 1.55 | 9.06 | 7.75 | 4.99 | 3.14 |
| Hm | — | — | — | — | 1.51 | — | — | 0.01 | 0.95 |
| Il | 5.16 | 7.72 | 5.83 | 6.02 | 1.15 | 6.43 | 4.67 | 1.84 | 1.02 |
| Ap | 0.82 | 1.39 | 1.23 | 1.16 | 0.21 | 1.89 | 1.63 | 0.82 | 0.16 |

Tab.1 - continued

R I F T   S E R I E S

| | MAIN ETHIOPIAN RIFT | | | | | | | AFAR RIFT | | | | | | | | |
|---|---|---|---|---|---|---|---|---|---|---|---|---|---|---|---|---|
| VOLCANIC FORMATION | FURSA | ANCHAR | BALCHI | | BOFA | WONJI | | MABLA | DALHA | AFAR STRAT. SERIES | | AXIAL RANGES | | | TRANSVERSAL RANGE | |
| COLUMN | 10 | 11 | 12 | 13 | 14 | 15 | 16 | 17 | 18 | 19 | 20 | 21 | 22 | 23 | 24 | 25 |
| $SiO_2$ | 50.55 | 46.95 | 69.61 | 64.35 | 47.73 | 47.71 | 68.55 | 74.91 | 49.40 | 49.19 | 72.54 | 47.57 | 67.86 | 72.85 | 47.02 | 61.56 |
| $TiO_2$ | 2.65 | 2.86 | 0.44 | 0.55 | 2.28 | 2.13 | 0.41 | 0.18 | 2.94 | 3.02 | 0.24 | 2.87 | 0.42 | 0.14 | 2.72 | 0.57 |
| $Al_2O_3$ | 13.76 | 15.91 | 11.78 | 15.04 | 16.47 | 15.44 | 11.97 | 12.15 | 13.08 | 13.48 | 12.75 | 13.82 | 12.72 | 13.13 | 16.40 | 15.39 |
| $Fe_2O_3$ | 3.62 | 6.13 | 3.79 | 3.48 | 3.92 | 3.41 | 2.76 | 1.45 | 6.42 | 4.91 | 1.89 | 3.71 | 1.87 | 1.35 | 4.45 | 3.17 |
| FeO | 8.80 | 6.50 | 1.58 | 1.00 | 7.66 | 7.75 | 3.29 | 0.50 | 7.44 | 8.44 | 1.00 | 9.81 | 4.60 | 0.39 | 6.27 | 4.00 |
| MnO | 0.20 | 0.20 | 0.20 | 0.15 | 0.17 | 0.18 | 0.28 | 0.02 | 0.21 | 0.23 | 0.07 | 0.22 | 0.20 | 0.06 | 0.18 | 0.22 |
| MgO | 4.73 | 5.08 | 0.25 | 0.33 | 6.22 | 7.72 | 0.11 | 0.20 | 5.66 | 4.89 | 0.22 | 6.79 | 0.58 | 0.21 | 6.08 | 0.58 |
| CaO | 8.83 | 9.38 | 0.64 | 1.73 | 10.02 | 10.38 | 0.69 | 0.48 | 10.16 | 9.68 | 1.04 | 9.35 | 2.31 | 1.02 | 10.17 | 3.68 |
| $Na_2O$ | 3.16 | 3.74 | 4.65 | 5.10 | 3.29 | 3.00 | 6.40 | 4.65 | 2.69 | 3.04 | 4.57 | 2.82 | 4.78 | 4.70 | 3.45 | 5.38 |
| $K_2O$ | 1.13 | 0.83 | 4.60 | 4.76 | 0.76 | 0.84 | 4.32 | 4.10 | 0.41 | 0.86 | 4.06 | 0.46 | 2.91 | 4.35 | 1.37 | 3.31 |
| $P_2O_5$ | 0.62 | 0.66 | 0.05 | 0.06 | 0.37 | 0.42 | 0.04 | 0.02 | 0.36 | 0.61 | 0.03 | 0.42 | 0.07 | 0.02 | 0.52 | 0.12 |
| $H_2O^+$ | 1.59 | 1.42 | 2.66 | 3.16 | 0.77 | 0.58 | 0.44 | 1.24 | 1.20 | 1.14 | 1.49 | 1.17 | 1.67 | 2.12 | 1.25 | 1.77 |
| Total | 99.54 | 99.66 | 100.25 | 99.71 | 99.66 | 99.56 | 99.26 | 100.03 | 99.97 | 99.49 | 99.90 | 99.00 | 99.93 | 100.34 | 99.88 | 99.75 |
| Analysed rocks n° | 11 | 12 | 42 | 5 | 8 | 41 | 124 | 6 | 3 | 17 | 13 | 11 | 2 | 2 | 3 | 3 |
| Q | 3.58 | — | 24.73 | 13.32 | — | — | 17.67 | 31.34 | 6.75 | 3.83 | 28.52 | — | 21.67 | 27.23 | — | 8.55 |
| Or | 6.67 | 4.90 | 27.18 | 28.13 | 4.49 | 4.96 | 25.53 | 24.23 | 2.42 | 5.08 | 23.99 | 2.71 | 17.19 | 25.70 | 8.09 | 19.56 |
| Ab | 26.73 | 31.64 | 34.98 | 43.15 | 27.83 | 25.38 | 37.52 | 39.34 | 22.76 | 25.72 | 38.67 | 23.86 | 40.44 | 39.77 | 25.69 | 45.52 |
| An | 19.94 | 24.17 | — | 4.08 | 27.92 | 26.18 | — | 0.17 | 22.40 | 20.59 | 2.28 | 23.69 | 4.65 | 1.88 | 25.21 | 8.06 |
| Ac | — | — | 3.84 | — | — | — | 7.98 | — | — | — | — | — | — | — | — | — |
| Ns | — | — | — | — | — | — | 1.76 | — | — | — | — | — | — | — | — | — |
| Ne | — | — | — | — | — | — | — | — | — | — | — | — | — | — | 1.92 | — |
| Di: Wo | 8.54 | 7.53 | 1.17 | 0.95 | 8.08 | 9.42 | 1.32 | 0.57 | 10.70 | 9.78 | 0.64 | 8.33 | 2.64 | 0.34 | 9.12 | 3.92 |
| Di: En | 4.64 | 5.65 | 0.62 | 0.82 | 5.12 | 6.14 | 0.06 | 0.49 | 7.64 | 5.91 | 0.64 | 4.87 | 0.51 | 0.29 | 6.65 | 0.83 |
| Di: Fs | 3.61 | 1.12 | 0.61 | — | 2.44 | 2.63 | 1.41 | — | 2.11 | 3.34 | — | 3.05 | 2.33 | — | 1.61 | 3.36 |
| Wo | — | — | 0.01 | 0.76 | — | — | — | 0.29 | — | — | 0.47 | — | — | 0.87 | — | — |
| Hy: En | 7.13 | 3.98 | — | — | 2.52 | 2.00 | 0.20 | — | 6.44 | 6.26 | — | 11.82 | 0.93 | — | — | 0.61 |
| Hy: Fs | 5.55 | 0.79 | — | — | 1.20 | 0.85 | 4.47 | — | 1.78 | 3.53 | — | 7.42 | 4.24 | — | — | 2.47 |
| Ol: Fo | — | 2.11 | — | — | 5.48 | 7.76 | — | — | — | — | — | 0.14 | — | — | 5.94 | — |
| Ol: Fa | — | 0.46 | — | — | 2.88 | 3.66 | — | — | — | — | — | 0.10 | — | — | 1.59 | — |
| Mt | 5.24 | 8.88 | 3.56 | 2.11 | 5.68 | 4.94 | — | 1.15 | 9.30 | 7.11 | 2.74 | 5.37 | 2.71 | 1.04 | 6.45 | 1.69 |
| Hm | — | — | — | 2.01 | — | — | — | 0.67 | — | — | — | — | — | 0.62 | — | — |
| Il | 5.03 | 5.43 | 0.83 | 1.04 | 4.33 | 4.04 | 0.77 | 0.34 | 5.58 | 5.73 | 0.46 | 5.46 | 0.79 | 0.26 | 5.16 | 1.08 |
| Ap | 1.23 | 1.56 | 0.11 | 0.14 | 0.87 | 0.99 | 0.99 | 0.04 | 0.85 | 1.44 | 0.07 | 0.98 | 0.16 | 0.09 | 1.23 | 0.28 |

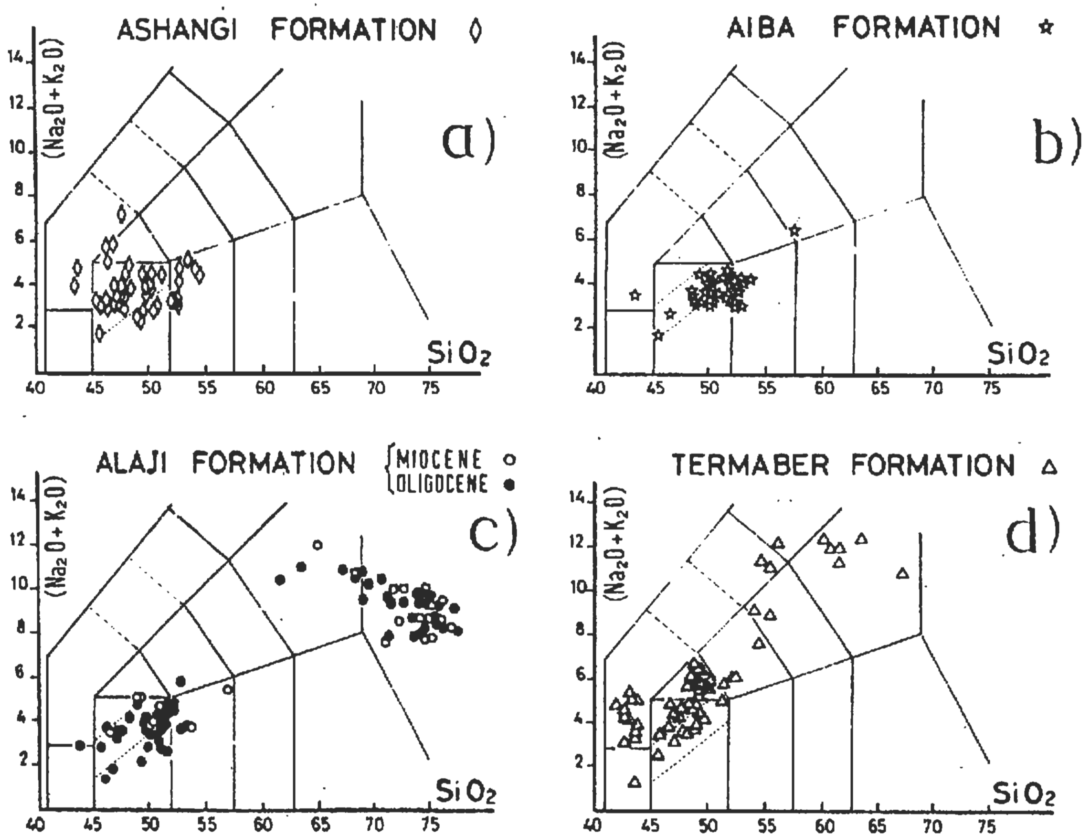


Fig. 6 - Total alkalis vs. silica diagram for plateau (Trap) volcanites of type area (after MOHR and ZANETTIN, 1988; data from ZANETTIN et al., 1976). Dashed lines: boundaries of transitional basalt field (see Fig. 2). Note gap between basalts and rhyolites of Alaji Formation.

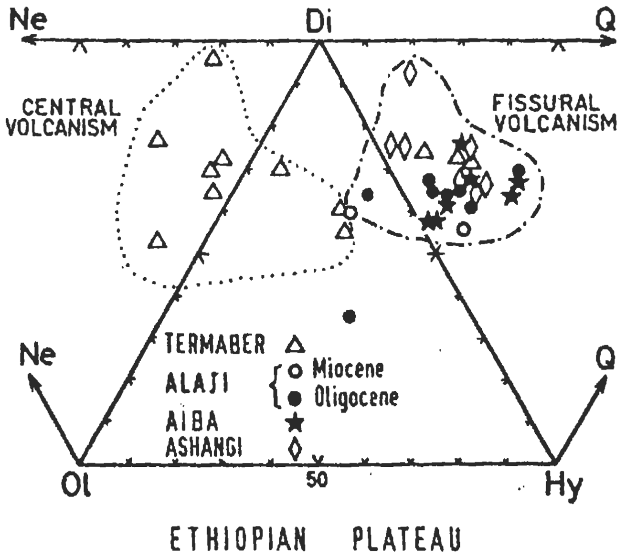


Fig. 7 - Normative plot of Ethiopian plateau basalts (after MOHR and ZANETTIN, 1988). Only basalts emitted from central volcanoes (Termaber Formation) show a predominantly alkaline character.

plateau (Alaji Formation) peralkaline silicics associated with transitional and transitional-tholeiitic basalts are less abundant (60%) and correspond essentially to comendites (Fig. 16).

An origin for these silicics through low-pressure fractionation of transitional basaltic magma is the most obvious genetic hypothesis, and is reinforced by the similarity of the $Sr^{87}/Sr^{86}$ isotope ratio for the basic and acidic rocks occurring in association (e.g., Ethiopian rift):

| | Basalts | Silicics |
|---|---|---|
| Ethiopian rift: | | |
| - Boseti Center | 0.7040 | 0.7040 |
| (BROTZU et al., 1980c) | | |
| - Afar Rift: | | |
| (BARBERI et al., 1980c) | | |
| Erta Ale (axial) | 0.7034 | 0.7041 |
| Manda Hararo (axial) | 0.7037 | 0.7040 |
| Stratoid series | 0.7036 | 0.705 |
| Ethiopian plateau: | | |
| (CAVAZZINI, unpublished) | | |
| Alaji Formation | 0.7037-0.7041 | 0.7042-0.7061 |

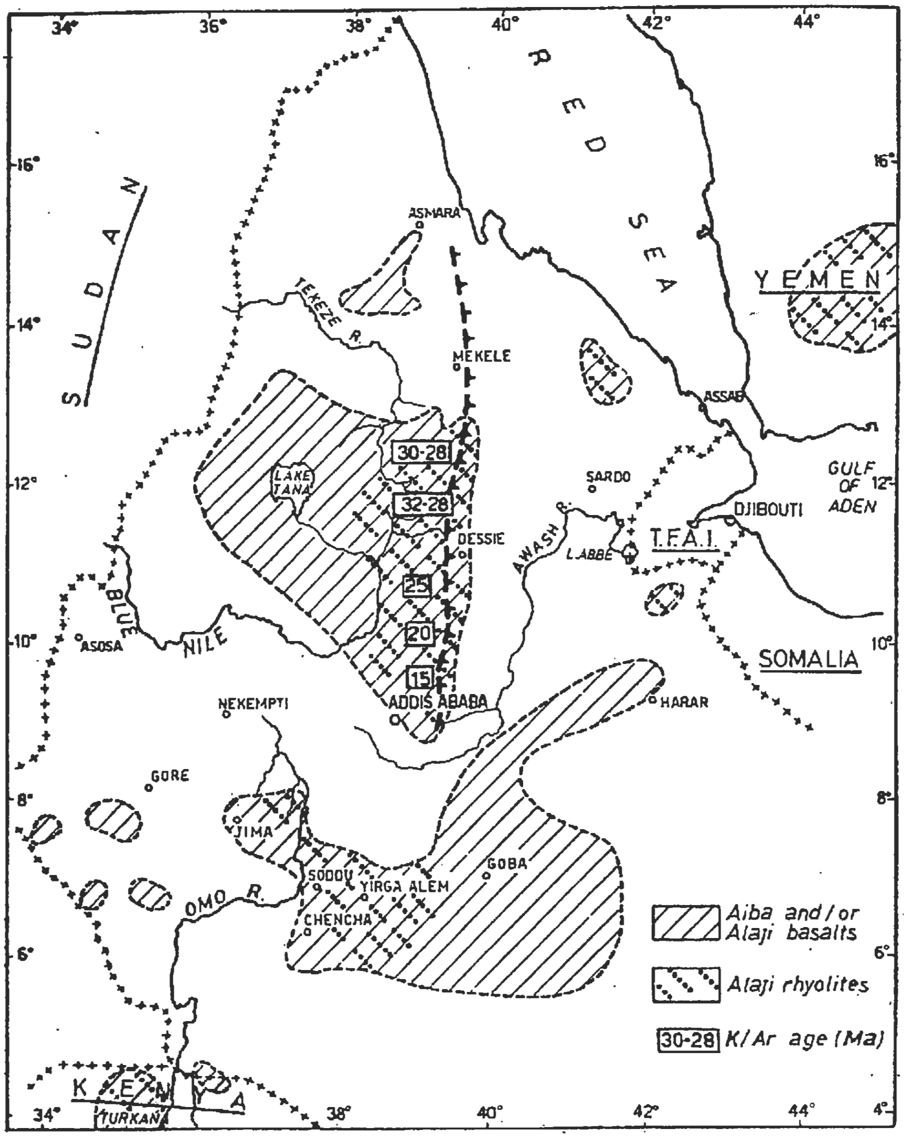


Fig. 8 - Distribution of Aiba, Alaji and coeval volcanites (32-15 Ma). Figures show that age of youngest rhyolites emitted at different points of edge of W Afar escarpment decreases towards S (migration of volcanism). These ages are also thought to represent formation age of escarpment.

A similar genesis is easily applied to the intermediate and acidic rocks that, associated in decreasing volumes with the basalts, form volcanic edifices in the axial zones of the rifts. Instead, some doubts may arise regarding the rhyolites occurring in the stratoid sequences from the plateau (Alaji Formation) and the rifts (Balchi Formation; Afar stratoid series), because of the absence or scarcity of rocks of intermediate composition (57-65% $SiO_2$). Even if the fractionation model still seems to be the more probable, an alternative model, based on partial melting of the basalts emplaced at the Moho, has been suggested by BETTON and COX (1979) to explain the origin of silicics occurring in similar associations.

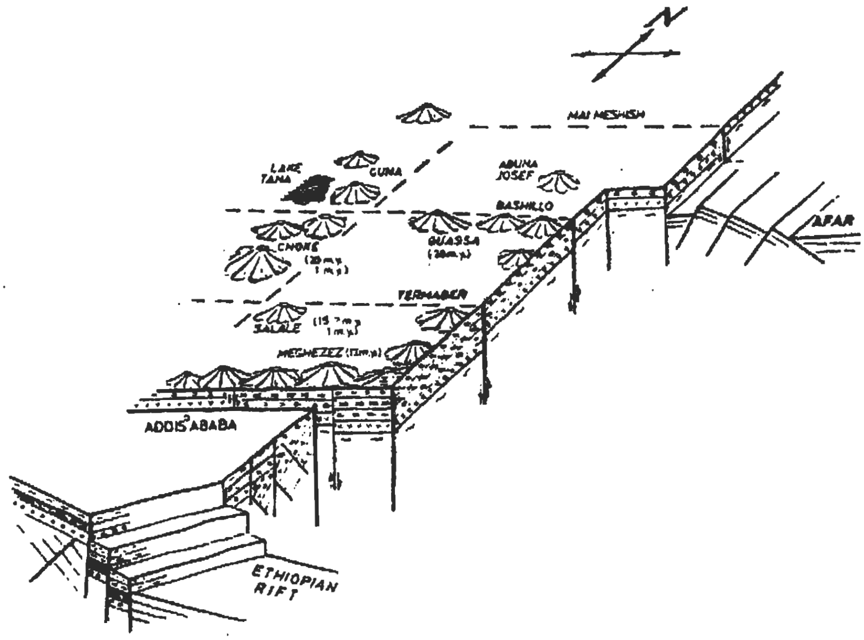


Fig. 9 - Distribution of shield volcanoes (Termaber Formation) in type area (after ZANETTIN et al., 1978). In belt close to W Afar margin, their age decreases from N to S (Mt. Guassa 28 Ma; Mt. Meghezez 13 Ma). Progressive shifting of fissural volcanism to S and E caused maximum thickening of volcanic pile in region of Addis Ababa.

### Alkali basalts

Close chemical similarities (major elements) (Fig. 15) also exist between the alkaline basalts occurring in the plateau (Oligocene to Miocene shield volcanoes of the Termaber Formation; Table 1, col. 7) and in the Afar floor (Quaternary transversal ranges; Table 1, col. 24).

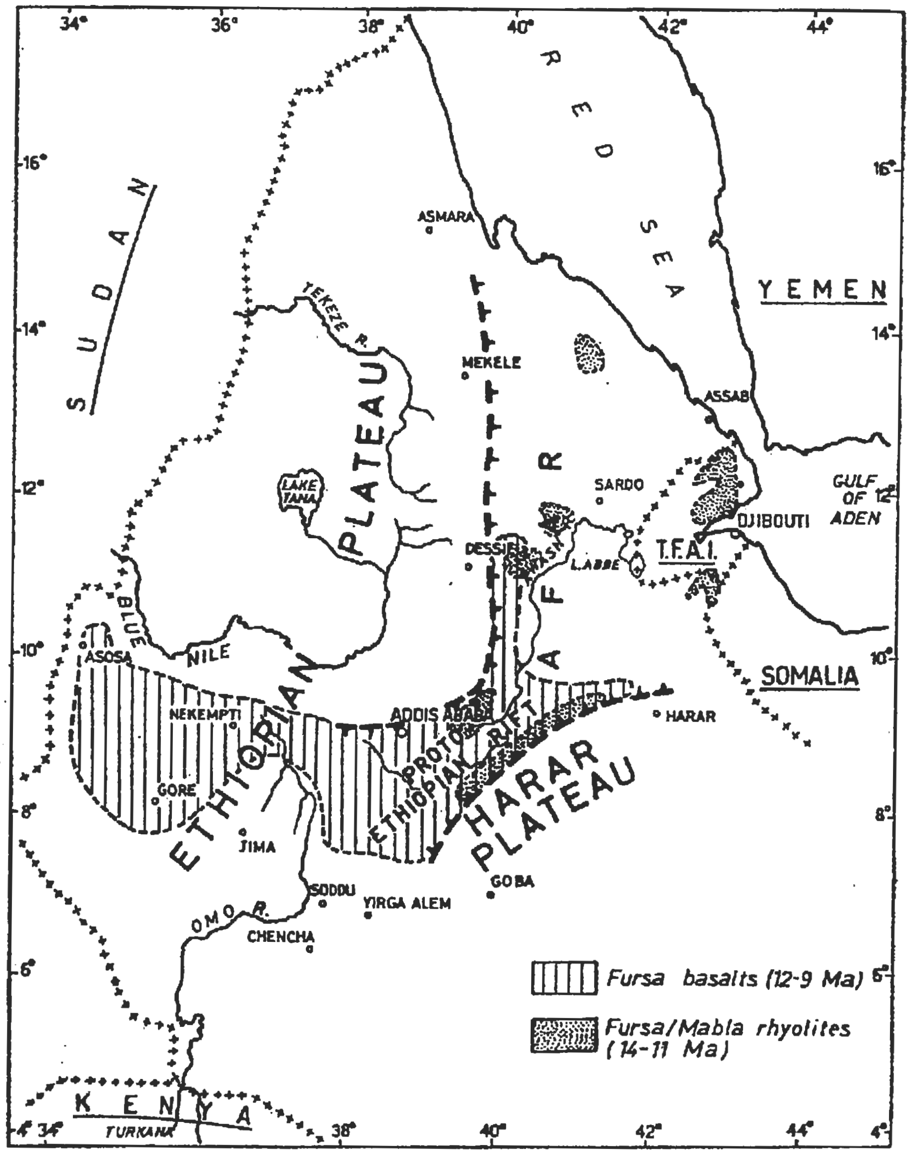


Fig. 10 - Distribution of Mabla rhyolites and Fursa basalts. W of Addis Ababa Fursa basalts were emitted in an elongated belt, interpreted as a rift that later disappeared (parallel to Ashangi paleorift of Fig. 5).

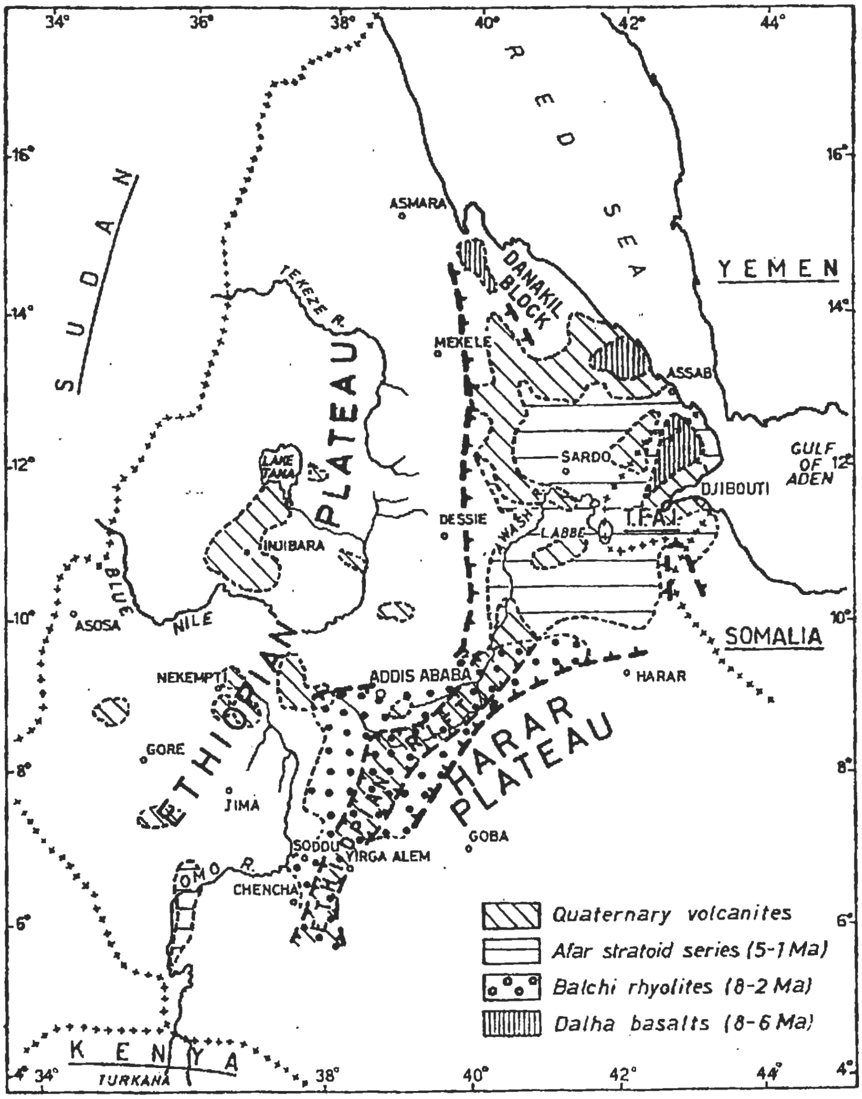


Fig. 11 - Distribution of Balchi and Afar volcanites. Note that Quaternary volcanism took place not only on rift floor but also in western Ethiopian plateau (Lake Tana area).

On the contrary, appreciable differences exist between the evolved products of these similar basalts: the Termaber mugearites, benmoreites and trachytes are richer in $Al_2O_3$ and alkalis and poorer in $FeO_{tot}$ and CaO than the equivalent rocks from the transversal ranges. Such differences may be clearly explained by the fractionation of the alkali basalts of the Afar transversal ranges under a lower $fO_2$ with respect to the Termaber basalts, and then by earlier crystallization of the plagioclase and consequent iron enrichment. Also as regards the rocks of the transitional series, iron enrichment is higher in Afar than in the plateau; we can therefore say that the lowermost $fO_2$ of the entire Ethiopian volcanic province took place in Afar.

## STRUCTURAL EVOLUTION OF THE ETHIOPIAN VOLCANIC PROVINCE

According to the classic tectonic model, the formation of a rift system includes the following stages: a) the territory is uplifted in the form of an elongated dome; b) volcanism begins along the crest of the dome; c) the crest subsides, forming a rift. For the Ethiopian Volcanic Province MERLA (1963), AZZAROLI (1968), BAKER et al. (1972) and ZANETTIN et al. (1978) defined a different model, summarized in Fig. 17:

A) a flat, low-lying territory was homogeneously fractured and then covered by volcanics;
B) the uplift of two opposite blocks, separated by a long belt lying at a lower level, caused the appearance of a very wide rift (proto-rift), to which volcanism was confined;
C) further repeated risings of the peripheral strips of the rift floor caused narrowing of the rift itself. At the same time, the rift floor thinned out until continental spreading was complete.

Fig. 18 shows the detailed evolution of the western Afar escarpment. Two stages of uplift of the territory are distinguished, both accompanied by block-tilting with antithetic faults. As a result, the escarpment became higher and wider and the rift narrower.

The appearance of the Ethiopian plateau and Afar rift seems to have occurred through a sequence of chronologically distinct uplifts (beginning from the north) of blocks bordered by major faults trending c. N-S and by minor faults or flexures transversal to the present escarpment, as shown in Fig. 19.

As regards the relationship between tectonic and volcanic activity, it may be said that: 1) territorial uplift was preceded by emission of ignimbrites from fissures parallel to the future escarpment; 2) fissural volcanism, both acidic and basic (transitional basalts) died out in the uplifted territories, while it continued elsewhere (i.e., to the E and S); 3) in the course of the uplift alkaline basic and intermediate lavas built up shield volcanoes, mainly located at the border of the uplifted blocks.

Weaker volcanic activity lasted until the Quaternary in the Ethiopian plateau, along a belt overlapping the old Ashangi rift, where the thermal gradient is very high (60°C/km) (BERKHOLD et al., 1975; ZANETTIN et al., 1980b).

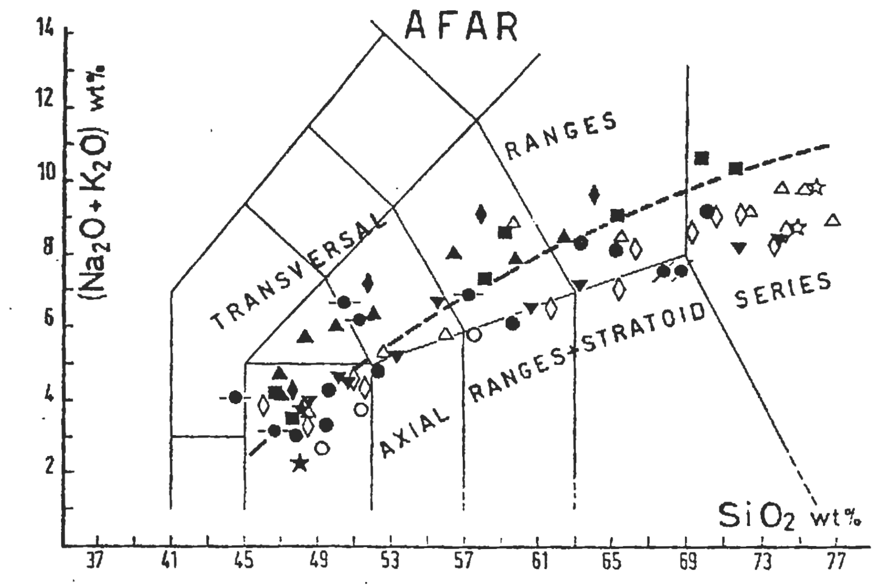


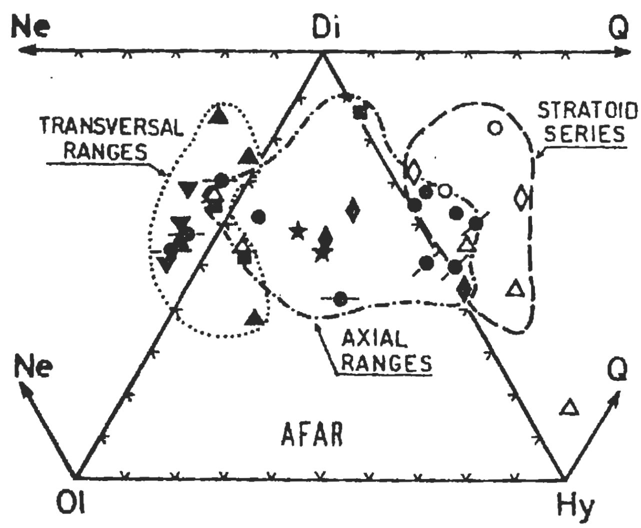


Fig. 12 - TAS diagram and normative plot for volcanic rocks of Afar floor (after MOHR and ZANETTIN, 1988; data from BARBERI and VARET, 1970; BARBERI et al., 1975; DE FINO et al., 1973, 1978; STIELTJES et al., 1976; FERRARA and SANTACROCE, 1980; JUSTIN-VISENTIN and ZANETTIN, unpublished). Diagrams indicate difference in composition of lavas emitted in different structural settings.

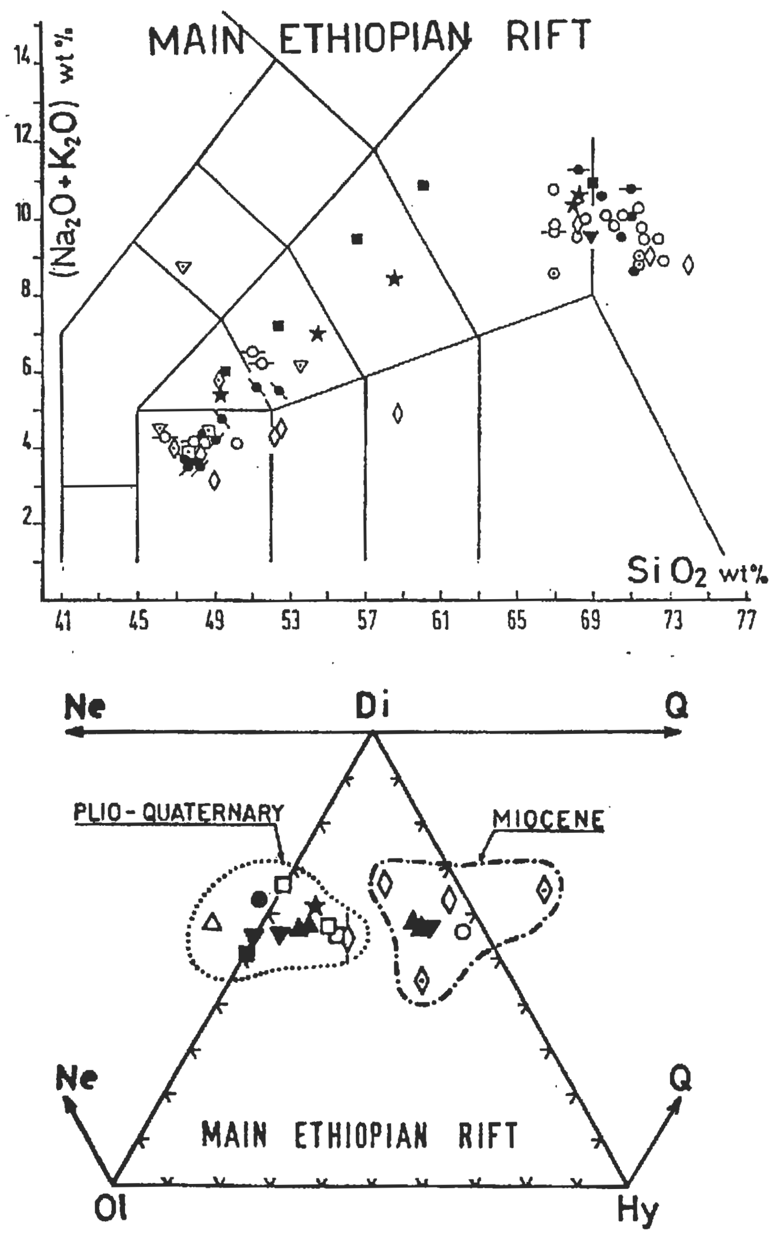


Fig. 13 - TAS diagram and normative plot for volcanic rocks of Main Ethiopian Rift (after MOHR and ZANETTIN, 1988; data from BROTZU et al., 1980; JUSTIN-VISENTIN and ZANETTIN, unpublished). Plio-Quaternary volcanics include Bofa basalts and rocks of Wonji Group.

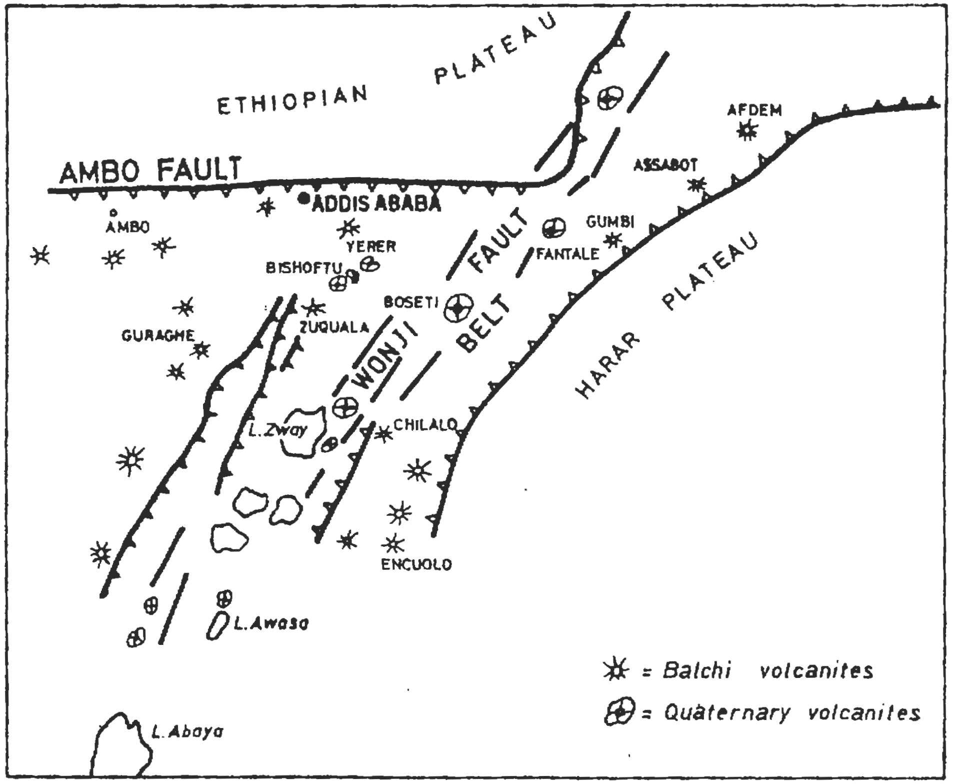


Fig. 14 - Volcanoes of Ethiopian rift floor. Note that volcanoes belonging to Balchi Formation occur on outer-most uplifted parts of rift, while younger, Quaternary volcanoes lie along axial belt of rift (Wonji fault belt).

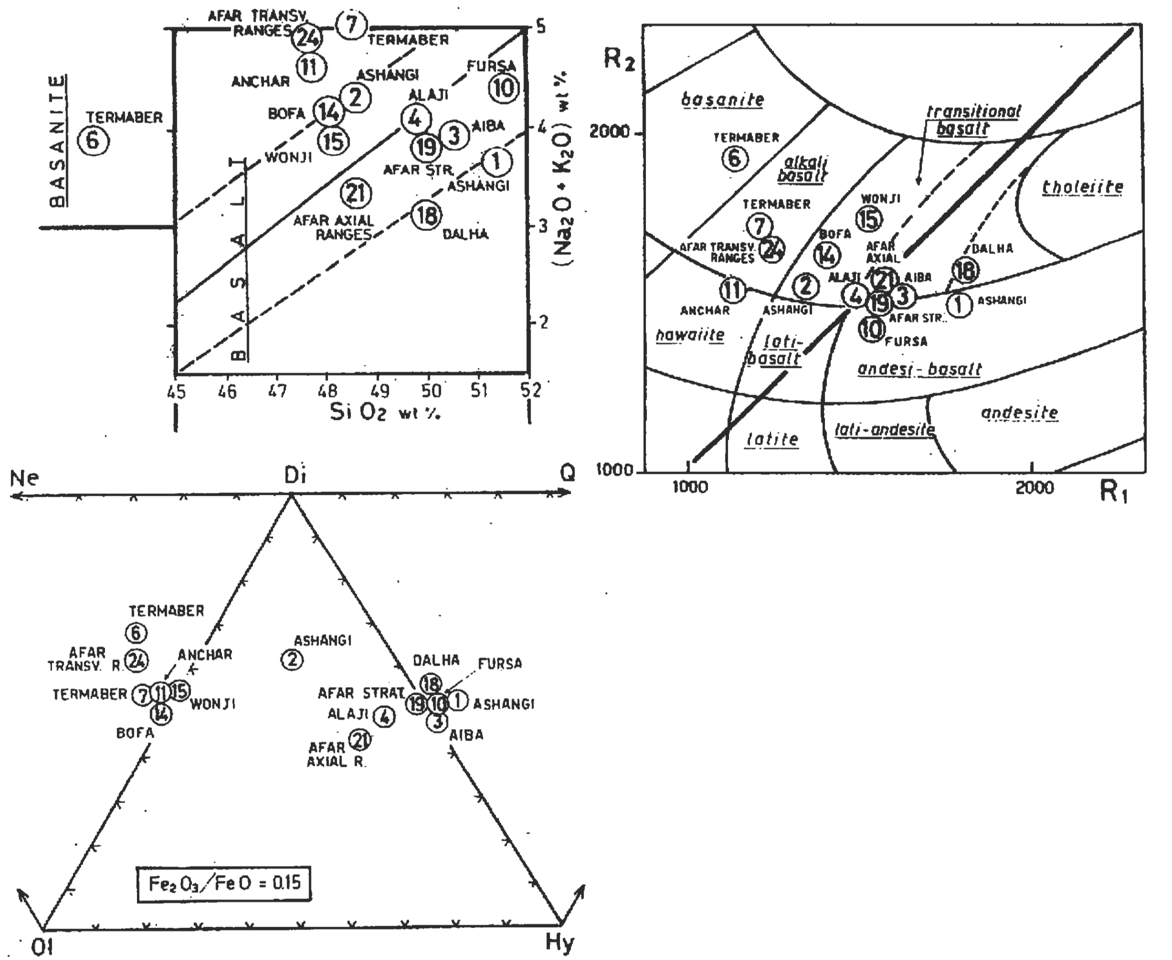


Fig. 15 - TAS and DE LA ROCHE diagrams and normative plots for basic volcanites of Ethiopian province. Lavas emitted in connection with fissural (transitional basalts of varying affinity) and central (alkali basalts and basanites) volcanism have similar compositions, independently of age and thickness of crust. Note that in normative plot (where $Fe_2O_3/FeO = 0.15$) transitional basalts with mild tholeiitic affinity plot close to plane of silica saturation and those with clear alkaline affinity close to plane of undersaturation.

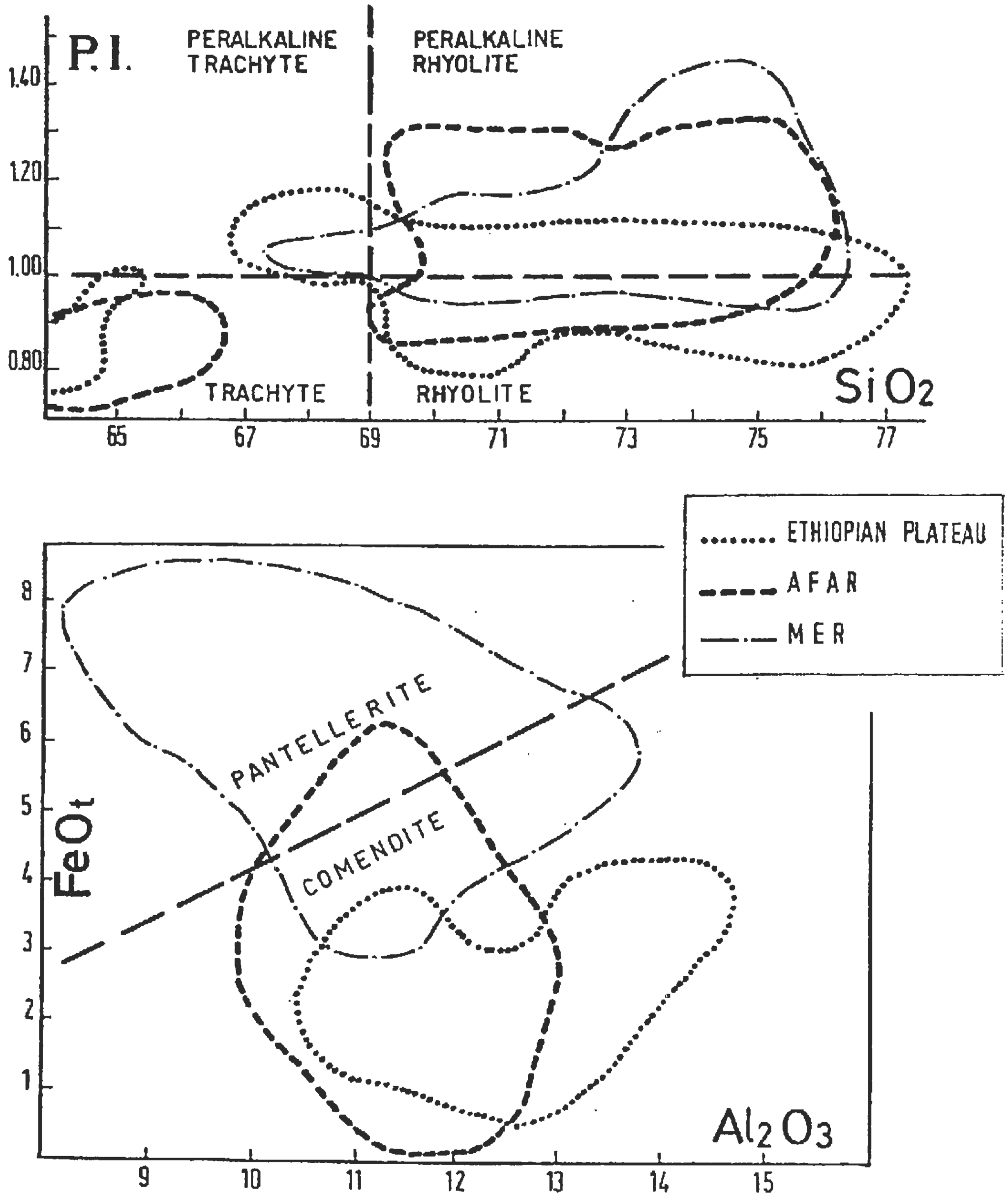


Fig. 16 - Peralkalinity index (P.I.) of silicic volcanic rocks, generally close to 1.0, slightly increases from Ethiopian Plateau to Afar and Ethiopian rifts. Accordingly, peralkaline rocks change from comendite to pantellerite.

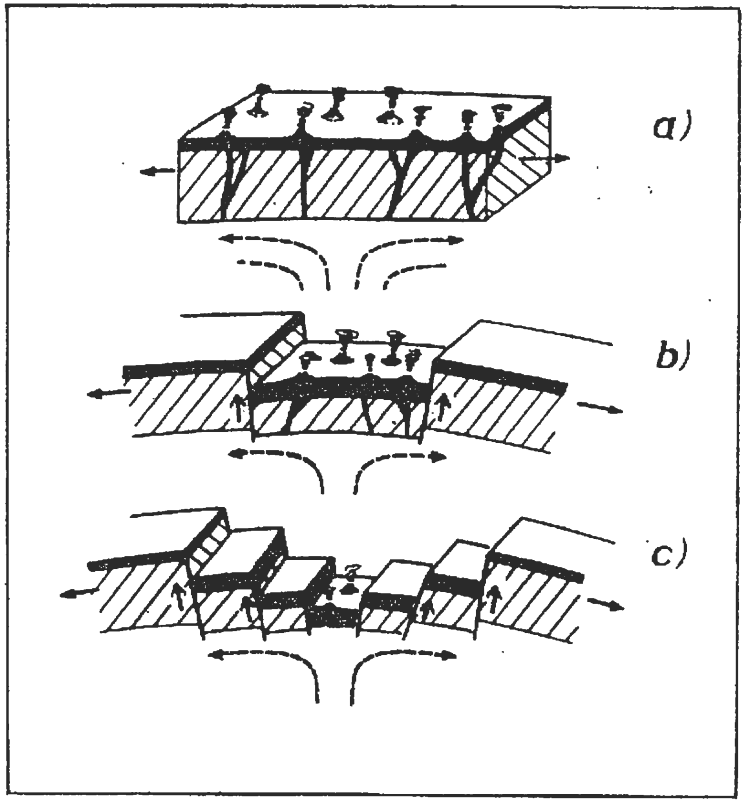


Fig. 17 - Ultrasimplified sketch of tectonic evolution of Ethiopian volcanic province: a) peneplain; b) uplift of territory and formation of proto-rift; c) more evolved stages, up to oceanization.

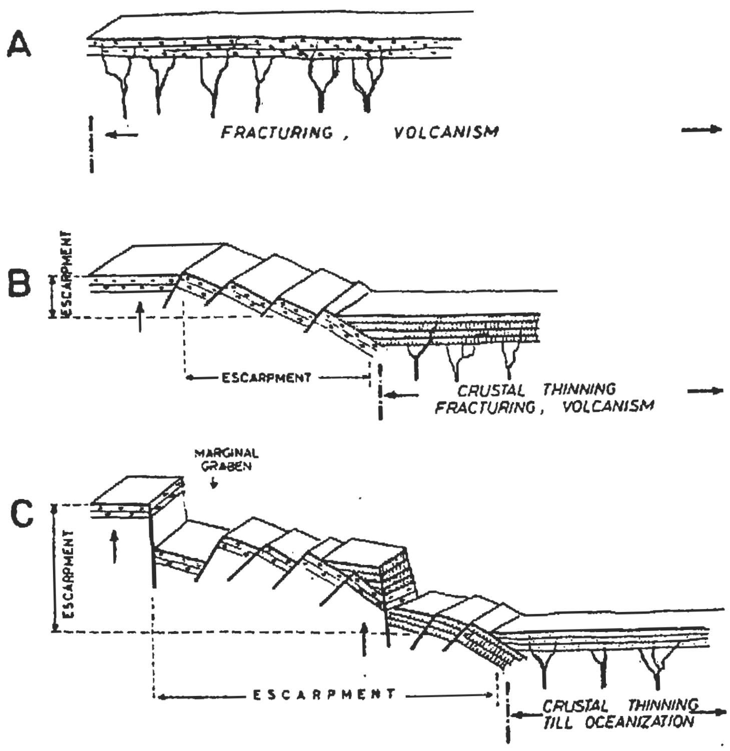


Fig. 18 - Tectonic and volcanic evolution of western margin of Afar: A) Fracturing, magmatic injection and volcanism are restricted to increasingly narrower belts; B) width and height of escarpment increase, while rift narrows; C) narrowing of rift is opposed by extension and thinning of crust. In central parts of Ethiopian Volcanic Province, escarpments are formed of blocks tilted towards rift (antithetic faults), while in outermost parts (i.e., approaching Red Sea, Gulf of Aden and Lake Abaya to south) blocks are tilted towards plateaus (synthetic faults) (after ZANETTIN et al., 1978).

## ORIGIN OF ETHIOPIAN BASALTS

Two alternative models have been proposed to explain the origin of the Ethiopian basic magmas. The first presupposes an originally homogeneous mantle, the second an inhomogeneous mantle.

The initial content of Eu, La, Ta, Tb, Th and Zr has been calculated for the source materials which, through partial melting, produced respectively the Ashangi, Aiba, Alaji and Termaber basaltic magmas (PICCIRILLO et al., 1979). Data show that, in the course of repeated melting processes, the mantle was progressively depleted in incompatible elements. Obviously, the composition of the basalt emitted at the surface largely depends on both degree of melting and later fractionation processes.

As a result of the progressive depletion of hygromagmatophile elements, the degree of melting required to produce basalts of comparable composition decreased in time.

According to GASS (1970) model, which postulates a homogeneous mantle in a territory subjected to progressive crustal thinning, the thinner the crust, the lower the $Sr^{87}/Sr^{86}$ isotope ratio of the emitted basalts. The lowest ratios are shown by the basalts of oceanic ridges.

This model does not seem applicable to the Afar rift, since the transitional basalts of the axial ranges, where the crust is thought to be very thin or absent (BARBERI et al., 1980) show higher isotope ratios than the coeval alkali basalts occurring in marginal areas where the crust should be thicker (e.g., Assab). In order to explain this discrepancy, it has been hypothesized that the composition of the mantle underlying the Afar floor changes with depth. The transitional basalts of the axial ranges formed through a high degree of melting of the lherzolite from the upper, more radiogenic zone. At the same time, the alkali basalts of the marginal zones originated by means of a lower degree of melting of source material from a deeper, less radiogenic zone.

Another genetic hypothesis can indirectly be put forward on the basis of observed (ZANETTIN et al., 1974) geochemical similarities (major elements) between the Ethiopian transitional flood basalts and the Hawaiian "tholeiites" (infraplate "hot-spot" basalts) (GREEN, 1989). If these similarities were confirmed for minor and trace elements too, the Ethiopian transitional magmas may have an origin similar to that inferred for the Hawaiian magmas: "partial melting of metasomatically enriched source region (at the lithosphere-asthenosphere boundary) in the presence of small but significant contents of water + $CO_2$" (GREEN, 1989).

## RELATIONSHIP BETWEEN STRUCTURAL SETTING AND BASALT COMPOSITION

Geophysical data, both gravimetric (MAKRIS et al., 1975) and seismic, show that the thickness of the continental crust under the Ethiopian plateau is about 40 km. It is

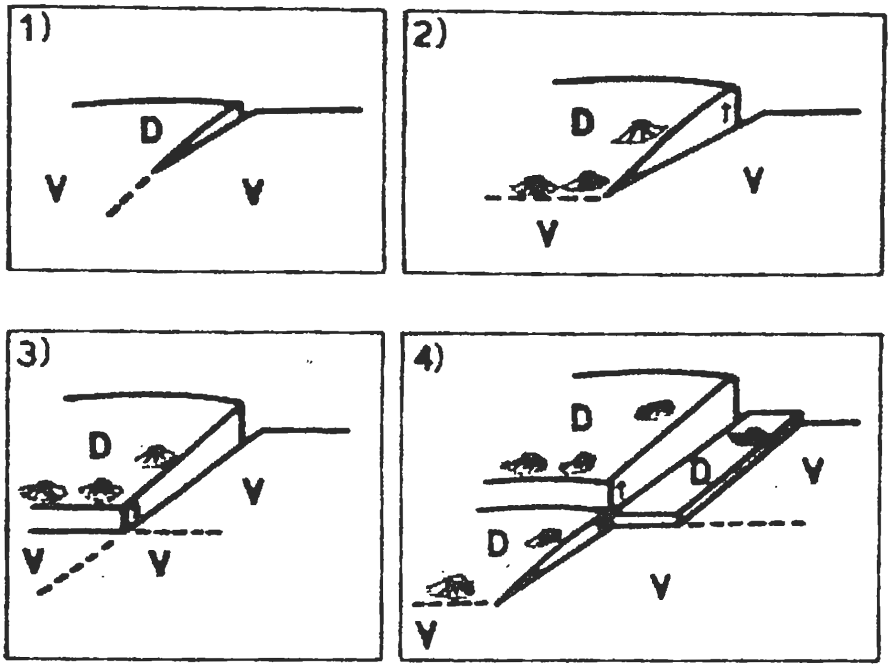


Fig. 19 - Tectonic evolution of central-eastern Ethiopian plateau (type area). Lifting of plateau occurred "block by block" starting from northern regions. Each block is defined by faults parallel and transversal to escarpment. Fissural silicic volcanism (V) died out (D) in uplifted regions, while alkaline lavas built shield volcanoes along faults (after ZANETTIN et al., 1978).

already thinned to 25-15 km in the Ethiopian rift and to 20-5 km in the Afar, where the minimum thickness has been found in the central sector. The Red Sea and Gulf of Aden rifts already have an oceanic character.

This crustal thinning is due to the spreading rate of the Arabian peninsula to the NE and of the Somalian plate to the south. The rate is 0.5 cm/year in the northern part of the Ethiopian rift (MOHR, 1977) and 2 cm/year in the Red Sea (PHILLIPS, 1970). Intermediate rates (1 cm/year) have been suggested for the Afar, which may still be thought of as a continental rift, locally in the course of incipient oceanization.

According to the model proposed by GASS (1970) for the Afro-Arabian rift system, the stronger the tholeiitic character of basalts emitted in a certain area, the stronger the crustal thinning in the same area. Where continental spreading is effective, true tholeiitic basalts should be emitted.

It has been said (BARBERI and VARET, 1975) that the axial ranges of the Afar correspond to oceanic rifts, but the basalts emitted there have a transitional rather than of a tholeiitic character. However, as already mentioned, the Afar transitional basalts are almost indistinguishable from those of the Ethiopian plateau, where the continental crust is very thick; their occurrence cannot therefore represent evidence of an oceanization process.

In any case, as the fissural transitional basalts of Ethiopia are in obvious connection with extensive movements, it has been hypothesized that a relationship exists between intensity of extension and degree of tholeiiticity of the basalts emitted. Following this concept, we may state that the emission of the transitional-tholeiitic basalts of Ashangi (c. 40 Ma), Aiba (c. 30 Ma), Fursa (c. 10 Ma) and the Afar stratoid series (c. 4 Ma) coincided with particularly strong episodes of extensive movements (STYLES and HALL, 1980; COCHRAN, 1983; GIRDLER and UNDERWOOD, 1985).

Among the recent basalts, the most tholeiitic characters are shown by the transitional basalts of Asal, representing a direct extension of the spreading axis of the Gulf of Tajura, while the basalts of the oceanic ridges of the Red Sea and the Gulf of Aden are actually tholeiitic (GASS, 1970).

## ACKNOWLEDGMENTS

Thanks are due to Profs. E. JUSTIN-VISENTIN, G. BELLIENI and Dr. A. FIORETTI for their collaboration in processing chemical data, and to G. MEZZACASA for his analytical and drafting work.

## REFERENCES

ABBATE E. and SAGRI M. (1969). Dati e considerazioni sul margine orientale dell'altopiano etiopico nelle province del Tigrai e del Wollo. Boll. Soc. Geol. Ital., 88: 489-497.

AZZAROLI A. (1968). On the evolution of the Gulf of Aden. XXIII Intern. Geol. Congr., 1: 125-134.

BAKER B.H., MOHR P.A. and WILLIAMS L.A.J. (1972). Geology of the Eastern Rift System of Africa. Geol. Soc. Am. Spec. Paper 136: 67 pp.

BARBERI F. and VARET J. (19759. Recent volcanic units of Afar and their structural significance. In: Afar Depression of Ethiopia (eds. A. PILGER and A. ROESLER), 1: 174-177. Schweizerbart.

BARBERI F. and SANTACROCE R. (1980). The Afar Stratoid Series and the magmatic evolution of the East African rift system. Bull. Soc. Geol. Fr., 22: 891-899.

BARBERI F., SANTACROCE R. and VARET J. (1974). Silicic peralkaline volcanic rocks of the Afar Depression (Ethiopia). Bull. Volcan., 38: 755-790.

BARBERI F., FERRARA G., SANTACROCE R. and VARET J. (1975a). Structural evolution of the Afar triple junction. In Afar Depression of Ethiopia (eds. A. PILGER and A. ROESLER), 38-54. Schweizerbart.

BARBERI F., CIVETTA L. and VARET. J. (1980). Sr isotopic composition of Afar volcanics and its implications for mantle evolution. Earth Planet. Sci. Lett., 50: 247-259.

BELLIENI G., JUSTIN-VISENTIN E., ZANETTIN B., PICCIRILLO. F. and RADICATI DI BROZOLO F. (1981). Oligocene transitional tholeiitic magmatism in Northern Turkana (Kenya): comparison with the coeval Ethiopian volcanism. Bull. Volcan., 44: 411-427.

BERHE S.M., DESTA B., NICOLETTI M. and TEFERRA M. (1987). Geology, geochronology and geodynamic implications of the Cenozoic magmatic province in W and SE Ethiopia. Journ. Geol. Soc. London., 44: 213-226.

BERKTOLD A., HAAK V. and ANGENHEISTER G. (1975). Afar: Geophysics - Magnetotelluric measurements in the Afar area. In: Afar Depression of Ethiopia (eds. A. PILGER and A. ROESLER), 1: 66-79. Schweizebart.

BETTON P.J. and COX K.G. (1979). Production of rhyolites at continental margins: an example from the Lebombo Monocline. 18th Congr. Geol. Soc. S. Afr. Abstract. 29-32.

BROTZU P., MORBIDELLI L., PICCIRILLO E.M. and TRAVERSA G. (1974a). Petrographical and chemical researches on the stratoid volcanics of the main Ethiopian rift. Mem. Museo Trid. Sci. Nat., 20: 100-122.

BROTZU P., MORBIDELLI L., PICCIRILLO E.M. and TRAVERSA G. (1974b). Petrological features of Boseti Mountains: a complex sistem in the axial portion of the main Ethiopian rift. Bull. Volcan., 38: 1-29.

BROTZU P., GANZERLI-VALENTINI M.T., MORBIDELLI L., PICCIRILLO E.M., STELLA R. and TRAVERSA G. (1980a). Quaternary basaltic volcanism in the northern part of the main Ethiopian rift (from 8° to 9° Lat. N.) Atti Convegni Lincei., 47: 293-315.

BROTZU P., KAZMIN V., MORBIDELLI L., PICCIRILLO E.M., SEIFE BERHE M. and TRAVERSA G. (1980). Petrochemistry of the volcanics in the northern part of the main Ethiopian rift. Atti Convegni Lincei., 47: 367-386.

BROTZU P., MORBIDELLI L., PICCIRILLO E.M. and TRAVERSA G. (1980). Volcanological and magmatological evidence of the Boseti volcanic complex (main Ethiopian rift). Atti Conveqni Lincei., 47: 317-366.

CIVETTA L., LA VOLPE L. and LIRER L. (1978). K/Ar ages of the Yemen Plateau volcanics. J. Volcan. Geotherm. Res., 4: 307-314.

COCHRAN J.R. (1983). A model for the development of the Red Sea. Am. Assoc. Petrol. Geol. Bull., 67: 41-69.

DAVIDSON A. and REX D.C. (1980). Age of volcanism and rifting in southwestern Ethiopia. Nature., 283: 654-658.

DE FINO M., LA VOLPE L. and LIRER L. (1973). Volcanology and petrology of the Assab Range. Bull. Volcan., 37: 95-110.

DE FINO M., LA VOLPE L. and LIRER L. (1978). Geology and volcanology of the Edd-Bahar Assoli area (Ethiopia). Bull. Volcan., 41: 1-11.

DI PAOLA G.M. (1972). The Ethiopian rift valley (between 7°00' and 8°40' lat. North). Bull. Volcan., 36: 517-560.

GASS I.G. (1970). The evolution of volcanism in the junction area of the Red Sea, Gulf of Aden and Ethiopian rifts. Phil. Trans. Roy. Soc. London, A267: 369-381.

GIRDLER R.W. and STYLES P. (1978). Seafloor spreading in the western Gulf of Aden. Nature, 271: 615-617.

GIRDLER R.W. and UNDERWOOD M. (1985). The evolution of early oceanic lithosphere in the southern Red Sea. Tectonophysics, 116: 95-108.

GREEN D.H. (1989). The earth's lithosphere and asthenosphere: concepts and constraints derived from petrology and high-pressure experiments (in press).

JUCH D. (1975). Geology of the south-eastern escarpment of the Ethiopia between 39° and 42° long. East. In: Afar Depression of Ethiopia (eds. PILGER A. and ROESLER A.), 310-316.

JUSTIN-VISENTIN E., NICOLETTI M., TOLOMEO L. and ZANETTIN B. (1974). Miocene and Pliocene volcanic rocks of the Addis Ababa Debra Berhan area (Ethiopia). Bull. Volcan., 38: 237-253.

KAZMIN V., BERHE M., NICOLETTI M. and PETRUCCIANI C. (1980). Evolution of the northern part of the Ethiopian rift. Atti Convegni Lincei, 47: 275-292.

LE RAS M.J., LE MAITRE R.W., STRECKEISEN A. and ZANETTIN B. (1986). A chemical classification of volcanic rocks based on the total Alkali-Silica diagram. Journ. Petr. Oxford., 27: 745-750.

MAKRIS J., MENZEL H., ZIMMERMANN J. and GOUIN P. (1975). Gravity field and crustal structure of North Ethiopia. In: Afar Depression of Ethiopia (eds. A. PILGER and A. ROESLER), 135-144. Schweizerbart.

MERLA G. (1963). Missione geologica nell' Etiopia meridionale del Consiglio Nazionale delle Ricerche, 1959-1960. Notizie geomorfologiche e geologiche. Giorn. Geol. Am. Museo Geol. Bologna, 31: 1-56.

MERLA G., ABBATE E., CANUTI P., SAGRI M. and TACCONI P. (1973). Geological map of Ethiopia and Somalia (1:2,000,000). C.N.R., Firenze.

MOHR P. (1967). The Ethiopian rift system. Bull. Geophys. Obs. Addis Ababa, 11: 1-65.

MOHR P. (1972). Regional significance of volcanic geochemistry in the Afar triple junction, Ethiopia. Bull Geol. Soc. Am. 83: 213-222

MOHR P. (1977). 1974 Ethiopian rift geodymeter survey. Smiths. Astr. Observ., Spec. Rep. 376, Cambridge, Mass.

MOHR P. (1983). Ethiopian flood Basalt province. Nature, 303: 577-584.

MOHR P. and ZANETTIN B. (1988). The Ethiopian flood basalt province. In Continental flood basalts (Edited by MAC DOUGALL J.D.), 63-110. Kluver Acad. Pubbl.

MOORE J.M. and DAVIDSON A. (1978). Rift structure in southern Ethiopia. Tectonophysics, 46: 159-173.

OTTONELLO G., PICCARDO G.B. and TREUIL J. (1980). Nature of the deep crust and uppermost mantle unter the Assab region (Ethiopia): inferences from petrology and geochemistry of mafic-ultramafic inclusions. Atti Convegni Lincei, 47: 463-488.

PHILLIPS J.D. (1970). Magmatic anomalies in the Red Sea. Phil. Trans. Roy. Soc. London, 267: 205-217.

PICCIRILLO E.M., JUSTIN-VISENTIN E., ZANETTIN B., JORON J.L. and TREUIL M. (1979). Geodynamic evolution from plateau to rift: major and trace element geochemistry of the central eastern Ethiopian Plateau volcanics. Neues Jb. Geol. Palaont. Abh., 158: 139-179.

STIELTJES L., JORON J.L., TREUIL M. and VARET J. (1976). Le rift d' Asal, segment de dorsale émergé: discussion petrologique et geochimique. Bull. Soc. Geol. Fr., 4: 851-862.

STYLES P. and HALL S.A. (1980). A comparison of the seafloor spreading historics of the western Gulf of Aden and the central Red Sea. Atti Convegni Lincei, 47: 585-606.

YODER H.S. and TILLEY C.E. (1962). Origin of basalt magmas: an experimental study of natural and synthetic rock systems. J. Pelrol., 3: 342-532.

ZANETTIN B. (1984). Proposed new chemical classification of volcanic rocks. Episodes, 7: 19-20.

ZANETTIN B. and JUSTIN-VISENTIN E. (1974). The volcanic succession in central Ethiopia. 2. The volcanics of the western Afar Ethiopian rift margins. Mem. Ist. Geol. Miner. Univ. Padova, 31: 1-19.

ZANETTIN B. and JUSTIN-VISENTIN E. (1975). Tectonical and volcanological evolution of the western Afar margin (Ethiopia). In Afar Depression of Ethiopia (eds. A. PILGER and A. ROESLER), 300-309. Schweizerbart.

ZANETTIN B., GREGNANIN A., JUSTIN-VISENTIN E., MEZZACASA G. and PICCIRILLO E.M. (1974). Petrochemistry of the volcanic series of the central eastern Ethiopian Plateau and relationship between tectonics and magmatology. Mem. Ist. Geol. Miner. Univ. Padova, 31: 1-34.

ZANETTIN B., GREGNANIN A., JUSTIN-VISENTIN E., MEZZACASA G. and PICCIRILLO E.M. (1976). New chemical analyses of the Tertiary volcanics from the central Ethiopian Plateau. C.N.R., Ist. Min. Univ. Padova, 1-43.

ZANETTIN B., JUSTIN-VISENTIN E. AND PICCIRILLO E.M. (1978). Volcanic succession, tectonics and magmatology in central Ethiopia. Atti Mem. Accad. Patavina Sci. Lett. Arti, 90: 5-19.

ZANETTIN B., JUSTIN VISENTIN E., NICOLETTI M. and PICCIRILLO E.M. (1980a). Correlations among Ethiopian volcanic formations with special references to the chronological and stratigraphical problems of the "Trap Séries". Atti Convegni Lincei, 47: 231-252.

ZANETTIN B., JUSTIN-VISENTIN E. and PICCIRILLO E.M. (1980b). Migration of the Ethiopian continental rifts in the course of the Tertiary evolution of the Afro-Arabian rift system. Atti Convegni Lincei, 47: 253-265.

ZANETTIN B., JUSTINVISENTIN E., BELLIENI G., PICCIRILLO E.M. and RITA F. (1983). Le volcanisme du bassin du Nord-Turkana (Kenya): age, succession et evolution structurale. Bull. Centres Rech. Explor., Prod. Elf, Aquitaine, 7: 249-255.

*Final editing, January 1990*

From *Geology and mineral resources of Somalia and surrounding regions*, Ist. Agron. Oltremare, Firenze,. Relaz. e Monogr. 113, 311-322, 1993.

# K-AR AND FISSION TRACK AGES OF THE LAST VOLCANO TECTONIC PHASE IN THE ETHIOPIAN RIFT VALLEY (TULLU MOYE' AREA)

B. BIGAZZI *, F.P. BONADONNA *, G.M. DI PAOLA **, and A. GIULIANI *

* Istituto di Geocronologia e Geochimica Isotopica, C.N.R., Via C. Maffi 36, 56100 Pisa, Italy.

** United Nation, Department of Technical Cooperation for Development, Room DC 1-780, One U.N. Plaza, New York, N.Y. 10017, U.S.A.

ABSTRACT

New radiometric data indicate that in the Ethiopian Rift South of 8°30' N, fissural peralkaline silicic activity of regional extent developed in an extremely recent past (0.25-0.1 m.y. B.P.). Large volumes of transitional basaltic lavas, minor oversaturated trachytes and comenditic end members, related to fissural activity in well defined "en échelon" displaced areas (Tullu Moyè type), were also erupted mostly during the last 0.1 m.y. until historical times. During the same period one of the most intense phase of faulting affected the rift floor. An acceleration of the Somalian plate motion, and consequent increase in the crustal thinning process, is tentatively suggested to explain this major volcano tectonic phase which still affects the floor of the Ethiopian Rift Valley.

## INTRODUCTION

Among volcanic rocks, peralkaline silicic ignimbrites, unwelded pyroclastics and minor lavas related to fissural eruptions of regional extent are by far the most abundant products outcropping on the floor and, in a relatively minor quantity, on the margins (NW and SE plateaux) of the Ethiopian Rift Valley. Central volcanoes and large regional calderas made of pantelleritic pyroclastics and lavas within the Rift, also contribute to the mainly silicic peralkaline volcanic picture of this part of Ethiopia (DI PAOLA, 1972).

Radiometric data of Ethiopian Rift volcanic rocks (BLACK et al., 1974; CHESSEX et al., 1974; KUNZ et al., 1974; MORBIDELLI et al., 1974; SICHENBERG and SCHONFELD, 1974; SPIES, 1974; JONES, 1976) indicate that north of Lat. 8°30' N approx., basaltic activity developed since Upper Oligocene-Lower Miocene until present time, while fissural peralkaline silicic volcanism covers a time span from Middle-Upper Miocene to Early Pleistocene with a climax during Pliocene. South of Lat. 8°30' N, only three radiometric data of rift floor volcanic rocks were up to now available (WENDORF et al., 1975). Owing to the lack of sufficient radiometric date south of this latitude, silicic peralkaline fissure activity has never been considered younger than Late Pliocene-Early Pleistocene all over the Ethiopian rift.

The aim of this paper is to show that the last fissural peralkaline silicic products, at least in the central part of the Ethiopian rift (Tullu Moyè area), are of one order of magnitude younger than their equivalents found up to now further north (0.1-0.2 m.y., instead of 1.5-2.0 m.y.). This implies that an important volcano tectonic phase, still affecting the rift floor, initiated only about two hundred thousand years ago.

## GEOLOGICAL SUMMARY OF THE TULLU MOYE' AREA

Some well defined en echelon displaced areas, where the most intense recent tensional tectonics (NNE-SSW trending) and related volcanic activity occurred and still occur, can be observed all along the floor of the Ethiopian Rift Valley. The Tullu Moyè, with its 2,000 km$^2$ surface, is one of the most representative of such areas (DI PAOLA, 1976; BIZOUARD and DI PAOLA, 1978).

The Tullu Moyè area (Fig. 1) is located in the central part of the Ethiopian Rift Valley (8°00' - 8°30' N; 39°00' - 39°15' E) close to the escarpment of the south-eastern Ethiopian plateau. A series of huge normal step faults lowers the average altitude of the southeastern plateau (2,500 m a.s.l.) to the 1,500-1,600 m a.s.l. of the rift floor at this latitude. Big central volcanoes such as Cilallo, Badda, etc., made of hawaiitic, mugearitic and alkali trachytic lava flows (DI PAOLA, 1973, 1976; MOHR and POTTER, 1976) stand above the Tertiary flood basalts of the plateau near the edge of the escarpment.

In the Tullu Moyè area the most recent volcanic activity developed intensively in two distinct parts of the rift floor :

a) an eastern one where a wide variety of different magmas (from mildly alkali basalts to comendites) erupted almost exclusively through a fissure swarm trending NNE-SSW in a very close time space association. The great number of recent normal faults and gaping fissures which affects this part of the Tullu Moyè area as well as the record of an eruption two centuries ago (DI PAOLA, 1976), or even later (GOUIN, 1979), indicate that this is the presently active axis of the structure.
b) a western one where volcanic activity built some small central volcanoes (Bora-Bericcio Complex) whose pyroclastics and lavas, almost exclusively pantelleritic, underlie those of the eastern part.

Some transverse (NW-SE) short normal faults through which part of the pantelleritic products were erupted, affect this western part of the Tullu Moyè area.

Other pantelleritic pyroclastics and lavas belonging to a 9 x 8 km large regional caldera (Gadamsà) located just at the northern limit of the eastern basaltic field, seem to be older than those of Bora-Bericcio Complex eventhough no direct stratigraphic relations between the two exist.

In both parts of the Tullu Moyè area, the recent volcanic rocks overlie a floor of pantelleritic ignimbrites and lavas. Ignimbrites, in turn, cover a mugearitic flow of the

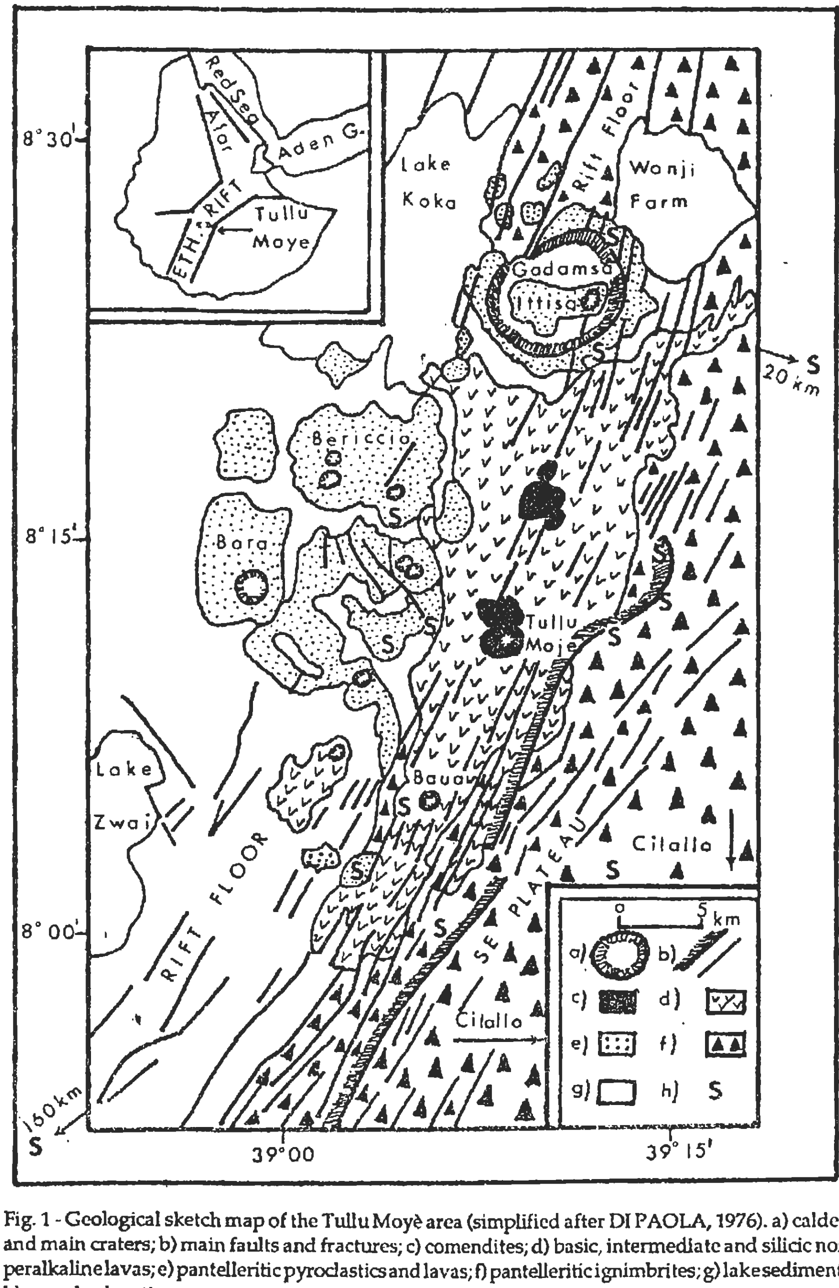


Fig. 1 - Geological sketch map of the Tullu Moyè area (simplified after DI PAOLA, 1976). a) caldera and main craters; b) main faults and fractures; c) comendites; d) basic, intermediate and silicic non-peralkaline lavas; e) pantelleritic pyroclastics and lavas; f) pantelleritic ignimbrites; g) lake sediments; h) samples location

western base of Cilallo near the edge of the eastern plateau and the precaldera pantelleritic lavas of Gadamsà.

The general stratigraphic sequence of the Tullu Moyè area is summarized in Fig. 2.

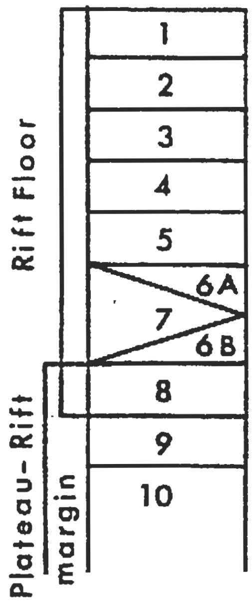


Fig. 2 - General stratigraphic sequence of the Tullu Moyè area (slightly modified after DI PAOLA, 1976). 1) fissural comenditic perlites and pumice cones; 2) trachytic and/or dark trachytic flows; 3) aphyric hawaiites and mildly alkali basalt flows and spatter cones 4) trachyrhyolitic flows; 5) megaplagioclase rich hawaiitic flows; 6A and 6B) pantelleritic obsidians, perlites and pumice of the Bora-Bericcio complex and NW-SE fissural activity; 7) fluvio-lacustrine sediments; 8) pantelleritic ignimbrites, lavas and pumice; 9) mugearitic flow of the western base of Cilallo; 10) flood basalts of possible Tertiary trap series (strongly weathered).

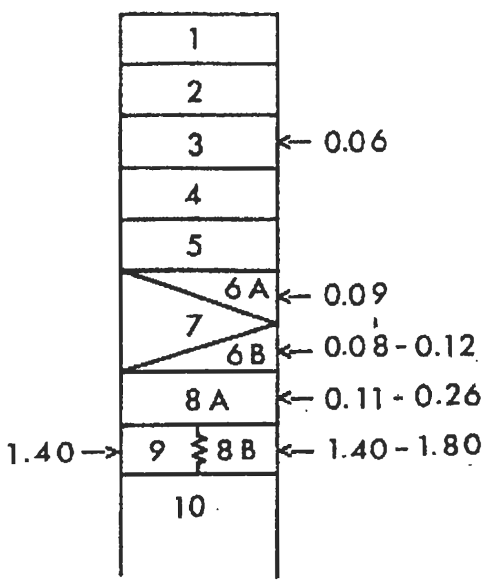


Fig. 3 - General stratigraphic sequence of the Tullu Moyè area corrected on the basis of present radiometric data. Ages in m.y. (see text and Tables 1 and 2). Same legend as in Fig. 2.

Table 1 - K-Ar and fission track ages of Ethiopian Rift volcanic rocks.

| Sample | K-Ar * | | | | Fission tracks | | | |
|---|---|---|---|---|---|---|---|---|
| | K(%) | (ml)rad $^{40}Ar$/gr K $\times 10^{-6}$ | (%)rad $^{40}Ar$ | Age (m.y.) | Age (m.y.) | Fossil tracks (dens./cm$^2$) | Induced ** tracks (density/cm$^2$) $\times 10^3$ | Fossil/induced size tracks ratio |
| RV 1A | 3.89 | 6.90 | 4 | (WR)1.77±0.44 | 1.60 ± 0.17 | 1080 | 50 | 0.87 |
| RV 22 | 3.99 | 7.02 | 34 | (AF)1.80±0.09 | 1.53 ± 0.16 | 1280 | 65 | 0.84 |
| RV 46 | 4.04 | 5.82 | 27 | (AF)1.49±0.07 | - | - | - | - |
| RV 108 | 3.83 | 5.51 | 19 | (AF)1.41±0.07 | - | - | - | - |
| RV 50 | 1.55 | 5.10<br>5.56 | 10<br>9.5 | (WR)1.31±0.13<br>(WR)1.43±0.14 | - | - | - | - |
| RV 211 | - | - | - | - | 0.428 ± 0.050<br>0.466 ± 0.056 | 760<br>830 | 139<br>143 | 0.86<br>0.85 |
| RV 264A *** | 3.64 | 2.05 | 1 | (SG)0.526±0.131 | 0.163 ± 0.027(R)<br>0.063 ± 0.013(E) | 100<br>42 | 84<br>84 | (+)<br>0.47 |
| RV 359 | 3.75 | 0.32 | 2 | (WR)0.082±0.021 | 0.267 ± 0.040<br>0.256 ± 0.030 | 315<br>320 | 117<br>108 | 0.76<br>0.82 |
| RV 365 | - | - | - | - | 0.212 ± 0.032 | 175 | 59 | 0.89 |
| RV 277 | - | - | - | - | 0.115 ± 0.016 | 140 | 98 | 0.86 |
| RV 51 | 3.42 | 0.72 | 2 | (AF)0.185±0.046 | - | - | - | - |
| RV 67 | 3.52 | 0.43 | 3 | (AF)0.110±0.027 | - | - | - | - |
| RV 305 | - | - | - | - | 0.124 ± 0.014<br>0.096 ± 0.015 | 110<br>60 | 77<br>70 | 0.81<br>0.73 |
| RV 226 | - | - | - | - | 0.092 ± 0.012 | 130 | 113 | 0.86 |
| RV 245 | - | - | - | - | 0.091 ± 0.011<br>0.083 ± 0.011 | 165<br>165 | 140<br>137 | 0.86<br>0.91 |

* Potassium analyses by A.A. (analyst : A. Pescia, CNR Pisa). $^{40}K/K = 1.17 \times 10^{-4}$; $\lambda_\varepsilon = 0.581 \times 10^{-10}\ yr^{-1}$ ; $\lambda_\beta = 4.96 \times 10^{-10}\ yr^{-1}$ (Steiger and Jäger, 1977). ** Referred to a neutron dose of $10^{15}$ neut./cm$^2$.

*** R = age of the rock ; E = age of the phreatic explosion. (+) This value has not been reported because of the bimodal distribution of size tracks.

WR = Whole rock ; AF = Alkali feldspar separated ; SG = Separated glass.

Table 2 - Location and petrography of samples analysed in Table 1.

| Sample | Location and geological setting* | Rock type | Petrography |
|---|---|---|---|
| RV 1A | Dyke cutting ignimbrites and pumice along the rift-plateau eastern escarpment (8) | Pantellerite | Crystal-free obsidian |
| RV 22 | Compact glassy "fiamma" of an ignimbritic unit along the rift-plateau eastern escarpment (8) | Pantellerite | Anorthoclase, acmitic Cpx and magnetite slightly porphyritic obsidian |
| RV 46 | Ignimbrite above RV 22 along the rift-plateau eastern escarpment (8) | Pantellerite | Anorthoclase, acmitic Cpx, alkali amphibole and magnetite porphyritic. Completely devitrified groundmass. |
| RV 108 | Ignimbrite along the rift-plateau eastern escarpment about 30 km ESE of Gadamsà caldera (8) | Pantellerite | Anorthoclase, quartz, acmitic Cpx, aenigmatite and fayalite porphyritic. Partly devitrified groundmass. |
| RV 50 | Lava flow at the western base of Cilallo volcano (9) on top of the eastern plateau | Mugearite | Olivine, plagioclase, augitic Cpx, Fe-Ti oxides and apatite subaphyric microcrystalline. |
| RV 211 | Lava flow at the eastern base of Duguna volcano (about 200 km SW of Tullu Moyè crater) | Pantellerite | Crystal free obsidian |
| RV 264A | Compact glassy "fiamma" of an ignimbritic unit at the bottom of Baua phreatic explosion crater (8) | Pantellerite | Anorthoclase and acmitic Cpx slightly porphyritic obsidian |

* The number in parentheses refers to the stratigraphic position of Fig. 2.

Table 2 - continued

| Sample | Location and geological setting * | Rock type | Petrography |
|---|---|---|---|
| RV 359 | Precaldera lava flow on the SE rim of Gadamsà caldera (8) | Pantellerite | Obsidian with rare anorthoclase phenocrysts |
| RV 365 | Precaldera lava flow on the NE rim of Gadamsà caldera (8) | Pantellerite | Anorthoclase, acmitic Cpx, fayalite and magnetite slightly porphyritic obsidian. Some alkali feldspar microlites and Cpx in the groundmass |
| RV 277 | Compact glassy "fiamma" of an ignimbrite on the rift floor at the southern limit of Tullu Moyè basaltic field near the foot of the rift-plateau eastern escarpment (8) | Pantellerite | Obsidian with rare anorthoclase phenocrysts. |
| RV 51 | Ignimbrite covering RV 50, same locality (8) | Pantellerite | Anorthoclase and aenigmatite porphyritic. Partly devitrified groundmass. |
| RV 67 | Lava dome in the southern part of the Bora-Bericcio complex (6B) | Pantellerite | Anorthoclase and acmitic Cpx slightly porphyritic obsidian. Anorthoclase microlites, Cpx and aenigmatite in the groundmass |
| RV 305 | Block within pumice fall in the middle of Bora-Bericcio complex (6B) | Pantellerite | Crystal free obsidian |
| RV 226 | Lava dome of NW-SE fissural activity of the Bora-Bericcio complex (6A) | Pantellerite | Anorthoclase, quartz, acmitic Cpx, aenigmatite and fayalite slightly porphyriti obsidian. Few alkali feldspar microlites in the groundmass |
| RV 245 | Lava flow of the NW-SE fissural activity of the Bora-Bericcio complex (6B) | Pantellerite | Anorthoclase, acmitic Cpx and aenigmatite slightly porphyri tic obsidian |

* The number in parentheses refers to the stratigraphic position of Fig.2

## GEOCHRONOLOGY

K-Ar and fission track ages of Tullu Moyè volcanic rocks are listed in Table 1, while in Table 2, locations geological settings and brief petrographic descriptions of the same samples are reported. Sample RV 211, belonging to the base of Duguna, a rather important pantelleritic central volcano of another active area of the rift floor about 200 km SW of Tullu Moyè, has been reported for comparison. Argon analyses were performed by isotope dilution using a Reynolds type mass spectrometer statically operating.

Fission track age determinations have been performed using an already classical technique. Samples have been etched with HF 20 % for 90 seconds at 40°C and fission tracks have been counted in transmitted light. The amount of neutron dose has been determined using the standard SRM 963 of the National Bureau of Standards and the value of the decay constant used is $6.9 \times 10^{-17}$ years. All the analysed samples have shown a weak fading rate and, except for RV 264 A, the fission tracks distribution in all of them is unimodal. Apparent ages have been corrected according to STORZER and WAGNER (1969) using a curve obtained in the same etching conditions as those utilized for counting the fission tracks.

The bimodal distribution of fission tracks shown by sample RV 264 A indicates that this rock must have been subjected to a rather important geologic event, therefore two ages have been determined for this sample using the same correction curve; that of the eruption and that of the later event.

## DISCUSSION OF RADIOMETRIC RESULTS

A fairly good agreement between the results obtained with the two methods is evident for samples RV 1 A and RV 22 while an important discrepancy appears for samples RV 264 A and RV 359 (Table 1). However the too high atmospheric contamination revealed by these two samples makes their K-Ar ages quite suspicious, while fission track results appear to be much more acceptable.

The observed bimodal distribution of fission tracks in sample RV 264A finds a satisfactory explanation on a volcanological basis. This sample in fact is a compact glassy "fiamma" of a thick ignimbritic unit visible at the base of a 500 m large and 50 m deep phreatic explosion crater (Baua), located in the central southern part of the Tullu Moyè area. The violent shock produced by the phreatic explosion might account for the observed phenomenon.

Compairing the stratigraphy of Fig. 2 with the ages listed in Table 1, the following considerations emerge :

1) Owing to the strong lithological, petrographic, chemical and geochemical similarities of the several ignimbritic units outcropping all over the Tullu Moyè area and to the structural style of this region that frequently prevents any stratigraphic differentiation

between plateau and rift floor units, DI PAOLA (1976) erroneously considered such activity as a unique Late Pliocene-Early Pleistocene phase. Actually it is evident from the present data that a second phase of pantelleritic fissural activity (ignimbrites and lavas) occurred in a much more recent time within the rift and perhaps also on top of the eastern plateau (Table 1, 2) provided that the K-Ar age of RV 51 is not invalidated by the very high atmospheric contamination of this sample. Anyway the present ages found for this recent activity are in good agreement with those found for two crystal ash layers, not related to any central volcano, of the Gademota Formation (rift floor, about 50 km SW of Tullu Moyè; WENDORF et al., 1975).
The present data therefore allow a much better definition of the general stratigraphic sequence of the Tullu Moyè area as shown in Fig. 3.

2) The age of the western base of Cilallo volcano is in a rather good agreement with the neighbouring dyke swarm of the Sagatu ridge (MOHR and POTTER, 1976) and it seems to be more or less coeval with the first ignimbritic phase outcropping in this area.
3) The collapse of Gadamsa caldera is younger than 0.2 m.y..
4) The age of lake sediments interbedded with Bora-Bericcio pantelleritic pyroclastics and lavas is about 0.1 m.y.. This age perfectly coincide with that suggested by LAURY and ALBRITTON (1975) for the highest level reached by a large lake which in the past occupied all the central part of the Ethiopian Rift.
5) Post-caldera pantelleritic perlites and pumice, inside Gadamsà, were erupted between 0.2 and 0.1 m.y.. Some of these products, in fact, are covered by remnants of lake sediments which stand some tens of metres above the present caldera floor. Post-caldera activity probably continued after the dessication of the lake (later than 0.1 m.y.) as indicated by the well preserved, sediments uncovered, Ittisà crater.
6) All the volcanic products from unit 6B to unit 1 in Fig. 3 started erupting 0.1 m.y. B.P. and the activity continued until historical times. Consequently the ages of the great number of faults which affect these products, sometimes with vertical throws of several tens of metres, are younger than 0.1 m.y..
7) Baua phreatic explosion crater formed about sixty thousand years ago.

## CONCLUSIONS

Although its genesis and mechanism of eruption are not fully understood yet, large scale peralkaline silicic volcanism and magmatism seems to be the marker of important stages of crustal thinning and opening of continental rifts (BARBERI et al., 1972; MAC DONALD, 1974). The extremely young age of the last eruption of such products in the Tullu Moyè area might therefore indicate that a major phase of opening occurred very recently within the rift floor.

Present data are unsufficient to attempt a satisfactory reconstruction of the volcanic and tectonic history of the Ethiopian Rift. However, in order to explain this new major phase it can be tentatively suggested that this might be related to an acceleration of the Somalian plate motion. In this assumption, a significant increase in the crustal thinning process along the active axis of the rift should have initiated, according to the present date, 0.25 m.y. B.P. and it should be still in progress. This could account both for the present spectacular tensional tectonics affecting the floor of the Ethiopian Rift and, as already noticed by BIZOUARD and DI PAOLA (1978), for the significant lowering of potassium and rubidium content observed in the last erupted basic and intermediate magmas, as well as for the exclusively comenditic composition (instead of pantelleritic of the historical and sub-historical end members of the Tullu Moyè fractionation series

REFERENCES

BARBERI F., BORSI S., FERRARA G., MARINELLI G., SANTACROCE R., TAZIEFF H. and VARET J. (1972): Evolution of the Danakil Depression (Afar, Ethiopia) in light of radiometric age determinations. J. Geol., 80: 720-729.

BIZOUARD H. and DI PAOLA G.M. (1978). Mineralogy of the Tullu Moyè active volcanic area (Arussi: Ethiopian Rift Valley). In : E.R. NEUMANN and I.B. RAMBERG (Eds), Petrology and Geochemistry of Continental Rifts, 1: 87-100.

BLACK R., MORTON W.H. and REX D.C. (1975). Block tilting and volcanism within the Afar in the light of recent K-Ar age data. In : PILGER and ROSLER (Eds), Afar Depression of Ethiopia, 1: 296-300, Schweizerbart'sche Verlag Stuttgart.

CHESSEX R., DELALOYE M., MULLER J. and WEIDMANN M. (1975). Evolution of the volcanic region of Ali Sabieh (T.F.A.I.) in the light of K-Ar age determinations. In: PILGER and ROSLER (Eds), Afar Depression of Ethiopia 1: 221-227, Schweizerbart'sche Verlag, Stuttgart.

DI PAOLA G.M. (1976). Geological map of the Tullu Moyè active volcanic area (Arussi: Ethiopian Rift Valley), 1:75.000, C.N.R. Pisa.

GOUIN P. (1979). Earthquake history of Ethiopia and the Horn of Africa. I.D.R.C., 118e, Ottawa.

JONES P.W. (1976). Age of the lower flood basalts of the Ethiopian Plateau. Nature, 261, 567-569.

KUNZ K., KREUZER H. and MULLER P. (1975). Potassium-Argon age determinations of the trap basalt of the south-eastern part of the Afar Rift. In : PILGER and ROSLER (Eds), Afar Depression of Ethiopia, 1: 370-374. Schweizerbart'sche Verlag, Stuttgart.

LAURY R.L. and ALBRITTON C.C. Jr. (1975). Geology of Middle Stone Age archeological sites in the main Ethiopian Rift Valley. Geol. Soc. of Am. Bull., 86: 999-1011.

MAC DONALD R. (1974). Tectonic settings and magma associations. In : D.K. BAILE, F. BARBERI and R. MAC DONALD (Eds), Oversaturated peralkaline volcanic rocks. Bull. Volcan., 38\3: 575-593.

MOHR P.A. and POTTER E.C. (1976). The Sagatu ridge dyke swanm, Ethiopian Rift margin. J. Volc. Geotherm. Res., 1: 55-71.
MORBIDELLI L., NICOLETTI M., PETRUCCIANI C. and PICCIRILLO E.M. (1975). Ethiopian south-eastern plateau and related escarpment: K-Ar ages of th main volcanic events (Main Ethiopian Rift from 8°10' to 9°00' lat. north In: PILGER and ROSLER (Eds), Afar Depression of Ethiopia, 1: 362-369. Schweizerhart'sche Verlag, Stuttgart.
SICKENBERG O. and SCHONFELD M. (1975). The Chorora formation-Lower Pliocene limnical sediments in the Southern Afar (Ethiopia). In: PILGER and ROSLER (Eds), Afar Depression of Ethiopia, 1: 277-284. Schweizerbart'sch Verlag, Stuttgart.
SPIES O. (1975). Inclusion-bearing Pliocene peralkaline silicic ignimbrites frc south-west of Mt Ayelu, Southern Afar (Ethiopia). In: PILGER and ROSLER (Eds), Afar Depression of Ethiopia, 1, 334-340, Schweizerbart'sche Verlag, Stuttgart.
STEIGER R.H. and JAGER E. (1977). Subcommission on geochronology: convention on the use of decay constants in geo- and cosmochronology. E.P.S.L., 36: 359-362.
STORZER D. and WAGNER G.A. (1969). Correction of thermal lowered fission track ages of tektites. E.P.S.L., 5: 463-468.
WENDORF F., LAURY R.L., ALBRITTON C.C., SCHILD R., HAINES C.V., DAMON P.E., SHAFIQULLAH M. and SCARBOROUGH R. (1975). Dates for the Middle Stone Age of East Africa. Science, 187: 740-742.

*Final editing, January 1990*

From *Geology and mineral resources of Somalia and surrounding regions*, Ist. Agron. Oltremare, Firenze, Relaz. e Monogr. 113, 323-338, 1993.

# THE KELLA HORST: ITS ORIGIN AND SIGNIFICANCE IN CRUSTAL ATTENUATION AND MAGMATIC PROCESSES IN THE ETHIOPIAN RIFT VALLEY

G.M. Di Paola *, Seife-Michael Berhe ** and V.Arno ***

* United Nations, Department of Technical Cooperation for Development, Room DC-1-780, One U.N. Plaza, New-York, N.Y. 10017, USA.

** Ethiopian Institute of Geological Surveys, Ministry of Mines, Energy andWater Resources, P.O. Box 486, Addis Ababa,Ethiopia.
Present address: Department of Earth Science, The Open University, Walton Hall, Milton Keynes MK7 6AA, U.K.

*** Dipartimento di Scienze della Terra, Università di Pisa, Via Santa Maria 53, 56100 Pisa, Italy.
Present address: Geotermica Italiana S.R.L., Lungarno Mediceo 16, 56100 Pisa, Italy.

ABSTRACT

The Kella Horst, a Precambrian crystalline basement covered by typical Ethiopian Mesozoic marine sediments has been discovered close to the western escarpment of the Ethiopian Rift Valley, 110 km S-SW of Addis Ababa. Its unexpected occurrence raises challenging questions about its origin and significance in the evolution of the Ethiopian Rift south of the Addis Ababa latitude.

The present lack of radiometric dating for the thick, widespread Tertiary basaltic formation outcropping around Kella prevents to establish a definite correlation with similar Ethiopian formations known to span from pre-Oligocene to middle-Miocene (ZANETTIN and JUSTIN-VISENTIN, 1975). However the evidence that the pre-Tertiary rocks at Kella are directly covered by a 3.0 m.y. old volcanic unit (ignimbrite) rather than by much older basalts suggests that at least prior to 10-12 m.y. ago the Kella Horst was a topographic feature much more prominent than at present. Based on stratigraphic and tectonic considerations, the Kella Horst is interpreted as a crustal block intimately associated with the present extensional movements of the Ethiopian Rift rather than as a recent uplift. Comparing the tectonic style and petrological character of the Pleistocene Holocene basaltic activity of the eastern and western margins of the Rift at the latitude of Kella, an asymmetric crustal structure is tentatively proposed.

## INTRODUCTION

In Ethiopia the Precambrian basement, frequently covered by Mesozoic marine sediments, outcrops in many parts of the western and eastern plateaux and in minor extent along the escarpments bordering the oceanic Afar Depression and the continental Ethiopian Rift (DAINELLI, 1943; MOHR, 1962; ABBATE and SAGRI, 1969; ABBATE et al., 1969; DI PAOLA, 1972; BLACK et al., 1972; MERLA et al., 1973; KAZMIN, 1973; LEVITTE et al., 1974; BARBERI et al., 1975; BARBERI and VARET, 1977; BARBERI and VARET, 1978; MERLA et al. 1979).

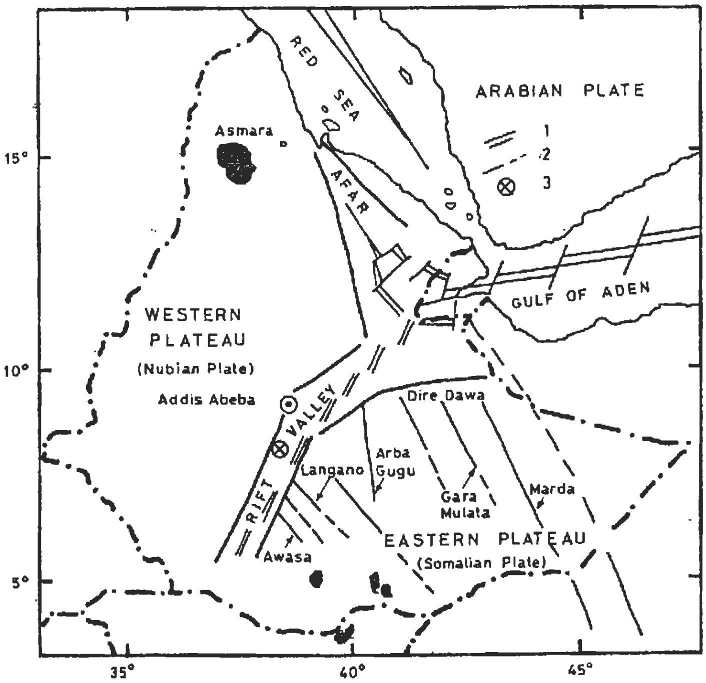


Fig. 1 - Structural sketch map of Ethiopia (modified after BARBERI and VARET (1977) and KAZMIN and SEIFE-MICHAEL BERHE (unpublished). 1) Main oceanic spreading axes and continental crust attenuation zones; 2) Main oceanic transform and continental transverse faults; 3) Location of the Kella Horst.

Along the 800 km of the Ethiopian Rift, the outcropping rocks were thought to be exclusively Tertiary and Quaternary volcanics (MERLA, 1962; DI PAOLA, 1972; MERLA et al., 1973; KAZMIN, 1973; ZANETTIN and JUSTIN-VISENTIN, 1973; ZANETTIN and JUSTIN-VISENTIN, 1975; MORBIDELLI et al., 1975), except for minor fluvio-lacustrine sediments mostly of Quaternary age (MOHR, 1962; KAZMIN, 1973; WENDORF et al., 1975; LAURY and ALBRITTON, 1975; DI PAOLA, 1976). Actually the Precambrian basement, covered by a typical sequence of Mesozoic marine sediments, outcrops also within the central portion of the Ethiopian Rift, close to its western

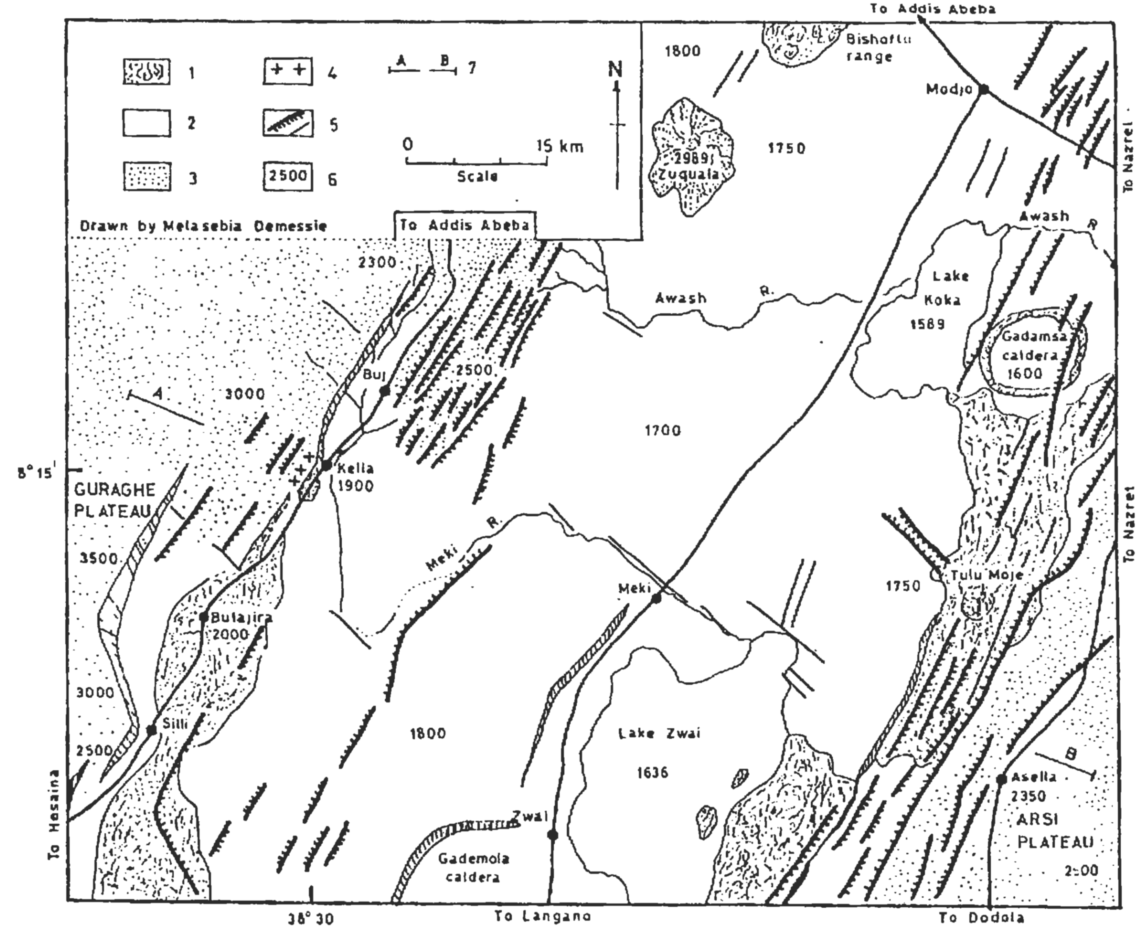


Fig. 2 - Simplified geological map of the central part of the Ethiopian Rift Valley. 1) Quaternary and historical fissure basalts (with related differentiation products along the eastern margin); 2) Plio-Quaternary peralkaline silicic ignimbrites, lavas, pyroclastics and peralkali trachytes (Zuquala) covered by pleistocene fluvio-lacustrine sediments; 3) Tertiary basalts, peralkaline silicic ignimbrites and lavas and alkali trachyte flows; 4) Precambrian crystalline basement covered by Mesozoic marine sediments at Kella (exaggerated); 5) Main faults; 6) Elevation in metres above sea level; 7) Cross section of Fig. 5.

margin (Fig. 1, 2). These pre-Tertiary rocks were found in June 1979 about 1 km West of the small town of Kella (Lat. 8° 15' N, Long. 38° 30' E, 1,900 m above sea level), 110 km S-SW of Addis Ababa, on the main road to Butajira and Hosaina (Fig. 1, 2). The main outcrop forms a block 4 km long, 1.5 km wide, dipping 20° West, bounded both by north-westerly and by north-easterly trending faults. In its maximum exposure (along a NE-SW trending recent fault scarp) the Kella Horst is constituted, from bottom to top by: 150 m of high grade metamorphic rocks (biotite gneiss cut by quartz-feldspathic pegmatitic veins); 150 m of Triassic Adigrat (BLANFORD, 1869) sandstone, resting unconformably on the underlying Precambrian; 30 m of shales and marls; 20 to 30 m of Jurassic Antalo (BLANFORD, 1869) limestone (Fig. 3).

The Antalo Limestone at Kella is directly overlain by a compact greenish grey, unstrained horizontal ignimbrite, alkali feldsparphyric, rich in xenoliths of upper Pliocene age (Table 1). Other ignimbritic units associated to viscous lavas follow upwards for about 400 meters.

All around the Kella Horst, the same ignimbrite is found to cover the top of the widespread Tertiary basaltic series of this area.

In its south-western part, the Kella Horst is cut by a deep river gorge which is partially filled with a Quaternary thin basaltic flow which originated about 2 km in the northwest.

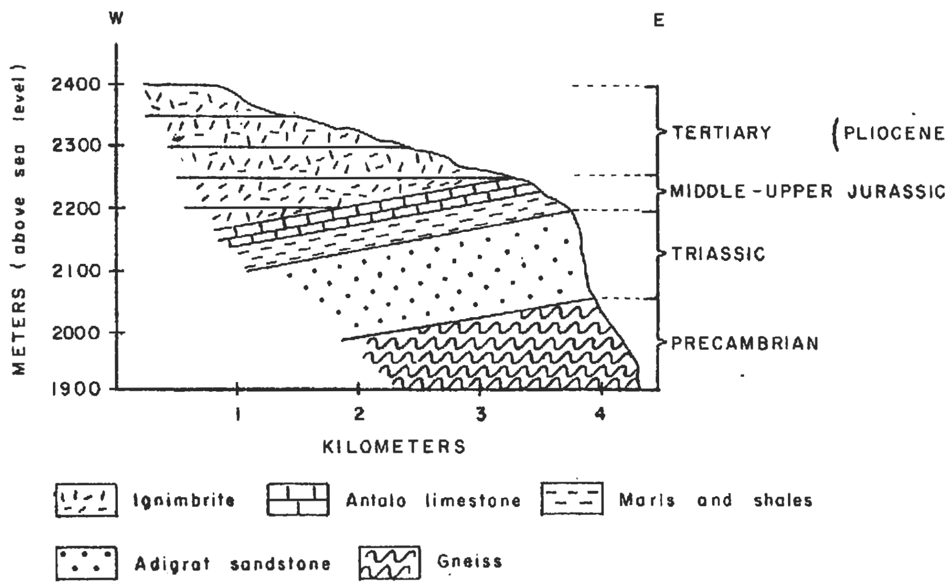


Fig. 3 - Stratigraphic sequence at Kella.

Three other minor outcrops, each a few hundred meters across, of pre-Tertiary rocks were also found 0.5, 2 and 4 km respectively northeast of the main outcrop, each one separated from the other by N-NW trending faults, somewhat obscured by the Tertiary volcanic cover. The exposures there are much less important than at the type locality because these blocks are far less elevated than the main one, therefore the Precambrian crystalline basement is not visible.

Table 1 - K/Ar dating of the alkali feldspar separated from the ignimbrite covering the pre-Tertiary rocks at Kella. Analysts: A. GIULIANI and A. PESCIA, C.N.R. Pisa, Italy. Petrography of the whole rocks (peralkali rhyolite): anorthoclase, quartz and oxidized aegirine phenocrysts. Alkali amphibole, aegirine, probable cossyrite and quartz-alkali feldspar intergrowths constitute the devitrified groundmass.

| Sample | % K | % rad. $^{40}AR$ | $\frac{ml\ rad.\ ^{40}Ar}{g\ K}$ | Age (m.y.) |
|---|---|---|---|---|
| BJ 6A | 3.73 | 70 | $1.176 \times 10^{-5}$ | $2.90 \pm 0.04$ |

REGIONAL TECTONICS AND VOLCANOLOGY

At the latitude of Kella, the Ethiopian Rift is about 80 km wide and the boundary between the western plateau and the rift floor is represented by an apparently curved master fault, the Guraghe Fault, 35 km long, located 10 to 20 km west and south-west of Kella (Fig. 2). This main fault has a visible vertical displacement exceeding 1,500 meters and it is quite affected by erosion. Numerous minor step faults are associated with the main one especially just NE and SW of it.

The apparent curvature of the Guraghe Fault is actually the result of an almost perpendicular junction of two main faults, trending NE-SW and NNW-SSE, respectively. Other apparently minor transverse faults, varying in trend from W-NW to N-NW and affecting either the Rift floor or the escarpments are also present. Transverse tectonic lineaments of regional importance (Marda, Gara Mulata, etc. of Fig. 1) have been identified on the Harari-Somali plateau (BLACK et al., 1974; PURCELL, 1976; KAZMIN and SEIFE, personal communication). These structures were active during the Precambrian with important strike-slip movements and the concomita formation of long, narrow grabens. During Tertiary times, on the contrary, vertical movements dominated, associated with minor dextral components especially during the last 10 million years.

In Central-northern Ethiopia important tensional movements and related major volcanic activity occurred in Early Tertiary with the formation of the Ashangi graben which later on began acting as a transcurrent structure transversal to the present Rift system of Ethiopia (ZANETTIN et al., 1980b). It is therefore tentatively suggested that the transverse (NNW-SSE) portion of the Guraghe Fault might have the same structural interpretation as above, although its age might be younger.

On the contrary, the boundary between the eastern Plateau at the latitude of Kella and the rift floor is constituted by a series of sharp step faults whose total visible vertical displacement does not exceed 1,000 meters, and they appear to be much younger than those along the western margin of the Rift.

The rocks outcropping along the western margin of the Rift in the area surrounding the Kella Horst, including the 1,500 meters high Guraghe fault scarp, are Tertiary fissure basalts covered by silicic alkaline and peralkaline ignimbrites, ash flows and lavas, associated with minor trachyte lava flows. This thick volcanic sequence is assumed to be generically Tertiary in age judging from its high degree of weathering, erosion and deep faulting. Despite many attempts, basaltic samples suitable for radiometric dating were not found during the field work and there are no published data for the basaltic volcanism of this area. Therefore it is not possible to establish a firm correlation between this basaltic formation and the stratigraphy, age of major volcanic events and related tectonic implications that ZANETTIN and JUSTIN-VISENTIN (1973); ZANETTIN et al. (1974); ZANETTIN and JUSTIN-VISENTIN (1975); MORBIDELLI et al. (1975); ZANETTIN et al. (1978); ZANETTIN et al. (1980a); ZANETTIN et al. (1980 b) have provided for almost all Ethiopian Plateaux and Rift volcanism.

Just where the Rift floor proper begins, the Butajira-Silti range (Fig. 2), about 80 km long (from Kella south-westward) and 10 km wide of Quaternary alkali basalt products made up of scoria cones, layered tephra, lava flows, phreatomagmatic explosion craters and related pyroclastics has developed along a NNE-SSW fissure swarm (DI PAOLA, 1972). No differentiated products such as trachytes and/or rhyolites related to this basaltic magma have been found all along this range. The last basaltic flows in this area look so young that a maximum age of a few thousand years is suggested.

The basalts of Butajira-Silti rest on ignimbrites which represent, at least in some parts of this area, the downfaulted top of the Tertiary series. Pliocene and Plio-Pleistocene peralkaline silicic ignimbrites (Balchi rhyolites of ZANETTIN and JUSTIN-VISENTIN, 1975) are the dominant products of the entire Ethiopian rift floor (DI PAOLA, 1972 ; MORBIDELLI et al., 1975; BIGAZZI et al., this volume).

Another range of Quaternary fissure alkali basalts and subordinate alkali trachytes, located close to the western escarpment is found some 50 km north-eastward from Kella (Fig. 2) along another NNE-SSW fissure swarm displaced some 20 km to the East (Bishoftu formation of ZANETTIN and JUSTIN-VISENTIN, 1973). This displacement is probably related to the presence of relatively old transverse tectonic lines marked, at present, by the rectilinear NW-SE segments of the Awash and Meki river courses

(Fig. 2). Also there, the last basaltic eruptions appear not to be older than few thousand years.

On the contrary, close to the eastern margin of the rift (Fig. 2) the Tullu Moyè area (DI PAOLA, 1976; BIZOUARD and DI PAOLA, 1978) displays an important and quite different volcanic activity (transitional basalts with associated differentiation products up to comenditic end members) developed from 0.1 m.y. ago until historical time (DI PAOLA, 1976; BIGAZZI et al., this volume; GOUIN, 1979) along a NNE-SSW fissure swarm affecting the Plio-Pleistocene ignimbrites of the Rift floor. Other areas, showing almost identical features have developed in very recent times all along the Ethiopian Rift (Wonji Fault belt of MOHR, 1962) with a right en echelon displacement, SSW and NNE of Tullu Moyè. The Butajira-Silti and Bishoftu ranges appear therefore located well outside the axis of the Wonji Fault belt (See Fig. 2).

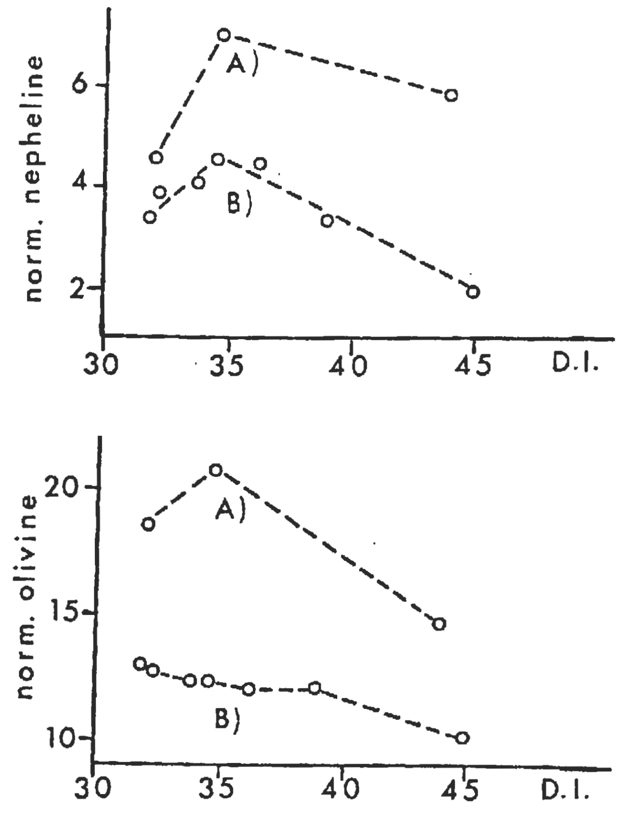


Fig. 4 - Normative nepheline and olivine v/s Differentiation Index: A) Butajira-Silti range (this paper); B) Tullu Moyè (DI PAOLA, unpublished data).

## STRUCTURAL AND MAGMATIC IMPLICATIONS

Many authors (DAINELLI, 1943; MOHR, 1962; MERLA et al., 1973; KAZMIN, 1973; MERLA et al., 1979) have indicated that the Afro-Arabian Precambrian basement was an almost completely peneplained, low lying surface at the beginning of the Permo-Triassic marine transgression. Only in Somalia have important troughs proved to exist at that time (MERLA et al., 1973; MERLA et al., 1979). However there are clear evidences that tectonic activity, pre or syn-Mesozoic transgression, produced important morphotectonic differences in many parts of the Precambrian surface in Ethiopia too, at least in its eastern half. This is shown by the abrupt change of thickness of the Mesozoic sediments found in adjacent areas of the Eastern Plateau (Harar).

A second cycle of erosion and peneplanation is also believed (MERLA et al., 1979) to have occurred during Tertiary just before the onset of volcanism related to the initiation of rifting along the Red Sea-Afar-Gulf of Aden and Ethiopian Rift system. The presence of the Kella Horst therefore suggests that important (Lower-middle Tertiary ?) tectonic movements must have affected the uplifted Afro-Arabian dome in Ethiopia, especially in its central part (Guraghe area) and in the North (Wollo-Tigre regions).

However the evidence that at Kella the pre-Tertiary rocks are directly covered by a 3.0 m.y. old ignimbrite and not by the stratigraphically lower unit of the surrounding Tertiary basaltic formation (visible thickness in excess of 1.000 meters) opens a challenging problem for what concerns its origin. In fact following ZANETTIN and JUSTIN-VISENTIN (1975) and ZANETTIN et al. (1978) classification of Ethiopian volcanics, the basalts outcropping along the western Rift margin at the latitude of Kella could be as old as the Ashangi series (pre-Oligocene) or as young as the Fursa basalt formation (10-12 m.y. B. P.)

There are therefore three possibilities to explain the genesis of the Kella Horst:

1) The very beginning of the volcanic activity in this area coincides with the Fursa basalts. In this case the Kella Horst must have been a prominent topographic feature at least 12 m.y. B.P..
2) The very beginning of the volcanic activity in this area coincides with the Ashangi basalts. In this case the Kella Horst must have been a prominent topographic feature already in pre-Oligocene time.
3) The Kella Horst was uplifted sometimes during Oligocene after the onset of the Ashangi series (or later after the eruption of the Aiba formation). In this case the absence of a basaltic cover and of the underlying "Upper Sandstone" (MOHR, 1962; MERLA et al., 1973; KAZMIN, 1973; MERLA et al., 1979) at Kella could be attributed to a long period of erosion. If this would be the case, the surrounding Tertiary basaltic formation outcropping along the Guraghe fault scarp, and to the West of the Kella Horst, must be younger than the Ashangi (or the Aiba) series (as if they were, they would have been eroded as well). Therefore also in this case the Kella Horst must have been a prominent topographic feature at least 12 m.y. B.P. or even earlier.

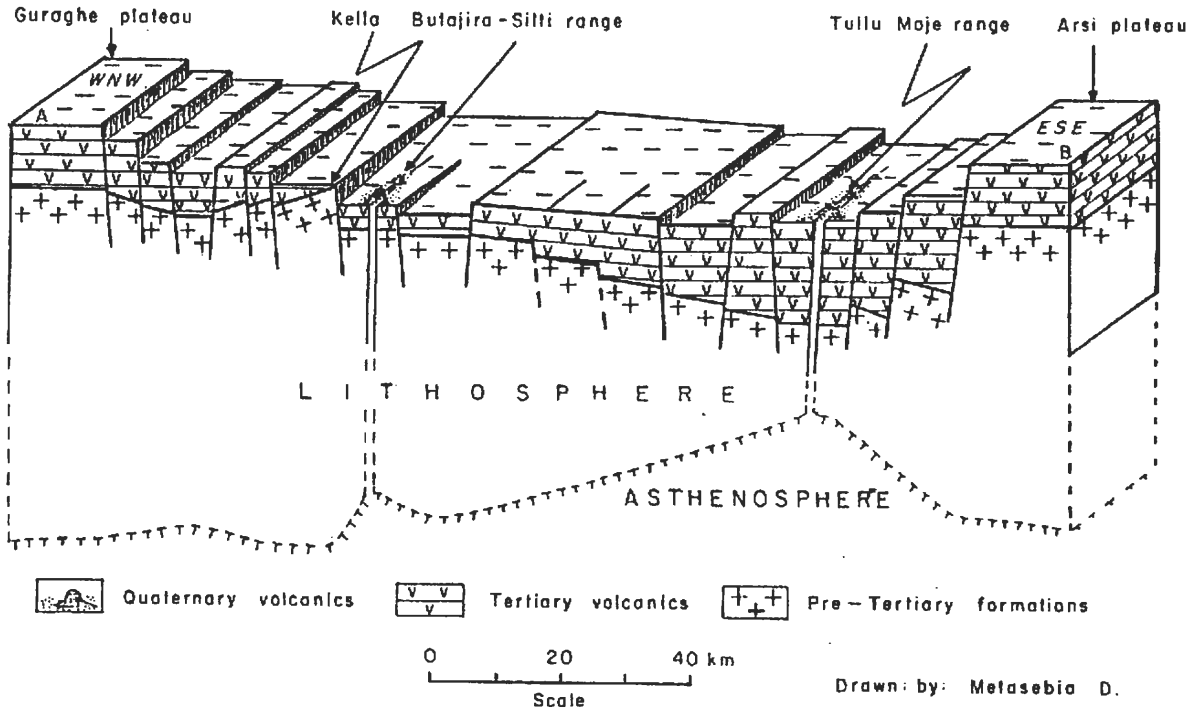


Fig. 5 - Qualitative interpretation of the crustal structure accross the Ethiopian Rift at the latitude of Kella.

In the absence of radiometric dating for the Tertiary basalts of this area, the first conservative assumption is proposed, also because the eruption of the Fursa basalts seems to be related to important tectonic movements that initiated the opening of the Ethiopian Rift (ZANETTIN and JUSTIN-VISENTIN, 1975). Therefore prior to the beginning of the Tertiary basaltic activity in the Guraghe area, Kella probably represented the northern edge of a deep, relatively narrow graben (the "Guraghe graben") trending roughly NW-SE, i.e. transversal to the present NNE-SSW Ethiopian Rift. Under these structural and morphological circumstances the Tertiary basalts of this area must have piled up within the Guraghe graben without reaching the top of the Kella Horst. The topographic gap was progressively filled by the concomitant accumulation of basaltic flows within the Guraghe graben and by the reduction in elevation of the Kella Horst due to erosion and NE-SW downfaulting related to the progressive widening of the Ethiopian Rift. Eventually the topography of the Kella Horst was sufficiently reduced to allow the 3.0 m.y. old ignimbrite to cover its top.

The above interpretation is suggested by the following considerations:

1. Along the 1.500 metres high Guraghe fault scarp only volcanic rocks outcrop and, as usual in Ethiopia, the Tertiary basalts constitute the lowest and thickest portion of the sequence. At Kella, on the contrary, the first volcanic unit directly covering the pre-Tertiary rocks is a peralkaline silicic ignimbrite which only 2 km to the West and 4 km to the S-SW (outside the limit of pre-Tertiary rocks) is found to cover a weathered basaltic flow. This latter cannot represent the base of the Tertiary basaltic series of this area because few km further to the SW the same stratigraphic situation is observed and the sequence becomes thicker and thicker with the outcropping of progressively older and older basalts, while the contact between the ignimbrite and the underlying basaltic formation is found at progressively higher and higher elevations as the Guraghe fault is approached and climbed.
2. The radiometric age (Table 1) of the ignimbrite directly covering the Kella Horst confirmes the stratigraphic and tectonic situation as it is much younger (only 3 m.y. B.P.) even than the last major pre\syn Rift opening related volcanic activity of Ethiopia (i.e. the Fursa basalts of ZANETTIN and JUSTIN-VISENTIN, 1975).

From the above discussion it follows that contrary to the current interpretation of other similar structures in the East African Rift System (LEVITTE ET AL., 1974; CHAPMAN et al., 1978), the Kella Horst does not seem to be related to an uplift of basement rocks during the Rift formation. It could be rather a structural feature which pre-existed as a morphological high either in early Tertiary time or at the latest in Miocene. Later on, the Kella Horst began to act as a block intimately associated with the Rift floor, being progressively sliced and downfaulted by the tensional movements which are still widening the Ethiopian Rift (MOHR et al., 1978).

This is furthermore suggested by the other minor outcrops of pre-Tertiary rocks visible just to the NE of the main one at Kella. Their considerably lower topographic elevation (200 meters) is in fact exclusively due to downfaulting and not to a higher degree of erosion since the thickness of the top pre-Tertiary rocks (Antalo Limestone)

Table 2 - XRF chemical analyses and CIPW norm of recent basic volcanic rocks from the Butajira-Silti range (MgO by A.A.; FeO by tritation; L.O.I. gravimetric). CIPW norm for sample BJ 5 recalculated assuming $Fe_2O_3/FeO$ ratio equal to 0.15. BJ 16: Pleistocene alkali basalt flow covering the Triassic Adigrat Sandstone of the Kella Horst on the bottom of bottom of a deep river gorge (plagioclase-olivine porphiritic in a microcrystalline groundmass. Presence of small ultramafic nodules). BJ 2: Holocene alkali basalt flow, 7 Km NE of town of Butajira (olivine, pleochroic augite and plagioclase porphyritic in a microcrystalline groundmass. Presence of small ultrmafic nodules). BJ 5: Pleistocene-Holocene (?) hawaiite flow jumping a fault scarp 4 Km SE of the town of Silti (Plagioclase-olivine phrophyritic in a microcrystalline groundmass).

| | BJ 16 | BJ 2 | BJ 5 |
|---|---|---|---|
| $SiO_2$ | 46.94 | 47.34 | 48.50 |
| $TiO_2$ | 2.45 | 2.22 | 2.84 |
| $Al_2O_3$ | 16.55 | 17.48 | 18.11 |
| $Fe_2O_3$ | 1.30 | 0.00 | 3.64 |
| FeO | 8.93 | 9.22 | 6.39 |
| MnO | 0.17 | 0.15 | 0.16 |
| MgO | 8.56 | 8.41 | 5.57 |
| CaO | 9.57 | 9.10 | 7.58 |
| $Na_2O$ | 3.68 | 4.13 | 4.76 |
| $K_2O$ | 0.81 | 0.95 | 1.40 |
| $P_2O_5$ | 0.44 | 0.56 | 0.59 |
| L.O.I. | 0.60 | 0.43 | 0.45 |
| Or | 4.79 | 5.61 | 8.34 |
| ab | 22.73 | 21.99 | 29.60 |
| an | 26.25 | 26.36 | 23.63 |
| ne | 4.55 | 7.01 | 5.82 |
| di (wo | 7.66 | 6.31 | 4.53 |
| di (en | 4.68 | 3.66 | 2.45 |
| di (fs | 2.55 | 2.37 | 1.92 |
| ol (fo | 11.65 | 12.11 | 8.02 |
| ol (fa | 6.99 | 8.63 | 6.68 |
| mt | 1.88 | - | 1.86 |
| il | 4.65 | 4.22 | 5.32 |
| ap | 1.04 | 1.33 | 1.34 |
| D.I. | 32.06 | 34.61 | 43.76 |

is the same as at the type locality. Its present occurrence might be related to the major Rift faulting and largest domal uplift which occurred in Ethiopia in Plio-Pleistocene time (BAKER et al., 1978) and it might be interpreted as the pre-Tertiary rocks of Aisha in the Afar depression (BLACK et al., 1972). In that sense, the term "Horst" utilized in this paper is probably not strictly correct (as it is generally utilized to describe an uplift or an unbroken remnant of crustal rocks) but a more specific term has not yet been proposed.

Eventhough involved in the crustal attenuation process of the Ethiopian Rift, the pre-Tertiary rocks found at Kella suggest that along the western margin of the Rift the thickness of the lithosphere might be greater than along the eastern margin as a result of a lower extensional rate. Geophysical data for Ethiopia (BERCKHEMER et al., 1975; BERKTOLD et al., 1975; MAKRIS et al., 1975; RUEGG, 1975; SEARLE, 1975) are almost all related to the Afar depression and neighbouring plateaux. The few concerning the Ethiopian Rift South of Addis Ababa (SEARLE and GOUIN, 1972) are not sufficient to allow the quantification of a crustal model. Therefore the one presented in Fig. 5 has to be regarded as qualitative and somewhat provocative. The crustal asymmetry tentatively proposed in Fig. 5 is suggested primarily by the presence of basement rocks at Kella and secondarily by the following petrochemical considerations:

1. The extremely recent basalts of the Butajira-Silti range are distinctly more alkalic (Table 2, Fig. 4) than the coeval fissure basalts of the Tullu Moyè and other similar areas located along the eastern margin of the Ethiopian Rift.
2. Complete differentiation series up to peralkali rhyolites closely associated in time and space with the Quaternary basalts are widespread along the Eastern margin of the Rift (DI PAOLA, 1976; BIZOUARD and DI PAOLA, 1978; BROTZU et al., 1980a; BROTZU et al., 1980b) while they are totally absent among the Quaternary basalts of the Butajira-Silti range.

These features may suggest a significantly shallower source in the mantle (COOMBS, 1963; GREEN and RINGWOOD, 1967), i.e. a possible faster rate of lithosphere attenuation (GASS, 1970) for eastern margin Quaternary basalts relative to the coeval basalts of the western margin of the Rift.

On the other hand, it has to be pointed out that PICCIRILLO et al. (1979) on the basis of major and trace elements analyses of Plateau and Rift basalts of Ethiopia, have shown that the chemistry of basaltic melts are more likely related to the intensity of extension movements rather than to crustal thickness. While the results of PICCIRILLO et al. (1979) are quite convincing there is another evidence that supports the possibility of a thinner crust and consequent higher heat flow along the Eastern margin of the Ethiopian Rift. As a matter of fact all geothermal manifestations, South of the Addis Abeba latitude, are clearly related to the recent fissural volcanism and tensional tectonics of the eastern margin of the Rift (Tullu Moyè type areas), including the recently (1985) proven existence of a high enthalpy geothermal field in the Langano-Aluto area. On the contrary, no relevant hydrothermal manifestations are known to exist along the corresponding western margin, despite the presence of the extremely

recent and extensive volcanic activity previously mentioned (Butajira-Silti and Bishoftu ranges).
Another evidence of a possible faster rate of crustal attenuation along the eastern margin of the Ethiopian Rift is provided by the large number of extremely recent normal faults, open fissures and tilted blocks that can be observed in the Tullu Moyè and Zwai-Langano areas. On the contrary, along the Butajira-Silti range only minor recent faulting and no tilting is present. Pending the availability of deep penetration geophysical data for the Ethiopian Rift South of the Addis Ababa latitude, the above tentative interpretation has to be regarded as a proposed working hypothesis for future detailed investigations by East African Earth scientists.

## REFERENCES

ABBATE E. and SAGRI M. (1969). Dati e considerazioni sul margine orientale dell'altipiano etiopico nelle province del Tigrai e del Wollo. Boll. Soc. Geol. Ital., 88: 489-497.

ABBATE E., FACIBENI P., GREGNANIN A., MERLA G. and SAGRI M. (1969). Basalt flows and related sandstones in the Socota area (Northern Ethiopia). Boll. Soc. Geol. Ital., 88: 499-516.

BAKER B.H., MOHR P.A. and WILLIANS L.A.J. (1972). Geology of the Eastern Rift System. Geol. Soc. America Sp. Paper, 136.

BARBERI F., FERRARA G., SANTACROCE R. and VARET J. (1975). Structural evolution of the Afar triple junction. In: Afar Depression of Ethiopia, I, (Edited by PILGER and ROSLER), 38-54. E. Schweizerbart'sche Verlag, Stuttgart.

BARBERI F. and VARET J. (1977). Volcanism of Afar: small scale plate tectonics implications. Geol. Soc. Am. Bull., 88: 1251-1266.

BARBERI F. and VARET J. (1978). The Afar Rift junction. In: Petrology and geochemistry of continental rifts (Edited by NEUMANN E.R. and RAMBERG I.B.), 55-69. D. Reidel Publishing Co., Dordrecht, Holland.

BERCKHEMER H., BAIER B., BARTELSEN H., BEHLE A., BURKHARDT H., GEBRANDE H., MAKRIS J., MENZEL H., MILLER H. and VEES R. (1975). Deep seismic sounding in the Afar region and on the highland of Ethiopia In: Afar Depression of Ethiopia, II, (Edited by PILGER and ROSLER), 89-107. E. Schweizerbart'sche Verlag, Stuttgart.

BERKTOLD A., HAAK V. and ENGENHEISTER G. (1975). Magnetotelluric measurements in the Afar area. In: Afar Depression of Ethiopia, I, (Edited by PILGER and ROSLER), 66-79. E. Schweizerbart'sche Verlag, Stuttgart.

BIGAZZI G., BONADDONA F.P., DI PAOLA G.M. and GIULIANI A. (This volume). K-Ar and fission track ages of the last volcano tectonic phase in the Ethiopian Rift Valley (Tullu Moyè area).

BIZOUARD H. and DI PAOLA G.M. (1978). Mineralogy of the Tullu Moyè active volcanic area (Arussi: Ethiopian Rift Valley). In: Petrology and geochemistry of continental rifts (Edited by NEUMANN E.R. and RAMBERG I.B.), 87-100. D. Reidel Publishing Co., Dordrecht, Holland.

BLACK R., MORTON W.H. and VARET J. (1972). New data on Afar tectonics. Nat. Phys. Sci., 240: 170-173.

BLACK R., MORTON W.J. and TSEGAYE HAILU (1974). Early structures around the Afar triple junction. Nature, 248: 496-497.

BLANFORD W.T. (1869). On the geology of a portion of Abyssinia. Quart. J. Geol. Soc. London, 25: 401-406.

BROTZU P., MORBIDELLI L., PICCIRILLO E.M. and TRAVERSA G. (1980 a). Volcanological and magmatological evidence of the Boseti volcanic complex (main Ethiopian Rift). In: Geodynamic evolution of the Afro-Arabic Rift System. Acc. Naz. Lincei, Roma.

BROTZU P., KAZMIN V., MORBIDELLI L., PICCIRILLO E.M., SEIFE M.B. and TRAVERSA G. (1980 b). Petrochemistry of the volcanics in the Northern part of the main Ethiopian Rift. In: Geodynamic evolution of the AfroArabic Rift System. Acc. Naz. Lincei, Roma.

CHAPMAN G.R., LIPPART S.J. and MARTYN J.E. (1978). The stratigraphy and structure of the Kamasia range, Kenya Rift Valley. J. Geol. Soc. London, 135: 265-281.

COOMBS D.A. (1963). Trends and affinities of basaltic magmas and pyroxenes as illustrated on the diopside-olivine-silica diagram. Min. Soc. Amer. Spec. Pap.I, 227-250.

DAINELLI G. (1943). Geologia ell'Africa Orientale. 4 volumi. R. Accad. d'Italia, Roma.

DI PAOLA G.M. (1972). The Ethiopian Rift Valley (between 7°00' and 8 40' lat. North). Bull. Volcanol., 36, 4: 517-560.

DI PAOLA G.M. (1976). Geological map of the Tullu Moyè active volcanic area 1:75,000 (Arussi: Ethiopian Rift Valley). CNR, Pisa.

GASS I.G. (1970). The evolution of volcanism in the junction area of the Red Sea, Gulf of Aden and Ethiopian rifts. Phil. Trans. Roy. Soc.London, A, 267: 369-381.

GOUIN P. (1979). Earthquake history of Ethiopia and the Horn of Africa. IDRC, 118 e, Ottawa.

GREEN D.H. and RINGWOOD A.E. (1967). The genesis of basaltic magmas. Contr. Mineral. and Petrol., 15: 103-190.

KAZMIN V. (1973). Geological map of Ethiopia 1:2,000,000 with comments. Geological Survey of Ethiopia.

LAURY R.L, and ALBRITTON C.C. Jr. (1975). Geology of Middle Stone Age archeological sites in the main Ethiopian Rift Valley. Geol. Soc. of Am. Bull. 86: 999-1011.

LEVITTE D., COLUMBA J. and MOHR P. (1974). Reconnaissance geology of the Armaro Horst, Southern Ethiopian Rift. Geol. Soc. of Amer. Bull., 85: 417-42

MAKRIS J., MENZEL H., ZIMMERMANN J. and GOUIN P. (1975). Gravity field and crustal structure of North Ethiopia. In: Afar Depression of Ethiopia, I (Edited by PILGER and ROSLER), 135-144. E. Schweizerbart'sche Verlag, Stuttgart.

MERLA G., ABBATE E., CANUTI P., SAGRI M. and TACCONI P. (1973). Geological map of Ethiopia and Somalia 1: 2.000.000. CNR, Firenze.

MERLA G., ABBATE E., AZZAROLI A., BRUNI P., CANUTI P., FAZZUOLI M., SAGRI M. and TACCONI P. (1979). A geologic map of Ethiopia and Somalia 1973, 1:2,000,000 and comments with a map of major landforms. CNR, Firenze.

MOHR P. A. (1962). The Ethiopian rift system. Bull. Geophys. Obs. Addis Ababa Univesity, 5: 33-62.

MOHR P.A., GIRNIUS A. and RALFF J. (1978). Present day strain rates at the northern end of the Ethiopian Rift Valley. Tectonophysics, 44: 141-160.

MORBIDELLI L., NICOLETTI M., PETRUCCIANI C. and PICCIRILLO E.M. (1975). Ethiopian south-eastern plateau and related escarpment: K/Ar ages of the main volcanic events (Main Ethiopian Rift from 8 10' to 9 00' Lat north). In: Afar Depression of Ethiopia, I, (Edited by PILGER and ROSLER), 362-369. E. Schweizerbart'sche Verlag, Stuttgart.

PICCIRILLO E.M., JUSTIN-VISENTIN E., ZANETTIN B., JORON J.L. and TREUIL M. (1979). Geodynamic evolution from Plateau to Rift: major and trace element geochemistry of the Central Eastern Ethiopian plateau volcanics. N. Jb. Geol. Palaont. Abh., 158: 139-179.

PURCELL P.G. (1976). The Marda Fault Zone, Ethiopia. Nature, 261: 569-571.

RUEGG J.C. (1975). Main results about the crustal and upper mantle structure of the Djibouti region (T.F.A.I.). In: Afar Depression of Ethiopia, I, (Edited by PILGER and ROSLER), 120-134. E. Schweizerbart' sche Verlag, Stuttgart.

SEARLE R.C. and GOUIN P. (1972). A gravity survey of the central part of the Ethiopian Rift Valley. Tectonophysics, 15: 41-52.

SEARLE R.C. (1975). The dispersion of surface waves across southern Afar. In: Afar Depression of Ethiopia, I, (Edited by PILGER and ROSLER), 113-120. E. Schweizerbart'sche Verlag, Stuttgart.

WENDORF F., LAURY R.L., ALBRITTON C.C., SCHILD R., HAINES C.V., DAMON P.E., SHAFIQULLAH M. and SCARBOROUGH R. (1975). Dates for the Middle stone Age of East Africa. Science, 187: 740-742.

ZANETTIN B. and JUSTIN-VISENTIN E. (1973). Serie di vulcaniti etiopiche: 1 - La serie dell'altipiano etiopico centro-orientale. Boll. Soc. Geol. Ital., 92: 313-327.

ZANETTIN B., GREGNANIN A., JUSTIN-VISENTIN E., NICOLETTI M., PETRUCCIANI C., PICCIRILLO E.M. and TOLOMEO L. (1974). Migration of the Oligocene-Miocene ignimbritic volcanism in the central Ethiopian plateau. N. Jb. Geol. Palaont. Mh., 9: 567-574.

ZANETTIN B. and JUSTIN-VISENTIN E. (1975). Tectonical and volcanological evolution of the Western Afar margin (Ethiopia). In: Afar Depression of Ethiopia, 1, (Edited By PILGER and ROSLER), 300-309. E. Schweizerbart'sche Verlag, Stuttgart.

ZANETTIN B., JUSTIN-VISENTIN E., NICOLETTI M. and PETRUCCIANI C. (1978). The evolution of the Chencha escarpment and the Ganjuli graben (Lake Abaya) in southern Ethiopian Rift. N. Jb. Geol. Palaont. Mh. 8: 473-490.

ZANETTIN B., JUSTIN-VISENTIN E., NICOLETI M. and PICCIRILLO E.M. (1980a). Correlations among Ethiopian volcanic formations with special references to the chronological and stratigraphical problems of the "Trap Series". In: Geodynamic evolution of the Afro-Arabic Rift System. Acc. Naz. Lincei, Roma.

ZANETTIN B., JUSTIN-VISENTIN E. and PICCIRILLO E.M. (1980b). Migration of the Ethiopian continental Rifts in the course of the Tertiary evolution of the Afro-Arabian Rift System. In: Geodynamic evolution of the Afro-Arabic System. Acc. Naz. Lincei, Roma.

*Final editing, January 1990*

From *Geology and mineral resources of Somalia and surrounding regions*, Ist. Agron. Oltremare, Firenze, Relaz. e Monogr. 113, 339-344, 1993.

# ARFVEDSONITE FROM A PERALKALINE RHYOLITE (MOJO, ETHIOPIA)

G. FERRARIS

Dipartimento di Scienze della Terra, Sezione di Mineralogia e Cristallografia, Università di Torino, Via S. Massimo 24, 10123 Torino, Italy.

## ABSTRACT

Combined chemical and X-ray single-crystal analyses indicate that an amphibole from a peralkaline rhyolite of Mojo (Ethiopia) is arfvedsonite with crystallochemical formula $(Na_{0.76}K_{0.23})(Na_{1.75}Ca_{0.22}Mn_{0.03})(Fe^{2+}_{3.59}Fe^{3+}_{0.91}Na_{0.14}Mn_{0.34}Al_{0.02})(Si_{7.97}Al_{0.03})O_{22}(OH)_{0.28}F_{1.72}$. The temperature of crystallization is estimated to lie in the range 600-700 °C under conditions of low oxygen fugacity.

## INTRODUCTION

Arfvedsonite is an alkali amphibole with ideal composition $Na_3Fe^{2+}_4Fe^{3+}Si_8O_{22}(OH)_2$. It is usually found in plutonic rocks (DEER et al., 1967), but its occurrence in volcanic rocks has been reported as well (DE ANGELIS, 1923; LONSDALE, 1940; WHITTEN, 1954). Similarities, complicated by a variable behaviour, make difficult its distinction from riebeckite $Na_2 Fe^{2+}_3 Fe^{3+}_2 Si_8O_{22}(OH)_2$.

On the basis of unpublished X-ray data (UNGARETTI, personal communication) and detailed microprobe studies (WONES and GILBERT, 1982), several samples of supposed riebeckite turned out to be arfvedsonite. This mineral, therefore, could be more common than previously suspected. The distinction between riebeckite and arfvedsonite may be especially useful in documenting changes in oxygen fugacity during final crystallization (WONES and GILBERT, 1982).

## EXPERIMENTAL DATA

### OCCURRENCE

The sample used for this research has been collected in a quarry located on the right side of the road from Bishoftu to Mojo (Shewa, Ethiopia), 9.5 km before the junction to the Lake Zway. In this area MORTON et al. (1979) give for ignimbrites and olivine

Table 1 - Rock bulk composition of a Mojo rhyolite.

| | % weight | | ppm | | ppm |
|---|---|---|---|---|---|
| $SiO_2$ | 71.47 | Ba | 378 | Zr | 739 |
| $Al_2O_3$ | 11.87 | Be | 4.8 | La | 96.1 |
| $Fe_2O_3$ | 4.89 | Co | 44 | Nd | 86.9 |
| MnO | 0.23 | Cr | 8 | Eu | 2.8 |
| MgO | 0.13 | Cu | 29 | Dy | 15.9 |
| CaO | 0.34 | Nb | 93 | Yb | 10.2 |
| $Na_2O$ | 4.60 | Ni | 8 | Ce | 239.3 |
| $K_2O$ | 4.93 | Rb | 138 | Sm | 19.5 |
| $TiO_2$ | 0.32 | Sc | 7.6 | Gd | 14.9 |
| $P_2O_5$ | 0.06 | Sr | 13 | Er | 8.6 |
| L.O.I. | 1.41 | V | <5 | Lu | 1.3 |
| Total | 100.25 | Zn | 186 | Y | 101.8 |

CIPW weight norm: Q 26.59, or 29.14, ab 33.61, di 0.70, wo 0.08, ac 4.68, il 0.49, hem 3.27, ti 0.15, ap 0.14.

Table 2 - Average % weight of six microprobe chemical analyses of long (1) and short (2) prismatic crystals of arfvedsonite from Mojo.

| | 1 | 2 |
|---|---|---|
| $SiO_2$ | 49.56 | 50.60 |
| $TiO_2$ | - | - |
| $Al_2O_3$ | 0.14 | 0.11 |
| $Cr_2O_3$ | 0.01 | 0.03 |
| FeO | 33.03 | 32.34 |
| MgO | 0.01 | 0.01 |
| MnO | 2.64 | 2.62 |
| CaO | 1.78 | 1.25 |
| $K_2O$ | 1.51 | 1.69 |
| $Na_2O$ | 8.58 | 8.87 |
| $H_2O$ | n.d. | n.d. |
| F | n.d. | n.d. |
| Total | 97.26 | 97.52 |

basalts an age younger than 3 Myr. The quarry exploits the rhyolite of a subvolcanic dome, where columnar joints indicate a low rate of cooling in presence of an active fluid. Pockets and fissures occur frequently; their surfaces are coated by a black film of haematite on which millimetric crystals of amphibole have abundantly grown.

Microscopic examination of the rock shows an oligoporphyric trachytic texture, with few phenocrysts of sanidine scattered in a ground mass mainly consisting of sanidine. Frequent microcracks are partially or completely filled with haematite concretions, arfvedsonite, and high-temperature quartz. Arfvedsonite and interstitial skeletal quartz also occur in the rock. Around microcracks the minerals are stained by limonitic products. Other minerals are: sanidine (main phase); aegirine (quite common); rare aenigmatite (cossyrite), sometimes included in sanidine phenocrysts; very rare fayalite; magnetite as inclusion in phenocrysts of sanidine. A skeletal phase associated with aegirine was not identified. On the basis of the microscopic and chemical analyses the rock can be classified as a peralkaline rhyolite (comenditic type). The rock chemical data were obtained by means of X-ray fluorescence and plasma-emission (RE) techniques: they are shown in Table 1.

Arfvedsonite occurs both as phenocrysts on the surface of macro- and micro-fissures and as interstitial microliths. The former, up to 1 mm in length, shows two

Table 3 - X-ray powder pattern of arfvedsonite from Mojo; Guinier-Lenné camera, CuKa radiation. The observed interplanar spacings ($d_{obs}$) are compared with those calculated ($d_{calc}$), for the shown indices (hkl), with the unit-cell parameters reported in the text. $I_{obs}$ are the observed intensities on relative scale. Single-starred values are broad lines; the double-starred value belongs to haematite.

| dobs(Å) | d calc (Å) | hKl | Iobs |
|---|---|---|---|
| 8.47 | 8.489 | 110 | 9 |
| 4.87 | 4.887 4.806 | 111 200 | 3 |
| 4.50 | 4.525 4.477 | 040 021 | 5* |
| 4.04 | 4.041 | 111 | 1 |
| 3.83 | 3.884 | 131 | 1 |
| 3.41 | 3.417 3.400 | 131 041 | 6 |
| 3.24 | 3.295 | 240 | 1 |
| 3.15 | 3.155 | 310 | 5* |
| 2.722 | 2.7369 2.7267 | 331 151 | 8 |
| 2.702** | | | 1 |
| 2.629 | 2.6240 | 112 | 2 |
| 2.600 | 2.6033 2.5890 | 061 241 | 5 |
| 2.539 | 2.5377 | 202 | 10 |
| 2.332 | 2.3419 2.3313 2.3292 | 351 112 421 | 2 |
| 2.273 | 2.2758 2.2627 | 312 080 | 4 |
| 2.178 | 2.1810 | 261 | 2 |
| 2.071 | 2.0726 | 202 | 3 |
| 1.695 | 1.6942 1.6889 | 133 282 | 4* |
| 1.586 | 1.6019 1.5867 | 600 153 | 7 |
| 1.518 | 1.5200 1.5176 | 551 263 | 5 |
| 1.316 | 1.3170 1.3152 | 751 114 | 3 |
| 1.288 | 1.2909 1.2883 1.2878 | 353 134 004 | 3 |
| 1.267 | 1 2689 | 404 | 2 |

different shapes: long crystals with tabular to prismatic habit, and short prismatic crystals. No substantial differences have been detected between the two forms by chemical (Table 2), powder (Table 3) and single-crystal X-ray diffraction, and microscopic analyses.

### Arfvedsonite chemical data

Microprobe analyses performed on the two types of amphibole crystals supplied the chemical data shown in Table 2. These data were recalculated on the basis of 24(O, OH) in the cell and by taking $H_2O$ as difference to 100%, obtaining the following formulas:

long crystals:

$(Na_{2.67}\ K_{0.31}\ Ca_{0.31})\ S_{3.29}(Fe_{4.43}\ Mn_{0.36}\ Al_{0.01})\ S_{4.80}\ (Si_{7.96}\ Al_{0.04})\ S_{8.00}$
$O_{21.08}(OH\ )_{2.92}$

short crystals:

$(Na_{2.75}\ K_{0.34}\ Ca_{0.21})S_{3.30}(Fe_{4.33}\ Mn_{0.35}\ Al_{0.02})\ S_{4.70}$
$Si_{8.10}\ O_{21.35}\ (OH)_{2.65}$

No substantial compositional zoning was detected within the analysed crystals.

The small amount of Al and a content of Si close to 8 atoms per f.u., exclude a substantial substitution of Al in the tetrahedral chains of the structure. The sum of the larger cations (Na, K, Ca) is greater than 3 and a presence of them in octahedral sites must be expected, also because (Fe+Mn+Al) < 5. Not enough material was available for an analytical determination of $Fe^{3+}$, $H_2O$ and F.

### X-ray analysis

The unit-cell parameters were obtained from single-crystal X-ray diffractometry, and have the following values a = 9.008(3), b = 18.1012(6), c = 5.3062(2) Å, b = 103.88(3)°; space group C2/m.

No differences between the two groups of crystals were detected by X-ray powder analysis. The indexing of the powder pattern (Table 3) was performed by comparison of the measured interplanar spacings ($d_{obs}$) with those calculated ($d_{calc}$) from the unit-cell parameters; the diffraction intensities measured on single crystal were also taken into account, when multiple indexing was possible.

In order to establish the crystallochemical formula, an X-ray single-crystal study was performed in the framework of a research program on amphiboles. Several crystals belonging to the two groups (long and short prismatic crystals) were tested, finding no substantial differences. With the diffraction intensities collected on a short-prismatic crystal a crystal-structure refinement was performed (R = 0.0144 for 2453 reflections). Through the refinement of the number of electrons per crystallographic site, the consideration of the bond lengths, their correlations, and cell parameters, it can be concluded that, in the octahedral strip, $Fe^{3+}$ and (Na+Mn) lie in M2 and M3 sites, respectively. The following crystallochemical formula is deduced from the crystal-structure refinement

$(Na_{0.76}\,K_{0.23})(\,Na_{1.75}\,Ca_{0.22}\,Mn_{0.03})(Fe^{2+}{}_{3.59}\;Fe^{3+}{}_{0.91}\;Na_{0.14}\;Mn_{0.34}\;Al_{0.02})\;(Si_{7.97}\;Al_{0.03})\;O_{22}(OH)_{0.28}\;F_{1.72}$

## CONCLUSIONS

According to an experimental study by ERNST (1962), oxygen fugacity strongly controls the character of the riebeckite-arfvedsonite solid solution series. This author found that at higher oxygen fugacity, in presence of haematite, the amphibole is riebeckite with a relatively low thermal stability that would not normally permit coexistence with silicate liquid. Under conditions of lower oxygen fugacity, the amphibole becomes more arfvedsonitic with concomitant increase in thermal stability; arfvedsonite was found to coexist with the liquid at about 700 °C. Obviously, availability of Na could also control the type of amphibole which can crystallize.

The occurrence of high-temperature quartz and interstitial arfvedsonite suggests that the crystallization temperature of the rhyolite could lie in the range 600-700 °C, under conditions of low oxygen fugacity. The presence in the fissures of arfvedsonite with haematite as products of an active fluid, seems to contradict the ERNST (1962) results; however, arfvedsonite occurring within macro- and micro-fissures is clearly grown on the film of haematite and, therefore, the crystallization of the two minerals is not simultaneous.

## ACKNOWLEDGMENTS

I am grateful to E. CALLEGARI (Torino) for the optical analysis and valuable suggestions and to L. UNGARETTI (Pavia) for letting me use results from its research on the crystal chemistry of amphiboles. This research has been supported by M.P.I. 40% grants.

## REFERENCES

DE ANGELIS M. (1923). Note di petrografia dancala. Atti della Società Italiana di Scienze Naturali e del Museo Civico di Storia Naturale, Milano, 62: 179-200.

DEER W.A., HOWIE R.A. and ZUSSMAN J. (1967). Rock-Forming Minerals, vol. 2. Longmans, London, U.R.

ERNST W.C. (1962). Synthesis, stability, and occurrence of riebeckite and riebeckite-arfvedsonite solid solutions. J. Geol. 70: 689-736.

LONSDALE J.T. (1940). Igneous rocks of the Terlingua-Solitario region, Texas. Bull. Geol. Soc. Amer. 51: 1539-1626.

MORTON W.H., MITCHELL J.G., REX D.C. and MOHOR P. (1979). Riftward younging of volcanic units in the Addis Ababa region, Ethiopian Rift Valley. Nature 280: 284-288.

WHITTEN E.H. (1954). Two arfvedsonitic rhyolite intrusions from Cloghaneely, Co. Donegal. Min. Mag. 30: 393-399.

WONES D.R. and GILBERT M.C. (1982). Amphiboles in the igneous environment. In: Reviews in Mineralogy, Amphiboles: Petrology and Experimental Phase Relations (Edited by VEBLEN D. R. and RIBBE H., 355-390). Min. Soc. of America, Chelsea, U.S.A.

*Final editing, January 1990*

From *Geology and mineral resources of Somalia and surrounding regions*, Ist. Agron. Oltremare, Firenze, Relaz. e Monogr. 113, 345-356, 1993.

# THE CONTINUING STORY OF THE FRAGMENTATION OF GONDWANA: A CONTRIBUTION FROM SOMALIA

A.H.A. DUALEH * and A.E.M. NAIRN **

* Department of Geology, Somali National University, P.O. Box 1081, Mogadishu, Somalia.

** Earth Sciences and Resources Institute, University of South Carolina, Columbia, SC 29208, USA.

ABSTRACT

Well records from the northeast coast and near offshore of Somalia support the hypothesis of an easterly cratonic continuation which persisted unit Middle Cretaceous time. As the onset of the southward drift of Madagascar in the Late Jurassic is established by recognition of the M anomaly sequence in the Gulf of Somalia, it is proposed that the ridge and fracture pattern by which this separation was accomplished broke up Greater India and left part still attached to Northeastern Somalia. This situation persisted until Middle Cretaceous time when a split developed dose to the present coastline of Somalia. The now-separated northern fragment of Greater India once more became part of the Indian Plate, though separated from peninsular India by about 1,000 Km.

## INTRODUCTION

We have recently examined the well logs of Guardafu-1, Ras Binnah, Hafun-1, and Hafun Terrestre (Fig. 1) from Northeastern Somalia. These can be partly tied by data from seven offshore seismic lines and have been compared with data from the Obbia, Garad Mare, and Sagaleh wells from the Somali embayment. The data from these wells are shown in Fig. 2, which illustrates two important points: 1) that north of the Hamurre escarpment the Jurassic section is either absent or reduced to shallow water environments (BOSELLINI, 1986) and 2) the onset of the Middle Cretaceous marine section in Northeastern Somalia is nearly synchronous within the limits of dating.

## DATA

### THE WELLS

The wells drilled in the coastal and offshore region of Northeastern Somalia are not numerous (Fig. 1) and only a few of these penetrate to the basement. The HAT-1 (Hafun

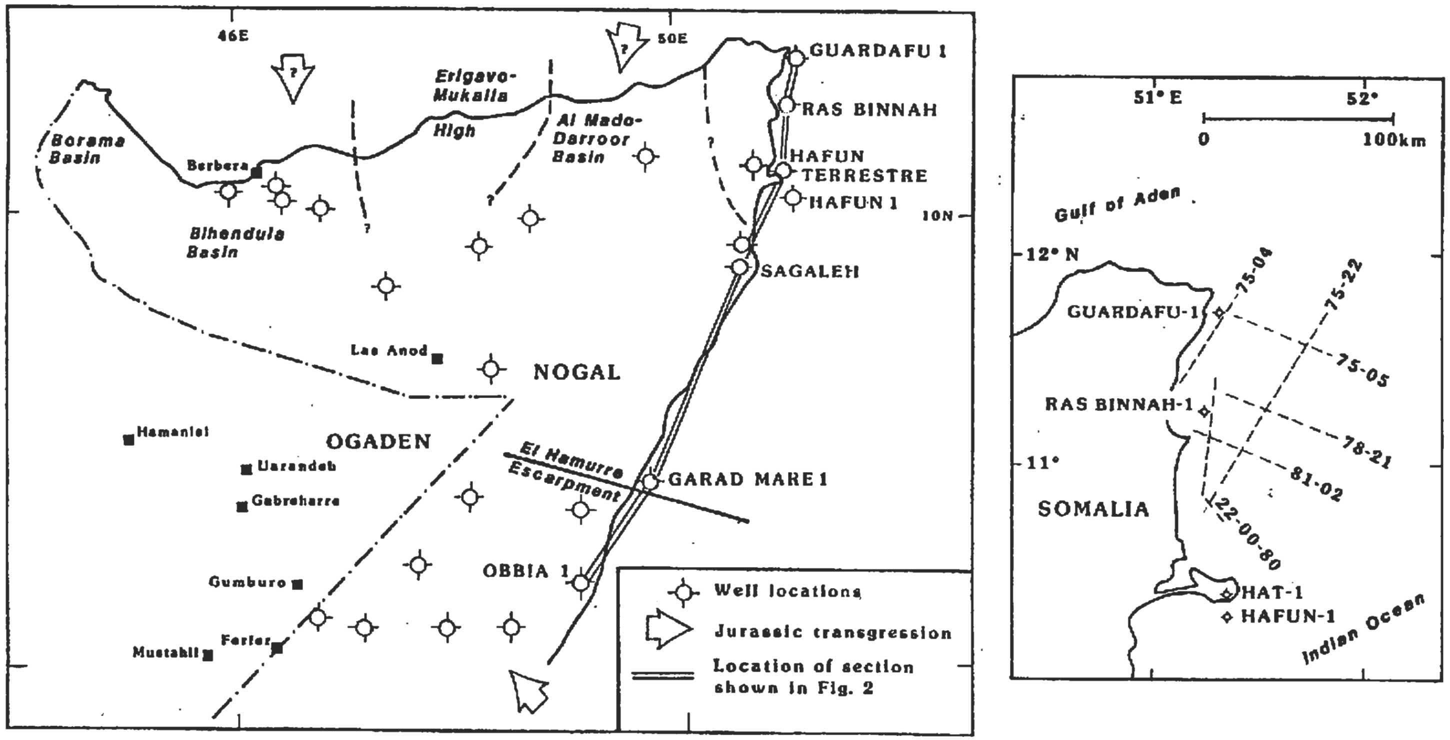


Fig. 1 - Location of wells and the seismic lines used in the present study.

Terrestre) and Ras Binnah-1 wells both reach basement, whereas drilling at Ha-l (Hafun 1) and Guardafu-1 stopped while still within the Cretaceous.

Although Jurassic beds were recorded in Hat-1 and Ras Binnah-1, the thick marine sequences of the Garad Mare-1 and Sagaleh wells to the south (Fig. 1) are not encountered. In Hat-1, the basement is covered by more than 300 meters of undated pyroclastics and basaltic flows conformably overlain by a 120 meter sandstone (the Adigrat Sandstone) identified from microfloral remains as Late Triassic or Early Jurassic. The sandstone is overlain by marine Aptian sands and limestones fromed in a restricted supratidal to intertidal regime. These shallow water conditions persisted into the Cenomanian. There is a break above, as the Cenomanian beds are followed by shallow water Eocene carbonates which give way to basinal shales, continuing until Late Oligocene with only short, shallow water intervals.

In the Ras Binnah-1 well, in contrast, a wholly marine, restricted platform sequence directly overlies Precambrian diorite; it is dated as latest Jurassic to Neocomian in age. The fauna is non diagnostic, but an erosional unconformity below the Aptian indicates the Neocomian must be incomplete. The Aptian-Eocene beds are deeper water to bathyal shale and marl.

As might be anticipated from its location, the Hafun-l well sequence is basically the same as Hat-1, except that the Middle Oligocene section is missing. As beds formed in deeper water conditions occur above and below, this lacuna is presumed to be a starved basin-nondepositional event.

The Guardafu-l well bottomed in Barremian after penetrating a 3,300 meter marine section below Early Oligocene; this section consists mainly of pelagic limestones and fine deep marine clastics. One unconformity is seen, between Maastrichtian and Late Paleocene, but sedimentary discontinuities are shown by marked variation in lithotypes, depositional environments and sedimentation rates.

The simplified lithologic sections are shown in Fig. 2 to demonstrate the lithological contrasts with sections in wells farther to the south.

### Seismic Stratigraphy

Although six seismic lines were available, only one was migrated and non passed through the locations of the available wells. In consequence, conventional subsurface analysis was not possible. However, two major seismo-stratigraphic sequences were recognized: one Mesozioc (Cretaceous and older units), the other Cenozoic (Paleocene-Recent). The latter may be further broken down, at some places, into sequences of Paleocene-Eocene sediments and post-Eocene sediments (Fig. 3). These identifications were based upon well velocity surveys of the nearby wells (Ras Binnah-1 and Guardafu-l) and the recognition of regional geologic units.

The basic structure from Hafun northward is of a Cretaceous high at Hafun and a relative high at Ras Binnah, with an intervening shallow basin. Guardafu lies within a depression. South of Hafun is a zone in which shallow marine carbonates were

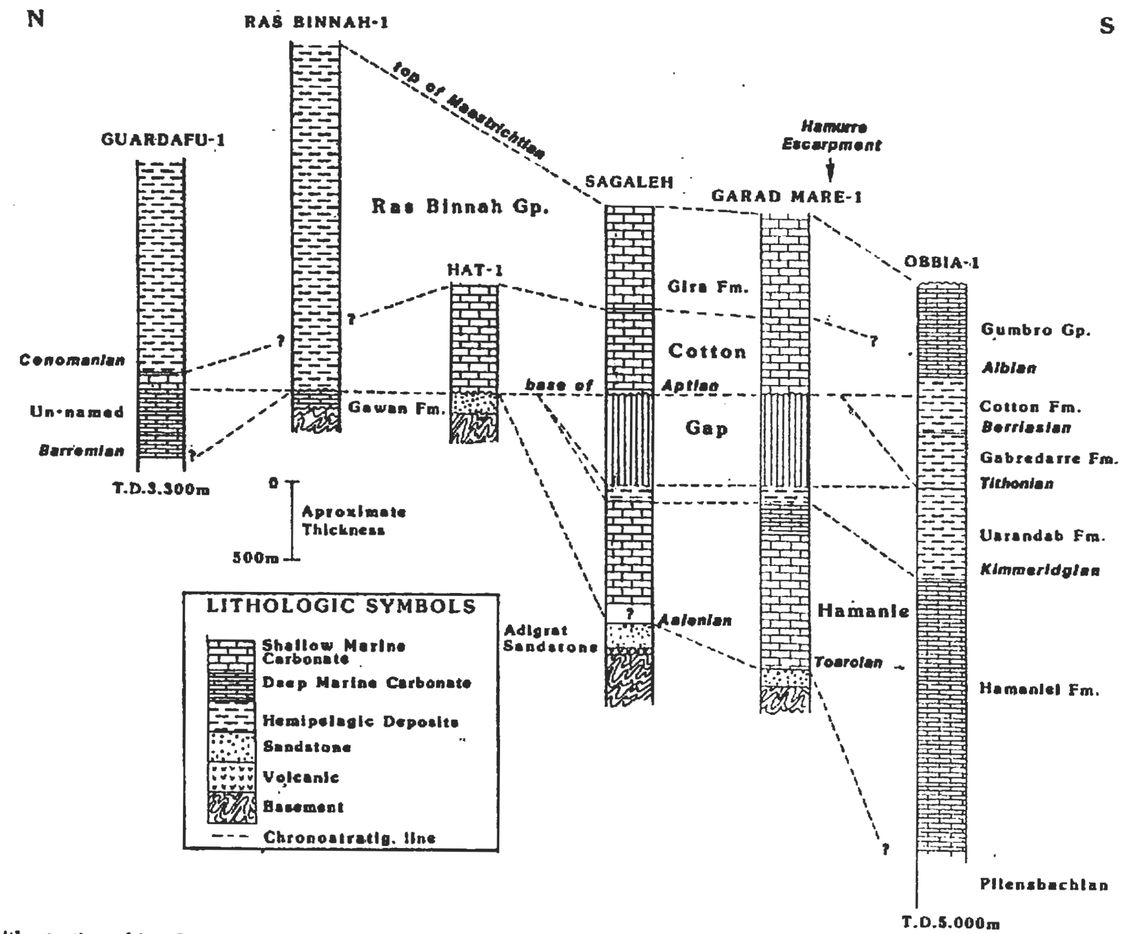


Fig. 2 - Lithostratigraphic columns of wells discussed in the text. The wells that penetrate basement are indicated by a symbol. The TD of wells not reaching basement is given.

deposited during Aptian-Maastrichtian times, but which subsequently, in Paleocene times, became a zone of deep water.

### Basin History

Utilizing a computer program developed by Dr. I. LERCHE (University of South Carolina), it was possible to quantify the development of the basin along the northeastern coast of Somalia by breaking down subsidence into a tectonic component and one due to sediment and water loading. In the case of Somalia, the results must be regarded as provisional because of uncertainties affecting the input parameters - i.e., the assumption that the basement is highly compacted and that the same applies to rocks below TD, which is clearly not always true, and also assumptions concerning porosity, geothermal gradient, etc. Despite the uncertainties, some general conclusions on subsidence rates can be drawn.

At the southern end of the northeastern Somali coastal section, represented by the Hat-1 (Fig. 5a) and Hafun-1 wells, the geohistory curves show relative stability from about 90 m.y. to about 50 m.y., followed by more rapid subsidence. At the northern end, in contrast, Guardafu-1 (Fig. 5b) and Ras Binnah-1 show slow subsidence rates, 2-3 cm/1,000 years, through the Cretaceous on to about 50 m.y. when they, too, indicate the same order of subsidence (10 cm/1,000 years). This more rapid subsidence ended before the cessation of subsidence farther south. The only additional feature is the occurrence of a short Middle Cretaceous episode of rapid subsidence (9 cm/1000 years) seen in the Hat-1 and the Hafun-1 wells.

## DISCUSSION

The distribution of the deeper and shallower water Jurassic facies in the Somali embayment and surrounding area led (BOSELLINI, 1986) to infer invasion of the Mandera-Lugh basin in Southwestern Somalia from the south and east. This is in stark contrast to the commonly indicated transgression from the north and east (ARKELL, 1973). Bosellini version requires transgression west of the Bur Acaba high across a sill that separates the Mandera-Lugh basin from the Lamu embayment (BELTRANDI and PYRE, 1973). No geological evidence, however, has been presented which would discriminate between this model and the more usual pattern of transgression from the north and east into the Borama, Bihendula, and Al Mado-Darroor basins in Northern Somalia, linking with the Mandera-Lugh basin across the Ogaden and/or Northeastern Somalia (Fig. 1). This latter model is an interpretation of the generalized paleogeographic model and shows extension from the ancestral Tuwaiq Bay (BELTRANDI and PYRE 1973).

The timing of this Jurassic transgression and the occurrence of deeper water facies in the Somali embayment coincide with the split and separation of East and West

RB 75-22

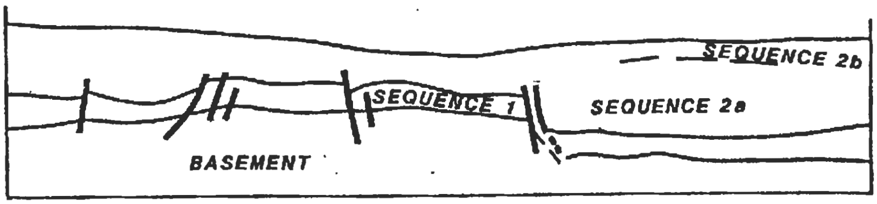


RB 75-21

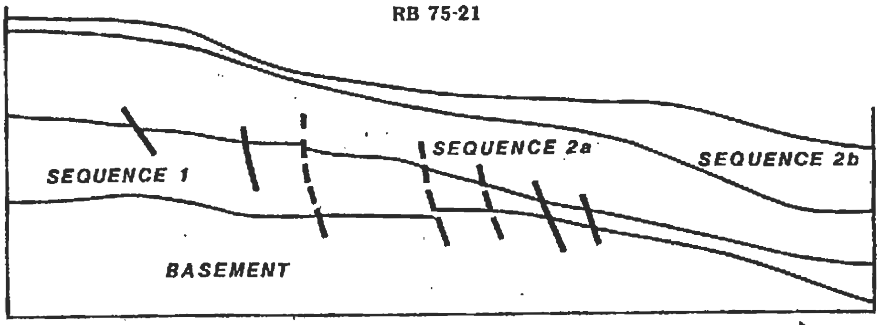


Fig. 3 - Seismic units identified on lines RB75-21 and RB75-22. The location of the lines is indicated in the inset map of Fig.1.

Gondwana, but is not usually considered in the discussion of the displacement of Madagascar. The original debate concerning a northerly location for Madagascar (Fig. 6a) and timing of its southerly drift (SMITH, 1976; TARLING and KENT, 1976; SCRUTTON, 1978; KAMEN-KAYE, 1982) has subsided since the discovery of the M anomaly sequence in the Gulf of Somalia (RABINOWITZ et al., 1983) and Mozambique basin (SEGOUFIN, 1980) and the presentation of paleomagnetic data (MC ELHINNY et al., 1976). This southerly movement was accomplished along lengthy transforms separated by short spreading segments of which the Davie, Dhow, and VLCC are remnants (BUNCE et al., 1973).

The absence of marine Jurassic in some parts of the coastal and near offshore areas of Northeastern Somalia and thin shallow marine deposits in other places indicates that the new plate margin did not extend north-eastward, despite the implication of shallow marine environments in some paleogeographic figures and the trends shown in some tectonic models (DIETZ and HOLDEN, 1970; SMITH and HALLAM, 1970). This issue is resolved by having a Greater India (CRAWFORD, 1974; AUDLEY-CHARLES, 1983; POWELL et al., 1980) (Fig. 5a), with the separation of the southern from the northern part resulting from a continuation of the Jurassic fracture pattern (Fig. 5b). Thus, by the

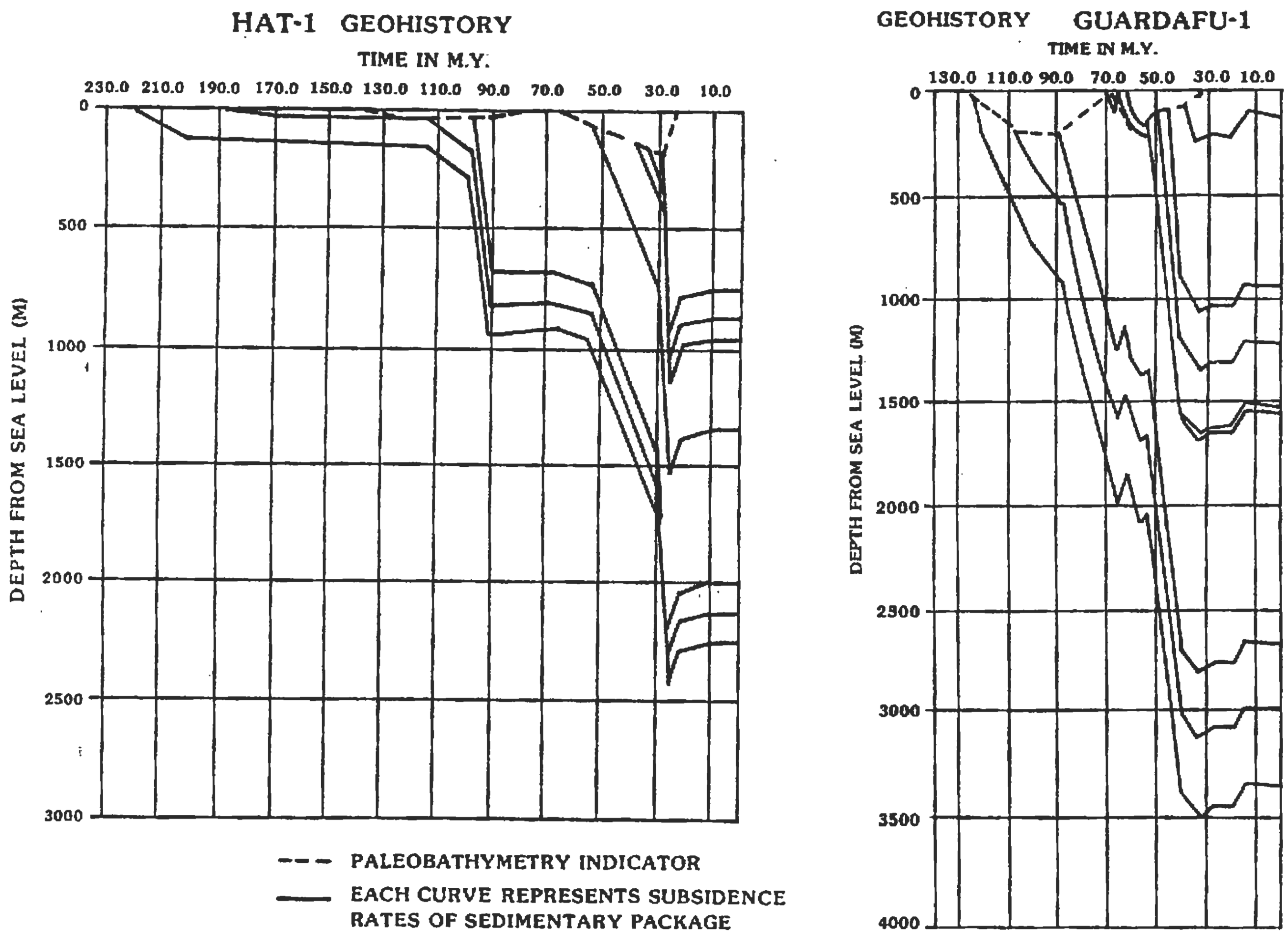


Fig. 4 - Geohistory curves for a) Hat-1, and b) Guardafu-1 showing subsidence rates.

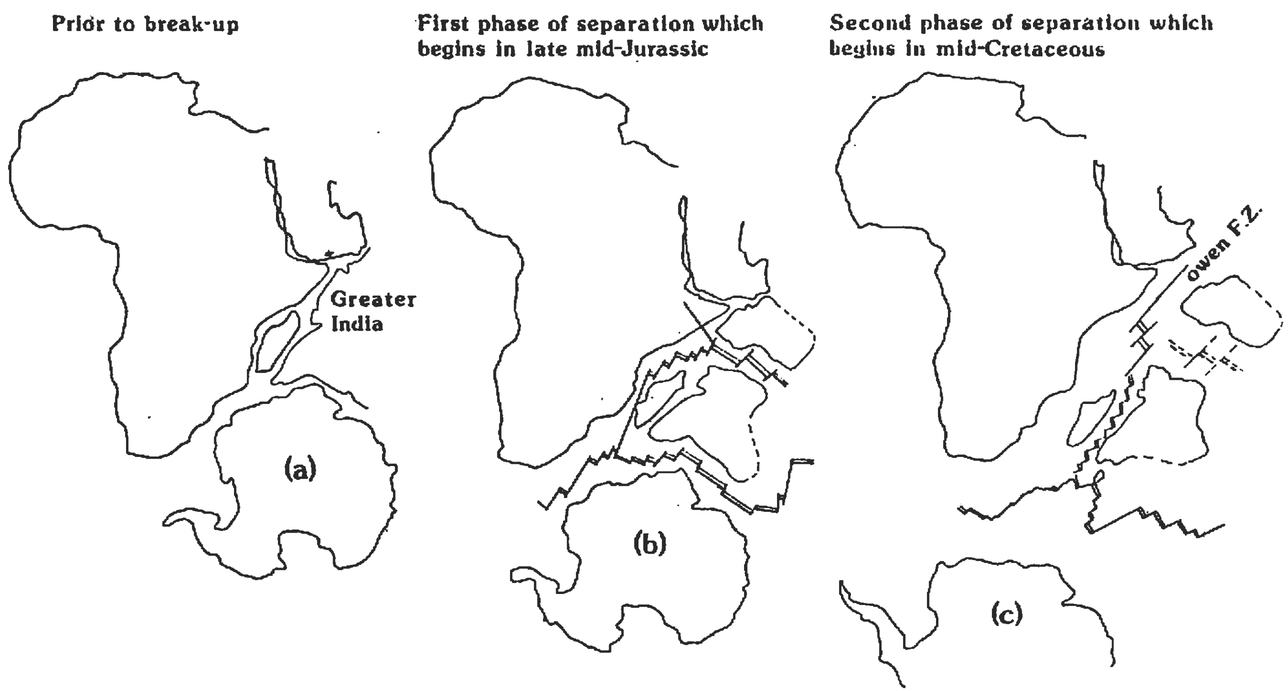


Fig. 5 - The two stage development of the Indian Ocean coast of Somalia. The basic figures are taken from NORTON and SCLATER and have been modified to show the proposed fracture-ridge pattern: a) prior to breakup; b) the Middle-upper Jurassic split with the separation of Greater India into two and the development of the Somali Embayment; and c) the phase beginning in the Middle Cretaceous with the separation of northern Greater India from Somalia and of India from Madgascar.

time Madagascar had reached its present southerly location off the African coast, the two parts of Greater India were separated by over 1,000 km (Fig. 5c).

The second major event recorded by the well data from northeastern Somalia is the nearly synchronous appearance of a Middle Cretaceous marine section. Only in the northernmost well, Guardafu-l, is there evidence of earlier (Barremian) marine beds. The later occurrence of marine Cretaceous onshore to the west (e.g., in the Las Anod well) suggests transgression from the eastern quadrant. From the geology of the Al Mado-Darroor basin in Northern Somalia it appears that this transgression did not extend as far west as the Erigavo-Mukalla high (Fig. 1). Subsequently through the rest of the Cretaceous (Aptian-Maastrichtian), subsidence curves indicate a rapid deepening in the present coastal area of northern Somalia, ranging from 25 to 150 m/m.y. (DUALEH, 1986).

In the plate tectonic context, we equate the occurrence of the marine section with the development of a fracture zone parallel to the present coast (Fig. 5c), a development with which the Owen fracture zone and the posited continuation of the onshore South Bur fault (BOSELLINI et al., 1982) are presumed to be related. Much clearer evidence of this Cretaceous fracture appears along the Arabian Sea coast of the Arabian Peninsula, at that time continuous with northeastern Somalia. This split closely coincides in time with the separation of India from Madagascar and with the separation of South America from Africa. The result of this change in spreading pattern, which left Madagascar locked in its present position with respect to the African craton, reunited the two parts of India on the same plate, although now separated by in excess of 1,000 km of oceanic crust. The northerly movement of this Indian plate as it subducted under Eurasia ultimately led to the accretion of the northern part of Greater India (as one or more fragments) to the Eurasian continent, followed by the later collision of the southern segment.

## CONCLUSIONS

This discussion is necessarily qualitative, for the minor crustal fragments such as the Seychelles have not been taken into account (MATTHEWS and DAVIES, 1966; MILLER and MUDIE, 1961). Nor do we consider the possibility that the northern part of Greater India was split into an easterly Tibetan and a westerly Afghan-Iranian block or blocks. It also is not yet possible, from present geologic data, to ascertain whether the Mandera-Lugh, Al Mado-Darroor, Bihendula, and Borama basins may be considered as half-grabens that resulted from the original tensional fracturing of Somalia preceding the phase of Jurassic marine invasion and the beginning of spreading. We plan to use additional seismic and well data in combination with field studies to develop a quantitative model.

ACKNOWLEDGMENTS

Most of the work on which this is based was carried out during the tenure of a Fulbright Fellowship (AHAD) on data, provided by courtesy of the Ministry of Mining and Hydrology, Mogadishu. We also wish to thank Drs. I. LERCHE and S. SCHAMEL for critical comments and encouragement.

## REFERENCES

ARKELL W.J. (1973). Jurassic Geology of the World. (Eds. OLIVER and BOYD), London, 806 pp.

AUDLEY-CHARLES M.G. (1983) Reconstruction of eastern Gondwanaland. Nature, 306: 48-50.

BELLIENI G., HAYDER A., SASSI F.P., IBRAHIM H. and ZIRPOLI G. (1982). Caratteri geochimico-petrografici dei graniti dei Bur (Somalia meridionale). Univ. Naz. Somala. Quad. Geol. Somalia, 6: 33-50.

BELTRANDI M.D. and PYRE A. (1973). Geological evolution of Southwest Somalia. In: Bassins Sedimentaires du Littoral Africain. Pt. 2. Littoral Austral et Oriental (Edited by G. BLANT). Assoc. serv. geol. Africaine. Paris, 159-178.

BLANT G. (1973). Structure et paleogeographie due littoral meridional et oriental. In: Bassins Sedimentaires du Littoral Africain. Pt. 2. Littoral Austral et Oriental (Edited by G. BLANT). Assoc. serv. geol. Africaine, Paris, 192-231.

BOSELLINI A. (1986). East Africa continental Margins. Geology, 1: 76-78; see, in particular, his Fig. 3.

BUNCE E.T., LANGSETH M.G., CHASE R.L. and EWING M. (1973). Structure of the Western Somali Basin. Jour. Geophys. Res., 72: 2547-2555.

CRAWFORD A. R. (1974). A greater Gondwanaland. Science, 184: 1179-1181.

DIETZ R.S. and HOLDEN J.C. (1970). Reconstruction of Pangaea: Breakup and dispersal of continents, Permian to present. Jour. Geophys. Res., 75: 4939-4956.

DUALEH A. (1986). Geological and stratigraphic evolution of the Northeast Somalia continental margin and adjacent areas. Unpublished thesis. University of South Carolina, 129 pp.

KAMEN-KAYE M. (1982). Mozambique-Madagascar gosyncline I: deposition and architecture. J. Petrol. Geol., 5: 3-30.

MATTHEWS D.H. and DAVIES D. (1966). Geophysical studies of the Seychelles Bank. Trans. Roy. Soc. London, 259A, 227-239.

MC ELHINNY M.W., EMBLETON B.J.J., DALY L. and POSSI J.P. (1976). Paleomagnetic evidence for the location of Madagascar in Gondwanaland. Geology, 4: 455-457.

MILLER J.A. and MUDIE J.D. (1961). Potassium-argon age determinations on granite from the island of Mahé in the Seychelles Archipelago. Nature, 192: 1174-1175.

NORTON I.O. and SCLATER J.G. (1979). A model for the evolution of the Indian Ocean and the break-up of Gondwanaland. Jour. Geophys. Res., 84: 6803-6830.

POWELL C.M., JOHNSON B.D. and VEEVERS J.J. (1980). A revised fit of East and West Gondwanaland. Tectonophysics, 63: 13-29.

RABINOWITZ P.D., COFFIN M.F. and FALVEY D. (1983). The separation of Madagascar and Africa. Science, 220: 67-69.

SCRUTTON R.A. (1978). Davie fracture zone and the movement of Madagascar. Earth Planet. Sci. Letts., 39: 84-88.

SEGOUFIN J. (1980). La transition entre le canal de Mozambique et le bassin de Madagascar. Bull. soc. geol. Fr., 22: 469-479.

SMITH A.G. and HALLAM A. (1970). The fit of the southern continents. Nature, 225: 139-144.

SMITH P. J. (1976). Madagascar issue settled. Nature, 259: 80

TARLING D.H. and KENT P.E. (1976). The Madagascar controversy still lives. Nature, 261: 304-305.

*Final editing, January 1990*

From *Geology and mineral resources of Somalia and surrounding regions*, Ist. Agron. Oltremare, Firenze, Relaz. e Monogr. 113, 357-368, 1993.

# NEOGENE REACTIVATION OF OLDER STRUCTURAL FEATURES IN NORTHERN SOMALIA: INFERENCES FROM LANDSAT INTERPRETATION

J.W. GRANATH, P.E. BUCHHOLZ, KHALID A. SOOFI and R.S.U. SMITH

Conoco Inc., Ponca City, OK 74601, USA.

ABSTRACT

A mosaic of 11 individual Landsat scenes was digitally created for most of Northern Somalia. The quality of each scene was improved by contrast enhancement procedures, by subsampling the data at a resolution of 50 m instead of 80 m, and by application of a high pass filtering algorithm. The mosaic itself was created by standardizing the colour balance of the 11 scenes, while preserving the proportional intensities of the three bands for each pixel. The resulting image is particularly amenable to a photogeologic approach to its interpretation. Most of the traditionally recognized stratigraphic units in Northern Somalia have a characteristic textural and/or tonal signature. The Neogene tectonic features, broadly related to opening of the Gulf of Aden, are particularly evident in the image.

The style and locus of Neogene deformation was apparently influenced by Mesozoic and older tectonics. Three "sectors" of contrasting structural style can be recognized along the north coast. In the west, the Guban appears to be a reactivated Mesozoic basin that underwent extension in front of the Golis Escarpment, insulating the plateau to the south from Tertiary deformation. The Ahl Medo Escarpment marks the shoulder of the Gulf rift the central sector, localizing it to the north of the Erigavo stable block. East of 49 degrees E, the shoulder lies offshore and appears to connect eastward to outcrops of Precambrian rocks on Socotra Island. The Darror Basin shows Tertiary reactivation, insulating areas to the south from deformation. The style of transition between these three "sectors" suggests low-angle detachment tectonics characterize the opening of the Gulf. Varying degrees of reactivation are reflected as far inboard as the Nogal Valley.

## INTRODUCTION

In the course of petroleum exploration in Northern Somalia, eleven individual Landsat scenes have been integrated into a mosaic for use as a synoptic overview of the regional geology. In this paper we would like to describe the characteristics of the mosaic, particularly how it was assembled, and illustrate its use in analysing Tertiary tectonics. The interpretation benefits from surface geological studies and early phases of exploration in Blocks 27, 28, and 29, all inboard from the coast.

## IMAGE CREATION

### Description of Landsat Images

The first of the Landsat series of satellites was launched in 1972. One of the instruments onboard these satellites is a multispectral scanner (MSS). MSS acquires data in both the visible and infrared spectrum. There are two bands in the visible region (red and green) and two in the infrared spectrum (far-infrared and near-infrared). For this study only three of the four available bands were used: green, red, and far-infrared.

The nominal resolution of the MSS scanner is about 80 meters. Each scene covers about 185 by 185 square kilometres on the ground. Eleven MSS scenes were acquired for this mosaic, which covers about 150,000 square kilometres. Table 1 lists the Landsat scenes that were used to create a mosaic that covers most of Northern Somalia from just west of Berbera east to the Indian Ocean.

Table 1 - Landsat scenes used in mosaic. *Parts of two scenes (161/54) spliced together.

| Path | Row | Date collected |
|---|---|---|
| 164 | 53 | 18 Oct 1984 |
| 175 | 52 | 10 Nov 1978 |
| 175 | 53 | 26 Feb 1979 |
| 175 | 54 | 3 Jan 1979 |
| 162 | 52 | 30 Jan 1984 |
| 162 | 53 | 30 Jan 1984 |
| 174 | 54 | 25 Jan 1979 |
| 161 | 52 | 20 Jan 1985 |
| 161 | 53 | 20 Jan 1986 |
| 161 | 54 | 20 Feb 1986 |
| | | 17 Jan 1985* |
| 173 | 55 | 19 Jan 1979 |

### Processing and Plotting of the Imagery

The final image was created by digitally "mosaicking" the eleven individual scenes, each of which was contrast enhanced, high pass filtered and finally plotted on negative film. These steps are explained in some detail below:

*Mosaicking*. Even though the resolution of MSS is 80 meters, the data were resembled to a 50 meter pixel, which did not add any new information but made it possible to plot the image at enlarged scales. After resembling the data, each scene was digitally mosaicked to create one large file of the whole area. The seam lines of the MSS scenes were carefully feathered to remove the edge effects. The feathering was done in

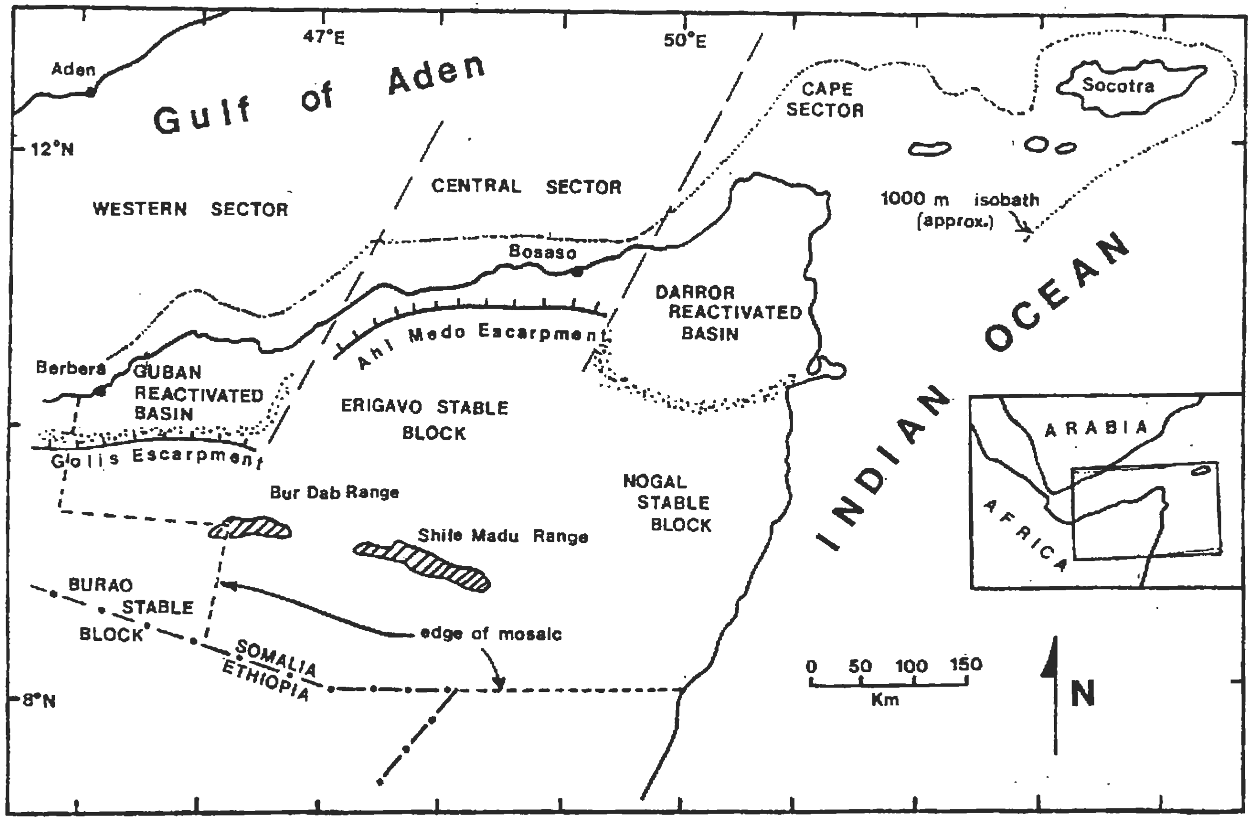


Fig. 1 - Sketch map of northern Somalia showing the major tectonic features identified from the Landsat mosaic. The northern coastal area can be divided into three sectors, each showing a different structural style and (by inference) a different relationship to the shoulder of the Gulf of Aden. The boundaries between the three sectors can be traced offshore to major fracture zones on the floor of the Gulf (northeasterly oriented dashed lines). The area covered by the mosaic is outlined. See text for further discussion.

such a way so that spectral differences between different bands were preserved as much as possible. The final mosaic represents a careful compromise between digital feathering of the seam lines and preservation of spectral differences between bands.

*Enhancement.* After the images were digitally combined into one image, it was contrast enhanced. The data as collected were concentrated into the lower portions, or dimmer parts of the detectable range of brightness. That range is a linear gray shade scale assigned values of DN (or density) of 0 to 255. The enhancement was done by preserving the lowest DN of each band at 0 and expanding the highest DN value out to the maximum possible value of 255. Gray shade values between were linearly interpolated. This process usually increases the contrast of the image sufficiently, but if the image is too dark or too bright (i.e. dominated by either the low or high end of the range), then the lower or upper DN values must be clipped. In the case of the Somalia mosaic, both bright and dark areas had to be subdued in such a way. Several cutoff DN values were tried for optimum contrast enhancement and the final values were chosen to emphasize the major features of the Blocks 27, 28, and 29, the concession area. As a result, the mountains along the northern coast appear slightly darker than the optimum.

*Filtering.* The image was further processed by a "high pass" filter to sharpen the edges. The filter was applied to blocks of data composed of 51 by 51 pixels. The resulting image looked rather harsh. Therefore the original mosaic (contrast enhanced) was added back to the filtered image to produce the final mosaic.

*Plotting.* The final mosaic was plotted on three 8 by 10 film negative-sheets using a laser plotter. Various final prints have been created by projecting these negatives to the desired scale. The initial false colour version was created at 1:500,000, but subsequent prints have been enlarged to 1:250,000. The mosaic can be enlarged in principle to 1:100,000 without serious degradation of the image.

## CHARACTERISTICS OF THE IMAGERY

A characteristic of the colour balance used in the mosaic is its fidelity to the major units in the stratigraphy of Northern Somalia. Although we may not be able to identify precisely the origin of spectral data that give rise to the tonal and textural signatures in the image, we have been able to develop an empirical scheme for recognition of stratigraphic units, and to use that scheme to build a geological map. The map units correspond in general to the principal stratigraphic units, but it should be emphasized that the boundaries in such an approach are basically tonal/textural in nature and correspond to formal stratigraphic boundaries only insofar as they faithfully reflect the physical basis on which the stratigraphy has been recognized. Our empirical scheme was guided by field experience. At the scale used in the image analysis, system-level units can be distinguished for the pre-Tertiary: the Precambrian crystalline basement, the Jurassic carbonate sequence of the Berbera region, largely recognized from the

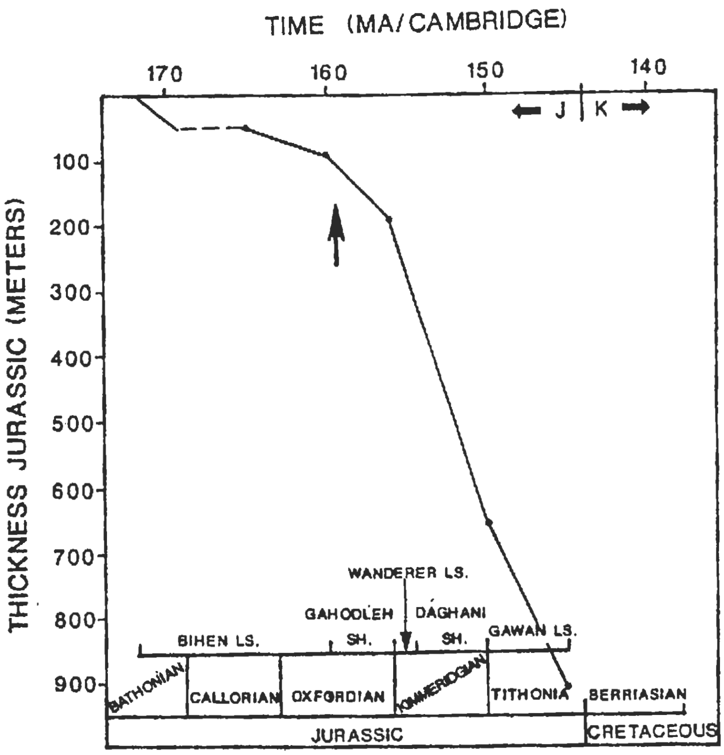


Fig. 2 - Deposition vs. time ("geohistory") diagram for the Bihendula Jurassic section. The curves represent "raw" thicknesses, uncorrected for compaction. Absolute ages are from HARLAND et al. (1982). Solid curve is drawn using data from MACFADYEN (1933), as reported in ARKELL (1956). More recently the Bihen-Gahodleh-Wanderer part of the section has been dated by BUSCAGLIONE and FAZZUOLI (1987) and by A.S. HUSSEIN and MONECHI (1987): their dates are used to construct the lower (dotted) curve at the tip of the arrow. In either case, the acceleration of sedimentation 155 to 160 ma suggests the onset of a tectonically controlled depositional basin within the broad late Jurassic carbonate platform ordinarily recognized in northeast Africa.

Bihendula section, and the Cretaceous section of clastics. The Precambrian is expressed in brown to blue shades and has a distinctive textural character that reflects the steep plunges of the polyphase-deformed metamorphic assemblage. Particularly along the Golis, the Precambrian bears a red tinge reflecting the lusher vegetation there. The Jurassic tends to have a grey to buff colour and a smooth texture, the Cretaceous green hues reflecting the red coloration of the rocks themselves and a rough or pitted texture.

The tripartite division of the Eocene, Auradu-Taleh-Karkar, is reflected in a range

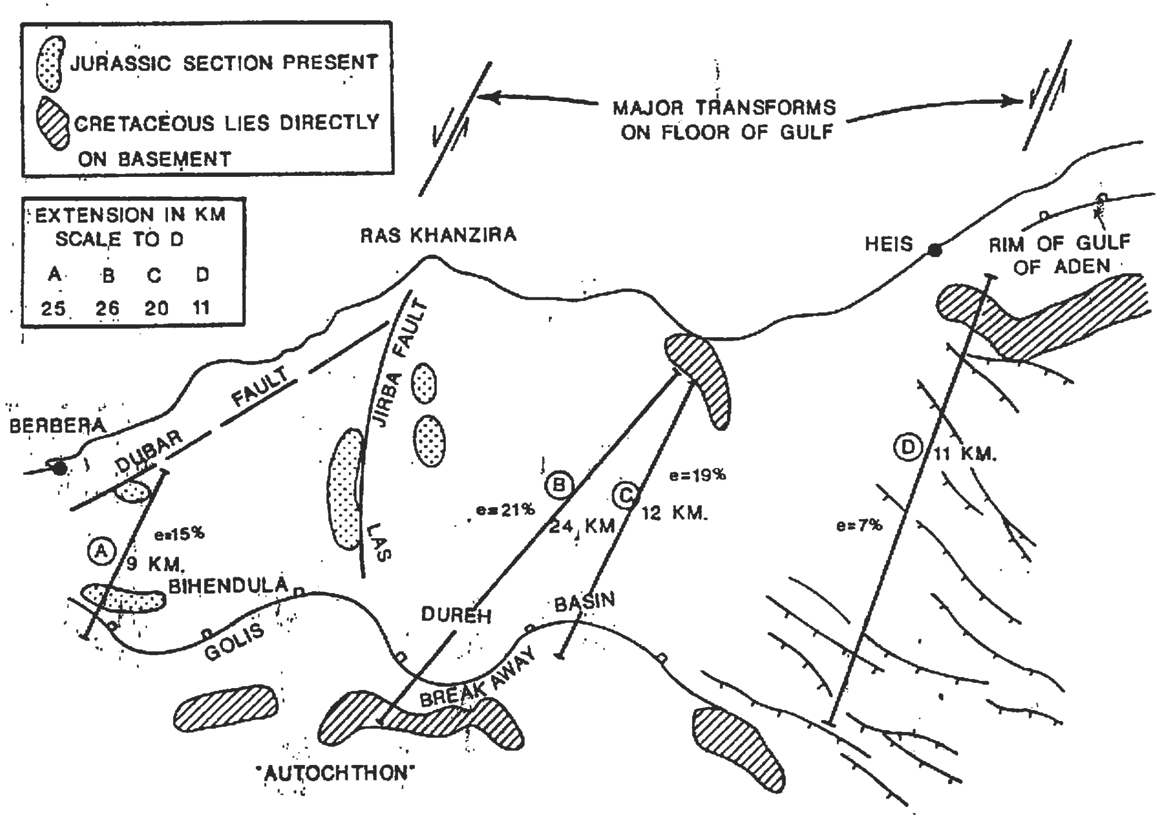


Fig. 3 - Tectonic sketch map of the Guban region showing the locations of four cross sections (A through D) and their respective amounts of extension in both percentage and km. Section B is presented in Fig. 6, and section D in Figs. 4; 5. For purposes of comparison between the sections, the amount of extension in each section has been scaled to the length of section D, and displayed in the box at upper left. The locations of Jurassic section are shown stippled, presumably roughly outlining the older Mesozoic basin suggested by Fig. 1. Locations of a thin Cretaceous section lying directly on basement presumably lie outside the confines of that basin. See text for further discussion.

of tonal signature that allows in a broad way to photogeologically map within the extensive Eocene outcrop on the plateau. The Auradu tends to be pink to buff in colour with a texture that directly reflects the rough weathering style and the cliff-forming character of the limestones. The Taleh, and to a degree the upper part of the Auradu, shows up as a chalky white somewhat washed out unit with some pale olive green horizons near the base. The texture in the imagery is granular. The Karkar is perhaps the most distinctive of the three, with a brownish yellow to rusty brown coloration and a fine mottled texture. The badlands style of outcrop along the edge of Karkar outcrop belts is easily detected in the imagery.

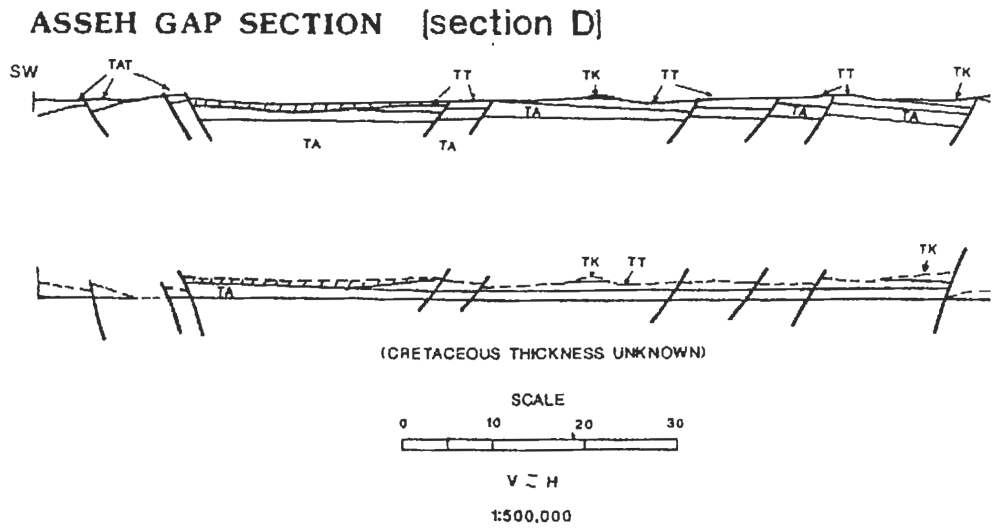


Fig. 4 - Southern half of the Bur Dab-Ahl Medo Escarpment cross section (section D in Fig. 3) across the Asseh Gap region. The location is shown in Fig. 3, but note that the southern end of the section in Fig. 3 corresponds to the arrow in this figure. PT = Proterozoic basement, K = Cretaceous, TA = Tertiary Auradu, TAT = Tertiary Auradu-Taleh, TT = Tertiary Taleh, TK = Tertiary Karkar, cross hatched pattern is young valley fill. Section has been drawn so as to be both restorable and balanced.

## TECTONIC FEATURES OF NORTHERN SOMALIA

The tectonic features in the imagery are dominated by features of mid-to late Tertiary age, broadly identifiable with early extension presaging the opening of the Gulf of Aden, and with the opening itself. Three sectors are apparent along the north coast (Fig. 1). In the west, the Golis Escarpment and the tilted fault block terrane of the Guban is easily distinguished and readily identified as the shoulder of the Gulf rift and an onshore salient of Gulf extended terrane, respectively. To the south of the Golis is

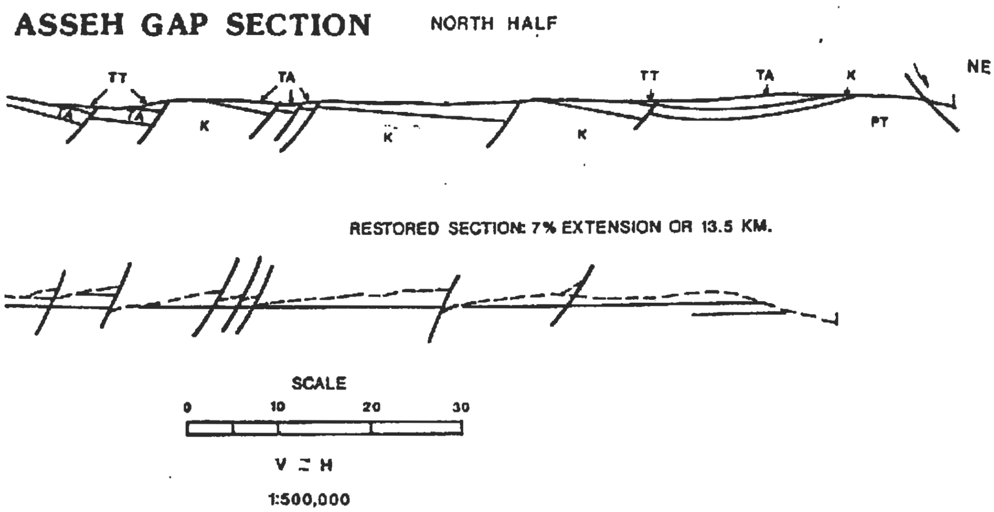


Fig. 5 - Northern half of the Asseh Gap structural section. See Fig. 4 for description.

a relatively stable block bearing gentle Tertiary deformation. We call this block the Burao stable block. Between about 47 and 49 degrees East, the Ahl Medo escarpment plays a similar role to that of the Golis, but is stepped north toward the coast along the northern fringe of the Erigavo "High" or stable block. East of 49 degrees, in the Cape sector, Tertiary deformation can be clearly seen in the Darror-Segaleh Basin, outlining the shape of the older basin. There is no obvious escarpment or shoulder to the Aden rifting onshore in this sector, but the continental shelf extends farther seaward from the coast than it does to the west. Consequently we have entertained the possibility that Socotra Island lies along a shallowly buried ridge of Precambrian rocks offshore, in a position analogous to the Golis and Ahl Medo escarpments.

Pre-Tertiary tectonic features have apparently played a role in extension leading to the opening of the Gulf. Neogene reactivation is particularly clearly shown in the density and orientation of lineaments in the processed imagery that coincide with known pre-Tertiary structures.

In the west, the Guban appears to have been the location of a tectonically controlled depocenter of Jurassic age, judging from the rapid acceleration of depositional rate in the Early Kimmeridgian (Fig. 2) and the rapid thinning of Mesozoic stratigraphic units across the Golis escarpment (Fig. 3). We propose that renewed extension in the Guban area in Tertiary time was concentrated along the locus of the older depositional basin, and insulated the Burao block to the south from significant extensional strains. In the central sector, the Ahl Medo escarpment is localized along the north edge of the Erigavo block within which little Tertiary deformation is apparent. On the south edge of the

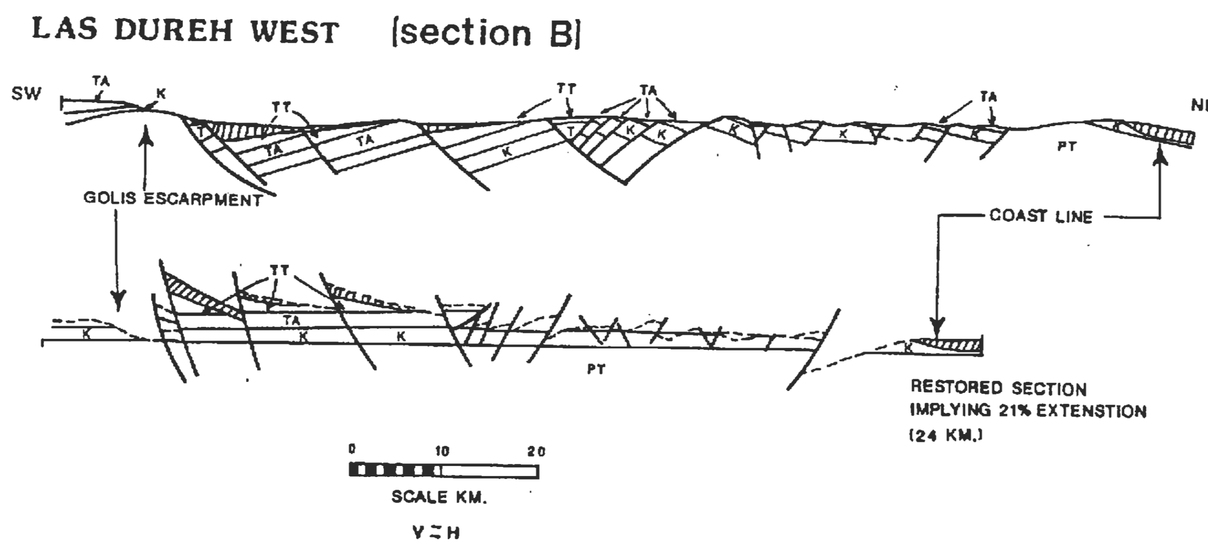


Fig. 6 - The Las Dureh West structure section, section B in Fig. 3. See Fig. 4 for identification of units, and text for further discussion.

Erigavo block, however, the Bur Dab and Shile Madu Ranges were uplifted along apparently older structural trends.

In the east, the Darror Basin localized Tertiary deformation inboard from the plate margin. The Nogal stable block suffered some block faulting during the Tertiary, but it is less severe than demonstrated by the Bur Dab and Shile Madu Ranges to the west. The Darror essentially plays a similar role as the older basin in the Guban, but instead is located behind the rift shoulder rather than in front of it.

## Geology of the Guban

One of the more prominent physiographic and interesting geological features of Northern Somalia is the Guban, and its eastward transition into the Erigavo stable block serves to illustrate the accommodation of differential extension as the shoulder of the Gulf rift steps to the north. The Guban is characterized by basin-and-range style topography, the ranges being the tips of tilted fault blocks surrounded by Tertiary and Quaternary clastic valley fill. The southern edge of the Guban is bordered by the Golis Escarpment, which marks the southern rim of the Gulf of Aden where a strip of Precambrian basement is exposed. Because the Golis is also the northern edge of the Burao block (as described above), the fault system along the foot of the Golis Escarpment marks the trace of the upper crustal breakaway to which the faults within the Guban are genetically related. We dub this fault system the Golis fault.

The eastern end of the Guban is covered by the mosaic, but a portion of the transition from the Guban to highlands of the central sector is, unfortunately covered by clouds. Nevertheless, it is apparent that the transition is not marked by a discrete northeasterly trending fault system, but rather appears to be characterized by a progressive decrease in throw on the northwesterly trending faults that bound rotated blocks within the Guban (Fig. 3). A gradual increase in surface elevation parallels the transition, and near the coast, Precambrian rocks are again exposed in the rim of the Gulf of Aden along the Ahl Medo escarpment. A restored cross section from the Bur Dab Range across this transition to the west end of the Ahl Medo escarpment (Figs. 4; 5), suggests 7% or 13.5 km of extension. Eleven km of that extension is concentrated north of the end of the Golis escarpment, so that only 2.5 km of extension is represented by faulting in the upper Nogal Valley.

The amount of extension in the Guban (Fig. 3) is somewhat greater, on the order of 20%. The Guban itself is segmented by a network of strike-slip faults that are best recognized through combining ground-based studies with imagery interpretation. Two such faults are apparent in the area covered by the mosaic. One (herein named the Dubar fault) enters the area of the image about 20 km south of Berbera, and skirts several coastal ranges in a northeasterly direction to join the second (the Jirba fault) on Ras Khanzira. The trace of the Dubar fault is clear on the S.O.E.C. mapping southeast of Berbera, but its extension across the coastal plain to the northeast is best marked by a tonal and textural signature in the orbital imagery. The Jirba fault diverges from the

Golis fault system along the western side of the Las Dureh Basin and runs along the eastern side of the "Jirba" Range toward Ras Khanzira to join the Dubar fault. Several folds within the sedimentary section along the fault lie at various angles to the trace, indicating its fundamentally strike-slip character.

Between those accommodation faults, the blocks of the Guban are bounded by more or less coherently grouped normal faults, which can occur at a variety of angular relations to the strike-slip faults. Consequently, a complicated displacement field and history is evident, with components of oblique slip probably the norm on most of the normal faults (see, for example, the discussion between BOSWORTH, 1986, and LISTER et al., 1986).

Three cross sections have been constructed across parts of the Guban between the accommodation faults (Fig. 3). One of the sections is presented here (Fig. 6). The locations of the others are shown in Fig. 3. Note that the amount of extension in the Las Dureh West section is about 21% or 24 km, in contrast to the values along the Asseh Gap section (Fig. 5). The other sections in the Guban also show larger extensions, percentage wise, than the Asseh Gap section. But because each is shorter than the Asseh Gap section, the amount of extension in each has been scaled to the length of the Asseh Gap section for comparison purposes only (values in the box on Fig. 3). These values are not values of measured extension, but rather projected estimates if the sections were as long as the Asseh Gap section.

The interesting thing about these sections is the rather abrupt decrease in the amount of upper crustal extension between the Las Dureh and Asseh Gap sections, yet no clearly defined northeasterly trending fault marks that abrupt change. In conventional vertical graben tectonics, such lateral differences would ordinarily necessitate strike-slip faults to accommodate the differential displacement of the rift margins, the orientation of the faults paralleling the direction of extension. In this case, the suggestion is that all of this portion of Northern Somalia lies within an inhomogeneously extended upper crustal plate within which differential extension can be accommodated by oblique slip on families of obliquely oriented faults. The upper plate may be underlain by a common detachment surface at mid-crustal levels, as is commonly becoming recognized in other extensional terranes. The degree to which displacement varies on that detachment surface may reflect the degree to which Tertiary extensional strains are localized by older structures, as described earlier in this text. Could elements of the detachment reach as far to the south as the Bur Dab and Shile Madu Ranges?

ACKNOWLEDGMENTS

We would like to thank the conveners of GEOSOM '87 for the opportunity to share our thoughts on Somali tectonics, especially in such an early stage of their development, and the many geoscientists who have influenced our thinking. Conoco Inc. very graciously has allowed the release of this contribution.

REFERENCES


ABDI SALAH HUSSEIN and MONECHI S. (1987). Calcareous nannofossils of middle to late Jurassic sediments in north-western and central Somalia (abs.). GEOSOM '87. Somali National University. Dept. of Geology, 13.

ARKELL W.J. (1956). Jurassic Geology of the World. OLIVER and BOYD Ltd., Edinburgh and London, 806 pp.

BOSWORTH W. (1986). Comment on "Detachment faulting and the evolution of passive continental margins". Geology, 14: 890-891.

BUSCAGLIONE L. and FAZZUOLI M. (1987). Jurassic Carbonate Microfacies of Somalia. Dipartimento di Scienze della Terra. Università di Firenze, 109 pp.

HARLAND W.B., COX A.V., LLEWELLYN P.G., PICKTON C.A.G., SMITH A.G., and WALTERS R. (1982). A Geologic Time Scale. Cambridge University Press. Cambridge, 131 pp.

LISTER G.S., ETHERIDGE M.A. and SYMONDS P.A. (1986). Reply on "Detachment faulting and the evolution of passive continental margins". Geology, 14: 891-892.

MACFADYEN W.A. (1933). The geology of British Somaliland with a geological map 1:1,000,000. Crown Agents. London, 87 pp.


*Final editing, January 1990*

From *Geology and mineral resources of Somalia and surrounding regions*, Ist. Agron. Oltremare, Firenze, Relaz. e Monogr. 113, 369-378, 1993.

# FISSION-TRACK AGES AND THE UPLIFT OF THE SOMALI PLATEAU

E. ABBATE *, G. BIGAZZI **, P. NORELLI **, C. QUERCIOLI ** and D. VISONÀ ***

* Dipartimento Scienze della Terra, Universita' di Firenze, Via La Pira 4, 50121 Firenze, Italia

** Istituto Geocronologia e Geochimica Isotopica, CNR, Via C. Maffi 36, 56100 Pisa, Italia

*** Dipartimento di Mineralogia e Petrologia, Universita' di Padova, Corso Garibaldi 37, 35100 Padova, Italia

## ABSTRACT

Apatite concentrates from three Younger Granites outcrops ( Daymolëh Weyn, Daimoleh Yare and Bur Wadaba) in the crystalline basement of the northern Somali plateau escarpment gave Tertiary fission-track ages. The apatites were separated from the same granite samples which already supplied a Rb/Sr w.r. isochron of about 550 Ma. The obtained fission-track ages, which are thought to reflect cooling due to regional uplift and erosion, exhibit some differences: while five samples collected from the two Daymolehs range in age from 19.6 to 22.9 Ma, the only one sample from the Bur Wadaba yields an age of 41.8 Ma. Since these age differences cannot be explained on the basis of difference in altitude, it is likely that the uplift was not coeval along the northern Somali plateau margin, but had possibly local inception since Late Eocene and more continuous pulses during Early Miocene.

## INTRODUCTION AND GEOLOGIC HISTORY

Although there are many rifted plate margins flanked by basement uplifts, temporal and causal relationships between uplift and rifting are still unclear. To get new information on these processes we sampled three Paleozoic Panafrican granites in the Northern Somali basement along the escarpment facing the Gulf of Aden. Fission-track ages were obtained from the apatites of the granites and we used them to constrain times and rates of uplift. In fact, at temperatures less than 100 °C , fission tracks are preserved in the apatite crystals and their increase in number is a time function. The fission-track ages records the time (cooling age) since the apatite was last at its track annealing temperature (NAESER and FORBES, 1986). It can be assumed that uplift and concomitant erosion were responsible for this transition toward lower temperatures. Unfortunately, a straightforward age interpretation is hampered by the occurrence of a zone, extending about 30 °C, in which the tracks are only partially preserved (see below).

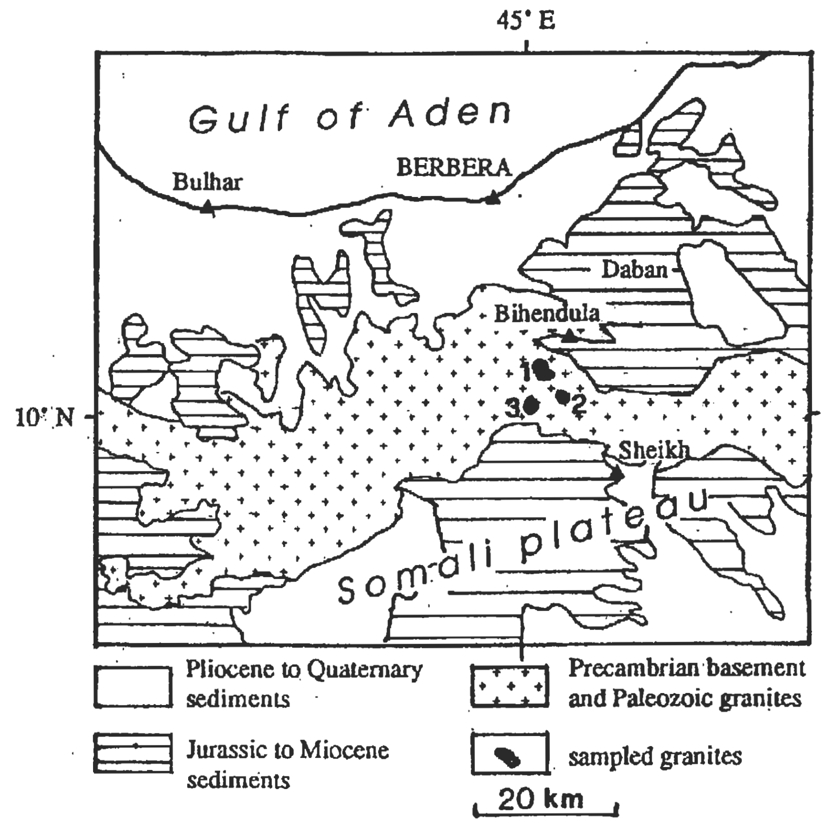


Fig. 1 - Geologic sketch map of the Berbera- Sheikh area. Dated granites: 1- Daimoleh Weyn; 2 - Daimoleh Yare; 3- Bur Wadaba.

The granites, which are all biotitic, often porphyritic and slightly foliated, are intruded in the Precambrian Qabri Bahar Complex of Northern Somalia (HUNT, 1960; VISONÀ et al., 1984), north of the Sheikh escarpment (Fig. 1). They now emerge from the lowland country rock as prominent inselbergs (Daimoleh Weyn, Daimoleh Yare and Bur Wadaba). Limitedly to the Daimoleh Weyn, radiometric datings are available. A Rb/Sr whole rock isochron provided an age of about 550 Myr (FERRARA et al.,1985), while K/Ar analyses on the biotites gave an age of about 500 Myr (SNELLING, 1967; FERRARA et al.,1985).

Basement and granites were peneplained and presently rest beneath thick Mesozoic to Paleogene, mostly shallow-marine or continental deposits. This succession was so widespread to cover both Northern Somalia and Southern Arabia. The rifting phase, which eventually gave rise to the Gulf of Aden, began in the Oligocene and was followed by sea floor spreading during the Early Miocene ( see ref. in ABBATE et al., 1986).

## ANALYTICAL METHODS

Apatite separates in the size of 75-100 microns were obtained from six rock samples of about 3 kg each using conventional heavy liquids and magnetic techniques. For each sample a portion of grains was heated to remove fossil fission tracks and irradiated in the LENA reactor of the Pavia University.

For age measurements the population method has been used: fossil and induced track densities have been determined in two different portions and counted on unit surface on the apatite crystals 300 to 1,480 grains for the spontaneous tracks and 80 to 220 grains for the induced tracks have been analysed.

Although the number of the tracks (and grains) is significant, the experimental uncertainty on the age, which includes the counting error only (one standard deviation) is relatively high ( about 5-6%). This is due to the fact that countings do not follow a Poisson distribution. The Chi-square test applied to the comparison between observed and corresponding Poissonian distributions has shown significant deviations. This is confirmed by the comparison between the percentages of column $\bar{\bar{S}}'$ and the corresponding Poisson errors (s with $(1/n_s)^{1/2}$ and i with $(1/n_I)^{1/2}$) taken also into consideration the number of grains to which they refer. The Chi-square test, assuming the counting mean as expected value (see BIGAZZI et al., 1986), leads to values significantly higher than the counting number as indicated by the Chi-square test applied to the Poisson distributions. This means that there are, as commonly happens, significant variations in uranium content in different apatite crystals.

Some apatite crystals include small zircons much richer in uranium. In some cases the tracks from the zircon radiate into the closest portion of the apatite crystal. In other cases the tracks are unevenly distributed on the surface of the same grain, suggesting inhomogeneities in uranium content. This contrasts with the relatively uniform track distribution of the apatites apparently devoid of zircon crystals. Whereas the first grains were discarded, the others were analysed because the apatite crystals would not have been treated in the same way for both spontaneous and induced tracks, owing to different $r_s$ and $r_I$ densities.

Apatite analytical results are shown in Table 1. Ages fall into two groups. The first includes samples from the Daimoleh Weyn and the Daimoleh Yare, the second the only sample from the Bur Wadaba.

Experimental uncertainties prevent establishing whether age differencies within the first group are significant, or, more precisely, whether the S-83/153 sample is actually younger than the others of the same group. Observed differencies are, in fact, compatible with statistical scattering.

Table 1 - Fission track ages of apatite samples from Daymoleh Weyn (S83-153, S83-151 and S84-88, approximate elevation 880m), Daimoleh Yare (83-156 and S83-182, approximate elevation 900m) and Bur Wadaba (S83-189, approximate elevation 1,040m) granites.

| Sample | $\rho_S$ ($n_S$) | $\rho_I$ ($n_I$) | $\bar{S}'$ - % s | i | S | I | Age Ma |
|---|---|---|---|---|---|---|---|
| S83-153 | 49800 (1013) | 1038000 (3283) | 3.7 | 4.2 | 905 | 130 | 19.6 $\pm$ 1.1 |
| S83-151 | 95600 (842) | 1881000 (2435) | 3.5 | 5.1 | 1480 | 220 | 22.7 $\pm$ 1.4 |
| S84-88 | 73400 (1160) | 1478000 (3242) | 3.8 | 3.4 | 689 | 170 | 21.9 $\pm$ 1.1 |
| S83-156 | 77900 (857) | 1590000 (2922) | 4.2 | 3.7 | 450 | 140 | 22.7 $\pm$ 1.3 |
| S83-182 | 139000 (1020) | 2678000 (2946) | 4.4 | 4.6 | 300 | 80 | 22.9 $\pm$ 1.4 |
| S83-189 | 299000 (2188) | 3161000 (3581) | 3.1 | 3.8 | 574 | 200 | 41.8 $\pm$ 2.0 |

$r_s$ ($r_I$): spontaneous (induced) track density, tracks/cm$^2$; $n_s$ ($n_I$): number of spontaneous (induced tracks); $\bar{S}'$%: relative standard error of the mean of spontaneous (s) and induced (i) track counting. The fission tracks were calculated with the following parameters: decay constant of $^{238}U$ spontaneous fission, $\lambda_F = 6.85 \times 10^{-17} a^{-1}$; cross section for $^{235}U$ induced fission, $\sigma = 5.802 \times 10^{-22}$ cm$^2$; isotopic ratio $^{238}U/^{235}/U = 137.88$. The neutron fluence, referred to SRM 963a standard of NBS, was $7.18 \times 10^{15}$ neut/cm$^2$. Irradiated and non-irradiated apatites were included in epoxy resin and polished. Samples S-83/153, S-83/151, S-84/88 and S-83/182 were etched for 45" in 5% $HNO_3$ at 20°C; sample S-83/156 and S-83/109 for 60" in the same conditions.

## TEMPERATURE AND TRACK FADING IN THE APATITE

Extrapolation to geologic times of annealing experiments, carried out in laboratories, and the study of natural fading in well samples at different depths indicate that for times of the order of tens of millions years tracks begin to fade at about 70° C, and are thoroughly unstable at temperature greater than 125° C (WAGNER, 1968; NAESER and FAUL, 1969; WAGNER and REIMER, 1972; NAGPAUL et al., 1974; NAESER and

FORBES, 1976; NAESER, 1979; BRIGGS et al., 1980; NAESER, 1980; GLEADOW and DUDDY, 1981).

Closing temperature are dependent from the time interval during which the apatites reside in the partial annealing zone (i.e. in the zone between the fading inception and the total fading).

For relatively high, cooling temperatures, as in the case of mountain building, a closing temperature of about 120° C has been proposed for the apatites (WAGNER et al.,1977; ZEITLER et al.,1982). However, chemical variations in a mineral phase can significantly influence the closing temperature (POUPEAU,1981).

Recent papers agree in assuming a closing temperature of 120° $\pm$ 20°C during the uplift processes (CARPENA, 1985, HURFORD, 1986). Thus we can infer that the ages in Table 1 are indicative of the time in which temperature was lower than the above-mentioned closing temperature.

How much a residence in the partial annealing zone influences fission-track ages can be commonly judged through the analysis of the length of the confined tracks (GLEADOW et al., 1986). This was not possible for our samples due to the paucity of confined tracks. Anyhow; the similar length of fossil and induced tracks would indicate a residence in the partial annealing zone too short to modify significantly the cooling ages.

## INTERPRETATION OF FISSION TRACK RESULTS

Apatite fission track ages are sensibly younger than the ages of granite crystallization (550 Myr) or metamorphism (500 Myr). To explain this difference, let us sketchly summarize the geological history of the region punctuated by repeated uplifts, denudations and burials (Fig. 2).

Between the intrusion of the Early Paleozoic granites into the Precambrian basement and the regional Middle Jurassic peneplanation, there is an extended chronological hiatus: Judging from conterminous regions (Ethiopia and Arabia) it is likely that further sedimentary cycles, possibly with periglacial episodes, occurred during that time interval.

Thus, repeated track resets can be envisaged until the major erosional phase marked by the important unconformity between the basement and the Middle Jurassic Adigrat Sandstones. The latter were deposited in a transitional environment and were followed by a thick succession of prevalently shallow-marine limestones, in turn overlain by the terrestrial Yesomma Sandstones (Fig. 2,I).

Taking into consideration the total thickness of sediments and their depositional environment, we can assume a generalized uniform subsidence, which probably brought about an annealing of the tracks in the apatites of the Daimoleh and Wadaba granites.

Early Cretaceous regional reconstructions indicate that, while the Yesomma Sandstones were being deposited, the region was vigorously blockfaulted (Fig. 2,II)

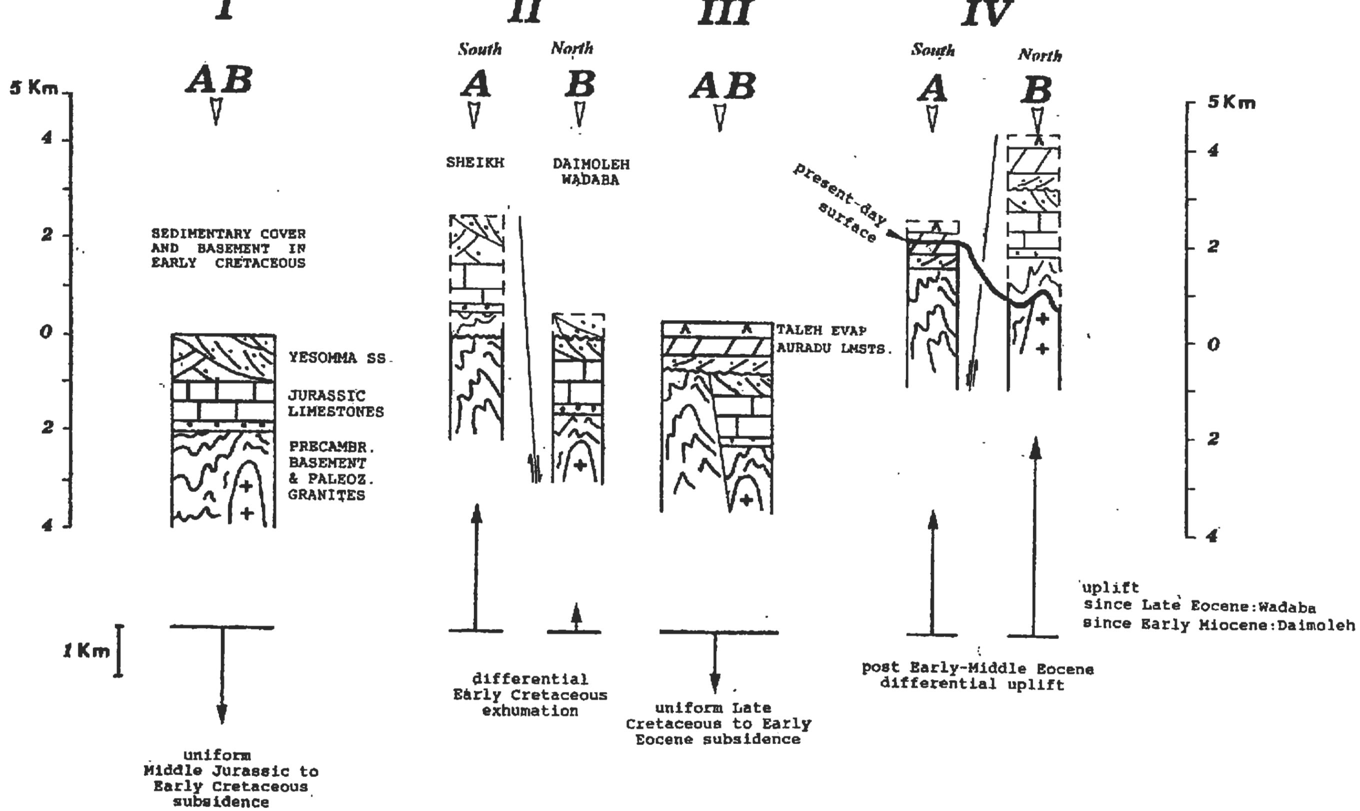

I
AB
II
South
A
North
B
III
AB
IV
South
A
North
B
5 Km
4
2
0
2
4
1 Km
SEDIMENTARY COVER AND BASEMENT IN EARLY CRETACEOUS
YESOMMA SS.
JURASSIC LIMESTONES
PRECAMBR. BASEMENT & PALEOZ. GRANITES
SHEIKH
DAIMOLEH WADABA
TALEH EVAP
AURADU LMSTS.
present-day surface
uniform Middle Jurassic to Early Cretaceous subsidence
differential Early Cretaceous exhumation
uniform Late Cretaceous to Early Eocene subsidence
post Early-Middle Eocene differential uplift
uplift
since Late Eocene:Wadaba
since Early Miocene:Daimoleh

(ABBATE and BRUNI, in press). This induced an intense denudation in the uplifted Sheikh area (A in fig. 2,II), where an erosion down to the basement occurred. On the contrary, on a short distance further north (e.g. Bihendula), the thick Jurassic to Early Cretaceous sedimentary cover was preserved in downfaulted blocks (Fig. 2,II).

Although no clear-cut relations are visible in the field because of post-Eocene faulting and erosion, the present location of the granite bodies would suggest that they belong to the basement of the downfaulted block.

Still during the Early Cretaceous, terrestrial sandstones accumulate and were followed by shallow-marine sediments until Early-Middle Eocene (Fig. 2,III).

The whole sedimentary pile reached such a thickness that the Daimoleh and Wadaba granites were buried beneath the track annealing zone during this phase of renewed subsidence.

Subsequently, the whole Northern Somalia continental margin, including the Sheikh and Daimoleh/Wadaba areas (A and B in Fig. 2,IV), was uplifted in connection with the Gulf of Aden development. For the Sheikh area (A in Fig. 2,IV) an uplift of at least 2,000 m has to be assumed with respect to the sea level, since shallow-water sediments are presently found at elevations close to 2,000 m. An even higher vertical displacement (about 4,000 m) is inferred for the Daimoleh/Wadaba block (B in Fig. 2, IV), which was a horst bounded to the south by the Sheikh plateau (A in Fig. 2, IV) and to the north by the downfaulted Bihendula block. This block was a prominent exception in the structure of the margin characterized by a general stepping down from the edge of the plateau to the coastal lowlands.

The different fission track ages for the Wadaba and Daimoleh granites (Table 1) cannot be explained on the basis of difference in altitude, but rather indicate that each of the two areas behaved differently. The Wadaba granite moved upward across the track accumulation zone toward the end of the Eocene (about 40 Ma), whereas for the Daimoleh this rise was delayed until the Early Miocene (about 20 Ma). It is likely that the two blocks were disconnected by an intervening fault zone.

This reconstructed sequence of events has to be matched with the information obtained from the sedimentary and structural history of the adjacent (to the north) Daban basin (ABBATE et al., 1986).

While the Daimoleh datings agree with an uplift of the basin shoulder testified by remarkable clastic supply at the end of the Oligocene and the beginning of the Miocene, it is more difficult to refer a Wadaba uplift during the Late Eocene to significant clastic deposition in the nearby basin. At this point further datings and analyses would be needed to exclude the possibility that the available dating could be considered as mixed age.

Some inferences about uplift rates can be put forward. Assuming a mean surface temperature of 20°C and a paleogeothermal gradient of 30° C, the 100°C isotherm is met at about 3,000m. Thus, the uplift rate was about 0.15mm/y for the Daimolehs, and half that value for the Wadaba. Rates of 0.1-0.2 mm/yr have been found for the uplift of the Sinai crystalline basement (KOHN and EYAL, 1981).

## CONCLUSIONS

1) Two (Daimoleh Weyn and Daimoleh Yare) out of three Early Paleozoic granites intruded in the Precambrian basement along the Somali continental margin of the Gulf of Aden gave Early Miocene fission track ages. They confirm that at least since then the uplift of the shoulders of the rift was active, as also suggested by the sedimentary and structural evolution of the adjacent Daban basin.

A third dating (Wadaba granite) would indicate an uplift back at the boundary between Middle and Late Eocene. Although this fits with difficulty in the geological history of the region and would need further confirmations, it could be assumed that precocious, possibly local, uplifts occurred in some sectors of the continental margin.

On a more regional scale, the rifting seems to coexist with the uplift.

2) The last track annealing in the apatites occurred in Paleocene/Middle Eocene times when the granites were buried under a cover of at least 3,000 m. Such a thickness was the result of the Tertiary sedimentation above Mesozoic deposits (a thick Bihendula-type succession) and underlying basement. It is worth noting that one must assume a prolongation of the Bihendula complete section as far south as to the granites outcrops in order to provide a sufficiently thick thermal cover.

3) In the general down-stepping structure of the margin from the plateau toward the Gulf of Aden the Wadaba/Daimoleh block was a horst higher than the edge of the nearby plateau.

## REFERENCES

ABBATE E., BRUNI P., FAZZUOLI M. and SAGRI M. (1986). The Gulf of Aden continental margin of Northern Somalia: Tertiary sedimentation, rifting and drifting. Mem. Soc. Geol. It., 31: 427-445.

BIGAZZI G., BONADONNA F.P. and HADLER NETO J.C. (1986). Contribution to statistics in fission tracks counting. Nucl. Tracks, 11: 123-136.

BRIGGS N.D., NAESER C.W. and MAC CULLOCH T. (1980). Thermal history of sedimentary basins by fission track dating. Fission Track Dating Workshop, Pisa, Abstracts, edited by G.Bigazzi, Istituto di Geocronologia e Geochimica Isotopica - CNR, reproduced in Nucl. Tracks, 5: 235-237 (1981).

CARPENA J., (1985). Tectonic interpretation of an inverse gradient of zircon fission track-ages with respect to altitude: alpine thermal history of the Gran Paradiso basement. Contrib. Mineral. Petrol., 92: 413-427.

FERRARA G., TONARINI S., SASSI F.P. and VISONÀ D. (1985). Sull'età del massiccio granitico di Daymoleh (Somalia Settentrionale). Univ. Naz. Somala. Quaderni Geologia Somalia, 8: 233-241.

GLEADOW A.J.W. and DUDDY I.R. (1981). A natural long-term annealing experiment for apatite. Nucl. Tracks, 5: 169-174.

GLEADOW A.J.W., DUDDY I.R., GREEN P.F. and LOVERING J.F. (1986). Confined fission track lengths in apatite: a diagnostic tool for thermal history analysis. Contrib. Mineral. Petrol., 94: 405-415.

HUNT J.A. (1960). Report on the geology of the Berbera - Shikh area, Berbera and Burao district. Somaliland Protect. Geol. Survey Rept., 4: 27 pp.

HURFORD A.J. (1986). Cooling and uplift patterns in the Lepontine Alps, South Central Switzerland and an age of vertical movement on the Insubric fault line. Contrib. Mineral. Petrol., 90: 413- 427.

KOHN B.P. and EYAL M. (1981). History of uplift of the crystalline basement of Sinai and its relation to opening of the Red Sea as revealed by fission track dating of apatites. Earth Planet. Sci. Letters, 52: 129-141.

MASON J.E. (1962). Report on the Geology of the area north of Hargeisa and Laferug. Somaliland Protect. Geol. Survey Rept. 7: 34p.

NAESER C.W. (1979). Fission track dating and geologic annealing of fission tracks. in E. JAEGER and J.C. HUNZIKER, Lecture in Isotope Geology, Springer Verlag, Berlin, 154-169.

NAESER C.W. (1980). The fading of fission tracks in the geologic environment.Data from deep drill-holes. Fission Track Dating Workshop, Pisa, Abstracts, edited by G. BIGAZZI, Istituto di Geocronologia e Geochimica Isotopica - CNR, reproduced in Nucl. Tracks, 5, 248-250 (1981).

NAESER C.W. and FAUL H. (1969). Fission track annealing in apatite and sphene. J. Geophys. Res., 74: 705-710.

NAESER C.W. and FORBES R.B. (1976). Variation of fission-track ages with depth in two deep drill holes. EOS Trans. AGU, 57: 1-35.

NAGPAUL K.K., MEHTA P.P. and GUPTA M.L. (1974). Annealing studies on radiation damage in biotite, apatite and sphene and corrections to fission track ages. Pure and Applied Geophysics, 112: 131-139.

POUPEAU G. (1981). Precision, Accuracy and Meaning of fission track Ages. Proc. Indian Acad. Sci., Earth Planet. Sci. Lett. PL, 403-406.

SNELLING N.J. (1967). Age determination results. in GREENWOOD J.E. and BLEACKLEY C. (eds.) Geology of the Arabian Peninsula, Aden Protectorate. U.S.Geol.Survey Prof. Paper 560-C, 693-695.

VISONÀ D., ABDULLAHI H.M., HAWA H.H., IBRAHIM H.A. and SAID A.A. (1984). Nuovi dati di campagna sul basamento cristallino della Somalia settentrionale (Escursione settembre-novembre 1983) Univ Naz. Somala. Quaderni Geologia Somalia, 7: 273-293.

WAGNER G.A. (1968). Fission Track Dating of Apatites. Earth Planet.. Sci. Lett. 4: 411-415.

WAGNER G.A. and REIMER G.M. (1972). Fission tracks tectonics: the tectonic interpretation of fission track apatite ages. Earth Planet. Sci. Lett., 14: 263-268.

WAGNER G.A., REIMER G.M. and JAEGER E., (1977). Cooling ages derived by apatite fission track, mica Rb/Sr and K/Ar dating: the uplift and cooling history of the Central Alps. Mem. Ist. Geol. Miner. Univ. Padova, 30: 27 pp.
ZEITLER P., TAHIR KHELI RAK, NAESER C.W. and JOHNSON N.M. (1982). Unroofing history of a suture zone in the Himalaya of Pakistan by means of fission track annealing ages. Earth Planet. Sc. Lett. 57: 227-240.

*Final editing, January 1990*

From *Geology and mineral resources of Somalia and surrounding regions*, Ist. Agron. Oltremare, Firenze, Relaz. e Monogr. 113, 379-388, 1993.

# TECTONIC TRANSPRESSION IN THE GEDO REGION (SOUTHERN SOMALIA)

ALI KASSIM MOHAMED *, L. CARMIGNANI ** and P. FANTOZZI **

* Department of Geology, National Somali University, P.O. Box 1081, Mogadishu, Somalia.
Present address: Dipartimento di Scienze della Terra, Università di Siena, Via delle Cerchia 3, 53100 Siena, Italy.

** Dipartimento di Scienze della Terra, Università di Siena, Via delle Cerchia 3, 3100 Siena, Italy.

## ABSTRACT

The Gedo Region (SW Somalia) is crossed by two parallel deformed belts 2-5 km wide and more than 100 km long, extending from Luuq to Kenya. Detailed field mapping shows that each belt contains a pattern of folds and faults similar to those occurring in a right wrench zone with a transpression component.

The main elements supporting this interpretation are:

- a deformation limited to an elongated belt (wrench zone);
- a series of "en échelon" folds inclined at a low angle to the wrench zone;
- synthetic faults inclined at a low angle to the wrench zone but in the opposite direction from the folds.

In particular, the elements supporting the existence of a transpression component are:

- presence of evident anticlines parallel to the synthetic-slip faults (positive flower structures);
- absence of antithetic strike-slip faults.

Geophysical surveys carried out and petroleum wells drilled in the area suggest that the two wrench zones have reactivated the marginal faults of the pre-Jurassic graben (Luuq-Mandera Basin).

## GEOLOGICAL SETTING

Two main sedimentary basins may be recognized in Southern Somalia (Fig. 1): the NE-SW-trending Mesozoic-Tertiary Somali Coastal Basin, and the NNE-SSW-trending Mesozoic Luuq-Mandera Basin. Both are separated by the so-called "Bur Region", a wide elliptical area where the basement rises to the surface.

The central part of the Luuq-Mandera Basin outcrops in the Gedo Region, and is bounded to the SE by the structural high of the Bur Region and to the west by the crystalline basement of NE Kenya. In the axial zone of the basin, an oil exploration borehole found 4,400 m of sedimentary Cretaceous to Triassic rocks without reaching the basement and also a thick detritic and evaporitic succession under the mainly carbonatic formations (BURMAH OIL COMPANY, 1973; BELTRANDI and PYRE, 1975). This is an important subsiding elongated area which, at least at the beginning of the Mesozoic, was invaded by the sea during the dismembering of Gondwana.

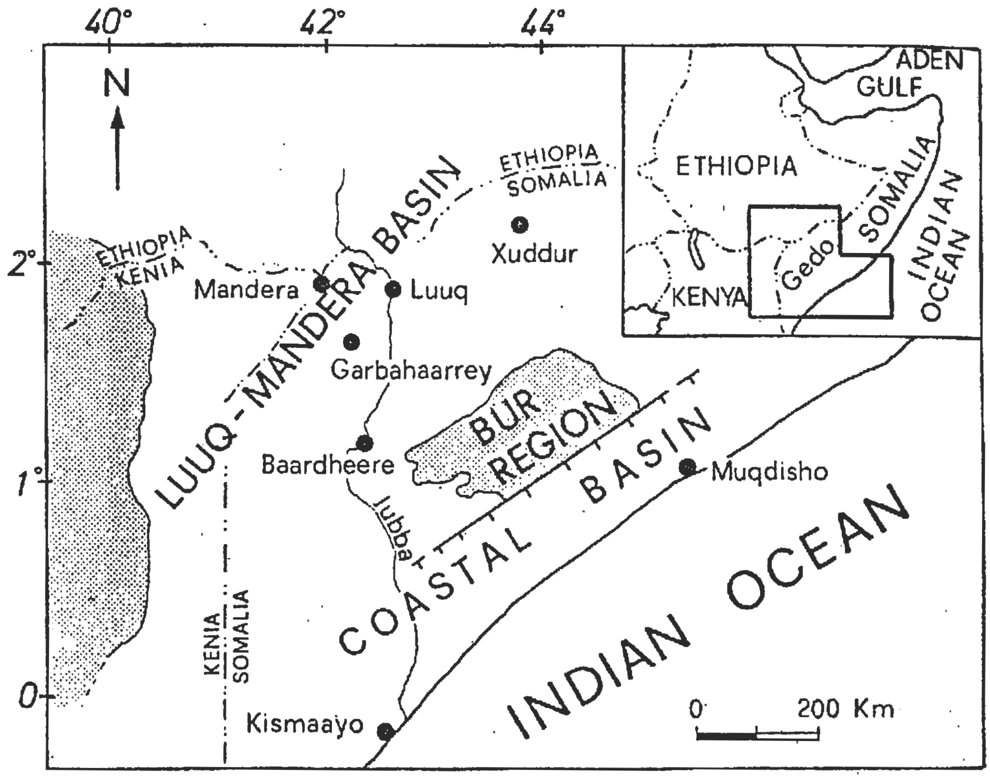


Fig. 1 - Location map.

The Luuq-Mandera Basin has been described by many authors (BARBIERI, 1968, 1970; BELTRANDI and PYRE, 1975; CANUTI et al., 1979; ANGELUCCI et al., 1981; CARMIGNANI et al., 1983), to whom we refer readers for a more complete discussion of its sedimentary evolution.

In the Gedo Region only the upper part of the succession of the Luuq-Mandera Basin outcrops. From the oldest to the most recent, the outcropping formations are:

- Anole (Caanole) Formation: consisting mainly of marl and marly limestone with some layers of fossiliferous calcilutite and calcareous sandstone. Pelecypods, gasteropods, brachiopods, ammonites, belemnites and foraminifers indicate a Late

Callovian to Late Oxfordian age. The formation may mainly be referred to deep shelf conditions (open sea phase of the sedimentary cycle).

- Uegit (Waajid) Formation: mainly consisting of oolitic calcarenite, bioclastic calcilutite and oncoidal calcilutite, ranging in thickness from 600 to 650 m. Fossils are pelecypods, gasteropods, brachiopods, echinoderms, corals, calcareous algae and foraminifers, ranging in age from Late Oxfordian-Kimmeridgian to Early Portlandian. The main depositional environment may be referred to a restricted platform and more rarely to open platform or even shallow shelf.
- Garbaharre (Garbahaarrey) Formation: this formation, sub-divided by BARBIERI (1968) into two members, the lower Busul (Bossul) and upper Mao (Macow) members, is closely connected with the regressive phase of the Early Cretaceous. The lower member mainly consists of calcarenite, calcilutite and quartzose sandstone, and the upper one of gypsum, anhydrite, shale, calcarenite and sandstone. The thickness of the whole formation is about 600 m.

The Mao member makes a lateral transition towards the SE, to the so-called "Ambar Sandstone".

The region was no longer submerged by the sea after the Cretaceous regression. More recent deposits (Tertiary?) are limited to some outcrops of lacustrine sandy clays (Faanweyn Formation) and fluvial deposits (Kuuredka Formation) covered by basalt flows (ABDIRAHIM et al., 1987, ALI KASSIM M. et al., 1987). These formations are of uncertain age, but are in any case clearly discordant on the underlying Mesozoic series.

Overall, the structure of the region is very simple: north-west of the Bur Region the sedimentary cover dips gently NW for more than 100 km, as far as the Luuq-Garbahaarrey areas. Further west, the stratification dips SE and E, and then the Precambrian basement outcrops again beyond the frontier with Kenya. The main structure of the Jubba valley upstream from Baardheere is therefore a wide syncline between two crystalline outcrops. Its core is made up of the great Cretaceous formations outcropping between Garbahaarrey and Luuq (Tomalo Syncline).

Aereomagnetic surveys have shown that the axis of the syncline approximately coincides with the axial zone of the Luuq-Mandera Basin, where the sedimentary cover is more than 3,000 m thick (BELTRANDI and PYRE, 1975).

This simple regional structure is complicated by two NE-SW-trending highly deformed belts about 10 km wide, extending both NW and SE of the Tomalo Syncline and including various systems of faults and folds, sometimes with steeply dipping limbs (Fig. 2).

The north-east or Sengif Belt is essentially composed of a long anticline bounded on both sides by two faults. Starting from the Mandera area, it extends into Kenya and is about 110 km long. The south-west or Garbahaarrey Belt is more than 130 km long. The belts cut across an enormous practically undeformed area and are the most interesting tectonic structures of the region.

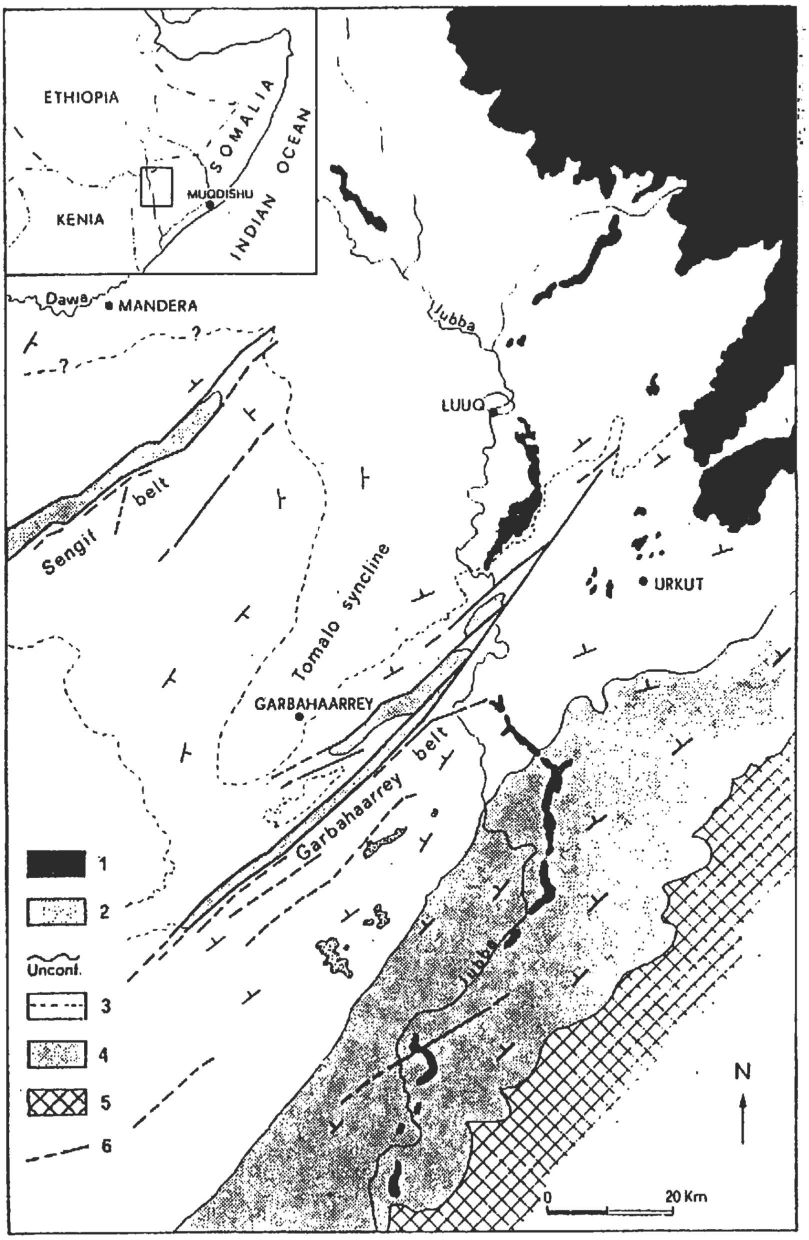


Fig. 2 - Geological sketch-map of Gedo Region. 1: Basalt; 2: Faanweyn Formation; 3: Busul Member/ Mao Member and Ambar Sandstone; 4: Uegit Formation; 5: Anole Formation; 6: Fault.

GARBAHAARREY BELT

BELTRANDI and PYRE (1975) made an initial attempt at interpreting the two belts of the Gedo Region. In these authors' opinion, the belts are essentially the result of movements along a system of normal faults. According to this hypothesis the various anticlines and synclines inside the belts correspond to small horsts and grabens. Their uplift is attributed to the flow of pre-Jurassic evaporites from the axial zone of the basin towards its periphery during the development of the Tomalo Syncline.

A detailed geological map of the Gedo Region has been completed in the last few years. Summarized in Fig. 3, this map shows that the Garbahaarrey Belt has a relatively complex structure in which various systems of faults and folds may be recognized. The relations between these systems indicate that the structural setting of the belt is due to wrenching tectonics with a transpression component. The basic structural patterns of wrenching are simple and well-documented in many regions. The main elements of the basic wrench pattern are:

- deformation, limited to a narrow belt: the "wrench zone";
- the "main wrench fault", parallel or sub-parallel to the wrench zone;
- "en échelon" folds, inclined at low angles to the wrench zone;
- a "conjugated strike-slip fault", including a "synthetic fault" inclined at a low angle to the wrench zone but in the opposite direction from the "en échelon" folds and "antithetic faults", nearly perpendicular to the wrench zone.

A close examination of the structural map (Fig. 3) shows that the Garbahaarrey Belt contains many elements of a right-slip wrench zone, i.e.:

- the so-called "Garbahaarrey Fault", about 100 km long and parallel to the deformed belt, may represent the main wrench fault;
- there is a set of "en échelon" folds in the north-east part of the belt between Luuq and Urkut;
- synthetic strike-slip faults with orientation compatible with a right-slip wrench zone are well developed all along the belt.

The Garbahaarrey Belt shows many features of a right-slip wrench zone, but some very obvious structural elements cannot be interpreted as due to a simple movement of the parallel wrench type. These elements are:

- the presence of an important system of folds parallel to the synthetic faults;
- systematic and sharp changes in direction of the axes of the latter system of folds;
- the almost complete absence of antithetic strike-slip faults;
- the angle between the strike of the wrench zone and the fold axis of the set of "en échelon" folds is less than 30°;
- far smaller than that predicted by the theory for a true simple shear.

These structural characteristics indicate that the right-hand movement was accompanied by shortening normal to the wrench zone (Fig. 3).

In transpression experiments with clay models, the angle between "en échelon" fold axes and wrench faults is approximately 30° (WILSON et al., 1973); SANDERSON

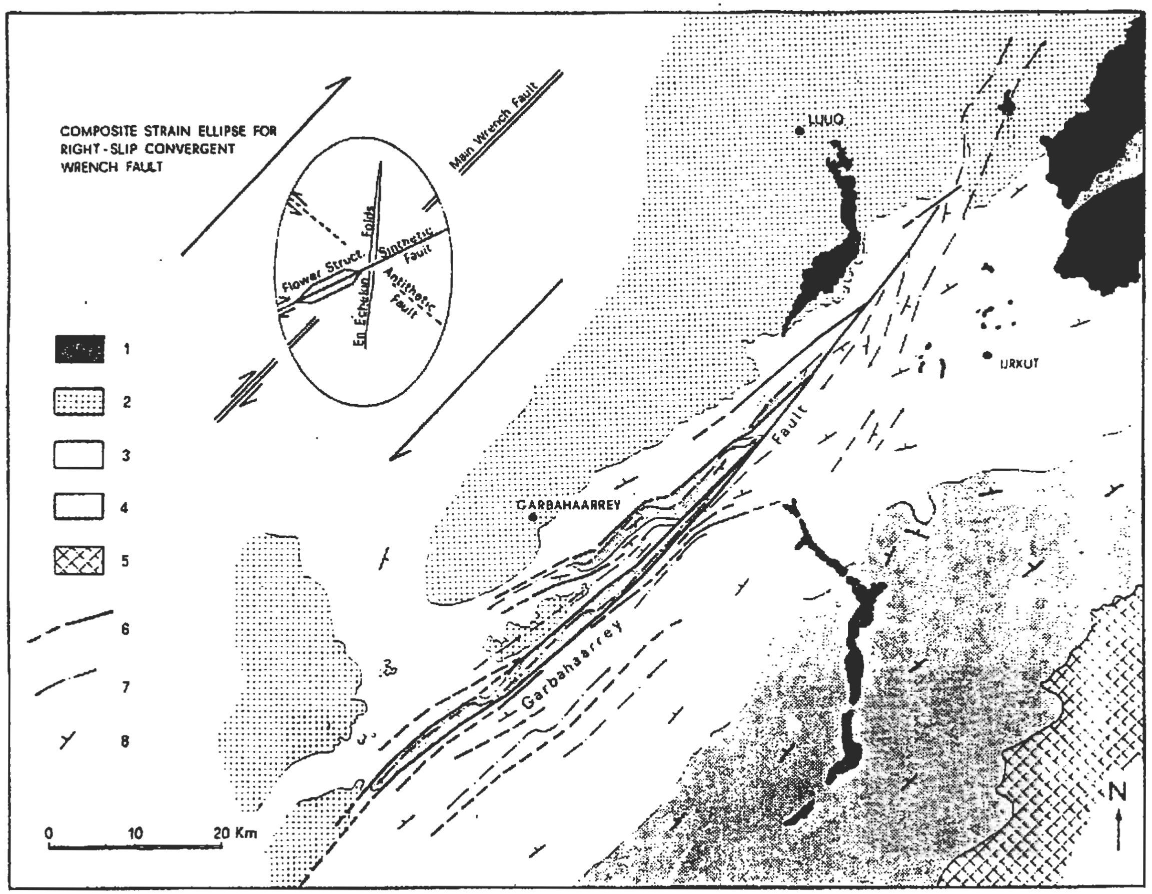


Fig. 3 - Geological map of Garbahaarrey belt and composite strain ellipse for right-slip convergent wrench fault. 1: Basalt; 2: Mao Member and Ambar Sandstone; 3: Busul Member; 4: Uegit Formation; 5: Anole Formation; 6: Faults; 7: Fold axis showing direction of plunge; 8: Bedding attitude.

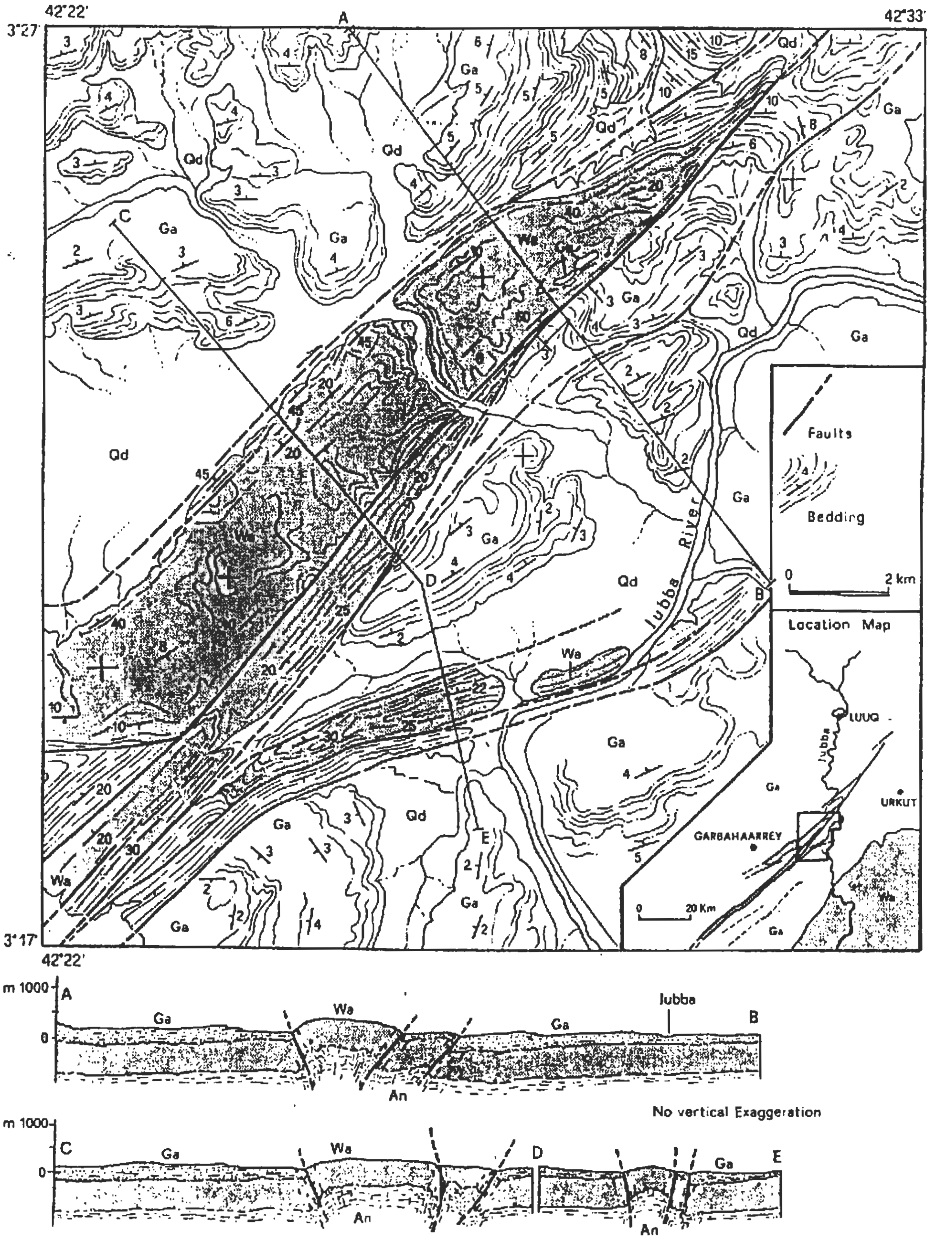


Fig. 4 - Structure of Garbahaarrey belt east of Garbahaarrey. Qd: Quaternary deposits; Ga : Garbahaarrey Formation; Wa: Uegit Formation; An: Anole Formation.

and MARCHINI (1984) showed that a wrench shear zone accompanied by horizontal shortening across the shear plane allows angles far smaller than 45° between "en échelon" fold axes and shear zones.

Convergent wrenching, on whatever scale, tends to enhance compressive structures, i.e., folds and synthetic strike-slip faults. In their clay model of a convergent wrench fault, WILCOX et al. (1973) reproduced a structure which was generally similar to that of the Garbahaarrey Belt. In an early stage of movement of this experiment, "en échelon" folds were well developed and a few synthetic fractures formed. At a later stage, the "en echelon" folds were offset along the synthetic faults and a few antithetic faults also formed, although their importance in the deformation was minimal. The model also revealed a complex thrusting of the wedges squeezed off the wrench zone by convergence.

Between Luuq and Urkut an "en échelon" anticline is cut and displaced by a synthetic fault (Fig. 3), as in the above experiment.

However, the structures which best reveal the compressive component of the Garbahaarrey wrench zone is the system of folds parallel to the synthetic faults which caused the limestone of the Uegit Formation to outcrop (Figs. 2, 3).

Anticlines bordered by a series of convex upward reversed or thrust faults have been shown in many wrench zones (SYLVESTER et al., 1976) and have also been obtained in convergent wrench models (WILCOX et al., 1973). The cross-sectional appearance of the overall structure has led to the name "flower structure".

The attitude of the faults measured in some localities appears on the large-scale map, and the general geological setting of the Garbahaarrey Belt indicates that the largest anticlines are flower structures (Fig. 4). The sharp and systematic variations of axial direction characterizing these folds in both the Garbahaarrey and Sengif Belts also occur in convergent wrench models (see fig. 13 B in WILCOX et al., 1973). These torsions are probably features acquired in the late phase of wrench zone evolution: their form and asymmetry recall drag folds which, due to the right-hand movement, folded already existing folds and faults.

An equally detailed geological map of the Sengif Belt is not available. However, partly on the basis of Landsat images and some surveys, we believe that it too has a structure very similar to that of the Garbahaarrey Belt. The two belts are similar in size and equal in direction; the Sengif Belt also contains faults and folds which show systematic variations in axial direction which are identical to those of the Garbahaarrey Belt.

## CONCLUSIONS

The Garbahaarrey and Sengif Belts are two convergent right wrench zones. Although the age of movement is uncertain, it is definitely later than the Early Cretaceous: the Mao member is clearly folded in the north-eastern extremities of both belts. Instead, no upper chronological limit may be set, because the ages of the discordant sedimentary Faanweyn and Kuuredka Formations and the radiometric ages of the Jubba valley basalts are still uncertain (ALI KASSIM M. et al., 1987; ABDIRAHIM M. et al., 1987).

Geophysical soundings (BELTRANDI and PYRE, 1975) and Well Hol 1 (BURMAH OIL COMPANY, 1973) have shown the existence of a NE-SW-trending Triassic basin composing the oldest part of the Luuq-Mandera Basin, the axis of which runs between the two deformed belts. This coincidence between the location and orientation of the Triassic basin with the belts deformed after the Early Cretaceous suggests that these different structures are related. Old normal Triassic faults (the two marginal faults of the basin?) may have been reactivated as wrench faults after the Early Cretaceous.

It is difficult to place these movements in a larger regional context, mainly because of their uncertain age. Moreover, right-hand movements along pre-existing NE-SW-trending discontinuities of the basement may have been caused by very different shortening directions on a regional scale. The facts that the two belts are probably Tertiary in age and their relative nearness to the East African Rift lead us to relate them to these large structures. It seems improbable that these structures are linked to the formation of the SE Somali continental margin. According to BOSELLINI (1989), sea-floor spreading between Africa and the Madagascar-India-Seychelles block began in Callovian-Early Oxfordian times and is thus much older than the flower structures of the Luuq-Mandera Basin.

## ACKNOWLEDGMENTS

Research carried out with grants from the Italian Ministero degli Affari Esteri, Dipartimento per la Cooperazione allo Sviluppo.

## REFERENCES

ABDIRAHIM M.M., ALI KASSIM M., CARMIGNANI L. and COLTORTI M. (This volume). The geomorphological evolution of the upper Jubba Valley in Southern Somalia.

ALI KASSIM M., BELLIENI G., CARMIGNANI L., FANTOZZI P., FERRARA G., JUSTIN VISENTIN E., TONARINI S. and ZANETTIN B. (This volume). Flood basalts of the Gedo Region (Southern Somalia): geology, petrology and isotopic geochemistry.

ANGELUCCI A., BARBIERI F., MAXAMED C.M., CARUUSH M.C. and PICCOLI G. (1981). Preliminary report on the Jurassic sequence in the Gedo and Bay Regions (South-western Somalia). Univ. Naz. Somala, Quad. Geol. Somalia, 4: 115-154.

BARBIERI F. (1968). Jurassic microfacies in Western Somalia. Riv. It. Paleont. Stratigr., 74: 805-826.

BARBIERI F. (1970). La stratigraphie du Mésozoique dans la région du Giuba en Somalie. Actes IV Coll. Africain Micropalaéont., Abidjan, 45-50, Nice.

BELTRANDI M.D. and PYRE A. (1975). Geologic evolution of South-west Somalia. In: Sedimentary Basins of African Coasts. Part 2: South and East Coasts (Edited by BLANT G.), Ass. Serv. Geol., 159-178.

BOSELLINI A. (1989). The continental margins of Somalia: their structural evolution and sequence stratigraphy. Mem. Sci. Geol. Padova, 41: 373-458.

BURMAH OIL CO. (1973). Hol. No. 1 - Completion Report. Burmah Oil Somalia Ltd., Muqdishu, 71 pp.

CANUTI P., FAZZUOLI M. and TACCONI P. (1979). Geological outlines between Juba and Webi Shebeli rivers (South-western Somalia). Geodynamic Evolution of the Afro-Arabian Rift System. Acc. Naz. Lincei and C.N.R., 120 pp.

CARMIGNANI L., ALI KASSIM M. and FANTOZZI P. (1983). Nota preliminare sul rilevamento della regione di Gedo (alta valle del Giuba, Somalia meridionale). Univ. Naz. Somala, Quad. Geol. Somalia, 6: 85-109.

SANDERSON D.J. and MARCHINI W.R.D. (1984). Transpression. J. Struct. Geol., 6: 449-458.

SYLVESTER A.G. and SMITH R.R. (1976). Tectonic transpression and basement controlled deformation in the San Andreas Fault Zone, Salton Trough, California. A.A.P.G., 60: 2081-2102.

WILCOX R.E., HARDING T.P. and SEELY D.R. (1973). Basic wrench tectonics. A.A.P.G., 57: 74-96.

*Final editing, January 1990*

From *Geology and mineral resources of Somalia and surrounding regions*, Ist. Agron. Oltremare, Firenze, Relaz. e Monogr. **113**, 671-686, 1993.

# A GEOLOGICAL MODEL FOR GROUND WATER RESEARCH IN THE SHABEELLE VALLEY (SOMALIA)

E. Sommavilla *, G. Masè *, S. Marchesi **, Ali Kassim ***, Hussen Salad *** and Ibrahim Mohamed Farah***

* Dipartimento di Scienze Geologiche e Paleontologiche, Università di Ferrara, Corso Ercole I d' Este 32, 44100 Ferrara, Italy.

** I.G.T., Trento.

***Department of Geology, Somali National University, P.O. Box 1081, Mogadishu, Somalia.

ABSTRACT

The authors were asked by U.N.H.C.R. to assess the possible presence, quality and potentiality of ground water in an area where a refugee settlement was being planned.

First of all, a geological investigation was carried out, aimed to define a geological model for the region. For this purpose, satellite images (MMS, Bands 5 and 7) and "False Colour Composites" (from Bands 4, 5 and 7) proved very useful, along with photogeological and field survey. In addition, the main lithological and geomorphological units (paleodunal sandy soils, paleochannels, loamy flood-plains etc.) were defined as a basis for the land-use study.

The model led to the important discovery of an ancient hydrogeological system, mainly consisting of buried paleochannels with a NW-SE direction, originating in the "Buur inselbergs region" and dating back to a time when the Shabeelle paleoriver did not the studied area, but flowed into Indian Ocean much further to the north. The upstream reaches of this paleodrainage still coincide partly with the present hydrographic network. Hence the paleochannels are possible aquifers recharged by the Buur drainage.

The paleochannels are still visible, in the satellite images, upstream of the area selected for the settlement. In this area, they are buried under the alluvium carried by the present Shabeelle after its diversion toward SE, and have been detected, localized and measured thanks to geophysical methods.

Three pilot wells have been drilled in the middle of the paleochannels.

The data collected from the wells and the petrographycal and mineralogical study of the samples confirmed the geological model and the foreseen location of the sands and gravel source-area in the Buur region: two catchment areas (3,500 km² and 3,800 km² wide) which recharge two different aquifers in the project area.

The third borehole has been drilled in the second aquifer (which is confined with static level at 4.5 m below ground) and turned out to be a production well with fresh water probably sufficient for the whole settlement.

The surprisingly good result of this study is due to the adopted method which supplied a geological model, reliable for a vast region where, according to previous researches, good water was extremely rare and available only by chance.

available water are concerned. For example, in Hiiraan Region (Central Somalia), the Shabeelle river, ponds and hygienically unacceptable wells are the only water sources, with very few exceptions: three or four major centres, supplied by means of motor pumps (of difficult maintenance and with very low "life expectancy") and only one village with a properly covered hand-dug well, equipped with a hand pump.

The wells frequently encounter saline water, due to the abundance of evaporitic rocks (Main Gypsum and Ferfer Formations) and to the salts dissolved by the rivers from these rocks and spread in the alluvial plains by the evaporating flood waters. In Southern Somalia, the situation is even more dramatic.

The so far commonly pursued solution was to drill. A huge number of boreholes were drilled, with enormous losses, due to the scarcity of fresh deep water and sometimes to insufficient previous geological studies. And even the few successful wells did not give adequate results, because of maintenance difficulties.

This is way the authors decided to study the shallow and surface waters, which obviously are economically and technologically more accessible. We faced also the technological problem of their exploitation by testing some low technology systems, like infiltration trenches and galleries, subsurface dams, sun powered ultraviolet purification plants etc.

Large areas of Central and Southern Somalia were first studied from the geomorphological point of view by means of satellite images. Then a field survey was carried out, and numerous trenches were dug the hydrogeological data and the technical exploitation tests will be discussed in another paper. We had also the opportunity to gain first-hand stratigraphic informations on the Shabeelle valley alluvium by assisting several drilling operations. It should be printed out that, of the lithologic logs available from the previous drilled wells, very few can be used for a geological study, due to mistakes or omissions. E.g., continental duricrusts (caliche) are often defined as calcareous gravel or limestone (implying "marine"), and varval lacustrine deposits are sometimes mistaken for marine marls; gravel and sand are usually recorded without any compositional or textural indication.

The obtained data led to outline a possible morphological history of the Shabeelle Valley and of its surface and sub-surface waters. It is just a rough hypothesis, but worthy of being verified. If confirmed and completed by further observations, it could become an important geomorphological model for the hydrogeological research.

## NEOTECTONIC EVENTS

First of all, some evidence of two major recent tectonic movements, accountable for morphological changes, was recognized (Fig. 1).

Fig. 1 - Reactivated tectonic features (Marda Fault Zone and Jalalaqsi Fault) and localities mentioned in the text.

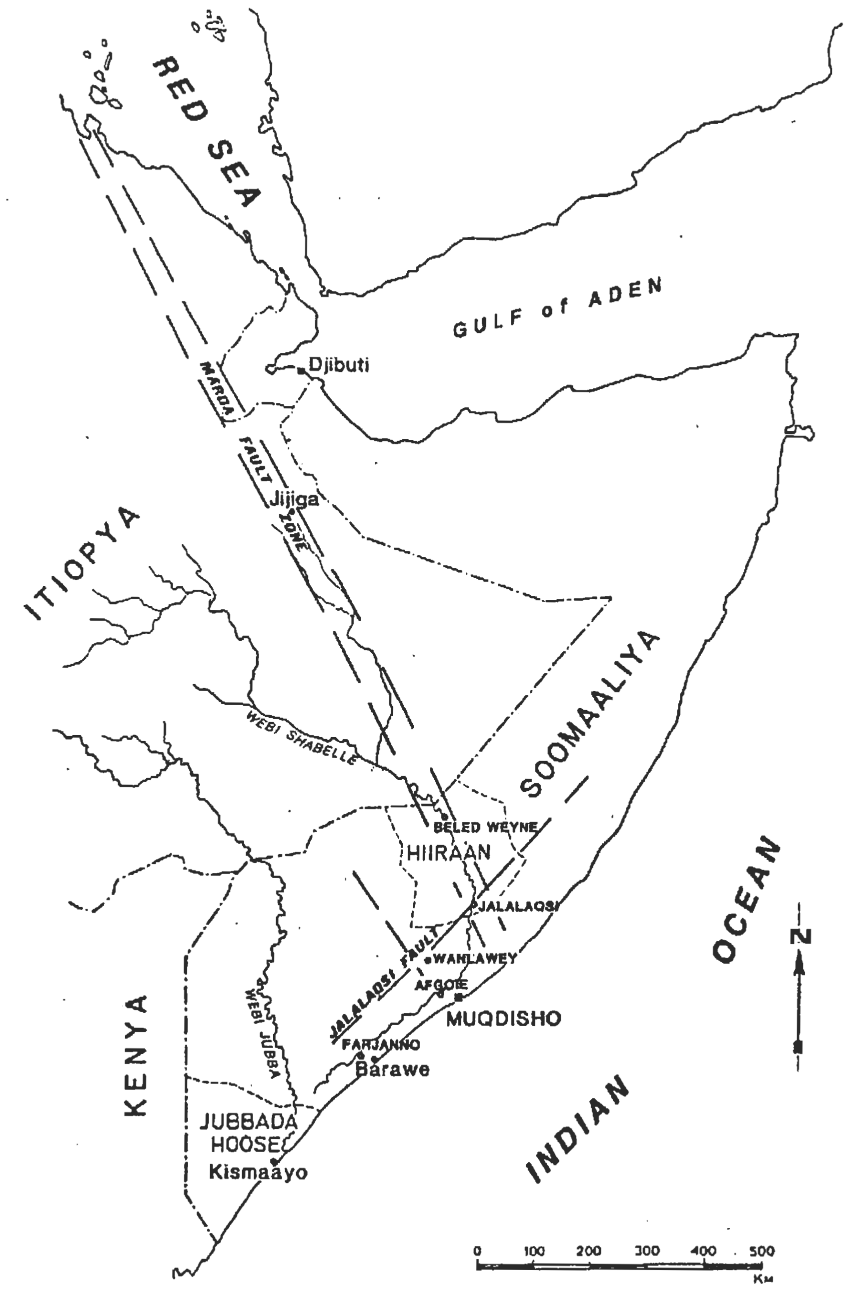
RED SEA
GULF of ADEN
Djibuti
MARDA FAULT ZONE
Jijiga
ITIOPYA
WEBI SHABELLE
SOOMAALIYA
BELED WEYNE
HIIRAAN
JALALAQSI
WANLAWEY
AFGOIE
JALALAQSI FAULT
MUQDISHO
FARJANNO
Barawe
WEBI JUBBA
KENYA
JUBBADA HOOSE
Kismaayo
INDIAN
OCEAN
N
0 100 200 300 400 500
KM

NNW-SSE FAULT SYSTEM

Lineations of a NNW-SSE oriented structure are clearly shown in the satellite images between the Ethiopia border (north of Beled Weyne) and Jalalaqsi. These faults correspond to the south-eastern part of the Marda Range Graben, which extends toward NNW, through Jijigga, reaching the western coast of the Red Sea (BLACK et al., 1974; PURCELL, 1976). This structure is about 1500 Km long and dates back to the Precambrian. In Somalia, records are known of late Mesozoic activity.

The satellite images lineations are clearly visible even where recent detritus covers the bed-rock. Therefore, very recent movements must have taken place. Two major lines are visible: one on the western side of the valley, about 45 Km from the river, and the other 20 Km to the east.

The NNW-SSE graben is obviously responsible, in the Hiiraan Region, for the main drainage. In addition to the present Shabeelle Valley, a paleo-valley is clearly visible from the satellite images along the western lineation. Thick coarse alluvial beds occur at Ceel Cali, a village located in the middle of this paleo-valley, and no present drainage could be accountable for such a deposit. It should be noted that these gravels and sands are probably the only aquifers of acceptable quality of the whole western portion of the Hiiraan Region, which is hydrogeologically very negative, as nearly all the outcropping rocks are saline.

The eastern line, which passes about 20 Km from the Shabeelle River, is accountable for a morphologic shelf and for some drainage anomalies, such as the disappearing hydrographic network, which have been observed by FRANCESCHETTI and ABDULKADIR S. DORRE (1983).

The following morphogenetic events may be explained if a neotectonic movement is hypothesized along the NNW-SSE lines:

- a relief rejuvenation which recently took place on the left side of the Shabeelle Valley, marked by coarse alluvial deposits lying upon clayey paleo-soils; alluvial fans have been formed by gravel and sand where the torrential basins face the river plain;
- another rejuvenation that occurred more recently in the same zone, marked by the fact that the present torrential beds are cut into the fans, at the depth of about two metres; probably due to the same event, the major fans seem to have been cut off at their lower border, as it may be inferred from the presence of a small escarpment.

NE-SW FAULT SYSTEM

Recent tectonic movements can be hypothesized in the eastern (Indian) coastal belt. As will be said later, there is evidence of two opposite movements: the uplifting of coastal blocks and the sinking of an interior zone. These two events may easily be accepted as a consequence of a single tilting movement along a rotational fault. The tilting produced a semi-graben structure (see SOMMAVILLA et al., 1988). The Jalalaqsi Fault, which is the major distensive structure connected to the separation of

Madagascar and India from Eastern Africa, could have acted as the hinge of the movement. Obviously, a rejuvenation should be hypothesized, as the Jalalaqsi tectonism is of Mesozoic-Early Tertiary age.

The following data support the hypothesis of this neotectonic event:

- the occurrence of marine or transitional semi-lithified sediments, outcropping on the coastal ridge at heights of several tens of metres above the sea level (see Geological Map in ANGELUCCI et al., 1983); these findings can not be mistaken with the result of a marine eustatic event, as some author has tried to assert, because, apart from general considerations, the sea would have invaded, in very recent times, the whole Shabeelle plain, where no marine sediments are present;
- some NE-SW lineaments, clearly visible from the satellite images on the recent alluvial and proluvial sediments, along a stripe between Jalalaqsi, Wanlaweyn and the southern flank of the Buur inselbergs; such a feature may only be explained as due to neotectonic movements, since the main tectonic activity came to an end tens of millions of years ago, and the faults are buried under more than one thousand metres of post-tectonic sediments; it is worth noting that occurrence of differential compaction, which may sometimes account for a surface appearance of buried synsedimentary faults, seems to be very unlikely, as hundreds of metres of coarse sediments (gravel and sands of the Merka Fm.) cover both sides of the fault;
- the very rapid pluristadial withdrawal of the sea, marked by a series of paleo-dunal ridges stretching parallel to the coast on a 30 Km wide belt and showing an increasing age from the coast toward the interior (they are more and more weathered and eroded);
- the dissection of the alluvial deposits of the middle Shabeelle Valley, effected by the river itself, which today runs at a depth of 6-7 m below the alluvial plain surface (while it is pensile in its lower course); only a downstream lowering of the ground level may account for this feature, since only graben tectonics are possible upstream, due to the NNW-SSE fault system;
- the evidence, obtained from the wells, of subsidence events that recently took place downstream from the Jalalaqsi Fault; in fact the stratigraphic logs show, in this area, clayey deposits (partly lacustrine), down to a depth of about 100 m.

The data in favour of the tilting (rotational) movement with the hinge on the Jalalaqsi Fault are as follows:

- the thickness of the clayey deposits, and consequently the depth of the graben, apparently increases from the coast toward the Jalalaqsi Fault, from about 50 m at Afgoye and Lambar Konton to 90-100 at Wanlaweyn: the top of the older sandy and gravelly alluvium lying under the clayey deposits, is encountered at a depth of about 100 m in the wells located 80 Km from the coast, while at a distance of 25 Km, it is found at 50 m; as these sediments came from NW (see SOMMAVILLA et al., 1988), these findings can not be explained without postulating a neotectonic movement, dated between the gravelly/sandy and the clayey deposits;
- the oldest courses of the NE-SW drainage are clearly shown, by the satellite images,

in the Wanlaweyn area, just southeast of the Jalalaqsi Fault, where, therefore, the first subsidence must have taken place; the diverted Shabeelle gradually migrated toward its present position after having filled the semi-graben.

## LANDSCAPE EVOLUTION

In conclusion, the main morphogenetic events and corresponding landscape evolution can be reconstructed, for Central Somalia. as follows:

1. For a long time, probably starting in the Late Miocene, the SE dipping morphology and the NW-SE faults system caused a southeastward oriented drainage network, with the exception of the Shabeelle course, which was conditioned by the old, but still active, NNW-SSE oriented Marda Range graben. The regime was higher than the present one, as in the wells, under recent clayey and silty deposits, paleo-channels are encountered with coarse sand and gravel. Southeastward oriented rivers were also present in the area where, later, the present Lower Shabeelle plain formed, as shown by SOMMAVILLA et al.(1988) for the Farjanno zone, in which extraordinary good aquifers were detected in the paleo-channels.
2. As a consequence of the rotational, neotectonic movement, hinged in the rejuvenated Jalalaqsi Fault, a marine regression took place in three or four stages, leaving as many coastal rows of dunes, which appear older and older from the shore to the interior. The Shabeelle River was gradually forced to divert from its normal (see BOSELLINI, 1989), tectonically accountable, southeastward course, to the present direction toward south-west. The diversion of the Shabeelle river is in fact much more easily explained by a coastal up-lifting, rather than by the usually invoked damming effect of the coastal dunes, which are themselves a consequence of the tectonic rising.
3. Due to the same neotectonic event, subsidence, with deposition of clayey and lacustrine sediments, occurred in a zone close to the Jalalaqsi Fault. The sedimentation rate was higher near the tectonic line and decreased southeastward; so a prism of fine sediments was formed with a thickness of about 100 m in its north-western side and vanishing to the SE.
4. Over-alluvial deposition took place in the Shabeelle Valley, upstream of the Jalalaqsi Fault, with thickness of some tens of metres. Either NE-SW or NNW-SSE movements can account for this morphological event, and also a combination of both of them.
5. The over-alluvial deposits have been later dissected by the Shabeelle River to a maximum depth of 6-7 m. This was likely due to a new downstream lowering of the ground level, since uplifting movements are not to be expected in a graben structure.
6. A sudden change of the stream energy occurred very recently on the eastern slope of the Shabeelle Valley. Gravelly fans formed upon a clayey paleo-soil where the lateral torrents face the Shabeelle plain. This event could correspond to the Holocene Pan-African humid phase (see BELLUOMINI et al., 1980); but a relief rejuvenation,

caused by a remobilization of the eastern NNW-SSE line, can better account for the quick and sharp change.

7. Finally a dissection of the gravelly alluvium took place, as the present beds are cut into the fans to a depth of about 2 m. Therefore, a last movement should be hypothesized, causing a lowering on the valley bottom.

REFERENCES

ANGELUCCI A., ABDULKADIR MOHAMED M. and ROBBA E. (1983). A preliminary Report on the quaternary Sequence in the coastal Area of Benadir (Central Somalia). Univ. Naz. Somala. Quaderni di Geologia della Somalia, 7.

BELLUOMINI G., ESU D., MANFRA L. and MATTEUCCI R. (1980). Gasteropodi dulcicoli e terrestri nell' isola di Dahlad Kebir. Testimonianze di una fase umida olocenica nelle Isole Dahlak, Mar Rosso. Boll. Malac.,16, 11-12: 369-390.

BOSELLINI A. (1989). The continental Margins of East Africa. Their structural Evolution and stratigraphical Sequences. Mem. Sci. Geol. Padova, 41: 373-458.

BLACK R., MORTON W.H. and TSEGAYE HAILU (1974). Early Structures around the Afar Triple Junction. Nature, 248: 496-497.

CANUTI P., FAZZUOLI M. and TACCONI P. (1979). Geological outlines of the Region between Juba and Webi Shebeli Rivers (Southeastern Somalia). Int. Con. "Geodyn. Evol. of the Afro-Arabian Rift System". Acc. Naz. Lincei e C.N.R., Roma, Italy.

DAL PRÀ A., BENVENUTI G., OMAR SHIRE I., OSMAN MOHAMED A., MUMIN M. GOD and AHMED YUSUF I. (1983). Hydrogeological Investigation in the surroundings area of Qorioley on the Shabeelle River. Univ. Naz. Somala. Quademi di Geologia della Somalia, 7.

FAILLACE C. (1964). Le risorse idriche sotterranee dei comprensori agricoli di Afgoy e Genale. Rivista di Agricoltura Subtropicale e Tropicale. Firenze, Italy, LVIII, n. 10-12.

FAILLACE C. (1964). Surface and ground water of Shebelle Valley. Ministry of Public Works, Mogadishu, Somalia.

FAILLACE C. (1983). Groundwater conditions of Beled Weyne Area and potential water sources for Township water supply. Ministry of Mineral and Water Resources. Mogadishu, Somalia.

FAILLACE C. (1986). Water quality data book of Somalia. Hydrogeology and water quality of Southern Somalia. G.T.Z, Roma, Italy.

FAILLACE C. (1987). Water quality data book of Somalia: Hydrogeology and water quality of Middle Somalia. G.T.Z, Roma, Italy.

FRANCESCHETTI B. and DORRE ABDULKADIR S. (1983). Indagine preliminare sulla potenzialità idrica dei bacini torrentizi situati sulla sinistra dell' Uebi Scebeli, tra Halgen e il pozzo di Ceel Gal. e sulle possibilità di realizzare in essi delle riserve d'acqua. Univ. Naz. Somala. Quaderni di Geologia della Somalia, 7.

HUNT J.A. (1955). Report on geological work carried out in connection with the proposed sub-surface dams, Hargeisa. Geol. Surv. Somaliland Prot., Westminster, U.K. and Nairobi, Kenya. I: 70 pp.

JOHONSON J.H. (1978). A conceptual Review of Somalia's Groundwater Resources. FAO.

LOW J. and Others (1985). A Baseline Survey in Sablaale District. Lower Shabeelle Region Somalia. EURO ACTION-ACORD, Mogadishu, Somalia.

MC DONALD and Partners (1982). Farjanno Settlement Project Land Evaluation. Report to NRC and UNHCR, Cambridge, U.K.

POZZI R. (1979). Studio geologico applicato e geofisico per dighe subalvee nel distretto del Nogal (Somalia Settentrionale). Mem. Sc. Geol. Padova, Italy, 32: 33 pp..

POZZI R. (1981). Lineamenti di Idrogeologia della Somalia. Univ. Naz. Somala. Quaderni di Geologia della Somalia, 7.

POZZI R., BENVENUTI G., GATTI G. and IBRAHIM MAHAMED FARAH (1983). Water Supply and agricultural use: a proposal for the adoption of sub-surface dams in Somalia. In: Proc. II Int. Congr. Somali Studies, Vol. II "Aspects of development" (Edited by LABAHN T.), Hamburg, Germany.

POZZI R., BENVENUTI G., MAHAMED C.X. and SHUURIUJE C.I. (1983). Groundwater resources in Central Somalia. Univ. Naz. Somala. Quaderni di Geologia della Somalia, 7.

PURCELL P.G. (1976). The Marda Fault Zone Ethiopia. Nature 261: 569-571.

SOMMAVILLA E., MASÈ G., MARCHESI S., CALI KASSIM, HUSSEN SALAD and IBRAHIM MAHAMED FARAH (1988). Hydrogeology in the Shabeelle Valley (Somalia) through. Geology, Geomorphology and Geophysics (in print).

*Final editing, January 1990*

From *Geology and mineral resources of Somalia and surrounding regions*, Ist. Agron. Oltremare, Firenze, Relaz. e Monogr. 113, 397-416, 1993.

# REGIONAL GRAVITY STUDY OF SOMALIA

A.S. DORRE * and A. RAPOLLA **

* Department of Geology, Somali National University, P.O. Box 1081, Mogadishu, Somalia.

** Dipartimento di Geofisica e Vulcanologia, Università di Napoli, Largo San Marcellino 10, 80134 Napoli, Italy.

ABSTRACT

Procedures and results concerning a regional gravity survey carried out on Southern, Central and Northeastern Somalia are presented in this paper. The aim of this research was to unify the pre-existing inhomogeneously distributed gravity data of Somalia under a single base station network. The compilation of the previous gravity data obtained from the surveys aimed to hydrocarbon researches with those made by the authors during 1984-1985 allowed to draw a Bouguer map of Somalia. A preliminary Free-air map, compiled by using only the data taken by the authors, is also presented.

A two dimensional filtering analysis has been then carried out on the Bouguer gravity anomaly data. The aim was to investigate the characteristics of the long wavelength gravity field of Somalia and particularly to delineate the regional pattern of the Moho discontinuity in that region. The results suggest that a higher-than 200 km wavelength component is the dominant regional gravity anomaly. It is interpreted to be caused by the variable morphology of the Moho in Somalia. It has been seen that the mean depth of the Moho throughout the country is about 30 Km, except on southeasternmost of Somalia where its depth decreases on less than 24 Km. A sharp decrease is also observed toward the coastal areas.

## GEOLOGICAL SETTING

Somalia lies along the east coast of Africa between latitudes 1.5° S and 12° N and between longitudes 41 °E and 51 °E. It occupies a territory of about 638,000 km². Somalia as other structurally related areas of East Africa, has been an environment of great development of marine and continental deposits. It is underlain principally by Mesozoic and Tertiary sedimentary rocks deposited unconformably on Precambrian metamorphic and igneous rocks. Quaternary and Holocene alluvial and eluvial deposits cover much of the southern coastal area. The Precambrian rocks are exposed in the northern block-fault mountains and in the broad uplift of the Bur Region, in Southern Somalia.

Structurally East African region is mainly dominated by the apparently fault-controlled southwest trending region of the Indian Ocean, the rifted and block-faulted,

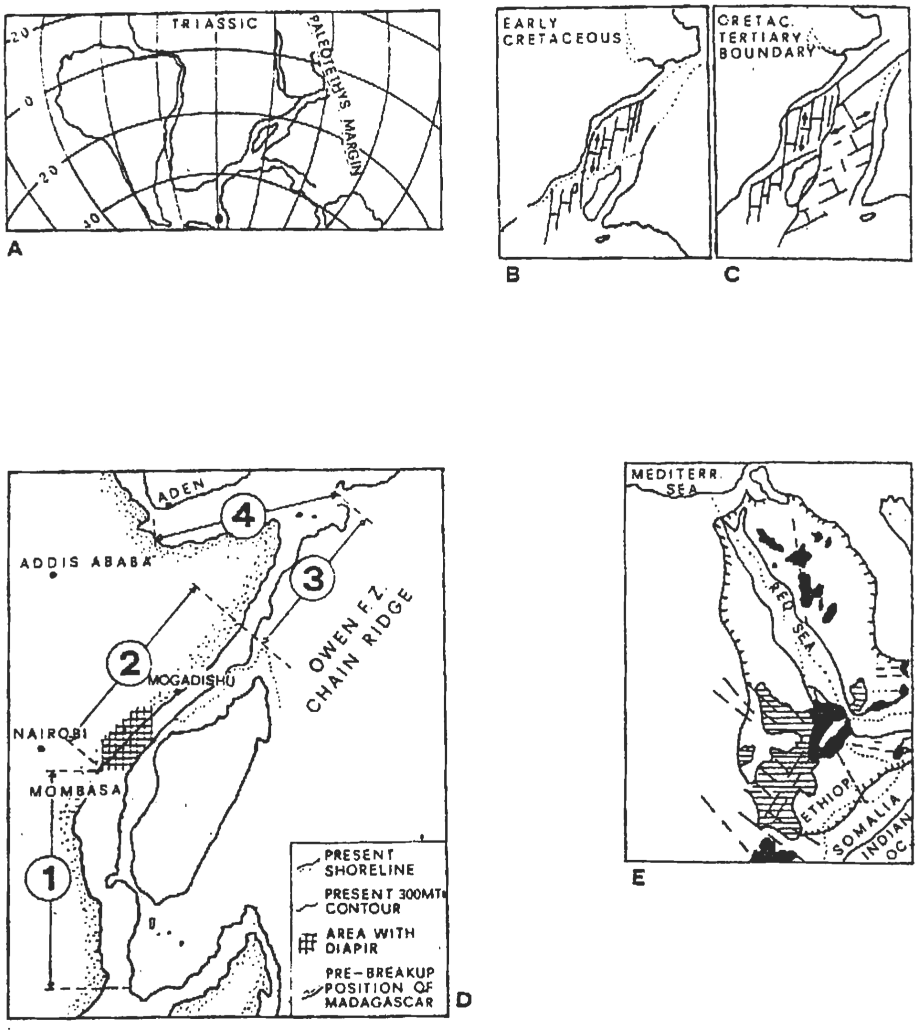


Fig. 1 - Geodynamic history of the East African Region from Triassic to Recent (A-D; after BOSELLINI, 1986) and structural map of the Afro-Arabian Dome (E).

east-northeast trending margin of the Gulf of Aden and the complexly faulted East African Rift on the west (Fig. 1). These structures were formed by major crustal plate movements related to the break-up of Madagascar and to the formation of the north-western margin of the Indian Ocean, the Gulf of Aden and Red Sea. These tectonic features are characterized by normal faulting and isostatic subsidence related to the regional extension.

Somalia, which is bordered by two of these regional structures (the north-western margin of the Indian Ocean and the Gulf of Aden) can not, geodynamically, be independent on the various tectonic effects due to this regional extension. It is believed that the coexistence of Precambrian crystalline basements with the more recent Tertiary sediments is caused by an unequal downward of the sialic crust during the Mesozoic and successive Tertiary ingression (MERLA et al., 1979). This unequality has consequently caused upheavals which formed the basement uplifts. But, unfortunately, a better insight of this belief has not been fully clarified yet. This fact is due to the lack of deep crustal studies which are necessary elements for the proper comprehension of the evolutionary history of this region. It has been, therefore, considered essential to begin regional geophysical studies in Somalia. Such studies are aimed to contribute to fill up the void of data which now exists between the African Rift bordered countries of East Africa and the Indian Ocean, two areas which are important for the geodynamic study of the region and particularly for the solution of the controversial problem of the break-up of Madagascar from the eastern coast of Africa.

## GRAVITY OBSERVATIONS

During 1984 and 1985, 830 gravity stations, 69 of which were base stations, were set on southern, Central and Northeastern Somalia (RAPOLLA et al., 1985, 1986). The measurements were taken along roads and tracks which were accessible and which were more or less perpendicular to the main regional structures. The gravity values of each station was determined from an average of at least three measurements; the mean distance between adjacent stations was 5 Km. Such spacing seemed adequate, given the aim of the survey. The gravity readings were made by a thermally compensated Worden Master Gravimeter. Prior to the field use, it was first calibrated on the Egyptian Embassy-Afgoi calibration run, previously established by the Somali Gulf Oil Company (VAN DAMME, 1962). The absolute gravity values of these two stations were g = 978072.20 mGal for the Egyptian Embassy-Mogadishu base station and g = 978035.90 mGal for the Afgoi base station. These gravity values were referred to Postdam absolute gravity value. The take-off point, the Egyptian Embassy base station, was itself tied to the Mogadishu former International Airport fundamental gravity station which had been established by HARDING in 1950 (VAN DAMME, 1962). Unfortunately, the exact position of the latter was not recognized with certainty due to the many improvements and reorganisations made at the Airport. The available figure of WOODS HOLE OCEANOGRAPHIC INSTITUTE by WOOLARD (adopted by VAN DAMME, 1962) was as follows:

Site: at the base of the flagpole on the runway-side of the terminal.

| | |
|---|---|
| Latitude: 2°1.0' N | Longitude: 45°19' E |
| Elevation: 27 ft | Gravity: 978076.90 mGal |

This station was part of the Woods Hole Worldwide Gravity Networh (MASON SMITH and ANDREWS, 1962). In Mogadishu, there was another fundamental base station which was also tied to Mogadishu former Airport base station and to the Egyptian Embassy base station and it was utilized in this survey as a check point. This station is the "AGIP Circle" base with an absolute gravity value of 978077.66 mGal.

Both available base stations in Mogadishu, that is the Egyptian Embassy and the AGIP Circle - base station, were unfortunately located in areas of intense day-time traffic. Therefore, it was thought proper to establish a new base station at ex-Gaheyr Campus of Somali National University in Mogadishu. This was made by several night-time connections. The Somali National University base (S.N.U.) resulted to have a gravity value of 978058.80 mGal. The monographs of the above mentioned stations are reported in Fig. 2.

During 1987, in cooperation with the University of Leeds, a gravity tie was made between London Heathrow and Mogadishu Egyptian Embassy base stations and then between the latter and AGIP base station at Darin (NE Somalia). During this survey another base station was established in the new University Campus in Mogadishu, in correspondence of the geophysical section.

The gravity value of the new University base is 978065.11 mGal. The London-Mogadishu tie gave a negative discrepancy of 0.9 mGal on the new Egyptian Embassy base value in respect to its older value. This may be due to the oldness of this base. Consequently, all gravity readings in Somalia might be added to 0.9 mGal (GREEN and DORRE, 1987). For facility reasons, S.N.U. base station was chosen as a take-off point for all the discrepancies successively established base stations throughout the country. For comparative reasons, several gravity bases, established by the previous hydrocarbon exploration surveys (VAN DAMME, 1964), were reoccupied discrepancies were generally negligible. Errors in base stations were minimized by network adjustment. The gravity differences between grid and base stations were determined by single observation at the former and then to the nearest base station, within a time interval of generally less than two hours; this being the normal time allowed so that the run may be corrected for linear drift.

Heights of gravity stations were determined by means of an accurate micro barometric survey which was carried out by a precision Paulin System altimeter. For the altimetric measurements a single base and leap-frog method was employed. The levelling network was tied, wherever possible, to trigonometric points and bench marks. Locations of the base stations were determined using the existing very accurate 1:100,000 topographic maps.

Bouguer density of 2.2 $g/cm^3$ was assumed for all areas except the Bur Region

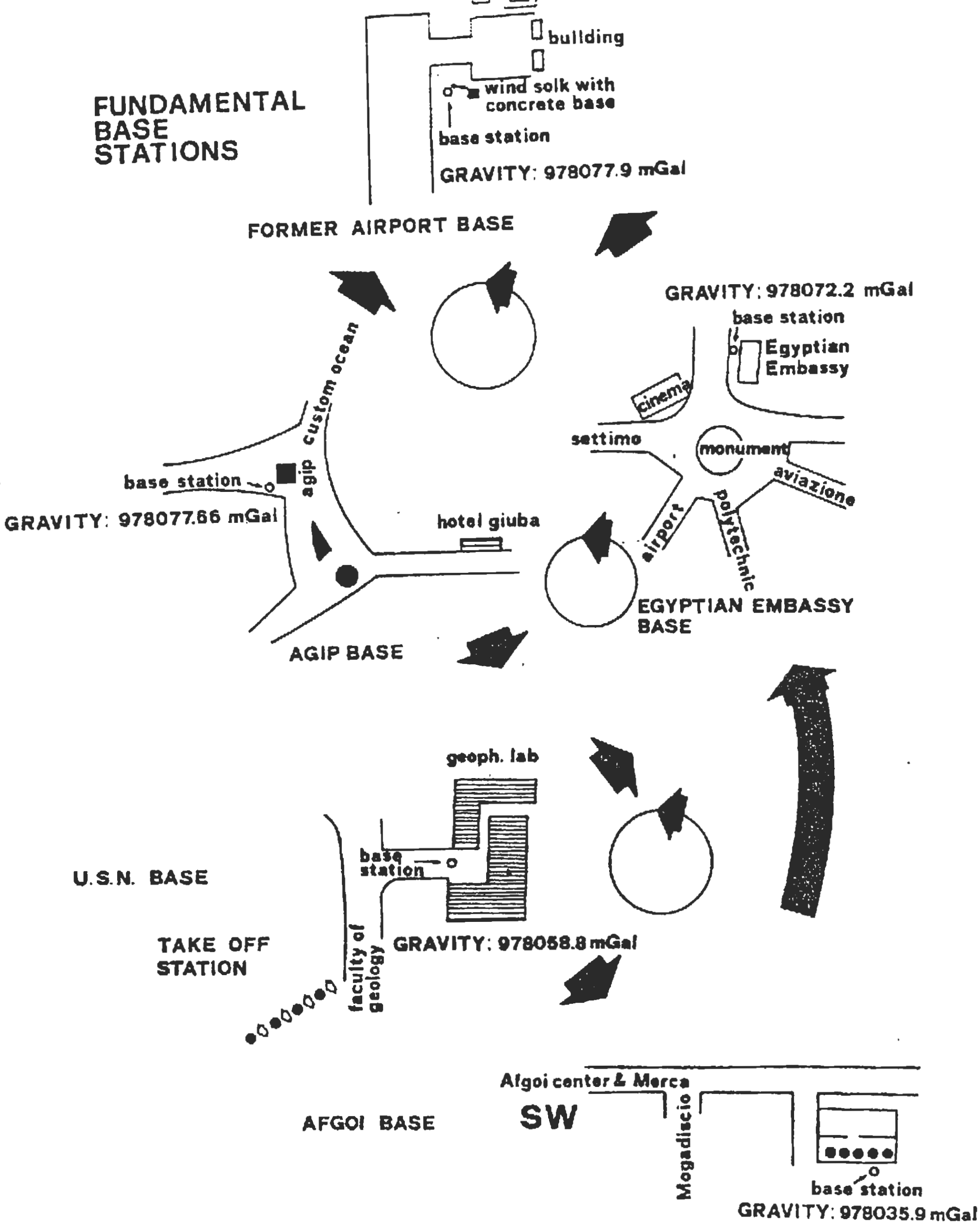


Fig. 2 - Monographics of fundamental base stations used for the Gravity Survey of 1985 - 1986.

(Southern Somalia) where 2.3 g/cm$^3$ density was used. In fact, in the Bur Region, the crystalline basement rises nearer to the surface and sometimes outcrops as isolated inselbergs. It is mostly covered by low density thick Quaternary sediments. This justifies the use of density value smaller than the normal basement density figures. Anyway, these density figures were those utilized by various oil companies which worked in Somalia and whose data were used for the compilation of our Bouguer map. We also consider that such density values are compatible with the geological features of Somalia. For the sake of comparison with the previous data, the theoretical gravity and consequently the Bouguer anomaly of each station, was derived from the International Gravity Formula of 1930.

Due to lack of large scale topographic maps, topographic corrections were not applied to the data. Anyway, this was considered to be not critical given the extreme flatness of the studied area.

In order to integrate our data with those of the oil companies and reduce all of them under the common reference station in Mogadishu, we correlated the data along some of our profiles with the data of the corresponding profiles of the oil companies. This correlating technique is illustrated on Fig. 3. It shows the correlation between our data (S.N.U.) with those of Conoco in north-eastern Somalia. A simple translating shift of -390 mGal was made on Conoco data in order to get values coherent with ours. This kind of correlation was the only possible as it was not available to us the precise locations of the base stations of the oil companies.

## FREE-AIR ANOMALY MAP

Free-air anomaly map (Fig. 4) has been constructed over the studied area (DORRE and RAPOLLA, 1987). This map is based only on the gravity survey of the Department of Geology of Somali National University as the gravity data listing of the areas covered by the oil companies was not available to us. Contours of equal anomaly were drawn at intervals of 10 mGal. Areas for which gravity values and heights were not available and significant interpolation was not possible are delineated by broken lines.

The main figures of this map are: the belt of gravity high with a maximum higher than 30 mGal in the northern part of the studied area; an appreciable negative value of the order of -30 mGal in Central Somalia; and a broad anomalous positive feature in the south. Although, due to lack of good reasonable coverage of data, we did not make a quantitative interpretation of these anomalies, it seems that at least some parts of Somalia is yet to arrive to an isostatic equilibrium.

## BOUGUER ANOMALY MAP

The compilation of our data and the homogenized data of oil companies allowed to draw the Bouguer map of Somalia which is presented in two sheets: the northern

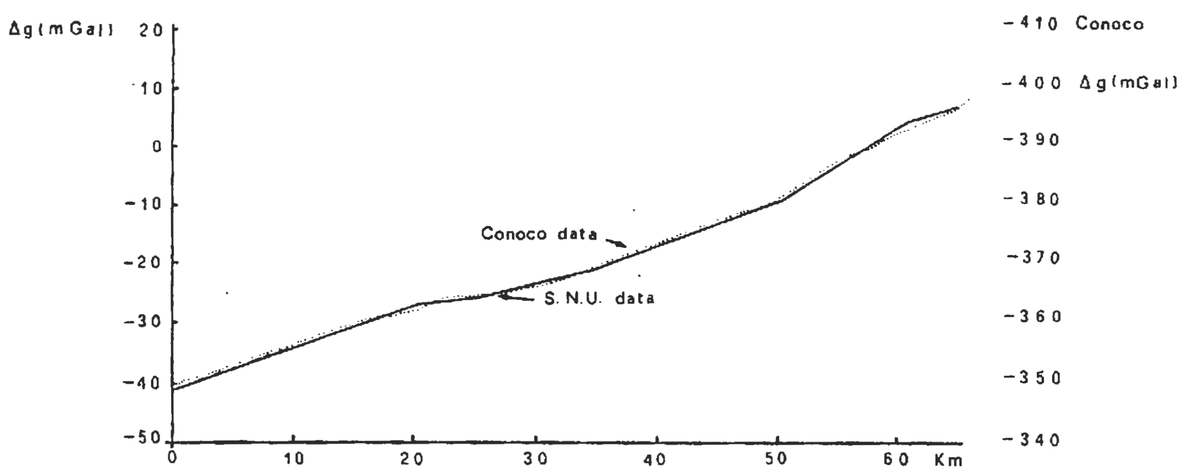


Fig.3 - Observed gravity values from the Garowe-Awrculus intersection to Eyl. Data from Conoco Survey and S.N.U. Survey are shown. A good fitting is obtained by shifting -390 mGal on Conoco data.

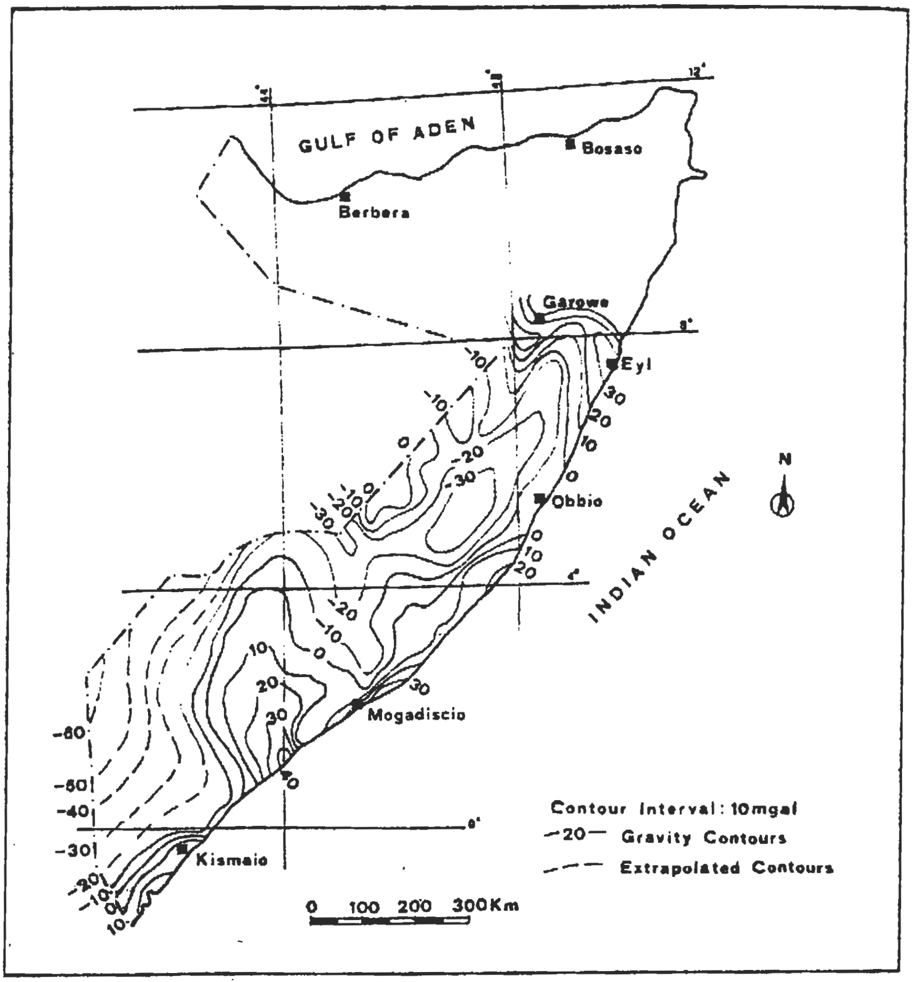


Fig. 4 - Free-air Anomaly map of Somalia.

sheet and the southern sheet (Figs. 5, 6). Both sheets are contoured at 5 mGal interval and show the presence of a long wavelenght negative anomaly which is superimposed on smaller positive anomalies. Both sheets show a seaward increase of the gravity anomalies as one would expect, but there are also other relevant regional anomalies For example, Central Somalia is dominated by a broad negative gravity low which attains values lower than -30 mGal. In the south-eastern most areas, the gravity anomaly gets its highest values, higher than 35 mGal. This anomaly begins on the coastal areas and

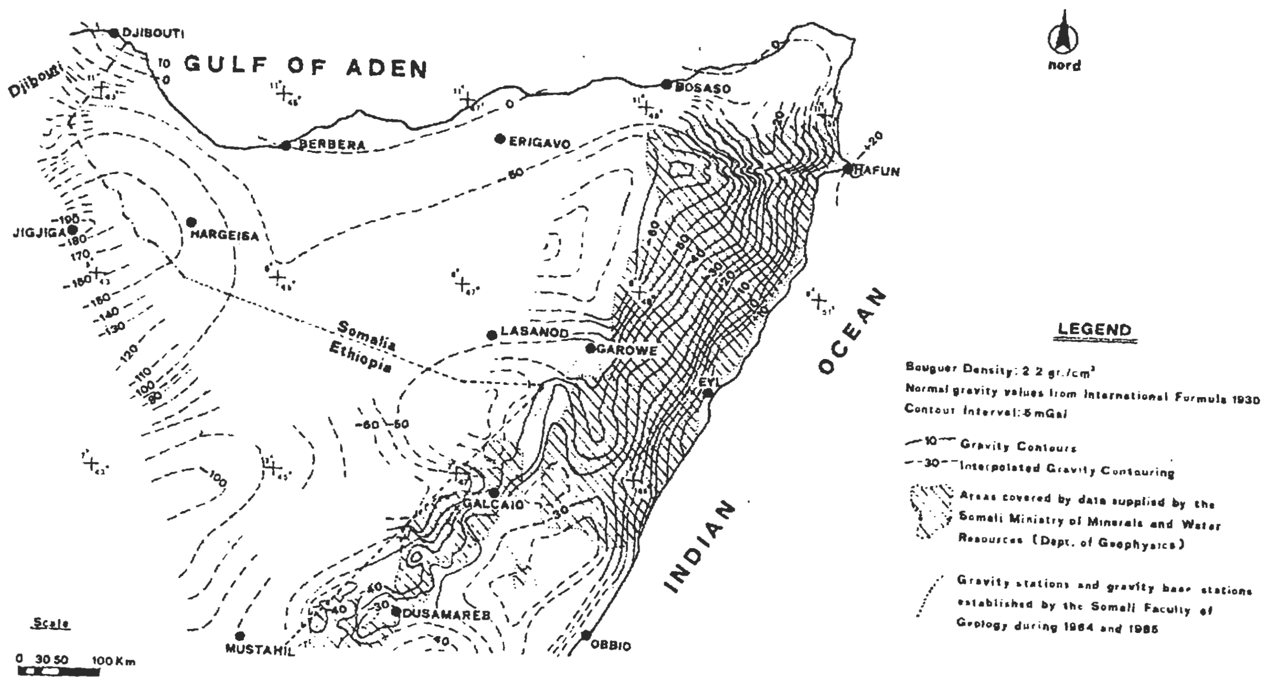


Fig. 5 - Gravimetric map of Northern Somalia.

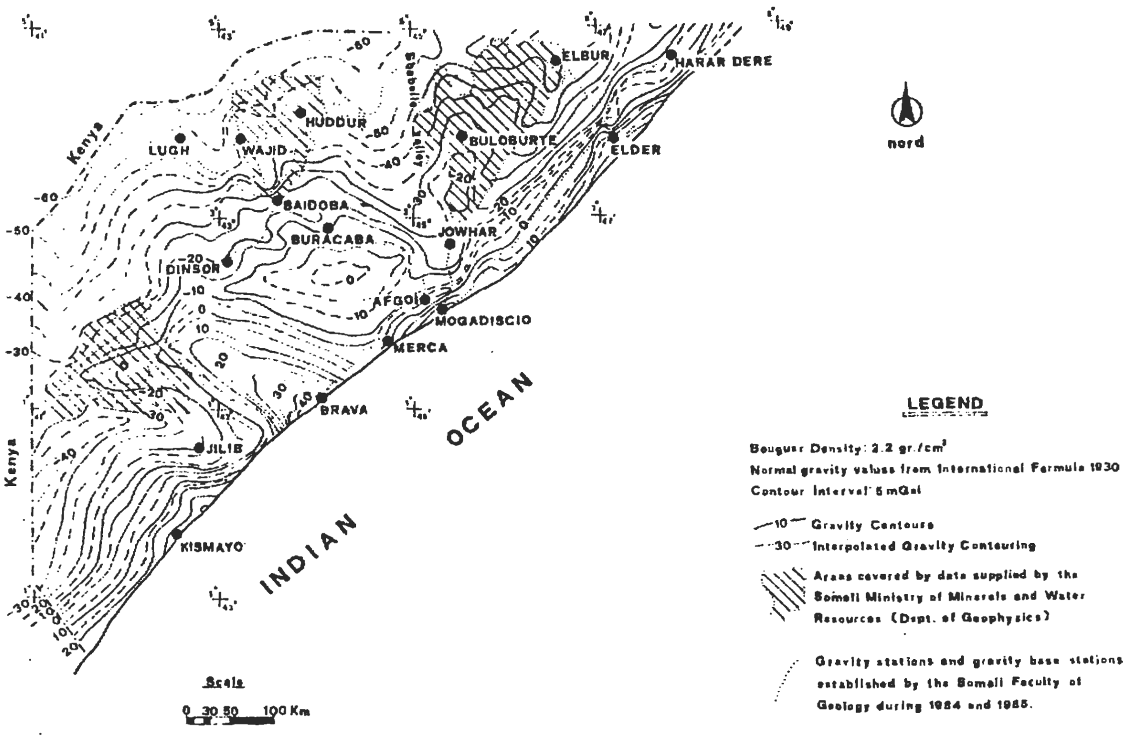


Fig. 6 - Gravimetric map of Southern Somalia.

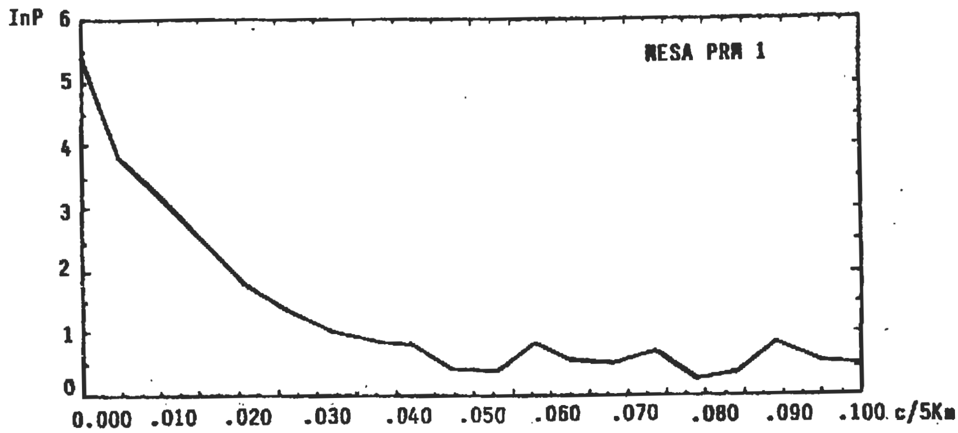


Fig. 7 - Mesa spectrum of the Bouguer Gravity profile between B/Uen and Mogadishu.

curves inland with its magnitude dropping about zero after nearly 200 km from the coast. It has a width larger than 75 km. Toward south-west, it passes to a small positive closure. Toward south, at about Kismaio, the magnitude of this anomaly decreases to values of about 25 mGal. There is also a relative high in corrispondence of the Bur basement.

A cursory look of the contour-lines of the southern sheet reveals that the dominant east-west trend in the south is replaced by south-north trending isogals in correspondence of Shabeele Valley where the continuity of the Mardha transcorrent fault of Ethiopia may be assumed. A gravity low is present in south-west Somalia in correspondence of the Lugh-Mandera basin. These great and small irregularities of the gravity field of Somalia indicate the existance of intermediate and deep seated crustal inhomogenities.

## DATA ANALYSIS

The gravity data set which was utilized for this study was based on values obtained by digitizing the Bouguer anomaly maps of Somalia with a square grid of 20 km x 20 km. As in every potential field data, the gravity data comprise anomalies caused by deeper bodies and those due to shallower structures. Therefore, in order to single out the anomaly due to the Moho, data were first filtered out of the high frequency components for diminishing the aliasing effect and then we estimated the wavelength of the gravity component due to such source. This is necessary in order to filter out the undesired anomalies mainly due to shallower structures. In order to isolate the desired wavelength, the Maximum Entropy (ME) and Fast Fourier Transform (FFT) analyses were made along selected profiles. Figs. 7 and 8 represent two typical examples of such

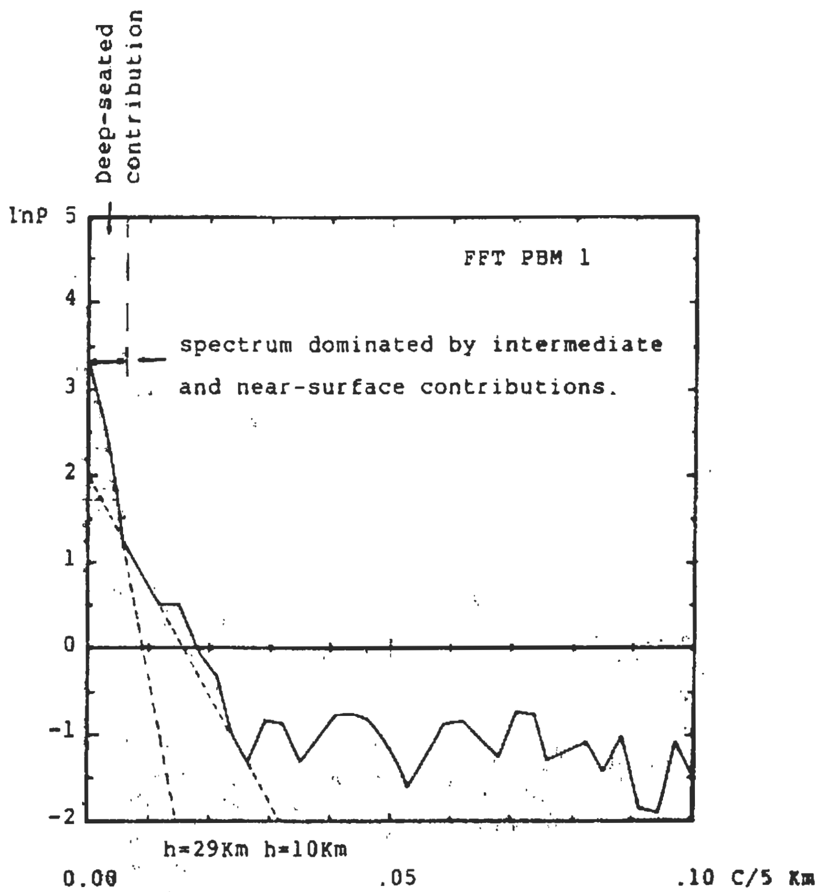


Fig. 8 - FFT spectrum of the Bouguer Gravity profile between B/Uen and Mogadishu. The power spectrum related to deep sources is indicated. Average depths of the deep-seated and intermediate sources calculated by SPECTOR and GRANT (1970) method are also shown.

spectral factorization. They show that the main long wavelength gravity component can be distinguished from the intermediate and higher frequencies. By applying to the FFT and modifications of GRANT and SPECTOR (1970), we estimated a value of about 30 km as the mean average depth of the deep seated anomaly source. However, as often happens, the examination of the spectra relative to several profiles showed that those spectra do not correlate perfectly each other. This therefore, prevented us to choose a unique cut-off to be used in the successive phase of filtering. Hence, we made along various gravity profiles several filtering attempts, using cut-off wavelengths within the

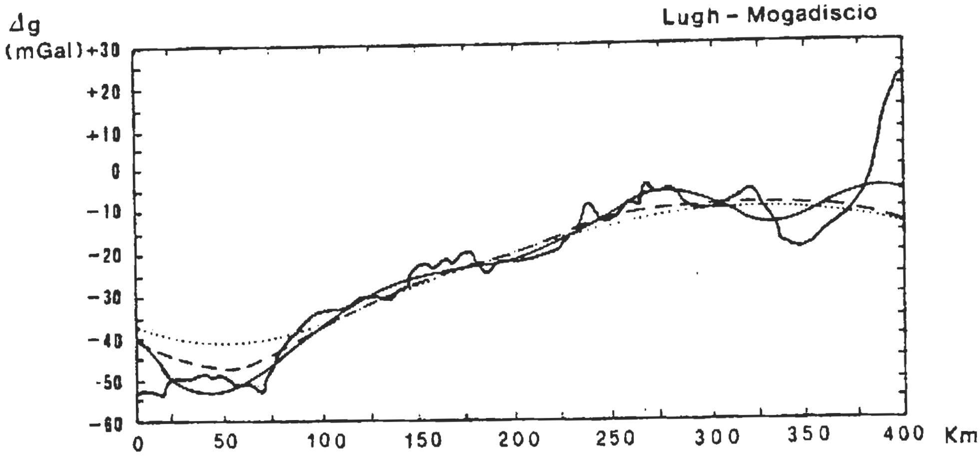


Fig. 9 - Observed gravity anomaly between Lugh and Mogadishu (solid line) and filtered anomaly: 100 Km (continous line), λ >200 Km (dashed line) and λ >300 Km (dotted line).

within the range suggested by the spectral analyses. Fig. 9 displays a representative profile showing the effects of the various cut-offs made on the gravity profile between Lugh and Mogadishu. This test, as well as the others, suggested that a cut-off wavelength higher than 200 km was the most suitable value to be used for filtering out the shallower effects, leaving alone the Moho gravity effect. Using this value, a two-dimensional filtering was applied to the whole gravity map of Somalia (Fig. 10).

To perform a quantitative interpretation to reveal the geometry of such deep seated anomaly, seven profiles were chosen from the filtered map. Due to lack of any Moho depth calibration point within Somalia, some of our profiles were extended to Harar area (in Ethiopia), where the Moho depth was previously calculated to be approximately 34 km (MAKRIS et al., 1972). The remaining profiles were connected to the previous ones.

These gravity profiles were modelled by using a computer program developed on the basis of the Talwani algorithim (TALWANI, 1959) for the computation of two-dimensional model of arbitrary shape. The program makes use of the least square iterative procedure for the best fitting between the observed and computed anomalies of the model (RAPOLLA, 1982). A simple two layer model with a density contrast of 0.3 g/cm$^3$ (assuming average densities of 3.0 g/cm$^3$ and 3.3 g/cm$^3$ for the crust and the mantle, respectively) were utilized as the first guess model. A series of iterations was made until the computed and the observed gravity curves agreed throughout the profile with a negligible tolerance. A representative best fitted computed and observed gravity curves with the corresponding model are reported in Fig. 11. Obviously, the results are affected by the well-know non uniqueness which affects the interpretations of all potential field data.

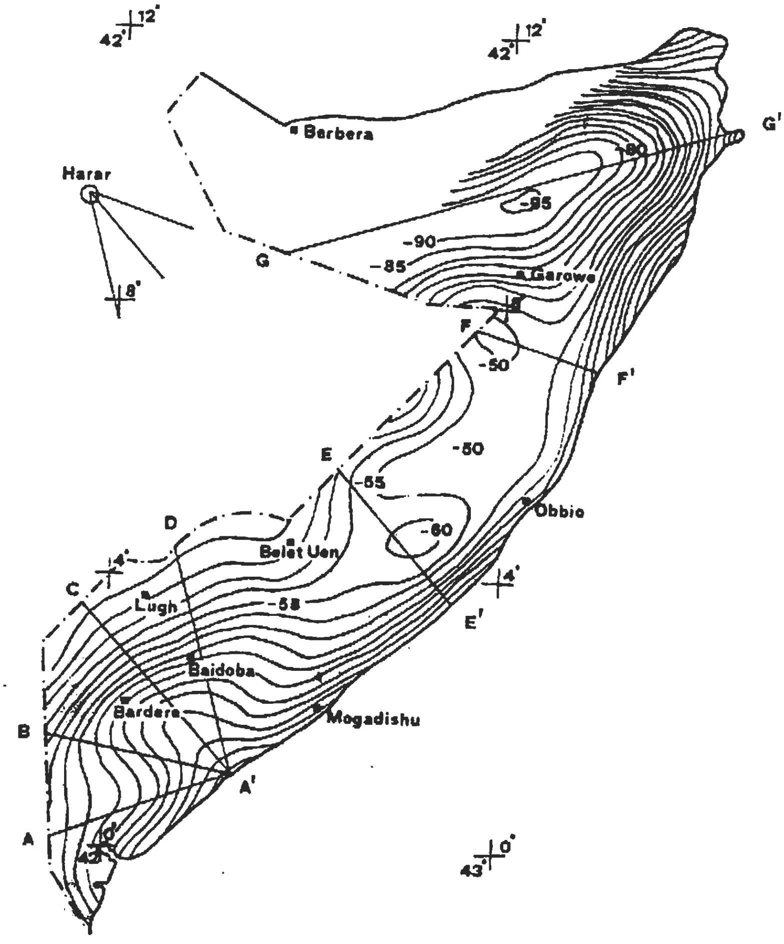


Fig. 10 - Filtered anomaly field of Somalia (λ >200 Km).

## MOHO DEPTH MAP OF SOMALIA

For the purpose of presenting the regional morphological trend of the Moho, a map whose contours show the depth to the Moho of Somalia was prepared. It was the result of the digitization of the above described Moho depth models, plotted and then contoured at 0.5 km interval (Fig. 12).

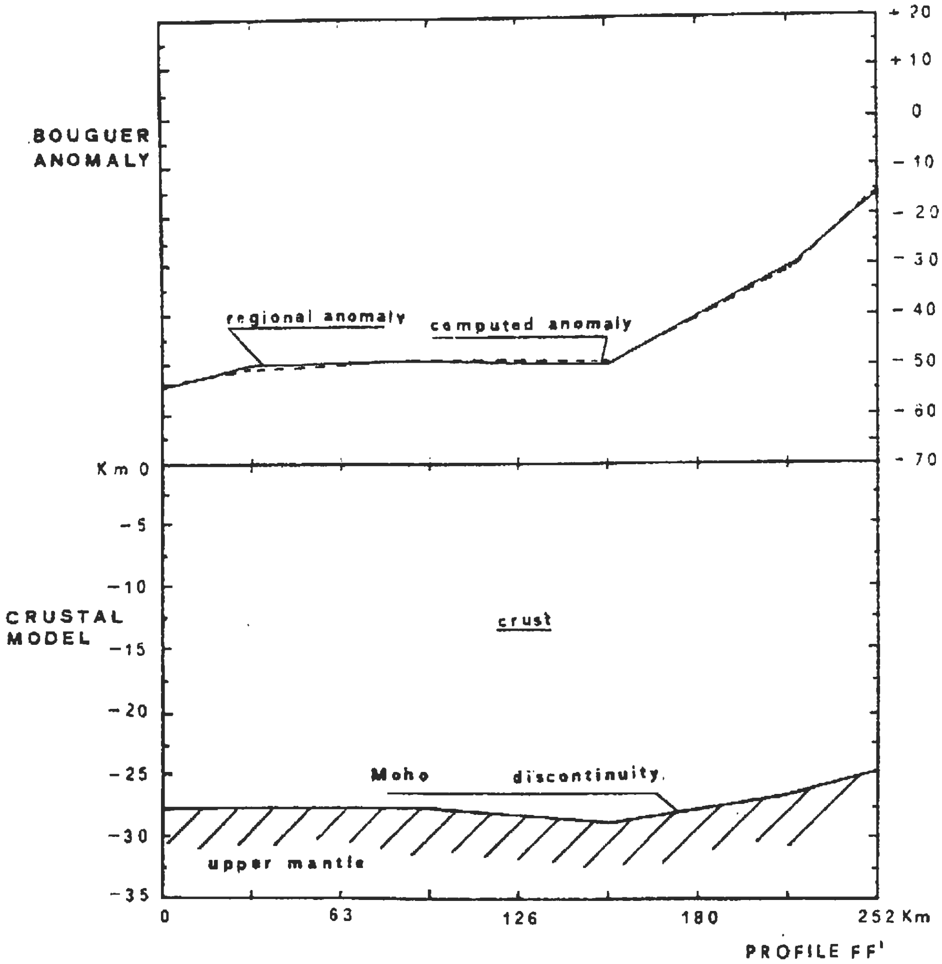


Fig. 11 - A) Observed (filtered) and fitted gravity profile FF'. B) The interpreted Moho discontinuity ($\Delta$ RHO = 0.3 g/cm$^3$).

Considering the main morphological feature of the Moho surface for the territory of Somalia, we may distinguish two wide regions having higher Moho (up to 35 km) depth in the north-eastern part and in the southern part of Somalia. Another interesting feature is the presence of a large Moho depression in Central Somalia in correspondence of the Central Somalia Embayment. An area characterized by a lower Moho depth (less than 25 km) is located along the southern coast of Somalia from the Kenyan border to

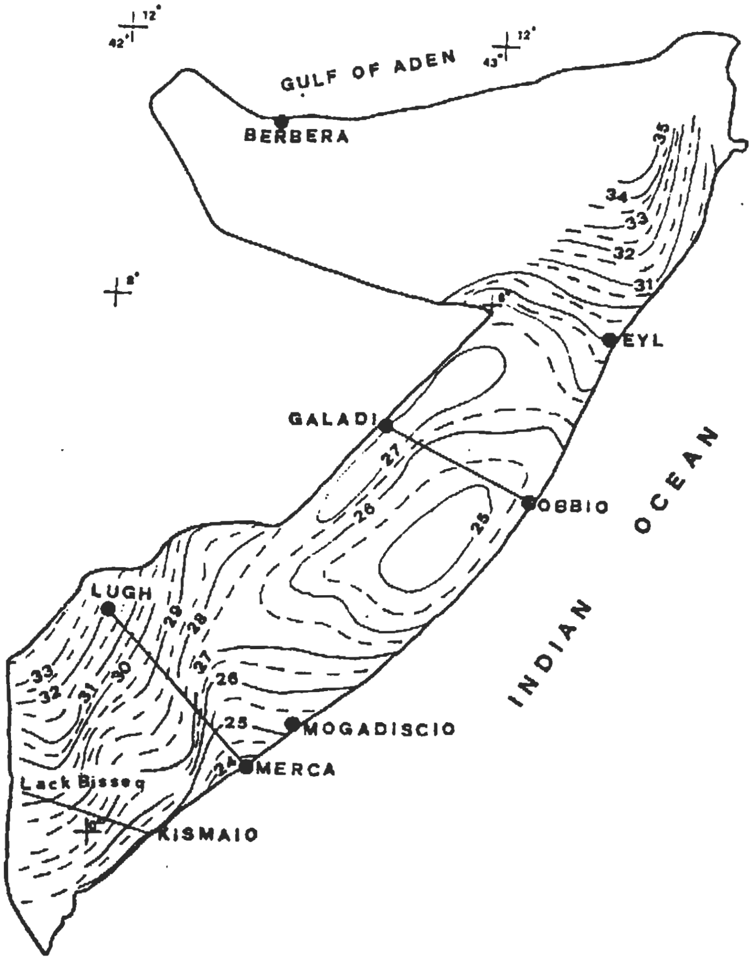


Fig. 12 - The Moho depth of Somalia (density contrast = 0.3 g/cm³). - - - - - - - Contour lines (Km).

about Mogadishu. The depth of the Moho in Northeastern Somalia may be related to the increasing topographic relief; on the contrary, the increase observed in Southwest Somalia is geographically correspondent to the Lugh-Mandera basin.

In order to present at least a preliminary correlation between the surface morphology of the Moho with that of the basement in Somalia, three schematic cross-sections based on our Moho depth results and those of Schluemann upper crust geological sections in Somalia (1983) were prepared.

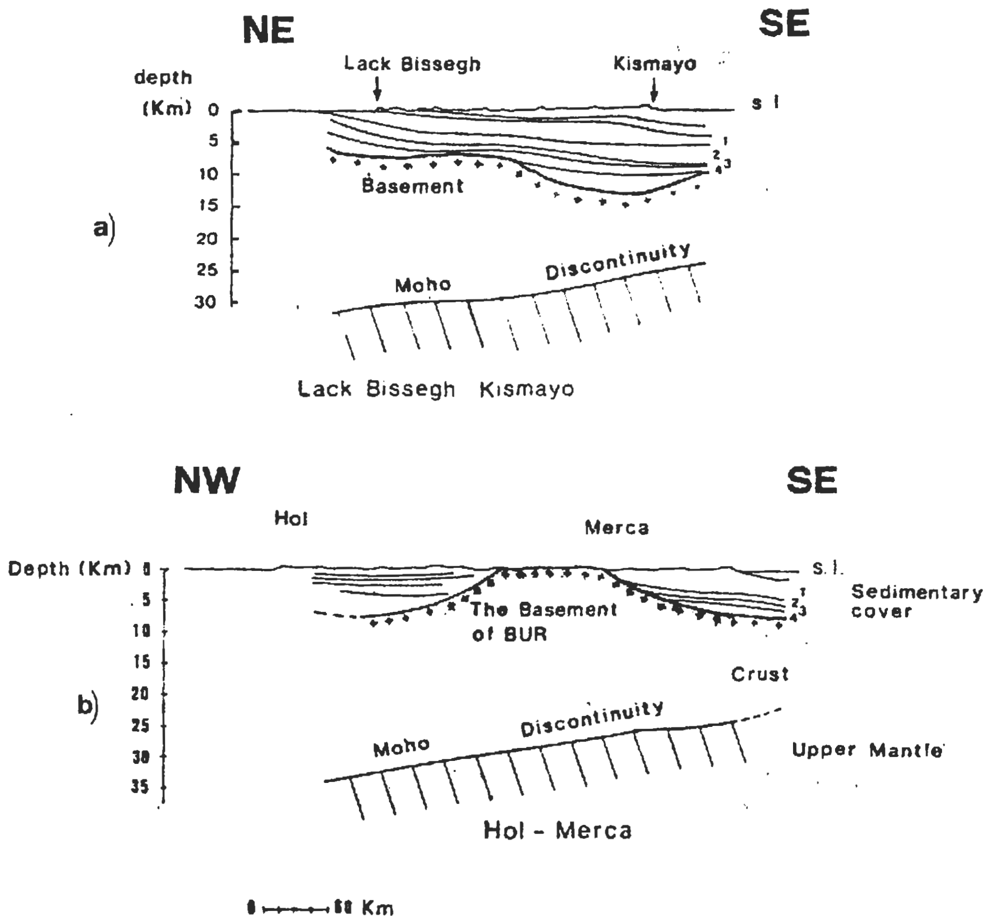


Fig. 13 - Crustal model deduced from gravity data (shallow geologic section after SCHUNEMANN, 1983). 1. Tertiary; 2. Cretaceous; 3. Jurassic; 4. Karoo/Adigrat.

The first section (Fig. 13a) begins on Lack Bissegh area near the Somali-Kenya border area and ends on the coastal areas of Kismaio in Somalia. The thickness of the basement thins from more than 25 km on the border areas to less than 15 km before the coastal area. This clearly shows the existence of relevant crustal attenuation from the border area of Kenya and Somalia to the coast.

The second section (Fig. 13b) starts from the Hol well near Lugh (Southwest Somalia), passes through the Bur crystalline basement uplift and arrives to the coastal

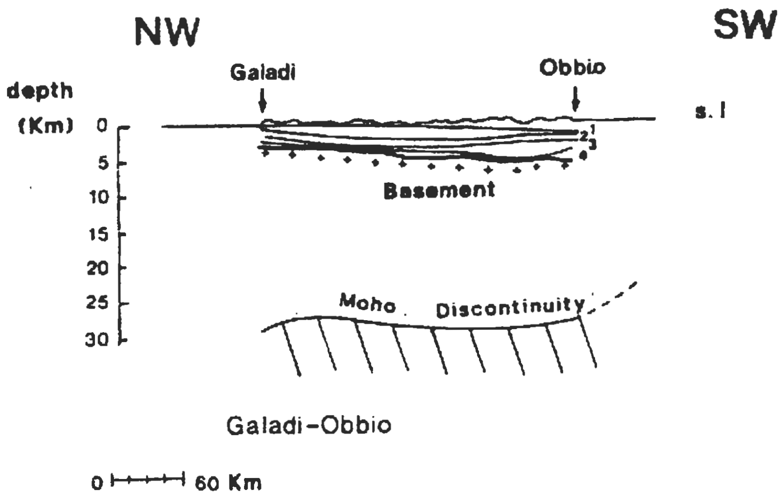


Fig. 14 - Crustal Model deduced from gravity data (shallow geologic section after SCHUNEMANN, 1983). 1. Tertiary ; 2. Cretaceous; 3. Jurassic; 4. Karoo/Adigrat.

area of Merca. The Moho morphology rises from 35 km in Lugh area to about 25 km in Merca. It is interesting to note that the Moho morphology seems not to be effected by the morphology of the top of the basement. This basement outcrops in Bur area and reaches a depth more than 8 km in the Lugh basin.

The last section (Fig. 14) is the one connecting Galadi near the Ethiopia and Somali border on Central Somalia to the coastal area of Obbio. Here, although a depressed Moho surface is seen, the change of morphology is very gradual: it changes from a maximum depth of 28 km to a minimum depth of 29 km and then rises to 28 km again.

## CONCLUSIONS

The completion of the first Free-air and Bouguer gravity anomaly maps of Somalia is important as it enables to gain a better insight regarding the existence and the development of intracratonic structures in Somalia. The anomalous features on these maps reveal that the region is by far more complex than supposed. Therefore, further geological and geophysical studies should be made especially on Southern Somalia where there are both positive Free-air and Bouguer anomalies and northern part of the studied area where, for about 100 km, inland incurved isogals disturb the regular north-east trending anomalies.

Since the density contrast used for the computation of the Moho depth is based on few literature data about the regional geology and geophysics of the neighbouring countries rather than on seismic determinations made in Somalia and since there is a lack of any information on the Moho depth in Somalia to be utilized as constrains points in the interpreted earth model, the obtained Moho depth map of Somalia should be considered only as preliminary. However, it gives valuable input data and guideline for the planning of the future geophysical and geodynamic researches in Somalia. More precise and detailed results about the crustal structures of this region will be hopefully determined when also the intermediate wavelength gravity components of the gravity field of Somalia are taken into account, especially where detailed gravity data exists and where other supportive geophysical data become available. It is our programme to carry out such a study along main geotraverses in the framework of the Global Geotransect Project of the International Litosphere Programme.

ACKNOWLEDGMENTS

A number of people, many more than we can mention here, have helped us both directly and indirectly in the process of preparing this work. First, our colleagues of the Department of Geology of Somali National University and University of Naples particularly Drs. HASSAN M.M. and ROBERTI N. for their essential field work participation. We owe all of them a debt of gratitude for encouraging us to undertake such a major effort. Their prodding questions and challenging criticism helped us to obtain plausible results from a work without precedent in Somalia.

The authors would like to express their sincere gratitude to Prof. F. SASSI of the Technical Committee of the Italian Ministry of Foreign Affairs for the strong encouragement he gave us during all phase of this research. We, moreover, gratefully acknowledge the financial contribution of the Italian Ministry of Foreign Affairs, Department for Cooperation and Development and of the Somali National University.

We pay tribute to the Somali Ministry of Mines which kindly put on at our disposal many geological and geophysical data necessary for the completion of this paper.

## REFERENCES

BOSELLINI A. (1986). East Africa continental margins. Geology, 14: 76-78.

DORRE A.S. and RAPOLLA A. (1987). Free-air and Bouguer maps of Somalia. Univ. Naz. Somala. Quad. Geol. Somalia, 10, in press.

GREEN C.M. and DORRE A.S. (1987). Gravity tie between AGIP survey of NE Somalia and Somali national gravity base station network. Unpublished report.

MAKRIS J., MENZEL H., ZIMMERMANN J. and GOUIN P. (1974). Gravity field and crustal structure of north Ethiopia. Tectonophysics, 15.

MASON SMITH D. and ANDREWS E.M. (1962). East Africa gravity base systems. Geophys. Jour. Roy. Astro. Soc.,Vol. 7(1).

MERLA G., ABBATE E., AZZAROLI A., BRUNI P., CANUTI P., FAZZUOLI M., SAGRI M. and TACCONI P. (1979). Geological map of Ethiopia and Somalia (1973), 1:2,000,000 and comment with a map of major landforms. C.N.R. Italy. Centro Stampa, Firenze, 95 pp..

RAPOLLA A, DORRE A.S., CARRARA E., ROBERTI N. and HASSAN M. (1986). Studio gravimetrico e magnetico della Somalia: descrizione della rete gravimetrica di base della Somalia centro-meridionale. Univ. Naz. Somala. Quad. Geol. Somalia, 9 .

RAPOLLA A. (1982). Some aspects of the interpretation of the gravity data for the study of regional and local structures. In: The solution of the inverse problem in geophysical interpretation. Plenum Press, London.

RAPOLLA A., DORRE A.S. and HASSAN M. (1986). Studio gravimetrico della Somalia: descrizione della rete gravimetrica di base della Somalia centrale e nord orientale. Univ. Naz. Somala. Quad. Geol. Somalia, 9.

SCHUNEMANN H.W. (1985). Exploration for oil in Somalia. Univ. Naz. Somala. Quad. Geol. Somalia, 8.

SPECTOR A. and GRANT F.S. (1970): Statistical models for interpretating aeromagnetic data. Goophysics, 35.

TALWANI M., WORZOL J.L. and LANDISMAN M. (1959). Rapid gravity computation for 2-dimensional bodies with applications to the Mendocino fracture zone. J. Geophys. Res., 64.

VAN DAMME A.M. (1962). Gravimeter calibration bases Mogadishu. Unpublished report. Geophysical Department the Ministry of Minerals and Water Rosources, Mogadishu.

VAN DAMME A.M. (1964). Gravity base net of Somali Gulf Oil Company. Unpublished report. Geophysical Department of the Ministry of Minerals and Water Resources, Mogadishu.

*Final editing, January 1990*

Finito di stampare
nel maggio 1994
dalla Litografia I.P., Firenze